

# Diastolic Relaxation of the Heart

# Diastolic Relaxation of the Heart

*Basic Research and Current Applications for  
Clinical Cardiology*

*Edited by*

WILLIAM GROSSMAN

BEVERLY H. LORELL



Martinus Nijhoff Publishing

A Member of the Kluwer Academic Publishers Group

BOSTON DORDRECHT LANCASTER

## DISTRIBUTORS

for the United States and Canada: Kluwer Academic Publishers, 101 Philip Drive, Assinippi Park, Norwell, MA, 02061, USA

for the UK and Ireland: Kluwer Academic Publishers, MTP Press Limited, Falcon House, Queen Square, Lancaster LA1 1RN, UK

for all other countries: Kluwer Academic Publishers Group, Distribution Centre, P.O. Box 322, 3300 AH Dordrecht, The Netherlands

## Library of Congress Cataloguing in Publication Data

Diastolic relaxation of the heart.

“Edited compilation of the scientific presentations given at an International Symposium on the Physiology of Diastole in Health and Disease, Sept. 11–14, 1986 in Cambridge, Massachusetts”—Pref.

Includes index.

1. Diastole (Cardiac cycle)—Congresses. 2. Congestive heart failure—Congresses. I. Grossman, William, 1940–. II. Lorell, Beverly. III. International Symposium on the Physiology of Diastole in Health and Disease (1986 : Cambridge, Mass.) [DNLM: 1. Myocardial Contraction—congresses. WG 280 D541 1986]

QP114.D5D53 1987 616.1'2907 87-18466

ISBN 978-1-4615-6834-6 ISBN 978-1-4615-6832-2 (eBook)

DOI 10.1007/978-1-4615-6832-2

Copyright © 1988 by Martinus Nijhoff Publishing, Boston

Second Printing 1989

Softcover reprint of the hardcover 1st edition 1989

All rights reserved. No part of this publication may be reproduced, stored in a retrieval system, or transmitted in any form or any means, mechanical, photocopying, recording, or otherwise, without the prior written permission of the publishers, Martinus Nijhoff Publishing, 101 Philip Drive, Assinippi Park, Norwell, MA 02061, USA

# Contents

Preface	viii
Contributing Authors	ix

## PART I: Cell Biology of Diastole

1. Cellular Mechanisms of Relaxation: Lessons From Frogs, Birds, and Mammals WILLIAM H. BARRY	3
2. Sarcoplasmic Reticular Control of Cardiac Contraction and Relaxation ARNOLD M. KATZ	11
3. Calcium and Cardiac Relaxation JAMES P. MORGAN, RODERICK MACKINNON, MAURICE BRIGGS, <i>and</i> JUDITH K. GWATHMEY	17
4. Variable Calcium Sensitivity of the Mammalian Cardiac Contractile System SAUL WINEGRAD, GEORGE MCCLELLAN, ANDREA WEISBERG, STEVEN WEINDLING, <i>and</i> LIN ER LIN	27
5. Is Ischemic Contracture Preceded by a Rise in Free Calcium? WILLIAM H. BARRY	33
6. The Effect of Regional Myocardial Heterogeneity on the Economy of Isometric Relaxation NORMAN R. ALPERT <i>and</i> LOUIS A. MULIERI	39
7. Functional Sequelae of Diastolic Sarcoplasmic Reticulum Ca <sup>2+</sup> Release in the Myocardium EDWARD G. LAKATTA, MAURIZIO C. CAPAGROSSI, ARTHUR A. KORT, <i>and</i> MICHAEL D. STERN	49

## PART II: Physiologic Modifiers of Relaxation in Experimental Models

8. Hypoxia and Relaxation WINIFRED G. NAYLER, DARREN J. BUCKLEY, <i>and</i> JENNIFER S. ELZ	67
9. Ischemic/Hypoxic and Reperfusion/Reoxygenation Contractures: Mechanisms A.H. HENDERSON	73
10. Load Dependence of Relaxation DIRK L. BRUTSAERT <i>and</i> STANISLAS U. SYS	83

11. The Effects of Cardiac Hypertrophy on Intracellular  $\text{Ca}^{2+}$  Handling  
 JAMES P. MORGAN, RODERICK MACKINNON, MARC FELDMAN, WILLIAM  
 GROSSMAN, *and* JUDITH K. GWATHMEY 97

### PART III: Evaluation of Relaxation and Compliance in the Intact Heart

12. Diastolic Myocardial Mechanics and the Regulation of Cardiac Performance  
 J. SCOTT RANKIN, J. WILLIAM GAYNOR, MICHAEL P. FENDEY,  
 DONALD D. GLOWER, JOHN A. SPRATT, GEORGE S. TYSON, GEORGE W.  
 MAIER, CRAIG O. OLSEN, THOMAS N. SKELTON *and* THOMAS M. BASHORE 111
13. Evaluation of Time Course of Left Ventricular Isovolumic Relaxation in Man  
 JOSEPH P. MURGO, WILLIAM E. CRAIG, ARES PASIPOULARIDES 125
14. Loading Conditions and Left Ventricular Relaxation  
 WILLIAM H. GAASCH, MICHAEL R. ZILE, ALVIN S. BLAUSTEIN *and*  
 OSCAR H. L. BING 133
15. Influence of Pressure and Volume Overload on Diastolic Compliance  
 H. P. KRAYENBUEHL, O. M. HESS, M. RITTER, J. SCHNEIDER,  
 E. S. MONRAD, *and* J. GRIMM 143
16. Influence of the Pericardium on Diastolic Compliance  
 MARTIN M. LEWINTER 151
17. Implications of Pericardial Pressure for the Evaluation of Diastolic  
 Dysfunction  
 JOHN V. TYBERG, NAIRNE W. SCOTT-DOUGLAS, INS KINGMA,  
 MOUHIEDDIN TRABOULSI, *and* ELDON R. SMITH 163
18. Comparative Effects of Ischemia and Hypoxia on Ventricular Relaxation  
 in Isolated Perfused Hearts  
 CARL S. APSTEIN, LAURA F. WEXLER, W. MARK VOGEL,  
 ELLEN O. WEINBERG *and* JOANNE S. INGWALL 169
19. Effects of Hypoxia on Relaxation of the Hypertrophied Ventricle  
 BEVERLY H. LORELL, LAURA F. WEXLER, SHIN-ICHI MOMOMURA, ELLEN  
 WEINBERG, JOANNE INGWALL, *and* CARL S. APSTEIN 185
20. Relaxation and Diastolic Distensibility of the Regionally Ischemic Left  
 Ventricle  
 WILLIAM GROSSMAN 193

### PART IV: Clinical Disorders of Diastolic Relaxation and Compliance

21. Altered Diastolic Distensibility During Angina Pectoris  
 SHIGETAKE SASAYAMA 207
22. Diastolic Function During Exercise-Induced Ischemia in Man  
 JOHN D. CARROLL, OTTO M. HESS, *and* HANS PETER KRAYENBUEHL 217

23. Left Ventricular Filling in Ischemic and Hypertrophic Heart Disease ROBERT O. BONOW	231
24. Regional Diastolic Dysfunction in Coronary Artery Disease: Clinical and Therapeutic Implications HUBERT POULEUR AND MICHAEL ROUSSEAU	245
25. Ejection, Filling, and Diastasis During Transluminal Occlusion in Man: Consideration on Global and Regional Left Ventricular Function PATRICK W. SERRUYS, WILLIAM WIJNS, FEDERICO PISCIONE, PIM DE FEYTER, <i>and</i> PAUL G. HUGENHOLTZ	255
26. Diastolic Ventricular Function in Primary and Secondary Hypertrophy: The Influence of Verapamil W. H. BLEIFELD	281
27. Failure of Inactivation of Hypertrophied Myocardium: A Cause of Impaired Left Ventricular Filling in Hypertrophic Cardiomyopathy and Aortic Stenosis WALTER J. PAULUS, STANISLAS U. SYS, PAUL NELLENS, GUY R. HENRICKX, <i>and</i> ERIC ANDRIES	291
Index	305

# Preface

This book represents an edited compilation of the scientific presentations given at an International Symposium on the Physiology of Diastole in Health and Disease, September 11 to 14, 1986, in Cambridge, Massachusetts. Numerous studies have documented the importance of diastolic dysfunction in clinical heart disease. In recent years clinicians have become increasingly aware that many patients with congestive heart failure have completely normal myocardial contractile function. In these patients, inotropic agents provide no clinical benefit and may in fact exacerbate clinical manifestations of heart failure. These patients, who may be regarded as having diastolic heart failure, represent a major therapeutic challenge today. It has also become increasingly apparent that a variety of pathologic processes can result in diastolic dysfunction sufficient to cause congestive heart failure. These include pathologic processes *extrinsic* to the ventricular myocardium (e.g., constrictive pericarditis) as well anatomic and pathologic alterations within the ventricular wall (e.g., fibrosis, amyloidosis). However, an exciting body of information has emerged that supports the concept that altered intracellular function within myocytes may play a role in the diastolic dysfunction of many patients with heart failure.

The intracellular processes that control myocardial relaxation have been rapidly delineated in recent years. A central role for sarcoplasmic reticular calcium sequestration has been clearly established. Moreover, the role of disturbed intracellular calcium handling associated with a variety of pathologic processes has been increasingly documented in both experimental animals and humans. The available data suggest to us that diastole should be regarded as a high-energy state, because the myocardial contractile proteins can only relax in the presence of very low intracellular calcium concentrations (i.e.,  $10^{-7}$  M), and substantial energy expenditure is required to maintain this very low cytosolic calcium concentration in myocytes bathed by an extracellular fluid whose calcium concentration is approximately  $10^{-3}$  M. Considered from this point of view, the transition from diastole to systole that occurs with each heart beat may be

viewed as rolling downhill from an uphill or high-energy state. This transition results from the opening of membrane pores that allow calcium to rush into the cytosol, triggering excitation-contraction coupling. If the energy available to sarcoplasmic reticular and sarcolemmal calcium pumps was insufficient to remove this calcium from the cytosol and restore the 10,000-fold calcium gradient, characteristic of the "resting" myocyte, we would live for one glorious systole and die in cardiac rigor. The well-known phenomenon of rigor mortis reminds us that for skeletal muscles as well relaxation is the high-energy state and permanent contraction is the inevitable downhill state for muscle that can no longer produce adenosine triphosphate. Given these considerations, it should hardly be surprising that a variety of pathophysiologic states which impair membrane energy metabolism or adversely alter the functional capacity of intracellular calcium pumps will be associated with some impairment of myocardial relaxation.

The material presented in this book summarizes current knowledge concerning the biological basis for understanding diastolic relaxation and compliance. In addition to cellular biology, the importance of mechanical factors such as ventricular interaction, coronary vascular turgor, and the pericardium are emphasized. Finally, the relevance of an understanding of diastolic physiology to clinical practice is presented. Evaluation of diastolic relaxation and compliance in the intact heart is a controversial subject, and some of the methodologic issues are addressed by a variety of experts in this field. We hope that this book will serve as a stimulus to further investigation, as well as a compendium of current knowledge concerning cardiac diastole. We are deeply grateful to Dr. Eugene Braunwald, who has enthusiastically supported our research efforts in this area over the past 12 years, as well as to our many colleagues whose work is summarized in these pages.

William Grossman, M.D.  
Beverly H. Lorell, M.D.  
Boston, Massachusetts

# Contributing Authors

Norman R. Alpert, Ph.D., Professor of  
Physiology,  
Chairman, Department of Physiology and  
Biophysics,  
University of Vermont College of Medicine,  
Burlington, VT.

Carl S. Apstein, M.D., Professor of Medicine,  
Director, Cardiac Muscle Research Laboratory,  
Boston University School of Medicine;  
Chief, Section of Cardiology,  
Boston City Hospital,  
Boston, MA.

William H. Barry, M.D., Nora Eccles Harrison  
Professor of Medicine, Chief, Division of  
Cardiology,  
University of Utah Medical Center,  
Salt Lake City, UT.

Walter H. Bleifeld, M.D., Direktor der  
Abteilung Kardiologie der Medizinischen  
Klinik,  
Universitäts-Krankenhaus Eppendorf,  
Hamburg, West Germany.

Robert O. Bonow, M.D., Senior Investigator,  
Chief, Nuclear Cardiology Section,  
Cardiology Branch,  
National Heart, Lung, and Blood Institute,  
Bethesda, MD.

Dirk L. Brutsaert, M.D., Professor of  
Physiology,  
Univitaire Instelling Antwerpen,  
Edegem, Belgium.

John D. Carroll, M.D., Assistant Professor of  
Medicine,  
The University of Chicago Hospital,  
Chicago, IL.

William H. Gaasch, M.D., Professor of  
Medicine,  
Tufts University School of Medicine;  
Chief of Cardiology,  
Veteran's Administration Medical Center,  
Boston, MA.

William Grossman, M.D., Herman Dana  
Professor of Medicine,  
Harvard Medical School; Chief, Cardiovascular  
Division,  
Beth Israel Hospital,  
Boston, MA.

Andrew Henderson, F.R.C.P., Sir Thomas  
Lewis Chair Professor of Cardiology,  
University of Wales College of Medicine;  
Head, Department of Cardiology,  
British Heart Foundation,  
Heath Park, Cardiff, Wales.

Arnold M. Katz, M.D., Professor of Medicine,  
Head, Division of Cardiology,  
The University of Connecticut Health Center,  
Farmington, CT.

Hans P. Krayenbuehl, M.D., Professor of  
Cardiology,  
Medical Policlinic of the University,  
Zurich, Switzerland.

Edward G. Lakatta, M.D., Associate Professor  
of Medicine,  
Johns Hopkins School of Medicine;  
Associate Professor of Physiology,  
University of Maryland School of Medicine;  
Chief, Laboratory of Cardiovascular Science,  
Gerontology Research Center,  
National Institute on Aging,  
National Institutes of Health,  
Baltimore, MD.

Martin M. LeWinter, M.D., Professor of  
Medicine,  
University of Vermont College of Medicine;  
Director, Cardiology Unit,  
Medical Center Hospital of Vermont,  
Burlington, VT.

Beverly H. Lorell, M.D.,  
Assistant Professor of Medicine,  
Harvard Medical School;  
Co-Director, Hemodynamic Research  
Laboratory,  
Beth Israel Hospital,  
Boston, MA.

James P. Morgan, M.D., Ph.D., Assistant  
Professor of Medicine,  
Harvard Medical School;  
Cardiovascular Division,  
Beth Israel Hospital,  
Boston, MA.

Joseph P. Murgu, M.D., Director, Cardiology  
Research and Technology, Texas Heart  
Institute,  
St. Luke's Episcopal Hospital,  
Houston, TX.

Winifred G. Nayler, D.Sc., NH and MRC  
Principal Research Investigator,  
Department of Medicine,  
The University of Melbourne,  
Austin Hospital,  
Heidelberg, Victoria, Australia.

Walter J. Paulus, M.D., Ph.D., Cardiologisch  
Centrum,  
O.L.V. Ziekenhuis,  
Moorselbaan,  
Aalst, Belgium.

Hubert Pouleur, M.D., Department of  
Physiology and Cardiology,  
University of Louvain, School of Medicine,  
Av. Hippocrate, 55,  
B-1200 Brussels, Belgium.

J. Scott Rankin, M.D., Assistant Professor of  
Surgery and Physiology,  
Duke University Medical Center,  
Durham, NC.

Shigetake Sasayama, M.D., Professor of  
Medicine,  
The Second Department of Internal Medicine,  
Toyama Medical and Pharmaceutical  
University,  
Toyama, Japan.

Patrick W. Serruys, M.D., Ph.D., Co-  
Director, Cardiac Catheterization Laboratory,  
Thoraxcenter,  
Erasmus University,  
Roderdam, The Netherlands.

John V. Tyberg, M.D., Ph.D., Professor of  
Medicine and Medical Physiology,  
The University of Calgary,  
Calgary, Alberta, Canada.

Saul Winegrad, M.D., Professor of Physiology,  
School of Medicine,  
University of Pennsylvania,  
Philadelphia, PA.

---

PART I. CELL BIOLOGY  
OF DIASTOLE

---

---

# 1. CELLULAR MECHANISMS OF RELAXATION: LESSONS FROM FROGS, BIRDS, AND MAMMALS

---

William H. Barry

Much progress has been made in the elucidation of the cellular mechanisms of development and relaxation of twitch tension in cardiac muscle. The onset of contraction is preceded by a rise in cytosolic calcium ion concentration,  $[Ca^{2+}]_i$  [1]. This rise in  $[Ca^{2+}]_i$  in mammalian ventricular myocytes appears primarily to be due to release of  $Ca^{2+}$  from intracellular stores contained within the sarcoplasmic reticulum (SR), the release being triggered by influx of extracellular  $Ca^{2+}$  across the sarcolemma via the slow calcium channel during phase 2 of the cardiac action potential. In frog myocardium, little of the  $Ca^{2+}$  involved in excitation-contraction coupling is derived from intracellular stores because of a very sparse SR, and therefore most of the rise in  $[Ca^{2+}]_i$  occurs because of transsarcolemmal  $Ca^{2+}$  influx via the slow  $Ca^{2+}$  channel and possibly via an electrogenic  $Na^+-Ca^{2+}$  exchange [2]. Calcium bound to sarcolemmal sites may also be of importance in the excitation-contraction coupling process [3], possibly by providing a source for  $Ca^{2+}$  influx.

Relaxation of developed tension results from a fall in  $[Ca^{2+}]_i$ , which allows dissociation of  $Ca^{2+}$  from troponin and subsequent cross-bridge detachment dependent on adenosine triphosphate (ATP) binding to the contractile proteins. The initial fall in  $[Ca^{2+}]_i$  in the

mammalian myocardial cell is believed to be due to ATP-dependent uptake of  $Ca^{2+}$  by an SR  $Ca^{2+}$  pump of high affinity and high  $Ca^{2+}$  transport capacity [4]. However, an amount of  $Ca^{2+}$  equal to that entering from the extracellular space during the onset of contraction must be extruded from the cell subsequently, to avoid a progressive gain in cellular calcium content [5]. Therefore, relaxation of the myocardial cell may be considered to have two components from a theoretical standpoint: first, an initial rapid relaxation most likely due to intracellular reuptake of  $Ca^{2+}$  by SR, and second,  $Ca^{2+}$  extrusion from the cell across the sarcolemma. In this chapter, I will describe recent experiments performed on cultured chick embryo ventricular cells, which elucidate the relative importance of different transsarcolemmal  $Ca^{2+}$  extrusion mechanisms during relaxation.

## *Methods*

### TISSUE CULTURE

The experiments to be described were performed on monolayer cultures of spontaneously contracting chick embryo ventricular cells, prepared as previously described [6]. Briefly, hearts of 10-day-old chick embryos were removed, minced, and placed in  $Ca^{2+}$  and  $Mg^{2+}$ -free solution. The cells were isolated by four cycles of trypsinization, resuspended in culture medium, and placed in plastic petri dishes containing circular glass overslips. After 3 to 4 days of culture, confluent layers of spontaneously contracting cells developed.

Supported in part by National Institutes of Health Grant HL30478.

Grossman, William, and Lorell, Beverly H. (eds.), *Diastolic Relaxation of the Heart*. Copyright © 1987. Martinus Nijhoff Publishing. All rights reserved.

### MEASUREMENT OF CONTRACTION AND RELAXATION

Measurement of relaxation and contraction of individual cells in the culture were assessed by the use of an optical video system as described [7]. Coverslips with attached monolayers were placed in a perfusion chamber in which the medium bathing a segment of the culture could be changed with a time constant of 1 to 2 seconds. The chamber was placed on the stage of an inverted phase-contrast microscope enclosed in a Lucite box in which a temperature of 37°C was maintained. Cells were magnified with a 40× objective, and the image was monitored by a low-light-level television camera, connected to a video motion detector. The motion detector measured motion along a selected raster-line segment, and the output of the motion detector was calibrated to indicate actual microns of motion.

### MEASUREMENT OF CALCIUM EFFLUX

In the experiments to be described,  $\text{Ca}^{2+}$  efflux was measured by labeling the cells with  $^{45}\text{Ca}$  tracer to equilibrium and then washing the cells to remove the extracellular label. The coverslip cultures were then placed serially in 2-ml aliquots of efflux medium for 5 seconds in each. The  $^{45}\text{Ca}$  efflux was calculated as fractional loss of  $^{45}\text{Ca}$  counts for each 5-second time point. For further details, see Barry and colleagues [7].

### MEASUREMENT OF CHANGES IN $[\text{Ca}^{2+}]_i$

Changes in  $[\text{Ca}^{2+}]_i$  were detected using the new fluorescent probe, Indo-1 [8, 9]. Cells were exposed to the acetoxymethyl ester form (Indo-1 AM) of the fluorescent probe. This membrane-permeable compound diffuses into the cell, where the ester groups are cleaved by intracellular esterases, leaving the Indo-1 molecule free to bind to  $\text{Ca}^{2+}$ . Cells were excited at a wavelength of 360 nm, and fluorescence at 410 and 480 nm was detected using photomultiplier tubes. The fluorescence intensity increases at 410 nm with increasing  $[\text{Ca}^{2+}]_i$ ; and decreases at 480 nm with increasing  $[\text{Ca}^{2+}]_i$ ; therefore, the ratio of the fluorescence intensities at these two wavelengths was used as an index of free  $[\text{Ca}^{2+}]_i$  concentration.

### Results

When the contractile activity of spontaneously beating cultured ventricular cells within a

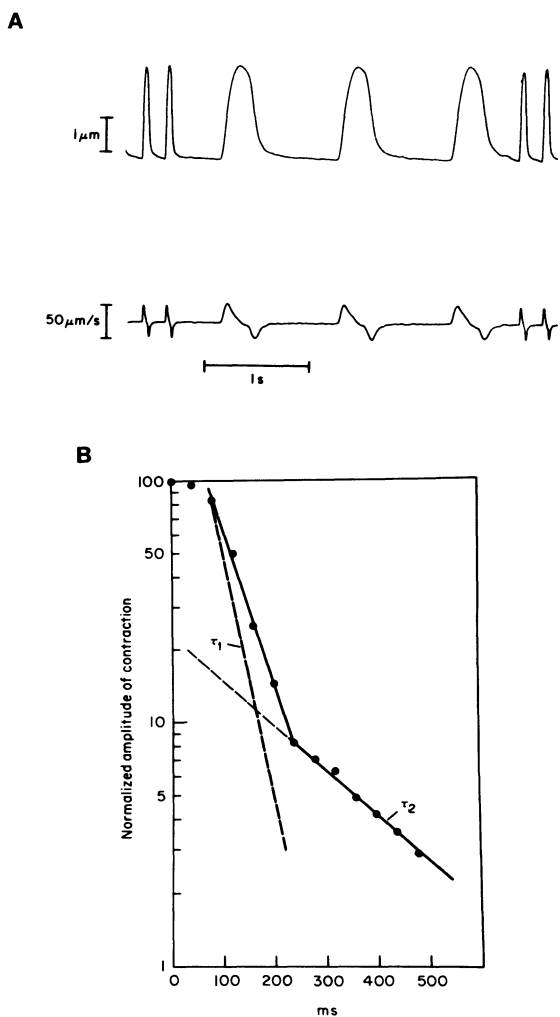


FIGURE 1-1. Two phases of relaxation. A. Contraction and relaxation of a cultured heart cell, as measured by cell motion. An initial rapid phase of relaxation (I) is followed by a slow phase (II) that continues until the next contraction. The lower tracing in panel A is the first derivative of the cell motion trace. Recorder speed was reduced by a factor of five at the beginning and end of the recording. B. Estimation of the time constants  $T_1$  and  $T_2$  of relaxation, from the cell motion trace shown in panel A. Cell motion is plotted on a log scale, beginning at peak amplitude of contraction and extending through diastole. Complete relaxation was assumed to have occurred at the end of diastole.  $T_1$  is 30 to 40 msec, whereas  $T_2$  is about 200 msec. (Adapted from Miura et al. [5].)

monolayer is monitored, two distinct phases of relaxation are apparent, as seen in Figure 1-1. There is an initial rapid phase of relaxation followed by a slow phase that continues until the next contraction. The time constant of the rapid phase of relaxation is 30 to 40 msec, and the time constant of the second slower phase is longer. The exact magnitude of this slower time constant is difficult to determine, however, because the cells are continuing to relax at the onset of the next contraction, and therefore the position of complete relaxation is unknown. It is important to note that two phases of relaxation have also been detected in cultured aggregates of chick embryo ventricular cells by Clusin [10] and in isolated dissociated adult ventricular myocytes [11].

It has been suggested that this second slow

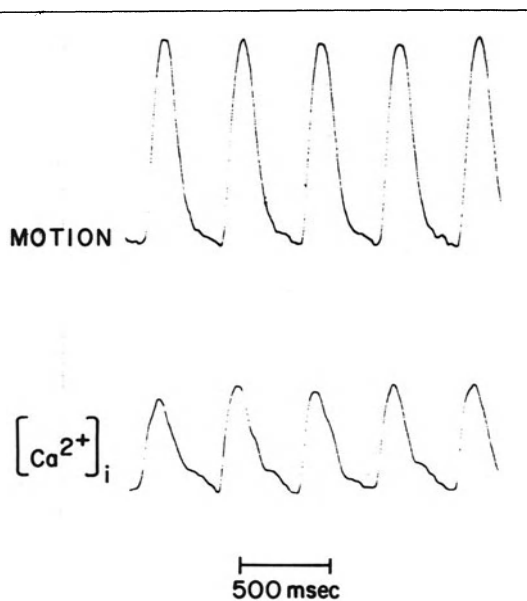


FIGURE 1-2. Simultaneous Cell motion (upper trace) and changes in  $[Ca^{2+}]_i$  (lower trace) in a monolayer of cultured heart cells. The  $[Ca^{2+}]_i$  signal is the ratio of fluorescence intensities at 410 and 480 nm of cells loaded with Indo-1 and excited at 360 nm. Calibration studies using a  $Ca^{2+}$  ionophore and  $Ca^{2+}$ -buffered solutions indicate an average systolic  $[Ca^{2+}]_i$  of 780 nM, and end-diastolic  $[Ca^{2+}]_i$  of 240 nM [9]. Note that  $[Ca^{2+}]_i$  continues to fall slowly throughout diastole, after an initial more rapid decline.

phase of relaxation is not a viscoelastic phenomenon but rather represents a decline in  $Ca^{2+}$ -dependent contractile force [5, 10]. In this regard, recent studies in our laboratory using Indo-1 have confirmed that this slow phase of relaxation is associated with a fall in  $[Ca^{2+}]_i$  [9], as illustrated in Figure 1-2.

Thus, in intact cultured ventricular myocytes, both the decline in  $[Ca^{2+}]_i$  and the corresponding mechanical relaxation of the cell appear to occur in two distinct phases with markedly different time constants. Although the initial rapid phase appears to be accounted for by SR uptake of  $Ca^{2+}$  [4], the mechanism(s) responsible for the second slower phase of relaxation have not been established. It has been proposed by Clusin [10] and Muira et al. [5] that the second phase of relaxation might represent  $Ca^{2+}$  extrusion via  $Na^+-Ca^{2+}$  exchange. However, subsequent experiments demonstrated that cultured heart cells can maintain an efflux of  $Ca^{2+}$  at a normal rate in the presence of zero extracellular  $Na^+$ , a finding that suggests that  $Na^+$ -dependent  $Ca^{2+}$  extrusion may be relatively unimportant in these cells [12]. Thus, the slow phase of relaxation could be due to another extrusion mechanism such as the sarcolemmal  $Ca^{2+}$ -ATPase calcium pump.

As shown in Table 1-1, work recently summarized by Carafoli [4] has demonstrated that while the  $Na^+-Ca^{2+}$  exchanger has a relatively low affinity for  $Ca^{2+}$ , it has a much higher maximum transport rate than the sarcolemmal  $Ca^{2+}$ -ATPase. These results, which were based on studies performed on vesicles prepared from adult mammalian myocardial sarcolemmal membranes, suggested that the  $Ca^{2+}$  pump was a low-capacity, high-affinity transport system, whereas the  $Na^+-Ca^{2+}$  exchanger was a relatively low-affinity but high-capacity transport system. A major question remained regarding the extent to which either one or both of these  $Ca^{2+}$  extrusion systems contributes to the slow phase of relaxation.

To approach this question we performed the experiment [7] shown in Figure 1-3. In this experiment, cultured heart cells were first exposed to nominal zero  $Na^+$ , zero  $Ca^{2+}$  solution ( $[Ca^{2+}] = 1-5 \mu M$ ). This resulted in oscillatory mechanical activity consistent with SR  $Ca^{2+}$  overload [13]. However, the cells remained in a relaxed position. Abrupt exposure to 20 mM caffeine in the absence of extracellular  $Na^+$ , caused a contracture, which relaxed slowly (Fi-

TABLE 1-1. Kinetic Properties of Myocardial  $\text{Ca}^{2+}$ -Transporters

	K <sub>m</sub> ( $\mu\text{M}$ )	V <sub>max</sub> (nmol/mg/sec)	% Total $\text{Ca}^{2+}$ Uptake
SR $\text{Ca}^{2+}$ -ATPase	0.1-0.5	20-30	88.0
SL $\text{Na}^{+}$ - $\text{Ca}^{2+}$ Exchanger	2-20	15-30	4.9
SL $\text{Ca}^{2+}$ -ATPase	0.5	0.5	0.7
Mitochondria			
Electrophoretic uptake in situ	15-30	< 0.5	6.3
$\text{Na}^{+}$ - $\text{Ca}^{2+}$ exchanger	13	0.2	

K<sub>m</sub> = concentration at which enzyme activity is one-half V<sub>max</sub>; V<sub>max</sub> = maximum activity rate; SR = sarcoplasmic reticulum; SL = sarcolemma. (From Carafoli [4]).

gure 1-3A). As shown in Figure 1-3B, exposure to caffeine under these conditions also increased  $^{45}\text{Ca}$  efflux. Under identical conditions, exposure of cells to caffeine plus  $\text{Na}^{+}$  (140 mM) produced a smaller contracture that relaxed much more rapidly (Figure 1-3C) and a more rapid  $^{45}\text{Ca}$  efflux (Figure 1-3D).

Data from several experiments are summarized in Table 1-2. Cells relaxed more rapidly in 140 mM  $\text{Na}^{+}$  than in the absence of  $\text{Na}^{+}$ , and this effect of  $\text{Na}^{+}$  was antagonized by  $\text{La}^{3+}$ , an inhibitor of  $\text{Na}^{+}$ - $\text{Ca}^{2+}$  exchange. These findings indicate that there is an  $\text{Na}^{+}$ -independent,  $\text{Ca}^{2+}$  extrusion system in these cultured heart cells, which is capable of extruding  $\text{Ca}^{2+}$  against a considerable electrochemical concentration gradient. This system presumably is a  $\text{Ca}^{2+}$ -ATPase calcium pump. However, the rate of relaxation of tension that this system is able to produce is inadequate to account for the second slow phase of relaxation in intact beating cells. The results in which  $\text{Na}^{+}$  was resupplied simultaneously with caffeine exposure indicate that  $\text{Na}^{+}$ - $\text{Ca}^{2+}$  exchange can extrude  $\text{Ca}^{2+}$  more rapidly and produce more rapid relaxation of the caffeine contracture. The time constant for this relaxation is similar to that noted for the second phase of relaxation in intact cells. These data, taken together, show that the sarcolemmal  $\text{Ca}^{2+}$  pump is incapable of contributing to phasic relaxation in these cells but support the hypothesis that the second, slow phase of relaxation is due to  $\text{Ca}^{2+}$  extrusion across the sarcolemma via  $\text{Na}^{+}$ - $\text{Ca}^{2+}$  exchange.

### Discussion

The results shown above demonstrate the presence of two kinetically distinct phases of relaxation of cultured ventricular cells. This finding is consistent with the presence of two distinct

mechanisms by which cytoplasmic  $[\text{Ca}^{2+}]$  is lowered during diastole. It is known that intact adult avian myocardium resembles mammalian myocardium in that it possesses a well-developed SR [14]. Studies by Holland [15] have demonstrated  $\text{Ca}^{2+}$ -dependent SR ATPase in cell cultures of chick heart. In addition, recent studies in our laboratory [16] have demonstrated that the contractile amplitude of cultured heart cells is influenced by ryanodine and caffeine in such a way as to suggest that the SR plays a significant role in excitation-contraction coupling in these cells. Therefore, it seems reasonable to ascribe the rapid phase of myocardial cell relaxation to  $\text{Ca}^{2+}$  uptake by SR, as suggested previously.

The second, slower phase of relaxation seems to be due to  $\text{Ca}^{2+}$  extrusion from the cell by  $\text{Na}^{+}$ - $\text{Ca}^{2+}$  exchange. It is of interest to note that studies by Roulet and co-workers [17] have demonstrated that relaxation of frog atrium, which has a very sparse functional SR, as mentioned previously, is primarily dependent on the extracellular  $\text{Na}^{+}$  concentration. The relaxation of frog ventricle after repolarization from a voltage-clamp pulse was ten times more rapid in the presence of  $\text{Na}^{+}$  than in its absence, a result which is very consistent with our own findings (Table 1-2) and which further supports the conclusion that  $\text{Na}^{+}$ - $\text{Ca}^{2+}$  exchange is involved in relaxation of twitch tension.

These results also suggest that cardiac glycosides, which increase net  $^{45}\text{Ca}$  uptake and content [18], do so primarily by slowing the rate of  $\text{Ca}^{2+}$  efflux occurring each beat via  $\text{Na}^{+}$ - $\text{Ca}^{2+}$  exchange. This occurs because with inhibition of the  $\text{Na}^{+}$  pump, and consequent increase in intracellular  $[\text{Na}^{+}]$ , less electrochemical energy from the  $\text{Na}^{+}$  gradient is available for the  $\text{Na}^{+}$ - $\text{Ca}^{2+}$  exchanger to extrude  $\text{Ca}^{2+}$ . Additionally, a cardiac glycoside-

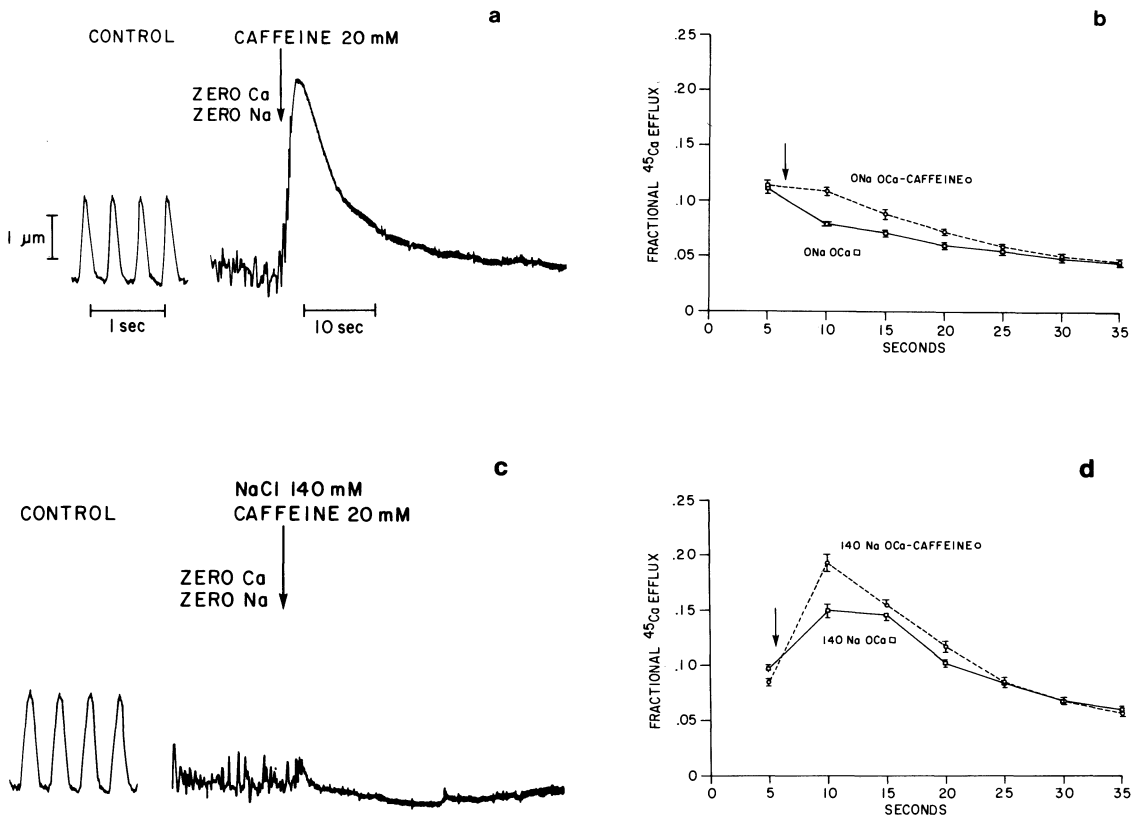


FIGURE 1-3. a. Effect of abrupt exposure to caffeine on cell motion in the absence of extracellular Na<sup>+</sup>. Control contractions at fast paper speed are shown on left. Oscillatory mechanical activity developed in zero Na<sup>+</sup>, nominal zero Ca<sup>2+</sup> solution. Caffeine exposure (vertical arrow) caused a large contracture, which relaxed over 20 to 30 seconds. b. Effect of abrupt exposure to caffeine on <sup>45</sup>Ca efflux. Control efflux in zero Na<sup>+</sup>, nominal zero Ca<sup>2+</sup> solution is shown on bottom (squares). Caffeine exposure (vertical arrow) in the absence of extracellular Na<sup>+</sup> caused an increased efflux of <sup>45</sup>Ca, which lasted for about 20 seconds. c. Effect of abrupt exposure to caffeine plus 140 mM Na<sup>+</sup> on motion. The combination of caffeine plus Na<sup>+</sup> produced a smaller, more rapidly relaxing contracture. This was the same cell as shown in A, after recovery in normal HEPES-buffered medium. d. Effect of abrupt exposure to caffeine and Na<sup>+</sup> on <sup>45</sup>Ca efflux. 140 mM Na<sup>+</sup> plus caffeine produced an increase in Ca<sup>2+</sup> efflux relative to that seen on resupply of Na<sup>+</sup> alone, the major portion of which occurred within 5 seconds [7].

TABLE 1-2. Effects of Na and La on Caffeine Contracture<sup>a</sup>

	Caffeine Contracture (μm)	Relaxation t1/2 (sec)
0 Na <sup>+</sup> , 0 Ca <sup>2+</sup>	3.94 ± 0.90 (p < .05)	8.60 ± 1.22 (p < .001)
140 mM Na <sup>+</sup> , 0 Ca <sup>2+</sup>	1.53 ± 0.50	0.77 ± 0.09
140 mM Na <sup>+</sup> , 0 Ca <sup>2+</sup> , 1 mM La <sup>3+</sup>	2.28 ± 0.93	6.51 ± 2.18

<sup>a</sup> n = 7; p values shown indicate a paired t-test comparison of zero Na<sup>+</sup>, zero Ca<sup>2+</sup> vs. 140 mM Na<sup>+</sup>, zero Ca<sup>2+</sup> groups. The non-paired t test, showed no significant differences between the zero Na<sup>+</sup>, zero Ca<sup>2+</sup>, 140 mM Na<sup>+</sup>, zero Ca<sup>2+</sup>, 1 mM La<sup>3+</sup> groups.

induced increase in  $[Na^+]_i$  may cause a small increase in  $Ca^{2+}$  influx via  $Na^+-Ca^{2+}$  exchange each beat, during the initial phase of the action potential after membrane depolarization but before the  $[Ca^{2+}]_i$  transient due to SR  $Ca^{2+}$  release [18]. It should be noted, however, that experiments with extracellular  $Ca^{2+}$  indicators do not support a major role for enhanced  $Ca^{2+}$  influx via  $Na^+-Ca^{2+}$  exchange as a mechanism for strophanthidin-induced inotropy [19].

Relaxation of myocardial cells in the absence of functioning SR and in the absence of extracellular  $Na^+$  is very slow indeed, but does occur [see Figure 1–3A]. It is not clear whether this relaxation is due to  $Ca^{2+}$  extrusion by the  $Ca^{2+}$ -ATPase calcium pump (although this clearly could play a role), or could represent  $Ca^{2+}$  binding to proteins within the cell [20] or to mitochondria. Mitochondria have a large capacity for  $Ca^{2+}$  but have very slow rates of  $Ca^{2+}$  uptake and release [4]. It is therefore believed that under usual circumstances,  $Ca^{2+}$  uptake by mitochondria serves primarily to buffer the cell against  $Ca^{2+}$  changes at higher  $Ca^{2+}$  levels in the cytosol, as might occur during marked and prolonged inhibition of the  $Na^+$  pump, rather than to contribute to phasic changes in  $Ca^{2+}$  during excitation contraction coupling [21, 22].

Many lessons remain to be learned about relaxation, and its integration with excitation-contraction coupling. As pointed out by Carafoli [4], very little is known about the  $Ca^{2+}$  release channels in the SR. Furthermore, the importance of cAMP-dependent phosphorylation of SR, relative to calmodulin-modulated phosphorylation and protein kinase C-modulated phosphorylation of phospholamban, in regulating  $Ca^{2+}$  uptake by the SR under physiologic and pathologic conditions remains uncertain. Finally, mechanisms involved in the translocation of  $Ca^{2+}$  from the uptake site of SR to  $Ca^{2+}$  release sites are uncertain. It is clear that all these components of the SR system must function in an integrated way to provide normal relaxation as well as contraction.

## References

1. Fabiato A, Fabiato F (1979). Calcium and cardiac excitation-contraction coupling. *Annu Rev Physiol* 41:473–484.
2. Horakova M, Vassort G (1979). Na–Ca exchange in the regulation of cardiac contractility. *J Gen Physiol* 73:403–424.
3. Langer GA, Nudd LM (1983). Effects of cations, phospholipases, and neuraminidase on calcium binding to “gas-dissected” membranes from cultured cardiac cells. *Circ Res* 53:482–490.
4. Carafoli E (1985). The homeostasis of calcium in heart cells. *J Mol Cell Cardiol* 17:203–212.
5. Miura DS, Biedert S, Barry WH (1981). Effects of calcium overload on relaxation in cultured heart cells. *J Mol Cell Cardiol* 13:949–961.
6. Barry WH, Pober J, Marsh JD, Frankel SR, Smith TW (1980). Effects of graded hypoxia on contraction of cultured chick embryo ventricular cells. *Am J Physiol* 239:H651–H657.
7. Barry WH, Rasmussen CAF Jr, Ishida H, Bridge JHB (1986). External Na-independent Ca extrusion in cultured ventricular cells. *J Gen Physiol* 88:393–411, 1986.
8. Gryniewicz G, Poenie M, Tsien RY (1985). A new generation of  $Ca^{2+}$  indicators with greatly improved fluorescence properties. *J Biol Chem* 260:3440–3450.
9. Peeters GA, Hlady V, Bridge JHB, Barry WH (1986). Simultaneous measurement of calcium transients and cell motion in cultured cells. *Am J Physiol*, (in press).
10. Clusin WT (1981). The mechanical activity of chick embryonic myocardial cell aggregates. *J Physiol* 320:149–174.
11. Isenberg G (1982). Ca entry and contraction as studied in isolated bovine ventricular myocytes. *Z Naturforsch* 37:502–512.
12. Barry WH, Smith TW (1984). Movement of  $Ca^{2+}$  across the sarcolemma: effects of abrupt exposure to zero external Na concentration. *J Mol Cell Cardiol* 16:155–164.
13. Lakatta EG, Capogrossi MC, Kort AA, Stern MD (1985). Spontaneous myocardial calcium oscillations: Overview with emphasis on ryanodine and caffeine. *Fed Proc* 44:2977–2983.
14. Manasek FJ (1969). Histogenesis of the embryonic myocardium. *Am J Cardiol* 25:149–168.
15. Holland PC (1979). Biosynthesis of the  $Ca^{2+}$  and  $Mg^{2+}$ —dependent adenosine triphosphatase of sarcoplasmic reticulum in cell cultures of embryonic chick heart. *J Biol Chem* 254:7604–7610.
16. Rasmussen CAF Jr, Sutko JL, Barry WH (1987). Effects of ryanodine and caffeine on contractility, membrane voltage, and calcium exchange in cultured heart cells. *Circ Res* 60:495–504.
17. Roulet MJ, Mongo KG, Vassort G, Ventura-Clapier R (1979). The dependence of twitch relaxation on sodium ions and on internal  $Ca^{2+}$  stores in voltage clamped frog atrial fibers. *Pfluegers Arch* 379:259–268.

18. Barry WH, Hasin Y, Smith TW (1985). Sodium pump inhibition, enhanced calcium influx via sodium-calcium exchange, and positive inotropic response in cultured heart cells. *Circ Res* 56:231-241.
19. Cleeman L, Pizarro G, Morad M (1984). Optical measurements of extra-cellular calcium depletion during a single heart beat. *Science* 226:172-177.
20. Robertson SP, Johnson JD, Potter JD (1981). The time course of  $\text{Ca}^{2+}$  exchange with calmodulin, troponin, parvalbumin and myosin in response to transient increases in  $\text{Ca}^{2+}$ . *Biophys J* 34:559-569.
21. Fabiato A (1983). Calcium-induced release of calcium from the cardiac sarcoplasmic reticulum. *Am J Physiol* 245:C1-C14.
22. Fabiato A (1984). Effects of spermine in skinned cardiac cells suggest that mitochondria do not participate in beat-to-beat  $\text{Ca}^{2+}$  regulation in intact cardiac cells but control  $\{\text{free } \text{Ca}^{2+}\}$ . *J Gen Physiol* 84:37-38a (abstract).

## 2. SARCOPLASMIC RETICULAR CONTROL OF CARDIAC CONTRACTION AND RELAXATION

Arnold M. Katz

Any analysis of cardiac relaxation requires an understanding of the role of the sarcoplasmic reticulum (SR) in removing activator  $\text{Ca}^{2+}$  from the cytosol at the end of systole. The precise relationship between  $\text{Ca}^{2+}$  uptake into this intracellular membrane system and the changes in muscle length and tension that occur during diastole remains incompletely understood, but it is generally accepted that relaxation begins when cytosolic  $\text{Ca}^{2+}$  is reduced by the calcium pump of the SR.

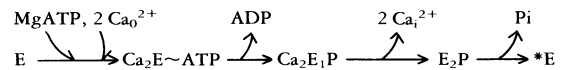
This chapter reviews briefly the handling of  $\text{Ca}^{2+}$  by the SR and focuses on the properties of the calcium pump ATPase, which is the major intrinsic protein in these membranes. The role of the SR in the release of activator  $\text{Ca}^{2+}$  at the start of systole is also described; however, this process is much less well understood than that of  $\text{Ca}^{2+}$  uptake.

The SR is an intracellular membrane system that is specialized for its role of regulating cytosolic  $\text{Ca}^{2+}$  concentration. These membranes cause cardiac muscle to relax by pumping  $\text{Ca}^{2+}$  "uphill" against a concentration gradient, while by mediating a "downhill"  $\text{Ca}^{2+}$  release from stores in the SR these membranes also initiate contraction. The transport of  $\text{Ca}^{2+}$  by the SR is effected by an ATP-dependent calcium pump whose molecular properties have been extensively characterized.

### *The Calcium Pump of the SR*

The  $\text{Ca}^{2+}$ -transport reaction of the SR has been studied mainly in skeletal muscle vesicular preparations [1–4].  $\text{Ca}^{2+}$  transport by cardiac SR is generally similar to that of skeletal muscle [5], with the important exception that the cardiac system is more highly regulated and can be modified by such influences as protein kinase-mediated phosphorylation [6, 7].

The calcium pump ATPase reaction proceeds through several steps that involve the interaction of  $\text{Ca}^{2+}$  and ATP with the  $\sim 100,000$  dalton calcium pump ATPase protein. As shown in the scheme below,  $\text{Ca}^{2+}$  uptake begins when  $\text{Ca}^{2+}$  and ATP bind to the outer surface of the calcium pump ATPase (E), after which the terminal high-energy phosphate of ATP is transferred to the protein to form sequentially at least two different phosphoenzyme intermediates.



The initial formation of a  $\text{Ca}_2\text{E}\sim\text{ATP}$  intermediate is followed by the liberation of adenosine diphosphate (ADP), which rapidly converts this intermediate to the high-energy acyl phosphoenzyme denoted  $\text{E}_1\text{P}$ .  $\text{Ca}^{2+}$  remains bound with high affinity to  $\text{E}_1\text{P}$  at its low activity (i.e., as  $\text{Ca}_0^{2+}$ ). Thus, the energy of the terminal phosphate bond of ATP is retained in  $\text{E}_1\text{P}$ , which is a high-energy phosphoenzyme.

The key step in  $\text{Ca}^{2+}$  transport occurs when  $\text{E}_1\text{P}$  moves the two bound  $\text{Ca}^{2+}$  ions across the membrane bilayer at the same time that the affinity of the enzyme-bound  $\text{Ca}^{2+}$  becomes reduced. This allows  $\text{Ca}^{2+}$  to be released in the

Supported by Program Project Grant HL-33026 from the National Heart, Lung and Blood Institute.  
Grossman, William, and Lorell, Beverly H. (eds.), *Diastolic Relaxation of the Heart*. Copyright © 1987. Martinus Nijhoff Publishing. All rights reserved.

region of higher  $\text{Ca}^{2+}$  concentration within the SR  $[\text{Ca}^{2+}]_i$  while a different phosphoenzyme ( $\text{E}_2\text{P}$ , a low-energy reaction intermediate) is formed at this step of the reaction.  $\text{E}_2\text{P}$  is then hydrolysed to form  $^*\text{E}$  and inorganic phosphate. A conformational change in the calcium-pump ATPase ( $^*\text{E}-\text{E}$  transition) then occurs before the  $\text{Ca}^{2+}$  transport cycle can begin again. Because all steps in this reaction scheme are reversible, under special conditions the calcium-pump ATPase can be made to catalyze  $\text{Ca}^{2+}$  efflux from  $\text{Ca}^{2+}$ -filled SR vesicles.

The mechanism responsible for the conformational change in the ATPase protein that utilizes the energy of the acyl phosphate bond of  $\text{E}_1\text{P}$  to move  $\text{Ca}^{2+}$  across the SR membrane remains poorly understood. This key step of the active transport process may involve a large entropy change that occurs when the high-energy phosphoenzyme  $\text{E}_1\text{P}$  is converted to  $\text{E}_2\text{P}$ , but how such an entropy change, or other mechanism, actually causes  $\text{Ca}^{2+}$  to be transported uphill, against a concentration gradient, is not known. One possible mechanism is shown in Figure 2-1, where the movement of  $\text{Ca}^{2+}$  is shown to occur in a manner similar to that which raises a boat in a canal lock.

ATP has two distinct functions in the reactions of the calcium pump. At lower concentrations the nucleotide is a substrate that provides energy for the active transport of  $\text{Ca}^{2+}$ , whereas at higher concentrations ATP acts as an allosteric regulator that stimulates the overall transport reaction (see [7] for references). It is important to appreciate that the two ATP binding sites have different affinities; the substrate (high affinity) site has a  $K_d$  of  $\sim 1 \mu\text{M}$  while the allosteric regulatory (low affinity) site has a  $K_d$  of  $\sim 500 \mu\text{M}$ .

The allosteric effect of ATP appears to be relevant to physiologic, and especially pathophysiologic effects on  $\text{Ca}^{2+}$  transport by the SR. For example, during states of "energy starvation" such as occur in the ischemic or chronically overloaded heart, relaxation may be slowed by a modest fall in ATP concentration to levels low enough to reduce the allosteric effect of the nucleotide but not so low as to impair the substrate functions of ATP.

### *$\text{Ca}^{2+}$ Release from the SR*

Although  $\text{Ca}^{2+}$  release from the SR has been studied extensively over the past decade [8, 9],

and it is generally accepted that the terminal cisternae represent the site from which  $\text{Ca}^{2+}$  is released from the SR [10], the stimulus that initiates the  $\text{Ca}^{2+}$  release that constitutes the final step in excitation-contraction coupling is not yet fully understood. Three different mechanisms have been proposed to account for the initiation of this  $\text{Ca}^{2+}$  release: first, increased  $\text{Ca}^{2+}$  concentration at the cytosolic surface of the SR that occurs when  $\text{Ca}^{2+}$  enters the cell by way of sarcolemmal calcium channels (" $\text{Ca}^{2+}$ -induced  $\text{Ca}^{2+}$  release"); second, an increase in the  $\text{Ca}^{2+}$  permeability of the SR, caused by the sudden change in electrical potential across the sarcolemmal or t-tubular membrane during the action potential (" $\text{depolarization-induced Ca}^{2+}$ -release"); and third, a mechanical coupling between the membranes of the SR and sarcolemma; for example, depolarization of the t-tubular membrane might modify a structural connection between the t-tubular membrane and that of the terminal cisternae SR so as to "unplug" a channel that allows  $\text{Ca}^{2+}$  to flow out of the SR. At this time, a  $\text{Ca}^{2+}$ -induced  $\text{Ca}^{2+}$  release appears to be most important in the myocardium.

In addition to the uncertainty regarding the mechanism that initiates  $\text{Ca}^{2+}$  release from the SR, the nature of the channel through which  $\text{Ca}^{2+}$  leaves the SR remains to be defined [11]. Two general types of  $\text{Ca}^{2+}$  release channel have been proposed: a special "channel" that mediates passive  $\text{Ca}^{2+}$  flux out of the SR; or that the calcium-pump ATPase itself is the  $\text{Ca}^{2+}$  channel that allows  $\text{Ca}^{2+}$  to move "downhill" out of the  $\text{Ca}^{2+}$ -filled SR. As pointed out above, the calcium-pump ATPase, the predominant species of protein in the SR membrane, can catalyze a downhill flux of  $\text{Ca}^{2+}$  across these membranes; however, this  $\text{Ca}^{2+}$  efflux is slow [12]. The finding that ryanodine, which specifically inhibits  $\text{Ca}^{2+}$  release from the SR; binds to a limited number of sites in SR fractions derived from the terminal cisternae suggests the presence of a calcium channel in this region of the SR [13].

### *Implications of the Energetics of Calcium Transport by the SR*

As is discussed at length elsewhere in this volume, relaxation abnormalities play a major role in the pathophysiology of many forms of cardiac disease, including heart failure, and

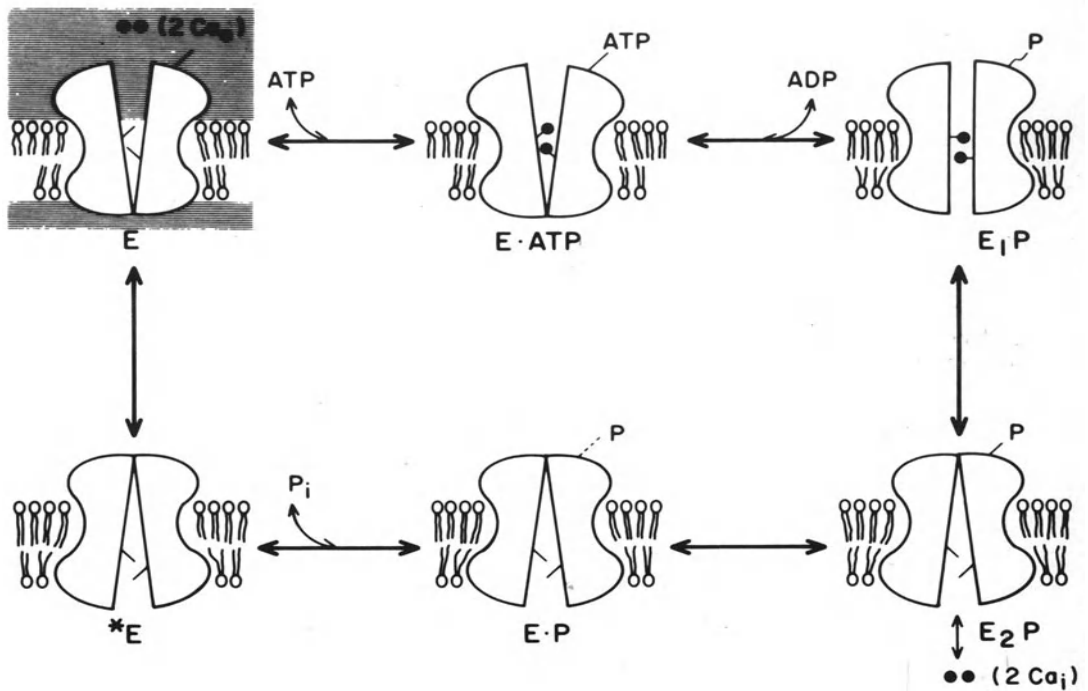


FIGURE 2-1. Schematic diagram of the reaction mechanism of the calcium pump ATPase reaction of the sarcoplasmic reticulum (SR). Beginning in the upper left corner, 2 moles of calcium and 1 mole of ATP bind to the calcium-pump ATPase protein to form the E-ATP complex. Hydrolysis of ATP and release of ADP leads to the formation of  $E_1P$ , the ADP-sensitive phosphorylated intermediate in which the 2 moles of calcium are occluded. The next step, formation of the ADP-insensitive  $E_2P$ , is accompanied by the translocation of the 2 moles of calcium into the lumen of the SR. This is followed by destabilization of the bond linking  $\text{P}_i$  to the enzyme and formation of E·P. Release of  $\text{P}_i$  forms  $E^*$ , a state of the calcium-pump ATPase protein that differs from E. The transition from  $E^*$  to E allows the calcium-pump ATPase protein again to bind 2 moles of calcium and 1 mole of ATP. All of these reactions can run in reverse, so that under special conditions the "downhill" efflux of calcium can be coupled to the resynthesis of ATP from ADP and  $\text{P}_i$ . (Reprinted from Katz et al. [17].)

relaxation is more severely impaired than contraction in the ischemic and overloaded heart. These findings reflect the greater effect of a deficit in chemical energy to slow the  $\text{Ca}^{2+}$  fluxes across the SR that occur during relaxation rather than during contraction, and also reflect a greater reserve capacity for the  $\text{Ca}^{2+}$  fluxes involved in systole than those involved in diastole.

The greater sensitivity of the  $\text{Ca}^{2+}$  fluxes involved in relaxation to an energy deficit is readily understood when it is remembered that delivery of activator  $\text{Ca}^{2+}$  to the contractile proteins is a passive process; whereas relaxation

requires that  $\text{Ca}^{2+}$  be transported actively against a concentration gradient. Thus, activation is initiated by the intrinsically rapid diffusion of  $\text{Ca}^{2+}$  through membrane channels from the extracellular space and SR, where  $\text{Ca}^{2+}$  concentration is in the millimolar range, into the cytosol, where  $\text{Ca}^{2+}$  concentration is approximately  $0.1\ \mu\text{M}$ . The downhill fluxes of activator  $\text{Ca}^{2+}$  are much faster than the active transport of  $\text{Ca}^{2+}$  that effects relaxation (Table 2-1). For example,  $\text{Ca}^{2+}$  entry via a single sarcolemmal calcium channel is approximately 3,000,000 ions/second [14], while ATP-dependent  $\text{Ca}^{2+}$  transport by a single calcium

TABLE 2-1. Balances Between  $\text{Ca}^{2+}$  Fluxes During Activation and Relaxation in the Myocardium

Surface areas of membranes in the myocardium ( $\mu\text{m}^2/\mu\text{m}^3$ )	
SL:	~0.3
SR:	~1.2
Densities of $\text{Ca}^{2+}$ channels and $\text{Ca}^{2+}$ pump sites (sites/ $\mu\text{m}^2$ )	
$\text{Ca}^{2+}$ channels in the cardiac SL	1-5
$\text{Ca}^{2+}$ pump proteins in cardiac SR	6000
Number of sites/ $\mu\text{m}^3$ [A $\times$ B]	
SL plus t-tubules	~1
SR	~7000
Rates of $\text{Ca}^{2+}$ fluxes involved in activation and relaxation (ions/sec)	
Activation (flux through a $\text{Ca}^{2+}$ channel)	~3,000,000
Relaxation (flux by a $\text{Ca}^{2+}$ pump site)	~30
"Ca <sup>2+</sup> flux reserve capacity" (ions/sec· $\mu\text{m}^3$ ) [C $\times$ D]	
Activation	~3,000,000
Relaxation	~210,000

SL = Sarcolemma and t-tubules; SR = sarcoplasmic reticulum. (Modified from Smith et al. [16].)

pump site of the SR is approximately 30 ions/second [15], 1/100,000 the rate of  $\text{Ca}^{2+}$  entry through a  $\text{Ca}^{2+}$  channel. Although the relative slowness of the  $\text{Ca}^{2+}$  fluxes responsible for relaxation is partially overcome by a very high density of  $\text{Ca}^{2+}$  pump proteins in the membranes of the SR (see Table 2-1), the myocardium remains susceptible to an imbalance between the rates of  $\text{Ca}^{2+}$  entry and removal from the cytosol.

The greater inhibition of relaxation than contraction when the rate of energy utilization exceeds that of energy production probably reflects not only the smaller "reserve" capacity for  $\text{Ca}^{2+}$  removal from within the myocardial cell, but also the fact that a deficit in myocardial ATP supply slows the  $\text{Ca}^{2+}$  pump of the SR and so delays  $\text{Ca}^{2+}$  removal from the contractile proteins. As pointed out above, even a small decrease in ATP supply can impair relaxation by the allosteric effect of ATP to stimulate the  $\text{Ca}^{2+}$  pump. A profound fall in ATP concentration, to levels below those of the  $K_m$  of the site at which ATP serves as the energy donor for the active transport of  $\text{Ca}^{2+}$ , would lead to contraction. Thus, relaxation (lusitropic) abnormalities tend to be more prominent than contraction (inotropic) abnormalities in hearts in which energy demand has outstripped energy delivery to the SR.

## References

1. Tada M, Yamamoto T, Tonomura Y (1978). Molecular mechanism of active calcium transport by sarcoplasmic reticulum. *Physiol Rev* 58:1-79.
2. Martin DW, Tanford C (1981). Phosphorylation of calcium adenosine triphosphatase by inorganic phosphate: van't Hoff analysis of enthalpy changes. *Biochem* 20:4597-4602.
3. Inesi G (1981). The sarcoplasmic reticulum of skeletal and cardiac muscle. In Dowben RM, Shay JW (eds): *Cell and Muscle Motility*. Plenum, New York:63-97.
4. Ikemoto N (1982). Structure and function of the calcium pump protein of sarcoplasmic reticulum. *Annu Rev Physiol* 44:297-317.
5. Shigekawa M, Wakabayashi S, Nakamura H (1983). Reaction mechanism of  $\text{Ca}^{2+}$ -dependent adenosine triphosphatase of sarcoplasmic reticulum. *J Biol Chem* 258:8698-8707.
6. Tada M, Katz AM (1982). Phosphorylation of the sarcoplasmic reticulum and sarcolemma: *Annu Rev Physiol* 44:401-423.
7. Katz AM, Takenaka H, Watras J (1986). The sarcoplasmic reticulum. In Fozzard H, et al (eds): *The Heart and Cardiovascular System*. New York: Raven Press.
8. Endo M (1977). Calcium release from the sarcoplasmic reticulum. *Physiol Rev* 57:71-108.
9. Fabiato A (1983). Calcium-induced release of calcium from the cardiac sarcoplasmic reticulum. *Am J Physiol* 245:C1-C14.
10. Somlyo AV, Gonzalez-Serratos H, McClellan G, Somlyo AP (1981). Calcium release and ionic changes in the sarcoplasmic reticulum of tetanized muscle: An electron-probe study. *J Cell Biol* 90:577-594.
11. Martonosi A (1984). Mechanisms of  $\text{Ca}^{2+}$  release from sarcoplasmic reticulum of skeletal muscle. *Physiol Rev* 64:1240-1320.
12. Katz AM, Repke DI, Fudyma G, Shigekawa M (1977). Control of calcium efflux from sarcoplasmic reticulum vesicles by external calcium. *J Biol Chem* 252:4210-4212.
13. Fleischer S, Ogunbunmi EM, Dixon MC, Fleer EAM (1985). Localization of  $\text{Ca}^{2+}$  release channels with ryanodine in junctional terminal cisternae of sarcoplasmic reticulum of fast skeletal muscle. *Proc Acad Sci USA* 82:7256-7259.
14. Tsien RW (1983). Calcium channels in excitable cell membranes. *Annu Rev Physiol* 45:341-358.
15. Shigekawa M, Finegan J-AM, Katz AM (1976). Calcium transport ATPase of canine cardiac sarcoplasmic reticulum: A comparison with that of rabbit fast skeletal muscle sarcoplasmic reticulum. *J Biol Chem* 251:6894-6900.

16. Smith V-E, Weisfeldt ML, Katz AM (1986) Relaxation and diastolic properties of the heart. In Fozzard H, et al (eds): *The Heart and Cardiovascular System*. New York: Raven Press.
17. Katz AM, Messineo FC, Nash-Adler P (1986). Effects of amphiphilic substances on sarcoplasmic reticulum function. In Entman ML, Van Winkle WB: *Sarcoplasmic Reticulum in Muscle Physiology*, vol II. Boca Raton, FL: CRC Press, pp 123–139.

---

### 3. CALCIUM AND CARDIAC RELAXATION

---

James P. Morgan, Roderick MacKinnon, Maurice Briggs,  
Judith K. Gwathmey

Excitation-contraction coupling in the heart can be divided into four steps as shown in Figure 3-1. First, an action potential depolarizes the sarcolemma. Second, this depolarization releases  $\text{Ca}^{2+}$  from the subsarcolemmal cisternae of the sarcoplasmic reticulum (SR), allows entry of calcium from outside the sarcolemma, or both. Third,  $\text{Ca}^{2+}$  diffuses to troponin-C on the thin filaments, and, by a complex sequence of events, the binding of calcium to this regulatory protein permits actin and myosin to interact. Fourth, relaxation occurs when the SR reaccumulates  $\text{Ca}^{2+}$ , causing it to dissociate from troponin C. The  $\text{Na}^+$ - $\text{Ca}^{2+}$  exchanger and  $\text{Ca}^{2+}$  pump, both located on the sarcolemma, ultimately restore  $\text{Ca}^{2+}$  to resting levels. The cellular mechanisms involved in each step are still not completely understood and in some cases remain subject to considerable controversy. Various aspects of the excitation-contraction process are considered in detail in several excellent reviews (1-4).

Although the scheme outlined in Figure 3-1 is useful for describing the  $\text{Ca}^{2+}$  fluxes that occur during contraction-relaxation cycles in the heart, it largely ignores other important regulatory mechanisms that are not directly involved with intracellular  $\text{Ca}^{2+}$  handling. Blinks and Endoh have recently presented a more comprehensive model for considering the regulation of cardiac contractile performance which incor-

The work was supported in part by HL31117, HL31704, HL07374, HL36797, and a Grant-in-Aid from the American Heart Association, Massachusetts Affiliate. Dr. Morgan is the recipient of a Research Career Development Award (HL01611).

Grossman, William, and Lorell, Beverly H. (eds.), *Diastolic Relaxation of the Heart*. Copyright © 1987. Martinus Nijhoff Publishing. All rights reserved.

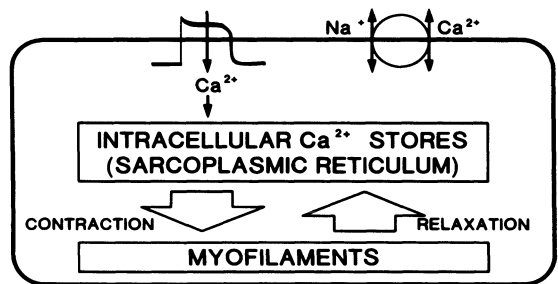


FIGURE 3-1. Major steps of excitation-contraction coupling in mammalian working myocardium. (From Morgan et al. [13], with permission.)

porates these additional mechanisms [5]. This scheme approaches cardiac contraction and relaxation from the vantage point of troponin-C, as shown in Table 3-1. As viewed in this way, the regulation of cardiac contractile performance can be divided into three types of mechanisms. First, the inotropic and lusitropic states of the heart may be changed by altering the amplitude or time course of the  $\text{Ca}^{2+}$  transient by the processes described in the preceding paragraph. For example, a stronger contraction may occur through the release of additional amounts of activator calcium from the SR or a positive lusitropic effect may develop if the rate of resequestration of  $\text{Ca}^{2+}$  by the SR is increased. These sorts of mechanisms, which are directly concerned with intracellular  $\text{Ca}^{2+}$  handling, are grouped together by Blinks and Endoh as "upstream" mechanisms. Second, regulation of cardiac contractile performance may occur through altering the affinity of troponin-C for

$\text{Ca}^{2+}$ , an effect that might come about through changes in the state of phosphorylation of troponin-I, which is itself regulated by a variety of  $\text{Ca}^{2+}$  and cyclic adenosine monophosphate (cAMP)-dependent protein kinases. Third, the contractile performance of the heart may be regulated by altering the response of the myofilaments to any given level of occupancy of the  $\text{Ca}^{2+}$  binding sites on troponin-C. The existence of this sort of regulatory mechanism in the heart has been demonstrated for changes in cyclic nucleotide concentrations and, in certain circumstances, with changes in intracellular adenosine triphosphate (ATP) levels [6]. It is likely that additional, as yet undefined, "downstream" processes are operative in the heart under normal and pathophysiologic conditions. As noted by Blinks and Endoh, it is often difficult to separate mechanisms IIA and IIB (see Table 3-1) in the intact cardiac muscle cell; however, they can be conveniently considered together as factors that may alter the  $\text{Ca}^{2+}$ -sensitivity of the contractile apparatus.

In summary, aside from changes in the intrinsic rates of energy utilization within the cell, an intervention that alters the inotropic or lusitropic properties of cardiac muscle must in general either alter the intracellular  $\text{Ca}^{2+}$  level itself, change the response of the contractile apparatus to  $\text{Ca}^{2+}$ , or exert both effects. We will review evidence supporting the importance of both general types of regulatory mechanisms in intact cardiac muscle preparations from animals and human beings.

### Methods

The effects of an intervention on intracellular  $\text{Ca}^{2+}$  levels and on the  $\text{Ca}^{2+}$ -sensitivity of the contractile apparatus can be determined by simultaneously measuring the intracellular calcium transient and force development. The experiments presented in this chapter were performed using the bioluminescent protein aequorin as a calcium indicator. Aequorin emits light when it combines with  $\text{Ca}^{2+}$ ; the light emission can be used as an index of intracellular  $\text{Ca}^{2+}$  levels. The preparation of aequorin for laboratory use and the kinetics of its reaction with calcium have been described in detail elsewhere [7]. Aequorin was introduced into the cytoplasm of mammalian cardiac muscle preparations from a variety of different species by microinjection or by a chemical loading techni-

TABLE 3-1. Regulation of Cardiac Contractile Performance

- 
- |     |   |
|-----|---|
| I.  | Regulation of intracellular $\text{Ca}^{2+}$ handling—<br>Altering the amplitude or time course of the $\text{Ca}^{2+}$ transient ("upstream mechanisms") |
| II. | $\text{Ca}^{2+}$ -sensitivity of the contractile apparatus  |
| A.  | Altering the affinity of troponin-C for $\text{Ca}^{2+}$  |
| B.  | Altering the response of the myofilaments to any given level of occupancy of $\text{Ca}^{2+}$ binding sites on troponin C ("downstream mechanisms")       |
- 

Modified from Blinks and Endoh [5].

que [8]. After loading, the light emitted by the injected aequorin was recorded simultaneously with tension in a specially designed apparatus [9]. Although a large number of cells can be loaded with aequorin, shot noise is prominent, and it is usually necessary to average successive signals (from 16 to several hundred depending on light intensity) to obtain a satisfactory signal-to-noise ratio. Despite these limitations, calcium transients have been recorded with aequorin in a variety of cardiac tissues. These include ventricular strips from *Amphiuma tri-dactylum* [10] and frogs [11], canine Purkinje fibers [12], and papillary muscles, strips of trabeculae carneae cordis, and atrial pectinate muscles from the cat, ferret, rat, dog, rabbit and human beings [10, 13, 14].

Interpretation of aequorin signals is complicated by the nonlinearity of the light response, which is directly proportional to the photoprotein concentration but increases logarithmically in proportion to the free calcium concentration, that is, as  $[\text{Ca}^{2+}]^n$ . Over the range of  $\text{Ca}^{2+}$  concentrations relevant to the experiments described in this report,  $n$  is equal to 2.5; thus, a 5.7-fold increase in light will be produced by a two-fold increase in the  $\text{Ca}^{2+}$  concentration. An important consequence of this nonlinear relation is that if the  $\text{Ca}^{2+}$  concentration is not uniform in a given cell, the intensity of the light emission will be higher than it would be if the same amount of calcium were distributed uniformly. In other words, the amplitude of the aequorin signal will be dominated by regions of the cell that contain the highest  $\text{Ca}^{2+}$  concentrations (entry and release sites) and, except under conditions in which the intracellular calcium concentration reaches a steady state, such as during tetanus in cardiac muscle, does not necessarily reflect the  $\text{Ca}^{2+}$  concentration

immediately surrounding the myofilaments. Under most experimental conditions, the aequorin signal recorded during isometric twitches in mammalian working myocardium appears to predominantly reflect the release and uptake of  $Ca^{2+}$  by the SR [10]. Although other methods for measuring  $Ca^{2+}$  are available, including metallochromic and fluorescent indicators and  $Ca^{2+}$ -selective electrodes, photoproteins like aequorin have several advantages for use in physiologic systems; these have been reviewed in detail by Blinks and colleagues [7].

*Results and Discussion*

Most interventions that alter the strength of contraction of mammalian working myocardium also change the amplitude of the aequorin signal in the same direction [10]. Similarly, changes in the time course of the aequorin signal are usually qualitatively similar to changes in the time course of the corresponding contraction. The effects of a large number of positive inotropic drugs have been studied with regard to their actions on the amplitude and time course of tension development and the corresponding  $Ca^{2+}$  transient, and the results serve to illustrate the general correlation between the configuration of the twitch and its corresponding calcium transient [15]. As shown in Table 3-2, each positive inotropic drug appears to produce one of four distinct patterns of light and tension responses. Agents that produce pattern I include the beta-agonists, papaverine, cholera toxin, isobutylmethylxanthine, and dibutyryl cAMP; agents that produce pattern II are theophylline and caffeine; pattern III, digitalis, increased  $[Ca^{2+}]_0$ , and vanadate; pattern IV, amrinone and milrinone. These patterns are

consistent with known actions of the various agents on the release of  $Ca^{2+}$  from intracellular stores, rate of calcium uptake by the SR, and  $Ca^{2+}$ -sensitivity of the myofilaments (Table 3-3). Figure 3-2 shows the effects of representative drugs producing each of the four patterns on the same papillary muscle.

As shown in Table 3-2 and Figure 3-2, for agents producing the pattern II response (i.e., caffeine and theophylline) a discrepancy is apparent between the effects of these agents on the amplitude of the calcium transient recorded with aequorin and peak developed tension. As shown in Figure 3-2, for caffeine, although peak developed tension is markedly increased compared to control, the amplitude of the calcium transient is actually diminished. Fortunately, these apparently discrepant results can be understood if one considers the effects of caffeine and theophylline on the sensitivity of the contractile elements to  $Ca^{2+}$  in "skinned" or hyperpermeable cardiac muscle preparations [6]. In these sorts of experiments, through mechanical or chemical means the sarcolemma is removed as a diffusion barrier; intracellular organelles can be destroyed by treatment with a mild detergent. The preparation that remains consists primarily of the contractile apparatus, which can then be exposed to a series of  $Ca^{2+}$  buffers to establish the calcium-force relationship. On the basis of such experiments, it can be demonstrated that caffeine and theophylline shift the calcium-force relationship to the left, indicating an increase in the sensitivity of the contractile apparatus to  $Ca^{2+}$  [16, 17]. Our results in aequorin-loaded preparations can therefore be explained, assuming that caffeine and theophylline produce a similar sensitization of the myofilaments to  $Ca^{2+}$  in the intact cell.

TABLE 3-2. Four Patterns of Light and Tension Responses Produced by Positive Inotropic Agents in the Cat Papillary Muscle

Pattern w/Example	Light			Tension		
	Peak	Time to Peak	T <sub>1/2</sub>	Peak	Time to Peak	T <sub>1/2</sub>
I. Isoproterenol	↑ ↑ ↑	↓	↓ ↓	↑ ↑ ↑	↓ ↓	↓ ↓
II. Theophylline	↓ ↑	↑ ↑	↑ ↑	↑ ↑ ↑	↑ ↑	↑ ↑
III. Digitalis	↑ ↑	↔	↔	↑ ↑	↔	↔
IV. Amrinone	↑ ↑	↑	↓	↑ ↑	↔	↓

T<sub>1/2</sub> = half-time for decline from peak: ↑ = increase; ↓ = decrease; ↔ = no change. The number of arrows indicates the relative maximal change or rate of change of each variable. (From Morgan et al. [13], with permission.)

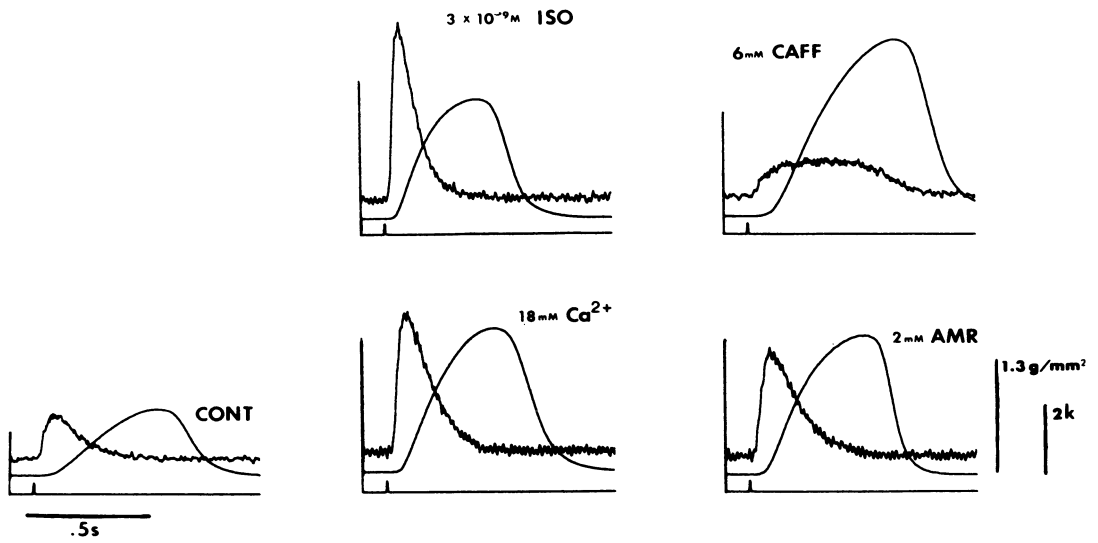


Figure 3-2 also shows that caffeine markedly prolongs the time course of the calcium transient, and the question naturally arises whether or not the increased amplitude of the twitch may be related to prolonged interaction between  $Ca^{2+}$  and troponin-C. This does not appear to be the case, based on results obtained with the alkaloid ryanodine, an agent that blocks the release of  $Ca^{2+}$  from intracellular stores but does not affect the sensitivity of the contractile apparatus to  $Ca^{2+}$  [10]. The effects of ryanodine on force and  $[Ca^{2+}]_i$  are shown in Figure 3-3. Note that although, as with caffeine, the time course of light and tension are prolonged, ryanodine has a *negative* inotropic effect as

FIGURE 3-2. Comparative effects of agents producing response patterns I through IV (see Table 3-2) in an isometric cat papillary muscle preparation. The upper, noisy trace in each panel is the aequorin signal, and the lower, smooth trace is the tension trace. Each trace represents 64 averaged responses at 4-second intervals of stimulation; temperature was 38°C. Cont = control; ISO = isoproterenol; Caff = caffeine; AMR = amrinone. (From Morgan and Morgan [10], with permission.)

expected on the basis of the change in the amplitude of the  $Ca^{2+}$  transient, because it does not increase the sensitivity of the myofilaments to  $Ca^{2+}$ .

Although “skinned” and hyperpermeable cardiac muscle preparations remain the “gold

TABLE 3-3. Subcellular Actions of Inotropic Agents on Intracellular  $Ca^{2+}$  Handling and Proposed Mechanisms of Action

Pattern	Release from Stores	Reuptake by Stores	Sensitivity of Myofilaments	Proposed Mechanisms
I	↑ ↑ ↑	↑ ↓	↓	↑ cAMP
II	↓ ↓ ↑	↓ ↓	↑	↑ cGMP. ↑ cAMP. “direct” effects
III	↑ ↑	↔	↔	↑ Loading of $Ca^{2+}$ stores
IV	↑ ↑	↑	?	Unknown

cAMP = cyclic adenosine monophosphate; cGMP = cyclic guanine monophosphate. (From Morgan et al. [13], with permission.)

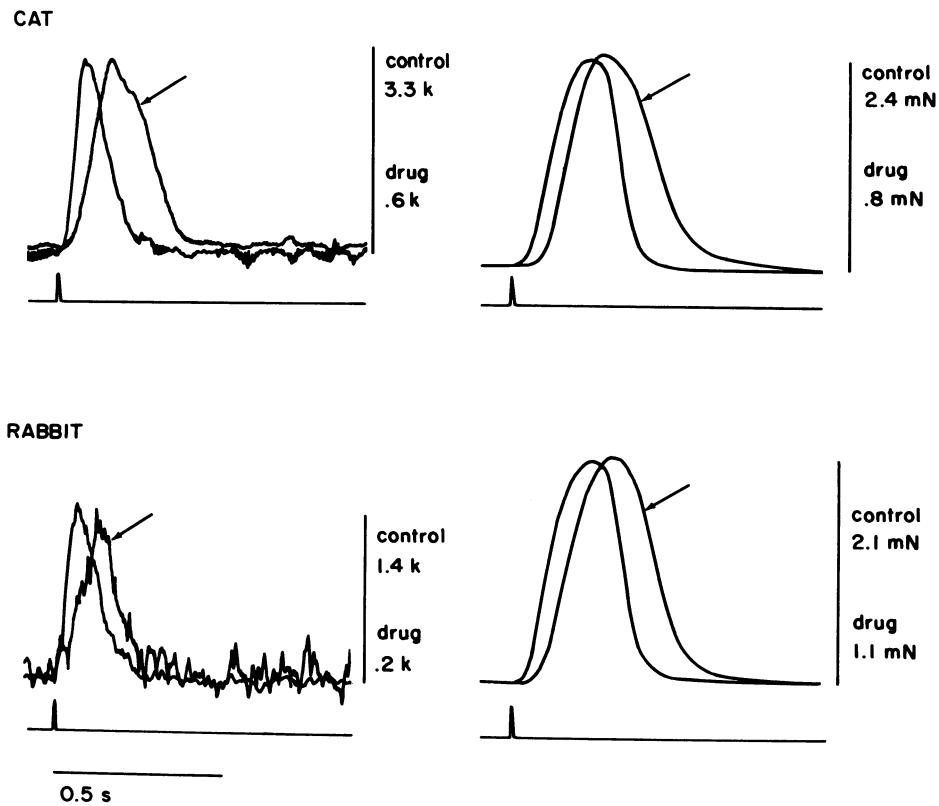


FIGURE 3-3. Influence of ryanodine,  $1 \times 10^{-6}$  M, on the time course of light and tension responses in cat and rabbit papillary muscles. Tracings recorded before and after (arrows) administration of the drug are superimposed with vertical scale adjusted to give the same peak amplitude. True amplitudes are indicated to the right. Note that although, as with caffeine, the time courses of light and tension are prolonged, ryanodine has a negative inotropic effect because it does not increase the sensitivity of the myofilaments to  $\text{Ca}^{2+}$ . Tension is expressed in millinewtons (mN); k = 1000 photon counts/second. (From Morgan and Morgan [10], with permission.)

standards" for determining the effects of interventions on the calcium sensitivity of the myofilaments, similar information can be obtained using aequorin in intact preparations, by comparing the peak amplitude of the aequorin light signal to the peak tension response [5, 18, 19]. Agents that do not affect the calcium sensitivity of the contractile apparatus in skinned-

muscle preparations produce force-vs.-light relationships that lie along the same line. This is illustrated in Figure 3-4 for points in the frequency-response curve before and after verapamil and for different doses of calcium. In contrast, agents that are known to decrease the sensitivity of the contractile apparatus to calcium produce a downward and rightward shift in the force-vs.-light relationship, as shown in Figure 3-4 for isoproterenol. On the other hand, agents that are known to increase the calcium sensitivity of the contractile apparatus produce a leftward shift in this relationship as illustrated in Figure 3-4 for caffeine. Although there are obvious limitations to this sort of analysis, which stem in part from the fact that most interventions produce significant changes in the time course of the calcium transient and twitch as well as in their amplitude, the results correlate quite well with those obtained in skinned or hyperpermeable cardiac muscle pre-

parations and provide a useful experimental approach for obtaining information about the calcium sensitivity of the contractile apparatus in intact preparations.

On the basis of force-vs.-calcium determinations in skinned, hyperpermeable, and aequorin-loaded preparations, it has been discovered that a variety of interventions can affect the calcium sensitivity of the contractile apparatus (Table 3-4). Each intervention produces apparently discrepant effects on the amplitude or time course of the intracellular calcium transient recorded with aequorin and isometric tension development. For example, although stretching an isometrically contracting muscle towards maximum length  $L_{\max}$  will produce marked increases in peak developed tension, the amplitude of the  $\text{Ca}^{2+}$  transient is practically unaffected by changes in muscle length [20]. In addition to caffeine and theophylline, differential effects on light and tension have been described for high concentrations of the calcium channel-blocking agents [21] phenylephrine [5], amrinone [22], sulmazole [23], and the hydrogen ion [24]. Changes in the time courses of the  $\text{Ca}^{2+}$  transient and the corresponding twitch are also usually parallel; however, stretch, particularly to lengths greater than  $L_{\max}$ , prolongs the mechanical activity of ventricular muscle, although the associated  $\text{Ca}^{2+}$  transient is slightly abbreviated [20]. Changing from isometric to isotonic loading conditions prolongs the  $\text{Ca}^{2+}$  transient but abbreviates the twitch [25].

The interventions discussed above that have differential effects on the  $\text{Ca}^{2+}$  transient and twitch appear to act by changing the  $\text{Ca}^{2+}$  sensitivity of the myofilaments; this effect is predominant over any additional changes the intervention might produce in the  $\text{Ca}^{2+}$  transient. For example, stretch [26], alkalosis [27], and caffeine [16] have been shown to increase the sensitivity of the myofilaments, an action that would be expected to increase the strength and prolong the time course of the twitch. On the other hand, acidosis [27] and decreases in muscle length [26] diminish the  $\text{Ca}^{2+}$  sensitivity of the myofilaments and might be expected to decrease the strength and abbreviate the time course of the twitch. Moreover, although in mammalian working myocardium, changes in the amplitude or time course of the aequorin signal generally reflect changes in calcium handling by the SR, the calcium transient may

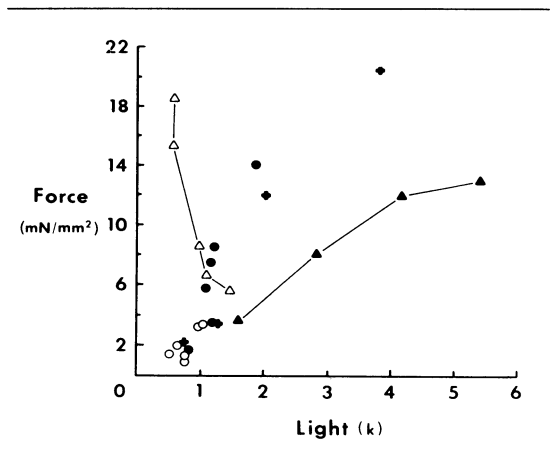


FIGURE 3-4. Plot of peak light against peak tension for several different inotropic agents applied to cat papillary muscle. The crosses represent points obtained from a calcium dose-response curve; the closed circles, points obtained from a frequency-response curve, and the open circles, a frequency-response curve in the presence of  $1 \times 10^{-6}$  M verapamil. The open triangles represent values obtained from a caffeine dose-response curve and the closed triangles represent values obtained from an isoproterenol dose-response curve. (From Morgan [19], with permission.)

be markedly affected by an increase or decrease in the  $\text{Ca}^{2+}$  affinity of troponin-C. If affinity is increased, troponin-C might be expected to release  $\text{Ca}^{2+}$  more slowly and therefore prolong the duration of the aequorin signal; decreases in affinity should have the opposite effect [25]. Such a change in the aequorin signal may be masked by additional effects of an intervention on intracellular  $\text{Ca}^{2+}$  handling. For example,

TABLE 3-4.  $\text{Ca}^{2+}$  Sensitivity of the Cardiac Contractile Apparatus

Increases $\text{Ca}^{2+}$ Sensitivity	Decreases $\text{Ca}^{2+}$ Sensitivity
Alkalosis	Acidosis
Stretch	cAMP
Caffeine	Calcium channel blockers (High dose)
Theophylline	Hypoxia
Sulmazole	
Alpha-adrenergic agonists	

although drugs that increase intracellular cAMP concentrations have been shown in skinned cardiac muscle preparations to markedly decrease the  $\text{Ca}^{2+}$  affinity of the myofilaments, they do not prolong the aequorin signal in intact muscles; marked abbreviation usually occurs, reflecting an increased rate of  $\text{Ca}^{2+}$  uptake by the SR [10].

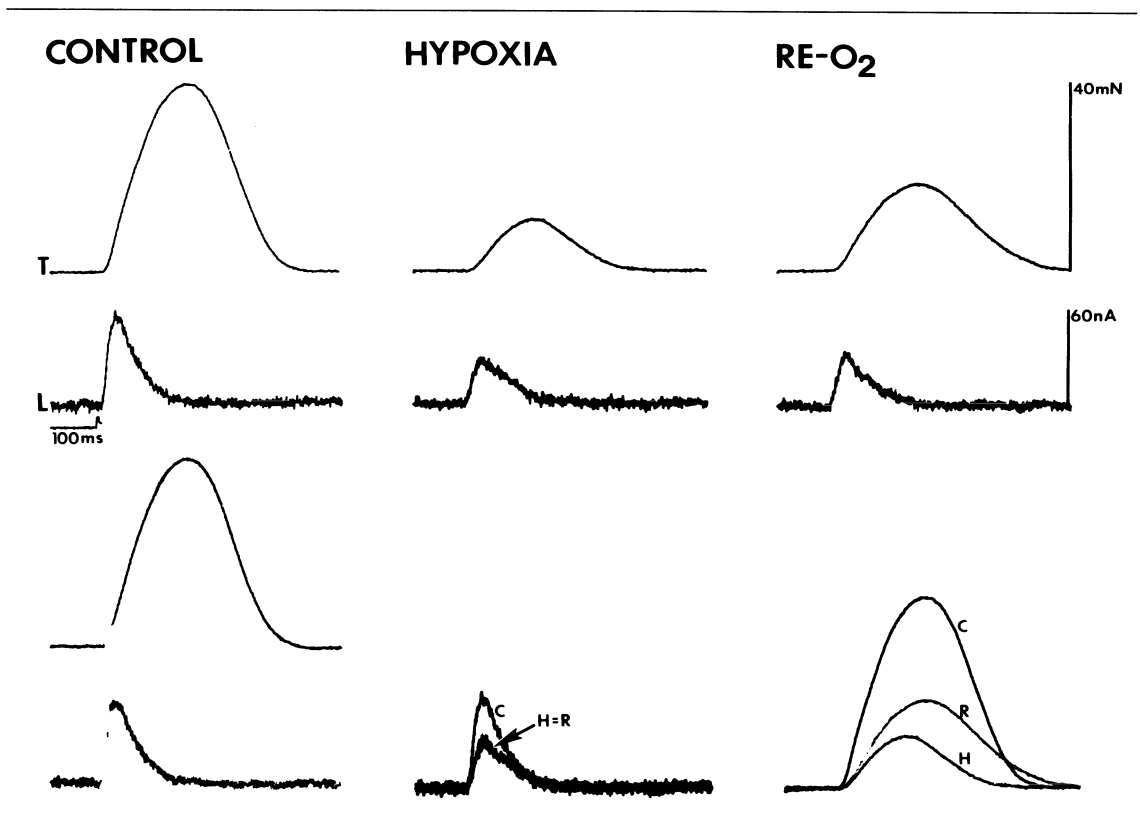
Striking examples of apparent dissociation between  $[\text{Ca}^{2+}]_i$  and mechanical activity are provided by comparison of the effects of hypoxia and reoxygenation on the amplitude and time course of the aequorin signal and isometric twitch. Exposing mammalian working myocardium to hypoxic conditions produces a negative inotropic effect accompanied by an abbreviation of isometric contraction. Reoxygenation completely reverses the negative inotropic effects caused by brief periods of hypoxia, but transiently prolongs isometric contraction and relaxation [28]. Changes in the amplitude and time course of contraction and relaxation have been demonstrated in the intact heart after reoxygenation of an hypoxic perfusate [29] or the release of a coronary artery ligature [28], as well as in isolated ventricular muscle from many mammalian species [28–31]. It has therefore been proposed that changes in mechanical activity induced by reoxygenation may be a major cause of systolic and diastolic dysfunction during recovery from transient ischemic episodes in animals and humans [28, 29].

The mechanisms responsible for these reversible, oxygen-dependent changes in tension development remain poorly understood. Because the calcium ion plays a key role as a second messenger in excitation-contraction coupling of cardiac muscle, it is reasonable to propose that alterations in the subcellular handling of  $\text{Ca}^{2+}$  might be the causative factor. A large body of experimental data has accumulated that is consistent with this hypothesis, including evidence of reoxygenation-induced increases in intracellular calcium concentrations and abnormal regulation of  $[\text{Ca}^{2+}]_i$  by the sarcolemma, SR and mitochondria [32]. On the other hand, Brutsaert and associates have reported a change in cross-bridge cycling rates during reoxygenation that cannot be fully explained by changes in the availability of activator  $\text{Ca}^{2+}$ , suggesting that reoxygenation has additional calcium-independent effects on the contractile apparatus [33]. Moreover, studies in ferret papillary

muscles loaded with the  $\text{Ca}^{2+}$  indicator aequorin have shown that changes in developed tension during hypoxia may occur without alteration of the corresponding  $\text{Ca}^{2+}$  transient [34]. We used aequorin to record intracellular  $\text{Ca}^{2+}$  transients during reoxygenation of hypoxic ferret ventricular muscle to determine whether the alterations in the amplitude and time course of the isometric contraction are mediated by changes in  $[\text{Ca}^{2+}]_i$  handling [35].

Ferret ventricular muscles ( $n = 5$ ) were stimulated to contract at 0.3 to 1 Hz in a bicarbonate-buffered salt solution at 30°C. The perfusate was bubbled with a mixture of 95%  $\text{O}_2/5\%$   $\text{CO}_2$  under control conditions and 95%  $\text{N}_2/5\%$   $\text{CO}_2$  to induce hypoxia. A typical experiment is shown in Figure 3–5. The peak light (i.e.,  $[\text{Ca}^{2+}]_i$ ) and peak tension were closely correlated under all conditions. In contrast, reoxygenation prolonged the duration of the contractile response by 1.5 to 2 times, but did not prolong the calcium transient. This indicates that reoxygenation-induced prolongation of relaxation cannot be attributed to changes in the time course of the  $[\text{Ca}^{2+}]_i$  transient, but may be related to an increased affinity of the contractile elements for  $\text{Ca}^{2+}$  or to other  $\text{Ca}^{2+}$ -independent factors governing the rate of cross-bridge cycling. It is unlikely that these results are simply an artifact due to differential oxygenation of superficial vs. core cells because cyanide (which produces uniform inhibition of oxidative phosphorylation throughout a preparation) and cyanide washout produced the same effects, respectively, as hypoxia and reoxygenation.

As suggested by Allen and Orchard [24], there are several mechanisms by which an intervention could interact with the contractile apparatus and alter its responsiveness to activator  $\text{Ca}^{2+}$ , including a competitive or noncompetitive interaction with  $\text{Ca}^{2+}$  at the level of troponin-C or an effect on the contractile proteins at some site other than troponin. A variety of changes in the intracellular milieu have been reported to occur during hypoxia and reoxygenation that could interact with the contractile apparatus at one or more sites, including shifts in the intracellular pH [36], inorganic phosphate [36], cyclic nucleotide [37], and high-energy phosphate concentrations [38] and the accumulation of free oxygen radicals [39]. Determination of which of these changes, if any, are responsible for the re-



oxygenation phenomena observed in our experiments must await additional study.

Up to this point, our discussion has focused on changes in calcium transients and phasic twitches. However, some investigators have proposed that increases in tonic tension development may also be important in certain pathophysiologic states such as ischemia. As shown in isolated papillary muscle preparations by Allen's group, an increase in tonic tension may or may not be associated with a change in intracellular  $[Ca^{2+}]_i$ . For example, in the presence of toxic doses of cardiac glycosides, increases in extracellular calcium will produce an increase in tonic tension development in an unstimulated ferret papillary muscle [40]. On the other hand, exposure of a preparation maintained in sodium-free medium to the metabolic inhibitor FCCP can produce a marked increase in tonic tension with no detectable change in intracellular  $Ca^{2+}$ . These two examples serve to illustrate the point

FIGURE 3-5. Intracellular  $Ca^{2+}$  transients during reoxygenation. The isometric twitch (T) and  $Ca^{2+}$  transient (L) were measured in a ferret right ventricular papillary muscle during a control period, during hypoxia, and during subsequent reoxygenation (RE- $O_2$ ). The muscle was stimulated to contract at 0.33 Hz and the temperature was 30°C. Hypoxia was induced by changing the gas mixture bubbling the bath from 95%  $O_2$  5%  $CO_2$  to 95%  $N_2$  5%  $CO_2$ . Control (C), hypoxia (H), and RE- $O_2$  (R) responses are superimposed in the middle and right panels of the lower half of the figure. T is expressed in milliNewtons- $mm^2$  and L is expressed in nanoamps.

that changes in tonic tension cannot always be attributed to changes in intracellular  $Ca^{2+}$ .

An interesting parallel can be drawn between the experiments discussed above and similar work done in vascular smooth muscle. Figure 3-6 shows the effects of two different types of interventions on intracellular  $Ca^{2+}$  and tonic tension development in a ferret portal-vein preparation. The lower panel shows the effects of depolarization with potassium. Note the

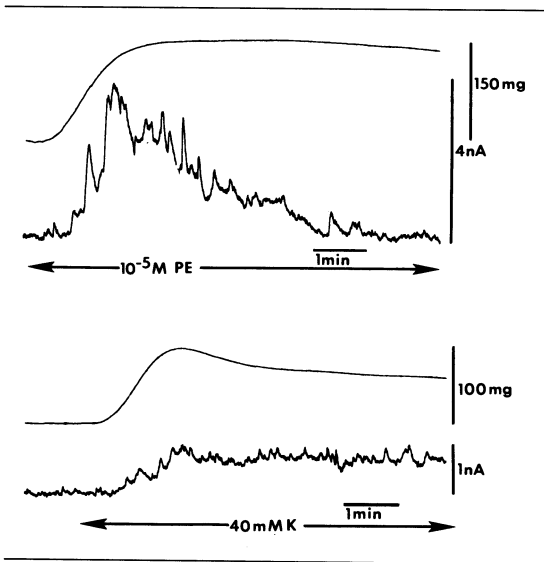


FIGURE 3-6. Effect of Phenylephrine (PE) and potassium ( $K^+$ ) depolarization on force (smooth traces) and the aequorin light signal (noisy traces) in vascular smooth muscle. Both sets of traces are from the same ferret portal-vein strip. Between the two sets of traces, the preparation was washed with drug-free physiologic saline solution for 1 hour. (From Morgan and Morgan [41], with permission.)

parallel and sustained rise in light and tension that occurs under the influence of this intervention. In contrast, the upper panel shows the effects of phenylephrine, which produces a rise in light and tension during the period of force development; but during the period of force maintenance, calcium falls towards resting levels while tension is maintained. This is a clear example of a situation in which force development is primarily dependent upon downstream mechanisms (i.e., formation of "latch state" between cross-bridges) rather than elevated levels of  $Ca^{2+}$  [41]. Although there are important differences between cardiac and vascular smooth muscle, it is not unreasonable to propose that similar downstream mechanisms may be playing a critical role in the regulation of contraction and relaxation processes of the heart under normal and pathophysiologic conditions.

In summary, a great deal of evidence supports the notion that cardiac contractile function is regulated by at least two major mechanisms (see

Table 3-1). It is clear that intracellular  $Ca^{2+}$  handling plays a central role in modulating the contraction-relaxation cycles of mammalian cardiac muscle. However, it is also becoming increasingly clear that changes in the  $Ca^{2+}$ -sensitivity of the myofilaments are also important. From both a clinical and an experimental standpoint, the examples discussed above illustrate the danger of drawing inferences about the amplitude and time course of the calcium transient from records of mechanical activity alone.

### References

1. Fozzard HA (1977). Heart excitation-contraction coupling. *Annu Rev Physiol* 39:201-220.
2. Chapman RA (1979). Excitation-contraction coupling in cardiac muscle. *Prog Biophys Mol Biol* 35:1-52.
3. Dhalla NS, Pierce GN, Anagia V, et al (1982). Calcium movements in relation to heart function. *Basic Res Cardiol* 77:117-139.
4. Langer GA, Frank JS, Philipson KO (1982). Ultrastructure and calcium exchange of the sarcolemma, sarcoplasmic reticulum and mitochondria of the myocardium. *Pharmacol Ther* 16:331-376.
5. Blinks JR, Endoh M (1986). Modification of myofibrillar responsiveness to  $Ca^{2+}$  as an inotropic mechanism. *Circulation* 73(suppl III):85-98.
6. Winegrad S (1984). Regulation of cardiac contractile proteins: Correlations between physiology and biochemistry. *Circ Res* 55:565-574.
7. Blinks JR, Wier WG, Hess P, Prendergast FG (1982). Measurement of  $Ca^{2+}$  concentrations in living cells. *Prog Biophys Mol Biol* 40:1-114.
8. Morgan JP, DeFeo TT, Morgan KG (1984) A chemical procedure for loading the calcium indicator aequorin into mammalian working myocardium. *Pfluegers Arch* 400:338-340.
9. Blinks JR (1984). Methods for monitoring  $Ca^{2+}$  concentrations with photoproteins in living cardiac cells. In Dhalla NS: *Methods for Studying Heart Membranes*, vol 2. Boca Raton, FL: CRC Press, pp 237-264.
10. Morgan JP, Morgan KG (1984). Calcium and cardiovascular function. *Am J Med* 77(5A):33-46.
11. Allen DG, Blinks JR (1978). Calcium transients in aequorin-injected frog cardiac muscle. *Nature* 269:509-513.
12. Wier WG (1980). Calcium transients during excitation-contraction coupling in mammalian heart: Aequorin signals of canine Purkinje fibers. *Science*; 1086-1087.

13. Morgan JP, Chesebro JH, Pluth JR, et al (1984). Intracellular calcium transients in human working myocardium as detected with aequorin. *Am J Cardiol* 3:410-418.
14. Allen DG, Kurihara S (1980). Calcium transients in mammalian ventricular muscle. *Eur Heart J* 1(suppl A):5-15.
15. Morgan JP, Blinks JR (1982). Intracellular  $Ca^{2+}$  transients in the cat papillary muscle. *Can J Physiol Pharmacol* 60:524-528.
16. Wendt IR, Stephenson DG (1983). Effects of caffeine on Ca-activated force production in skinned cardiac and skeletal muscle fibers of the rat. *Pfluegers Arch* 398:210-216.
17. McClellan GB, Winegrad S (1980). Cyclic nucleotide regulation of the contractile protein in mammalian cardiac muscle. *J Gen Physiol* 75:283-295.
18. Allen DG, Orchard CH (1984). Measurement of intracellular calcium concentration in heart muscle: The effects of inotropic interventions and hypoxia. *J Mol Cell Cardiol* 16:117-128.
19. Morgan JP (1985). The effects of digitalis on intracellular calcium transients in mammalian working myocardium as detected with aequorin. *J Mol Cell Cardiol* 17:1065-1075.
20. Allen DG, Kurihara S (1982). The effects of muscle length on intracellular calcium transients in mammalian cardiac muscle. *J Physiol (Lond)* 327:79-94.
21. Morgan JP, Wier WG, Hess P, Blinks JR (1983). Influence of  $Ca^{2+}$ -channel blocking agents on calcium transients and tension development in isolated mammalian heart muscle. *Circ Res* 52:47-52.
22. Morgan JP, Gwathmey JK, DeFeo TT, Morgan KG (1986). The effects of amrinone and related drugs on intracellular calcium in isolated mammalian cardiac and vascular smooth muscle. *Circulation* 73(suppl III):68-77.
23. Endoh M, Yanagisawa T, Taira N, Blinks JR (1986). Effects of new inotropic agents on cyclic nucleotide metabolism and calcium transients in canine ventricular muscle. *Circulation* 73(suppl III):117-133.
24. Allen DG, Orchard CH (1983). The effects of changes of pH on intracellular calcium transients in mammalian cardiac muscle. *J Physiol (Lond)* 335:555-567.
25. Housmans PR, Lee NKM, Blinks JR (1983). Active shortening retards the decline of the intracellular calcium transient in mammalian heart muscle. *Science* 221:159-161.
26. Hibberd MG, Jewell BR (1979). Length-dependence of the sensitivity of the contractile system to calcium in rat ventricular muscle. *J Physiol (Lond)* 290:30p-31p (abstract).
27. Fabiato A, Fabiato F (1978). Effects of pH on the myofilaments and the sarcoplasmic reticulum of skinned cells from cardiac and skeletal muscles. *J Physiol (Lond)* 276:233-255.
28. Bing OHL, Keefe MJ, Work MJ, et al (1970). Tension prolongation during recovery mechanics of cardiac contraction. *Am J Physiol* 218:1780-1787.
29. Blaustein AS, Gaasch WH (1981). Myocardial relaxation III. Reoxygenation mechanics in the intact dog heart. *Circ Res* 49:633-639.
30. Henderson AH, Brutsaert DL (1973). An analysis of the mechanical capabilities of heart muscle during hypoxia. *Cardiovasc Res* 7:763-776.
31. Tyberg JV, Yeatman LA, Parmley WW, et al (1970). Effects of hypoxia on mechanics of cardiac contraction. *Am J Physiol* 218:1780-1787.
32. Nayler WG, Poole-Wilson PA, Williams A (1979). Hypoxia and Calcium. *J Mol Cell Cardiol* 11:683-706.
33. Sys Su, Housmans PR, Van Ocker ER, Brutsaert DL (1984). Mechanisms of hypoxia-induced decrease of load dependence of relaxation in cat papillary muscle. *Pfluegers Archiv* 401:368-373.
34. Allen DG, Orchard CH (1983) Intracellular calcium concentration during hypoxia and metabolic inhibition in mammalian ventricular muscle. *J Physiol (Lond)* 339:107-122.
35. MacKinnon R, Gwathmey JK, Morgan JP (1987). Differential effects of reoxygenation on intracellular calcium and isometric tension. *Pfluegers Archiv* 409:448-453.
36. Allen DG, Morris PG, Orchard CH, Pirolo JS (1985). A nuclear magnetic resonance study of metabolism in the ferret heart during hypoxia and inhibition of glycolysis. *J Physiol (Lond)* 361:185-204.
37. Krause E, Wollenberger A (1980). Cyclic nucleotides in heart in acute myocardial ischemia and hypoxia. *Adv Cyclic Nucleotide Res* 12:49-60.
38. Veit P, Fuchs J, Zimmer G (1985). Uncoupler- and hypoxia-induced damage in working rat heart and its treatment: Observations with uncouplers of oxidative phosphorylation. *Basic Res Cardiol* 80:107-115.
39. Sjostrom K, Crapo JD (1983). Structural and biochemical adaptive changes in rat lungs after exposure to hypoxia. *Lab Invest* 48:68-79.
40. Allen DG, Eisner DA, Orchard CH (1984). Factors influencing free intracellular calcium concentration in quiescent ferret ventricular muscle. *J Physiol (Lond)* 350:615-630.
41. Morgan JP, Morgan KG (1984). Stimulus-specific patterns of intracellular calcium levels in smooth muscle of ferret portal vein. *J Physiol (Lond)* 351:155.

---

## 4. VARIABLE CALCIUM SENSITIVITY OF THE MAMMALIAN CARDIAC CONTRACTILE SYSTEM

---

Saul Winegrad, George McClellan, Andrea Weisberg,  
Steven Weindling, and Lin Er Lin

Activation of the contraction in cardiac muscle occurs as a result of a rise in the concentration of calcium in the immediate vicinity of the myofibrils. The sources of the calcium for this rise are the extracellular space and the sarcoplasmic reticulum. Within a specific range of concentration, in the vicinity of  $1\mu$  molar, the amount of force that is generated is dependent on the amplitude of the calcium concentration. The amplitude of the contraction, however, is also dependent on the affinity of the regulatory protein, troponin, for calcium. Developed force rises from zero to maximum with a change in concentration of calcium of approximately ten-fold, but the specific concentration range at which this occurs is dependent upon the properties of troponin, in particular, the affinity of the calcium binding site on one of the three subunits of the regulatory protein. A change in the range of calcium concentration that initiates contraction as a result of modification of the calcium-binding characteristics of troponin can be considered an alteration in calcium sensitivity. This can occur without any change in maximum calcium activity (Figure 4-1).

A change in the calcium sensitivity of the contractile system can produce important changes in the amount of tension developed during the cardiac contraction and in the rates of rise and fall of tension. Alteration of the affinity of the calcium-binding site on troponin can result

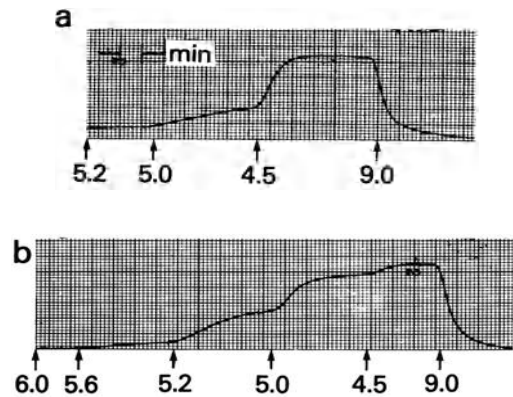


FIGURE 4-1. Force record of a bundle of hyper-permeable rat ventricular fibers. Numbers beneath the records indicate the pCa of the bathing solution. In the upper record (a), the calcium sensitivity is low; in the lower record (b), the calcium sensitivity is high as a result of dephosphorylation of troponin-I.

from either a change in the rate at which calcium binds to or is released by the binding site or a combination of both. The major impact of a change in calcium affinity on contraction has two fundamental causes. The maximum concentration of calcium achieved during a cardiac contraction probably rarely if ever rises to a level sufficient to produce maximum force. This has been shown by comparing the maximum force produced in isolated cardiac tissue with the maximum calcium-activated force in the same cells after the surface membrane has

Supported by grants HL16010, HL15835 and HL33294 from the National Institutes of Health.  
*Grossman, William, and Lorell, Beverly H. (eds.), Diastolic Relaxation of the Heart. Copyright © 1987. Martinus Nijhoff Publishing. All rights reserved.*

been removed as a diffusion barrier [1, 2]. Maximum calcium-activated force is at least twice that developed in the intact cell. The second reason is that the contraction generally does not last long enough for the cytosolic calcium concentration and the tension at that concentration to come to a steady state.

An example of the kind of effect a change in calcium sensitivity can have on the contraction is shown in Figure 4-2, illustrating consequences of a decrease in calcium sensitivity [3]. Here, estimated from direct measurements of the on- and off-rates of calcium binding by troponin under conditions where it is changed by beta-adrenergic activation, the response of the time course of saturation of calcium-binding sites on troponin to a change in the affinity is shown. In this case, the change in affinity is due exclusively to a faster rate of release of calcium by troponin. The kinetics of calcium uptake are changed very little, but there are major changes in the maximum level of saturation, the duration of the period during which some sites contain calcium, and the rate at which the proteins lose their calcium. Based on this type of analysis, one would expect that a decrease in calcium affinity from a faster off-rate would produce a lower level of maximum force, a shorter contraction, and a faster rate of relaxation. Experimental data support these inferences. On the other hand, increases in maximum force and slower rates of rise and fall in tension can be produced by modification of calcium sensitivity due to the appropriate changes in on- and off-rates of calcium binding by troponin.

Five different, potentially important mechanisms of change in calcium sensitivity in intact cardiac cells have been identified so far. These include phosphorylation of the inhibitory subunit of troponin, decrease in the concentration of adenosine triphosphate (ATP), increase in the resting length of the tissue, increase in the concentration of inorganic phosphate, and a change in the concentration of hydrogen ions.

### *Effects of Cyclic Adenosine Monophosphate (cAMP) on Calcium Sensitivity of Contractile Proteins*

When isolated myofibrils of cardiac muscle are exposed to cAMP and protein kinase, several sites on the contractile proteins are phosphorylated, but the primary site is the inhibitory

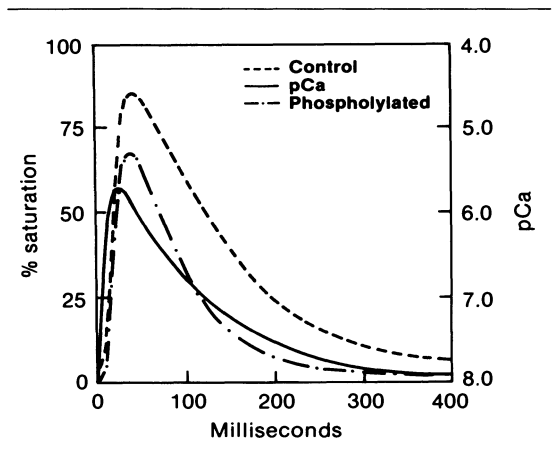
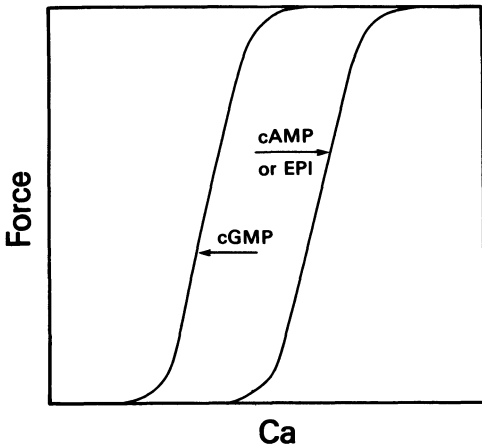


FIGURE 4-2. Consequences of a change in calcium sensitivity. The upper and middle curves are plots of the calculated changes in calcium binding (% saturation) by troponin with a change in calcium affinity resulting from phosphorylation of TNI. Solid curve depicts the change in the concentration of ionic calcium in the cytoplasm during a contraction.  $pCa =$  (From Robertson et al. [3]).

subunit of the regulatory protein troponin (TNI). Associated with this phosphorylation of TNI is an increase in the concentration of  $Ca^{2+}$  necessary to activate the actin-dependent ATPase activity of myosin [4-6]. A similar phosphorylation of TNI occurs when isolated perfused hearts are exposed to beta-adrenergic agonists. In this case the phosphorylation occurs very rapidly, with a time course that is similar to that of the onset of the inotropic action, but termination of the exposure to a beta-agonist causes an abrupt decline in contractility without an associated decline in the degree of phosphorylation of TNI.

The relationship of phosphorylation of TNI to tension development by the contractile system can be more rigorously studied in hyperpermeable cardiac cells. In this preparation, the surface membrane is made highly permeable to small molecules and ions without destroying the integrity of the membrane. The result is a preparation in which the concentration of calcium ions in the cytosol can be controlled by calcium buffer solutions added to a superfusion medium, but the adrenergic and cholinergic receptors in the membrane as well as important membrane enzymes like adenylate cyclase, guanylate cy-



**Ca Sensitivity Regulation**

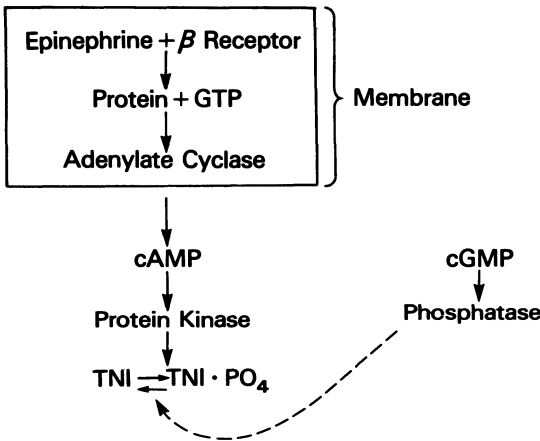


FIGURE 4-3. Calcium sensitivity regulation. Diagram of the mechanism of regulation of calcium sensitivity by phosphorylation of troponin-I (TNI) through adrenergic stimulation to produce cAMP or production of cGMP.

case, protein kinase, and phosphodiesterase remain functional [7].

**Role of Adrenergic Stimulation**

Exposure of hyperpermeable fibers to cAMP or to beta-agonists produces an increase in the con-

centration of  $Ca^{2+}$  required to activate tension [7]. The shape of the tension-calcium concentration relation is not changed, and the maximum force developed is not changed, but the whole curve is shifted to higher concentrations of  $Ca^{2+}$ . Removal of cAMP or the beta-agonist causes a reversal of the change in the calcium sensitivity of the contractile system. Addition of cyclic guanosine monophosphate (cGMP) produces an increase in  $Ca^{2+}$  sensitivity, again with no change in the maximum  $Ca^{2+}$ -activated force. These interrelationships are illustrated in Figure 4-3. The total range over which  $Ca^{2+}$  sensitivity can be shifted by the combined effect of the two cyclic nucleotides is approximately fivefold. The extent of the shift in calcium sensitivity is closely related to the amount phosphorylation of TNI [6]. This can be shown by exposing the bundles of hyperpermeable fibers to radioactively labeled ATP, and, after inducing changes in the calcium sensitivity with cyclic nucleotides, measuring the amount of  $P^{32}$  incorporated into TNI. The results show a very good correlation between the percentage of TNI phosphorylated and the change in  $Ca^{2+}$  sensitivity; the greater the degree of phosphorylation of TNI, the lower the  $Ca^{2+}$  sensitivity. In these experiments, care has been taken to first completely dephosphorylate TNI so that the incorporation of  $P^{32}$  is an accurate indication of the protein. The amount of phosphorylation of the protein. The protein kinase that is involved in this control mechanism is located in the surface membrane. The conclusion is drawn from studies of preparations in which the surface membrane has been removed, either manually or chemically, without major damage to the intracellular membranes or organelles. In these preparations, neither beta-agonists nor cAMP is able to alter calcium sensitivity. Interestingly enough, cGMP is still able to increase Ca sensitivity, indicating that its target molecule is not located in the surface membrane.

**Role of Cholinergic Stimulation**

Under certain circumstances, cholinergic stimulation can alter calcium sensitivity of hyperpermeable fibers [8]. Fibers with highest calcium sensitivity, achieved in the total absence of TNI phosphorylation, required approximately  $3 \mu M$   $Ca^{2+}$  for 50% of maximum force generation. Cholinergic stimulation of these fibers does not

alter  $\text{Ca}^{2+}$  sensitivity. However, cholinergic stimulation of fibers with lower levels of  $\text{Ca}^{2+}$  sensitivity raises sensitivity, and the lower the initial sensitivity, the larger the shift. These effects of cholinergic activity are completely inhibited by atropine, indicating that the mechanism of action is probably through muscarinic receptors. The effect of cholinergic stimulation appears to be dephosphorylation of already phosphorylated TNI. The extent to which cholinergic stimulation alters  $\text{Ca}^{2+}$  sensitivity is directly dependent upon the degree of TNI phosphorylation and indirectly dependent on the level of beta-adrenergic activity. In its dependence on existing beta-adrenergic tone, the extent of change in calcium sensitivity resembles the magnitude of the negative inotropic effect induced by cholinergic stimulation of intact hearts. In view of the dephosphorylating effect of cGMP and the known increase in cGMP produced by cholinergic stimulation, it is reasonable to assume that at least some of the effect of cholinergic stimulation is on the concentration of cGMP. It also may be due in part to the inhibition of adenylate cyclase in the membrane by activation of the inhibitory guanosine triphosphate (GTP)-binding subunit in the membrane.

Careful studies of the conformation of troponin, using a dansylated form of the molecule, have shown that phosphorylated troponin has a lower affinity for  $\text{Ca}^{2+}$  entirely as a result of a faster rate of release of bound  $\text{Ca}^{2+}$  with no significant change in the rate at which  $\text{Ca}^{2+}$  is bound by troponin [3]. Consequently, one would predict that the major effects of TNI phosphorylation would be on both the maximum force developed during a contraction and the rate of relaxation, with little change in the rate of rise of force. Calculations indicate that the amount of change in relaxation that should result from TNI phosphorylation is adequate to account for the increase in the rate of relaxation observed during beta-adrenergic stimulation of intact cells and the intact heart. It is interesting to note that beta-adrenergic stimulation also increases the slow inward  $\text{Ca}^{2+}$  current during the action potential, as well as the amplitude of the cytosolic rise in calcium concentration. These effects more than compensate for any negative effects of the decrease in  $\text{Ca}^{2+}$  sensitivity on the maximum force developed during beta-adrenergic stimulation.

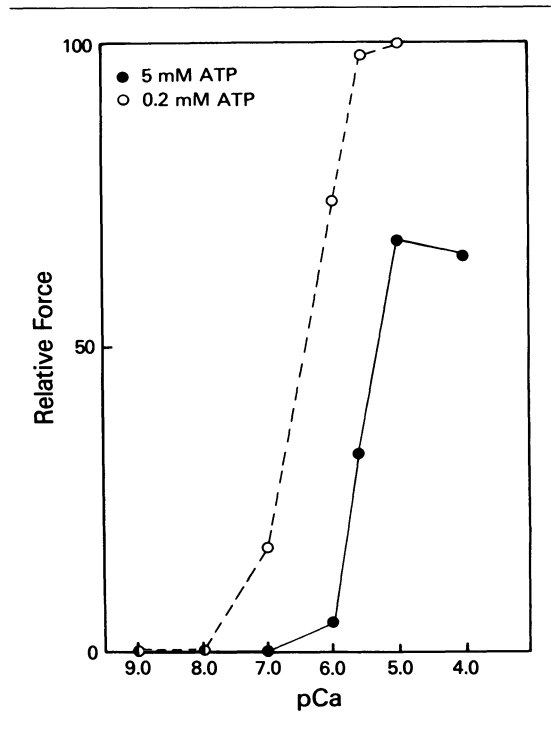


FIGURE 4-4. Effect of lowering the concentration of ATP on the calcium sensitivity of hyperpermeable cardiac fibers.

#### *Effects of ATP Concentration on the Calcium-Force Relation*

The calcium sensitivity of the contractile system can also be altered by a sufficient decrease in the concentration of ATP [7], as seen in Figure 4-4. As the concentration of ATP is reduced from its normal cytosolic value of 4 to 5 mM, maximum  $\text{Ca}^{2+}$ -activated force remains constant until ATP concentration is less than 1 mM. At that value, maximum  $\text{Ca}^{2+}$ -activated force begins to rise, and at an ATP concentration of 200  $\mu\text{M}$ , maximum  $\text{Ca}^{2+}$  activated force is about one-third greater than it is at normal ATP concentrations. At the same time, the  $\text{Ca}^{2+}$  sensitivity also shows a significant increase. At a concentration of 200  $\mu\text{M}$  ATP, maximum  $\text{Ca}^{2+}$  activation requires only about one-third or one-fourth of the concentration of  $\text{Ca}^{2+}$  that is necessary at 5 mM ATP. These effects of decreasing ATP concentration on

maximum  $\text{Ca}^{2+}$  activated force and  $\text{Ca}^{2+}$  sensitivity reach a maximum at about  $50 \mu\text{M}$  ATP; with further decrease in concentration of ATP, force begins to decline. Direct measurements of phosphorylated troponin show that phosphorylation of TNI is not required for this effect of ATP. The change in  $\text{Ca}^{2+}$  sensitivity can occur in the absence of a cell membrane, and therefore in the absence of the protein kinase that is active in the phosphorylation of TNI.

Unlike the changes in calcium sensitivity in response to beta-adrenergic and cholinergic stimulation that occur under normal, physiologic conditions, a change in  $\text{Ca}^{2+}$  sensitivity from low ATP concentration is unlikely to be seen in the normal, healthy heart because of the size of the decline in ATP concentration that is necessary. However, in metabolically stressed hearts, as those stressed by coronary artery disease, this mechanism may be active. Increases in resting tension during ischemia or hypoxia may occur from a rise in calcium sensitivity, leading to interaction between actin and myosin in the "resting" heart.

The way in which low ATP alters calcium sensitivity and maximum Ca-activated force is not entirely clear, but it seems to involve two components. Relaxation requires inhibition of the interaction of actin and myosin. Normally this occurs in the presence of adequate ATP by a steric block by tropomyosin of the sites on actin with which myosin interacts [9]. Binding of  $\text{Ca}^{2+}$  by troponin causes a movement of tropomyosin from this obstructing position to one that does not block the myosin interaction with actin. In the presence of a low concentration of ATP, the affinity of myosin for actin is so high—this is the basis of rigor interaction—that some myosin molecules bind to actin and shift tropomyosin out of its blocking position. One tropomyosin molecule blocks seven actin molecules. One or two rigor interactions may be sufficient to shift a tropomyosin molecule and open all seven actin molecules to myosin and produce a calcium-insensitive portion of the contractile system [10]. A second effect of low ATP concentration and the formation of rigor interactions is on the affinity of troponin for calcium. Through an allosteric effect, the interaction of myosin with actin increases the affinity of troponin for calcium. The reason for the increase in maximum  $\text{Ca}^{2+}$ -activated force is not clear, but it seems to be related to a change

in the force generators that results in a state of supercontractility. This was first observed in skeletal muscle by Bremel and Weber [10].

### *Effects of Resting Sarcomere Length on the Calcium-Force Relation*

The affinity of troponin for calcium is sensitive to the resting sarcomere length within the myofibrils [11]. As the sarcomere length is increased in cardiac fibers that have been treated with detergent to make the cells permeable to calcium-buffering systems, the  $\text{Ca}^{2+}$  sensitivity of contraction increases. This effect has also been shown in hyperpermeable fibers in which the cell membrane and intracellular membrane systems are still functional. Unlike the changes that result from TNI phosphorylation, the  $\text{Ca}^{2+}$  concentration required for maximum activation is unchanged. The curve relating tension to  $\text{Ca}^{2+}$  concentration is not simply shifted; its shape is also changed. Because the increase in  $\text{Ca}^{2+}$  sensitivity with increase in resting length can occur in the absence of a surface membrane, it cannot be due to TNI phosphorylation. Why this change in  $\text{Ca}^{2+}$  sensitivity occurs is not clear as yet.

The range of sarcomere lengths within which  $\text{Ca}^{2+}$  sensitivity depends on length is within the physiologic range, and it includes lengths developed during cardiac dilatation associated with pathologic states. The length-dependent response of  $\text{Ca}^{2+}$  sensitivity would provide a mechanism to resist the enlargement of the heart from an elevated diastolic pressure. A small number of force generators might be activated in the "resting," dilated heart leading to increased stiffness and a smaller change in size of the heart with increases in resting pressure.

### *Effect of pH and Inorganic Phosphate on the Calcium-Force Relation*

The calcium sensitivity of the contractile system is also sensitive to pH [1, 12]. This has been shown in both hyperpermeable fibers and in fibers from which the surface membrane has been manually removed. Calcium sensitivity is decreased by increasing acidity. A decrease in pH of 0.5 units will cause an increase in the concentration of  $\text{Ca}^{2+}$  required for 50% of maximum activation of about threefold. These

changes in  $\text{Ca}^{2+}$  sensitivity occur within the range that might exist inside cells during normal function and during metabolic stress, such as ischemia or hypoxia. Resting tension and actively developed tension could be affected.

The response of the cardiac contractile system to calcium ions is sensitive to the concentration of inorganic phosphate in the medium [13]. This influence is independent of any effect of pH or ionic strength in as much as it can be readily seen when changes in these two parameters have been prevented. A rise in the amount of phosphate added to the bathing medium from zero to 5 mM causes a reduction in maximum  $\text{Ca}^{2+}$ -activated force of about 45%, and further elevation of phosphate concentration causes a progressively larger drop in force so that in 20 mM phosphate, maximum  $\text{Ca}^{2+}$ -activated force has declined by almost 75%.

The *calcium* sensitivity of detergent-treated rat ventricular fibers is also depressed by increasing the concentration of phosphate. Raising the inorganic phosphate ions from zero to 20 mM doubles the concentration of calcium required to produce 50% of maximum  $\text{Ca}^{2+}$ -activated force. It results in an approximately symmetrical shift of the curve relating force to calcium concentration to higher concentrations of the activating ion.

In summary, it is now abundantly clear that the sensitivity of the contractile system to heart muscle can be altered by both physiologic and pathologic conditions, and that the changes induced can have major effects on the function of the heart. Both the maximum force developed during a contraction and the time course of the contraction can be influenced by the modification of the relation between developed force and calcium concentration.

### References

1. Winegrad S (1971). Studies of cardiac muscle with a high permeability to calcium produced by treatment with ethylene diamine-tetraacetic acid. *J Gen Physiol* 58:71-93.
2. Fabiato A, Fabiato F (1979). Tension developed and intracellular free calcium concentration reached during the twitch of an isolated cardiac cell with closed sarcolemma. *J Gen Physiol* 74:6a.
3. Robertson S, Johnson D, Holroyde M, et al (1982). The effect of troponin I phosphorylation on the Ca-binding properties of Ca-regulatory site of bovine cardiac troponin. *J Biol Chem* 257:260-263.
4. Holroyde MJ, Bowe E, Solaro RJ (1979). Modification of calcium requirements for activation of cardiac myofibrillar ATPase by cAMP dependent phosphorylation. *Biochim Biophys Acta* 586:63-69.
5. Ray K, England P (1976). Phosphorylation of the inhibitory subunit of troponin and its effect on calcium dependence of cardiac myofibril adenosine triphosphatase, *FEBS Lett* 70:11-17.
6. Mope L, McClellan G, Winegrad S (1980). Calcium sensitivity of the contractile system and phosphorylation of troponin in hyperpermeable cardiac cells. *J Gen Physiol* 75:271-282.
7. McClellan G, Winegrad S (1978). The regulation of calcium sensitivity of the contractile system in mammalian cardiac muscle. *J Gen Physiol* 72:734-764.
8. Horowitz R, Winegrad S (1983). Cholinergic regulation of calcium sensitivity in cardiac muscle. *J Mol Cell Cardiol* 16:277-280.
9. Huxley HE, Farugi AR, Kress M, et al (1982). Time resolved X-ray diffraction studies of the myosin layer-line reflections during muscle contraction. *J Mol Biol* 158:637-684.
10. Bremel R, Weber A (1972). Cooperation within actin filament in vertebrate skeletal muscle. *Nature New Biology* 238:97-101.
11. Hibberd M, Jewell B (1982). Calcium and length dependent force production in rat ventricular muscle. *J Physiol (Lond)* 329:527-540.
12. Fabiato A, Fabiato F (1978). Effects of pH on the myofilaments and the sarcoplasmic reticulum of skinned cells from cardiac and skeletal muscles. *J Physiol (Lond)* 276:233-255.
13. Kentish J (1986). The effects of inorganic phosphate and creatine phosphate on force production in skinned muscles from rat ventricle. *J Physiol* 370:585-604.

---

## 5. IS ISCHEMIC CONTRACTURE PRECEDED BY A RISE IN FREE CALCIUM?

---

William H. Barry

Initially during myocardial hypoxia or ischemia, development of contractile force declines. Ultimately the myocardial cell fails completely to develop contractile force and is usually fully relaxed at this stage [1]. With continued impairment of adenosine triphosphate (ATP) synthesis, the ischemic myocardial cell begins to develop an increase in resting tension. This increase in resting tension could be due to a rise in cytosolic free  $\text{Ca}^{2+}$  ion concentration,  $[\text{Ca}^{2+}]_i$ , or a fall in ATP concentration, which could produce rigor due to failure of actin-myosin cross-bridge dissociation [2].

A number of studies have investigated this issue. Lewis and colleagues [3] concluded from studies of elastic and viscous components of total myocardial stiffness that hypoxic contracture is not due solely to a rise in intracellular  $\text{Ca}^{2+}$ , but also to a rigor-type stiffness presumably due to ATP depletion. Holubarsch and associates [4] have concluded from studies of myocardial heat production during hypoxic and potassium chloride contracture that hypoxic contracture may not be due to an elevation in  $[\text{Ca}^{2+}]_i$ , but instead to rigor-like actin-myosin bonds. This conclusion is supported by the data of Allen and Orchard [5], who found no significant increase in aequorin luminescence in ferret papillary muscle during contracture induced by glycogen depletion and exposure to cyanide. In addition, Cobbold and Bourne [6] noted that cyanide plus 2-deoxyglucose produced contracture of isolated rat ventricular

myocytes within 10 minutes, before an increase in aequorin luminescence was noted.

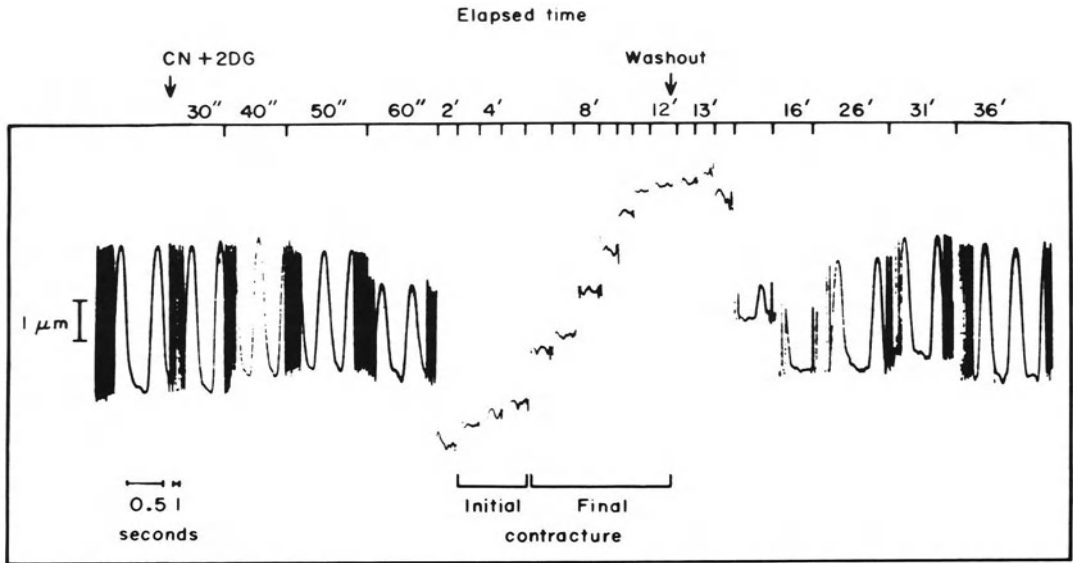
On the other hand, Dahl and Isenberg [7] noted that dinitrophenol produced within 2 to 6 minutes a parallel increase in  $[\text{Ca}^{2+}]_i$ , measured with a  $\text{Ca}^{2+}$  microelectrode, and electrical uncoupling in Purkinje fibers. Previous studies [8] have demonstrated that this uncoupling phenomenon coincides with development of contracture during hypoxia. In addition, Murphy and colleagues [9] reported that exposure to iodoacetate and an inhibitor of mitochondrial electron transport produced a rise in free  $[\text{Ca}^{2+}]_i$  in cultured chick embryo ventricular cells measured with the fluorescent  $\text{Ca}^{2+}$  indicator Quin-2 within 4 to 6 minutes. Snowdowne and coworkers [10] reported that hypoxia induced an increase in aequorin luminescence in dissociated myocytes within 4 to 5 minutes.

These apparent discrepancies led Clusin [11] to propose that perhaps the aequorin measurements were unreliable in this situation, because the aequorin luminescence is more sensitive to  $\text{Ca}^{2+}$  released from the sarcoplasmic reticulum (SR) than to uniformly distributed cytosolic  $\text{Ca}^{2+}$ . However, recent studies by Chapman [12] have also demonstrated that during contracture induced by mitochondrial inhibitors in ferret muscle, there was no detectable increase in  $[\text{Ca}^{2+}]_i$  measured with a  $\text{Ca}^{2+}$ -sensitive microelectrode.

We have approached this issue by utilizing the newly developed fluorescent  $\text{Ca}^{2+}$  indicator Indo-1 [13], to measure simultaneously changes in  $[\text{Ca}^{2+}]_i$  and development of contracture during metabolic inhibition of cultured ventricular cells. Our results suggest that there are two phases to the contracture associated with metabolic inhibition in these cells. An initial

Supported in part by the National Institutes of Health Grant HL30478.

Grossman, William, and Lorell, Beverly H. (eds.), *Diastolic Relaxation of the Heart*. Copyright © 1987. Martinus Nijhoff Publishing. All rights reserved.



relatively gradual phase is associated with a rise in  $[Ca^{2+}]_i$ ; a subsequent phase of contracture appears to be due to adenosine triphosphate (ATP) depletion.

### Methods

Ventricles from 10-day-old chick embryos were trypsinized, and the resulting cell suspension was cultured for 3 days as previously described [14]. During culturing, confluent cell layers developed in which over 80% of the cells had characteristics of myocytes and contracted spontaneously. Contraction and relaxation of individual cells within the cultured layers were quantitated by measurement of cell motion, using a phase-contrast microscope and video motion-detector as previously described [15]. Movement of an intracellular organelle, or a plastic microsphere adherent to the surface of the cell, was tracked in such a way so that an upward displacement of the motion signal corresponded to an increase in tension development.

Energy deprivation was produced by exposure of these cells to 1 mM cyanide and 20 mM 2-deoxyglucose (2DG) zero-glucose solution. Changes in  $[Ca^{2+}]_i$  were measured using the

FIGURE 5-1. Recordings of cell motion during superfusion with and washout of cyanide (CN) and 2-deoxyglucose (2DG). The times noted at the top of the figure indicate the interval after exposure to metabolic inhibitors. The initial stage of contracture development began at 3 minutes (3'), becoming accelerated 6' after exposure to CN and 2DG. Normal contractile activity returned after 20 minutes of washout. (From Hasin et al., [17].)

fluorescent  $Ca^{2+}$  indicator Indo-1 [13, 16]. Cells were exposed to  $10^{-5}$  Indo-1 AM for 15 minutes and then were washed free of dye. After approximately 1 hour, contractile activity returned to near control levels. Cells were placed subsequently in a perfusion chamber, where fluorescence intensity could be monitored at 410 and 480 nm, with excitation at 360 nm. An epifluorescence system attached to a Nikon phase-contrast microscope was used, which permitted simultaneous measurement of motion, using the video motion-detector, and changes in fluorescence intensity. With Indo-1, fluorescence intensity increases with increasing  $Ca^{2+}$  concentration at 410 nm, and decreases with increasing  $Ca^{2+}$  concentration at 480 nm. Therefore, the ratio of fluorescence intensities at 410 and 480 nm was used to indicate changes in  $[Ca^{2+}]_i$  levels.

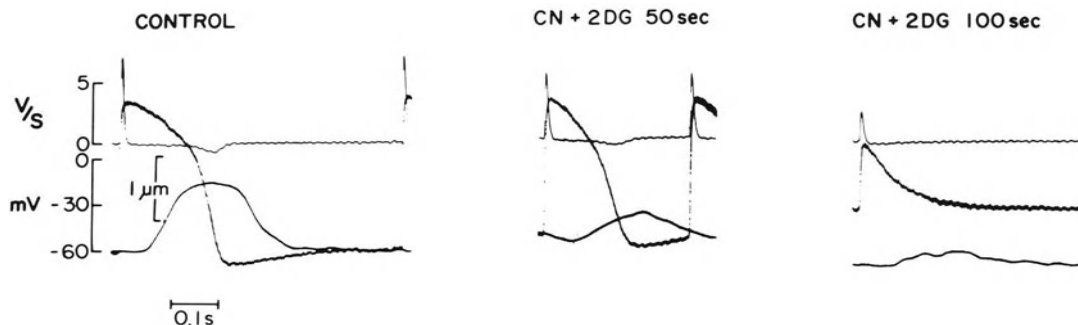


FIGURE 5-2. Effects of cyanide (CN) and 2-deoxyglucose (2DG) on membrane potential (mV), its first derivative (V/s), and cell motion ( $\mu\text{m}$ ). Note that depolarization of cell diastolic potential to  $-40$  mV occurred within 100 seconds of exposure to CN and 2DG. Membrane potentials were recorded with glass micropipettes (From Hasin and Barry, [18]).

### Results

Previous experiments in our laboratory have demonstrated that exposure of these cells to cyanide and 2DG produces a contracture that occurs in two stages, an initial slowly developing stage followed by a more rapid contracture development [17] as seen in Figure 5-1. This contracture is fully reversible, and contractile activity returns to normal within 20 to 30 minutes after washout of the inhibitors. The development of the initial contracture, and the onset of the final contracture, can be delayed by treatment *after* metabolic inhibition with  $\text{La}^{3+}$ , which inhibits Na-Ca exchange. Contracture onset was not affected by verapamil after metabolic inhibition. We therefore proposed that perhaps  $\text{Ca}^{2+}$  influx via Na-Ca exchange in the early phase of metabolic inhibition was contributing to contracture development in these cells [17].

Exposure to cyanide and 2DG results in rapid depolarization of the cells to approximately  $-40$  mV [18] as seen in Figure 5-2. Depolarization would tend to cause an increase in  $\text{Ca}^{2+}$  influx via Na-Ca exchange, because of the 3:1 stoichiometry of the exchanger, which results in this process being electrogenic [19]. Inhibition of the Na pump, which occurs within 4 to 5 minutes after cyanide and 2DG exposure (Figure

5-3) could also stimulate  $\text{Ca}^{2+}$  influx via the Na-Ca exchanger, because of a rise in  $[\text{Na}^+]_i$ .

To test the hypothesis that there is an initial increase in  $[\text{Ca}^{2+}]_i$  after metabolic inhibition, we performed the experiments shown in Figure 5-4. Exposure of the cells to cyanide and 2-DG resulted initially in failure of contraction, with increased relaxation. This is consistent with our previous findings. Shortly thereafter, there occurred a phase of progressive increase in  $[\text{Ca}^{2+}]_i$  that was associated with an increase in resting tension, manifested by a progressive upward movement of the motion signal. During this stage of initial contracture development, there was a reasonable correspondence between increases in  $[\text{Ca}^{2+}]_i$ , which was from 200 to 300 nM, and tension development. When  $[\text{Ca}^{2+}]_i$  levels reached approximately the same level as is present during normal beating, or about 300 nM [16] there occurred an accelerated rate of contracture, which was not associated with an increased rate of rise in  $[\text{Ca}^{2+}]_i$ . Of interest regarding this phase of contracture is that there were some coarse oscillatory movements noted as the contracture developed, which were also unassociated with any change in  $[\text{Ca}^{2+}]_i$ .

On abrupt reexposure to normal medium, there was an initial rapid phase of relaxation associated with fall in  $[\text{Ca}^{2+}]_i$ , followed by a slower phase of relaxation, presumably due to resynthesis of ATP, which can occur over this same time period [20]. Preliminary experiments in our laboratory [21] suggest that the fall in  $[\text{Ca}^{2+}]_i$  that occurs during washout of metabolic inhibitors is related to an increase in  $\text{Ca}^{2+}$

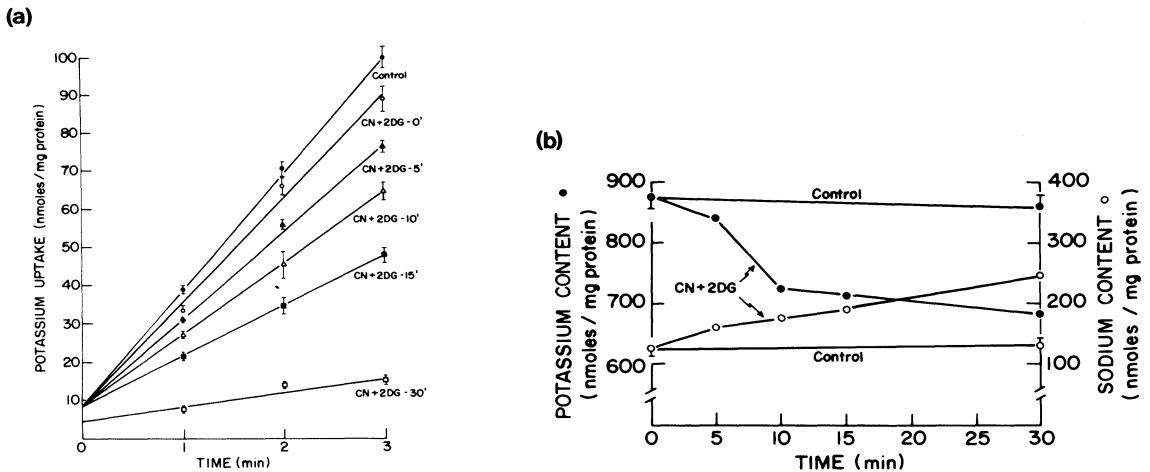


FIGURE 5-3. Effects of exposure to cyanide (CN) and 2-deoxyglucose (2DG) on  $K^+$  uptake (a) and  $K^+$  and  $Na^+$  contents (b) of cultured ventricular cells. Within 5 minutes after exposure to metabolic inhibitors, there was a significant impairment of  $K^+$  uptake and an increase in  $Na^+$  content. (From Hasin and Barry, [18].)

uptake by intracellular organelles, primarily in the sarcoplasmic reticulum, rather than transsarcolemmal  $Ca^{2+}$  efflux mediated by recovery of the  $Ca^{2+}$  pump.

### Discussion

Our findings are consistent with those of Allen and Orchard [5], which indicated that during energy deprivation contracture, a rise in  $[Ca^{2+}]_i$  alone could not account for the contracture tension-development observed. However, one of the limitations of the aequorin method is that it is relatively insensitive at diastolic levels of free  $Ca^{2+}$  and may be influenced by changes in  $Mg^{2+}$  concentration, which are unknown. Studies reported here using the newer fluorescent  $Ca^{2+}$  indicator Indo-1 indicate that the initial phase of contracture in cultured ventricular cells during energy depletion is in fact associated with an increase in  $[Ca^{2+}]_i$ . It is also apparent, however, that during the accelerated phase of contracture development, although  $[Ca^{2+}]_i$  continues to increase slightly, it does not reach a level sufficient to account for the tension development observed. Therefore, this accelerated phase of contracture probably is due to severe ATP depletion.

Our previous observations indicated that treatment of these cultured cells with  $La^{3+}$  after the onset of metabolic inhibition, could prolong the time required for development of the initial phase of contracture and the final contracture

[17]. This suggests that  $Ca^{2+}$  influx in these cells via Na-Ca exchange may well contribute to this initial rise in  $[Ca^{2+}]_i$ . An increase in  $[Ca^{2+}]_i$  in the early stage of metabolic inhibition could activate  $Ca^{2+}$ -sensitive ATPases, producing a more rapid and progressive decline in ATP stores, and thus contribute to the development of the contracture.

A role in this process for  $Ca^{2+}$  influx via Na-Ca exchange, or possibly by other pathways as well, is consistent with the observations of Nayler and associates [1] that a delay, attenuation, or even prevention of contracture, can be achieved when  $Ca^{2+}$  is removed from the extracellular medium before onset of contracture. Conrad and colleagues [22], observed that hypoxic contracture in the rat could be prevented by pretreatment with cobalt. In addition, Renlund and co-workers [23] have reported that a reduction in extracellular  $Na^+$  concentration, and thus presumably intracellular  $Na^+$  concentration, during ischemia resulted in a reduced development of contracture on reperfusion. Thus,  $Ca^{2+}$  influx may influence contracture both during and after recovery from ATP depletion.

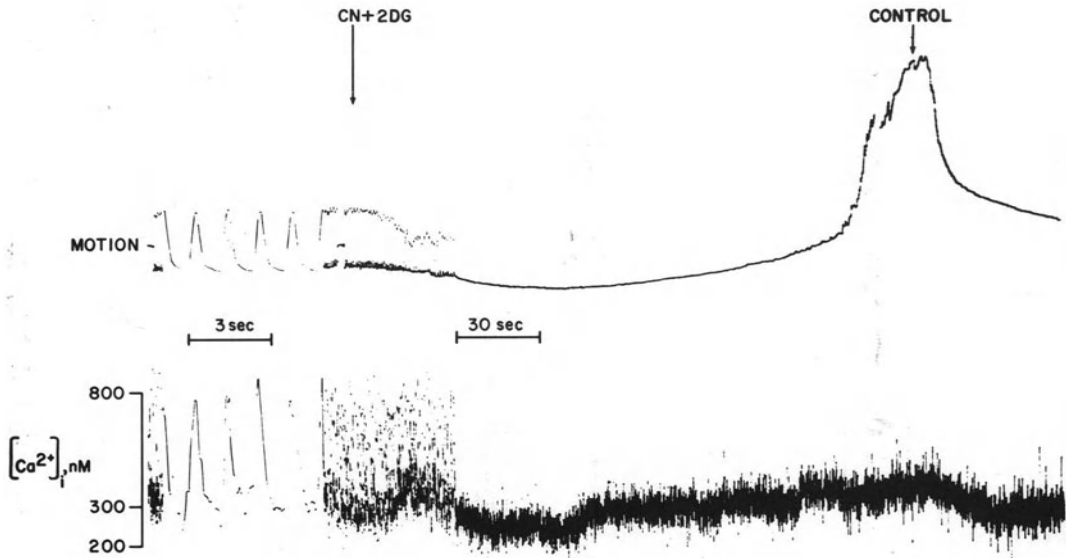


FIGURE 5-4. Simultaneous changes in cell motion (*upper trace*) and  $[Ca^{2+}]_i$  (*lower trace*) during exposure to cyanide (CN) and 2-deoxyglucose (2DG). The  $[Ca^{2+}]_i$  trace is the ratio of fluorescence intensities at 410/480 nm. The corresponding approximate values for  $[Ca^{2+}]_i$ , based on *in vivo* calibration data [16], are as indicated. The initial phase of contracture is associated with a rise in  $[Ca^{2+}]_i$ , whereas the subsequent accelerated phase is not. On washout, there is an immediate partial relaxation associated with a fall in  $[Ca^{2+}]_i$ , followed by a more gradual recovery towards a fully relaxed position.

We conclude that the initial phase of contracture during metabolic inhibition of ATP synthesis is associated with an increase in  $[Ca^{2+}]_i$ . This  $Ca^{2+}$  could derive from release from intracellular stores or from transsarcolemmal influx. It seems likely that this  $Ca^{2+}$  rise may contribute to ATP loss and the eventual development of an ATP-depletion contracture. Therefore, it may be possible to modulate the development of ischemic contracture by either diminishing or preventing this initial rise in  $Ca^{2+}$  or by increasing ATP stores, which are subsequently depleted by activation of  $Ca^{2+}$ -ATPases. Improved understanding of the mechanisms of ischemic contracture may help to define better ways to prevent and treat it and to understand its role in the development of cell death in intact tissue.

### References

1. Nayler WG, Poole-Wilson PA, Williams A (1979). Hypoxia and calcium. *J Mol Cell Cardiol* 11:683-706.
2. Grossman W, Barry WH (1980). Diastolic pressure-volume relations in the diseased heart. *Fed Proc* 39:148-155.
3. Lewis MJ, Housmans PR, Claes VA, Brutsaert DL, Henderson AH (1980). Myocardial stiffness during hypoxic and reoxygenation contracture. *Cardiovasc Res* 14:339-344.
4. Holubarsch CL, Alpert NR, Goulette R, Mulieri LA (1982). Heat production during hypoxic contracture of rat myocardium. *Circ Res* 51: 777-786.
5. Allen DG, Orchard CH (1983). Intracellular calcium concentration during hypoxia and metabolic inhibition in mammalian ventricular muscle. *J Physiol (Lond)* 339:107-122.
6. Cobbold PH, Bourne PK (1984). Aequorin measurements of free calcium in single heart cells. *Nature* 312:444-446.
7. Dahl G, Isenberg G (1980). Decoupling of heart muscle cells: Correlation with increased cytoplasmic calcium activity and with changes of nexus ultrastructure. *J Memb Biol* 53:C3-75.
8. Wojtczak J (1979). Contractures and increase in internal longitudinal resistance of cow ventricular muscle induced by hypoxia. *Circ Res* 44:88-95.
9. Murphy E, Jacob R, Lieberman M (1985).

- Cytosolic free calcium in chick heart cells. *J Mol Cell Cardiol* 17:221-231.
10. Snowdowne KW, Ertel RJ, Borle AB (1985). Measurement of cytosolic calcium with aequorin in dispersed rat ventricular cells. *J Mol Cell Cardiol* 17:233-241.
  11. Clusin WT (1985). Do caffeine and metabolic inhibitors increase free calcium in the heart? Interpretation of conflicting intracellular calcium measurements. *J Mol Cell Cardiol* 17: 213-220.
  12. Chapman RA (1986). Sodium/calcium exchange and intracellular calcium buffering in ferret myocardium: An ion-sensitive microelectrode study. *J Physiol (Lond)* 373:163-179.
  13. Barry WH, Pober J, Marsh JD, et al (1980). Effects of graded hypoxia on contraction of cultured chick embryo ventricular cells. *Am J Physiol* 239:H651-H657.
  14. Barry WH, Rasmussen CAF Jr, Ishida H, Bridge JHB (1986). External Na-independent Ca extrusion in cultured ventricular cells. *J Gen Physiol* 88:393-411.
  15. Gryniewicz G, Poenie M, Tsien RY (1985). A new generation of  $Ca^{2+}$  indicators with greatly improved fluorescence properties. *J Biol Chem* 260:3440-3450.
  16. Peeters GA, Hlady V, Bridge JHB, Barry WH (1987). Simultaneous measurements of calcium transients and cell motion in cultured heart cells. *Am J Physiol*, in press.
  17. Hasin Y, Doorey A, Barry WH (1984). Effects of calcium flux inhibitors on contracture and calcium content during inhibition of high energy phosphate production in cultured heart cells. *J Mol Cell Cardiol* 16:823-834.
  18. Hasin Y, Barry WH (1984). Myocardial metabolic inhibition and membrane potential, contraction, and potassium uptake. *Am J Physiol* 247:H322-H329.
  19. Reeves JP, Hale CC (1984). Stoichiometry of the cardiac Na-Ca exchange system. *J Biol Chem* 259:7733-7739.
  20. Doorey AJ, Barry WH (1983). The effects of inhibition of oxidative phosphorylation and glycolysis on contractility and high energy phosphate content in cultured chick heart cells. *Circ Res* 53:192-201.
  21. Cunningham MJ, Rasmussen CAF Jr, Sheck R, Barry WH (1985). Energy deprivation contracture in zero Na: Effects of resupply of Na or resynthesis of ATP on relaxation. *Circulation*. 72:III-345 (abstract).
  22. Conrad CH, Brooks WW, Ingwall JS, Bing OHL (1984). Inhibition of hypoxic myocardial contracture by cobalt in the rat. *J Mol Cell Cardiol* 16:34J-354.
  23. Renlund D, Gerstenblith G, Lakatta E, et al (1984). Perfusate sodium during ischemia-modified postischemic functional and metabolic recovery in the rabbit heart. *J Mol Cell Cardiol* 16:795-801.

---

## 6. THE EFFECT OF REGIONAL MYOCARDIAL HETEROGENEITY ON THE ECONOMY OF ISOMETRIC RELAXATION

---

Norman R. Alpert and Louis A. Mulieri

This chapter is directed at clarifying the relationship between regional myocardial heterogeneity and the economy of contraction and relaxation [1]. When heart muscle contracts and relaxes isometrically, there is considerable internal shortening and lengthening during the rise and fall of tension development [2]. In skeletal muscle, under those conditions where active muscle shortens and lengthens, the energetic cost of shortening is greater than that of lengthening [3–6]. Thus the economy of contraction is less than that of relaxation. If heart muscle is like skeletal muscle, one would expect the economy of relaxation to be greater than that of contraction. Inhomogeneity adds another dimension to this problem. Inhomogeneity is present in normal hearts and abounds under pathological conditions. In normal hearts there are geometric (apex to base) [7–10] and isoenzymic [11–16] differences. In the presence of regional ischemia, the stunned portion of the heart is much weaker than the nonstunned portion [17, 18]. When an infarct occurs, the noninfarcted remainder of heart may hypertrophy with the extent of the hypertrophic response being different in the various areas [19–22]. This heterogeneity results in a functional difference in myocytes or sarcomeres, which are in series with each other. How these differences affect the predicted increase in economy of isometric relaxation in contrast to contraction is the focus of this chapter.

*Grossman, William, and Lorell, Beverly H. (eds.), Diastolic Relaxation of the Heart. Copyright © 1987. Martinus Nijhoff Publishing. All rights reserved.*

### *Strategy*

We planned to produce the myocardial heterogeneity by using hearts of varying myosin isoenzyme composition. In rabbit heart, the adenosine triphosphatase (ATPase) activity of the contractile protein myosin (and therefore the velocity of shortening of the muscle) is determined primarily by its isoenzymic content. There are at least three isoenzymic forms of ventricular myosin. The  $V_1$  form has a high ATPase activity and is a homodimer consisting of two alpha chains [11]. The  $V_3$  form has a low ATPase activity and is a homodimer consisting of two beta chains, whereas the  $V_2$  form has intermediate ATPase activity and is a heterodimer consisting of one beta and one alpha chain [11]. It has previously been observed that myosin isoenzyme heterogeneity exists in young rabbits (1.5–2.0 kg) (about 90%  $V_3$ ) and in thyrotoxic rabbits (about 90%  $V_1$ ) [16, 23, 24]. Furthermore, in pressure-overloaded rabbit hearts, the affected myocardium consists of only one isoenzyme of myosin ( $V_3$ ) [16, 23, 24]. Accordingly, our plan was to use these three animal models: pressure-overloaded, control, and thyrotoxic rabbits to provide hearts that were (1) homogeneous, namely, the pressure-overloaded type (2) heterogeneous, i.e., the control and thyrotoxic types. The energy requirements of contraction and relaxation were assessed in these hearts using rapid, sensitive myothermal techniques and an analysis of the heat records, which separates the tension-dependent heat from the other components of the heat output [25–27].

## Methods

### ANIMAL MODELS

Young (1.5 kg), male, white New Zealand rabbits were divided into three groups. Pressure-overloaded hypertrophy is produced by twisting a spiral monel metal clip around the pulmonary artery and thus reducing the right ventricular outflow tract radius by 67%. The animal was allowed to recover from the surgery and the experiment was carried out 4 weeks after the operation [28, 29]. Thyrotoxicosis was produced by 14 daily intramuscular injections of L-thyroxine (0.2 mg/Kg) [23, 24]. The treatment was omitted on any day when the body weight was less than 80% of the control value.

### INTRAVENTRICULAR PRESSURE AND HEART WEIGHT MEASUREMENTS

Right ventricular pressures were measured in each of the animal models in the anesthetized closed-chest rabbit by means of a catheter attached to a Statham pressure strain gauge transducer. The right ventricular weight was obtained following sacrifice of the animal; the chest was opened and the heart removed for dissection of the papillary muscle. After removal of the papillary muscle, the right ventricle was dissected from the whole heart, quickly blotted to dryness, and weighed.

### RIGHT VENTRICULAR PAPILLARY MUSCLE MECHANICS

The rabbit was sacrificed by stunning and cervical dislocation, the chest was opened, and the heart was quickly removed and placed in oxygenated Krebs solution [30]. The right ventricle was opened and the papillary muscle exposed. Long, thin papillary muscles (>3.5 mm) were dissected free of the wall and mounted on the thermopile system so that the tendinous end of the muscle was attached to a stationary hook at the bottom of the thermopile while the cut end of the muscle was attached to a low-compliance, capacitance-force transducer [30, 31]. The muscle was placed so that the flat portion was in contact with the measuring junctions of the thermopile located in the central exposed region [30].

### PERCENT ISOMYOSIN AND CONTRACTILE PROTEIN ATPase ACTIVITY

Pyrophosphate gel electrophoresis was carried out using the methods described by Hoh and

colleagues [11] on homogenized ventricular tissue or purified myosin [32]. The percent of isomyosin was assessed from densitometer traces of the gels as previously described [16]. Calcium-stimulated myosin ATPase activity was assayed in 0.05 M KCl, 9 mM CaCl<sub>2</sub>, 4 mM ATP, and 0.05 M Tris buffer (pH 7.6). The assays were carried out at 25°C and were stopped by the addition of 0.5 ml of cold 20% HC10<sub>4</sub> [32].

### THERMAL MEASUREMENTS AND THEIR INTERPRETATION

Rapid, sensitive, thermal measurements on isolated papillary muscle provide a view of the time course of the biochemical processes taking place within the myocyte during the isometric twitch and recovery from that twitch. The key to making thermal measurements that can be resolved within a single beat was the development of a planar bismuth and antimony thermopile [30] of low thermal capacity and high sensitivity. The heat output of the muscle can be partitioned into resting or basal heat ( $H_B$ ) and activity-related heat ( $H_A$ ). The basal heat ( $H_B$ ) is a reflection of the energy requirements of all the processes involved in maintaining the normal integrity of the cell such as protection of ion gradients, organelle repair and replacement, cellular and intracellular restructuring, and general transport processes. The activity-related heat ( $H_A$ ) is liberated in two phases, an initial rapid phase and a secondary slower phase. As illustrated in Figure 6-1, the initial rapid phase is temporally associated with contraction and relaxation ( $\theta_1$ , panel A, Figure 6-1). The secondary slower phase is associated with recovery processes (panel A, Figure 6-1). The initial heat,  $I$ , is a reflection of ATP hydrolyzed by the myosin during the cyclic interaction of the myosin head with actin while producing force (tension-dependent heat, TDH) and the ATP hydrolyzed in pumping calcium ions from the cytosol (tension-independent heat, TIH). The recovery heat,  $R$ , is associated with the resynthesis by the mitochondria of ATP from the ADP produced during contraction and relaxation. The tension-independent heat (TIH) can be separated from the initial heat,  $I$ , by incubating the muscle in hyperosmotic mannitol or in a hyperosmotic mannitol diacetyl monoxime (BDM) Krebs solution. Under these conditions force is eliminated and the triggerable heat that remains is the tension-indepen-

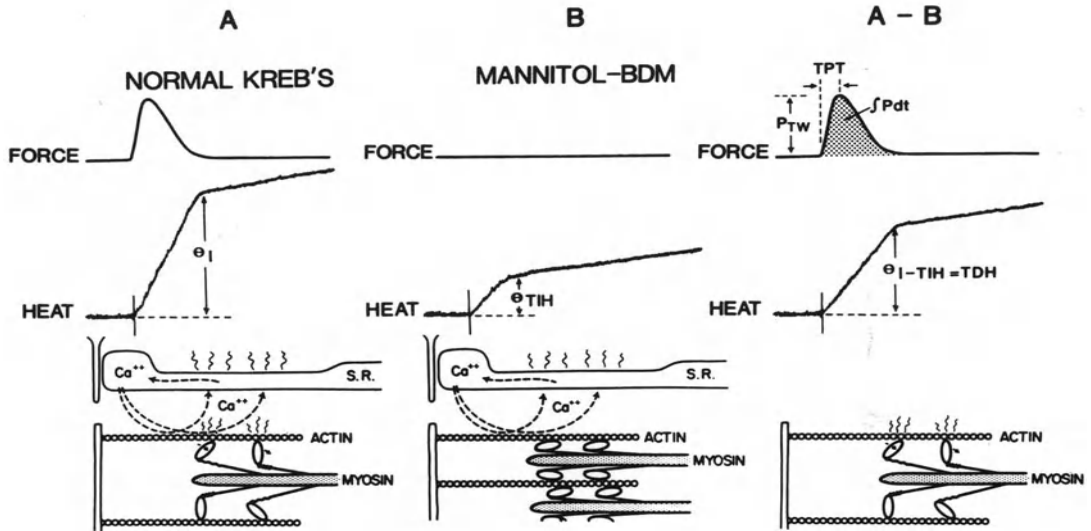


FIGURE 6-1. Isometric force, initial heat, and the partitioning of initial heat. Panel A is a record of heat and force from a papillary muscle incubated in normal Krebs solution. Records of the isometric force, the heat output, and a diagram illustrating the sources of the heat are presented from top to bottom. Panel B is a record of force (*above*) and heat (*middle*) from a papillary muscle incubated in hyperosmotic mannitol Krebs solution or hyperosmotic mannitol diacetyl monoxime (BDM) Krebs solution. Note that force is eliminated and triggerable heat remains. The diagram in Panel B (*bottom*) illustrates that the cross-bridge cycling has been eliminated and that the heat is liberated by the calcium pump activity. The heat associated with cross-bridge cycling (TDH) is obtained by subtracting the initial heat obtained in the mannitol BDM solution ( $\theta_{TIH}$ , Panel B) from that obtained in the normal Krebs solution ( $\theta_I$ , Panel A) (right panel, A-B). S.R. = sarcoplasmic reticulum; TPT = time to peak tension;  $P_{TW}$  = isometric peak twitch force;  $\int Pdt$  = tension-time integral.

dent heat ( $\theta_{TIH}$ , panel B, Figure 6-1). The tension dependent heat can be calculated by subtracting the tension independent heat from the initial heat ( $\theta_I - \theta_{TIH} = \theta_{TDH}$ , panel A - B, Figure 6-1).

#### THE ECONOMY OF CONTRACTION AND RELAXATION

The goal of this chapter is to compare the energetic requirements of the contraction and relaxation phases of the isometric twitch. This is possible because of the rapid time resolution of the heat-sensing elements of the vacuum-deposited bismuth-antimony thermopile system [30]. The protocol for dividing the tension-dependent heat output into the contraction and relaxation components is illustrated in Figure 6-2. The initial heat is recorded and is divided

into its contraction ( $I_C$ ) and relaxation ( $I_R$ ) phases (Figure 6-2). The papillary muscle is then incubated in the hyperosmotic mannitol Krebs solution (see Figure 6-1, Panel B). The triggerable tension-independent heat output is then partitioned into its contraction ( $TIH_C$ ) and relaxation ( $TIH_R$ ) phases (see Figure 6-2). The tension-dependent heat for contraction ( $TDH_C$ ) is obtained by subtracting the tension-independent heat for contraction ( $TIH_C$ ) from the initial heat for contraction ( $I_C$ ) (Figure 6-2). The tension-dependent heat for relaxation ( $TDH_R$ ) is obtained by subtracting the tension-independent heat for relaxation ( $TIH_R$ ) from the initial heat for relaxation ( $I_R$ ) (see Figure 6-2). The economy for isometric contraction is obtained by dividing the tension-time integral for contraction ( $\int Pdt_C$ ) by the tension-dependent heat for contraction ( $TDH_C$ ), while the economy of

relaxation ( $\int Pdt_R/TDH_R$ ) is obtained in a similar manner (see Figure 6-2).

### Results and Discussion

The objective of these studies was to examine the energetics of contraction and relaxation in homogeneous (pressure overloaded) and heterogeneous (control and thyrotoxic) heart papillary muscles. The data from each of the preparations will be presented in that order.

#### RIGHT VENTRICULAR HEART WEIGHT AND INTRAVENTRICULAR PRESSURES

The right ventricular heart weights for the pressure overloaded, control, and thyrotoxic preparations were  $1.70 \pm 0.13$ ,  $1.17 \pm 0.05$  and  $1.31 \pm 0.05$  grams, respectively. The pressure-overloaded and thyrotoxic hearts exhibited enlargement of the right ventricle of 45% and 12% relative to the control hearts. The systolic and diastolic pressures for the pressure overloaded and thyrotoxic hearts were greater than those for the control group (Table 6-1). No signs of congestion were present in any of the groups.

TABLE 6-1. Right Ventricular Systolic and Diastolic Pressure (RVP) in Pressure-Overloaded (P), Control (C), and Thyrotoxic (T) Rabbit Hearts

Model	RVP (mm Hg)	
	Systolic	Diastolic
P	$31.9 \pm 3.4$	$2.2 \pm 0.2$
C	$16.5 \pm 1.2$	$1.2 \pm 0.1$
T	$46.4 \pm 4.7$	$4.1 \pm 1.1$

TABLE 6-2. Isomyosin Composition and Calcium-Activated Myosin ATPase Activity for Pressure-Overloaded (P), Control (C), and Thyrotoxic Hearts (T)

Model	% $V_1$ Isomyosin*	Myosin ATPase ( $\mu\text{mol Pi mg}^{-1} \text{min}^{-1}$ )
P	$0 \pm 0$	$0.22 \pm 0.02$
C	$12 \pm 4$	$0.32 \pm 0.01$
T	$90 \pm 2$	$0.86 \pm 0.03$

\* There are three isoenzymes of myosin,  $V_1$ ,  $V_2$ , and  $V_3$ . From of densitometer traces of the polyacrylamide gel pattern, the percents  $V_1$ ,  $V_2$ , and  $V_3$  are ascertained. Half of the  $V_2$  trace is added to  $V_1$  and  $V_3$ . Accordingly, in this analysis the  $\% V_3 = 100 - \% V_1$ .

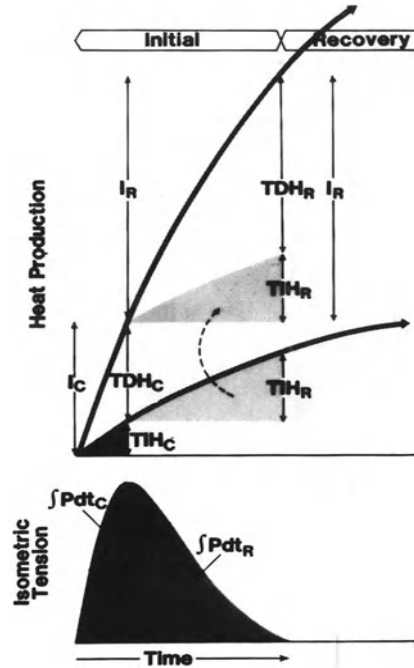


FIGURE 6-2. Tension-dependent heat and tension-time integral for contraction and relaxation. (See text for explanation and definition of the symbols.) Initial and recovery refer to the corresponding portions of heat output.

#### ISOMYOSIN COMPOSITION AND ATPase ACTIVITY

Hearts from the pressure-overloaded animals consisted of 100%  $V_3$  (0%  $V_1$ ) isomyosin and had an ATPase activity of  $0.22 \mu\text{mol Pi mg}^{-1} \text{min}^{-1}$ . The %  $V_1$  was greater in the control and thyrotoxic hearts as was the ATPase activity (Table 6-2). Thus animal preparations were available which were *homogeneous* with respect to the isomyosin profile (pressure overloaded, pure  $V_3$ ) and *heterogeneous* (control, 12%  $V_1$ -88%  $V_3$ ; thyrotoxic, 90%  $V_1$ -10%  $V_3$ ).

#### PAPILLARY MUSCLE MECHANICS

The times to peak tension (TPT) (Figure 6-1, upper right panel) for the pressure overloaded, control, and thyrotoxic animals were  $816 \pm 21$ ,  $627 \pm 20$ , and  $352 \pm 18$  msec, respectively. The peak twitch-tension and tension-time in-

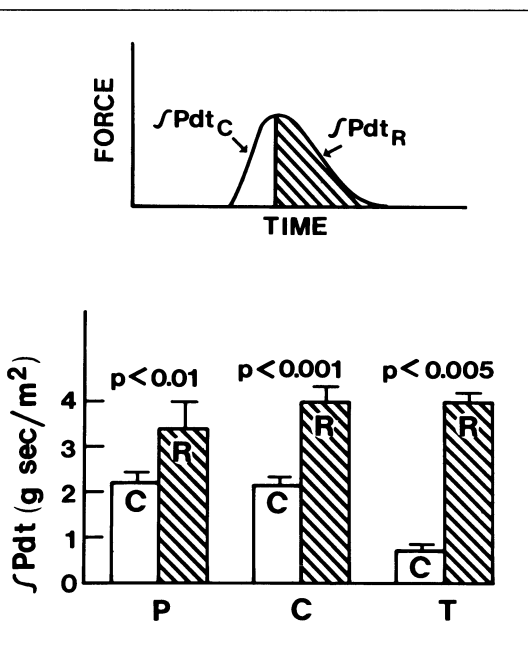


FIGURE 6-3. The relation between the tension-time integral for contraction ( $\int Pdt_C$ ) and relaxation ( $\int Pdt_R$ ) for pressure-overloaded (P), control (C), and thyrotoxic (T) rabbit hearts. The method for dividing the isometric tension-time integral into the contraction and relaxation phases is indicated above. The data for the contraction and relaxation tension-time integrals for each of the preparations are presented below. The standard error of the mean is indicated by the vertical lines. The significance level (paired *t* test) for the difference between the contraction and relaxation tension-time integral is presented above the data.

tegrals for the pressure-overloaded animals were 5.11 gm/mm<sup>2</sup> and 5.64 gsec/mm<sup>2</sup>, respectively. The twitch tension and tension-time integral were slightly but not significantly larger in the control animals and were significantly lower in the thyrotoxic animals (Table 6-3). The tension-time integral can be divided into a contraction and relaxation tension-time integral (Figure 6-2, 6-3). The tension-time integral for relaxation was greater than that for contraction in all three preparations (see Figure 6-3).

#### INITIAL AND TENSION-DEPENDENT HEAT

The initial and tension-dependent heats for the pressure-overloaded group were 1.20 and 1.00 mcal/gm, respectively. These values were

significantly higher in the control and thyrotoxic groups (Table 6-4). The tension-dependent heat can be divided into a contraction (TDH<sub>C</sub>) and relaxation (TDH<sub>R</sub>) phase (Figures 6-2, 6-4). The tension-dependent heat for contraction and relaxation is the same for the pressure-overloaded hearts (see Figure 6-4). For the control and thyrotoxic hearts the tension-dependent heat is greater for the relaxation phase than for the contraction phase (see Figure 6-4).

#### THE ECONOMY OF CONTRACTION AND RELAXATION

The economy of isometric contraction may be defined as the tension-time integral divided by the tension-dependent heat ( $E = \int Pdt/TDH$ ). Accordingly, the economy for the contraction phase of the twitch can be calculated and compared with that for the relaxation phase. The hypothesis guiding these experiments was that the economy of isometric relaxation would be greater than that of isometric contraction. In the homogeneous papillary muscles (pressure-overloaded, 100% V<sub>3</sub>), the economy of relaxation is greater than that of contraction (Figure 6-5). For the two heterogeneous groups, in the control hearts (88% V<sub>3</sub>, 12% V<sub>1</sub>) the economy of relaxation and contraction are identical, whereas in the thyrotoxic hearts (10% V<sub>3</sub>, 90% V<sub>1</sub>) relaxation economy is greater than contraction economy (see Figure 6-5).

TABLE 6-3. Papillary Muscle Isometric Force (P<sub>TW</sub>) and Tension-time Integral ( $\int Pdt$ ) for Pressure-Overloaded (P), Control (C), and Thyrotoxic (T) Rabbit Hearts

Model	P <sub>TW</sub> (gm mm <sup>-2</sup> )*	$\int Pdt$ (gm sec mm <sup>-2</sup> )
P	5.11 ± 0.47	5.64 ± 0.57
C	5.90 ± 0.25	6.12 ± 0.57
T	4.55 ± 0.76	4.83 ± 0.86

\* The isometric peak twitch force (P<sub>TW</sub>) is measured at a stimulus frequency of 0.2 Hz at a length where the active force is maximal.

TABLE 6-4. The Initial Heat (I) and Tension-Dependent Heat (TDH) for Pressure-Overloaded (P), Control (C), and Thyrotoxic (T) Rabbit Hearts

Model	I (mcal gm <sup>-1</sup> )	TDH (mcal gm <sup>-1</sup> )
P	1.20 ± 0.12	1.00 ± 0.12
C	1.66 ± 0.10	1.30 ± 0.11
T	1.70 ± 0.20	1.40 ± 0.17

### ANALYSIS OF THE ECONOMY OF CONTRACTION AND RELAXATION IN TERMS OF THE ACTOMYOSIN CROSS-BRIDGE CYCLE

In muscle, heart as well as skeletal, force is developed when a myosin cross-bridge head, extending from the thick filament, attaches to the actin thin filament, rotates from the 90-degree to the 45-degree configuration, and thus stretches the compliant elements in the neck and tail region of the myosin molecule embedded in the thick filament. Thus, for isometric contraction or relaxation, the force developed is a function of the cycling rate and tension-time integral for each myosin cross-bridge head integrated over the duration of the twitch. An analysis of the isometric force, in terms of the cross-bridge cycle, from the mechanical and thermal data is based on three assumptions: (1) the enthalpy of ATP hydrolysis is the same in each preparation; (2) the number of myosin molecules in a unit half sarcomere is the same in each preparation; and (3) each time a myosin molecule goes through a complete cycle, developing its tension-time integral, one high-energy phosphate bond is hydrolyzed. The tension-time integral for the isolated papillary muscle for contraction and relaxation ( $\int Pdt_C$ ,  $\int Pdt_R$ ) can be defined in terms of the cross-bridge tension-time integral ( $\int sdt$ ) and the cycling frequency ( $f$ ) by equations 6.1a and 6.1b, where the symbols are defined as follows:  $\int Pdt_C$  and  $\int Pdt_R$  are the papillary muscle contraction and relaxation tension time integrals per  $\text{mm}^2$ , respectively;  $\int sdt_C$  and  $\int sdt_R$  are the average cross-bridge tension-time integrals for contraction and relaxation, respectively;  $f_C$  and  $f_R$  are the average cross-bridge cycling frequencies for contraction and relaxation, respectively;  $M$  is the number of myosin heads in a half sarcomere of muscle with a  $1 \text{ mm}^2$  cross-sectional area; and  $TT_C$  and  $TT_R$  are the duration of the contraction time and relaxation times, respectively.

$$\int Pdt_C = \int sdt_C \times f_C \times M \times TT_C \quad (6.1a)$$

$$\int Pdt_R = \int sdt_R \times f_R \times M \times TT_R \quad (6.1b)$$

Thermal and mechanical data are used to calculate  $f$  and  $\int sdt$  in the following manner. The frequency of cross-bridge cycling is defined by equation 6.2, where  $d(\text{TDH})/(\text{dt gm})$  is the average tension-dependent heat rate per gram of

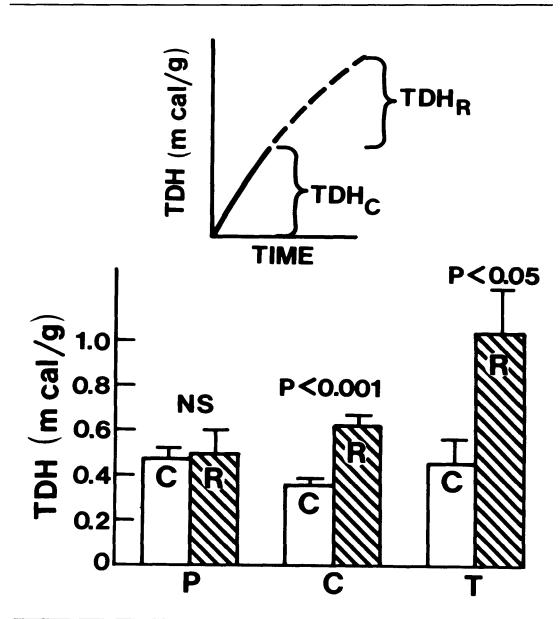


FIGURE 6-4. The tension-dependent heat (TDH) for contraction (C) and relaxation (R) for pressure-overloaded (P), control (C), and thyrotoxic (T) rabbit hearts. Above is the tension-dependent heat for contraction ( $\text{TDH}_C$ ) and relaxation ( $\text{TDH}_R$ ) reconstructed as described in Figure 6-2. The data for each of the preparations are presented below. The significance level for the difference between relaxation and contraction for each of the preparations is presented above the bar graph of the data (paired  $t$  test). The standard error of the mean is indicated by the vertical lines. NS = not significant.

muscle,  $W_{1/2 \text{ sarcomere}}$  is the weight of a half sarcomere with a cross-sectional area of  $1 \text{ mm}^2$ ,  $E^{-1}$  is the reciprocal molar enthalpy of the ATP hydrolysis involved in the cross-bridge cycle and  $M^{-1}$  is the moles of cross-bridge heads in a half sarcomere.

$$f = \frac{d(\text{TDH})(\text{dt gm}) \times W_{1/2 \text{ sarcomere}}}{E^{-1} \times M^{-1}} \quad (6.2)$$

The cross-bridge tension-time integral ( $\int sdt$ ) is defined by equation 6.3 where the tension time integral for the cross-bridge ( $\int sdt$ ) or the muscle  $\int Pdt$  represents that for the contraction or relaxation phases, the frequency ( $f$ ) is the average frequency for the contraction or relaxation phases and  $TT$  is the duration of the contraction or relaxation phases.

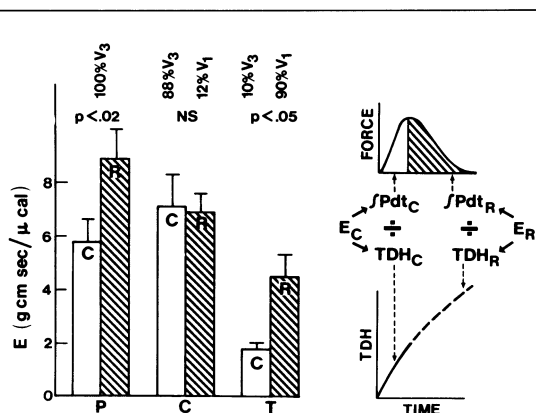


FIGURE 6-5. The economy of relaxation and contraction for pressure-overloaded (P), control (C), and thyrotoxic (T) rabbit hearts. The right panel depicts the method for calculating the economy of contraction and relaxation. The economy of contraction,  $E_C$ , is obtained by dividing the contraction tension-time integral ( $\int Pdt_C$ ) by the tension-dependent heat liberated during the contraction phase of the isometric twitch ( $TDH_C$ ). A similar calculation can be made for the relaxation phase ( $\int Pdt_R/TDH_R$ ). The open and cross-hatched bar graphs represent the contraction (C) and relaxation (R) phases, respectively.

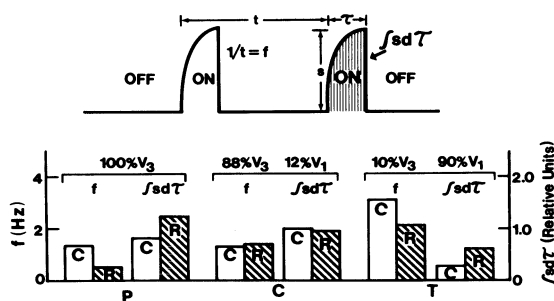


FIGURE 6-6. Cross-bridge cycling frequency ( $f$ ) and tension-time integral ( $\int s dt$ ) for contraction (C, open bar graph) and relaxation (R, cross-hatched bar graph). The upper panel diagrams the time course of force development for a single cross-bridge. Note there is an "off" period where the cross-bridge head is not attached to the actin, and a period of attachment and cross-bridge head rotation where force is developed "on" each cycle. The force is analyzed in terms of the frequency of cycling,  $1/t$ , where  $t$  is the time between cycles and the cross-bridge tension-time integral, where  $s$  is the force, and  $t$  is the "on" time. The myosin isoenzyme composition is indicated above the bar graphs for each group.

$$\int s dt = \int P dt / (f \times TT) \quad (6.3)$$

In the pressure-overloaded group of muscles, where relaxation is more economical than contraction, the average cross-bridge cycling frequency for relaxation is less than that for contraction, whereas the average cross-bridge tension-time integral is greater (Figure 6-6). In the control muscles, where the economy of isometric contraction and relaxation is identical, the frequency of cross-bridge cycling and the cross-bridge tension-time integral is also identical (Figure 6-6). In the thyrotoxic preparations, where relaxation economy is also greater than contraction economy, the average cross-bridge cycling frequency for relaxation is less than that for contraction, whereas the tension-time integral is greater (see Figure 6-6).

#### THE CONTRIBUTION OF HEART MUSCLE HETEROGENEITY TO THE ECONOMY OF CONTRACTION AND RELAXATION

The hypothesis that the economy of relaxation is greater than that of contraction is supported in the pressure overloaded homogeneous preparation and in the heterogeneous thyrotoxic hearts but is rejected for the heterogeneous control animals. In the pressure overloaded, pure V<sub>3</sub> hearts, the increase in relaxation economy can be interpreted at the cross-bridge level in terms of a decrease in the cycling frequency and an increase in the tension-time integral. These changes may be attributed to the effect of lengthening of the sarcomeres during the relaxation [2] on the kinetic properties of the actomyosin. In the same manner, similar changes in the kinetics during relaxation might account for the differences observed in cross-bridge frequency and tension-time integral in the thyrotoxic hearts. However, it is not clear why in control hearts the economies of relaxation and contraction are identical. This finding is especially puzzling considering that the myosin isoenzyme mixture for the control group (88% V<sub>3</sub>, 12% V<sub>1</sub>) is not substantially more heterogeneous than in the thyrotoxic hearts (90% V<sub>1</sub>, 10% V<sub>3</sub>).

To explain the paradoxical behavior of the control animals, we would like to offer a speculative hypothesis: the increased economy during lengthening may be related to the "give" phenomenon described by Flitney, Hirst, and Jones [33] or to the fact that thyrotoxic, i.e., V<sub>1</sub> containing, myocytes relax more rapidly (note the decrease in time to peak tension).

Flitney and colleagues changed the cross-bridge cycling rate in contracting skeletal muscle by altering the temperature at which the experiments were carried out. The activated muscle was subjected to steady stretches. The force,  $P_s$ , during the stretch was above isometric force,  $P_0$ , and increased as a function of the velocity of stretch. The force during stretch,  $P_s$ , rose to a critical point ( $V_c$ ) and then ceased to rise. A similar phenomenon has been observed in rabbit papillary muscle [34]. In this mode of force development, high forces are maintained with little or no cross-bridge cycling [6]. For the slowly cycling cross-bridges (low temperature), the critical velocity was lower and  $P_s/P_0$  was higher than for the faster cycling cross-bridges (higher temperature). In our model,  $V_3$  represents the slower cycling cross-bridges and  $V_1$  the faster cycling cross-bridges. During the rise of isometric tension in a pure preparation (pressure-overloaded) the sarcomeres shorten, and as expected the cross-bridge cycling rate increases while the tension-time integral decreases (Figure 6-7). From the peak of tension to complete relaxation, the elastic energy stored in the compliant elements lengthen the sarcomeres (Figure 6-7). The stretch produces the expected result of reducing the cycling rate and increasing the tension-time integral for the cross-bridges [4-6].

During the rise in tension of muscles consisting of a mixture of slow (strong) and fast (weak) sarcomeres, both the fast and the slow sarcomeres shorten against the series compliant elements (Figure 6-8). During the relaxation phase, the energy stored in the series' compliant elements extend the sarcomeres. The fast sarcomeres are extended preferentially over the slow sarcomeres because they have a lower  $P_s/P_0$  at the critical velocity or they are deactivated sooner. For the control muscles (see Figure 6-8), which have 88%  $V_3$  myosin (vertical stripes of the sarcomeres) and 12%  $V_1$  myosin (dotted sarcomeres), during relaxation only 12% of the sarcomeres would undergo the economical "give" phenomenon. The increase in economy for this small fraction of  $V_1$  sarcomeres would be outweighed by the unchanged economy of the 88% of the sarcomeres that continue to shorten during the relaxation period (see Figure 6-8). In the thyrotoxic hearts, where the isomyosin composition is reversed (90%  $V_1$ , 10%  $V_3$ ), the small fraction of sarcomeres (the slow  $V_3$ ) continues to shorten during relaxation, whereas

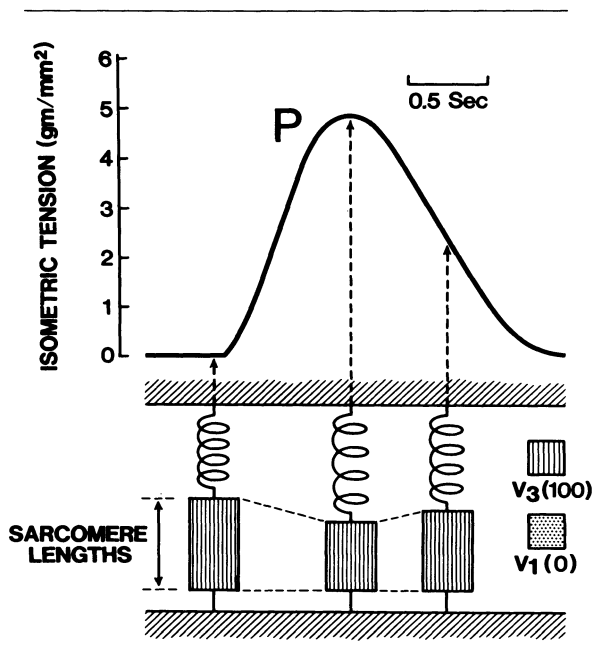


FIGURE 6-7. Papillary muscle isometric tension and a diagram of the sarcomere lengths in pressure-overloaded ( $P$ ) hearts. Above is the time course of the isometric tension. Below is a diagram of the changes in sarcomere lengths during contraction and relaxation. The isoenzyme percent composition (100%  $V_3$ ) is indicated by the vertical stripes.

the large  $V_1$  population undergoes the more economical give or stretch phenomenon (see Figure 6-8). Thus in this heterogeneous group the economy of relaxation is greater than that of contraction.

### Summary

The economy of relaxation is greater than that of contraction for the pressure-overloaded and thyrotoxic rabbit hearts. The economy of relaxation is equal to that of contraction in the control hearts. In the homogeneous preparations (pressure overloaded, 100%  $V_3$ ) where the economy of relaxation is greater than that of contraction, it is believed that the internal lengthening, which occurs during the relaxation phase of the isometric contraction, alters the actomyosin kinetics so as to reduce the cross-bridge cycling frequency and increase the cross-bridge tension-time integral. In the heterogeneous groups the

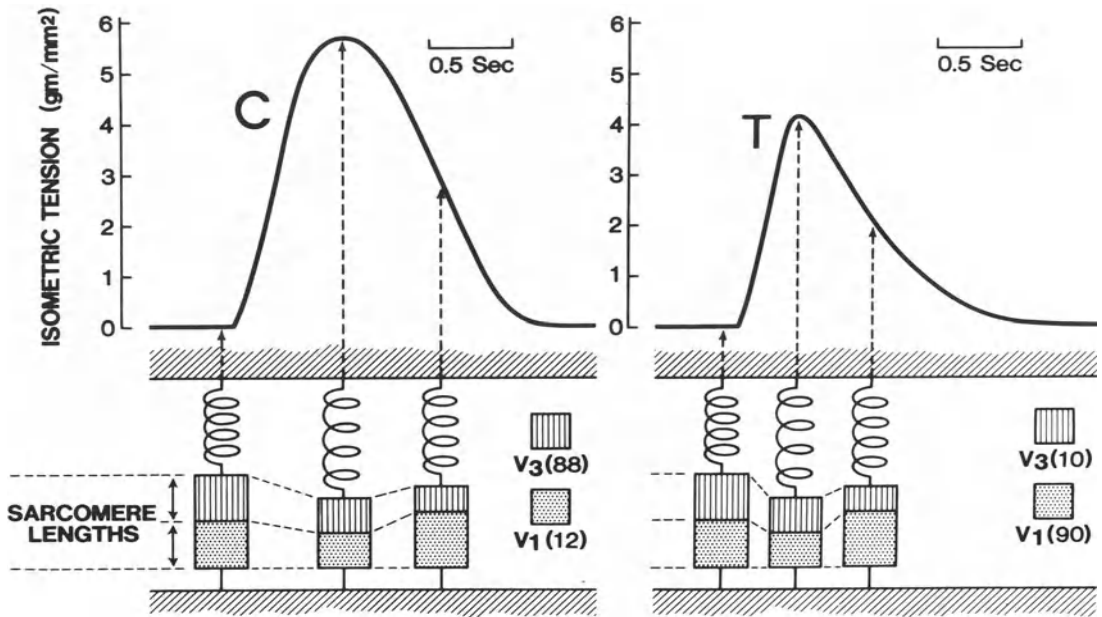


FIGURE 6-8. Papillary muscle isometric tension change and sarcomere length pattern for control (C) and thyrotoxic (T) hearts. Above is the time course of the isometric twitch. Below is the sarcomere length pattern during contraction and relaxation. The bars with the vertical stripes represent the %  $V_3$  and the  $V_3$  sarcomeres, the bars with the dots represent the %  $V_1$  and the  $V_1$  sarcomeres.

difference between the normal and thyrotoxic preparations is explained in terms of the interaction of faster cycling, weaker sarcomeres ( $V_1$ ) in series with slower-cycling, stronger sarcomeres ( $V_3$ ). The normal hearts consist of 88%  $V_3$  isomyosin. During relaxation, this portion of the heart continues to shorten, while the  $V_1$  portion is lengthened. The majority of the sarcomeres in these hearts are in the less economical shortening mode during relaxation, and thus relaxation and contraction exhibit identical economies. In contrast, in the thyrotoxic heart, the majority of the sarcomeres are made up of the weaker  $V_1$  type isoenzyme. In this preparation during relaxation, the minor portion of the muscle continues to shorten while the major portion is lengthened and thus put in the more economical mode of operation. In all of the preparations, cross-bridges continue to

cycle during relaxation, and there is a significant energy cost of relaxation. Heterogeneity (weak vs. strong, fast vs. slow) affects the economy of relaxation.

### References

1. Alpert NR, Mulieri LA, Litten RZ (1983). Isoenzyme contribution to economy of contraction and relaxation in normal and hypertrophied hearts. In Jacob R, Gulch RW, Kissling G (eds): *Cardiac Adaptation to Hemodynamic Overload and Stress*. Dr. D. Steinkopff Verlag, Darmstadt pp 147-157.
2. Kreuger JW, Pollack GH (1975). Myocardial sarcomere dynamics during isometric contraction. *J Physiol* 251:627-643.
3. Abbott BC, Aubert XM, Hill AV (1951). The absorption of work by muscle stretched during a single twitch or a short tetanus. *Proc Roy Soc B*, 139:86-104.
4. Abbott BC, Aubert XM (1951). Changes in energy in a muscle during very slow stretches. *Proc Soc Biol* 139:104-117.
5. Abbott BC, Bigland B, Ritchie JM (1952). The physiological cost of negative work. *J Physiol* 117:380-390.
6. Curtin N, Davies RE (1975). Very high tension with very little ATP breakdown by active

- skeletal muscle. *J Mechanochem Cell Mot* 3:147-154.
7. Burton AC (1957). The importance of the shape and size of the heart. *Am Heart J* 54:801-810.
  8. Burns JW, Covell JW, Myers R, Ross J (1971). Comparison of directly measured left ventricular wall stress and stress calculated from geometric reference figures. *Circ Res* 28:611-621.
  9. Streeter DD Jr, Hanna WT (1973). Engineering mechanics for successive states in canine left ventricular myocardium. *Circ Res* 33:639-655.
  10. Rankin JS, McHale PA, Arentzen CE, et al (1976). The three dimensional dynamic geometry of the left ventricle in the conscious dog. *Circ Res* 39:304-313.
  11. Hoh JFY, McGrath PA, Hale PT (1977). Electrophoretic analysis of multiple forms of rat cardiac myosin: Effects of hypophysectomy and thyroxine replacement. *J Mol Cell Cardiol* 10:1053-1076.
  12. Lompre AM, Mercadier JJ, Wisnewsky C, et al (1981). Species- and age-dependent changes in the relative amounts of cardiac myosin isozymes in mammals. *Dev Biol* 84:286-290.
  13. Mercadier JJ, Lompre AM, Wisnewsky C, et al (1981). Myosin isoenzymic changes in several models of rat cardiac hypertrophy. *Circ Res* 49:525-532.
  14. Sartore S, Gorza L, Pierobon S, et al (1981). Myosin types and fiber types in cardiac muscle/ventricular myocardium. *J Cell Biol* 88:226-233.
  15. Schiaffino S, Gorza L, Sartore S (1983). Distribution of myosin types in normal and hypertrophic hearts: An immunocytochemical approach. In Alpert NR (ed): *Myocardial Hypertrophy and Failure*. New York Raven Press, pp 149-166.
  16. Litten RZ, Martin BJ, Buchtal RH, et al (1985). Heterogeneity of myosin isozyme content of rabbit heart. *Circ Res* 57:406-414.
  17. Heyndrick GR, Millard RW, McRitchie RJ, et al (1975). Regional myocardial functional and electrophysiological alterations after brief coronary artery occlusion in conscious dogs. *J Clin Invest* 56:978-985.
  18. Herman MV, Heinle RA, Klein MD, Gorlin R (1967). Localized disorders in myocardial contraction. *N Engl J Med* 277:222-232.
  19. Heikkila J, Tabakin BS, Hugenholtz PG (1972). Quantification of function in normal and infarcted regions of the left ventricle. *Cardiovasc Res* 6:516-531.
  20. Turek Z, Granthner M, Kubat K, et al (1973). Arterial blood gases, muscle fiber diameter and intercapillary distance in cardiac hypertrophy of rats with an old myocardial infarction. *Pfluegers Arch* 376:209-215.
  21. Rubin SA, Fishbein MC, Swan HJC, Rabines A (1983). Compensatory hypertrophy in the heart after myocardial infarction in the rat. *J Am Coll Cardiol* 1:1435-1441.
  22. Anversa P, Loud AV, Levicky V, Guideri G (1985). Left ventricular failure induced by myocardial infarction. I. Myocyte hypertrophy. *Am J Physiol* 248:H876-H882.
  23. Alpert NR, Mulieri LA, Litten RZ (1979). Functional significance of altered myosin adenosine triphosphatase activity in enlarged hearts. *Am J Cardiol* 44:947-953.
  24. Litten RZ, Martin BJ, Low RB, Alpert NR (1982). Altered myosin isozyme patterns from pressure-overloaded and thyrotoxic hypertrophied rabbit hearts. *Circ Res* 50:856-864.
  25. Mulieri LA, Luhr G, Trefry J, Alpert NR (1977). Metal-film thermopiles for use with rabbit right ventricular papillary muscles. *Am J Physiol* 233:C146-156.
  26. Alpert NR, Mulieri LA (1981). The utilization of energy by the myocardium hypertrophied secondary to pressure overload. In Strauer BE (ed): *The Heart and Hypertension*. Berlin: Springer Verlag, pp 153-163.
  27. Alpert NR, Mulieri LA (1980). The functional significance of altered tension dependent heat in thyrotoxic myocardial hypertrophy. *Basic Res Cardiol* 75:179-184.
  28. Hamrell BB, Alpert NR (1977). The mechanical characteristics of hypertrophied rabbit cardiac muscle in the absence of congestive heart failure: the contractile and series elastic elements. *Circ Res* 40:20-25.
  29. Alpert NR, Mulieri LA (1982). Increased myothermal economy of isometric force generation in compensated cardiac hypertrophy induced by pulmonary artery constriction in the rabbit: A characterization of heat liberation in normal and hypertrophied right ventricular papillary muscles. *Circ Res* 50:491-500.
  30. Hamrell BB, Panaanen R, Trono J, Alpert NR (1975). A stable, sensitive, low-compliance capacitance force transducer. *J Appl Physiol* 38:190-193.
  31. Flitney GW, Hirst DG, Jones DA (1976). Effects of temperature and velocity of stretch on the maximum tension borne by the sarcomeres in contracting muscle. *J Physiol* 256:127-128P.
  32. Moss RL, Sollins MR, Julian FJ (1976). Calcium activation produces a characteristic response to stretch in both skeletal and cardiac muscle. *Nature* 260:619-621.

---

## 7. FUNCTIONAL SEQUELAE OF DIASTOLIC SARCOPLASMIC RETICULUM $\text{Ca}^{2+}$ RELEASE IN THE MYOCARDIUM

---

Edward G. Lakatta, Maurizio C. Capogrossi, Arthur A. Kort, and Michael D. Stern

Routine cardiac catheterization and angiography in patients with cardiac disease have permitted the measurement of not only systolic function but also of ventricular filling pressure and volume. The advent of ultrasound and radio-nuclide techniques has rendered the assessment of diastolic function, i.e. filling rates and volumes, and systolic function still more common. While these technological developments have verified the notion of variable diastolic compliance and the coexistence of "abnormal diastolic" function with normal or abnormal systolic "function," the nature of the former and its relation to the latter still remain obscure.

Coincident with advances in technology to measure ventricular function was the development of new concepts regarding mechanisms of excitation-contraction coupling in cardiac muscle, specifically those mechanisms that govern the  $\text{Ca}^{2+}$  homeostasis of myocardial cells. Although earlier studies of this sort had focused on the role of how enhanced cell  $\text{Ca}^{2+}$  loading, e.g., that mediated by "inotropic interventions," can lead to a stronger contraction during systole, more recent studies have been concerned with the role of  $\text{Ca}^{2+}$  in the modulation of diastolic function and its relationship to systolic function [1]. In particular, the phenomenon of spontaneous diastolic  $\text{Ca}^{2+}$  release from the sarcoplasmic reticulum (SR) into the myoplasm

has been shown to (a) cause decreased diastolic compliance [2-6], (b) initiate spontaneous action potentials that lead to arrhythmias [7-10], and (c) reduce the force of contraction during subsequent systoles [3, 11-15, 35]. Some aspects of these functional sequelae of spontaneous diastolic  $\text{Ca}^{2+}$  release will be reviewed here.

Figure 7-1 shows the response in a representative example of an isolated perfused isovolumic rat heart, stimulated regularly at a low frequency ( $20 \text{ min}^{-1}$ ), to increasing perfusate [ $\text{Ca}^{2+}$ ],  $\text{Ca}_0$ , and thus to increasing myocardial cell  $\text{Ca}^{2+}$  loading. Over the lower range of increasing  $\text{Ca}_0$ , i.e., up to about 2 mM, systolic pressure increases markedly and is accompanied by a modest increase in diastolic pressure; with further increases in  $\text{Ca}^{2+}$  loading (a to b in Figure 7-1A), systolic function increases only slightly and plateaus while diastolic pressure continues to increase. At  $\text{Ca}_0$  of 2 to 5 mM, diastolic compliance might be considered to be "abnormal," whereas systolic function appears to be unimpaired. Still further increases in  $\text{Ca}^{2+}$  loading (in Figure 1A) cause diastolic pressure to increase further and systolic pressure to be reduced from its optimal level. The myocardial energy consumption in this instance, however, is greater than at lower  $\text{Ca}_0$  [17, 18]. A biopsy of the heart at this stage would prove normal, and the reduced systolic and enhanced diastolic pressures observed at high cell  $\text{Ca}^{2+}$  loading are completely reversible upon reducing the  $\text{Ca}_0$ .

The lower part of Figure 7-1A depicts actual tracings at points a, b, and c in the upper panel.

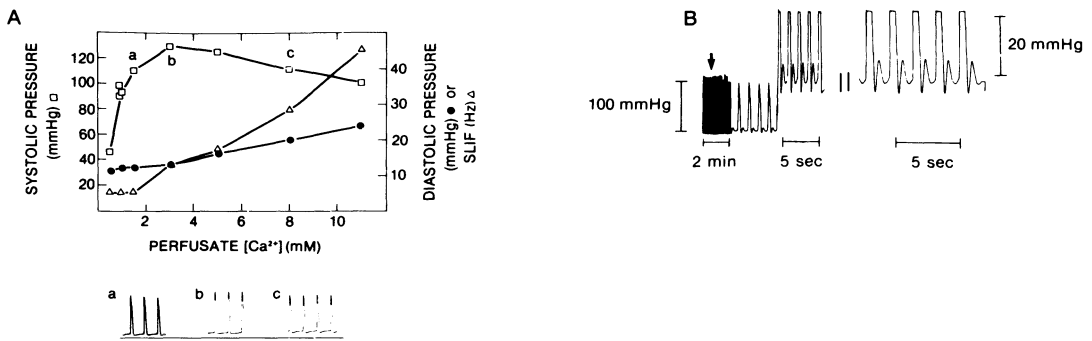


FIGURE 7-1. Response of isolated rat heart to increasing  $\text{Ca}^{2+}$  loading. A. The  $\text{Ca}^{2+}$  dependence of systolic and diastolic pressures and scattered light-intensity fluctuations (SLIF), a manifestation of spontaneous diastolic intracellular  $\text{Ca}^{2+}$  oscillations. The preparation was perfused retrograde from the aorta and rendered quiescent by an atrioventricular block and the addition of  $1 \mu\text{g/ml}$  propranolol to the perfusate. The left atrium was removed and a balloon was inserted into the left ventricle to maintain constant end-diastolic volume. Stimulation at  $20 \text{ min}^{-1}$  at  $37^\circ\text{C}$  produced isometric systoles. Actual records a, b, and c, are shown below. (See text for further details.) B. When the heart in panel A was perfused with a  $[\text{Ca}^{2+}]$  of  $15 \text{ mM}$ , the heart began to beat spontaneously (*arrow*), and the oscillation in diastolic pressure became more pronounced. (From Weiss and Lakatta [16].)

Note that even in the isovolumic mode (effected via a left ventricular balloon at constant volume) in the absence of atrial contraction, an increase in diastolic pressure occurs: it is lowest in early diastole and then drifts upward (a); with further  $\text{Ca}^{2+}$  loading (b and c), the rate and extent of rise is more marked. Figure 7-1B shows that a higher  $\text{Ca}_0$  than that depicted in panel A, causes spontaneous ventricular tachycardia to occur; the transient increase in diastolic pressure with time following the prior systole now passes through a maximum, decreases, and then begins to rise again, i.e., an “after-contraction” occurs, which gives rise to the next spontaneous systole. The variable diastolic compliance shown in this Figure is clearly  $\text{Ca}^{2+}$ -dependent.

The third parameter in Figure 7-1A is a measure of scattered light intensity fluctuations (SLIF) produced in a laser beam reflected from the heart [4, 5]. SLIF increase monotonically with increases in  $\text{Ca}_0$ . SLIF are caused by oscillatory diastolic  $\text{Ca}^{2+}$ -myofilament interactions resulting from spontaneous oscillations in intracellular  $[\text{Ca}^{2+}]$  or “CaOs” [4, 5, 19, 20]. To address the potential functional implications of diastolic CaOs, it is first necessary to consider some of their specific properties, which have been determined from studies in isolated cardiac muscle and myocytes.

### Characteristics of CaOs in Single Cardiac Cells

CaOs are caused by spontaneous oscillatory  $\text{Ca}^{2+}$  release from the SR [21–23]. Although SR  $\text{Ca}^{2+}$  release triggered by an action potential to cause systole is relatively synchronous within and among myocytes comprising cardiac tissue, spontaneous diastolic  $\text{Ca}^{2+}$  release, at a given instant, can be localized *within* cells (Figure 7-2B) and occurs heterogeneously *among* cells [5, 6, 19, 20]. This phenomenon can occur in all mammalian cardiac muscles, but the conditions required for its occurrence are species-dependent [20, 22, 24]. In rat preparations it occurs in the unstimulated state or during low rates of stimulation even when these preparations are bathed in physiologic  $\text{Ca}_0$ , i.e., under conditions in which the resting myoplasmic  $\text{Ca}^{2+}$  is as low as  $100 \text{ nM}$  [22, 25, 26]. Experimental maneuvers to increase the cell  $\text{Ca}^{2+}$  load are required for cardiac tissues from other mammalian species to exhibit CaOs [20, 22, 24]. The localized  $\text{Ca}^{2+}$ -myofilament interaction that results from spontaneous SR  $\text{Ca}^{2+}$  release causes localized sarcomere shortening that can be similar in magnitude to that during systole, but much of this myofilament displacement is not associated with shortening of the

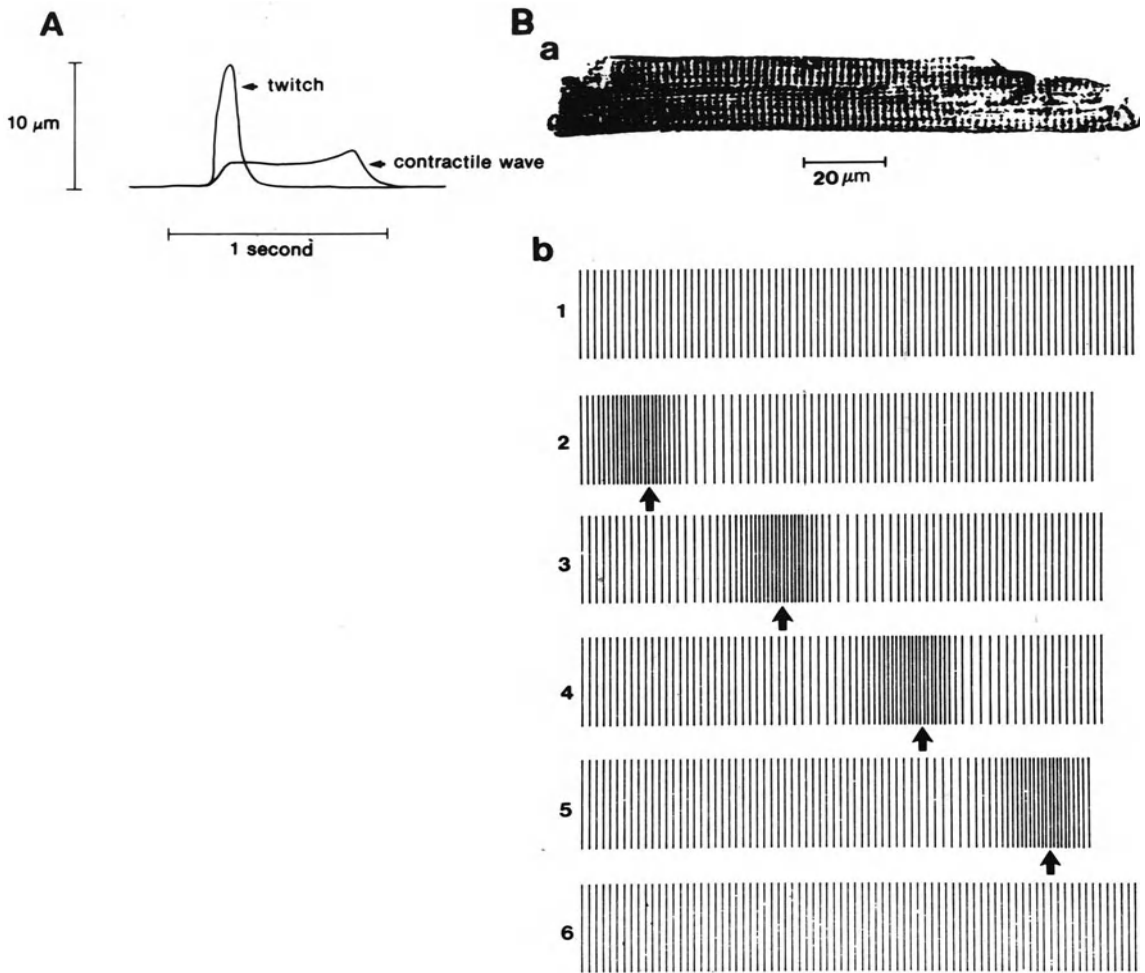


FIGURE 7-2. A. The displacement of a myocyte in response to an action-potential-mediated twitch coupled to that which occurs during spontaneous localized sarcoplasmic reticulum  $Ca^{2+}$  release. (From Capogrossi and Lakatta [14].) B. Part a: photomicrograph of a typical single rat cardiac myocyte used in studies described throughout the text. Part b: computer sequence of images showing the propagation of a contractile wave reconstructed from the magnified video image of a single myocyte. The cell is idealized as a row of sarcomeres. In tracing 1, where no contractile wave is present, sarcomere spacing is uniform. In tracings 2 to 6, a wave appears at the left end of the cell, propagates across the cell, and disappears at the right end. Note that the wave itself appears as a dark region of sarcomere shortening surrounded on both sides by light areas resulting from the stretching of the adjacent relaxed sarcomeres. When the wave is present, the ends of the myocyte shorten and correspond to the actual video analyzer output of Figure 7-2A. (From Kort et al. [19].)

myocyte (Figure 7-2A) or force production but rather is dissipated in stretching other areas within the cell in which myofilaments are relaxed because spontaneous  $\text{Ca}^{2+}$  release has not occurred in that locus at that instant. Thus, even though the localized increase in myoplasmic  $[\text{Ca}^{2+}]_i$ ,  $\text{Ca}_i$ , due to spontaneous  $\text{Ca}^{2+}$  release has been estimated to be at systolic levels [6, 23, 27-30] the resultant displacement at the ends of the cardiac myocyte is far less but of larger duration than that elicited by an action potential during systole (Figure 7-2A)

Figure 7-2B shows that the localized band of myofilament inactivity due to spontaneous  $\text{Ca}^{2+}$  release is not constant in its location but propagates through the cell at a fairly slow speed, i.e., about 100  $\mu\text{m}/\text{second}$  [19]. This indicates that when localized spontaneous  $\text{Ca}^{2+}$  release occurs within a myocyte it propagates as a wave by diffusion and initiates a further (regenerative) release of  $\text{Ca}^{2+}$  at the wave front [31]. The *heterogeneity* of spontaneous  $\text{Ca}^{2+}$  release (within and among cells in intact tissue, see below) is an important characteristic of CaOs with respect to their functional sequelae.

Spontaneous diastolic SR  $\text{Ca}^{2+}$  release recurs in an oscillatory fashion. Although its occurrence is asynchronous among cells, its recurrence within a given cardiac cell is not a random process, but is roughly *periodic* [1, 19, 21-23]. The oscillation frequencies that have been measured vary from  $< 0.1$  to 7-8 Hz [1]. A major determinant of the oscillation frequency is the rate at which SR can cycle  $\text{Ca}^{2+}$ , a major determinant of which is the quantity of  $\text{Ca}^{2+}$  available for pumping. This has been referred to as the cell " $\text{Ca}^{2+}$  load" [13, 19]. In single cardiac myocytes the frequency of CaOs can be measured directly by monitoring the occurrence of spontaneous contractile waves (Figure 7-3A). In intact cardiac muscle, direct monitoring of the frequency of CaOs is not always possible, but other techniques, i.e., SLIF measurements as in Figures 7-1, 7-3B and 7-4, can detect their presence. As the cell  $\text{Ca}^{2+}$  load increases, the increase in SLIF in intact tissue is proportional to the increase in contractile wave frequency in single cardiac myocytes (Figure 7-3B). Although this indirect method to sense CaOs in intact muscle is noninvasive, and its units are reported in Hz, it does not measure the actual frequency of the microscopic mechanical motion due to the underlying  $\text{Ca}^{2+}$  oscillations, but rather the product of the frequency and

amplitude of the underlying motion. Nonetheless, this technique is noninvasive and presently is the most sensitive method of detecting "low-frequency" CaOs in intact cardiac tissue.

### *CaOs Produce Diastolic Tonus*

Studies in intact isolated cardiac muscle have shown that the process of spontaneous  $\text{Ca}^{2+}$  release illustrated in Figure 7-2A for a single myocyte does not occur synchronously among cells [6, 19, 20]. The resultant heterogeneity of sarcomere lengths results in a blurring or disappearance of the sarcomere diffraction pattern as cell  $\text{Ca}^{2+}$  loading, resting force, and SLIF increase (Figure 7-4A). Thus, in multicellular cardiac preparations, the efficacy of the localized diastolic myofilament shortening to produce force is further dissipated because cells in which spontaneous  $\text{Ca}^{2+}$  release occurs are linked to completely relaxed cells in which no CaOs are occurring at that instant.

The actual frequency of CaOs in the intact muscle can be determined by a "noise" analysis of the fluctuations in optical density caused by the myofilament motion due to the underlying microscopic motion [19]. Examples of these fluctuations of optical density and of the simultaneously measured resting tension are illustrated in Figure 7-4B. A similar noise analysis coupled with the use of  $\text{Ca}^{2+}$ -sensitive indicators [27, 33] permits quantification of the spontaneous oscillations in myoplasmic  $\text{Ca}^{2+}$  [28, 32]. Figure 7-4C illustrates that the frequency of oscillations in luminescence of the chemiluminescent protein aequorin, which had been injected into multiple resting cells comprising the bulk preparation, is also the same as that in resting force.

In assessing how CaOs cause diastolic tonus, the concept of temporal summation of discrete oscillators needs to be considered. That the frequency of myofilament oscillation that underlie the increase in resting force are the same as those simultaneously measured in optical fluctuations (Figure 7-4B) or  $\text{Ca}_i$  (Figure 7-4C) indicates that the  $\text{Ca}^{2+}$ -dependent diastolic tonus in cardiac tissue is at least, in part, linked to the presence of CaOs and specifically to their frequency. A relatively simple mathematical model has shown that as the oscillation frequency of multiple independent oscillators (cells, areas within cells, or groups of cells) increases, the resultant summation effect causes an in-

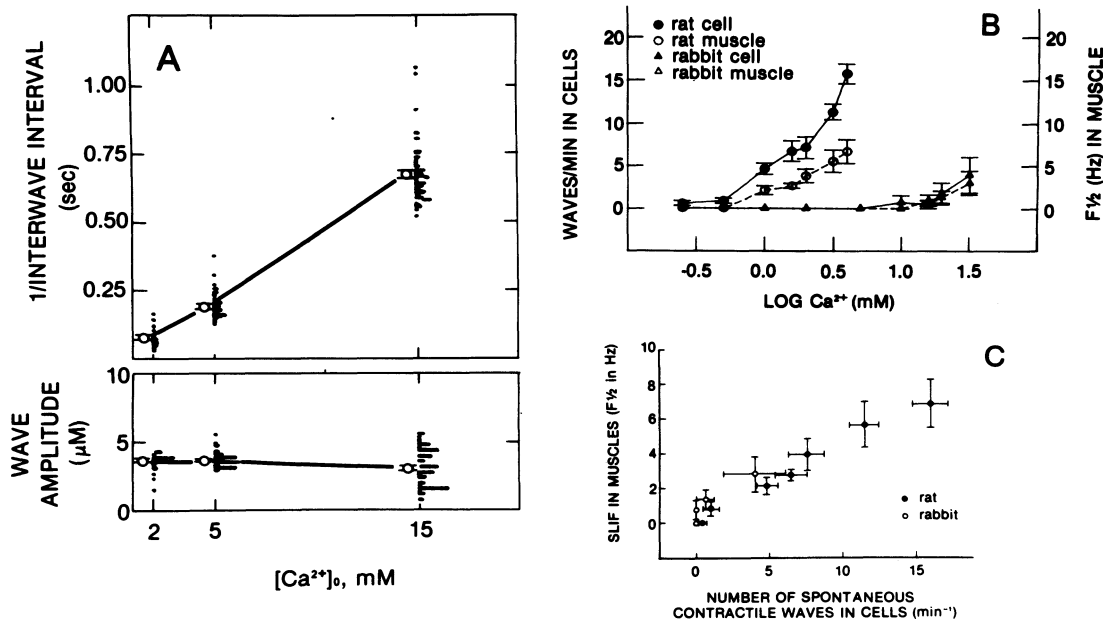


FIGURE 7-3. A. The effect of  $Ca_0$  on spontaneous contractile wave frequency (*top panel*) and amplitude (*lower panel*) as measured in a representative single rat cardiac myocyte (at 23°C). Multiple occurrences of a given value are continuously added to the right of the preceding measurement. The open circles are the mean  $\pm$  standard error of the mean (SEM) of all the values in that  $Ca_0$ . The solid points represent individual waves in a given  $Ca_0$  from Kort et al [19]. B. The increase in contractile wave frequency as the cell  $Ca^{2+}$  load is increased in myocytes is paralleled by an increase in frequency of scattered light-intensity fluctuations (SLIF) in intact muscles. Note the species differences in conditions required for CaOs to occur. C. Spontaneous wave frequency in myocytes and SLIF frequency in muscles measured across the range of  $Ca_0$  in rats and rabbits in panel B. (From Capogrossi et al. [24].)

crease in the instantaneous extent of myofilament interaction in tonus (Figure 7-5). This is a mechanism, at least in part, for the increase in resting force with  $Ca_0$  in Figure 7-4, or the increase in diastolic pressure with increasing  $Ca^{2+}$  loading of the intact heart in Figure 7-1. Thus, the increase in  $Ca^{2+}$ -dependent tonus with increasing cardiac cell  $Ca^{2+}$  loading in Figures 7-1 and 7-4 cannot be solely due to tonic  $Ca^{2+}$  myofilament interaction because as the cell  $Ca^{2+}$  load increases, the presence of a normal functioning SR initiates CaOs that can produce force over and above any tonic  $Ca^{2+}$ -dependent force. Figure 7-1B shows that in the presence of spontaneous  $Ca^{2+}$  release not only is the end-diastolic pressure  $Ca^{2+}$ -dependent, but the recovery of resting pressure following a twitch is oscillatory, i.e., hyperrelaxation followed by a gradual increase or overshoot (after-

contraction) can occur at high-cell  $Ca^{2+}$  loading. This can be explained on the basis of variations in the temporal synchronization within [14] and among [4] individual myocytes that occur with time following action-potential-mediated SR  $Ca^{2+}$  release to cause systole.

In summary, the  $Ca^{2+}$ -dependent diastolic tonus imparted to the myocardium by spontaneous  $Ca^{2+}$  release can be explained on the basis of its salient characteristics: (a) its presence is temporally heterogeneous within and among cells, but subject to variable degree of summation, and (b) its occurrence within a cell is roughly periodic, and the periodicity varies with  $Ca^{2+}$ , i.e., frequency of CaOs increases with increasing cell  $Ca^{2+}$  loading. The frequency of CaOs is a determinant of the extent of summation within and among cells [4, 6] and thus of the magnitude of the resultant  $Ca^{2+}$ -

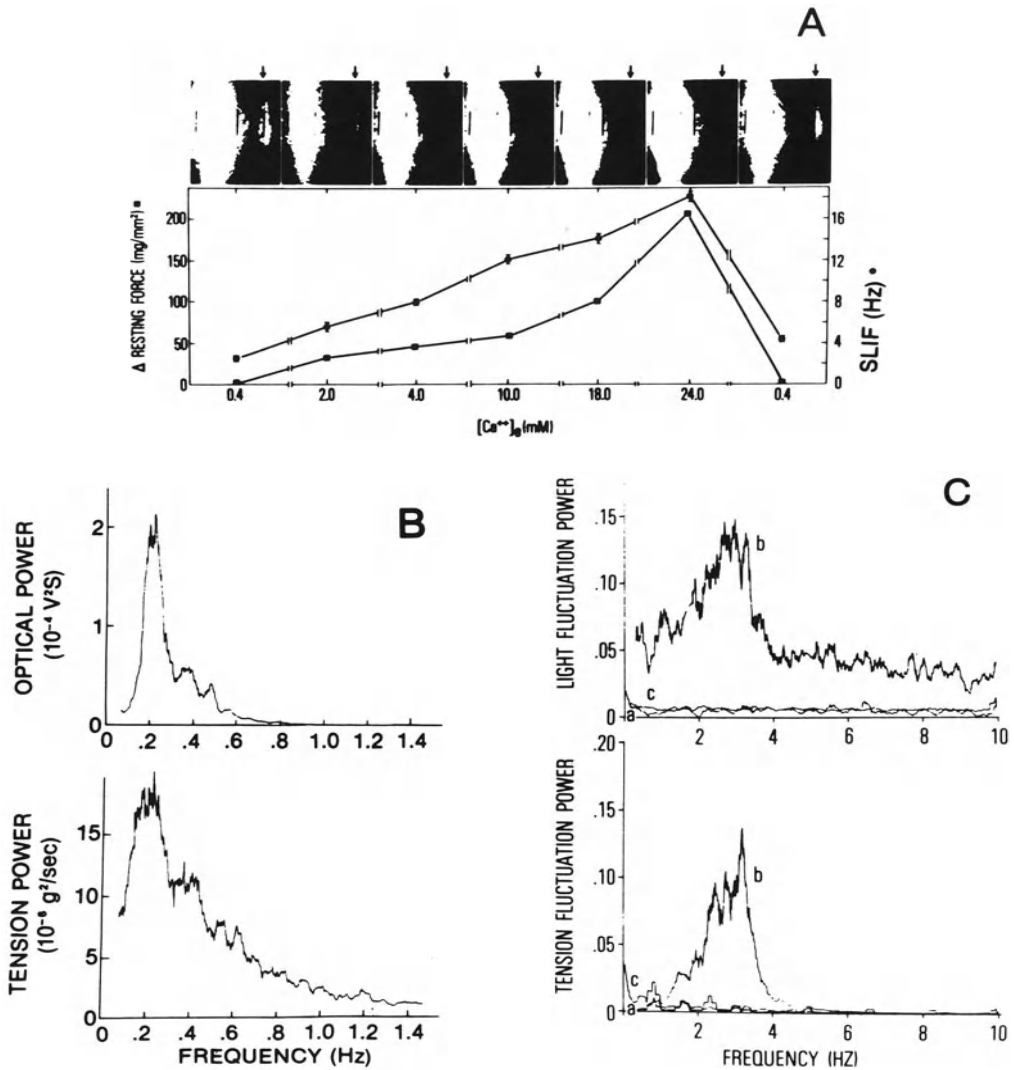


FIGURE 7-4. A. A representative example of the sarcomere diffraction pattern (*top panels*), frequency of scattered light-intensity fluctuations (SLIF) (F), and resting force (RF) (*lower panel*), measured over a wide range of  $Ca_0$  in a rat papillary muscle. Photographs of the diffraction pattern were made in the same area of the muscle at the same camera setting in each  $Ca_0$ . Arrow indicates the first order of diffraction.  $\Delta$ RF is the difference between RF in a given  $Ca_0$  and that in the reference  $Ca_0$  of 0.4 mM. (From Lakatta and Lappe (3).) B. The power spectrum of optical fluctuations caused by contractile wave displacement measured by a photoresistor placed upon the magnified image of the edge of an ultra-thin rat right ventricular papillary muscle unstimulated and bathed in  $Ca_0$  of 3.0 mM at 23°C (*top panel*) and that of the simultaneously measured tension fluctuations (*bottom panel*). The similarity in frequency for both peaks implies that a component of resting tension is generated by the contractile waves. (From Kort et al. [19].) C. Spectral analysis of aequorin luminescence (*top panel*) and tension (*bottom panel*) from a canine Purkinje fiber at rest (trace a) and during exposure to a solution low in  $Na^+$  to induce cell  $Ca^{2+}$  loading and exacerbate CaOs (trace b). Conditions in trace c are the same as in b, but the tissue had been preexposed to 1  $\mu$ M ryanodine, which abolishes the CaOs by disabling normal sarcoplasmic reticular function. (From Wier et al. [27] and Wier et al. [32].)

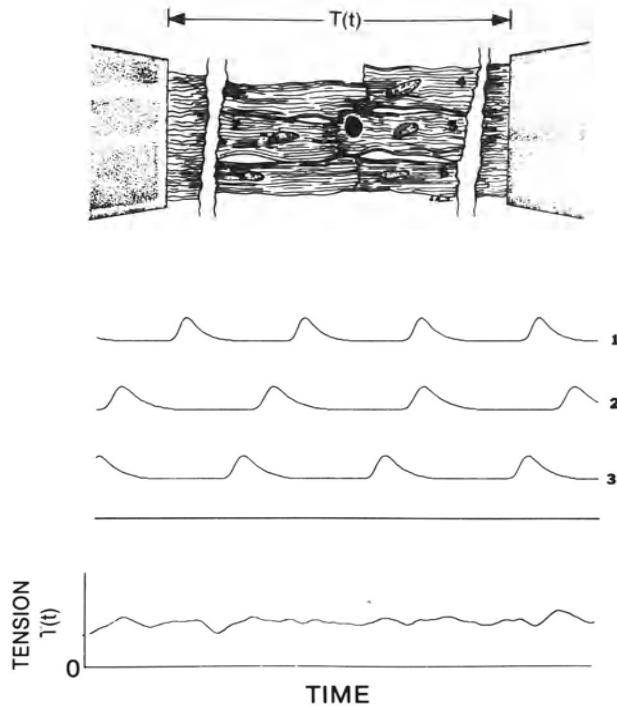


FIGURE 7-5. Model of independent cellular oscillators within intact cardiac tissue. The sum of independent periodic asynchronous CaOs in cells 1 through 3 summates to cause a fluctuating tension  $T(t)$ , measured at the ends of the preparation. The curve shown as  $T(t)$  in the lower part of the panel was computer-simulated by adding up 100 curves similar to curves 1 through 3 but with arbitrary phases and periods normally distributed about an average value. Note that this average tension is nonzero and thus contributes to the diastolic force. (From Stern et al. [4].)

dependent tonus. Changes in the extent of summation during diastole can produce oscillatory diastolic force, i.e., after-contraction.

### *How CaOs Can Interfere with Systolic Function*

Following action-potential-mediated synchronous  $\text{Ca}^{2+}$  release from the SR to cause a systole, restitution of various mechanisms is required for optimal  $\text{Ca}^{2+}$  release in a following systole. Though the precise nature of these mechanisms

remains to be elucidated, time-dependent re-filling of an SR  $\text{Ca}^{2+}$  release pool and removal of  $\text{Ca}^{2+}$  inhibition of the SR release channel appear to be rate-limiting factors. If the SR is the same source for both systolic  $\text{Ca}^{2+}$  release and for spontaneous diastolic  $\text{Ca}^{2+}$  release, or if these two processes share common release mechanisms, the coexistence of both types of release ought to affect each other.

In Figure 7-6 graded caffeine concentrations have been used to effect graded levels of SR  $\text{Ca}^{2+}$  depletion in order to examine the effects of depletion on the amplitude of cell displacement during the twitches elicited by action potentials and on that due to the contractile waves that result from spontaneous SR  $\text{Ca}^{2+}$  release. The relative reduction in both parameters with incremental caffeine concentrations is very similar. This suggests that these two forms of SR  $\text{Ca}^{2+}$  release do indeed share a common  $\text{Ca}^{2+}$  pool or release mechanisms. In intact muscle, both twitch force and SLIF frequency also exhibit proportional reductions in response to incremental caffeine concentrations [34].

Thus, the occurrence of spontaneous diastolic  $\text{Ca}^{2+}$  release might be expected to have an impact on twitch amplitude, and this effect ought to vary with time that elapses between the spontaneous diastolic release and the subsequent action potential. This has been found to be the case (Figure 7-7). Panel A shows that in cardiac myocytes when a spontaneous contractile wave occurs in diastole, the amplitude of contraction in the subsequent systoles decreases. Panel B shows that the effect of spontaneous diastolic  $\text{Ca}^{2+}$  release, manifested as the occurrence of a contractile wave, to reduce the extent of systolic cell shortening depends upon the time elapsed between the spontaneous release and the onset of the next systole. Other studies in myocytes have shown that the inotropic response to enhanced  $\text{Ca}_0$  peaks at that  $\text{Ca}_0$  at which spontaneous diastolic  $\text{Ca}^{2+}$  release first occurs in single myocytes (Figure 7-7C). This appears to be a mechanism for the limitation of systolic pressure as  $\text{Ca}_0$  (and SLIF) increase in Figure 7-1 [35, 36]. In fact, a simple mathematical model that assumes individual cells in a bulk myocardial tissue differ slightly in their threshold for spontaneous  $\text{Ca}^{2+}$  release predicts the effect of enhanced  $\text{Ca}_0$  depicted in Figure 7-1, i.e., that the excessive spontaneous  $\text{Ca}^{2+}$  release, manifest in Figure 7-1 as SLIF, will lead to compromised action-potential-triggered SR  $\text{Ca}^{2+}$  release and thus result in suboptimal force production on that basis; this will occur in the setting of enhanced resting force and after-contraction due to the summation of oscillations in different cells as described above [37]. An additional mechanism limits the systolic function when  $\text{CaOs}$  are present within intact myocardial tissue. Cells that have experienced a diastolic  $\text{Ca}^{2+}$  release and respond with a decreased  $\text{Ca}^{2+}$  release during the next systole, e.g., as in Figure 7-7A, are coupled to other myocytes in which no  $\text{CaOs}$  occurred during the previous diastole and in which greater  $\text{Ca}^{2+}$  release and thus greater systolic shortening occurs in response to an action potential. Cells that have less  $\text{Ca}^{2+}$  release are stretched by those with more  $\text{Ca}^{2+}$  release and thus essentially comprise islands of stray series compliance within the tissue. This compromises systolic force development even in cells that did not experience spontaneous  $\text{Ca}^{2+}$  release in the previous diastole [20, 36].

From Figure 7-7 it can be inferred that insofar as spontaneous diastolic SR  $\text{Ca}^{2+}$  release

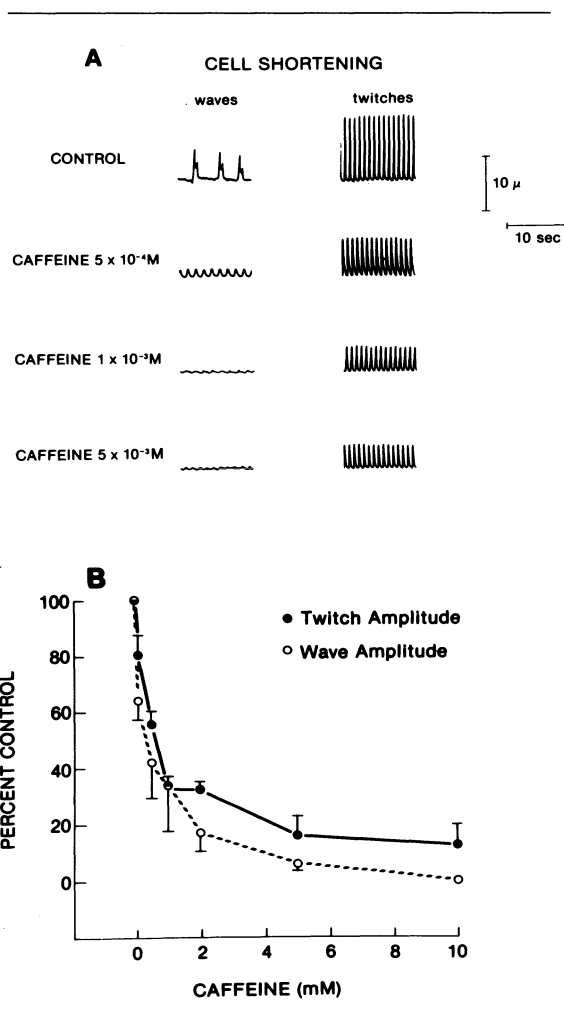


FIGURE 7-6. The effect of increasing caffeine on twitch (during stimulation at  $72 \text{ min}^{-1}$ ) and contractile wave amplitude (in the absence of stimulation) in single rat myocytes bathed in  $\text{Ca}_0$  of 1 mM. A. Tracings from a representative myocyte. B. Average effect of caffeine in four cells. In control cells, the amplitudes of twitch and wave were  $11.4 \pm 1.7$  and  $4.2 \pm 0.77 \mu\text{m}$ , respectively ( $\bar{X} \pm \text{SEM}$ ). (From Capogrossi et al. [13].)

can affect subsequent action-potential-triggered release; so too ought the latter affect the former. Figure 7-8A illustrates that this is indeed the case.  $\text{CaOs}$  do not appear in diastole when the rat cells bathed in physiologic ( $\text{Ca}_0$ ) are electrically stimulated at rates greater than  $24 \text{ min}^{-1}$ .

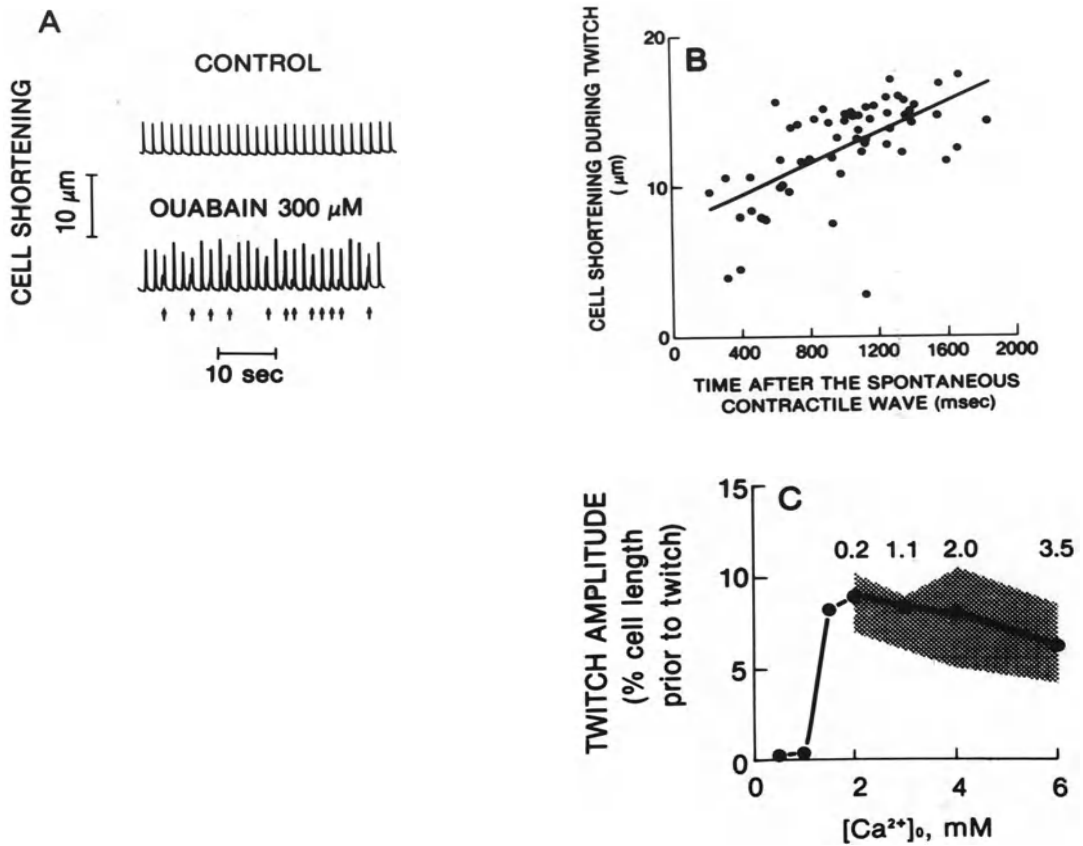


FIGURE 7-7. A. Chart recording of the extent of cell shortening during the twitch in response to electrical stimulation at  $36 \text{ min}^{-1}$  prior to (*upper*) and in the presence of ouabain (*lower*). Note that spontaneous diastolic contractile waves do not occur during stimulation prior to ouabain but do occur in its presence and that their occurrence is associated with a reduction in subsequent twitch amplitude (arrows indicate waves that are obvious even at the slow chart speed). (From Capogrossi et al. [13].) B. The extent of cell shortening during the twitch of a single rat myocyte varies with the time elapsed between the preceding spontaneous diastolic contractile wave and that twitch. (From Capogrossi et al. [13].) C. Representative example of an individual myocyte stimulated at 0.2 Hz in varying  $\text{Ca}_0$ . The line is the *average* twitch amplitude. The shaded area indicates the range of twitch amplitudes in a given  $\text{Ca}_0$  when spontaneous contractile waves appeared. Numbers above the shaded area are the average number of waves between two consecutive twitches at each  $\text{Ca}_0$ . (From Capogrossi et al. [35].)

Upon cessation of stimulation a delay interval (first arrow in figure) following the last twitch, i.e., the last action-potential-triggered SR  $\text{Ca}^{2+}$  release, elapses before the first spontaneous wave occurs (second arrow in figure). The duration of this "delay interval" is the critical determinant of whether spontaneous  $\text{Ca}^{2+}$  release will occur

in the diastolic period. When the delay interval is shorter than the interstimulus interval, spontaneous  $\text{Ca}^{2+}$  release will occur in diastole; conversely, when the interstimulus interval is less than the delay interval, the spontaneous SR  $\text{Ca}^{2+}$  release will be suppressed, i.e., "over-driven." The duration of the delay interval is

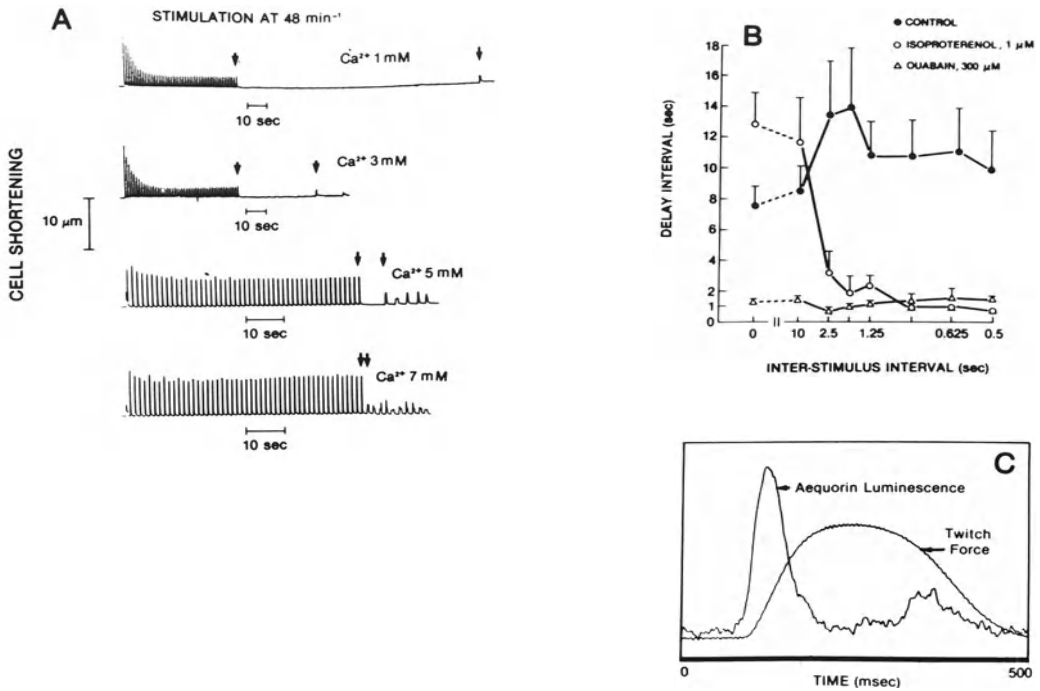


FIGURE 7-8. A. The effect of regular field stimulation ( $48 \text{ min}^{-1}$ ) of a rat myocyte bathed in  $\text{Ca}_0$  of 1 mM. Following stimulation, a delay interval elapses prior to the occurrence of a spontaneous contractile wave. At the lower ( $\text{Ca}_0$ ), the duration (arrows) of the delay interval, i.e., the interval from the last stimulated twitch to the first spontaneous oscillation (contractile wave), is longer than the average interwave interval after several minutes of rest. At higher  $\text{Ca}_0$ , the latter is greater than the former. (From Capogrossi and Lakatta [14].) B. The average effect ( $\bar{X} \pm \text{SEM}$ ) of ouabain ( $300 \mu\text{M}$ ) or isoproterenol ( $1 \mu\text{M}$ ) on the interwave interval at rest (interstimulus interval of zero) and on the delay interval following 1 minute of electrical stimulation of four rat myocytes at varying frequencies in  $\text{Ca}_0$  of 2 mM. The magnitude of the variance about the control curve is due to differences among the cells in the stimulation rate at which the maximum delay interval occurred. In the presence of drug, if the delay interval was less than the interstimulus interval, waves appeared between twitches in the diastolic periods. (From Capogrossi et al. [13].) C. Spontaneous  $\text{Ca}^{2+}$  release can occur during the twitch itself. Aequorin luminescence and tension in a ferret papillary muscle in which several cells were injected with aequorin. The functional implications, (and possibly the factors initiating) spontaneous  $\text{Ca}^{2+}$  release during a twitch, when the sarcolemma may be partially depolarized, might be expected to differ from a release occurring between twitches. (From McIvor et al. [38].)

not fixed, but, like the wave period at rest in Figure 7-3A, is affected by the cell " $\text{Ca}^{2+}$  load," a parameter dependent on  $\text{Ca}_0$ , frequency of stimulation, and the presence of certain drugs that can affect  $\text{Ca}^{2+}$  metabolism. Figure 7-8A shows the effect of  $\text{Ca}_0$  to decrease the delay interval following stimulation at a given frequency. Figure 7-8B shows the effects of isoproterenol and ouabain during stimulation across a range of frequencies. Beta-adrenergic stimulation, as might be expected, decreases the

delay interval due to the net cell  $\text{Ca}^{2+}$  gain resulting from the enhanced  $\text{Ca}^{2+}$  influx via the slow  $\text{Ca}^{2+}$  inward channel during repetitive depolarization. However, when electrical stimulation is terminated, this effect dissipates; (the interwave interval at rest is actually increased above the control level (see Figure 7-8B)). In contrast, the increase in cell  $\text{Ca}^{2+}$  during in response to cardiac glycosides occurs via the Na-Ca exchanger. Thus, in contrast to isoproterenol, cell  $\text{Ca}^{2+}$  gain can occur in diastole

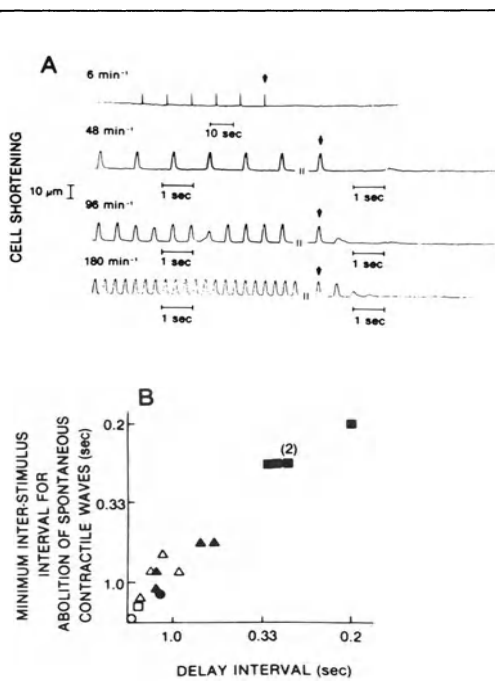


FIGURE 7-9. A. The effect of 1 minute of stimulation at varying frequencies on a representative *rabbit* myocyte bathed in  $Ca_0$  of 3 mM in the presence of 1  $\mu$ M isoproterenol. Arrow indicates the last stimulated twitch. B. The minimum interstimulus interval to suppress spontaneous waves in rat myocytes varies with the delay interval;  $Ca_0$  3 mM (○),  $Ca_0$  5 mM (□),  $Ca_0$  7 mM (●),  $Ca_0$  2 mM and 100 mM ouabain (△),  $Ca_0$  2 mM and 300 mM ouabain (▲),  $Ca_0$  2 mM and 1 mM isoproterenol (■) [13].

during stimulation and in the absence of stimulation as well. In the presence of glycosides, the interwave interval in the unstimulated state, as well as that during stimulation, is markedly reduced from control. The same holds true for increases in  $Ca_0$  (see Figure 7-8A).

Stimulation affects spontaneous  $Ca^{2+}$  release in intact cardiac muscle just as it does in single cardiac cells [3, 34, 39]. SLIF, which monitor the contractile waves that occur within individual cells in which spontaneous  $Ca^{2+}$  release occurs, are suppressed by electrical stimulation in the absence of drugs or excessive  $Ca_0$  [34, 39]. Following cessation of stimulation, a delay interval of several seconds must elapse following stimulation before SLIF reappear. In the presence of Na-K inhibition or enhanced  $Ca_0$ , SLIF both at rest and immediately following the prior

contraction during stimulation are enhanced [3, 34, 39]. Isoproterenol, as in single cardiac cells, decreases or does not affect SLIF in the unstimulated state, but markedly augments SLIF in the diastolic period during stimulation [34]. Figure 7-8C shows that spontaneous  $Ca^{2+}$  release in the intact muscle monitored by aequorin luminescence, can occur during the relaxation phase of the twitch and thus can be a determinant of relaxation of the twitch in  $Ca^{2+}$  overload states.

Thus, in addition to increasing the inotropic state of cardiac muscle,  $Ca_0$ , cardiac glycosides, and isoproterenol decrease the delay interval and thus enhance the likelihood for spontaneous CaOs to occur in diastole. Figure 7-9A illustrates that the interaction between electrical stimulation and  $Ca_0$ s and the effect of isoproterenol on them demonstrated above in rat cells occurs in rabbit cells as well. In the cell in Figure 7-9A (upper panel), which was superfused with buffer containing 1  $\mu$ M isoproterenol, the following can be observed:

1. Waves are not present in the absence of stimulation because as also shown in the rat in Figure 7-8 (panel 13), isoproterenol, while increasing cell  $Ca^{2+}$  loading during stimulation, through accentuation of the slow inward current, and inducing a decrease in the delay interval does not increase the frequency of spontaneous contractile waves at rest.
2. No spontaneous contractile waves are observed during or following stimulation at 6  $min^{-1}$ .
3. A spontaneous wave occurs following stimulation at higher rates (48  $min^{-1}$ ), but the delay interval is longer than the interstimulus interval—thus no waves appear in the diastolic period and each twitch is of constant amplitude.
4. The delay interval decreases as the frequency of stimulation increases. At 96  $min^{-1}$  it is less than the interstimulus interval and, thus, at this frequency of stimulation, spontaneous contractile waves occur in between stimulated twitches. As shown in the rat in Figure 7-7A, when a wave precedes a twitch, the amplitude of that stimulated twitch decreases, and this produces an "alternans" in twitch amplitude which is well evident in the seventh twitch and, at closer observation, also in the third and fourth twitch.

5. During stimulation at  $180 \text{ min}^{-1}$  the interstimulus interval is less than the delay interval for spontaneous release, the waves are suppressed and twitch amplitude becomes uniform once again. Additionally, the initial waves following stimulation exhibit varying degrees of synchronization prior to a time-dependent reduction in their frequency and subsequent abolition at rest as demonstrated previously also in rat cells [14] (Figure 7-10C). Reducing the interstimulus interval to less than the delay interval "overdrive suppresses" the diastolic spontaneous  $\text{Ca}^{2+}$  release. Figure 7-9B shows that suppression of spontaneous diastolic  $\text{Ca}^{2+}$  release can be achieved across a broad range of delay intervals and thus a broad range of cell  $\text{Ca}^{2+}$  loading.

### *How CaOs Can Initiate Arrhythmias*

The spontaneous release of  $\text{Ca}^{2+}$  into the myoplasmic space not only results in a  $\text{Ca}^{2+}$  myofilament interaction but also allows  $\text{Ca}^{2+}$  to interact with sarcolemmal ion channels and carrier proteins. This  $\text{Ca}^{2+}$  modulation produces miniature inward currents in cardiac myocytes [40], and, thus, the occurrence of a spontaneous contractile wave in a single cardiac myocyte is accompanied by a small membrane depolarization (Figure 7-10A). When the resting-membrane potential is at the normal level, i.e., around  $-80 \text{ mV}$ , this depolarization is of insufficient magnitude to induce an action potential (because the threshold for action potentials is that for sufficient Na channels to open and this requires a depolarization to around  $-67 \text{ mV}$ ). However, certain circumstances increase the magnitude of the depolarization due to spontaneous  $\text{Ca}^{2+}$  release. Myocardial cells that are stimulated during high  $\text{Ca}^{2+}$  loading states, e.g., in the presence of glycosides, enhanced bathing ( $\text{Ca}_0$ ) or catecholamines, exhibit not only a decrease in the delay interval for spontaneous  $\text{Ca}^{2+}$  release to occur following prior stimulation, but also an enhanced probability for it to occur in more than a single focus, i.e., more than a single band of high  $\text{Ca}^{2+}$  is present within cells at a given time (Figures 7-10B and 7-10C). Thus, in this instance, compared to when spontaneous  $\text{Ca}^{2+}$  is released only at a single focus (unifocal CaOs) as in Figure 7-2 or 7-10A, a greater area of sarcolemma and thus more Na-Ca carrier or TI

channel proteins will be exposed to high  $[\text{Ca}^{2+}]$ . Because the myocyte length is not greater than  $150 \mu\text{m}$ , the  $\text{Ca}^{2+}$  modulation of sarcolemmal conductances produced by synchronized areas of spontaneous  $\text{Ca}^{2+}$  release within a myocyte summates to produce an augmented depolarization compared to that which accompanies a unifocal release [9, 10]. The augmented depolarization that accompanies multifocal, spontaneous, SR  $\text{Ca}^{2+}$  release sometimes is sufficient to trigger an action potential, even when the initial membrane potential is normal [9]. Similarly, the rapid application of caffeine to single ventricular myocytes at the normal membrane potential, which causes a relatively synchronous release of  $\text{Ca}^{2+}$  from the SR into the myoplasmic space, mimics the ability of multifocal, spontaneous, SR  $\text{Ca}^{2+}$  release to result in a depolarization sufficient on magnitude to elicit an action potential from normal resting-membrane potential [10]. At more positive membrane potentials, even the smaller depolarization that accompanies spontaneous  $\text{Ca}^{2+}$  release at a single focus can induce action potentials. It is noteworthy that during the reflow period following ischemia or reoxygenation following hypoxia [16, 41, 42] or acidosis in the presence of high-cell  $\text{Ca}^{2+}$  loading [8], the contractile wave frequency and accompanying sarcolemmal depolarization increases markedly. It has been suggested that some arrhythmias that occur during these conditions may be due to exaggerated spontaneous diastolic  $\text{Ca}^{2+}$  release [43]. An example of the exacerbation of spontaneous SR  $\text{Ca}^{2+}$  release by acidosis, which results in spontaneous action potentials is illustrated in Figure 7-10D.

In summary, there are abundant experimental data to indicate that the characteristics of spontaneous SR  $\text{Ca}^{2+}$  release are similar in a variety of cardiac preparations ranging from single cardiac ventricular cells to the intact isolated heart. Additionally, abundant evidence indicates that spontaneous SR  $\text{Ca}^{2+}$  release in diastole can have marked functional implications. Taken together, these studies provide support for the hypothesis that spontaneous  $\text{Ca}^{2+}$  release as a *single* mechanism (Figure 11) could underlie the three most common clinical signs of many forms of heart disease: increased diastolic tonus, normal or reduced systolic function; and an increased likelihood for the occurrence of ventricular extrasystoles and arrhythmias. Although we are not suggesting

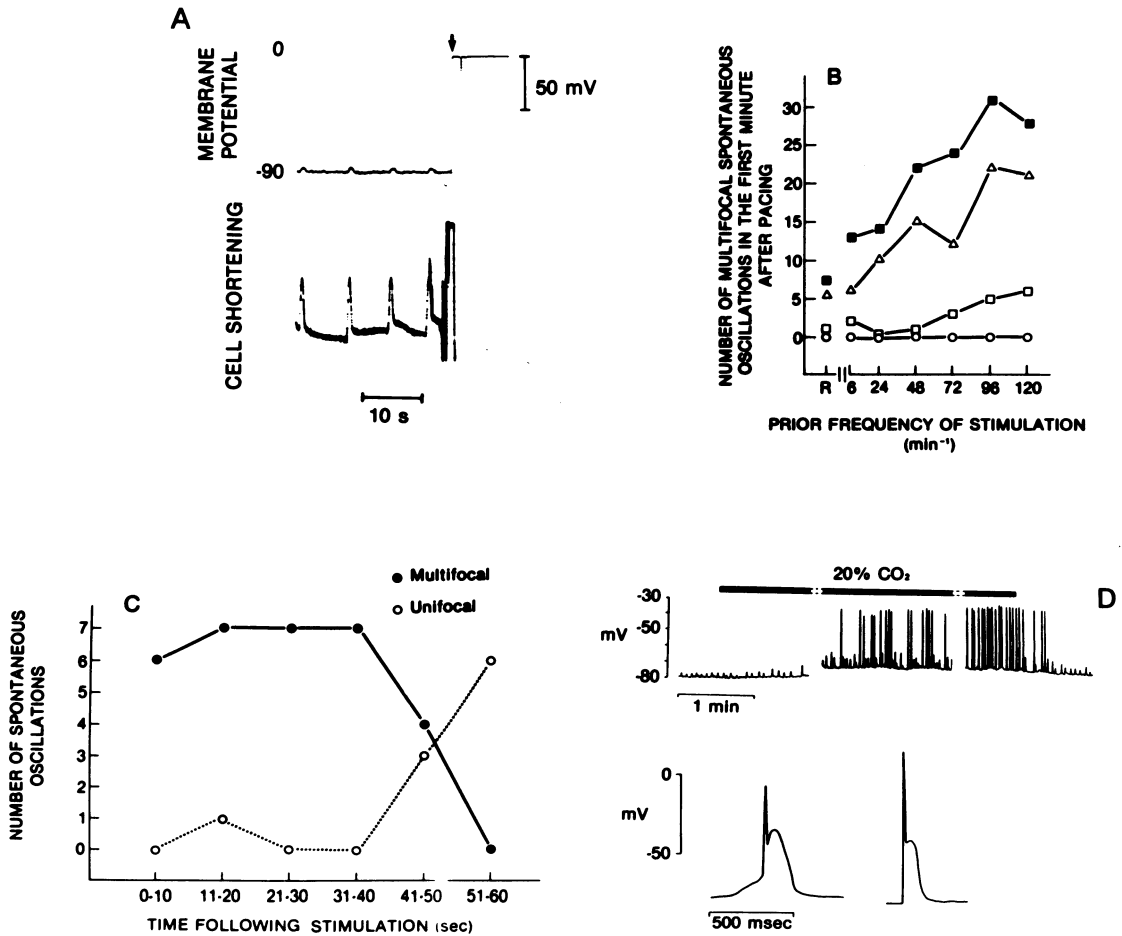


FIGURE 7-10. A. The spontaneous contractile waves in a typical ventricular myocyte bathed in  $Ca_0$  of 2.0 mM (lower panel) are accompanied by a small sarcolemmal depolarization (upper panel). At arrow, the electrode was removed from the cell and indicates that the membrane potential at which the waves occurred in this myocyte was  $-90$  mV from Capogrossi et al. [24]. B. and C. Representative rat myocytes stimulated for 1 minute at different rates and varying  $Ca_0$ . The likelihood for multifocal  $Ca^{2+}$  release to occur increases with increasing  $Ca_0$  and changes with the rate of stimulation (panel B). Multifocal wave decay following stimulation at  $96 \text{ min}^{-1}$  in 7 mM  $Ca_0$  and unifocal waves become predominant (panel C) from Capogrossi et al. [14]. D. The upper panel shows a chart recording of the membrane potential in an isolated rat myocyte ( $Ca_0 = 4 \text{ mM}$ ,  $37^\circ\text{C}$ ) before, during, and after acidosis produced by increasing perfusate ( $\text{CO}_2$ ) to 20% ( $[\text{HCO}_3^-] = 20 \text{ mM}$ ). Within 10 minutes of exposure to the acid solution: (1) Membrane potential had depolarized significantly from  $-79.3$  to  $-75.8$  mV; (2) the frequency of contractile waves and accompanying amplitude of the membrane depolarizations had increased by 31% and became large enough to frequently trigger an action potential shown in greater detail in the oscilloscope tracing in the left lower panel. An electrically stimulated action potential is shown for comparison in the right lower panel. These changes were reversible. The results suggest that the increased  $Ca_i$  during acidosis overrides the  $\text{H}^+$  suppression of sarcoplasmic reticular function and may be important in the genesis of acidosis-induced arrhythmias. (From Orchard et al. [43].)

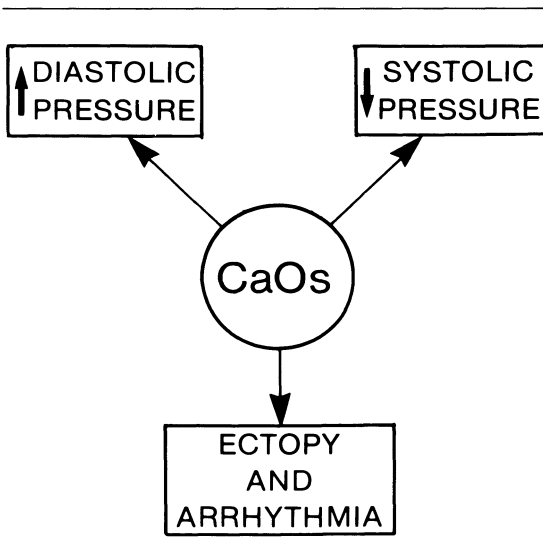


FIGURE 7-11. Relation between spontaneous diastolic  $\text{Ca}^{2+}$  oscillators (CaOs), as a single mechanism, and the control manifestations common to multiple cardiac disease states.

that spontaneous  $\text{Ca}^{2+}$  release is a unique mechanism for each of these clinical signs, as each can have other causes, no single pathophysiologic mechanism that has been implicated in heart failure, can, in a straightforward and documented manner, explain all three of these common and concurrent manifestations of multiple cardiac disease states. Thus, the conceptual framework regarding the functional implications of CaOs, as reviewed here, merits consideration in the interpretation of studies that seek to identify cellular mechanisms of cardiac disease.

### References

- Lakatta EG, Capogrossi MC, Kort AA, Stern MD (1985). Spontaneous myocardial  $\text{Ca}^{2+}$  oscillations: An overview with emphasis on ryanodine and caffeine. *Fed Proc* 44:2977-2983.
- Lappe DL, Lakatta EG (1980). Intensity fluctuation spectroscopy monitors contractile activation in "resting" cardiac muscle. *Science* 207:1369-1371.
- Lakatta EG, Lappe DL (1981). Diastolic scattered light fluctuation, resting force and twitch force in mammalian cardiac muscle. *J Physiol (Lond)* 315:369-394.
- Stern MD, Kort AA, Bhatnagar GM, Lakatta EG (1983). Scattered light intensity fluctuations in diastolic rat cardiac muscle caused by spontaneous  $\text{Ca}^{2+}$ -dependent cellular mechanical oscillations. *J Gen Physiol* 82:119-153.
- Stern MD, Weisman HF, Renlund DG, et al (1985). Cellular calcium oscillations in intact perfused hearts detected by laser light scattering: cellular mechanism for diastolic tone. *Circulation* 72(suppl III):296 (abstract).
- Kort AA, Lakatta EG, Marban E, et al (1985). Fluctuations in intracellular calcium concentration and their effect on tonic tension in canine cardiac Purkinje fibres. *J Physiol (Lond)* 367: 291-308.
- Kass RS, Tsien RW (1982). Fluctuations in membrane current driven by intracellular calcium in cardiac Purkinje fiber. *Biophys J* 38:259-269.
- Houser SR, Orchard CH, Capogrossi MC, et al (1986). Spontaneous  $\text{Ca}^{2+}$  oscillations during acidosis can produce action potentials in unstimulated cardiac myocytes. *Biophys J* 49:455a (abstract).
- Bahinski A, Capogrossi MC, Houser SR, Lakatta EG (1986). Multifocal spontaneous  $\text{Ca}^{2+}$  release can trigger a spontaneous action potential in single cardiac myocytes. *J Physiol (Lond)* 371: 196P (abstract).
- Houser SR, Capogrossi MC, Bahinshi A, Lakatta EG (1986). Spontaneous action potentials due to SR  $\text{Ca}^{2+}$  release in unstimulated rat cardiac myocytes. *Circulation* 74(suppl II):29 (abstract).
- Valdeolmillos M, Eisner DA (1985). The effects of ryanodine on calcium-overloaded sheep cardiac Purkinje fibers. *Circ Res* 56:452-456.
- Eisner DA, Valdeolmillos M (1986). A study of intracellular calcium oscillations in sheep cardiac Purkinje fibers measured at the single cell level. *J Physiol (Lond)* 372:539-556.
- Capogrossi MC, Suarez-Isla BA, Lakatta EG (1986). The interaction of electrically stimulated twitches and spontaneous contractile waves in single cardiac myocytes. *J Gen Physiol* (in press).
- Capogrossi MC, Lakatta EG (1985). Frequency modulation and synchronization of spontaneous oscillations in cardiac cells. *Am J Physiol* 248(Heart Circ Physiol 17):H12-H418.
- Allen DG, Eisner DA, Pirolo JS, Smith GL (1985). The relationship between intracellular calcium and contraction in calcium overloaded ferret papillary muscle. *J Physiol (Lond)* 364: 169-182.
- Weiss RG, Lakatta EG (1986). Temporal relationship of recovery of systolic contractile function, spontaneous diastolic calcium oscillations, and metabolism during reflow in rat

- myocardium. *Circulation* 74 (4), Part 2, II-67 (abstract).
17. Hoerter JA, Miceli MV, Renlund DG, et al (1986). A phosphorus-<sup>31</sup> nuclear magnetic resonance study of the metabolic, contractile, and ionic consequences of induced  $Ca^{2+}$  alterations in the isovolumic rat heart. *Circ Res* 58:539-551.
  18. Renlund DG, Lakatta EG, Mellits ED, Gerstenblith G (1985). Calcium-dependent enhancement of myocardial diastolic tone and energy utilization dissociates systolic work and oxygen consumption during low sodium perfusion. *Circ Res* 57:876-888.
  19. Kort AA, Capogrossi MC, Lakatta EG (1985). Frequency, amplitude, and propagation velocity of spontaneous  $Ca^{2+}$ -dependent contractile waves in intact adult rat cardiac muscle and isolated myocytes. *Circ Res* 57:844-855.
  20. Kort AA, Lakatta EG (1984). Calcium-dependent mechanical oscillations occur spontaneously in unstimulated mammalian cardiac tissues. *Circ Res* 54:396-404.
  21. Fabiato A, Fabiato F (1972). Excitation-contraction coupling of isolated cardiac fibers with disrupted or closed sarcolemma: Calcium dependent cyclic and tonic contractions. *Circ Res* 31:293-307.
  22. Chiesi M, Ho MM, Inesi G, et al (1981). Primary role of sarcoplasmic reticulum in phasic contractile activation of cardiac myocytes with shunted myolemma. *J Cell Biol* 91:728-742.
  23. Fabiato A (1985). Time and calcium dependence of activation and inactivation of calcium-induced release of calcium from the sarcoplasmic reticulum of a skinned canine cardiac Purkinje cell. *J Gen Physiol* 85:247-289.
  24. Capogrossi MC, Kort AA, Spurgeon HA, Lakatta EG (1986). Single adult rabbit and rat cardiac myocytes retain the  $Ca^{2+}$  and species dependent systolic and diastolic contractile properties of intact muscle. *J Gen Physiol* (in press).
  25. Fabiato A, Fabiato A (1975). Contractions induced by a calcium-triggered release of calcium from the sarcoplasmic reticulum of single skinned cardiac cells. *J Physiol (Lond)* 249:469-495.
  26. Fabiato A (1985). Rapid ionic modifications during the aequorin-detected calcium transient in a skinned canine cardiac Purkinje cell. *J Gen Physiol* 85:189-246.
  27. Wier WG, Kort AA, Stern MD, et al (1983). Cellular calcium fluctuations in mammalian heart: Direct evidence from noise analysis of aequorin signals in Purkinje fibers. *Proc Natl Acad Sci USA* 80:7367-7371.
  28. Orchard CH, Eisner DA, Allen DG (1983). Oscillations of intracellular  $Ca^{2+}$  in mammalian cardiac muscle. *Nature* 304:735-738.
  29. Cobbold PhH, Bourne PK (1984). Aequorin measurements of free calcium in single heart cells. *Nature* 312:444-446.
  30. Fabiato A (1981). Myoplasmic free calcium concentration reach during the twitch of a intact isolated cardiac cell and during calcium-induced release of calcium from the sarcoplasmic reticulum of a skinned cardiac cell from the adult rat or rabbit ventricle. *J Gen Physiol* 78:457-497.
  31. Stern MD, Capogrossi MC, Lakatta EG (1984). Propagated contractile waves in single cardiac myocytes modeled as regenerative calcium induced calcium release from the sarcoplasmic reticulum. *Biophys J* 45(2):94a (abstract).
  32. Wier WG, Yue DT, Marban E (1985). Effects of ryanodine on intracellular  $Ca^{2+}$  transients in mammalian cardiac muscle. *Fed Proc* 44:2989-2993.
  33. Allen DG, Eisner DA, Orchard DG (1984). Characterisation of oscillations of intracellular calcium concentration in ferret ventricular muscle. *J Physiol (Lond)* 352:113-128.
  34. Kort AA, Lakatta EG (1987). Bimodal effect of electrical stimulation on light fluctuations that monitor spontaneous sarcoplasmic reticulum  $Ca^{2+}$  release in rat cardiac muscle. (submitted for publication)
  35. Capogrossi MC, Lakatta EG, Spurgeon HA (1985). Spontaneous sarcoplasmic reticulum  $Ca^{2+}$  release limits the ability of  $Ca^{2+}$  to enhance twitch shortening in rat cardiac myocytes. *J Physiol (Lond)* 369:81P (abstract).
  36. Kort AA, Lakatta EG (1987). The relationship of spontaneous sarcoplasmic reticulum  $Ca^{2+}$  release to twitch tension in rat and rabbit cardiac muscle. (submitted for publication)
  37. Stern MD, Capogrossi MC, Lakatta EG (1987). A single model of spontaneous calcium release explains calcium- and rate-dependent saturation of contractility, oscillatory restitution of contractility and aftercontractions in heart muscle. *Biophys J* (in press).
  38. McIvor ME, Lakatta EG, Orchard CH (1986). Spontaneous  $Ca^{2+}$  release can occur during isometric twitch in cardiac muscle. *Biophys J* 49:463a (abstract).
  39. Kort AA, Lakatta EG (1985).  $Ca^{2+}$ -dependent oscillations in rat cardiac muscle: Transient state measurements following regular electrical depolarization. *Biophys J* 47:280 (abstract).
  40. Talo A, McIvor ME, Spurgeon HA, Lakatta E (1986). Membrane currents during spontaneous contractile waves in rat cardiac myocytes. *Fed Proc* 45(4):769 (abstract).
  41. Stern MD, Chien AM, Capogrossi MC, et al (1985). Direct observation of the "oxygen paradox" in single rat ventricular myocytes. *Circ*

- Res 56:899-903.
42. Renlund DG, Weisman HF, Gerstenblith G, et al (1985). Exaggerated ATP-dependent  $\text{Ca}^{2+}$  cycling sensed by laser spectroscopy during reperfusion. *Circulation* 72 (4), Part II, III-120 (abstract).
  43. Orchard CH, Houser SR, Kort AA, et al (1986). Acidosis facilitates spontaneous sarcoplasmic reticulum  $\text{Ca}^{2+}$  release in rat myocardium. *J Gen Physiol* (in press).

---

PART II. PHYSIOLOGIC  
MODIFIERS OF  
RELAXATION IN  
EXPERIMENTAL MODELS

---

---

## 8. HYPOXIA AND RELAXATION

---

Winifred G. Nayler, Darren J. Buckley, and Jennifer S. Elz

Hypoxia has a profound effect on the myocardium. Early changes include a decline in peak developed tension [1], depletion of the endogenous adenosine triphosphate (ATP) and creatine phosphate (CP) [2] reserves, an accumulation of protons [3], and a gain in  $\text{Na}^+$  and loss of  $\text{K}^+$  [4]. As the duration of the hypoxic episode progresses, other changes occur, including a gradual but sustained increase in end-diastolic resting tension. Many factors, including extracellular pH [5], temperature [6], and the glucose content of the perfusion buffer [7], have been shown to affect the rate of onset and the magnitude of this hypoxia-induced increase in end-diastolic resting tension (hypoxic contracture). Nevertheless its precise cause is uncertain. Basically there are two schools of thought: that the contracture occurs because there is inadequate ATP to facilitate cross-bridge detachment [8]; or that the contracture occurs because of a raised cytosolic  $\text{Ca}^{2+}$  [9].

There are at least three reasons why an increase in end-diastolic resting tension such as that which occurs during hypoxia is undesirable. First, it will impede left ventricular filling. Second, it may result in the physical occlusion of patent coronary blood vessels. Third, if, as some investigators believe [10], sustained contracture damages the sarcolemma, rendering it increasingly permeable, then the contracture that develops during hypoxia may contribute to the mechanisms that are responsible for the massive influx of  $\text{Ca}^{2+}$  that occurs upon reoxygenation [9].

This chapter is concerned with a series of experiments that were undertaken to further investigate the factors that are responsible for the contracture that develops during hypoxia (Figure 8-1). Three different approaches have been

followed. First, by reducing extracellular  $\text{Ca}^{2+}$  during the hypoxic episode we have investigated the importance of extra cellular  $\text{Ca}^{2+}$  in this response. Second, by adding ryanodine—a compound that inhibits  $\text{Ca}^{2+}$  release from the sarcoplasmic reticulum (SR) [11], we have determined whether  $\text{Ca}^{2+}$  from the SR is involved. Finally, by adding 2,3-butanedione monoxime (BDM) we have attempted to control contracture development, in the hope of establishing whether this avoids excessive  $\text{Ca}^{2+}$  gain upon reoxygenation. The major site of action of BDM is at the myofibrils, where it inhibits cross-bridge formation [12], possibly by decreasing the sensitivity of the myofibrils to  $\text{Ca}^{2+}$  [13]. BDM has a negative inotropic effect on both intact and skinned muscle fibers [13].

The results presented here indicate that the development of contracture during hypoxia is independent of extracellular  $\text{Ca}^{2+}$  and of  $\text{Ca}^{2+}$  release from the SR. In addition, the results show that conditions that attenuate the hypoxia-induced increase in resting tension do not necessarily prevent  $\text{Ca}^{2+}$  from being accumulated upon reoxygenation.

### *Methods*

Adult female (200–250 gm) Sprague-Dawley rats were used for these experiments. They were lightly anesthetized with a diethylether/ $\text{O}_2$  mixture and heparinized before their hearts were removed and placed in ice-cold Krebs-Henseleit buffer until contractions ceased. After any extraneous tissue was removed, the hearts were attached to a stainless steel cannula and then subjected to a non-recirculating Langendorff perfusion with a constant flow of 10 ml/min at 37°C. The hearts were allowed to beat spontaneously.

### PERFUSION BUFFERS

The perfusion buffers were prepared in distilled water and contained (in mM):

*Grossman, William, and Lorell, Beverly H. (eds.), Diastolic Relaxation of the Heart. Copyright © 1987. Martinus Nijhoff Publishing. All rights reserved.*

*Krebs-Henseleit buffer (K-H)*: NaCl, 119.0; NaHCO<sub>3</sub>, 25.0; KCl, 4.6; KH<sub>2</sub>PO<sub>4</sub>, 1.2; MgSO<sub>4</sub>, 1.2; CaCl<sub>2</sub>, 1.3; and glucose, 11.0.

*Glucose-free K-H*: This was prepared by omitting glucose from K-H and replacing it with 22.0 mM sucrose.

*Low Ca<sup>2+</sup>, glucose-free K-H*: This was prepared by reducing the Ca<sup>2+</sup> concentration from 1.3 to 0.1 mM.

*Glucose-free, BDM K-H*: This was prepared by adding 30 mM BDM to glucose-free K-H and increasing its CaCl<sub>2</sub> content to 2.6 mM. Preliminary experiments using a calcium ion-selective electrode (Model 93-20, Orion Research Incorporation, Cambridge, MA), in conjunction with an Orion 701A pH meter, indicate that 30 mM BDM lowers the free Ca<sup>2+</sup> concentration but that increasing the Ca<sup>2+</sup> content of K-H to 2.6 mM compensated for this.

The buffers were gassed with 95% O<sub>2</sub> + 5% CO<sub>2</sub> for aerobic conditions and with 95% N<sub>2</sub> + 5% CO<sub>2</sub> for hypoxic conditions.

#### PERFUSION SEQUENCES

Hearts were perfused with aerobic K-H for 30 minutes prior to being made hypoxic. Hypoxic perfusion was for 30 or 60 minutes with glucose-free K-H. In some experiments 10 μM ryanodine was added to the glucose-free K-H. In other experiments the Ca<sup>2+</sup> concentration was lowered to 0.1 mM, while in others 30 mM BDM was added. When required, the hypoxic hearts were reoxygenated by the reintroduction of aerobic K-H buffer. At the conclusion of each perfusion sequence, the hearts were analyzed for Ca<sup>2+</sup> or ATP and CP as described below.

#### MECHANICAL RECORDS

Throughout the entire period of perfusion, peak developed and end-diastolic resting tension were recorded by attaching a Narco F-60 Biosystem myograph to the left ventricular apex, as described elsewhere [14]. The output from the strain gauge was displayed on a Devices Physiograph Recorder (Narco Biosystems, Houston, TX). Hearts from which peak developed tension and end-diastolic tension were recorded were not used for the analysis of Ca<sup>2+</sup> or ATP and CP.

#### MEASUREMENT OF CELL Ca<sup>2+</sup>

After the appropriate perfusion sequence, the

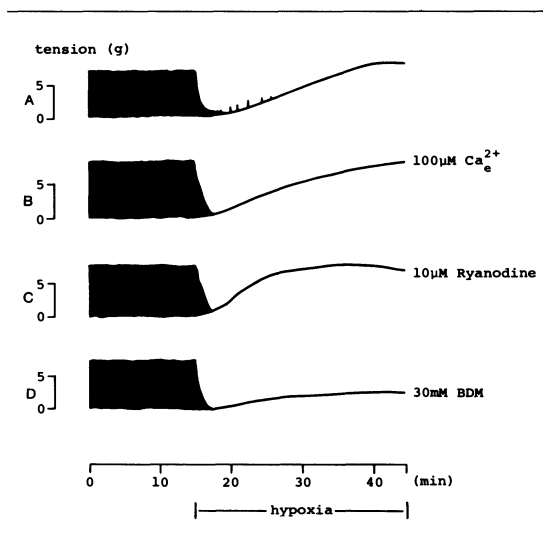


FIGURE 8-1. Factors responsible for contracture that develops during hypoxia. Tension records obtained from hearts which, after 30 minutes perfusion with aerobic Krebs-Henseleit buffer (K-H) were perfused with glucose-free hypoxic K-H (A), glucose-free hypoxic K-H containing 100 μM Ca<sup>2+</sup>, instead of 1.3 mM (B); 10 μM ryanodine (C); or 30 mM 2, 3-butanedione monoxime (BDM) (D). Note that BDM attenuated the hypoxic-induced rise in resting tension.

coronary vasculature was flushed with 10 ml of an ice-cold sucrose/histidine solution that had been pretreated with Dowex (50 W), as described by Alto and Dhalla [15]. This procedure was performed to minimize the contribution of extracellular Ca<sup>2+</sup> to the measured cell Ca<sup>2+</sup>. The hearts were blotted, and the ventricles dried to constant weight at 100°C. After dissolving the ventricles in concentrated HNO<sub>3</sub> and diluting with a KCl/LaCl<sub>3</sub> solution, the Ca<sup>2+</sup> content was measured by atomic absorption spectrophotometer at 422.7 nm, as described in detail previously [16].

#### MEASUREMENT OF TISSUE ATP AND CP

When tissue ATP and CP measurements were required, the hearts were snap-frozen between large stainless steel tongs precooled in liquid N<sub>2</sub>. ATP and CP were determined enzymatically, as described by Lamprecht and Trautshold [17], and Lamprecht and colleagues [18]. Results are expressed as μmol/gm dry weight.

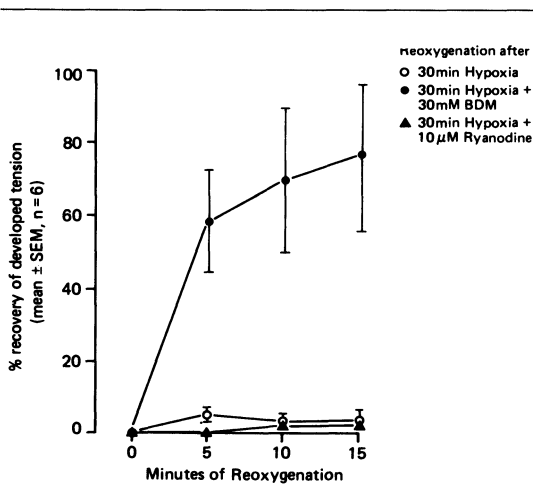


FIGURE 8-2. Effect of reoxygenation on recovery of developed tension. Recovery of active tension generation in hearts that were reoxygenated after 30 minutes of perfusion with glucose-free hypoxic Krebs-Henseleit buffer containing either 30 mM BDM or 10  $\mu$ M ryanodine. Each point is based on the mean  $\pm$  SEM of six separate experiments. Recovery is expressed as % based on tension developed immediately prior to making the hearts hypoxic.

## Results

### EFFECT OF LOW EXTRACELLULAR $Ca^{2+}$ , RYANODINE, AND BDM ON HYPOXIA-INDUCED CONTRACTURE

Figure 8-1 shows the effect of reducing extracellular  $Ca^{2+}$  from 1.3 to 0.1 mM, of adding 10  $\mu$ M ryanodine, and of adding 30 mM BDM on the hypoxia-induced increase in resting tension. In each case these interventions were introduced coincidentally with the switch from aerobic to hypoxic (glucose-free) perfusion. The upper trace (see Figure 8-1) relates to the increase in resting tension normally seen when hypoxic, glucose-free conditions are introduced. These traces show that reducing the extracellular  $Ca^{2+}$  to 0.1 mM or adding ryanodine had no effect on the hypoxia-induced increase in resting tension. BDM however, markedly reduced this contracture (see Figure 8-1).

### EFFECT OF LOW EXTRACELLULAR $Ca^{2+}$ , RYANODINE, AND BDM ON RECOVERY OF MECHANICAL FUNCTION DURING POSTHYPOXIC REOXYGENATION

Figure 8-2 shows that the reoxygenation of hearts that had been perfused with hypoxic, glucose-free K-H failed to result in any recovery of active tension development. Figure 8-2 also shows that, whereas adding ryanodine to the hypoxic perfusion buffer failed to provide any benefit in terms of the recovery of function upon reoxygenation, hearts that had been made hypoxic for 30 minutes in the presence of BDM recovered. Thus after 15 minutes of reoxygenation the "BDM-treated" hearts exhibited an active-tension-generating capacity approximately 80% of that of aerobically perfused hearts that had not been made hypoxic. The remainder of our experiments, therefore, were restricted to hearts that had been made hypoxic in the presence of BDM.

### EFFECT OF BDM DURING HYPOXIA ON THE REOXYGENATION-INDUCED GAIN IN $Ca^{2+}$

Figure 8-3A shows that the presence of BDM during the hypoxic episode failed to prevent a small gain in tissue  $Ca^{2+}$  during the hypoxic episode itself. This figure (Figure 8-3A) also shows that whereas the control hypoxic hearts accumulated excess  $Ca^{2+}$  upon reoxygenation after 30 minutes of hypoxia, hearts that had been hypoxic for 30 minutes in the presence of BDM did not accumulate  $Ca^{2+}$  during reoxygenation. Hence, the data presented so far show that an agent such as BDM, which attenuates the hypoxic-induced increase in resting tension, leaves the muscle in a condition that favors recovery of mechanical function upon reoxygenation and prevents reoxygenation-induced  $Ca^{2+}$  overload.

### EFFECT OF BDM ON THE LOSS OF ATP AND CP DURING 30 MINUTES OF HYPOXIA

Table 8-1 confirms that hearts that are perfused with glucose-free hypoxic K-H for 30 minutes become depleted of ATP and CP. Table 8-1 also shows that adding BDM during the hypoxic episode attenuates this loss of ATP and CP. Considering these results, therefore, it is impossible to conclude whether the ability of BDM to protect against reoxygenation-induced  $Ca^{2+}$  overload is due to its attenuation of the hypoxic-induced increase in resting tension.

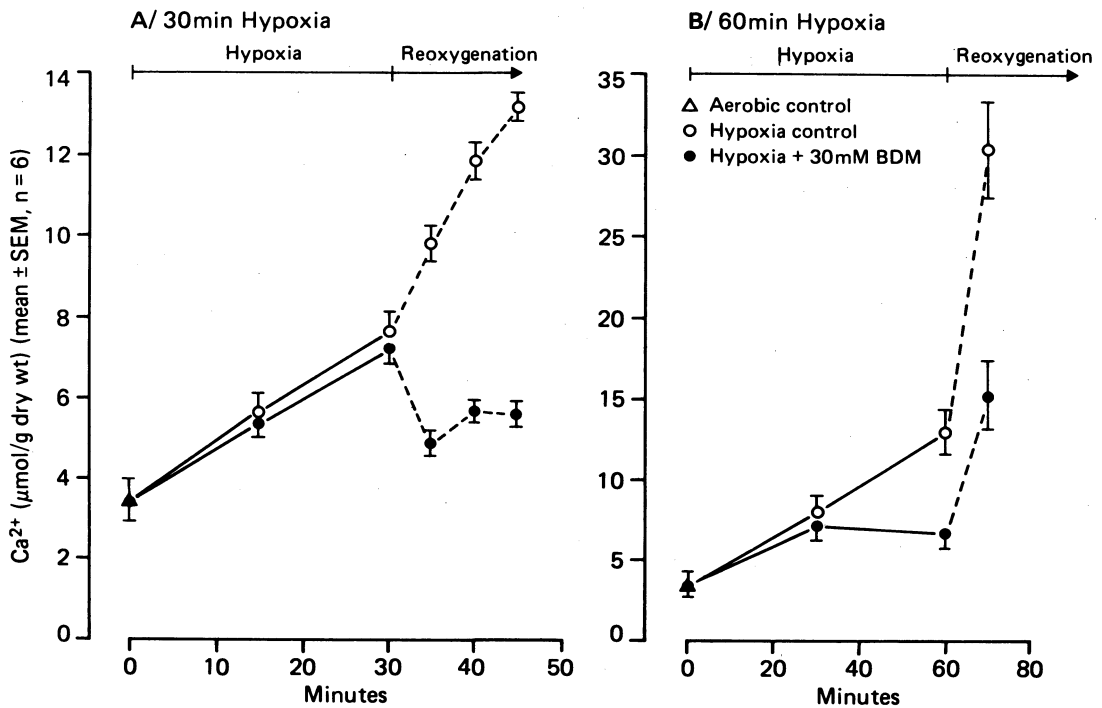


FIGURE 8-3. Effect of BDM on tissue  $\text{Ca}^{2+}$  during hypoxia and reoxygenation. Each point is mean  $\pm$  SEM of six separate experiments. In series A the hearts were hypoxic for 30 minutes and in series B for 60 minutes before being reoxygenated.

TABLE 8-1. Effect of BDM on Hypoxia-Induced Loss of ATP and CP<sup>a</sup>

Experiment	ATP <sup>b</sup>	CP <sup>b</sup>
Aerobic control	17.47 $\pm$ 1.14	32.25 $\pm$ 2.14
30 min hypoxia	2.26 $\pm$ 1.13	9.82 $\pm$ 3.06
30 min hypoxia + 30 mM BDM	10.11 $\pm$ 1.24	10.42 $\pm$ 1.04
60 min hypoxia	2.38 $\pm$ 1.06	6.54 $\pm$ 1.99
60 min hypoxia + 30 mM BDM	3.89 $\pm$ 0.56	12.49 $\pm$ 1.21

<sup>a</sup> Each result is mean  $\pm$  SEM of six separate experiments. The aerobic control values were obtained from hearts that had been perfused with aerobic Krebs—Henseleit buffer for 30 minutes.

<sup>b</sup>  $\mu\text{mol/gm}$  dry weight.

BDM = 2,3-butanedione monoxime; ATP = adenosine triphosphate; CP = creatine phosphate.

#### EFFECT OF BDM ON RECOVERY OF MECHANICAL FUNCTION, $\text{Ca}^{2+}$ GAIN, AND END-DIASTOLIC RESTING TENSION DURING REOXYGENATION AFTER 60 MINUTES OF HYPOXIA

Figure 8-4 shows that although BDM attenuated the hypoxic-induced rise in resting tension throughout 60 minutes of hypoxia, reoxygenation prompted a rapid rise in resting tension. At the same time there was no recovery of active tension generation (results not shown). Although BDM reduced the gain in  $\text{Ca}^{2+}$  during hypoxia, it failed to prevent  $\text{Ca}^{2+}$  from being accumulated at a relatively rapid rate (see Figure 8-3B) during reoxygenation. The relevant data in Table 8-1 show that after 60 minutes of hypoxia the ATP and CP content of even the BDM-treated hearts was now severely reduced. Thus, we have a condition in which BDM has

The alternative is that this attenuation of  $\text{Ca}^{2+}$  overload resulted from an improved preservation of the ATP and CP reserves. To explore this problem further, we have extended the period of hypoxia from 30 to 60 minutes.

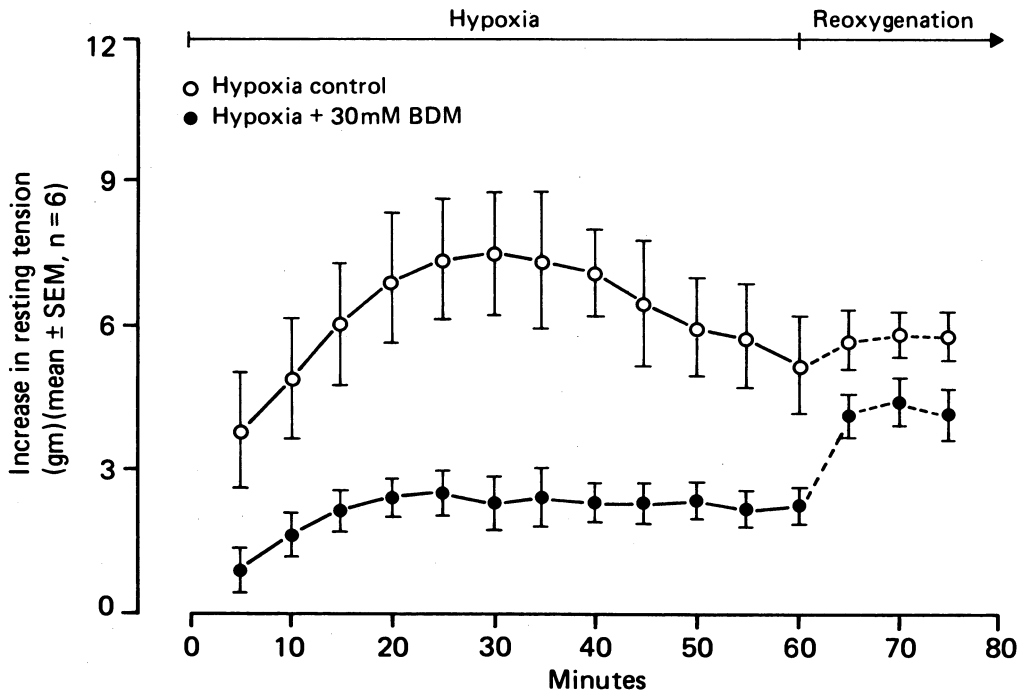


FIGURE 8-4. Effect of 30 mM BDM on the rise in resting tension caused by 60 minutes of hypoxia and on the response to reoxygenation. Each point represents the mean  $\pm$  SEM of six experiments.

attenuated the hypoxic-induced rise in resting tension but in which subsequent reoxygenation in the absence of BDM fails to stimulate active-tension generation but prompts a rapid increase in tissue  $\text{Ca}^{2+}$  and a rise in resting tension. Presumably, therefore, simply attenuating the hypoxic-induced rise in resting tension without simultaneously preserving the endogenous stores of ATP and CP does not prevent the occurrence of uncontrolled  $\text{Ca}^{2+}$  gain upon reoxygenation. Similarly, reducing the hypoxic-induced gain in  $\text{Ca}^{2+}$  does not prevent the uncontrolled  $\text{Ca}^{2+}$  gain upon reoxygenation. Hearts that had been hypoxic for 60 minutes in the presence of low  $\text{Ca}^{2+}$  K-H (0.1 mM) had a  $\text{Ca}^{2+}$  content of  $5.3 \pm 0.6 \mu\text{mol/gm}$  dry weight. However, after 5 minutes of reoxygenation with aerobic K-H this had increased to  $23.9 \pm 1.4 \mu\text{mol/gm}$  dry weight.

### Discussion

These results confirm the results of our earlier investigations [9, 19], which show that while isolated hearts gain only small amounts of  $\text{Ca}^{2+}$  during normothermic hypoxic perfusion, the reintroduction of oxygen is accompanied by a massive and apparently uncontrolled increase in cell  $\text{Ca}^{2+}$ . Despite this relatively small gain in cell  $\text{Ca}^{2+}$  during hypoxic perfusion, resting tension rises. It is unlikely that this hypoxic-induced increase in resting tension is due simply to an increase in cytosolic  $\text{Ca}^{2+}$ ; otherwise we would have expected either administering ryanodine or reducing the extracellular  $\text{Ca}^{2+}$  would have modified it. The aequorin experiments of Allen and Orchard [8] support this conclusion.

One of the interventions that was made here—namely, introducing BDM during the hypoxic episode—did attenuate the hypoxic-induced increase in resting tension. The BDM-treated hearts that were hypoxic for only 30 minutes recovered their active-tension-generating capacity upon reoxygenation and did not become overloaded with  $\text{Ca}^{2+}$ . At first glance it

is tempting to conclude that BDM, by preventing the hypoxia-induced rise in resting tension, protected the hearts so that on reoxygenation,  $\text{Ca}^{2+}$  overloading was avoided. There is, however, another plausible explanation for this "protective" role of BDM, namely, that ATP and CP reserves were well maintained in the BDM-treated hearts that had been hypoxic for only 30 minutes.

Extending the period of hypoxia to 60 minutes allowed us to distinguish between these possibilities. Thus, after 60 minutes of hypoxia, even in the presence of BDM, the endogenous reserves of ATP and CP were depleted, as seen in Table 8-1, but the rise in resting tension was still markedly attenuated. Under these conditions, reoxygenation failed to trigger the recovery of active-tension-generating capacity. Instead it prompted a marked rise in resting tension and a massive gain in  $\text{Ca}^{2+}$ .

Presumably, therefore, although BDM prevented the onset of massive contracture during hypoxia, the underlying defect that facilitated excess  $\text{Ca}^{2+}$  entry upon reoxygenation must persist.

## References

- Greene HL, Weisfeldt ML (1977). Determinants of hypoxic and posthypoxic contracture. *Am J Physiol* 232:H85-H94.
- Hearse DJ (1979). Oxygen deprivation and early myocardial contractile failure: Reassessment of the possible role of adenosine triphosphate. *Am J Cardiol* 44:1115-1121.
- Mattews PM, Taylor DJ, Radda GK (1986). Biochemical mechanisms of acute contractile failure in the hypoxic rat heart. *Cardiovasc Res* 20:13-19.
- McDonald TF, MacLeod DP (1973). Metabolism and electrical activity of anoxic ventricular muscle. *J Physiol* 229:559-582.
- Bing OH, Keefe JF, Wolk MJ, et al (1971). Tension prolongation during recovery from myocardial hypoxia. *J Clin Invest* 50:660-666.
- Harding DP, Poole-Wilson PA (1980). Calcium exchange in rabbit myocardium during and after hypoxia: effect of temperature and substrate. *Cardiovasc Res* 14:435-445.
- Bing OH, Apstein CS, Brooks WW (1975). Factors influencing tolerance of cardiac muscle to hypoxia. In Roy PE, Rona G (eds): *Recent Advances on Cardiac Structure and Metabolism*, vol 10. Baltimore: University Park Press, pp 343-354.
- Allen DG, Orchard CH (1983). Intracellular calcium concentration during hypoxia and metabolic inhibition in mammalian ventricular muscle. *J Physiol* 339:107-122.
- Nayler WG, Poole-Wilson PA, Williams A (1979). Hypoxia and calcium. *J Mol Cell Cardiol* 11:683-706.
- Ganote CE, Liu SY, Safavi S, Kaltenebach JD (1981). Anoxia, calcium and contracture as mediators of myocardial enzyme release. *J Mol Cell Cardiol* 13:93-106.
- Chamberlain BK, Volpe P, Fleischer S (1984). Inhibition of calcium-induced calcium release from purified cardiac sarcoplasmic reticulum vesicles. *J Biol Chem* 259:7547-7553.
- Blanchard EM, Mulieri LA, Alpert NR (1984). The effect of 2,3-butanedione monoxime (BDM) on the relation between initial heat and mechanical output of rabbit papillary muscle. *Biophys J* 45:48a.
- Li T, Sperelakis N, TenEick RE, Solaro JR (1985). Effects of diacetylmonoxime on cardiac excitation-contraction coupling. *J Exp Ther* 232:688-695.
- Nayler WG, Perry S, Daly MJ (1983). Cobalt, manganese and the calcium paradox. *J Mol Cell Cardiol* 15:735-747.
- Alto LE, Dhalla NS (1979). Myocardial cation contents during induction of calcium paradox. *Am J Physiol* 237:H713-H719.
- Nayler WG, Perry SE, Elz JS, Daly MJ (1984). Calcium, sodium and the calcium paradox. *Circ Res* 55:227-237.
- Lamprecht W, Trautschold I (1974). Adenosine-5'-triphosphate determination with hexokinase and glucose-6-phosphate dehydrogenase. In Bergmeyer (ed): *Methods of Enzymatic Analysis*, vol 4. New York: Academic Press, pp 2101-2110.
- Lamprecht W, Stein P, Heinz F, Weisser H (1974). Creatine phosphate determination with creatine kinase, hexokinase and glucose-6-phosphate dehydrogenase. In Bergmeyer HU (ed): *Method of Enzymatic Analysis*, vol 4. New York: Academic Press, pp 1777-1781.
- Nayler WG, Ferrari R, Poole-Wilson PA, Yezes CE (1979). A protective effect of a mild acidosis on hypoxic heart muscle. *J Mol Cell Cardiol* 11:1053-1071.

---

## 9. ISCHEMIC/HYPOXIC AND REPERFUSION/REOXYGENATION CONTRACTURES: MECHANISMS

---

A.H. Henderson

By the late 1960s it had become apparent that myocardial ischemia was associated with a reversible rise in end-diastolic pressure [1]. Whether this represented a change in myocardial stiffness was not then clear and was to remain controversial for some years: the complexities of dissociating hemodynamic from myocardial properties are not unique to systolic function. The observation nevertheless marked a renewal of interest in diastolic function whose importance had been rather neglected since before the days of Harvey.

### *Ischemic/Hypoxic Contracture*

Studies with isolated papillary muscle preparations allowed an experimental approach to the myocardial consequences of ischemia, free of the confounding influences of hemodynamic changes and of the vascular system and its contents. Not being perfused through a coronary bed, these preparations do not provide a total model of ischemia, but oxygen deprivation is a major and relevant component of ischemia. Observations on the effects of hypoxia and reoxygenation are thus essentially pertinent to ischemia and reperfusion. Importantly, hypoxia reproduces the phenomenon of contracture.

#### DEFINITION

Contracture is defined as a rise in resting force at constant length, or a reduction in resting length at constant force, i.e., an increase in resting myocardial stiffness. It differs from active contraction (which can be viewed in terms of

changing stiffness) only in that it is present at rest.

#### IS IT DUE TO CALCIUM?

Circumstantial evidence from a number of studies on the reversible contracture induced by hypoxia in rat papillary muscle preparations suggested that it was related to the severity of energy deprivation. Thus it was shown to be related to the duration and severity of oxygen deprivation, to be worse with free fatty acids than with glucose as exogenous substrate, and to correlate generally with the depression of systolic force development (though, interestingly, glucose had a relatively greater protective effect in respect of the contracture than of the contraction) [2, 3]; others reported that hypoxic contracture in stimulated, contracting preparations was increased by isoproterenol and decreased by verapamil and acidosis, effects attributed likewise to the changes in energy balance [4].

The alternative view that ischemic/hypoxic contracture might be due to raised levels of free calcium was nevertheless argued by others [5], in the light of evidence that calcium antagonists reduced hypoxic contracture in perfused hearts. This hypothesis was attractive because it offered therapeutic possibilities. It has become increasingly clear, however, that the protective effect of calcium antagonists in these perfused heart models is likely to be attributable predominantly and perhaps wholly to their energy-sparing negative inotropic effect.

Further experiments with rat papillary muscle preparations showed that hypoxic contracture was influenced by pH even in quiescent muscles and thus independently of its inotropic

*Grossman, William, and Lorell, Beverly H. (eds.), Diastolic Relaxation of the Heart. Copyright © 1987. Martinus Nijhoff Publishing. All rights reserved.*

effect: contracture was exaggerated at pH 7.8 [6] and reduced at pH 6.8 [7]. In resting as in stimulated muscles, hypoxic contracture was temperature-related, and slightly greater in contracting than quiescent muscles. In resting muscles its relationship to exogenous substrate persisted, it was not ameliorated by verapamil ( $10^{-4}$  M), propranolol ( $10^{-4}$  M) or lanthanum (2 mM), and not altered by elevating (to 7.5 mM) or reducing (to "zero") extracellular calcium; only in contracting muscles, and thus by implication where they altered energy consumption, did these interventions alter the severity of hypoxic contracture (Figure 9-1) [7]. These experiments therefore provided no evidence that hypoxic contracture was due to raised resting levels of calcium within the cell as influenced by the availability of extracellular calcium. Experiments were carried out to investigate whether calcium derived from an intracellular source might contribute, using caffeine as the tool to release calcium internally. High-dose caffeine (20 mM) had no effect on hypoxic contracture in resting rat papillary muscle preparations in the presence or absence of extracellular calcium [7]. In contracting preparations, by contrast, the addition even of a low dose of caffeine (2.5 mM), despite reducing active force development [8], led after a few minutes to obvious exaggeration of the hypoxic contracture (see Figure 9-1). Caffeine has been shown likewise to increase diastolic tension in a dog model of pacing-induced myocardial ischemia [9].

#### CAFFEINE

Caffeine has a number of effects on myocardium, in addition to its vasodilator action on vascular smooth muscle:

1. inhibits phosphodiesterase, thereby increasing cyclic adenosine monophosphate (cAMP) levels, which will (a) increase calcium influx through the slow channel, (b) enhance calcium uptake by sarcoplasmic reticulum (SR) so that more is available for subsequent contractions, and (c) reduce the affinity of troponin for calcium so that relaxation occurs earlier.
2. increases the permeability of the SR [10] so that calcium leak (a) can cause a transient contracture [11] associated with a rise in cytosolic calcium following the addition of high-dose caffeine [12], (b) impairs net calcium uptake, converting load-dependent

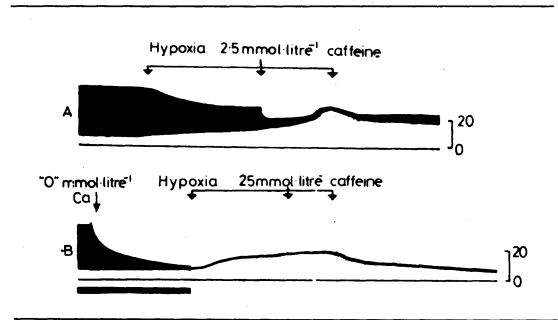


FIGURE 9-1. Slow paper-speed trace of force generated by rat papillary muscle preparation at  $29^{\circ}\text{C}$ , stimulated to contract isometrically at 0.2 Hz during the period shown by the lower solid bar. Bathing solution was replaced by solution containing no added calcium as shown. The preparation was subjected to 30 minutes of hypoxia. The lower trace shows that hypoxic contracture occurred in the "absence" of extracellular calcium, and in unstimulated as in contracting muscle. The addition of high-dose caffeine had no effect in unstimulated muscle. The upper trace shows that in stimulated contracting preparations caffeine depressed active-force development (as in oxygenated preparations) and then increased resting force.

relaxation of twitch contractions to activation-dependent relaxation [13] and slowing relaxation, (c) reduces the availability of intracellular calcium for subsequent beats, thus contributing a negative inotropic effect [8] associated with a reduction in the measured calcium transient [14] and accounting probably for the slowed onset of activation [15], and (d) increases adenosine triphosphatase (ATPase) activity and energy utilization by isolated preparations of SR [10].

3. shifts the force/calcium relationship of the contractile proteins thus increasing their calcium sensitivity [14, 16-19].

The resultant effects of caffeine will be species-frequency-dose- and temperature-dependent. Experimental findings with caffeine are thus difficult to interpret with certainty. The complexity of caffeine's actions means that additional measurements are needed to identify its resultant effects with certainty in any given situation. Its effects on the hypoxic contracture may be attributable to the additional calcium influx in contracting (but not resting) prepara-

tions at a time when SR function is likely to be impaired already by energy lack [20] and to become further impaired by caffeine; this will favor intracellular calcium overload, which may slow relaxation and increase resting levels of calcium to contribute actively to resting force; in addition, the increase in energy-dependent uptake of calcium into the leaky SR may increase energy utilization, whereas the energy-dependent uptake of excess calcium into mitochondria would result in a reduction of energy export from these organelles.

#### ACIDOSIS

The protective effect of acidosis even in resting muscles might in theory be attributable to an effect on energy production. However, acidosis is now known to reduce the tension response of the contractile proteins to calcium, acting in the reverse direction to caffeine.

#### DOES DELAYED RELAXATION CONTRIBUTE?

Delayed relaxation of contraction cannot contribute to the rise in resting tension of ischemic/hypoxic contracture in isolated muscle preparations. The duration of depolarization and contraction, which is relatively long at the slow frequencies of contraction employed in these isolated preparations, is markedly reduced by hypoxia (in marked contrast to what occurs on reperfusion/reoxygenation); moreover, hypoxic contracture was shown to develop equally in resting preparations. Nevertheless, there is evidence that relaxation is affected by hypoxia in that the normal load-dependent relaxation of mammalian myocardial contractions is lost [13]. Load-dependency of relaxation implies that cytosolic free-calcium levels have already been reduced so that cross-bridge detachment as influenced by mechanical loading is not followed by reactivation and is thus the rate-limiting step in mechanical relaxation. Loss of load-dependency implies that free calcium levels are maintained so that cross-bridge bonds can reform and the decline of free calcium becomes the rate-limiting step; this happens when calcium uptake by SR is impaired. Slight changes in SR function do not, on this analysis, influence the onset or rate of mechanical relaxation in normal mammalian muscle preparations, whereas they can when SR function is impaired—by caffeine or low ATP levels and possibly in myocardial hypertrophy, where biochemical evidence indicates impaired SR function.

At faster physiologic heart rates in vivo, the durations of depolarization and contraction are much shorter, and they are not obviously shortened by ischemia or hypoxia. Slowing of relaxation could therefore intrude importantly on the time that is available for diastolic filling (see Effects of Ischemia on Diastolic Stiffness In Vivo).

#### CALCIUM MEASUREMENTS

Measurements in isolated preparations showed no evidence of increase in net calcium influx during the course of hypoxic contracture [21]; however, measurable net influx probably depends on gross, energy-dependent deposition in mitochondria, such as occurs on reperfusion/reoxygenation and only to a small extent during ischemia [22]. Although there has been some conflict of data from direct measurements of intracellular free calcium, with different probes and in different experimental preparations, and there are uncertainties arising from heterogeneity of sampling with respect to intracellular calcium measurements in contrast to the lumped measurement of tension responses, most evidence seems now to indicate that resting free calcium levels do not rise measurably even with severe hypoxic contracture [23, 24]. In some instances a late rise of free calcium is seen but this probably reflects the onset of irreversible cell damage. These findings would seem to indicate that hypoxic contracture in these isolated preparations is not dependent on a rise in resting intracellular free calcium, and thus to confirm the earlier circumstantial evidence.

#### RIGOR

The alternative conclusion is that ischemic/hypoxic contracture is due to rigor. This view is supported by stiffness measurements. Rigor is characterized by the formation of cross-bridges between the contractile proteins whose lack of ATP prevents them from detaching as in normal cross-bridge cycling. It occurs at very low levels of ATP ( $< 16 \mu\text{M/gm}$  dry weight) [25–27]. Quick-release measurements in 1969 showed that hypoxic contracture was associated with an increase in relative stiffness, interpreted at the time in model terms as an increase in series-elastic-element stiffness [28]. This suggested that the mechanism underlying the rise in force is different from that which actively increases force during a contraction. The findings of the

quick-release data were confirmed and extended in a subsequent on-line study of myocardial stiffness in isolated papillary muscles, using electronic circuitry to analyze the responses to rapid (50–100 Hz), small-amplitude (0.1–0.25%  $l_{max}$ ) sinusoidal length perturbations (Figure 9–2) [29]. Stiffness increases as a linear function of tension during active force generation, according to the relationship:

$$dT/dl = kT + c$$

(where  $T$  is tension,  $l$  is length in  $l_{max}$ ,  $dT/dl$  is stiffness, and  $k$  and  $c$  are constants). The stiffness-tension relationship is unaffected by changes in resting length or inotropic state. During hypoxic contracture, however, the relationship is shifted, predominantly by an increase in the intercept  $c$ , representing stiffness at zero tension, the slope  $k$  altering little. The intercept “ $c$ ” was shown to be closely and linearly related to resting force, both as this increases during the course of hypoxic contracture and as it declines during reoxygenation, remaining unchanged unless contracture occurs—there was no suggestion of an early or late departure from this relationship and thus no suggestion that any component of the contracture was due to anything other than the phenomenon reflected in this changing intercept of the force-stiffness relationship. We conclude that hypoxic contracture is characterized by an additional component of stiffness, present in resting muscles and not participating in active force development. Ischemic/hypoxic contracture is thus attributable to the development of fixed (but reversible) rigor bonds.

#### BREAKING OF RIGOR BONDS

Quick systolic stretches had been observed to reduce resting force and increase active force development in papillary muscle preparations whose performance had declined in long experiments [30]. In the stiffness experiments, hypoxic contracture could be slightly but clearly reduced by a brief imposition of the rapid length perturbations during the interval between contractions, though this had no effect on resting force in the absence of hypoxic contracture; the reduction in resting force was then maintained and a further reduction could only be achieved after hypoxic contracture had further progressed; the slight reduction of contracture was associated with a corresponding reduction of the stiff-

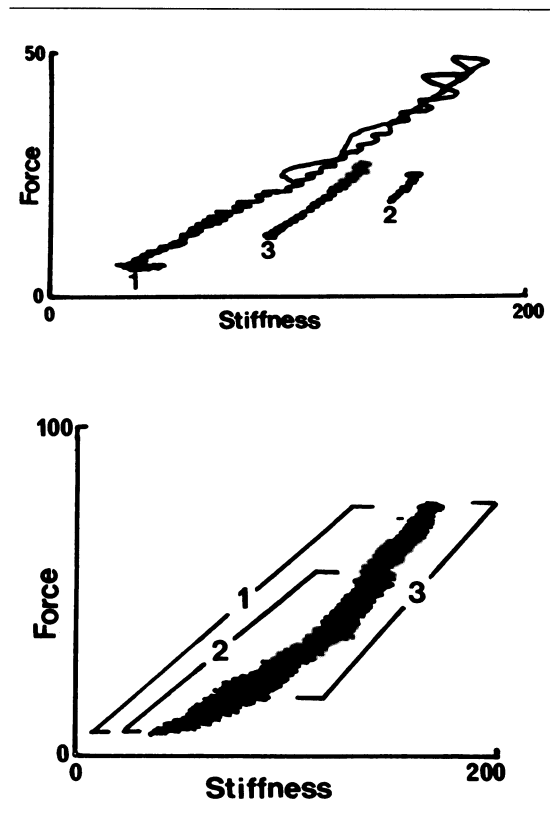


FIGURE 9–2. On-line traces of stiffness vs. force in three individual isometric contractions of representative papillary muscle preparations. Left trace (rat papillary muscle) shows, superimposed, (1) control, (2) 30 minutes of hypoxia, (3) 5 minutes of reoxygenation. Note that with hypoxic contracture the stiffness-force relationship is reversibly shifted, predominantly through a shift of the intercept at zero force. Right trace (cat papillary muscle in the presence of  $10^{-6}$  mM ouabain), shows superimposed (1) control, (2) 60 minutes of hypoxia, (3) 5 minutes of reoxygenation. Note that with reoxygenation contracture there is no change in the stiffness-force relationship.

ness constant  $c$ , consistent with mechanical breaking of rigor bonds [29]. Appreciating that ischemic fibers are subject to stretch by contraction of adjacent normal myocardium in the clinical setting, Apstein and Ogilby [31] showed in experiments with globally ischemic dog hearts that the imposition through an intraventricular balloon of systolic stretches could prevent the contracture that otherwise occurred.

Rigor thus appears to account for ischemic as well as for hypoxic contracture, but its consequences may be modified in vivo.

#### ADDITIONAL CONTRIBUTION OF CALCIUM TO ISCHEMIC/HYPOXIC CONTRACTURE

The demonstration that contracture is due primarily to rigor does not of course exclude an additional component which can be attributed to increased calcium levels in some circumstances. Such circumstances include severe ischemia with possibly irreversible damage of some cells in these heterogeneous preparations or experimental treatment with high-dose caffeine, or reperfusion, which is likely to occur in clinical situations with intermittent ischemia. Hearse and colleagues [26] were able in a perfused rat heart model to reduce the magnitude of ischemic contracture (though not delay its onset) at the same low level of high energy phosphates by reducing extracellular calcium or by D600, suggesting the possibility of an additional contribution of calcium to resting force, though a vascular effect cannot be excluded. Jarmakani and colleagues [27] studying anoxic perfused rabbit septa found that contracture was related primarily to low levels of high energy phosphates; however, they also found that it was slightly less at the same low energy levels when the preparations were not contracting or when extracellular calcium was absent, suggesting an additional contribution of calcium in this model too, perhaps by favoring the formation of rigor bonds at any given inadequate level of ATP. The data in this respect are inconclusive.

#### *Reperfusion/Reoxygenation Contracture*

It is now well known that reperfusion and reoxygenation paradoxically make things worse. They precipitate arrhythmias, ultrastructural cell damage, the release of cytoplasmic enzymes, massive influx of calcium and sodium, deposition of calcium within mitochondria, and contraction band necrosis. The question has been whether this reperfusion injury represents simply an accelerated manifestation of predestined damage from ischemia or whether it is actually caused by reperfusion and is thus potentially amenable to therapeutic prevention. This question is related to the mechanism of reperfusion injury and to the causal chain of events that reperfusion initiates.

There are of course important differences

between reperfusion and reoxygenation, related largely to the greater accumulation of metabolites and osmotic load with ischemia and the consequential transmembrane gradients and cell swelling on reperfusion. This is visibly obvious as explosive swelling on reperfusion of an isolated ischemic heart. The important erectile contribution of changes in coronary flow to overall left ventricle stiffness has been well documented [32]. Changes in vascular tone, the contribution of vascular contents, and the delivery of possible sources of free radicals from activated leukocytes or catecholamines all have to be considered. Nevertheless, reoxygenation and the generation of energy comprise an essential component of reperfusion. This can be studied in isolated preparations independently of complicating variables. Under appropriate conditions, reoxygenation causes contracture as an entity quite distinct from hypoxic contracture and thus separately amenable to experimental investigation. A comparison of hypoxic and reoxygenation contractures has been useful.

#### REPERFUSION REOXYGENATION CONTRACTURE IS CALCIUM-MEDIATED

There can be little doubt that reoxygenation contracture, as distinct from hypoxic contracture, is mediated primarily by raised resting-calcium levels within the cell. It can be more readily elicited in papillary muscle preparations if these are "primed" with cardiac glycosides. Reoxygenation of cat or rabbit papillary muscle preparations then causes an immediate severe rise in resting force associated with the subsequent decline and cessation of active contractile activity, from which the muscle cannot be recovered and which must be regarded as leading irreversibly to cell death (Figure 9-3) [6, 33, 34]. Reduction of extracellular calcium at the time of reoxygenation prevents reoxygenation contracture, whether the muscles are contracting or resting [6]. Verapamil  $10^{-4}$  M and lidoflazine ( $2 \cdot 10^{-5}$  M) introduced at the time of reoxygenation had no effect; diltiazem ( $10^{-4}$  M),  $Mg^{2+}$  (30 mM),  $Mn^{2+}$  (8 mM), or acidosis-reduced reoxygenation contracture without preventing its subsequent development [34]. These findings indicate that the contracture is mediated by calcium influx. They indicate also that it does not occur through the slow calcium channel, while suggesting that diltiazem may possess properties additional to those of a "calcium antagonist." The effects of  $Mg^{2+}$ ,

$Mn^{2+}$ , and  $H^+$  are attributable to nonspecific interference with calcium influx, possibly by interfering with  $Na/Ca$  exchange. None of these agents allowed recovery of contractile function in these experiments.

#### REOXYGENATION DAMAGE IS PREVENTABLE

Importantly, it was possible to prevent reoxygenation contracture and allow recovery of contractile function by protecting the muscle from calcium overload while allowing metabolic recovery: this could be achieved by lowering extracellular calcium at the time of reoxygenation (though not to a level that would damage the sarcolemma and lead to the "calcium paradox") and then gradually reintroducing it (see Figure 9-3) [33, 34]. This confirms findings that reperfusion damage could be reduced by similar temporary reduction of extracellular calcium [35] or exposure to EDTA [36] in perfused preparations, from which experiments it was not possible absolutely to exclude a vascular effect, and is consistent with observations that recovery of contractile function on reperfusion can be influenced by the  $Ca^{2+}$ ,  $K^+$ , and  $Mg^{2+}$  concentrations in the buffer used for reperfusion [37].

#### DOES DELAYED RELAXATION CONTRIBUTE?

In contrast with hypoxia, reoxygenation prolongs relaxation to a bizarre degree in isolated preparations [4, 38, 39]. Nevertheless, it is clear that reoxygenation contracture in these preparations cannot be directly attributed to inadequate relaxation because of the slow frequencies of contraction employed and because it occurs equally in resting preparations. Delayed relaxation and reoxygenation contracture may, however, both be manifestations of the same underlying problem of calcium overload within the cell. Reoxygenation contracture begins to develop at a time when active contraction is maintained, unlike hypoxic contracture when loss of active contraction precedes the development of contracture. Experimentally, relaxation on reoxygenation was further prolonged by ouabain (to increase intracellular sodium) and reduced by high-dose insulin in the absence of glucose (to promote sodium extrusion); the phenomenon is much less obvious in frog myocardium (unpublished observations), which possesses only sparse SR so that intracellular

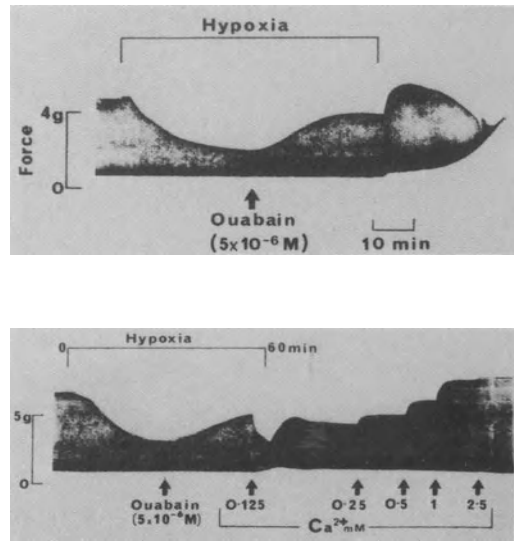


FIGURE 9-3. Slow paper-speed trace of cat papillary muscle preparation in the presence of ouabain added during a 60-minute period of hypoxia. Reoxygenation induces contracture with loss of contractile activity. This can be prevented with recovery of contractile activity by temporary reduction of extracellular calcium.

calcium control is presumably dependent more on other mechanisms, or in skeletal muscle, which shares with frog myocardium a poorer provision of mitochondria, suggesting the possibility of a mitochondrial role in the phenomenon [40].

#### STIFFNESS

Figure 9-2 shows that the stiffness-force relationship during reoxygenation contracture remained the same as during active force development, in direct contrast to the shift that characterizes hypoxic contracture [29]. This implies that the mechanism of the rise in resting force is similar to that of active force generation, i.e. it represents calcium-activated normal contraction, albeit tonic. Prolonged calcium-mediated contracture, as induced by high  $K^+$ , shows a gradual upward shift of the stiffness-force relationship after some minutes, as maintained calcium-mediated normal force generation leads to energy deficit and thus secondarily to rigor.

### CAUSES AND ROUTE OF CALCIUM INFLUX

Among possible mechanisms of the damaging influx of calcium that occurs on reperfusion/reoxygenation, Ganote and colleagues have argued that it is the force of contracture that causes mechanical rupture of sarcolemmal membranes, leading to massive calcium influx, leakage of large-molecular-weight enzymes and adenine nucleotides, and cell death [41]. This seems unlikely to be the whole story, however, because enzyme leakage occurs under conditions where reperfusion contracture does not occur, and extracellular markers show no loss of sarcolemmal integrity in some preparations exhibiting reperfusion/reoxygenation contracture [21, 42]; a study of the transmural cell damage showed moreover that contraction bands occurred predominantly in the mid-portion, whereas the sarcolemmal damage was diffuse [43]. Jennings and colleagues have recently shown that a combination of energy deprivation and osmotic swelling can cause sarcolemmal rupture, which does not occur with either insult alone, and they suggest that energy deprivation weakens the cytoskeleton [44, 45]—somewhat analogously to the mechanism proposed for the calcium paradox where lack of calcium weakens intercalated discs, and the reintroduction of calcium, either from extracellular or intracellular sources [46], leads to force generation sufficient to rupture the sarcolemma. Jennings and colleagues suggest that the osmotic load incurred during ischemia primes the cell for an explosive swelling with resultant mechanical stress once it is reperfused, although these effects are likely to be less marked on reoxygenation than on reperfusion. This is an attractive hypothesis to account for events with more severe ischemia but it is unlikely to account for the calcium influx that occurs during reoxygenation/reperfusion while sarcolemmal integrity is preserved (with respect to large molecules) and whose consequence in the form of contracture can be shown to be reversible. This influx of calcium cannot be due to gross loss of sarcolemmal integrity.

### FREE RADICALS

The role of oxygen-based free radicals is a subject of intense investigation at present. There are a number of possible sources, evidence that they can cause changes in sarcolemmal permeability to cations, and supportive circumstantial evidence, with species differences,

that prevention of radical formation or radical scavengers can reduce reperfusion damage.

### EXAGGERATED CALCIUM ENTRY THROUGH NORMAL CHANNELS

Loss of sarcolemmal structural or functional integrity may not in fact be a prerequisite for the increased calcium influx of reperfusion/reoxygenation. The pharmacologic evidence shows that it does not occur through the slow channels. It could, however, occur through  $\text{Ca}^{2+}/\text{Na}^{+}$  exchange which the gain of intracellular sodium during ischemia would favor. However, reperfusion causes the cell to gain sodium as well as calcium. Moreover, recent measurements have shown no evidence of sodium efflux associated with calcium influx (P.A. Poole-Wilson, personal communication). This is not necessarily incompatible with the hypothesis. Lazdunski and colleagues have proposed that the gain in intracellular sodium on reperfusion can be explained by the outward  $\text{H}^{+}$  gradient which then exists, with consequent activation of the  $\text{Na}^{+}/\text{H}^{+}$  antiporter; this would mean, at a time of depressed Na-K-ATPase activity, that sodium homeostasis is achieved by the  $\text{Na}^{+}/\text{Ca}^{2+}$  exchange system, leading to calcium influx but little net movement of sodium [47].

### *Effects of Ischemia on Diastolic Stiffness In Vivo*

The isolated muscle data show that (1) reversible rigor can account for the rise in resting stiffness that follows severe energy depletion; (2) the massive calcium entry which could cause tonic active tension is likely to reflect (a) the later development of irreversible cell damage, or (b) the ionic consequence of reperfusion; and (3) delayed relaxation does not contribute to the rise in resting tension in these models though it could in vivo. These models thus identify potential contributory mechanisms for a rise in diastolic stiffness of ischemic myocardium in vivo. The net effect of the changes induced by ischemia will obviously differ with the model and with circumstance. Isolated muscle preparations that are quiescent or contracting at low rates will clearly differ from perfused hearts contracting at physiologic rates; prolonged ischemia, from brief ischemic insult; global ischemia, from regional ischemia in which muscle is subject to stretching by the contractions of normal myocardium; paced global ischemia,

from ischemia that involves the natural pacemaker and leads to bradycardia. Whether the insult is ischemia or hypoxia, the severity of energy deprivation, frequency of contraction, temperature, interfiber creep, and breaking of rigor bonds must all be taken into consideration. In the intact heart, moreover, it is much more difficult to identify real changes in myocardial stiffness (active or passive). Effects of coronary turgor are important, chamber compliance that is influenced by the volume of other chambers within the pericardium must be distinguished from myocardial compliance, and acute changes in force must be related to the muscle length at which they are generated.

Brief periods of ischemia, such as occur clinically with angina or during angioplasty, have been studied experimentally in intact hearts and shown to cause a rise in end-diastolic stiffness within minutes [48, 49]. In this situation, endocardial ATP levels are only slightly depressed and are certainly not low enough to account for rigor without postulating a remarkable degree of compartmentalization within the cells. Moreover, interesting differences emerge between the effects of experimental coronary artery occlusion and of hypoxia or pacing-induced ischemia in regions of limited coronary perfusion reserve. Thus, coronary artery occlusion caused little or no rise in diastolic stiffness compared to a marked rise with hypoxia or pacing-induced ischemia. With coronary artery occlusion there was also a greater decline in systolic contraction such that the ischemic fibers were subject to stretch, a loss of coronary turgor which contributed to but did not appear wholly to account for the difference, and a greater loss of creatine phosphate and accumulation of metabolites such as phosphate and hydrogen ions—raising the possibility that acidosis and/or phosphate were depressing active tension through their known effect on the contractile protein response to calcium, with phosphate also acting as a buffer for calcium and thereby lowering free calcium levels.

The reason for the rise in diastolic stiffness with these brief (e.g., 3 minutes) periods of ischemia, at least when the ischemia is pacing-induced, is not entirely clear. There is circumstantial evidence that it may be related to calcium overload within the cell. The *in vivo* studies with ischemic models appear to show a general correlation between slowing of relaxation and a rise in diastolic stiffness. Activation-

dependent slowing of relaxation is thought to reflect impairment (at low ATP levels) and/or overloading of SR capacity to take up calcium. An extreme experimental example of this is provided by reoxygenation where the rise in resting tension is clearly calcium-mediated. Less extreme examples of calcium overloading in the cell are known to favour oscillatory, generally asynchronous, contractile activity in resting muscle, which can generate measurable tension. More sophisticated measurements of myocardial stiffness, by phase-plane analysis of velocity-length relationships on abrupt removal of load in isolated muscles, shows that it is related to the contractile state of the previous contraction and declines only very slowly over many minutes of rest (D.L. Brutsaert and A.H. Henderson, unpublished observations). It is a familiar experimental observation that pacing isolated buffer-perfused hearts to high frequency causes a rise in resting pressure (at constant volume), which is generally attributed to inadequate relaxation and which persists for a time when pacing is stopped. Contraction frequency will clearly influence net calcium influx into the cell and thus increase the calcium load on intracellular homeostatic control mechanisms. Calcium overload leading to raised free-calcium levels at rest and increased intracellular cycling of calcium cannot of course be considered in isolation from its consequences on the energy status of the cell, for calcium pumping will consume energy, and excess calcium can "steal" the potential export of mitochondrial energy to the cell. The observation that caffeine exaggerates the pacing-induced upward shift in the pressure-volume relationship in dogs with experimental coronary artery stenosis [9] provides circumstantial support for this view of events without rigorously testing it.

There is no clean demarcation between active tension development and resting diastolic tension, between active and resting stiffness, between contraction and contracture: the transition from peak levels of activation during systole to the resting state, which represents predominantly passive viscoelastic properties but some potential contribution of residual activity, is not an abrupt step. A delay in the decline of activation will intrude on diastolic filling relatively more at higher frequencies of contraction, damping the momentum of recoil, slowing early filling, and to a lesser extent reducing the adequacy of inactivation by the time of end-

diastole. The functionally important diastolic filling volumes will in turn reflect the interaction of changing load on this changing tension-length relationship.

### References

- Parker JO, Ledwich JR, West RO, Case RB (1969). Reversible cardiac failure during angina pectoris: Hemodynamic effects of atrial pacing in coronary artery disease. *Circulation* 39:745-757.
- Henderson AH, Most AS, Sonnenblick EH (1969). Depression of contractility in rat heart muscle by free fatty acids during hypoxia. *Lancet* 2:825-826.
- Henderson AH, Most AS, Parmley WW, et al (1970). Depression of myocardial contractility in rats by free fatty acids during hypoxia. *Circ Res* 16:439-449.
- Bing OHL, Brooks WW, Messer JV (1973). Heart muscle viability following hypoxia: Protective effect of acidosis. *Science* 180:1297-1298.
- Nayler WG, Poole-Wilson PA, Williams A (1979). Hypoxia and calcium. *J Mol Cell Cardiol* 11:683-706.
- Greene HL, Weisfeldt ML (1977). Determinants of hypoxic and posthypoxic myocardial contracture. *Am J Physiol* 232(5):H526-533.
- Lewis MJ, Grey AC, Henderson AH (1979). Determinants of hypoxic contracture in isolated heart muscle preparations. *Cardiovasc Res* 13: 86-94.
- Henderson AH, Brutsaert DL, Forman R, Sonnenblick EH (1974). Influence of caffeine on force development and force-frequency relations in cat and rat heart muscle. *Cardiovasc Res* 8:162-172.
- Paulus WJ, Serizawa T, Grossman W (1982). Altered left ventricular diastolic properties during pacing-induced ischemia in dogs with coronary stenoses. *Circ Res* 50:218-277.
- Blayney L, Thomas H, Muir J, Henderson AH (1978). Action of caffeine on calcium transport by isolated fractions of myofibrils, mitochondria, and sarcoplasmic reticulum from rabbit heart. *Circulation* 43:520-526.
- Chapman RA, Leoty C (1976). The time-dependent and dose-dependent effects of caffeine on the contraction of the ferret heart. *J Physiol* 256:287-314.
- Sorenson MM, Coelho HSL, Reuben JP (1986). Caffeine inhibition of calcium accumulation by the sarcoplasmic reticulum in mammalian skinned fibers. *J Membr Biol* 90:219-230.
- Chuck LHS, Goethals MA, Parmley WW, Brutsaert DL (1981). Load-insensitive relaxation caused by hypoxia in mammalian cardiac muscle. *Circ Res* 48:797-803.
- Konishi M, Kurihara S, Sakai T (1984). The effects of caffeine on tension development and intracellular calcium transients in rat ventricular muscle. *J Physiol* 355:605-618.
- Henderson AH, Claes VA, Brutsaert DL (1973). Influence of caffeine and other inotropic interventions on the onset of unloaded shortening velocity in mammalian heart muscle. *Circ Res* 33:291-302.
- Fabiato A, Fabiato F (1976). Techniques of skinned cardiac cells and of isolated cardiac fibres with disrupted sarcolemmas, with reference to the effects of catecholamines and of caffeine. *Rec Adv Stud Cardiac Struct Metab* 9:71-94.
- Wendt IR, Stephenson DG (1983). Effects of caffeine on Ca-activated force production in skinned cardiac and skeletal muscle fibres of the rat. *Pfluegers Arch* 398:210-216.
- Eisner DA, Valdeolmillos M (1984). The mechanism of the increase of tonic tension produced by caffeine in sheep cardiac Purkinje fibres. *J Physiol* 364:313-326.
- Delay M, Ribalet B, Vergara J (1986). Caffeine potentiation of calcium release in frog skeletal muscle fibres. *J Physiol* 375:535-559.
- Schwartz A, Sordahl LA, Entman et al (1973). Abnormal biochemistry in myocardial failure. *Am J Cardiol* 32:407-422.
- Harding DP, Poole-Wilson PA (1980). Calcium exchange in rabbit myocardium during and after hypoxia: Effect of temperature and substrate. *Cardiovasc Res* 14:435-445.
- Nayler WG (1981). The role of calcium in the ischemic myocardium. *Am J Pathol* 102: 262-270.
- Allen DG, Orchard CH (1983). Intracellular calcium concentration during hypoxia and metabolic inhibition in mammalian ventricular muscle. *J Physiol* 339:107-122.
- Allen DG, Orchard CH (1984). Measurements of intracellular calcium concentration in heart muscle: the effects of inotropic interventions and hypoxia. *J Mol Cell Cardiol* 16:117-128.
- Katz A, Tada M (1972). The "stone heart": A challenge to the biochemist. *Am J Cardiol* 29:578-580.
- Hearse DJ, Garlick PB, Humphrey SM (1977). Ischemic contracture of the myocardium: Mechanisms and prevention. *Am J Cardiol* 39:986-983.
- Jarmakani JM, Nagatomo T, Langer GA (1978). The effect of calcium and high-energy phosphate compounds on myocardial contracture in the newborn and adult rabbit. *J Mol Cell Cardiol* 10:1017-1029.
- Henderson AH, Parmley WW, Sonnenblick

- EH (1971). The series elasticity of heart muscle during hypoxia. *Cardiovasc Res* 5:10-14.
29. Lewis MJ, Housmans PR, Claes, VA, et al (1980). Myocardial stiffness during hypoxic and reoxygenation contracture. *Cardiovasc Res* 14: 339-344.
  30. Brutsaert DL, Vermeulen FE, Arntzenius AC, Hugenholz PG (1970). Recovery of the contractility of depressed cat papillary muscles by repeated quick stretch-release. *Arch Int Pharmacodyn Ther* 185:194-195.
  31. Apstein CS, Ogilby JD (1980). Effects of "paradoxical" systolic fiber stretch on ischemic, myocardial contracture, compliance, and contractility in the rabbit. *Circ Res* 46:745-754.
  32. Vogel WM, Briggs LL, Apstein CS (1985). Separation of inherent diastolic myocardial fiber tension and coronary vascular erectile contributions to wall stiffness of rabbit hearts damaged by ischemia, hypoxia, calcium paradox and reperfusion. *J Mol Cell Cardiol* 17:57-70.
  33. Chappell SP, Lewis MJ, Henderson AH (1983). Myocardial reoxygenation damage can be circumvented. *J Mol Cell Cardiol* 15 (suppl 1):329.
  34. Chappell SP, Lewis MJ, Henderson AH (1985). Myocardial reoxygenation damage: Can it be circumvented? *Cardiovasc Res* 19:299-303.
  35. Shine KL, Douglas AM (1983). Low calcium reperfusion of ischaemic myocardium. *J Mol Cell Cardiol* 15:251-260.
  36. Ogilby JD, Apstein CS (1983). Reversal of reperfusion injury with post-ischemia EDTA pulse therapy. *J Mol Cell Cardiol* 15 (suppl 1):330.
  37. Kuroda H, Ishiguro S, Mori T (1986). Optimal calcium concentration in the initial reperfusion for post-ischemic myocardial performance (calcium concentration during reperfusion). *J Mol Cell Cardiol* 18:625-633.
  38. Tyberg JV, Yeatman LA, Parmley WW, et al (1970). Effects of hypoxia on mechanics of cardiac contraction. *Am J Physiol* 218:1780-1788.
  39. Bing OHL, Keefe JF, Wolk MJ (1971). Tension prolongation during recovery from myocardial hypoxia. *J Clin Invest* 50:660-666.
  40. Bing OHL, Brooks WW, Messer JV (1976). Prolongation of tension on reoxygenation following myocardial hypoxia: A possible role for mitochondria in muscle relaxation. *J Mol Cell Cardiol* 8:205-215.
  41. Ganote CE, Kaltenbach JP (1979). Oxygen-induced enzyme release: Early events and a proposed mechanism. *J Mol Cell Cardiol* 11: 389-406.
  42. Bourdillon PDV, Poole-Wilson PA (1981). Effects of ischaemia and reperfusion on calcium exchange and mechanical function in isolated rabbit myocardium. *Cardiovasc Res* 15:121-130.
  43. Humphrey SA, Vanderwee MA (1986). Factors affecting the development of contraction band necrosis during reperfusion of the isolated isovolumic rat heart. *J Mol Cell Cardiol* 18: 319-329.
  44. Steenbergen C, Hill ML, Jennings RB (1985). Volume regulation and plasma membrane injury in aerobic, anaerobic, and ischemic myocardium in vitro. *Circ Res* 57:864-875.
  45. Jennings RB, Reimer KA, Steenbergen C (1986). Myocardial ischemia revisited: The osmolar load, membrane damage, and reperfusion. *J Mol Cell Cardiol* 18:769-780.
  46. Heide RSV, Altschuld RA, Lamka KG, Ganote CE (1986). Modification of caffeine-induced injury in  $Ca^{2+}$ -free perfused rat hearts. *Am J Pathol* 123:351-364.
  47. Lazdunski M, Frelin C, Vigne P (1985). The sodium/hydrogen exchange system in cardiac cells: Its biochemical and pharmacological properties and its role in regulating internal concentrations of sodium and internal pH. *J Mol Cell Cardiol* 17:1029-1042.
  48. Paulus WJ, Grossman W, Serizawa T et al (1985). Different effects of two types of ischemia on myocardial systolic and diastolic function. *Am J Physiol* 248 (Heart Circ Physiol 17): H719-H728.
  49. Monomura S, Ingwall JS, Parker JA, et al (1985). The relationship of high energy phosphates, tissue pH, and regional blood flow to diastolic distensibility in the ischemic dog myocardium. *Circ Res* 57:822-835.

---

# 10. LOAD DEPENDENCE OF RELAXATION

---

Dirk L. Brutsaert and Stanislas U. Sys

The mechanical performance of the heart as a muscular pump during systole depends on the contractile properties of the contraction phase and on the time of onset, speed, and extent of the relaxation phase. Relaxation of the heart is defined by the events during systole by which the heart, as a muscle and as a pump, returns to a precontractile configuration. Relaxation of cardiac muscle includes isometric force decline and isotonic lengthening. Relaxation of the ventricle as a pump encompasses the second part of ejection, isovolumic relaxation, and rapid filling (Figure 10-1). Similarly, as for the contraction phase, a triple control mechanism also operates during the relaxation phase [1]. Relaxation of cardiac muscle and of the ventricular pump is thus governed by the dynamic interaction of the sensitivity of the contractile apparatus to the prevailing load (load dependence) and the dissipating activation (inactivation). This interaction is modulated by the regional and temporal nonuniform distribution of load and inactivation.

The concept of a triple control of relaxation has been well described in the rigorously controlled experimental setting of isolated cardiac muscle [2]. Yet, although there is evidence for the presence of a similar triple control in the intact ventricle [3-6] the exact mechanical manifestation of it is not always clear from the analysis of isovolumic pressure decline and rapid filling. This is partly due to the additional feedback regulation in the intact heart on load and inactivation of such extrinsic mechanisms as the neurohumoral control and the coronary circulation, and, as recently shown, the endo-

cardial endothelium [7]. A second problem in dealing with relaxation in the intact ventricle relates to the fact that most of our studies on isolated muscle were done with the isotonic-isometric relaxation sequence instead of the more physiologic isometric-isotonic relaxation sequence. This latter sequence is more analogous to relaxation in the ventricle where pressure decline precedes rapid filling. A third problem in the intact heart derives from the typical auxotonic, rather than the strict isometric-isotonic, loading conditions throughout contraction and relaxation of systole. Although force decline predominates in the muscle fibers in the ventricular wall during pressure fall and lengthening during rapid filling, some length changes of the fibers already occur during pressure fall and some further force decline occurs during rapid filling. Because of these "auxotonic" conditions in the ventricle, velocity measurements, such as  $(-)\text{dP}/\text{dt}$ ,  $(-)\text{dV}/\text{dt}$ , etc., cannot be interpreted simply.

In this chapter, we will describe first how the concept of load dependence becomes mechanically manifest in isolated cardiac muscle, even in the presence of the more physiologic isometric-isotonic relaxation mode. Second, we will summarize our present insights into the cellular mechanisms of load dependence. Third, we will discuss some practical aspects of load dependence in the intact ventricle, (i.e., with respect to the interpretation of altered systolic loading profiles).

## *Load Dependence in Isolated Cardiac Muscle*

### AFTERLOADED TWITCHES

Figure 10-2 depicts the superimposed force and length traces of three twitches, i.e., an isotonic

*Grossman, William, and Lorell, Beverly H. (eds.), Diastolic Relaxation of the Heart. Copyright © 1987. Martinus Nijhoff Publishing. All rights reserved.*

twitch with preload only (twitch 1), an afterloaded isotonic twitch (twitches 2a and 2b), and an isometric twitch at constant length (twitch 3). As soon as the muscle starts lengthening at the onset of relaxation in the isotonic preloaded and afterloaded twitches with the isotonic-isometric relaxation mode (twitch 2a), lengthening proceeds at an increasingly faster rate with the result that isotonic twitches are always much shorter than the isometric twitch. Isotonic lengthening is always followed by an abrupt drop in force during subsequent isometric relaxation. When the muscle is allowed to first relax isometrically, such as in the isometric-isotonic relaxation mode (twitch 2b), isotonic lengthening is still very rapid compared to the contraction rate, but the rate of force decline is much slower than that in the twitch with the isotonic-isometric relaxation mode and closely parallels force decline in the isometric twitch (twitch 3). Hence, the abrupt drop in force in the twitch with isotonic-isometric relaxation sequence is the direct mechanical manifestation of force potential being lost during the preceding fast lengthening of the muscle. Fast lengthening and subsequent drop in force are, therefore, inherent properties of relaxation, and not, as previously thought [8–11], the mere consequence of some “shortening inactivation” during the contraction phase.

#### LOAD-CLAMPED TWITCHES

The separation in time during relaxation between isotonic lengthening of isotonic preloaded and afterloaded twitches and the isometric control twitch is more striking still when a sudden increment of load (load clamp) is imposed on the muscle. Figure 10–3A illustrates the effect of a small increment of load late in contraction on the lengthening and force decline of an afterloaded twitch. In the isotonic-isometric relaxation mode (Figure 10–3A, left), lengthening starts sooner, i.e., the muscle is not capable of sustaining this additional load any longer. The subsequent time course of relaxation depends on the amplitude and timing of the load clamp. For smaller load clamps, as in the example of Figure 10–3A, lengthening speed is decreased, and the time of onset as well as the speed of subsequent force decline are hardly affected. For somewhat larger or slightly later load clamps (see Figure 10–1 in ref [1]), lengthening speed strikingly increases with, as a limit, an almost instantaneous reextension of

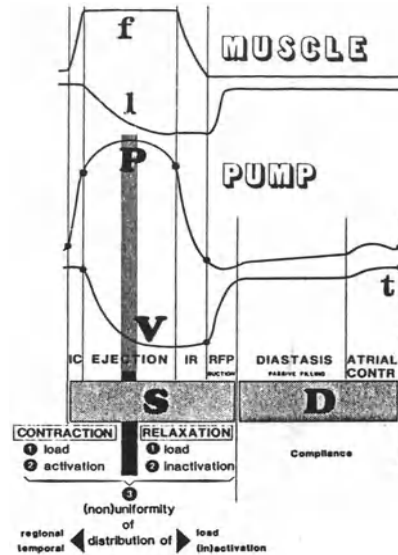


FIGURE 10–1. Triple control of systole of isolated cardiac muscle and of the ventricular pump of the heart. The time traces of force ( $f$ ) and length ( $l$ ) of an afterloaded twitch, obtained in isolated cardiac muscle with physiologically sequenced, i.e., isometric-isotonic relaxation, were photographically synchronized with the pressure ( $P$ ) and volume ( $V$ ) curves of the ventricle of the heart. This simplified diagram traces the analogy of the mechanics of contraction and relaxation between muscle and ventricular pump. Despite some evident shortcomings, such as the consideration of pressure instead of wall tension and the absence of auxotonic behavior in the muscle, it should be clear from the similar time courses that many concepts derived from experiments on isolated cardiac muscle must, by extrapolation, be taken into account in the evaluation of ventricular function.

Given the analogy between muscle and pump, the words systole ( $S$ ) and diastole ( $D$ ) of the heart as a muscular pump have been reinterpreted here in a conceptual rather than a phenomenologic sense [1]. Rapid filling phase (RFP) and isovolumic relaxation (IR) are, similarly as force decline and lengthening of the muscle, an integral part of relaxation of the muscular pump. Contraction and relaxation of the ventricle must be regarded as the two phases of systole in the same way as these constitute the two essential phases of an active twitch. The word diastole, from the Greek word meaning expansion in space, division, notch, separation in time should thus be reserved to mean the separation in time of two active contraction-relaxation (i.e., systolic) cycles.

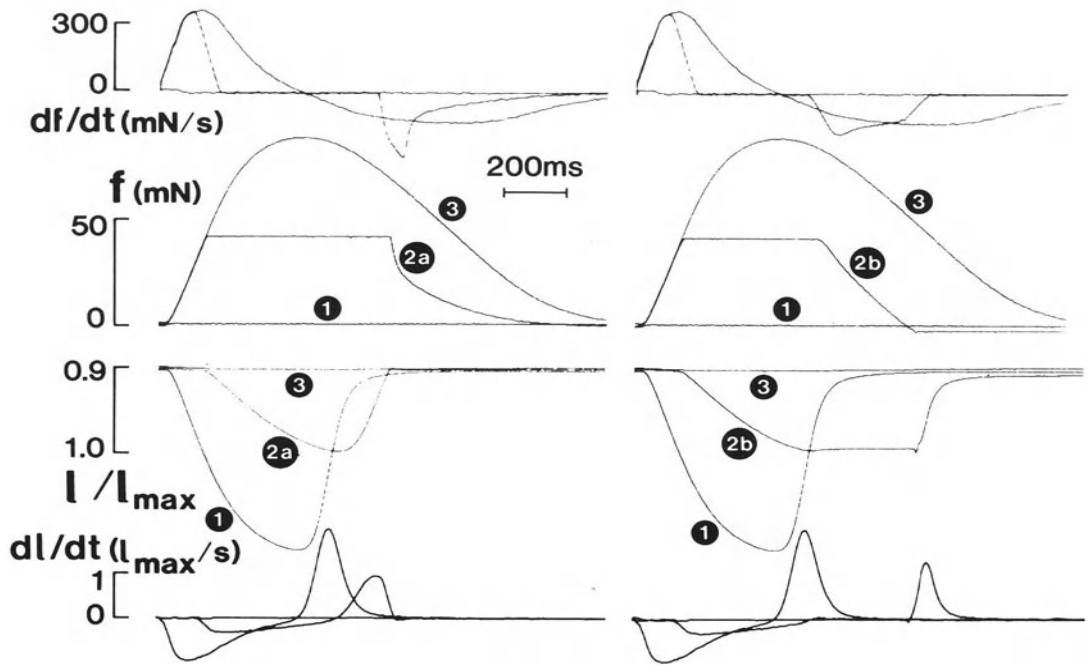


FIGURE 10-2. Force and length traces of an isotonic twitch at preload (twitch 1), an afterloaded twitch (twitches 2a and 2b), and an isometric twitch (twitch 3). The left side depicts afterloaded twitch 2a with familiar isotonic-isometric relaxation sequence, and the right, twitch 2b with same afterload, but with the more physiologic isometric-isotonic relaxation sequence.  $f$  = traces of force,  $df/dt$  = rate of force development; 1 = length;  $dl/dt$  = rate of length change. Muscle characteristics ( $29^{\circ}\text{C}$  and  $0.2\text{ Hz}$ ): length at  $l_{\text{max}}$  =  $10\text{ mm}$ ; mean cross-sectional area =  $0.65\text{ mm}^2$ , ratio of resting to total force at  $l_{\text{max}}$  =  $6.5\%$ .

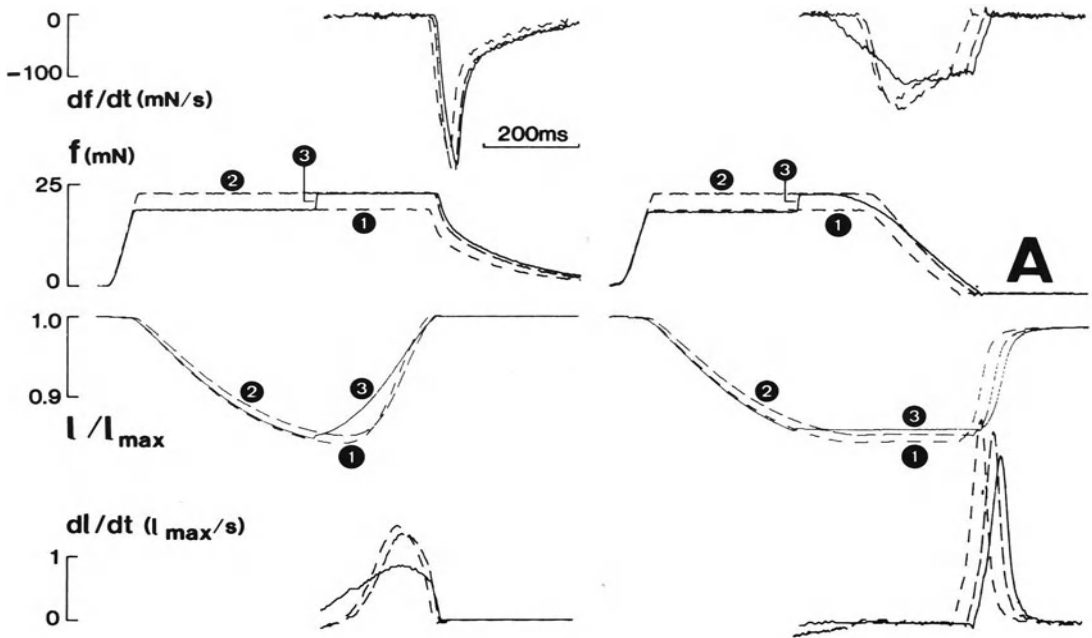
the muscle, followed by premature and faster force decline. In the isometric-isotonic relaxation mode (Figure 10-3A, right), force decline sets in sooner after the load clamp than in the two control afterloaded twitches; rate of force decline is slightly slower, and subsequent lengthening starts later and proceeds at a slower rate. For somewhat larger or slightly later load clamps (not shown), force decline remains slow, but subsequent lengthening may start sooner and progress at an increasingly faster rate.

Accordingly, after an increment in load late

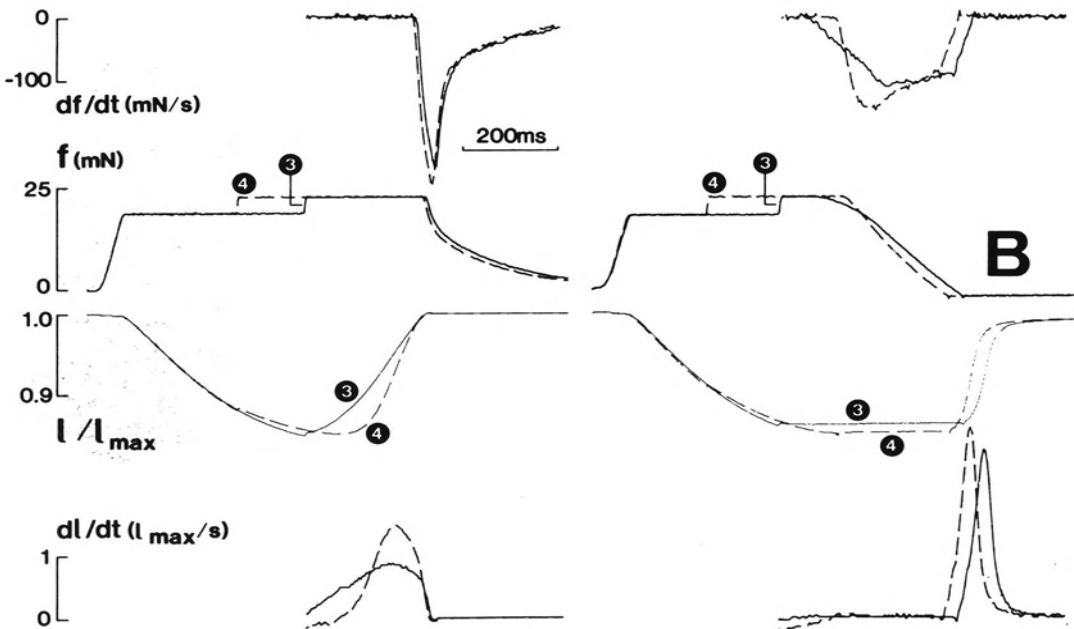
during a twitch, load dependence of relaxation may become manifest as an early onset of relaxation regardless of the relaxation mode. Rate of lengthening and rate of force decline will depend on the amplitude and timing of the load clamp and may often be affected in an opposite sense (see also Figure 10-12).

#### CONTRACTION LOAD VS. RELAXATION LOAD

The concept of load dependence of relaxation was derived from experiments in which effects of load (see Figure 10-2) or of changes in load (Figure 10-3A) occurred during the relaxation phase (relaxation load). However, when these changes in load were already established before or during the first two-thirds of the contraction phase (contraction load), the effects on relaxation were different and often opposite to those of late load increments (Figure 10-3B, lower). The onset of relaxation was always delayed at the higher load regardless of the relaxation mode, and therefore the net separation in time between the force decline in the afterloaded twitch and in the isometric twitch became smaller.



**A**



**B**

The transition from the effects on relaxation induced by contraction load to the opposite effects on relaxation induced by relaxation load occurs over a rather narrow time span which starts after approximately the first two-thirds of the contraction phase of the twitch [1]. It is important to be cognizant of such a transition zone when evaluating systolic performance, i.e., contraction and relaxation, of the intact heart (see also Figure 10–9).

### *Mechanisms of Load Dependence*

Relaxation is the return of the muscle to a pre-contraction configuration. At a cellular level this event can be seen as the consequence of inactivation. Inactivation is determined mainly by the life cycle of the cross-bridges between the actin and myosin filaments and by the efficient removal of  $\text{Ca}^{2+}$  by the sarcoplasmic reticulum (SR). These two processes are always operative and act in concert. Their respective contribution differs depending upon length and loading conditions. In isotonic twitches, in the presence of an efficient SR [12, 13], the prevailing load may become important in prematurely interrupting the cross-bridge life cycle, with subsequent rapid lengthening of the muscle and concomitant abbreviation of the twitch [14–16]. In isometric twitches, changes in sensitivity of the contractile proteins (CP), induced either by force development through cooperative activity [17] or by changes in initial muscle length [18], will predominate, thereby markedly affecting the duration of the CB life cycle and therefore force decline during relaxation.

We have seen that load dependence of relaxation of isolated cardiac muscle is manifested by the separation in time between rapid lengthening of isotonic (preloaded or afterloaded) twitches and the slower force decline of an

isometric twitch (Figure 10–4, left). Early isotonic lengthening of isotonic twitches and late isometric force decline of isometric twitches, together, determine the degree of their mutual separation in time, and thus constitute the two major aspects of load dependence of relaxation. Although, as we have said, the different processes that underlie these two aspects are closely linked and strikingly overlap, we have preferred, for didactic purposes, to discuss lengthening and force decline separately (Figure 10–4, right).

### LENGTHENING DURING RELAXATION

Rapid lengthening of muscle during isotonic relaxation is due to load-induced forcible detachment of the cross-bridges between actin and myosin filaments with subsequent sliding of these filaments back to their precontractile position [14–16]. The presence of an efficient SR is a prerequisite for this load-induced lengthening to become manifest [12, 13].

*Role of Load.* The effect of increased load on relaxation has been illustrated in Figure 10–3. Based on experimental data [14–16], load-induced lengthening has been conceived as a load-induced back-rotation and forcible detachment of still-attached cross-bridges when the relaxation load on the muscle exceeds the summed force level of these cross-bridges. This hypothetical importance of load can be tested further in experiments where the muscle is unloaded at an appropriate time, i.e., just prior to the onset of lengthening, and with an appropriate amount, i.e., sufficient to correct for the impending imbalance between load and force potential of the attached cross-bridge (Figure 10–5) [14–16]. Appropriate unloading delays the onset of lengthening, which now closely follows the time course of force decline in an isometric twitch.

*Role of SR.* The importance of the presence of a functional SR has been derived from a variety of experimental conditions where the SR was either scarcely developed [2], destroyed [12], or functionally inhibited [19] (Figure 10–6). In all these conditions, muscle lengthening is markedly delayed and closely follows the time course of force decline of an isometric twitch, thereby abolishing load dependence of relaxation.

FIGURE 10–3. Effect of load clamps on relaxation. A. Effect of a small increment in load (twitch 3) late in the twitch (relaxation load), on the time course of relaxation of an afterloaded twitch in the isotonic-isometric (*left*) and isometric-isotonic (*right*) relaxation mode. The two corresponding afterloaded control twitches are also shown (twitches 1 and 2). B. Effect of an increment in load early in the twitch (contraction load) (twitch 4). Muscle characteristics, abbreviations, and figure format (except for the scaling factors) are the same as in Figure 10–2. For clarity, only relaxation rates are depicted.

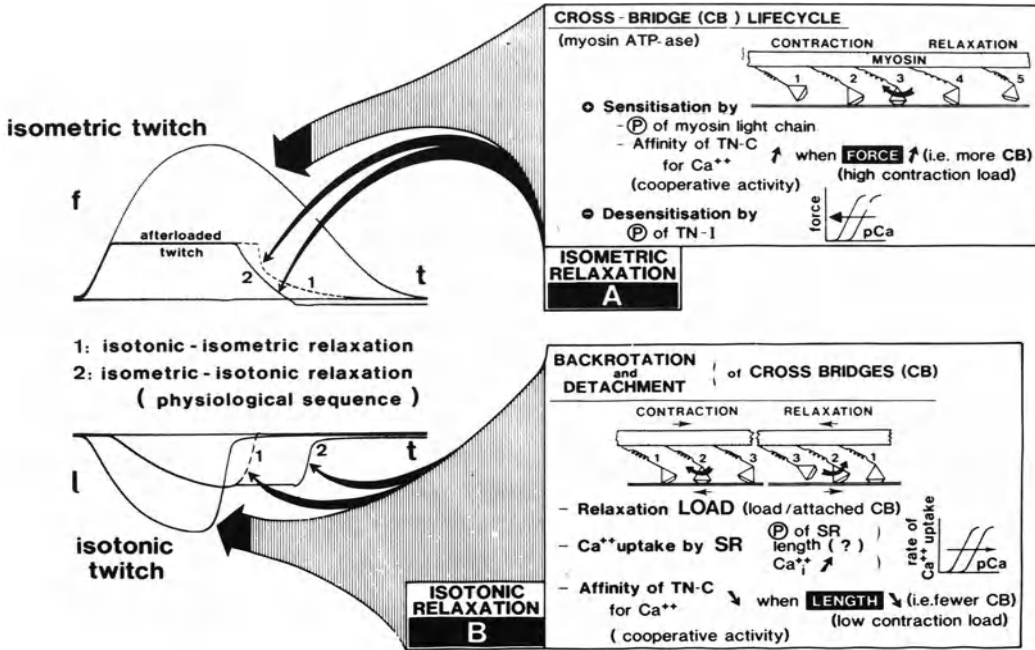
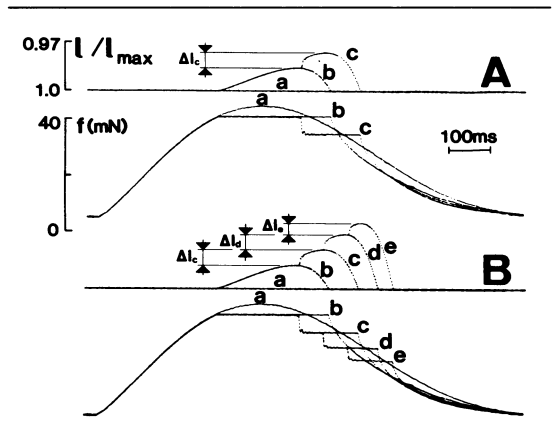


FIGURE 10-4. Mechanisms of load dependence of relaxation in isolated cardiac muscle. On the left, four twitches similar to the twitches in Figure 10-2 are superimposed and displayed as a reference for the panels to the right. A. Control of isometric relaxation or force decline (see text). B. Control of isotonic relaxation or lengthening (see text). ATP-ase = adenosine triphosphatase; TN-C = troponin-C; TN-I = troponin-I.

FIGURE 10-5. Effect of appropriate unloading clamp at peak shortening. A. Single unloading clamp from a high to a lower afterload (twitch c). The initial elastic shortening at the instant of the clamp is followed by some additional active shortening, thereby postponing the onset of lengthening and of subsequent force decline. The afterloaded control twitch (twitch b) is also displayed along with the isometric twitch (twitch a). B. Multiple unloading clamps. Two additional clamped twitches, i.e., with a double (twitch d) and with a triple (twitch e) clamp, are added to the twitches depicted in the upper panel. Note that lengthening and force decline are further postponed by additional unloading clamp. After an initial abrupt fall in force, due to disruption of some force potential during the preceding lengthening, subsequent force decline closely approximates the force decline in the isometric twitch. Muscle characteristics (29°C and 0.2 Hz): length at  $l_{max}$  = 7.0 mm; mean cross-sectional area = 1.0 mm<sup>2</sup>; ratio of resting to total force at,  $l_{max}$  = 10.4% (modified after [14] and [15]).



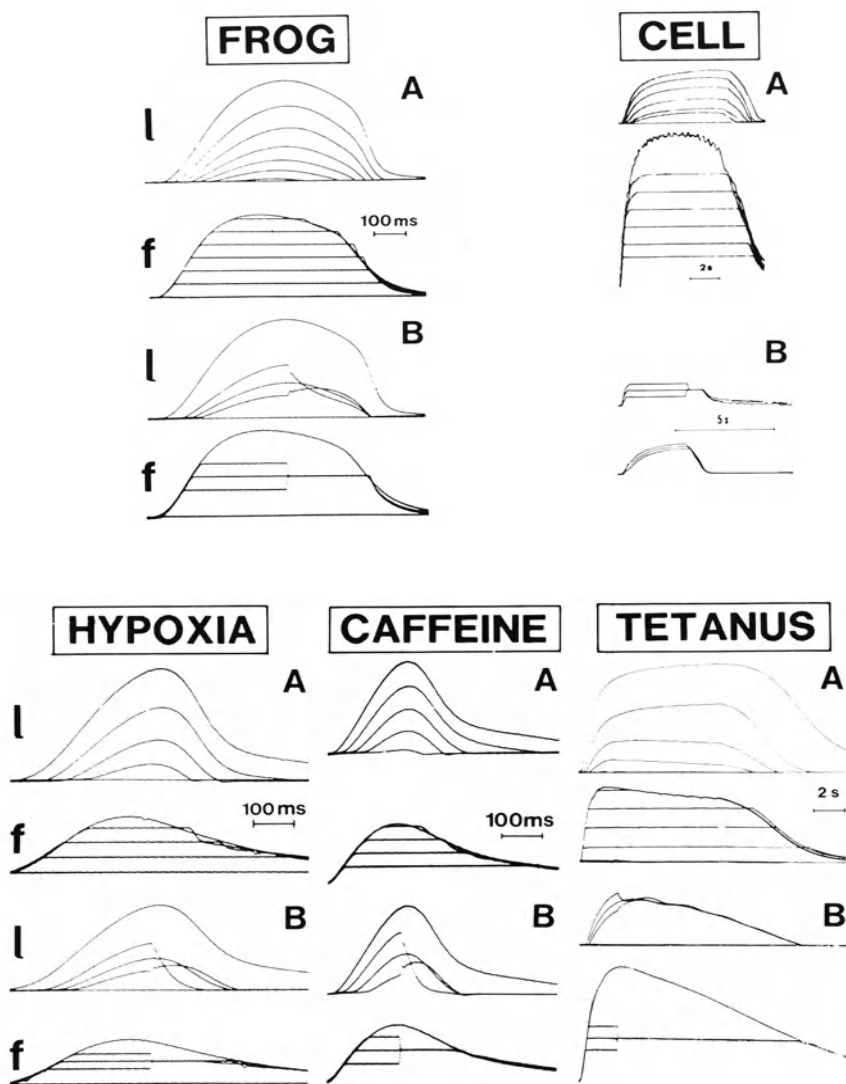


FIGURE 10-6. Importance of a functional sarcoplasmic reticulum (SR). Load dependence is diminished or absent in the absence of a functional, as in the frog where the SR is scarcely developed, in single cardiac cells where the SR had been destroyed by detergent treatment, in hypoxia where the SR is metabolically blocked and in the presence of caffeine and during tetanization where the SR had been inhibited. Load during afterloaded twitches *A* (panels), and load changes near peak shortening *B* (panels) illustrate that in all these conditions relaxation load has virtually no influence on twitch duration. *l* = length; *f* = force.

#### FORCE DECLINE DURING RELAXATION

The cross-bridge life cycle and modulation of its duration by changes in the sensitivity of the contractile proteins play a major role in determining force decline during relaxation. The number of cross-bridges and the duration of their cycle can be altered by various mechanisms, among which cooperative activity of the cross-bridges [17] or phosphorylation of myosin light chains or of troponin-I [20-22]. These

mechanisms will induce either so-called “sensitization of the CP” with delayed and slower force decline, or “desensitization of the CP” with earlier and faster decline [22].

Pharmacologic studies have shown that inotropic agents may act through such mechanisms [23]. Some new inotropic agents such as ARL-115 and UDCG-115 may sensitize the CP [24], while other agents, e.g., isoproterenol, may desensitize the CP by phosphorylation of troponin-I [22, 25]. In addition, some physiologic control mechanisms also act through changes in the sensitivity of the CP. For example, the process of force development itself may induce further force development through cooperative activity of the cross-bridges [17]. Decreasing length, by contrast, will desensitize the CP [18, 26, 27]. Moreover, the presence of an intact endocardium has recently been shown to enhance sensitization of the CP [7].

*Role of Cooperative Activity.* Experiments with the calcium-sensitive, bioluminescent protein aequorin [28] showed that, when active shortening was allowed at any time during a twitch, the free  $[Ca^{2+}]_i$  was higher than at comparable times in isometric twitches (Figure 10-7). Attachment of force-generating cross-bridges may indeed increase the affinity of troponin-C for calcium [29, 30] through cooperative activity of the cross-bridges [17]. By contrast, shortening of the muscle will decrease the affinity of troponin-C for calcium [29], so that the myofilaments will have less calcium bound at the end of a period of shortening than at a comparable time under isometric conditions. Since by that time the calcium transient is over, calcium cannot be regained by troponin-C, and the terminal phase of relaxation must take place with a reduced degree of activation [28].

Accordingly, in an isometric twitch, cooperative activity will, by a process of force development-induced increased affinity of troponin-C for calcium, tune up the development and maintenance of force throughout contraction and relaxation. On the other hand, in the isotonic twitch, cooperative activity will be reduced, thereby enhancing load-induced rapid lengthening in the presence of a functional SR. Similarly, decreasing initial muscle length (Figure 10-8) decreases peak isometric twitch force mainly through decreased sensitivity of CP [18, 26, 27].

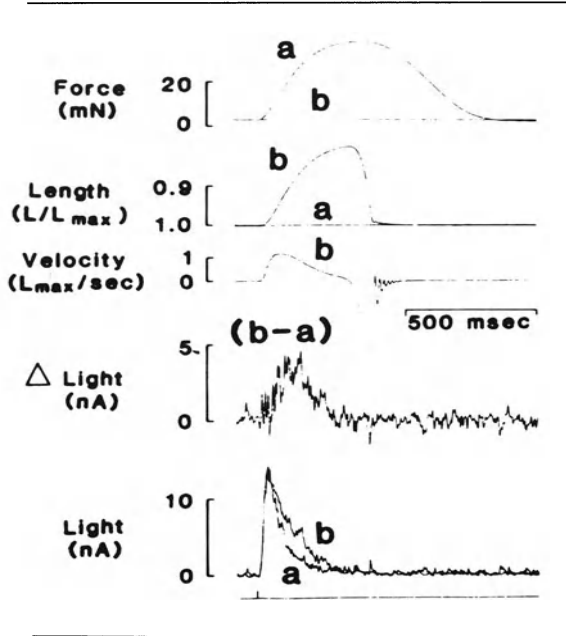


FIGURE 10-7. Aequorin signals of cat papillary muscle contracting against various loads. The tracings (from the top downward) show force, shortening, velocity of shortening, differential aequorin signal obtained by subtraction of the two averaged aequorin signals (b-a), and aequorin signals and stimulus. Tracings show two superimposed twitches, an isometric (a), and a preloaded isotonic twitch in which shortening occurred (b). The aequorin signals reach the same peak, but the decline of the aequorin signal ( $Ca^{2+}$  transient) is initially faster during force development (a) than during shortening (b). The total duration of the light signal is essentially the same in the two twitches. The light of shortening (the difference of the two light signals) becomes apparent some 35 ms after the onset of shortening. Muscle characteristics ( $30^{\circ}C$  and 0.25 Hz): length at  $l_{max} = 5.25$  mm; mean cross-sectional area =  $0.33$  mm<sup>2</sup>; ratio of resting to total tension at  $l_{max} = 7.9\%$  (from Housmans et al [28], with permission).

*Role of Endocardium.* We have recently shown [7] that the removal of a functional endocardium resulted in an immediate and irreversible abbreviation of isometric twitches with, except at the highest  $[Ca^{2+}]_0$ , a decrease in peak isometric force (see Figure 10-8). The pattern of changes, i.e., modulation of the onset of early force decline, induced by decreasing initial muscle length at each  $[Ca^{2+}]_0$  and by the

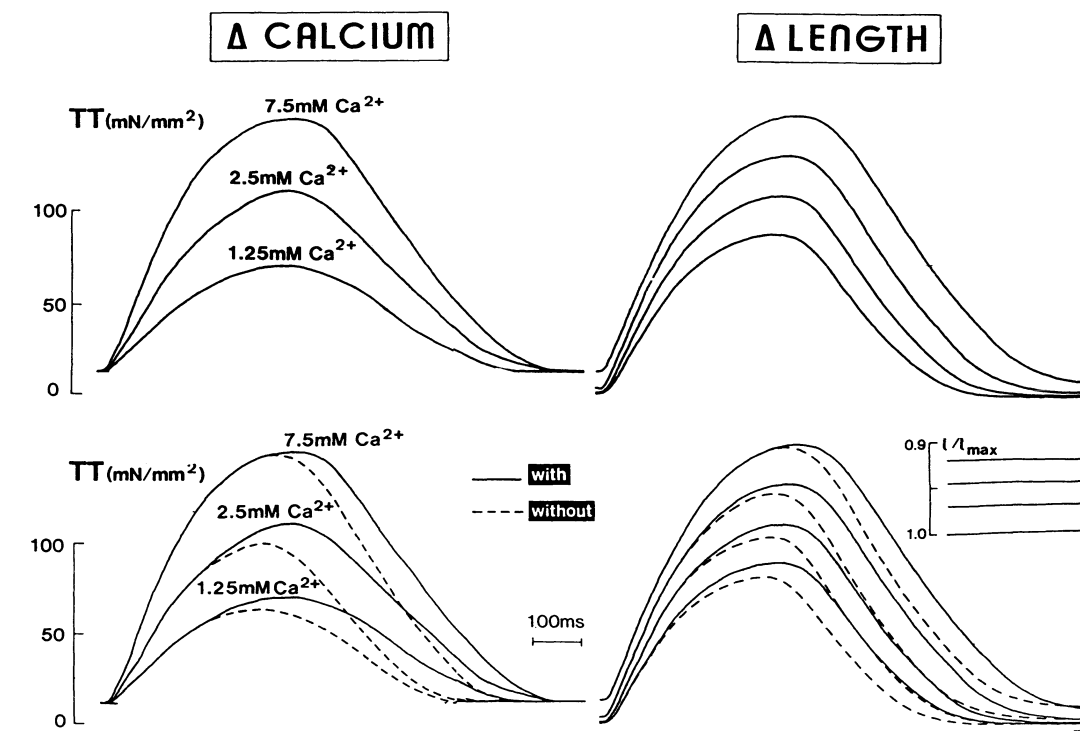


FIGURE 10-8. Effect of endocardium removal on relaxation. Removal of a functional endocardium (*dotted lines, lower panel*) induces an earlier relaxation, thereby reducing peak isometric twitch tension (TT). The control traces (*full lines, upper panel*) compare this effect of the effect of changes in external  $[Ca^{2+}]_0$  and of different initial muscle lengths on isometric twitches. Note that regardless of length and  $[Ca^{2+}]_0$ , removing a functional endocardium (*lower panel*) induces changes that resemble changing to shorter initial muscle length (*upper right*), but not changing to different  $[Ca^{2+}]_0$  (*upper left*). Muscle characteristics ( $29^\circ C$  and  $0.2$  Hz): length at  $l_{max} = 8$  mm; mean cross-sectional area =  $0.82$  mm<sup>2</sup>, ratio of resting to total force at  $l_{max}$  and  $2.5$  mM Ca = 10%.

removal of a functional endocardium are very similar. This similarity might suggest that the endocardium-mediated chain of events may also be mediated by changes in the sensitivity of the CP to  $Ca^{2+}$ . This hypothesis was supported further by the asymmetrical shift of the force- $[Ca^{2+}]_0$  relationship induced by the removal of a functional endocardium.

### Load Dependence in the Intact Ventricle

#### MECHANICAL EXPRESSION OF LOAD DEPENDENCE

The existence of load dependence in the intact ventricle has been well established [3-6, 31]. Some relevant experimental data from the literature are illustrated in Figure 10-9. As in isolated muscle (see Figure 10-3), sudden increments in load, either as pressure or as volume clamps, may delay the onset of pressure decline when applied early in the cardiac cycle (contraction load), but will induce premature pressure decline when applied late in ejection (relaxation load). Subsequent rate of pressure decline is faster after contraction load and slower after relaxation load, again analogous to the effect of changes in contraction load and relaxation load on the rate of force decline in after-loaded twitches of isolated muscle in the isometric-isotonic relaxation mode.

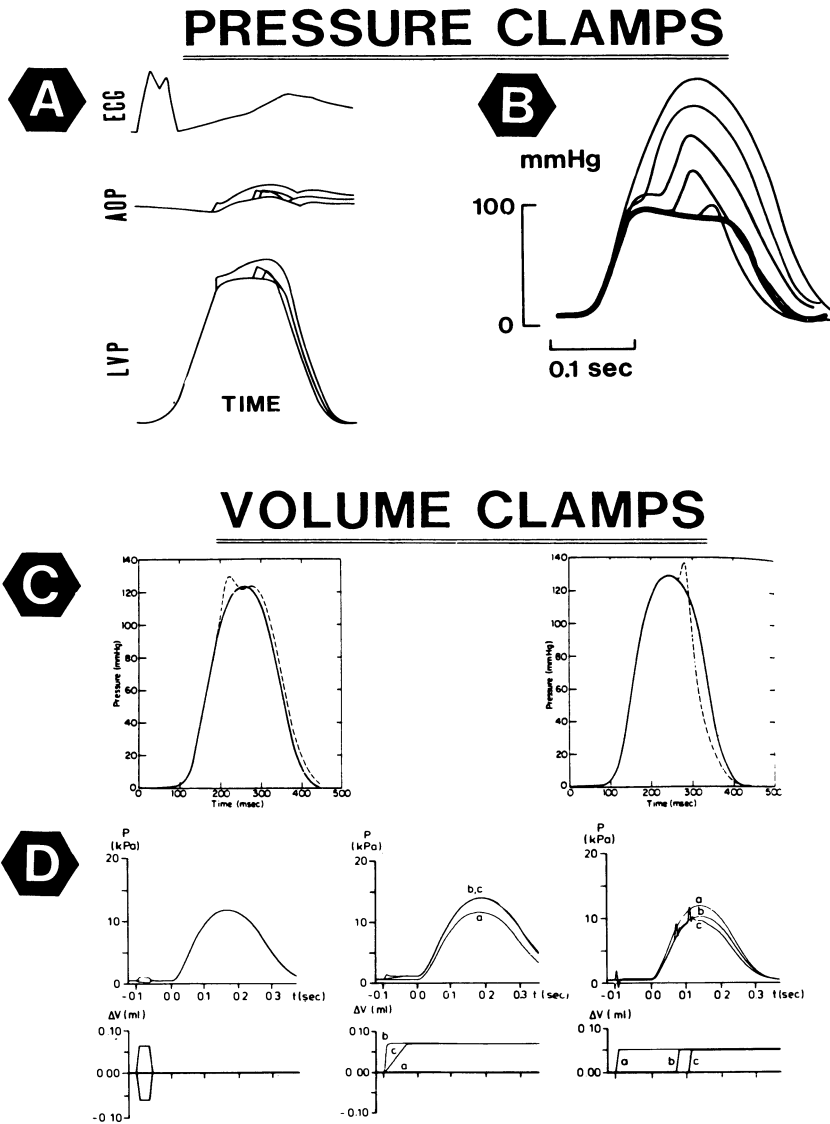


FIGURE 10-9. Mechanical expression of load dependence. Effects of pressure clamps (abrupt occlusion of the ascending aorta) and volume clamps (abrupt inflation of intracavitary balloon) on the time course of the pressure curve of the left ventricle in the intact heart. Data were retraced from literature (panel A, Brutsaert et al [3]; panel B, modified from Noble [4]; panel C, Gaasch et al [5]; panel D, Kil and Schiereck [6]).

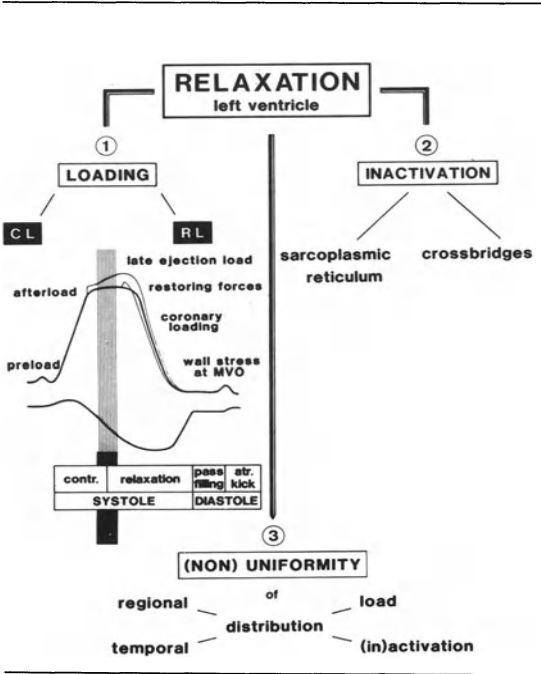


FIGURE 10-10. Triple control of relaxation of the ventricle as a muscular pump by loading, inactivation, and nonuniformity. CL = contraction load; RL = relaxation load; MVO = mitral valve opening.

Hence, similar to the triple control in isolated cardiac muscle, relaxation of the ventricle as a muscular pump is governed by the dynamic interplay of the sensitivity of the contractile system to the loading conditions (load dependence) and the dissipation of activation (inactivation), both modulated by some degree of nonuniformity (Figure 10-10).

IMPLICATIONS FOR INTERPRETATION OF RELAXATION INDICES

From the foregoing, it cannot be emphasized enough that the principles underlying force decline and rapid lengthening of isolated muscle, despite some unavoidable simplifications as stated before, ought to be taken into account when evaluating pressure fall or rapid filling in the whole ventricle. Moreover, one should not be surprised that in some conditions pressure fall and rapid filling may vary in an opposite sense with respect to timing of onset and to speed. These apparently contradictory findings are sometimes difficult to interpret in certain cardiac diseases, in particular in the presence of valvular lesions, where changes in the loading profile may dominate ventricular performance.

In Figure 10-1, we have emphasized the striking analogy between the time courses of force and pressure (tension) traces and of length and volume traces. In an attempt to demonstrate further how useful the study of isolated cardiac muscle can be in predicting ventricular function as a whole, in Figure 10-11 tension and volume traces obtained from published studies of mitral (MI) and aortic valvular insufficiency (AI) have been photographically synchronized with force and length traces of an afterloaded twitch from isolated muscle. The muscle was either unloaded early (Figure 10-11, left panel) or loaded late in the twitch (Figure 10-11, right panel). To help the reader understand how complex alterations of relaxation in the intact ventricle may be, depending on the type and complexity of the changed loading profile, similar abrupt unloading and loading clamps were imposed at three different times (early, medium, late) during an afterloaded twitch (Figure 10-12). Note that the early unloading (Figure 10-12, upper panel) and the late loading (Figure 10-12 lower panel) are analogous to MI and AI in Figure 10-11. Early and medium unloading of the muscle (see Figure 10-12, upper panel) are followed by a slower decline in force and faster lengthening,

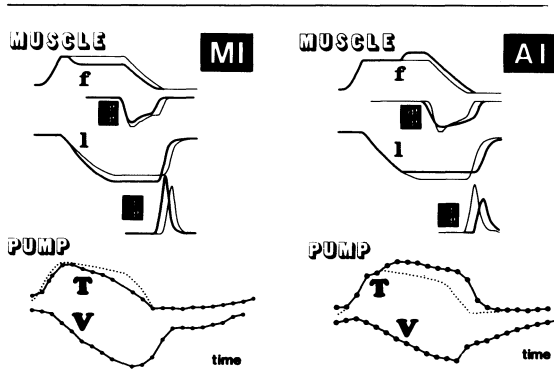
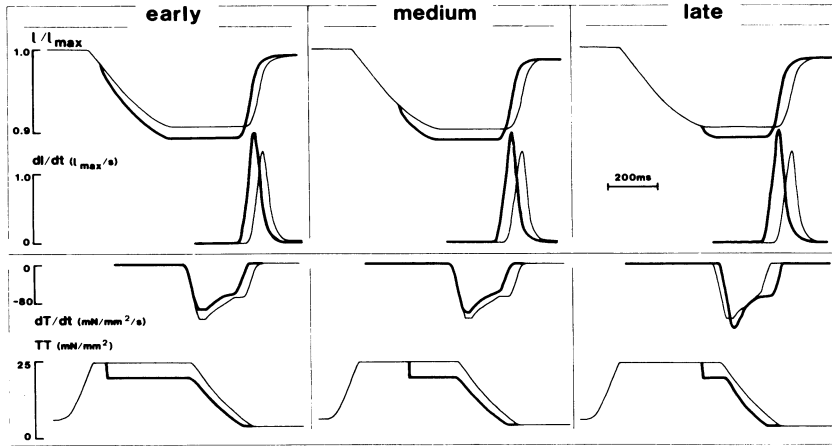
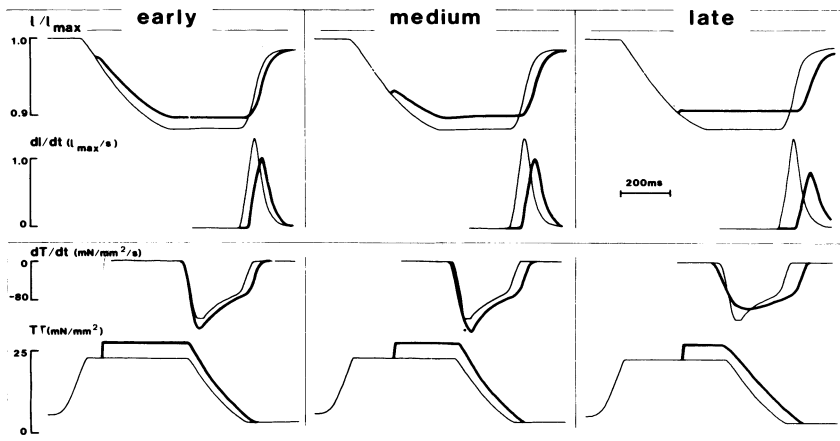


FIGURE 10-11. Loading profiles in mitral (MI) and aortic (AI) valvular insufficiency are compared to isolated muscle length and force traces of afterloaded twitches with an early unloading (as in MI) or a late loading (as in AI) clamp. Tension (T) and volume (V) data for MI and AI were adapted from actual traces in literature.  $df/dt$  = rate of force development;  $dl/dt$  = rate of length change.

### unloading clamps



### loading clamps



analogous to the slower tension fail and faster rapid filling typical for MI (see Figure 10-11). Late unloading of the muscle generally induces faster force decline and lengthening. Although early and medium loading of the muscle (see Figure 10-12, lower panel) are followed by faster force decline and slower lengthening, late loading may induce both slower force decline and slower lengthening, analogous to the delayed tension decline and slower filling typical for AI (see Figure 10-11). Yet, interpretation of

FIGURE 10-12. Spectrum of the influence on relaxation of unloading and loading clamps (*thick lines*) at various times during an afterloaded twitch (*fine lines*) with isometric-isotonic relaxation sequence. For clarity, emphasis is placed on relaxation.  $dl/dt$  = rate of length change;  $dT/dt$  = rate of tension change;  $TT$  = total tension.

relaxation indices in AI is not simple. First, transmitral flow during rapid filling—e.g., as measured by doppler or using mitral electromagnetic flowmeters—cannot be used as a measure of relaxation of the ventricle because

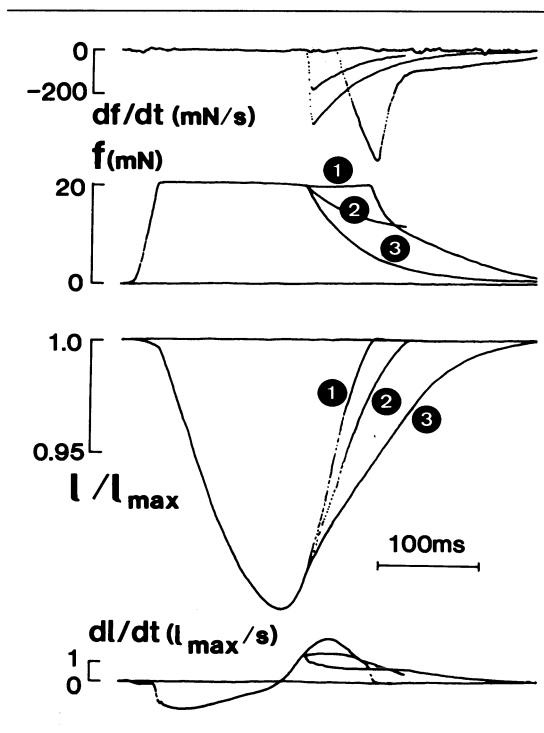


FIGURE 10-13. Two afterloaded isotonic twitches were made to relax auxotonically (twitches 2 and 3) and were superimposed on the baseline isotonic-isometric relaxation sequence (twitch 1), illustrating the analogy with different degrees of aortic insufficiency. Muscle characteristics ( $29^{\circ}\text{C}$  and  $0.1\text{ Hz}$ , rat papillary muscle): length at  $l_{\text{max}} = 7\text{ mm}$ ; mean cross-sectional area =  $1.16\text{ mm}^2$ , ratio of resting to force at  $l_{\text{max}} = 8.9\%$ .  $df/dt$  = rate of force change.

filling of the ventricle in AI will be the sum of transmitral flow plus the regurgitant fraction through the aortic valve. Second, an analysis of relaxation in AI may be further hampered by the marked "auxotonic" loading profile throughout pressure fall and filling. Some of this potential complexity is illustrated in Figure 10-13 showing traces of force and length with the respective first derivatives of three afterloaded twitches obtained in papillary muscle at  $37^{\circ}\text{C}$ . Twitch 1 is a control afterloaded twitch with isotonic-isometric relaxation sequence. Twitches 2 and 3 were equally afterloaded during contraction and the initial part or isotonic relengthening and were then made auxotonic. This situation would be analogous to two hemodynamic degrees of AI. With the higher load, and hence the higher

degree of AI (twitch 2), force decline is slower, but lengthening is more rapid. Alternatively, twitch 3 would be analogous to a lower regurgitant load, resulting in faster force decline and slower lengthening. Therefore, given the auxotonic conditions in the intact ventricle, rate of pressure decline and of filling cannot easily be interpreted in terms of muscle relaxation without taking into account concomitant dynamic changes in ventricular dimensions, as long as the loading on the myofilaments—thus the length of any elastic structure in series—is changing.

### References

1. Brutsaert DL, Rademakers FE, Sys SU (1984). Triple control of relaxation: Implications in cardiac disease. *Circulation* 69:190-196.
2. Brutsaert DL, De Clerck NM, Goethals MA, Housmans PR (1978). Relaxation of ventricular cardiac muscle. *J Physiol (Lond)* 283:469-480.
3. Brutsaert DL, Housmans PR, Goethals MA (1980). Dual control of relaxation in the ventricular function in the mammalian heart. *Circ Res* 47:637-652.
4. Noble MIM (1968). The contribution of blood momentum to left ventricular ejection in the dog. *Circ Res* 23:663-670.
5. Gaasch WH, Blaustein AS, Bing OHL (1985). Asynchronous (segmental early) relaxation of the left ventricle. *J Am Coll Cardiol* 5:891-897.
6. Kil PJM, Schiereck P (1983). Influence of the velocity of changes in end-diastolic volume on the Starling Mechanism of isolated left ventricles. *Pflugers Arch* 396:243-253.
7. Brutsaert DL, Meulemans AL, Sipido KR, Sys SU (1986). The endocardium is an important modulator of cardiac performance. (submitted).
8. Brady AJ (1968). Active state in cardiac muscle. *Physiol Rev* 48:570-600.
9. Edman KAP, Nilson E (1971). Time course of the active state in relation to muscle length and movement: A comparative study of skeletal muscle and myocardium. *Cardiovasc Res* 5:3-10.
10. Kaufmann RL, Lab MJ, Hennekes R, Krause H (1971). Feedback interaction of mechanical and electrical events in isolated mammalian ventricular myocardium. *Pflugers Arch* 324:100-123.
11. Brutsaert DL (1974). Force-velocity-length-time interrelationship of cardiac muscle. *Ciba Found Symp* 24:155-175.
12. Brutsaert DL, Claes VA, De Clerck NM (1978). Relaxation of mammalian single cardiac cells after pretreatment with the detergent Brij-58. *J Physiol (Lond)* 283:481-491.

13. Lecarpentier YC, Chuck LHS, Housmans PR, et al (1979). Nature of load dependence of relaxation in cardiac muscle. *Am J Physiol* 237: H455-H460.
14. Brutsaert DL, Housmans PR (1977). Load clamp analysis of maximal force potential of mammalian cardiac muscle. *J Physiol (Lond)* 271:587-603.
15. Brutsaert DL, Housmans PR (1979). Load-induced length transient of mammalian cardiac muscle. In Sugi H (ed): *Crossbridge mechanisms in Muscle Contraction*. Tokyo: University of Tokyo Press, pp 241-258.
16. Housmans PR, Brutsaert DL (1976). Three step yielding of load clamped mammalian cardiac muscle. *Nature* 262:56-58.
17. Weber AM, Murray JM (1973). Molecular control mechanisms in muscle contraction. *Physiol Rev* 53:612-673.
18. Hibberd MG, Jewell BR (1982). Calcium- and length-dependent force production in rat ventricular muscle. *J Physiol* 239:527-540.
19. Chuck LHS, Goethals MA, Parmley WW, Brutsaert DL (1981). Load insensitive relaxation caused by hypoxia in mammalian cardiac muscle. *Circ Res* 48:797-803.
20. Ray K, England D (1976). Phosphorylation of the inhibitory subunit of troponin and its effect on the calcium dependence of cardiac myofibril adenosine tri-phosphatase. *FEBS Lett* 70:11-17.
21. McClellan GB, Winegrad S (1978). The regulation of the calcium sensitivity of the contractile system in mammalian cardiac muscle. *J Gen Physiol* 72:737-764.
22. Winegrad S (1984). Regulation of cardiac contractile proteins: correlation between physiology and biochemistry. *Circ Res* 55:565-574.
23. Blinks JR, Endoh M (1986). Modification of myofibrillar responsiveness to  $Ca^{2+}$  as an inotropic mechanism. *Circulation* 75 (suppl III):85-98.
24. Ruegg JC (1986). Effects of new inotropic agents on  $Ca^{2+}$  sensitivity of contractile proteins. *Circulation* 73 (suppl III):78-84.
25. England PJ (1986). The adrenergic regulation of heart contraction and the role of calcium. *Proc 30th Congr IUPS (Vancouver, Canada)* 16:126.
26. Allen DG, Kentish JC (1985). The cellular basis of the length-tension relation in cardiac muscle. *J Mol Cell Cardiol* 17:821-840.
27. Kentish JC, Allen DG (1986). Changes in calcium concentration in skinned cardiac muscles subjected to length changes. *Proc 30th Congr IUPS (Vancouver, Canada)* 16:353.
28. Housmans PR, Lee NKM, Blinks JR (1983). Active shortening retards the decline of the intracellular calcium transient in mammalian heart muscle. *Science* 221:159-161.
29. Pan BS, Howe ER, Solaro J (1983). Calcium binding to troponin-C in loaded and unloaded myofilaments of chemically skinned heart muscle preparations. *Fed Proc* 42:574.
30. Hofmann PA, Fuchs F (1986). Evidence for a force-dependent component of  $Ca^{2+}$  binding to cardiac troponin-C. *Biophys J* 49:84a.
31. Wigle ED, Sasson Z, Henderson MA, et al (1985). Hypertrophic cardiomyopathy. The importance of the site and the extent of hypertrophy. A review. *Prog Cardiovasc Dis* 28: 1-83.

---

# 11. THE EFFECTS OF CARDIAC HYPERTROPHY ON INTRACELLULAR $Ca^{2+}$ HANDLING

---

James P. Morgan, Roderick MacKinnon, Marc Feldman,  
William Grossman, and Judith Gwathmey

The development of cardiac hypertrophy is associated with marked changes in contractile function in many mammalian species [1]. In isolated ventricular muscle, these changes usually manifest themselves as alterations in force generation and in the rate of relaxation [2]. The studies described in this chapter were designed to answer the question of whether the mechanical abnormalities of hypertrophied muscle are related to changes in intracellular  $Ca^{2+}$  handling. Four models of hypertrophy will be considered, including (1) pressure-overload right ventricular hypertrophy in ferrets, (2) alteration of the thyroid state in ferrets, (3) the compensatory hypertrophy that occurs in patients with heart failure, and (4) hypertrophic cardiomyopathy in humans.

## *Model I: Pressure-Overload Right Ventricular Hypertrophy in the Ferret*

One of the most extensively studied models of hypertrophy is produced by banding of the pulmonary artery in the cat to induce right ventricular pressure-overload [3, 4]. Mild degrees of banding produce a mild form of hypertrophy that is associated with normal contractile function; tighter banding produces more severe

hypertrophy in which contractile function is depressed; the most severe degrees of hypertrophy and contractile dysfunction are produced by banding of the pulmonary artery so that the percent remaining patent is 10% or less [5, 6]. We developed an alternative model of right ventricular pressure-overload hypertrophy in the ferret, a relatively less-expensive experimental animal that possesses several distinct advantages for cardiovascular studies, including the usual availability of multiple small papillary muscles from each heart. After successfully producing pressure-overload hypertrophy, we used aequorin to study the relationship of changes in intracellular  $Ca^{2+}$  handling to the alterations in contractile function that occur in isolated papillary muscles from this ferret model [7].

The banding procedure that we adapted to the ferret was initially developed for cats by Spann and colleagues [3, 4]. Young male ferrets ( $n = 9$ ) with a mean weight of  $0.60 \pm 0.04$  kg, and a mean age of  $70 \pm 10.5$  days were banded for use in these experiments. Under sterile conditions, the heart and pulmonary artery were exposed through an intercostal incision. To reduce the lumen of the pulmonary artery by 60 to 70%, a 2-mm (internal diameter) band was placed around the pulmonary artery and tied in place; greater degrees of constriction developed as the animals continued to grow and increase in body weight.

The banded animals were followed serially with radiographs to look for enlargement of the cardiac silhouette as evidence of hypertrophy. Animals that developed signs of congestive heart failure were excluded from the study. When enlargement of the cardiac silhouette

Supported in part by NIH grants HL31117, HL31704, HL07374, HL36797, and a Grant-in-Aid from the American Heart Association, Massachusetts Affiliate. Dr. Morgan is the recipient of a Research Career Development Award (HL01611).

Grossman, William, and Lorell, Beverly H. (eds.), *Diastolic Relaxation of the Heart*. Copyright © 1987. Martinus Nijhoff Publishing. All rights reserved.

developed, 1 to 5 months after the banding procedure, the hearts of the banded animals and their age-matched controls were excised for study. An appropriate right ventricular papillary muscle was removed and placed into a bath designed for aequorin experiments. Care was taken to select muscles with relatively cylindrical uniformity (diameters less than 1 mm) to ensure adequate oxygenation of central fibers. The muscles were suspended between two hooks—one stationary and the other attached to a Statham force transducer—for recording tension development. Muscles were stimulated to contract at 3-second intervals at 30°C, allowed to equilibrate for 1 hour, and then loaded with the bioluminescent  $\text{Ca}^{2+}$  indicator aequorin. Light and tension responses were recorded simultaneously, as described previously [8]. Because the light levels were very low and photomultiplier shot noise was prominent, it was necessary to average successive signals (from 16 to several hundred, depending on light intensity) to obtain a satisfactory signal-to-noise ratio. Comparison of the aequorin light signals from different muscles was performed by the method of fractional luminescence developed by Allen and Blinks [9]. The preparations were examined histologically for documentation of the degree of hypertrophy present.

Table 11-1 lists the heart weights and histologic features of the control and banded animals and shows that a significant degree of right ventricular hypertrophy developed in the banded animals. Figure 11-1 shows the aequorin light signals (i.e., intracellular calcium transients) and isometric tension tracings recorded in papillary muscles from a control and a hypertrophied ferret at three different concentrations of  $[\text{Ca}^{2+}]_0$ . Note that, in both muscles, the

aequorin signal consists of a single component that rises to a peak and declines towards baseline before the corresponding tension response.

To assess the effects of hypertrophy on the time course of isometric tension development and the aequorin light signal, we compared the time to peak light and tension, time to 50% decline from peak light and tension, and time to 80% decline from peak light and tension in papillary muscles from control and hypertrophied animals. As shown in Figure 11-2, hypertrophy was associated with a significant prolongation of each of these variables as compared to the control animals, except for time to peak light.

The time course of the aequorin light signal in mammalian working myocardium appears to predominantly reflect the release and uptake of calcium by the sarcoplasmic reticulum (SR) [10]. In general, drugs and interventions that inhibit the uptake (i.e., caffeine) or release (i.e., ryanodine) of  $\text{Ca}^{2+}$  by the SR prolong the duration of the aequorin light signal; conversely, those that increase the rate of uptake (i.e., isoproterenol) abbreviate the aequorin light signal [8, 10]. Our results indicate, therefore, that hypertrophy decreases the rate of  $\text{Ca}^{2+}$  uptake and perhaps also the rate of  $\text{Ca}^{2+}$  release by intracellular stores. This interpretation is consistent with reports of studies performed on isolated preparations of SR, which indicate that SR function, and  $\text{Ca}^{2+}$  accumulation, may be enhanced by the development of mild hypertrophy, but that more severe degrees of hypertrophy are associated with depression of function [11-14]. Attempts have been made to relate changes in  $\text{Ca}^{2+}$  uptake rates to alterations in the activity of  $\text{Ca}^{2+}$ -adenosinetriphosphatase (ATPase) isolated from SR vesicles, but the

TABLE 11-1. Weights and Histological Features of Cardiac Muscle from Control and Pulmonary-Artery-Banded Ferrets

	Heart Weight/ Body Weight	RV Weight/ Body Weight	Fiber Diameter ( $\mu$ )	Nuclear Area ( $\mu^2$ )	Nuclear Width ( $\mu$ )
Control	$0.369 \pm 0.014$ (n = 7) <sup>b</sup>	$0.075 \pm 0.004$ (n = 7)	$15.1 \pm 0.94$ (n = 50)	$59.7 \pm 3.4$ (n = 50)	$5.7 \pm 0.2$ (n = 50)
Banded (hypertrophied)	$0.448 \pm 0.036$ (n = 9)	$0.145 \pm 0.016$ (n = 9)	$22.8 \pm 1.0$ (n = 70)	$84.2 \pm 3.7$ (n = 70)	$6.7 \pm 0.2$ (n = 70)
<i>p</i> values <sup>c</sup>	< 0.05	< 0.001	< 0.001	< 0.002	< 0.002

<sup>a</sup> Results are expressed as mean  $\pm$  SE.

<sup>b</sup> n = number of preparations measured.

<sup>c</sup> *p* values were determined by Student's *t* test.

RV = right ventricle. (From Gwathmey and Morgan [7], with permission.)

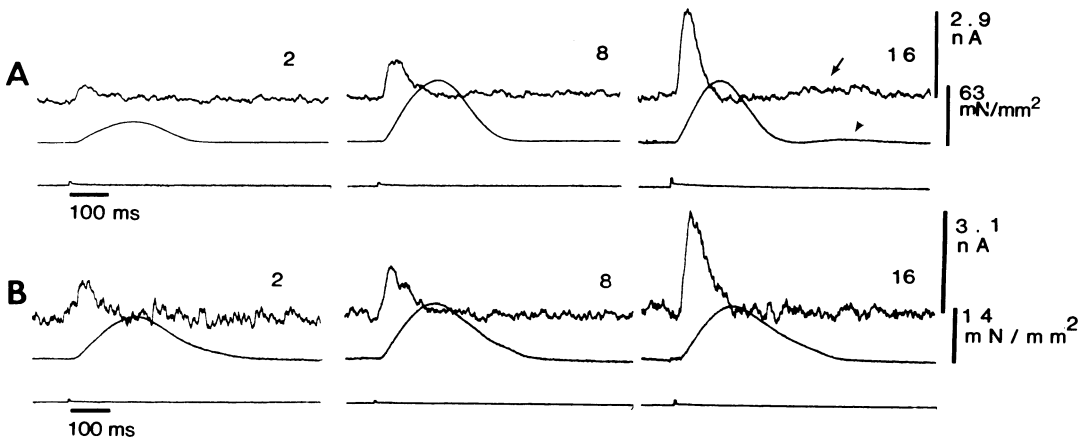


FIGURE 11-1. Aequorin Light Signals (*upper noisy traces*) and Tension Responses (*middle smooth trace*) in Control (A) and Hypertrophied (B) ferret papillary Muscles. The figure shows the responses to three different millimolar concentrations of  $\text{Ca}^{2+}$  in the perfusate, as indicated in the upper right corner of each panel. The lower trace in each panel is the stimulus artifact. The aequorin signal is expressed in nanoamperes (nA) of anode current recorded from the photomultiplier; tension is expressed in milliNewtons ( $\text{mN}/\text{mm}^2$ ) of cross-sectional area. Note the "afterglimmer" (*arrow*) in the light tracing and the aftercontraction (*arrowhead*) in the tension tracing that develop at 16 mM  $[\text{Ca}^{2+}]_0$  in the control. (From Gwathmey and Morgan [7], with permission.)

results are not yet conclusive [15]. Although it is not definitive proof of a cause-and-effect relationship (i.e., these results could be explained by a change in myosin isoenzymes or cross-bridge cycling rates), the prolonged time course of the calcium transient measured with aequorin correlates well with the prolonged relaxation of tension observed in the hypertrophied animals. Similar time-course changes and relaxation abnormalities have been reported in other animal models of hypertrophy as well as in cardiac hypertrophy in humans [16]. Moreover, preliminary electrophoretic measurements have indicated that hypertrophy in the ferret does not change the pattern of myosin isoenzymes; only a single isoenzyme ( $V_3$ ) has been identified [7].

As shown in Figure 11-3, isometric tension development in the hypertrophied muscles was significantly less than in the controls, and we

hypothesized that this might be due to a decreased availability of activator  $\text{Ca}^{2+}$  [7]. However, we tested this hypothesis by comparing the amplitudes of the aequorin light signals in papillary muscles from control and hypertrophied animals, using the method of fractional luminescence. We found that the results of this analysis in the two groups of ferrets were not significantly different, indicating that the availability of intracellular  $\text{Ca}^{2+}$  for activation of the myofilaments was not decreased in the hypertrophied animals. Moreover, as shown in Figure 11-4 the  $\text{Ca}^{2+}$ -tension and  $\text{Ca}^{2+}$ -peak light relationships at varying extracellular  $\text{Ca}^{2+}$  concentrations in the hypertrophied fibers were not shifted from the control curves, indicating that the *potency* of calcium as an agonist (which reflects in part the  $\text{Ca}^{2+}$  sensitivity of the myofilaments) was similar in the two groups of animals. The marked difference in the *efficacy* of  $\text{Ca}^{2+}$  in the two groups (as reflected by the maximum isometric tension response to  $\text{Ca}^{2+}$ ) appears to be due to a lesser ability of the hypertrophied papillary muscles to generate force at any given  $[\text{Ca}^{2+}]_0$ . This difference may be caused by factors not directly studied in our experiments, such as a decreased ability of the hypertrophied fibers to form cross-bridges or to changes in the morphometry or energetics of the cell. They do not appear to be due to changes in availability of intracellular  $\text{Ca}^{2+}$  for activation of the myofilaments or in the sensitivity of the myofilaments to  $\text{Ca}^{2+}$ . Our aequorin data also argue against an increase in the  $\text{Ca}^{2+}$  affinity

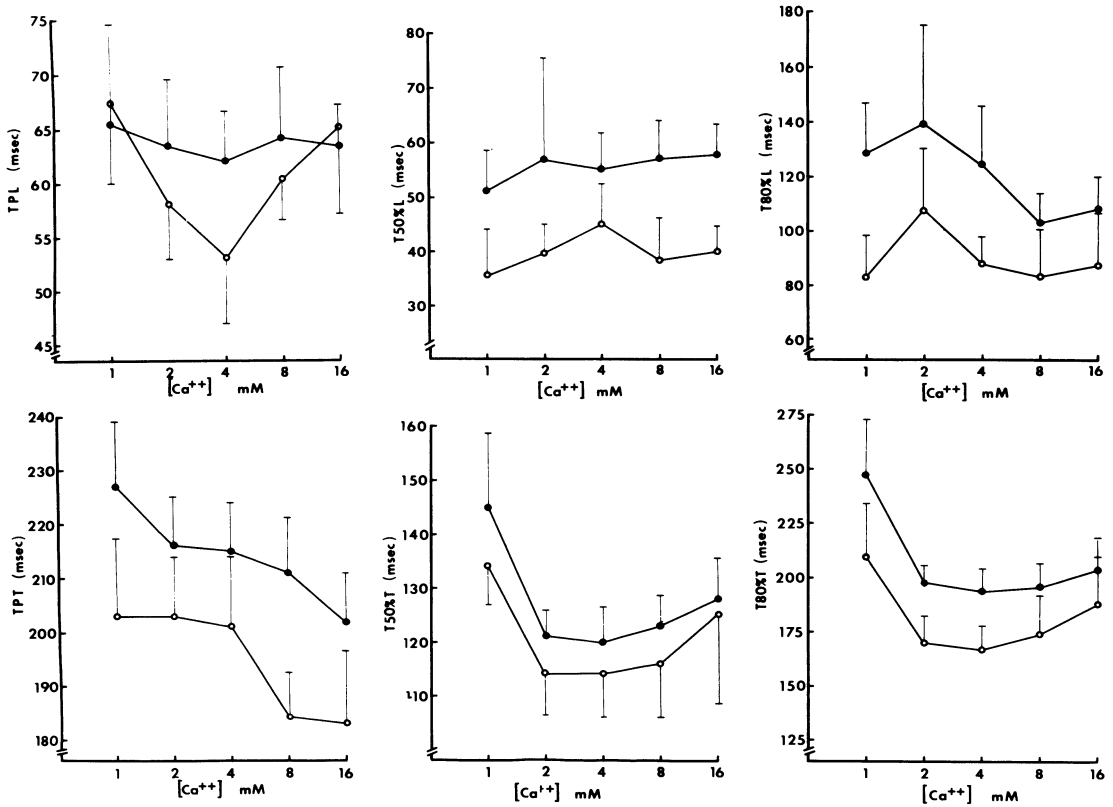


FIGURE 11-2. Time Course of the Aequorin Light Signals (*upper panels*) and Tension Responses (*lower panels*) in Control (*open circles*) and Hypertrophied (*filled circles*) Ferret Papillary Muscles. Concentration-effect curves for calcium are shown with regard to time to peak light (TPL), time to peak tension (TPT), time to 50% decline from peak light (T50%L), time to 50% decline from peak tension (T50%T), time to 80% decline from peak light (T80%L), and time to 80% decline from peak tension (T80%T). (From Gwathmey and Morgan [7], with permission.)

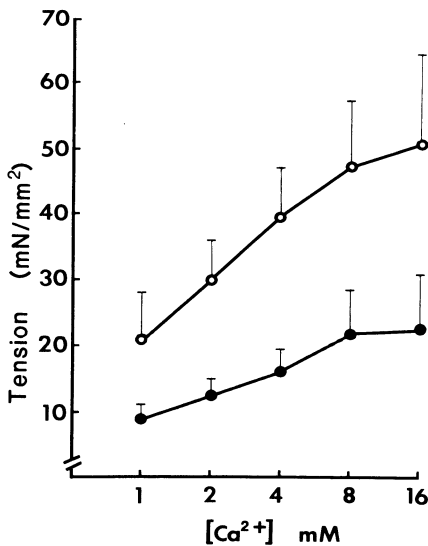


FIGURE 11-3. Concentration-Response Curve for Ca<sup>2+</sup> in Control (*open circles*) and Hypertrophied (*filled circles*) Ferret Papillary Muscles. The peak isometric tension developed at 3-second intervals of stimulation is plotted on the ordinate in mN/mm<sup>2</sup> of cross-sectional area. The millimolar calcium concentration in the perfusate is plotted in the abscissa. (From Gwathmey and Morgan [7], with permission.)

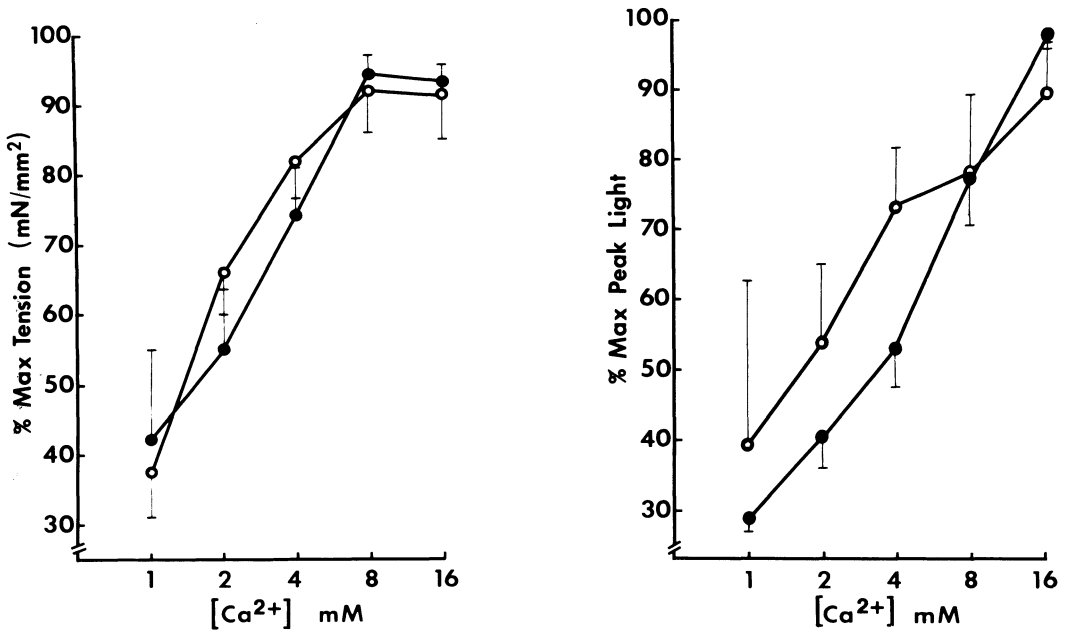


FIGURE 11-4. Concentration-response curve to  $Ca^{2+}$  in papillary muscles from control (open circles) and hypertrophied (filled circles) ferrets. The left panel shows the isometric tension response at 3-second intervals of stimulation displayed as a percent of the maximum tension response. The right panel shows the peak light response at 3-second intervals of stimulation represented as a percent of the maximum light response. (From Gwathmey and Morgan [7], with permission.)

of troponin-C as a potential cause of slowed relaxation in the hypertrophied preparations. Interventions that would be expected to decrease the off-rate of  $Ca^{2+}$  from its binding sites on troponin-C have been reported to abbreviate the duration of the aequorin signal [17, 18], in contrast to our hypertrophied preparations in which the duration of the aequorin signal was prolonged. On the other hand, it is possible that a prolongation of the  $Ca^{2+}$  transient resulting from abnormal calcium handling by intracellular stores could be of large enough relative magnitude to override and mask the effects of a change in the  $Ca^{2+}$  affinity of troponin-C. However, at the very least, our data indicate that a change in the  $Ca^{2+}$  affinity of troponin-C, if it occurs, is a less important determinant of the duration of isometric contraction in this

model of hypertrophy than changes in SR handling of calcium.

To summarize our studies with this model, our results indicate that the decreased amplitude of the peak isometric tension response recorded in the hypertrophied muscles is not due to a decreased availability of intracellular  $Ca^{2+}$  for activation of the myofilaments or to a decrease in the sensitivity of the myofilaments to  $Ca^{2+}$ . On the other hand, the prolonged time course of contraction and relaxation in the hypertrophied muscle correlates well with a similar prolongation of the calcium transient. We conclude, therefore, that changes in intracellular calcium handling can account for some but not all of the contractile changes seen in this ferret model of pressure-overload hypertrophy.

#### *Model II: Changes in the Thyroid State*

Thyroid hormone induces the development of cardiac hypertrophy and alters the contractile state of cardiac muscle; the change in the contractile state is characterized by an increase in the velocities of contraction and relaxation [19]. It has been suggested that thyroid hormone may affect contractility by altering the cellular

control of  $\text{Ca}^{2+}$ , an important second messenger in excitation-contraction coupling [20]. The thyroid state has been shown to influence the function of isolated cardiac SR. An increase in the rate of calcium uptake and adenosine triphosphate (ATP) hydrolysis by isolated cardiac SR has been demonstrated in the hyperthyroid state [21, 22]; in contrast, other investigators have described a diminished rate of calcium uptake by isolated cardiac SR following thyroxine treatment [23, 24]. Using the photo-protein aequorin, intracellular calcium levels during contraction and relaxation of cardiac muscle from hyperthyroid and euthyroid animals have been measured [25]. The results indicate that calcium handling in intact cardiac muscle is altered by the hyperthyroid state.

Nine 12-week-old male ferrets were injected subcutaneously with L-thyroxine, 0.3 mg/kg, daily for a period of 2 to 3 weeks. Eight age-matched control animals were either injected with vehicle for the same period of time or were not injected. There were no differences between the injected and noninjected controls. Hyperthyroid animals stopped gaining weight, whereas control animals continued to grow. Pre- and posttreatment weights in grams ( $\pm$ SD) were, respectively,  $983 \pm 184$  and  $1159 \pm 145$  for the controls and  $983 \pm 88$  and  $954 \pm 103$  for the hyperthyroid animals. The mean heart weight in grams ( $\pm$ SD) and mean heart weight/body weight ratio ( $\pm$ SD) were  $4.10 \pm 0.19$  and  $0.0038 \pm 0.0002$  for the controls and  $5.04 \pm 0.53$  and  $0.0053 \pm 0.0006$  for the hyperthyroid group, which is consistent with cardiac muscle hypertrophy as has been previously described during the development of the hyperthyroid state [26]. Right ventricular papillary muscle from control and hyperthyroid animals were prepared for aequorin studies exactly as described for the animals with pressure-overload.

The maximum tension achieved during isometric contraction was not altered by the hyperthyroid state (Table 11-2). The duration of contraction was abbreviated in muscles from hyperthyroid animals as indicated by a diminished time-to-peak tension and time to 80% relaxation from peak tension (Figure 11-5, Table 11-2). The time course of the calcium transient was also briefer in the thyroxine-treated ferrets. The relatively slow rate of aequorin's response to a change in calcium concentration means that during the rapid rise phase of the  $\text{Ca}^{2+}$  transient the signal does not

follow the true calcium concentration with fidelity [25]. Nevertheless, the rise phase of the calcium transient was detectably steeper in the hyperthyroid animals than in the controls. The decay phase of the calcium transient was markedly steeper in muscle from the hyperthyroid animals. The fractional luminescence [9],  $L/L_{\text{max}}$ , where  $L$  is the aequorin luminescence at the peak of the calcium transient and  $L_{\text{max}}$  is the maximum luminescence, was the same for the control and hyperthyroid animals (see Table 11-2). If cytoplasmic calcium concentration gradients at the peak of the calcium transient are similar in magnitude in both groups of animals, the equal  $L/L_{\text{max}}$  values indicate that the peak average cytoplasmic calcium concentration during contraction in cardiac muscle is not changed by the hyperthyroid state.

It is well established that the maximum rates of isometric tension development and relaxation in cardiac muscle are increased in the hyperthyroid state [27]. In a cross-species study of skeletal muscle, Barany showed that the myosin ATPase activity correlated with the speed of muscle shortening [28]. It has been shown in several species that thyroid-hormone treatment results in stimulation of cardiac muscle myosin ATPase [26]. In the rabbit heart, thyroxine

TABLE 11-2. Characteristics of the Isometric Contraction and the Calcium Transient in Cardiac Muscle from Control and Hyperthyroid Ferrets\*

	Control (n = 8)	Hyperthyroid (n = 9)
T (mN/mm <sup>2</sup> )	15.4 $\pm$ 7.2	16.2 $\pm$ 7.9
TPT (msec)	196 $\pm$ 23	153 $\pm$ 17*
RT <sub>0.8</sub> (msec)	171 $\pm$ 21	123 $\pm$ 16*
TPL (msec)	56 $\pm$ 6	47 $\pm$ 5*
RL <sub>0.8</sub> (msec)	93 $\pm$ 7	66 $\pm$ 6*
Log L/L <sub>max</sub>	-3.3 $\pm$ 0.1 (n = 4)	-3.4 $\pm$ 0.3 (n = 3)

\* All values are expressed as mean  $\pm$  standard deviation (\* $p$   $\pm$  0.002). T is the peak isometric tension in mN/mm<sup>2</sup> of muscle cross sectional area. Time to T (TPT) and time to an 80% relaxation from T (RT<sub>0.8</sub>) are measured in milliseconds. The time from stimulation to the peak of the calcium transient (TPL) and time to an 80% decay of the calcium transient (RL<sub>0.8</sub>) are also measured in milliseconds.  $L/L_{\text{max}}$  represents the ratio of the aequorin luminescence at the peak of the calcium transient over the  $L_{\text{max}}$  of the muscle that was calculated as described in the methods. Experiments were performed at 30°C, except for the measurement of  $L/L_{\text{max}}$  which was performed at 22°C (From MacKinnon and Morgan [25], with permission.)

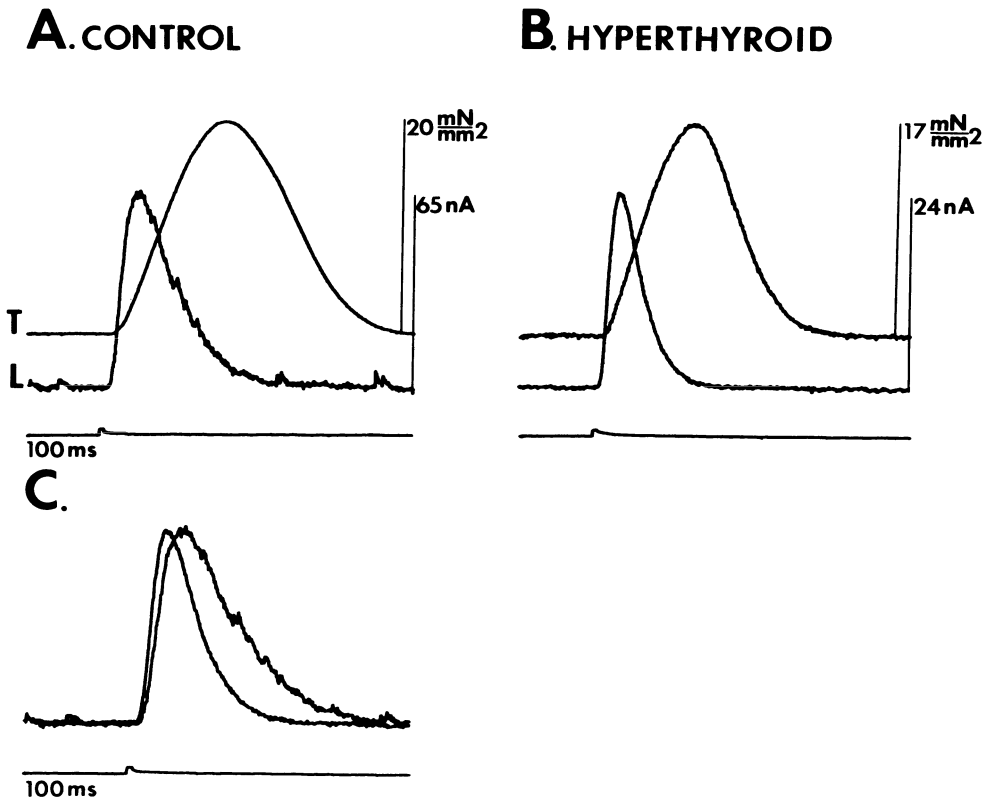


FIGURE 11-5. Isometric tension (T) and calcium transient (L) in the ferret papillary muscle. Tension is reported in units of  $\text{mN}/\text{mm}^2$ . The calcium transient is reported as nA. Signal averaging was used to increase the signal-to-noise ratio. The time from the start of the trace to the stimulus artifact is 100 ms. The muscle was from a control ferret (A) and from a thyroxine-treated ferret (B). In C, the calcium transients from A and B have been scaled to an equal amplitude and superimposed. Note the different time scale in C. (From MacKinnon and Morgan [25], with permission.)

induced the  $V_1$  myosin isozyme, and the relative amount of this myosin correlated with the speed of muscle shortening [29]. However, in the rat, thyroid hormone does not stimulate myosin ATPase, yet it does produce a velocity-related contractile change [30]. This suggests that there are other mechanisms that determine the rate of contraction and relaxation in cardiac muscle.

The experiments in aequorin-loaded muscles show that the cellular control of cytoplasmic

calcium concentration is altered by thyroid hormone. These results are consistent with the previous demonstration that the function of cardiac SR is influenced by the thyroid state. The faster rate of rise of the calcium transient in hyperthyroid animals could result from a thyroid hormone-induced increase in either the quantity of SR membrane, the calcium-conductance during the release phase, or the transmembrane calcium concentration gradient prior to release. It is likely that several factors contribute to the decline phase of the calcium transient, including the buffering of calcium by intracellular binding sites, removal by sarcolemmal mechanisms, and sequestration by the SR. The most important of these is probably the uptake of calcium by the SR [31]. The aequorin studies have clearly demonstrated that the decline phase of the calcium transient is accelerated by the hyperthyroid state. Because the removal of calcium from troponin-C is felt to

be a necessary condition for the relaxation of cardiac muscle, it follows that the calcium transient in the hyperthyroid state favors a more rapid relaxation. Our present description can only be qualitative, however, because a quantitative description of the relationship between the time course of the calcium transient and the tension response awaits more detailed knowledge of the events that translate a change in cytoplasmic calcium concentration into a change in force generation.

To summarize our studies with this model of hypertrophy, the hyperthyroid state results in a more rapid rise phase and decay phase of the calcium transient without apparently altering the peak level of free myoplasmic  $\text{Ca}^{2+}$  reached during contraction. The alteration of the control of intracellular calcium may represent an important mechanism by which thyroid hormone alters the mechanical properties of cardiac muscle, although other "downstream" mechanisms (such as a change in myosin isoenzymes) [32] may be important as well.

### *Models III and IV: Hypertrophy of Human Heart Muscle*

Specimens consisting predominantly of left and right ventricles without atria were obtained from 15 patients with end-stage biventricular failure undergoing cardiac transplantation for dilated cardiomyopathy (idiopathic,  $n = 6$ ; ischemic heart disease,  $n = 6$ ; myocardial deterioration after mitral valve replacement,  $n = 1$ ). Dilated hypertrophic hearts (weight 387–750 gm) were removed from 12 men and one woman, aged 33 to 58 years. To serve as controls, hearts free of gross pathology were obtained from six male and three female organ donors, aged 15 to 58 years, who died from noncardiac causes. Informed consent was obtained from all recipients and from the families of all prospective brain-dead organ donors, before transplantation or excision [33].

After the heart was removed from the thoracic cavity, the left and right ventricles were opened and experimental tissue was excised and placed into a container of oxygenated physiologic salt solution at room temperature. Thin trabeculae carneaе of less than 1.2 mm in diameter were selected for study. The muscles were subsequently handled exactly as described for ferret papillary muscles in the previous sections.

Histologic examination of trabeculae carneaе from the two groups documented that a substantial degree of compensatory hypertrophy was present in the hearts of patients with end-stage failure.

Figure 11–6 shows the light signal (i.e., intracellular  $\text{Ca}^{2+}$  transient), isometric twitch, and action potential recorded with an aequorin-loaded muscle from a control patient without heart failure; Figure 11–7 shows similar tracings from a patient with dilated cardiomyopathy. Compared to the controls, the myopathic muscles showed a prolongation of isometric tension development with a marked delay in relaxation and a corresponding prolongation of the  $\text{Ca}^{2+}$  transient. The light signal recorded from the control muscle in Figure 11–6 consisted of a single component that rose to a peak and then declined towards baseline before peak tension was reached. Similar aequorin signals have been recorded from nonfailing atrial and ventricular muscle [34] and appear to be typical of mammalian working myocardium [10]. In contrast, the light signals recorded from the myopathic muscles were not only prolonged compared to the controls but consisted of two temporally distinct components ( $L_1$  and  $L_2$ , Figure 11–7).  $L_2$  was minimal or absent in control preparations

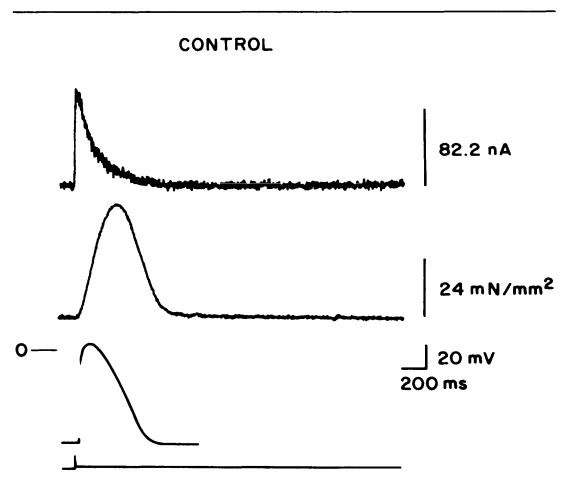


FIGURE 11–6. The aequorin signal (*upper panel*) and the isometric twitch (*middle panel*) recorded in a trabecula from a patient without cardiac disease. The action potential (*lower panel*) was recorded in a different trabecula from the same heart under the same experimental conditions.

DILATED CARDIOMYOPATHY

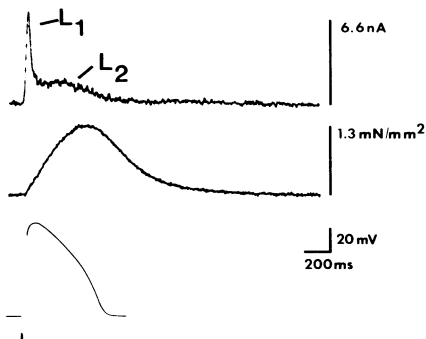
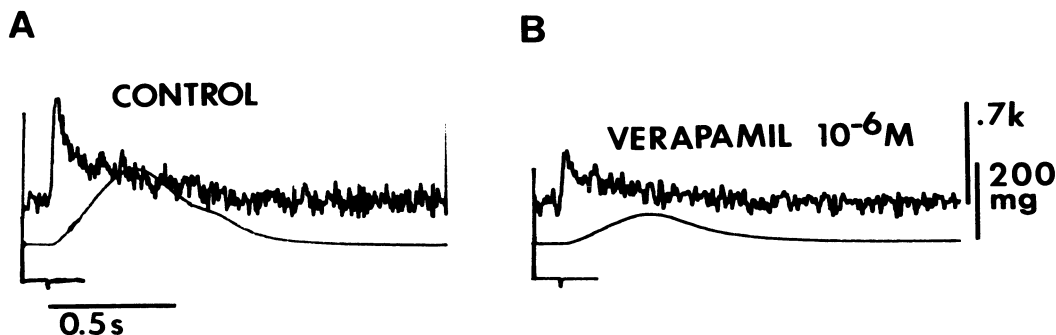


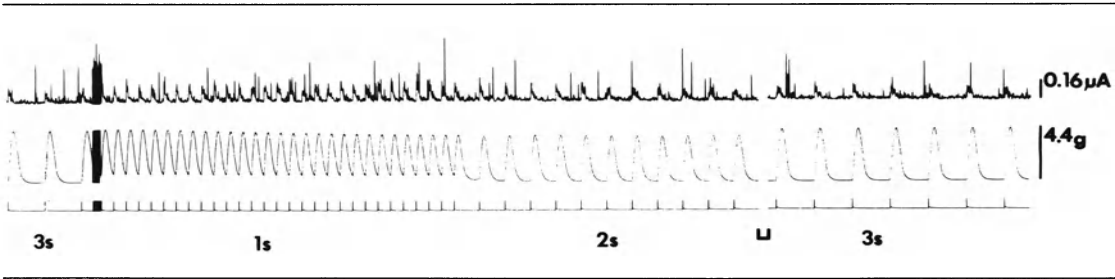
FIGURE 11-7. The aequorin signal (*upper panel*) isometric tension (*middle panel*), and action potential (*lower panel*) recorded in a trabecula from a patient with end-stage heart failure. L<sub>1</sub> and L<sub>2</sub> indicate the two components of the aequorin signal.

FIGURE 11-8. A. Aequorin signal and tension response in a small septal-based papillary muscle from a patient who underwent partial septectomy for idiopathic hypertrophic subaortic stenosis (35 gm of tissue removed). Stimulus interval = 4 seconds; 64 signals were averaged. B. Same muscle after addition of verapamil. Note that verapamil decreases the amplitude of the Ca<sup>2+</sup> transient but does not change its prolonged time course, suggesting that the underlying abnormality in Ca<sup>2+</sup> handling persists. However, the time course of the contractile response is returned towards normal. (From Morgan and Morgan [10], with permission.)

but was prominent in all of the myopathic muscles. These data indicate that the prolonged contraction of myopathic muscle *in vitro* as well as the myocardial relaxation abnormalities observed in patients with dilated cardiomyopathy [35] appear to correlate with changes in intracellular Ca<sup>2+</sup> handling. Similar abnormalities occur in the duration of the isometric twitch, action potential, and Ca<sup>2+</sup> transient recorded from trabeculae carneae of patients with hypertrophic cardiomyopathy [10] (Figure 11-8). These findings were present whether [36] or not [10] clinical signs of heart failure were present.

Although the mechanisms responsible for the generation of L<sub>1</sub> and L<sub>2</sub> are currently being investigated in our laboratory, the functional significance of the prolonged twitch is clearly shown in Figure 11-9. Note that at longer intervals of stimulation, complete relaxation occurs between twitches of this hypertrophied trabecula from a patient with dilated cardiomyopathy. However, at faster rates of stimulation, fusion occurs in the hypertrophied muscle, and both end-diastolic [Ca<sup>2+</sup>]<sub>i</sub> and tension rise. This effect is not observed in nonhypertrophied control preparations. The fusion phenomenon is exacerbated by interventions that increase intracellular Ca<sup>2+</sup>, such as elevated [Ca<sup>2+</sup>]<sub>o</sub> or digitalis; it is diminished by agents that increase the rate of uptake of Ca<sup>2+</sup> by the SR, including beta-adrenergic agonists and the adenylate cyclase activator forskolin. Note also that, not only does end-diastolic tension rise at the faster rates of stimulation, but peak active tension declines as the frequency approaches more physiologic rates. Assuming that a similar phe-





nomenon occurs in vivo, these data indicate that failure of the hypertrophied human heart may be largely due to impaired diastolic function.

**Summary**

In summary, these studies show that hypertrophy in four different disease states may be associated with a variety of alterations in the intracellular Ca<sup>2+</sup> transient. In general, hypertrophy-induced changes in the amplitude and time courses of the Ca<sup>2+</sup> transient correlate with similar changes in the mechanical twitch. However, additional factors altering the Ca<sup>2+</sup> sensitivity of the contractile apparatus and cardiac and extracellular structural changes also appear to be important.

**References**

1. Alpert NR (1983). Introduction. In Alpert NR (ed): *Perspectives in Cardiovascular Research, vol 7: Myocardial Hypertrophy and Failure*. New York: Raven Press, pp xxi-xxxv.
2. Mirsky I, Pfeffer JM, Pfeffer MA (1983). Mechanical properties of normal and hypertrophied myocardium: Is there a relationship between diastolic and systolic function? In Alpert NR (ed): *Perspectives in Cardiovascular Research, vol 7: Myocardial Hypertrophy and Failure*. New York: Raven Press, pp 39-55.
3. Spann JF, Buccino RA, Sonnenblick EH, Braunwald E (1967). Contractile state of cardiac muscle obtained from cats with experimentally produced ventricular hypertrophy and heart failure. *Circ Res* 21:341-354.
4. Spann JF, Covell JW, Eckberg DL, et al (1972). Contractile performance of the hypertrophied and chronically failing cat ventricle. *Am J Physiol* 223:1150-1157.
5. Cooper G, Tomanek RJ, Erdhardt JC, Marcus ML (1981). Chronic progressive overload of the cat right ventricle. *Circ Res* 48:488-497.
6. Spann JF (1983). Contractile and pump func-

FIGURE 11-9. Response of a hypertrophied trabecula from a patient with end-stage heart failure to increased rates of stimulation.

- tion of the pressure overloaded heart. In Alpert NR (ed): *Perspectives in Cardiovascular Research, vol 7: Myocardial Hypertrophy and Failure*. New York: Raven Press, pp 19-33.
7. Gwathmey JK, Morgan JP (1985). Altered calcium handling in experimental pressure-overload hypertrophy in the ferret. *Circ Res* 57:836-843.
8. Morgan JP, Blinks JR (1982). Intracellular Ca<sup>2+</sup> transients in the cat papillary muscle. *Can J Physiol Pharmacol* 60:524-528.
9. Allen DG, Blinks JR (1978). Calcium transients in aequorin injected frog cardiac muscle. *Nature* 273:509-513.
10. Morgan JP, Morgan KG (1984). Calcium and cardiovascular function: Intracellular calcium levels during contraction and relaxation of mammalian cardiac and vascular smooth muscle as detected with aequorin. *Am J Med* 77:33-46.
11. Shlafer M, Gelband H, Sung RF, et al (1978). Time-dependent alterations of myocardial microsomal yield and calcium accumulation in experimentally-induced right ventricular hypertrophy and failure. *J Mol Cell Cardiol* 10:395-407.
12. Sordahl LA, McCollum WB, Wood WG, Schwartz A (1978). Mitochondria and sarcoplasmic reticulum function in cardiac hypertrophy and failure. *Am J Physiol* 224:497-502.
13. Malhotra A, Penpargkul S, Schaible T, Scheuer J (1981). Contractile proteins and sarcoplasmic reticulum in physiologic cardiac hypertrophy. *Am J Physiol* 241:H263-H267.
14. Scheuer J (1983). Alteration in sarcoplasmic reticulum in cardiac hypertrophy. In Tarazi RC, Dunbar JB (ed): *Perspectives in Cardiovascular Research, vol 8: Cardiac Hypertrophy in Hypertension*. New York: Raven Press, pp 111-122.
15. Briggs NF, Wise RM, Feher JJ (1983). Diagnosis of alterations in sarcoplasmic reticulum function. In Alpert NR (ed): *Perspectives in Car-*

- diavascular Research, vol 7: Myocardial Hypertrophy and Failure.* New York: Raven Press, pp 513–525.
16. Paulus WJ, Brutsaert DL (1982). Relaxation abnormalities in cardiac hypertrophy. *Eur Heart J* 3:133–137.
  17. Allen DG, Orchard CH (1983). Intracellular calcium concentrations during hypoxia and metabolic inhibition in mammalian ventricular muscle. *J Physiol (Lond)* 339:107–122.
  18. Housmans PR, Lee NKM, Blinks JR (1983). Active shortening retards the decline of the intracellular calcium transient in mammalian heart muscle. *Science* 221:159–161.
  19. Buccino RA, Spann JF, Pool PE, et al (1967). Influence of the thyroid state on the intrinsic contractile properties and energy stores of the myocardium. *J Clin Invest* 46:1669–1681.
  20. Suko J (1971). Alterations of  $\text{Ca}^{2+}$  uptake and  $\text{Ca}^{2+}$ -activated ATPase of cardiac sarcoplasmic reticulum in hyper and hypothyroidism. *Biochim Biophys Acta* 252:324–327.
  21. Suko J (1973). The calcium pump of cardiac sarcoplasmic reticulum: Functional alterations at different levels of thyroid state in rabbits. *J Physiol (Lond)* 228:563–582.
  22. Limas CJ (1978). Enhanced phosphorylation of myocardial sarcoplasmic reticulum in experimental hyperthyroidism. *Am J Physiol* 234:H426–H431.
  23. Conway G, Heazlitt RA, Fowler NO, et al (1976). The effect of hyperthyroidism on the sarcoplasmic reticulum and myosin ATPase of dogs hearts. *J Mol Cell Cardiol* 8:39–51.
  24. Taskass IE, Szabo J, Nosztray K, et al (1985). Alterations of contractility and sarcoplasmic reticulum function of rat heart in experimental hypo- and hyperthyroidism. *Gen Physiol Biophys* 4:271–278.
  25. MacKinnon R, Morgan JP (1986). Influence of the thyroid state on the calcium transient in ventricular muscle. *Pfluegers Arch* 407:142–144.
  26. Morkin E, Flink IL (1983). Biochemical and physiologic effects of thyroid hormone on cardiac performance. *Prog Cardiovasc Dis* 25:435–464.
  27. Strauer BE, Scherpe A (1975). Experimental hyperthyroidism II: Mechanics of contraction and relaxation of isolated ventricular myocardium. *Basic Res Cardiol* 70:131–141.
  28. Barany M (1967). ATPase activity of myosin correlated with speed of muscle shortening. *J Gen Physiol (Suppl)* 50:196–216.
  29. Pagani ED, Julian FJ (1984). Rabbit papillary muscle myosin isozymes and the velocity of muscle shortening. *Circ Res* 54:586–594.
  30. Marriott ML, McNeill JH (1983). Effect of thyroid hormone treatment on responses of the isolated working rat heart. *Can J Physiol Pharmacol* 61:1382–1390.
  31. Solaro JR, Briggs FN (1974). Estimating the functional capabilities of sarcoplasmic reticulum in cardiac muscle. *Circ Res* 34:531–540.
  32. MacKinnon R, Allen P, Morgan JP (1986). The thyroid state influences myosin and calcium handling in ferret ventricle. *Circulation* 74 (suppl II):432.
  33. Feldman MD, Copelas L, Gwathmey JR, et al (1987). Pharmacologic evidence that deficient production of cyclic adenosine monophosphate may be the primary cause of contractile dysfunction in end-stage heart failure. *Circulation* 75:331–339.
  34. Morgan JP, Chesebro JH, Pluth JR, et al (1984). Intracellular calcium transients in human working myocardium as detected with aequorin. *J Am Coll Cardiol* 3:410–418.
  35. Grossman W, McLaurin LP, Rolett EL (1979). Alterations in left ventricular relaxation and diastolic compliance in congestive cardiomyopathy. *Cardiovasc Res* 13:514–522.
  36. Gwathmey JK, Copelas L, Grossman W, Morgan JP (1986). Calcium handling by normal and diseased human myocardium. *J Gen Physiol* 1986; 88:27a.
  37. Gwathmey JK, Copelas L, MacKinnon R, et al (1987). Abnormal intracellular calcium handling in myocardium from patients with end-stage heart failure. *Circ Res* 61:70–76.

---

PART III. EVALUATION  
OF RELAXATION AND  
COMPLIANCE IN THE  
INTACT HEART

---

---

## 12. DIASTOLIC MYOCARDIAL MECHANICS AND THE REGULATION OF CARDIAC PERFORMANCE

---

J. Scott Rankin, J. William Gaynor, Michael P. Feneley,  
Donald D. Glower, John A. Spratt, George S. Tyson, George W. Maier,  
Craig O. Olsen, Thomas N. Skelton, and Thomas M. Bashore

Over the past 15 years, the primary goal of our physiology laboratory has been to improve the understanding of basic myocardial function in both normal and diseased hearts. Very early in our studies, it became evident that existing descriptors of myocardial performance were deficient, and initial efforts were expended to develop basic models of ventricular geometry, diastolic properties, and systolic function. Later work has been directed toward applying these models to the study of pathophysiology in ischemic heart disease and chronic volume overload. Although this investigation is still in progress, enough information is currently available to provide insight into basic aspects of diastolic myocardial function, to propose several hypotheses on how the heart adapts to clinical heart disease, and to provide direction for future clinical investigation of myocardial mechanics in humans. This chapter will review these topics primarily through publications from our laboratory, each of which contains full references.

### *Proper Measurement of Diastolic Properties*

A detailed review of diastolic mechanics in the intact left ventricle has been published elsewhere [1]. For the purposes of this chapter,

diastole will be defined as that portion of the cardiac cycle in which all mechanical influences of systolic contraction are absent. In effect, this definition excludes relaxation characteristics, which are covered in other sections of this book. In the normal dog heart relaxation is essentially complete by the first diastolic minimum of left ventricular pressure, and half of rapid filling is accomplished during late relaxation before this pressure minimum [2, 3]. There is now evidence that active restorative forces associated with relaxation assist rapid filling during this period [4], and it is also clear that under pathologic conditions such as "demand ischemia," severely prolonged relaxation can limit ventricular "distensibility" throughout the filling period [5]. From our definition, however, this phenomenon would represent continuous systole, with the myocardium never reaching the completely relaxed state. Because the physiology of relaxation is reviewed in detail elsewhere, this chapter will concentrate instead on the mechanics of the fully relaxed phase, which we define as diastole.

Most would agree that diastolic properties are difficult to quantify in the closed-chest subject; it requires very precise measurement techniques as well as valid analytical models. Commonly overlooked factors necessary for acquiring meaningful data include: (1) assessment of intrathoracic pressure and calculation of transmural pressure in the closed chest state, (2) acquiring data over the full physiologic range of ventricular volumes, (3) employing an exponential elastic model in calculating compliance coefficients, (4) including only diastatic data to

Supported by NIH Grants HL09315, HL29436, and HL17670.

Grossman, William, and Lorell, Beverly H. (eds.), *Diastolic Relaxation of the Heart*. Copyright © 1987. Martinus Nijhoff Publishing. All rights reserved.

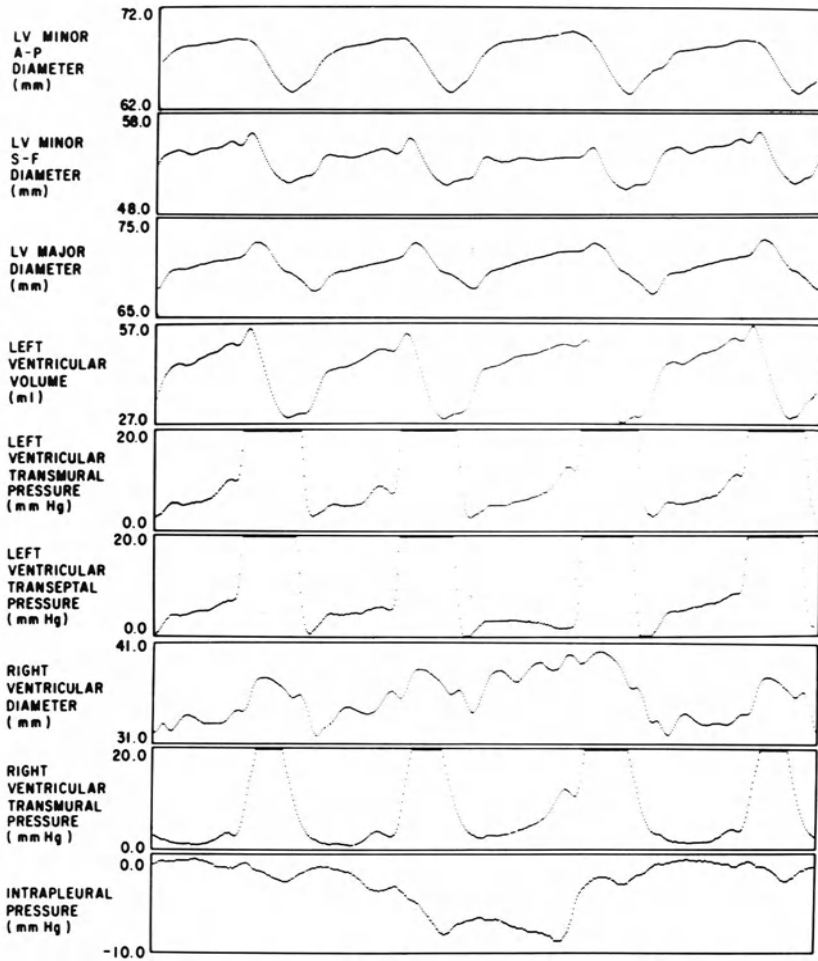


FIGURE 12-1. Multiple cardiac dimension and pressure measurements from a conscious dog during deep inspiration. While intracavitary ventricular pressures fall during inspiration, transmural end-diastolic ventricular pressures increase, consistent with the changes in end-diastolic volumes [6].

minimize viscous effects during rapid filling, (5) accounting for ventricular interaction and pericardial influences, and (6) properly normalizing forces and dimensions to account for differences in ventricular geometry.

The importance of intrathoracic pressure or the force external to the heart is illustrated in Figure 12-1, which depicts data recorded from a closed chest conscious dog during deep inspiration. Although all intrathoracic pressures fall markedly with inspiration, the decline in intracavitary left ventricular pressure is always inappropriate for ventricular dimensional alter-

ations; this apparent inconsistency is negated by subtracting intrapleural pressure from intracavitary values to calculate transmural left ventricular pressure [3, 6-8]. Measuring external pressure in humans poses a substantial problem but is just as important, because the absolute magnitude of diastolic ventricular pressure is on

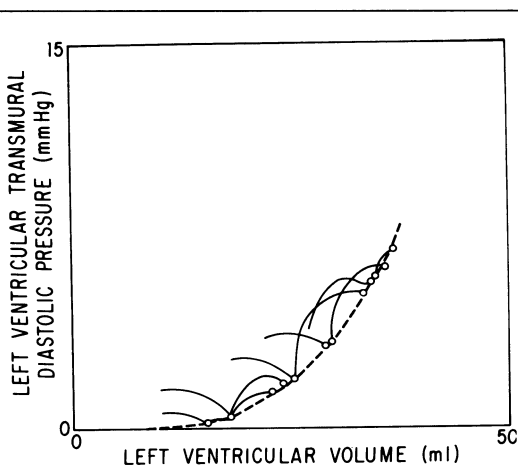


FIGURE 12-2. Diastolic left-ventricular transmural pressure-volume measurements from a conscious dog during vena caval occlusion. Diastatic points (open circles) were fitted with equation 12.1 to generate the static pressure-volume curve (dashed line). Pressure-volume data during rapid filling and atrial systole lie above the static relationship because of viscous effects [1, 3].

the same order as fluctuations in intrathoracic pressure with varying patterns of respiration. Under usual conditions, pericardial restraint probably is minimal, and simply measuring intrathoracic pressure will suffice [9]. Perhaps in future studies, the left pleural space could be cannulated anteriorly with a small introducer, and a 3F micromanometer could be passed to lie external to the left ventricular region of pericardium. Such a procedure should have negligible morbidity in humans and would provide the precision of transmural pressure measurements that is so critical for valid assessment of diastolic properties.

The next factor of importance is acquiring pressure and volume data over the full physiologic range. Figure 12-2 shows diastolic pressure-volume measurements over several dynamic diastoles during a transient vena caval occlusion in the conscious dog. With occlusion of the venae cavae, the heart rapidly empties over 15 to 20 seconds to an unstressed volume ( $V_0$ ), at which the diastolic transmural filling pressure is very close to zero mm Hg. From inspection of the data, it is obvious that simply fitting a single diastole with any sort of model would

yield an estimate of elastic properties very different from that obtained from the entire range of data. Thus, a wide range of measurements is critical. Transient vena caval occlusion may be the ideal method for varying ventricular volume in humans, because it produces negligible myocardial ischemia (Figure 12-3) and correlates well with steady-state information as seen in Figure 12-4 [9, 10]. A transient vena caval occlusion (15-20 seconds) is potentially safer than drug interventions for human application because of the very brief nature of the hemodynamic perturbation. Finally, the technique is more effective in generating a wide range of pressure and volume data which is so essential. Vena caval occlusion as a catheterization laboratory procedure should be investigated as a routine adjunct to diagnostic cardiac catheterization [11].

As with most biologic tissues, the relationship between diastolic ventricular pressure ( $P$ ) and volume ( $V$ ) or between myocardial force and length in the intact heart is exponential (Figures 12-2, 12-5). As such, some sort of exponential model must be used to describe the relationship numerically, and a modification of the equation formulated by Glantz has been ideal for this purpose:

$$P = \alpha \left( e^{\left\{ \beta \frac{V - V_0}{V_0} \right\}} - 1 \right),$$

where  $\alpha$  and  $\beta$  are elastic coefficients. This equation is appropriate for the intact heart because measured ventricular diastolic transmural pressure consistently has been found to be zero at a finite  $V_0$ , and the formula predicts this physiology. Diastolic properties can be quantified by the exponential elastic coefficients,  $\alpha$  and  $\beta$ , and, using standard nonlinear statistical routines [1, 3, 14], differences can be assessed objectively.

During rapid diastolic filling or atrial systole, measured ventricular pressure is always higher than predicted by the simple exponentially elastic relationship (Figure 12-2). This finding probably relates to viscous effects, where additional increments in pressure are required to stretch the muscle and to overcome internal frictional forces [1, 3, 15]. These viscous forces in the intact ventricle are approximately proportional to the myocardial lengthening rate and are most prominent during periods of dynamic filling. From a practical viewpoint, these effects are relevant to the measurement of diastolic properties and need to be considered in some

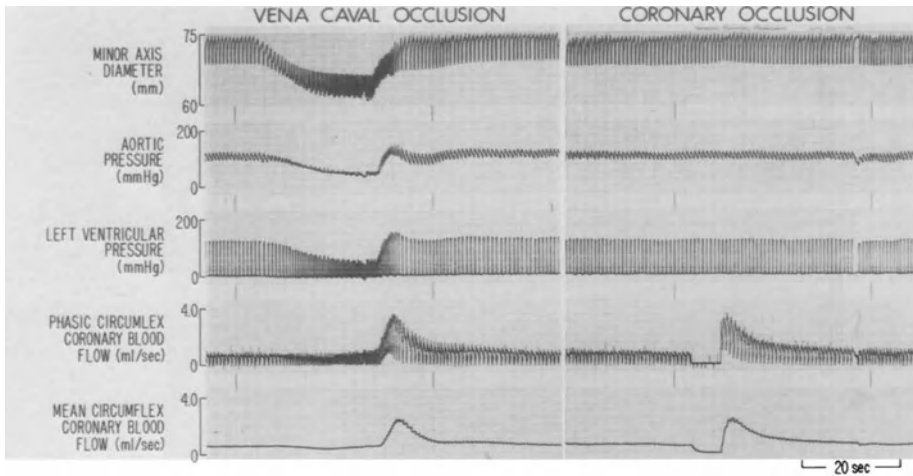


FIGURE 12-3. Ventricular dimensions, pressure, and coronary flow data from a conscious dog during a 20-second vena caval occlusion and during a 5-second coronary occlusion. Induced ischemia (as assessed by reactive hyperemia) from the vena caval occlusion is approximately equivalent to a 5-second coronary occlusion [1].

way. The simplest technique involves omitting dynamic data from the analysis and fitting only diastatic measurements ( $dL/dt < 5\%/second$ ) with the Glantz equation as shown in Figure 12-2.

To a certain extent, the cardiac ventricles function as a single unit during both systole and diastole [14]. Increasing right ventricular diastolic pressure and volume relative to the left ventricle shifts the interventricular septum leftward and alters left ventricular geometry (see Figure 12-1). The end result is a higher left ventricular diastolic transmural pressure at a given volume, or an apparent upward shift of the diastolic compliance curve (Figure 12-6). Thus, it is essential to minimize differential changes in right and left ventricular volumes (such as during inspiration) as data are recorded, and again the best method for accomplishing this goal is transient vena caval occlusion. Because the right ventricle empties rapidly at initiation of the occlusion, subsequent changes in left ventricular pressure and volume represent almost pure left ventricular physiology, devoid of interactive effects. Pericardial influences on ventricular filling under stable physiologic conditions probably are minimal and need not be considered [9]. However, the physiology in pathologic or acutely stressed situations is less clear.

The final factor to be considered is proper normalization of force and dimension data [1, 3, 16]. When dealing with different hearts or

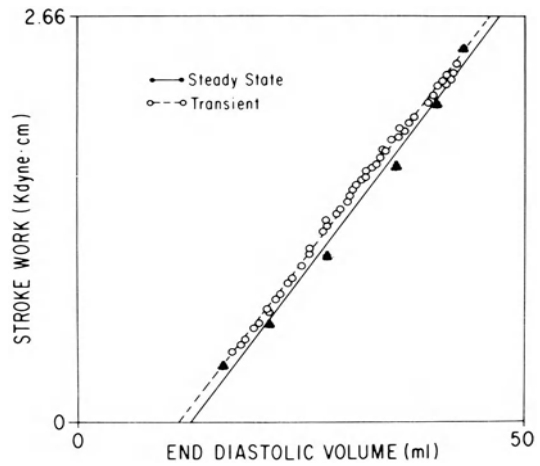


FIGURE 12-4. Left ventricular preload-recruitable stroke work relationships obtained in the isolated-perfused heart during steady-state decrements in end-diastolic volume (closed circles) and during simulated dynamic vena caval occlusion (open circles). The ventricle was emptied over 20 seconds during the simulated vena caval occlusion. Left-ventricular function data derived from dynamic decrements were not different from steady-state data [10].

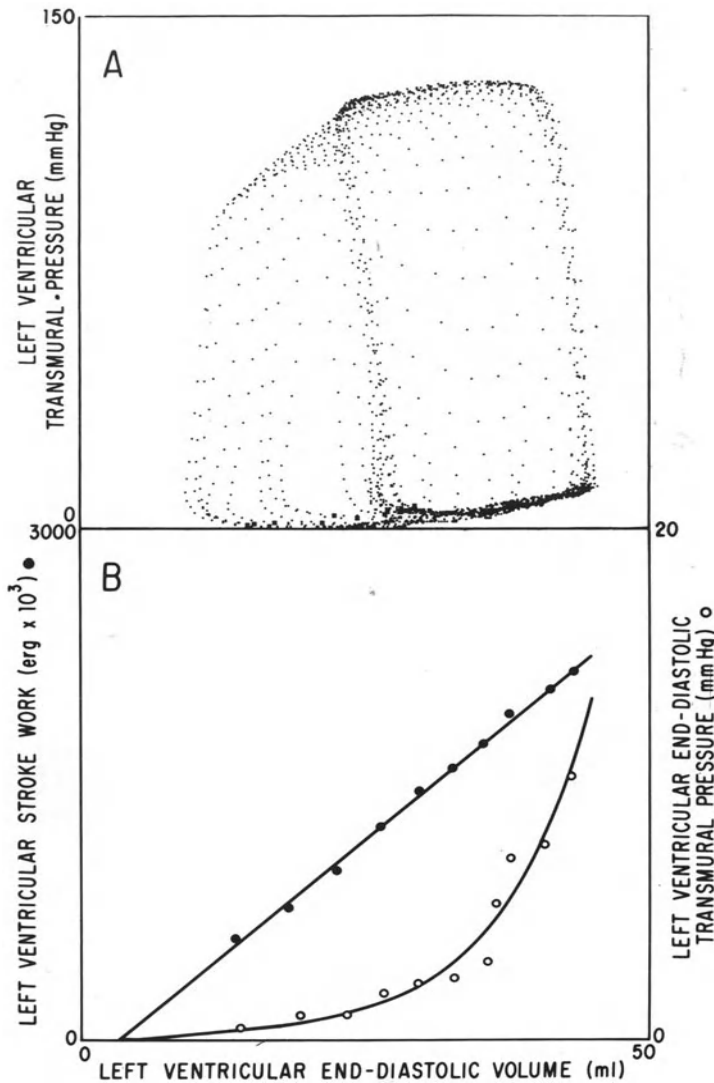


FIGURE 12-5. A. Dynamic left-ventricular pressure-volume loops obtained in the conscious dog during vena caval occlusion with data digitized at 200 Hz. B. Preload recruitable stroke work and diastolic pressure-volume curves [17].

with ventricles that are changing geometric characteristics with time, pressure and dimension measurements must be converted to wall stress ( $\sigma$ ) and strain ( $\epsilon$ ). Our group generally uses the ellipsoidal modification of Laplace's law to calculate stress:

$$\sigma = \frac{Pr_b}{b} \left[ 1 - \frac{r_b^3}{r_a^2(2r_b + b)} \right], \quad (12.2)$$

where  $r_b$  is minor axis midwall radius,  $r_a$  is major axis radius, and  $b$  is wall thickness. The Lagrangian strain formula is used to normalize dimensions:

$$\epsilon = \frac{\ell - \ell_0}{\ell_0}, \tag{12.3}$$

where  $\ell$  is the instantaneous minor axis mid-wall circumference and  $\ell_0$  is the unstressed circumference at 0 mm Hg diastolic transmural pressure. After conversion of pressures and dimensions to stress and strain, normalized myocardial elasticity can be calculated from equation 12.1, and myocardial properties of hearts with differing ventricular geometry can be compared.

An example of this principle is given by chronic volume overload [16]. After 1 week of a large aortocaval shunt in the conscious dog, significant ventricular dilatation and hypertrophy are evident (Figure 12-7). Inspection of the diastolic pressure-volume curve (Figure 12-8A) reveals a rightward shift of the relationship or an apparent increase in ventricular chamber compliance. To assess alterations in myocardial properties, however, measurements must be normalized for differences in chamber geometry. In fact, when diastolic stress-strain relationships are computed, the opposite result is evident (Figure 12-8B), and the diastolic curve is shifted to the left, suggesting a decrease in myocardial compliance. This simple example illustrates how important geometric normalization would be to proper interpretation of human pathophysiology.

### A Unified Approach to Quantification of Ventricular Function

In many respects, focusing exclusively on diastolic properties is misleading, because diastolic physiology is inextricably dependent on systolic function and vice versa. In fact, diastolic and systolic characteristics probably have a common basis at the level of the sacromere as outlined in the next section. To discuss diastolic and systolic function simultaneously, our group has devised the analysis shown in Figure 12-5. Raw digital pressure-volume loops from a conscious dog are shown in panel A for cardiac cycles during a vena caval occlusion. In panel B, the area of each pressure-volume loop is computed as net stroke work, and graphic analyses of systolic and diastolic function are illustrated on the same volume scale. The diastolic pressure-volume curve defines the chamber compliance characteristics, while the stroke work/end-

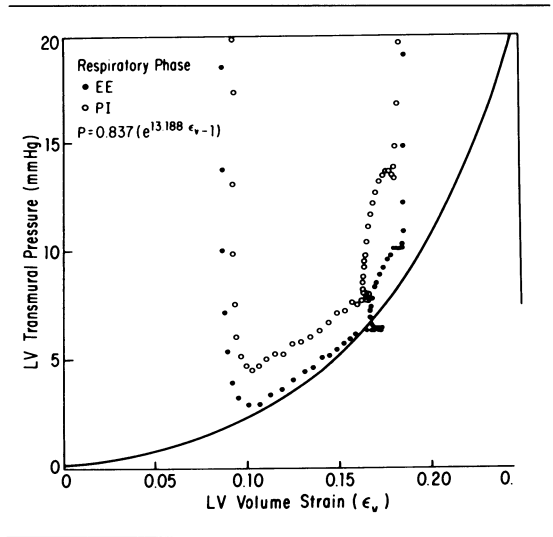


FIGURE 12-6. Diastolic left ventricular (LV) pressure-volume relationships obtained in a conscious dog during expiration (closed circles) and deep inspiration (open circles). Inspiration and leftward septal shifting (see Figure 12-1) were associated with an upward shift of the relationship [6].

diastolic volume or preload-recruitable stroke work (PRSW) relationship quantifies systolic function [17]. Specifically, the diastolic compliance curve determines the end-diastolic volume that is achievable with a given filling pressure, and the PRSW relationship defines the systolic external energy expenditure that is possible from a given end-diastolic volume. The slope of the PRSW curve is afterload-insensitive and responsive to changes in myocardial inotropism, while the  $x$ -intercept is approximately equivalent to diastolic  $V_0$  or the unstressed volume [17, 18]. From the pathophysiological viewpoint,  $V_0$  is in many respects the most relevant diastolic parameter, so that the PRSW curve *alone* provides a relatively complete and simultaneous assessment of diastolic and systolic function.

### Pathophysiology of Myocardial Ischemia

Myocardial compliance seems to be relatively passive and unaffected by acute pharmacologic interventions under normal conditions [1, 3, 19]. During acute ischemia, however, very rapid and profound changes occur in diastolic

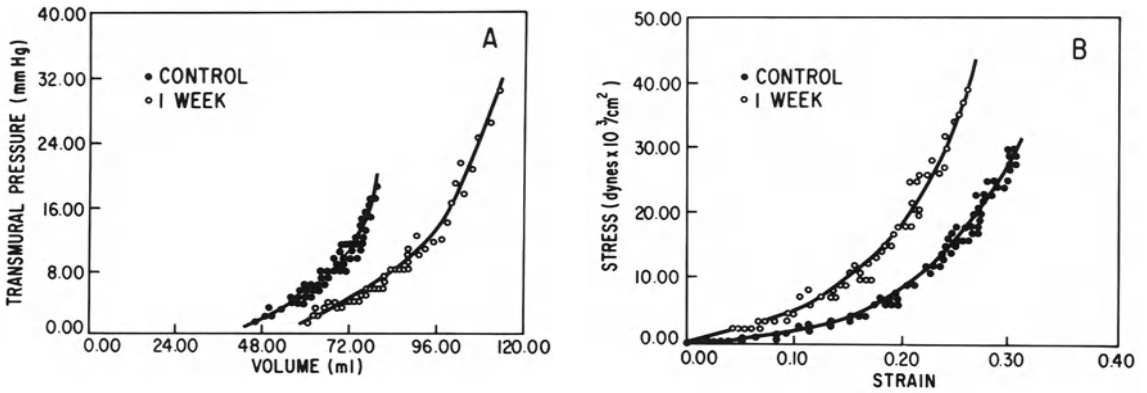


FIGURE 12-8. Diastolic left ventricular pressure-volume (A) and stress-strain (B) data obtained by vena caval occlusion in a conscious dog before and after 1 week of a large aortocaval shunt. Diastolic chamber and myocardial compliance characteristics change in opposite directions [1].

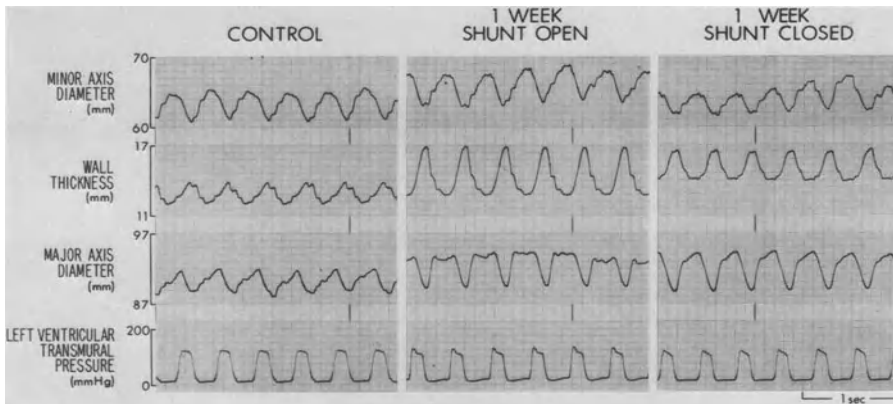


FIGURE 12-7. Analog left ventricular dimension and pressure data obtained during control conditions, after 1 week of a large aortocaval shunt, and after 1 week with the shunt acutely occluded. Significant ventricular dilatation and hypertrophy were evident, accounting for a 15% increase in myocardial mass [16].

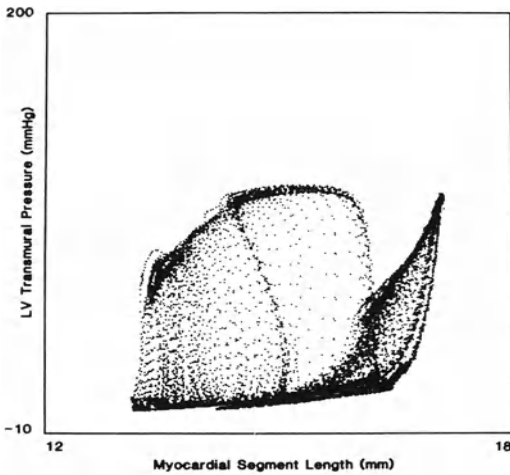


FIGURE 12-9. Dynamic left ventricular pressure-segment length loops obtained during vena caval occlusion during control conditions (*left set of loops*) and after an acute coronary occlusion (*right loops*). Collapse of the work loops and shifting to the right of the diastolic pressure-segment length relation are evident during ischemia [22].

properties, characterized by an increase in  $\ell_0$  and a shift to the right of the diastolic compliance curve (Figure 12-9). This phenomenon has been termed *ischemic-induced diastolic creep* [20]. Normalizing dimensions for the increase in  $\ell_0$  produces an upward shift of the diastolic pressure-strain relationship or a diminished compliance. Ischemic diastolic physiology can be described either by change in  $\ell_0$  or by alterations in the compliance coefficients, because the two parameters seem to be proportional. For practical purposes, simply assessing the changes in  $\ell_0$  provides a reasonably quantitative index of functional ischemic injury [21, 22].

Ischemic myocardial creep is characterized ultrastructurally by an overstretching of the sarcomere and the appearance of prominent I-bands [21]. Interestingly, reversal or recovery of the diastolic creep abnormality seems to be directly associated with recovery of systolic function (Figure 12-10), again suggesting a common ultrastructural basis. As opposed to normal conditions, pharmacologic interventions after ischemic injury acutely alter diastolic pro-

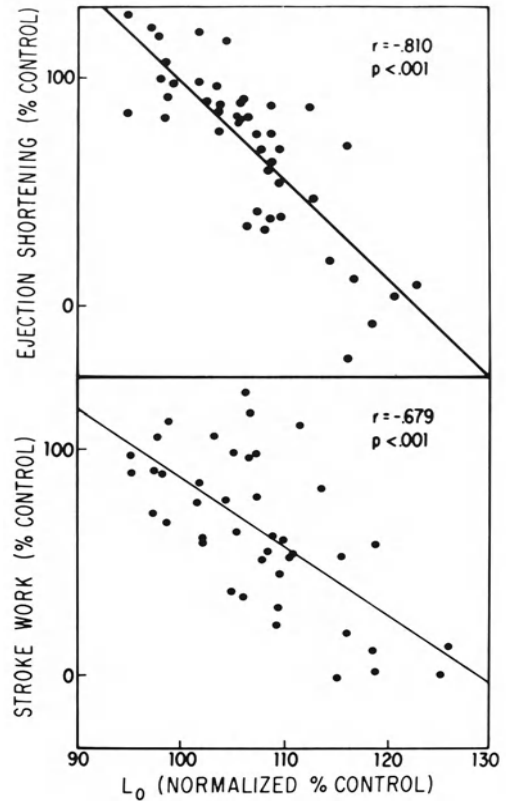


FIGURE 12-10. Myocardial function data obtained from eight dogs before and for 24 hours after a 15-minute coronary occlusion [21]. Depression and recovery of systolic function (change in segment shortening and stroke work) seemed to be directly related to the degree of diastolic creep (change in  $\ell_0$ ).

erties [23], while simultaneously producing a directionally similar and proportional effect on recovery of systolic function. This finding further substantiates the integral association of ischemic diastolic and systolic performance, with alterations in both perhaps reflecting a common ultrastructural factor such as sarcomere overstretching or abnormalities in actin-myosin cross-bridge registration [21].

A convenient method of simultaneously quantifying diastolic and systolic ischemic dysfunction is illustrated in Figure 12-11A. Ische-

mia alters the PRSW relationship both by increasing  $\ell_0$  (diastolic effects) and by decreasing the slope (systolic effects). Both alterations are associated with reduced work capacity and can be described simultaneously by changes in the area under the PRSW curve. A typical plot of myocardial functional recovery (PRSW area) after reversible ischemic injury is shown in Figure 12–11B. This model has been useful in

assessing the precise effects of hemodynamic interventions designed to alter recovery of myocardial function after ischemic injury [24]. In summary, alterations in diastolic mechanical properties and changes in  $\ell_0$  play a significant role in the pathophysiology of myocardial dysfunction during acute ischemia and reperfusion.

### Chronic Volume Overload

As described elsewhere [16, 25], volume overload acutely increases diastolic ventricular pressure and stroke volume. Cardiac output is maintained by a combination of Frank-Starling reserves (increasing end-diastolic volume) and inotropic reserves induced by sympathetic reflexes. The chronically elevated diastolic pressure, however, produces a time-dependent increase in diastolic ventricular dimensions at 0 m Hg transmural pressure, which also can be defined as creep. As opposed to ischemic creep, however, dimensional lengthening in volume overload is associated with an increased number of sarcomeres in series and parallel along with more normal sarcomere morphology [26]. The mechanism of this phenomenon is unclear but two hypotheses are possible. First, myocardial and sarcomere overstretching may occur at a very early stage, increasing systolic wall stress at a given pressure by altering ventricular geometry. Then, the elevated wall stress may stimulate sarcomere replication and the hypertrophy process [27–29]. Alternatively, elevated diastolic pressure may be a direct stimulus to hypertrophy without ever producing an “overstretched” state. Whichever mechanism is operative, hypertrophy in volume overload tends to produce wall thickening proportional to circumferential lengthening and to maintain a normal relationship between ventricular pressure and mural stress (Figure 12–12). This finding is characteristic of the “compensated” phase of adaptation, and several authors have postulated that inadequate hypertrophy, extreme geometric alterations, or both may be operative during the end-stage or decompensated phase [30, 31]. Thus, changes in diastolic geometry and mechanics play a major role in the adaptation of the heart to volume overload.

Mechanistic understanding of pathophysiology is important, but our final goal is to develop measures of myocardial performance that will be clinically useful in timing therapeutic interventions. The physiologic problem in volume

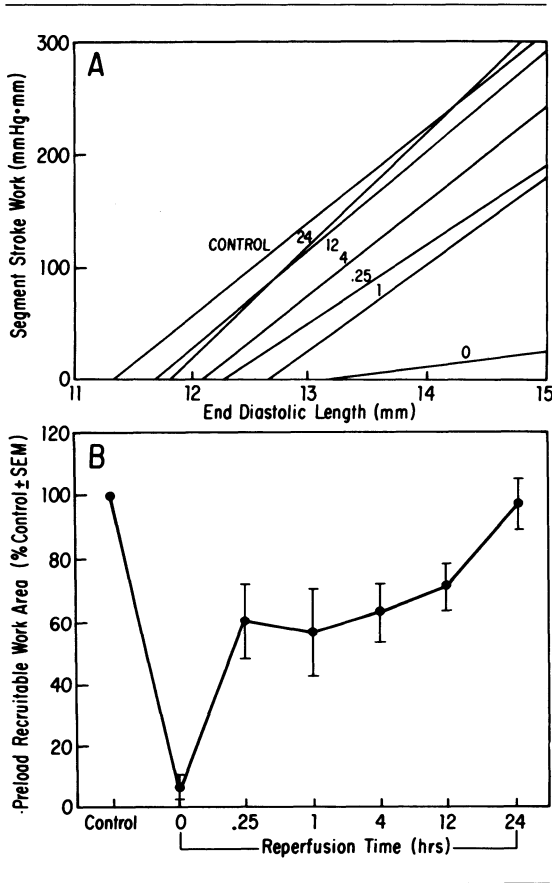
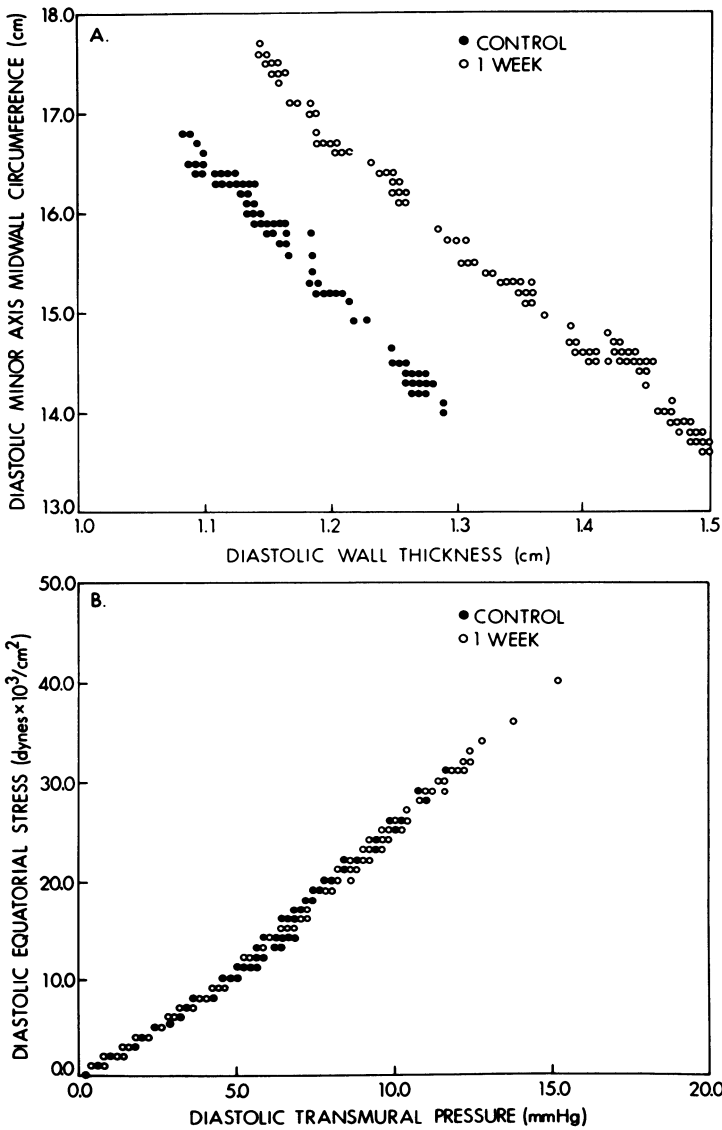


FIGURE 12–11. A. Regional left-ventricular preload-recruitable stroke work (PRSW) data obtained in the control state, during a 15-minute coronary occlusion, and at various times (0–24 hours) after complete reperfusion (panel A). Ischemia produced a rightward shift in the  $x$ -intercept and a decrease in PRSW slope (evident in line 0 at the start of reperfusion) which required 24 hours to recover. B. PRSW area data from eight dogs obtained during the same protocol, illustrating the time course of functional recovery after reversible ischemic injury [22].



overload and valvular heart disease in general is differentiating myocardial dysfunction from hemodynamic derangements induced by loading abnormalities. Clinical symptoms in volume overload correlate poorly with prognosis [32], and current indices of ventricular function, such as ejection fraction, are highly load-dependent. Thus, a load-insensitive method of quantifying myocardial performance would be desirable.

FIGURE 12-12. Left-ventricular minor axis midwall circumference and wall thickness relationships obtained by vena caval occlusion during control (*closed circles*) and after 1 week of a large aortocaval shunt (*open circles*). Hypertrophy and dilatation produced a shift in the relationship upward and to the right (*panel A*). In panel B, the wall thickening seemed to exactly compensate for the increased circumference, maintaining the relationship between left ventricular pressure and stress constant [1].

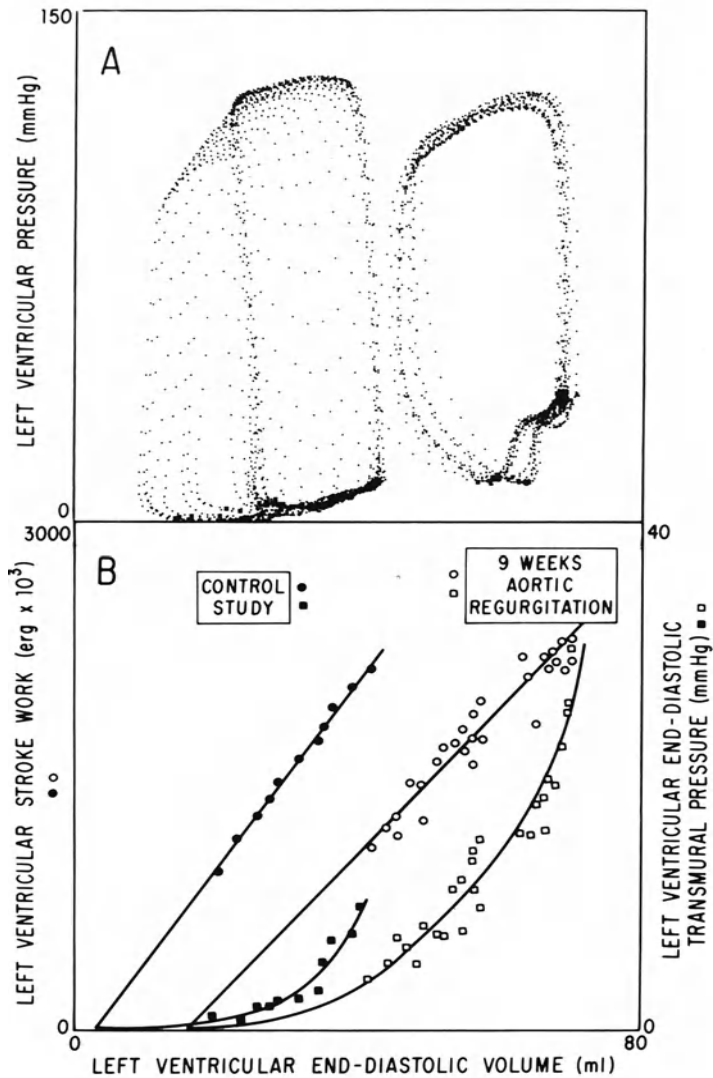


FIGURE 12-13. Left ventricular pressure-volume loops (*panel A*), and preload-recruitable stroke work and diastolic compliance curves (*panel B*) during control (*closed symbols*) and after 9 weeks of aortic valvular regurgitation (*open symbols*). Data were obtained during vena caval occlusion in a conscious dog. For clarity, only pre-occlusion pressure-volume loops are illustrated for the 9-week study [33].

To approach this problem, our group is currently employing a closed-chest chronically instrumented dog model of aortic valvular incompetence, which represents pure left-ventricular volume overload [33]. In Figure 12-13, control hemodynamic data are compared with those observed after 9 weeks of aortic regurgitation. Raw pressure-volume loops are illustrated in panel A, and derived PRSW and compliance

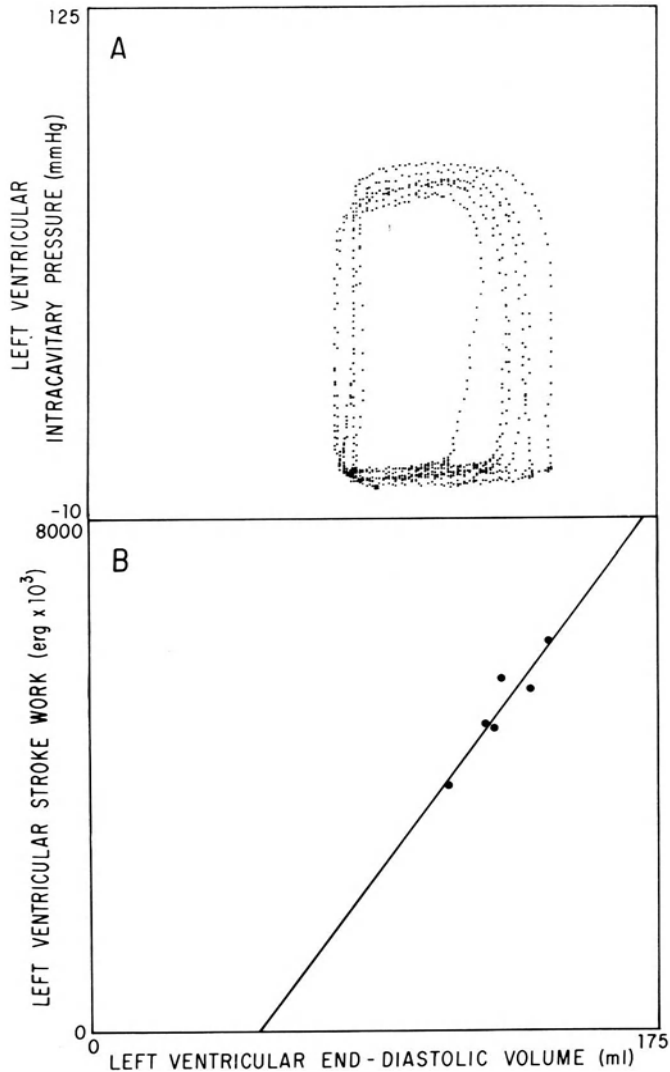


FIGURE 12-14. Left ventricular pressure-volume loops (*panel A*) and preload-recruitable stroke work relationships (*panel B*) obtained by digital subtraction ventriculography during a vena caval occlusion in man. See text for details.

curves are shown in panel B. As discussed previously, chronic volume overload is associated with an increase in  $V_0$  and a rightward shift of the diastolic pressure-volume relationship. The slope of the PRSW curve, however, is well-maintained, signifying a well-compensated adaptation. This change would be analogous to a reduced ejection fraction from ventricular dilatation but with preserved systolic perfor-

mance. Conversely, one might hypothesize that decompensation would reduce the slope of the relationship and that this parameter would be a useful index of intrinsic myocardial performance. Normalization of the analysis for chan-

ges in ventricular geometry and heart rate might be necessary and is easily accomplished [17]. It is hoped that either the magnitude of change in  $V_0$  normalized for body surface area, or the slope of the PRSW curve will have prognostic significance and clinical utility.

It is now possible to make detailed measurements of human myocardial function. Left ventricular pressure-volume loops obtained during transient inferior vena caval occlusion in a patient with normal left ventricular function are shown in Figure 12-14A. By pulsing small volumes of contrast into the left ventricle during each diastole, 30 seconds of continuous ventriculographic data were recorded on a digital disc during the course of a balloon occlusion of the inferior vena cava. Left ventricular volume was calculated with the digital-subtraction ventriculographic technique at 30-msec intervals [34], and intracavitary left ventricular pressure was obtained with a high-fidelity micromanometer. The data were smoothed with a poly-orthogonal transformation and expanded to 5-msec intervals by interpolation techniques. As shown in the dog, the human PRSW relationship (Figure 12-14B) seems highly linear, although only 40 to 50% of the curve is obtainable with isolated inferior vena caval occlusion. This range probably is sufficient to obtain meaningful data, whereas the range of end-systolic pressure-volume points (Figure 12-14A) seems inadequate [35]. Moreover, significant shifting of both diastolic and end-systolic intracavitary ventricular pressures was observed because of minor fluctuations in intrathoracic pressure. Such minor shifting of intracavitary pressure occurs despite attempts at stable breath-holding and clearly limits analysis of diastolic or end-systolic properties without intrapleural pressure measurements. Because the stroke work calculation is an integrated area of the pressure-volume loop, however, the PRSW relationship is relatively insensitive to minor alterations in intrapleural pressure. Therefore, the PRSW analysis may prove to be valid in humans from assessment of intracavitary pressure measurements alone. Although manual ventriculographic data reduction is still relatively tedious, the future development of automated edge detection programs, along with simultaneously digitized left ventricular pressure, may simplify the analysis complexity and facilitate calculation of human pressure-volume and PRSW relationships on a routine basis. Given the physiologic

advantages of this model [17], application of these techniques to future studies of clinical pathophysiology should provide important new insights.

In summary, diastolic myocardial mechanics are difficult to measure, but quantitative assessment is highly plausible with current technology. Alterations in diastolic properties play a major role in pathophysiology and adaptation of the heart to ischemic and valvular disorders. With several minor modifications in current diagnostic techniques and new approaches to functional modeling, quantification of intrinsic myocardial properties in humans now is possible. Such advances could significantly improve the care of patients with clinical heart disease.

### References

1. Rankin JS, Arentzen CE, Ring WS, et al (1980). The diastolic mechanical properties of the intact left ventricle. *Fed Proc* 39:141-147.
2. Rankin JS, McHale PA, Arentzen CE, et al (1976). The three-dimensional dynamic geometry of the left ventricle in the conscious dog. *Circ Res* 39:304-313.
3. Rankin JS, Arentzen CE, McHale PA, et al (1977). Viscoelastic properties of the diastolic left ventricle in the conscious dog. *Circ Res* 41:37-45.
4. Yellin EL, Masatsugu H, Yoran C, et al (1986). Left ventricular relaxation in the filling and nonfilling intact canine heart. *Am J Physiol* 250:H620-H629.
5. Momomura S, Bradley AB, Grossman W (1984). Left ventricular diastolic pressure-segment length relations and end-diastolic distensibility in dogs with coronary stenoses: An angina-physiology model. *Circ Res* 55:203-214.
6. Olsen CO, Tyson GS, Maier GW, et al (1985). Diminished stroke volume during inspiration: A reverse thoracic pump. *Circulation* 72:668-679.
7. Tyson GS Jr, Olsen CO, Maier GW, et al (1982). Dimensional characteristics of left ventricular function after coronary artery bypass grafting. *Circulation* 66(suppl I):16-25.
8. Rankin JS, Olsen CO, Arentzen CE, et al (1982). The effects of airway pressure on cardiac function in intact dogs and man. *Circulation* 66:108-120.
9. Tyson GS Jr, Maier GW, Olsen CO, et al (1984). Pericardial influences on ventricular filling in the conscious dog: An analysis based on pericardial pressure. *Circ Res* 54:173-184.
10. Snow ND, Burkhoff D, Glower DD, et al (1985). Evaluation of the vena caval occlusion

- technique for assessing systolic myocardial performance. *Circulation* 72(suppl III):III-341.
11. Bashore TM, Walker S, Van Fossen D, et al (1985). Use of inferior vena caval occlusion to acutely alter preload in man. *Circulation* 72 (suppl III):III-43.
  12. Glantz SA (1975). A constitutive equation for the passive properties in the left ventricle. *J Appl Physiol* 39:665-671.
  13. Olsen CO, Lee KL, Tyson GS, et al. Diastolic anisotropic properties of the left ventricle in the conscious dog. Submitted for publication.
  14. Olsen CO, Tyson GS, Maier GW, et al (1983). Dynamic ventricular interaction in the conscious dog. *Circ Res* 52:85-104.
  15. Rankin JS, Olsen CO (1980). The diastolic filling of the left ventricle. *Eur Heart J* 1:95-105.
  16. Olsen CO, Van Trigt P II, Rankin JS (1981). The dynamic geometry of the intact left ventricle. *Fed Proc* 40:2023-2030.
  17. Glower DD, Spratt JA, Snow ND, et al (1985). Linearity of the Frank-Starling relationship in the intact heart: The concept of preload recruitable stroke work. *Circulation* 71:994-1009.
  18. Spratt JA, Glower DD, Snow ND, et al (1984). Three-dimensional analysis of stroke work in conscious dog. *Circulation* 70(suppl II):936.
  19. Van Trigt P III, Olsen CO, Pellom GL, et al (1980). Do acute hemodynamic interventions alter diastolic mechanics of the left ventricle? *Circulation* 62(suppl III):778, 1980.
  20. Edwards CH II, Rankin JS, Ling D, et al (1981). The effect of ischemia on left ventricular regional function in the conscious dog. *Am J Physiol* 240:H413-H420.
  21. Glower DD, Wolfe JA, Spratt JA, et al ( ). Relationship between reversal of diastolic creep and recovery of systolic function after ischemic myocardial injury in the conscious dog. *Circ Res*: in press.
  22. Glower DD, Spratt JA, Kabas JS, et al. Quantification of regional myocardial function after acute ischemic injury: Application of preload recruitable stroke work. *Am J Physiol*: in press.
  23. Kabas JS, Glower DD, Spratt JA, et al (1985). Effects of afterload and inotropic state on diastolic properties after ischemic injury. *Circulation* 72(suppl III):III-283.
  24. Kabas JS, Glower DD, Spratt JS, et al (1985). Effects of dopamine on functional recovery after reversible ischemic myocardial injury. *Surg Forum*: 36:185.
  25. Rankin JS, Ring WS, Arentzen CE, et al (1977). The functional reserves of the left ventricle in chronic volume overload. *Circulation* 56(suppl II):906.
  26. Ross J Jr (1974). Adaptation of the left ventricle to chronic volume overload. *Circ Res* 34 and 35(suppl II):64-70.
  27. Linzbach AJ (1960). Heart failure from the point of view of quantitative anatomy. *Am J Cardiol* 5:370-382.
  28. Hood WP Jr, Rackley CE, Rolett EL (1963). Wall stress in the normal and hypertrophied human left ventricle. *Am J Physiol* 22:550-558.
  29. Grossman W, Jones D, McLaurin LP (1975). Wall stress and patterns of hypertrophy in the human left ventricle. *J Clin Invest* 56:56-64.
  30. Gaasch WH, Andrias CW, Levine JH (1978). Chronic aortic regurgitation: The effect of aortic valve replacement on left ventricular volume, mass and function. *Circulation* 58:825-836.
  31. Rankin JS (1980). The chamber dynamics of the intact left ventricle. In Baan J, Arntzenius AC, Yellin ED, (eds): *Cardiac Dynamics*. London: Martinus Nijhoff Publishers, pp 95-106.
  32. Rankin JS (1986). Mitral and tricuspid valve disease. In Sabiston DC Jr (ed): *A Textbook of Surgery*, 13th ed. Philadelphia: Saunders, 2344-2373.
  33. Gaynor JW: Unpublished data.
  34. Rankin JS, Newman GE, Muhlbaier LH, et al (1985). The effects of coronary revascularization of left ventricular function in ischemic heart disease. *J Thorac Cardiovasc Surg* 90:818-832. 1985.
  35. Spratt JA, Tyson GS, Glower DD, et al. The end-systolic pressure-volume relationship in conscious dogs. *Circulation*: In press.

---

# 13. EVALUATION OF TIME COURSE OF LEFT VENTRICULAR ISOVOLUMIC RELAXATION IN HUMANS

---

William E. Craig, Joseph P. Murgo, and Ares Pasipoularides

Weiss and coworkers [1] first determined, in an open-chest, right-heart-bypass animal model, that left-ventricular-pressure decay during isovolumic relaxation can be approximated by a monoexponential function. Their technique required that the derived or best-fit monoexponential curve for the pressure data decay asymptotically toward zero pressure. [1, 2]. Subsequent evaluation of the time course of pressure fall during isovolumic relaxation has questioned whether the monoexponential decay of isovolumic pressure decline should proceed to a zero or nonzero asymptote [3–5]. Inherent in this calculation is the assumption that pressure decline during isovolumic relaxation is monoexponential. This postulate is empiric and is not necessarily predicated by any physiologic mechanism [6]. However, in those cases where a monoexponential model applies, calculation of the time constant provides a single index which characterizes the shape of the pressure curve during isovolumic relaxation. Such an index is important if the effects of relaxation on diastolic performance and overall cardiac function are to be evaluated in diseases such as hypertrophic cardiomyopathy and exercise-induced myocardial ischemia.

The goal of this chapter is to describe the most appropriate calculation of the time constant in those instances where isovolumic pressure decay can be fit by a monoexponential

model. In those instances, the value of the time constant should be dependent only upon the shape of the isovolumic pressure decline during isovolumic relaxation. Additionally, suitable methods to assess whether a monoexponential model is applicable to the isovolumic pressure decline in any given ventricle will be considered.

Some insight into the difficulties encountered in calculation of the time constant are illustrated in Figure 13–1. This figure illustrates the problem generated in calculating the time constant using a technique that a priori requires pressure to decay toward a zero asymptote. Panel A displays a data set simulating a monoexponential pressure decay during isovolumic relaxation. Panel B illustrates the curve derived from the zero asymptote model that best fits the original data points. In Panel C, each point in the original data set has been shifted downward by a constant value, as might occur by a change in intrathoracic pressure associated with respiration. It is important to emphasize that the shapes of both data sets are identical and, therefore, have identical decay rates. However, as shown in Panel D, when the time constant is now calculated with the same zero asymptote model, the best-fit curve for the new data set yields a different value than that obtained in Panel B. Therefore, when using the zero asymptote model, a serious problem is encountered. *Apparent* changes in the value of the time constant may actually be due only to changes of intrathoracic pressure or be the result of other interventions that shift the entire left ventricular pressure curve without actually changing the *shape* of the curve during isovolumic relaxation.

It is thus imperative that any calculation of the time constant depend solely upon the shape

The views expressed herein are those of the authors and do not necessarily reflect the views of the U.S. Department of the Army or the U.S. Department of Defense.  
Grossman, William, and Lorell, Beverly H. (eds.), *Diastolic Relaxation of the Heart*. Copyright © 1987. Martinus Nijhoff Publishing. All rights reserved.

or actual rate of pressure decay of the pressure curve during isovolumic relaxation.

*Methods*

A monoexponential model that accounts for shifts of the entire pressure curve is shown in Figure 13-2. This figure illustrates that any given monoexponential decay may proceed toward an asymptote other than zero. In this figure, that asymptote is labeled  $P_B$  and is the theoretical baseline pressure toward which the monoexponential function decays. This model eliminates the a priori assumption that the isovolumic portion of left ventricular pressure decays toward zero. The equation that now describes pressure decay during isovolumic relaxation is [3]:

$$P(t) = P_0 e^{-kt} + P_B \tag{13.1}$$

$P_0$  represents the initial value of pressure with respect to  $P_B$ .

Given this equation to describe isovolumic pressure decline, Figure 13-3 illustrates one method of calculating the time constant from equation 12-1. As shown, if one takes the first derivative of this equation, it is apparent that the resulting equation for  $dp/dt$  has the same exponential decay rate as the original pressure equation:

$$dp/dt = -kP_0 e^{-kt} \tag{13.2}$$

A semilog plot of the  $dp/dt$  equation yields a straight line, the slope of which yields the time constant (TC). In practice these data are obtained by digitizing the first derivative signal, rather than left ventricular pressure itself, and then submitting the resultant semilog plot of first derivative data with respect to time to a least-squares linear regression analysis. It should be noted that all values for  $dp/dt$  must first be multiplied by a “-1,” since it is impossible to take the natural logarithm of a negative number.

The variables  $P_0$  and  $P_B$  for a given left ventricular pressure curve can be calculated once the value of the time constant is obtained. Since the pressure curve is given by equation 13.1 and  $k$  is known, for any given value of  $t$ ,  $e^{-kt}$  can be calculated. Left ventricular pressure is read from the recorded pressure curve at any  $t$ . Thus, for a linear relationship between  $P(t)$  and the calcula-

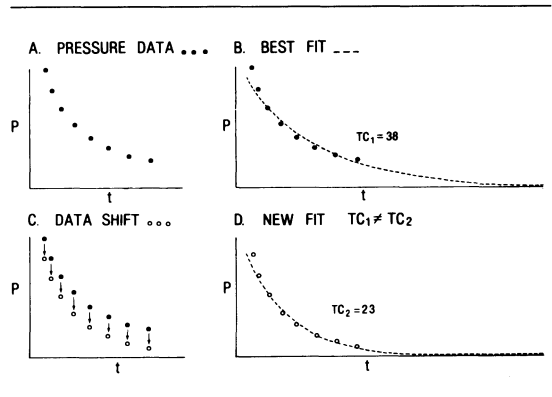


FIGURE 13-1. Schematic illustrating problems with zero asymptote model. (A) Simulated pressure data points with monoexponential decay. (B) Best-fit curve and time constant (TC) obtained from zero asymptote model. (C) Each point from panel A shifted down by constant value to yield a new data set with same monoexponential decay. (D) New best-fit curve and time constant when the same zero asymptote model is applied as in B.

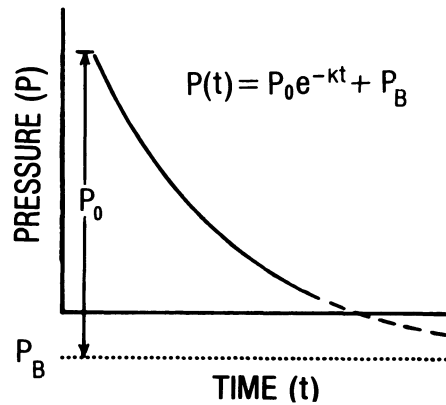


FIGURE 13-2. Monoexponential model accounting for possible shifts of entire pressure curve.  $P(t)$  represents actual pressure at any time ( $t$ ).  $P_B$  = theoretical baseline toward which monoexponential function decays;  $P_0$  = initial value of pressure measured relative to  $P_B$ ;  $k$  = variable defining rate of decay.

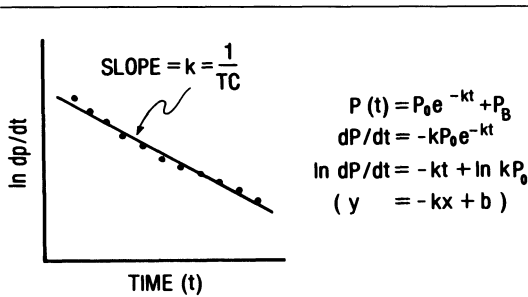


FIGURE 13-3. Illustration of variable asymptote technique to calculate the time constant (TC) from equation 13.1. First derivative of equation 13.1 ( $dp/dt$ ) yields on equation with the same decay rate, but eliminates the constant  $P_B$ , the theoretical nonzero asymptote. Thus, the  $dp/dt$  curve will always decay toward zero but will have the same decay rate as the pressure curve. Least-squares linear regression analysis from a semilog plot of  $dp/dt$  vs. time yields slope  $k$ . Note that all values of  $dp/dt$  have been first multiplied by “-1”.

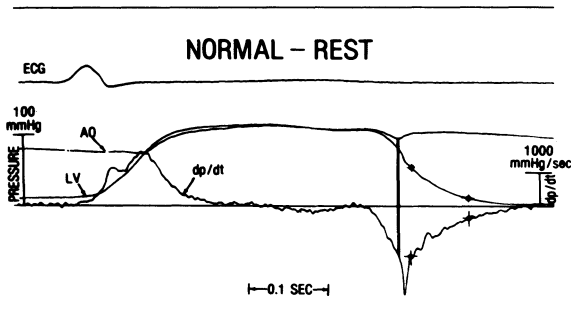


FIGURE 13-4. Representative cardiac catheterization data used to calculate time constant. Aortic (AO) and left ventricular (LV) pressures obtained by micromanometric techniques. First derivative of LV pressure ( $dp/dt$ ) obtained by electronic differentiation at 160 Hz. ECG = electrocardiogram. Paper speed was set at 1000 mm/sec.

ted values of  $e^{-kt}$ ,  $P_0$  and  $P_B$  can be obtained by linear regression techniques.

Once the values of all variables have been obtained, how well the exponential model fits the actual left ventricular pressure data can be determined. At any  $t$ , the predicted pressure can be compared to the actual pressure. If such a comparison is performed for multiple data

points, then a standard deviation of the actual data from the predicted curve can be obtained by standard statistical techniques. It is important to note that the value of this standard deviation helps quantify how well the exponential model fits the actual data.

Figure 13-4 is a representative beat from which data were obtained to calculate the time constant. Simultaneous left ventricular and aortic pressures were obtained by retrograde catheterization of the left ventricle using micromanometer techniques. Pressure signals were amplified by Honeywell Accudata 143 amplifiers and left ventricular pressure was electronically differentiated with a Honeywell Accudata 132 differentiator at a frequency response of 160 Hz. At this frequency response, the differentiator has a calculated time constant of less than 1 msec. All data were recorded on a Honeywell 1858 fiberoptic strip chart recorder at a paper speed of 1,000 mm/second. Ten consecutive beats were analyzed using a Hewlett-Packard 9864 digitizer. As illustrated in Figure 13-4, it is important to note that the onset of isovolumic relaxation used for the calculation of the time constant was chosen *after* aortic valve closure and peak negative  $dp/dt$  to avoid transients in the signals occurring at the time of valve closure. [7, 8]. The termination of the isovolumic relaxation period was defined as that point when mitral valve opening occurs, as estimated from a simultaneously recorded pulmonary capillary wedge pressure (not illustrated in the figure). The value of the time constant was then obtained from the least-squares linear regression analysis using the semilog plot of  $dp/dt$  vs. time, as described above. For comparison, some time-constant values were also calculated utilizing the technique described by Weiss and coworkers, which assumes a zero asymptote [1, 2].

## Results

Figure 13-5 demonstrates that in normal human ventricles, the monoexponential model is suitable for characterizing left ventricular pressure decline during isovolumic relaxation, and that the monoexponential model which does not assume a zero asymptote more accurately fits the actual data. Beats analyzed from normal ventricles consistently demonstrated a better fit to the nonzero asymptote model.

Figure 13-6 shows the results of applying the time constant calculation to normal ventricles using both the zero and nonzero asymptote methods [3]. Ten patients with no evidence of cardiovascular disease were studied during rest and supine submaximal bicycle exercise. Additionally five of the patients were studied during isoproterenol infusion. Results were obtained using the calculation technique that forces decay toward a zero asymptote and by the technique that does not assume a zero asymptote. Significantly different values of the isovolumic relaxation time constant were obtained by the two techniques in all cases, and it is noted worthy that the nonzero asymptote model yields higher values.

Figure 13-7 represents the results obtained in a specific subset of patients with coronary artery disease [9]. The patients included in this study had no prior evidence of myocardial infarction, but demonstrated more than 70% obstruction of all three major coronary arteries on angiography. They were on no medications at the time of catheterization, demonstrated normal hemodynamics at rest, and developed abnormal diastolic function with exercise, while maintaining normal indices of systolic function. The upper panel of Figure 13-7 compares the response of left ventricular end-diastolic pressure to supine submaximal exercise both in the normal and subjects in those with coronary artery disease. The bottom panel of the figure compares the corresponding values of the time constant, which was calculated using the nonzero asymptote model. In the normal subjects, left ventricular end-diastolic pressure (LVEDP) remained normal with exercise, whereas it became significantly elevated in the coronary artery disease group. The time constant data reveal that, although the coronary artery disease group had normal time constants at rest, values of the time constant failed to show a reduction with exercise, as was seen in normal subjects.

Application of the nonzero asymptote model for calculation of the time constant in patients with hypertrophic cardiomyopathy (HCM) is shown in Figure 13-8 [10]. The bar graphs in this figure show the time constants obtained both in normal subjects and in patients with HCM as well as corresponding values for peak positive and peak negative dp/dt. The data indicate that patients with HCM have computed time constants that are significantly elevated compared to normal subjects at rest and during

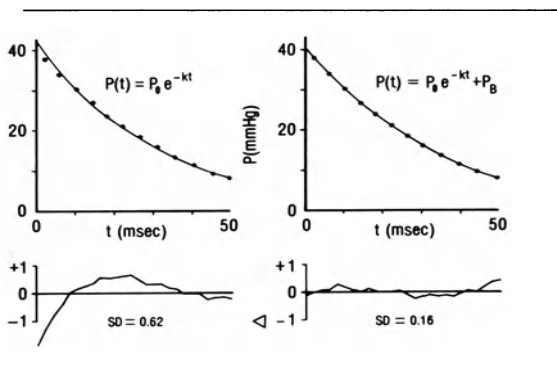


FIGURE 13-5. Representative example of ventricular pressure during isovolumic relaxation given by solid circles in upper portion of figure. The left panel illustrates the fit of the curve derived from the zero asymptote model to actual data points. The right panel gives the curve derived from nonzero asymptote model. The lower panels show the difference between predicted curves and actual data. SD = standard deviation.

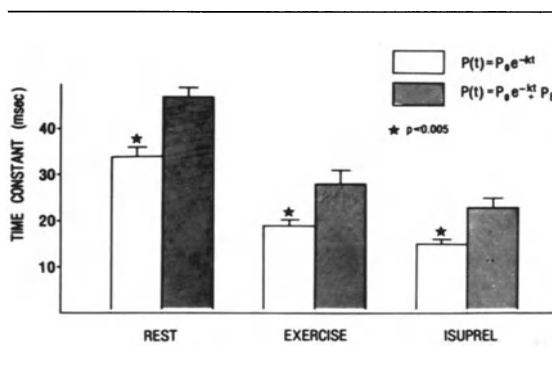


FIGURE 13-6. Time constants obtained from normal subjects studied at rest, during supine bicycle exercise, and during isoproterenol infusion (Isuprel). Hatched bars represent time constants from nonzero asymptote model and clear bars the time constants from the zero asymptote model. Brackets denote standard deviations.

exercise. These abnormalities do correlate with abnormal levels of peak negative dp/dt in patients with HCM, although levels for peak positive dp/dt are similar to normal.

Table 13-1 shows the values for the asymptote,  $P_B$ , as well as the time constants obtained

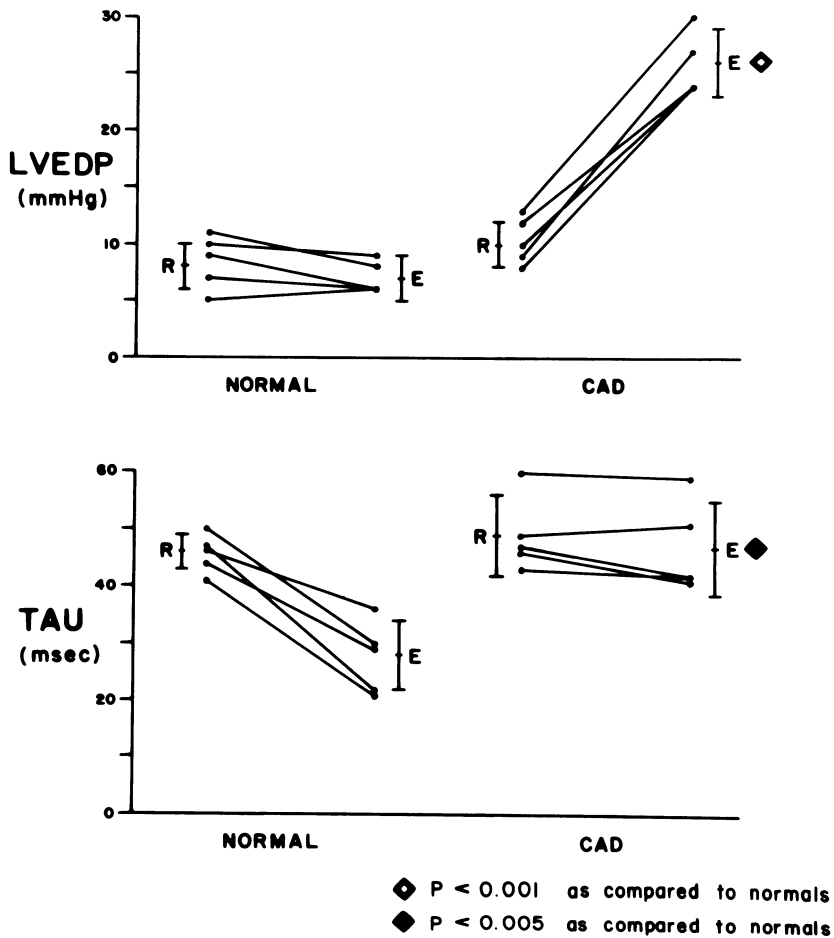


FIGURE 13-7. Results of left ventricular end-diastolic pressure (LVEDP) and time constant (TAU) obtained in normal subjects and a select group of patients with coronary artery disease (CAD). Subjects were studied at rest (R) and during supine submaximal bicycle exercise (E).

when the nonzero asymptote model is applied to normal subjects and patients with HCM. Although the values of  $P_B$  at rest and exercise for normal subjects are within the physiologic range expected for extramural forces, the values of  $P_B$  in HCM are implausible.

Analysis of the suitability of the monoexponential model for patients with HCM is examined in Figure 13-9. This figure is a phase-plane plot of  $dp/dt$  vs. left ventricular pressure

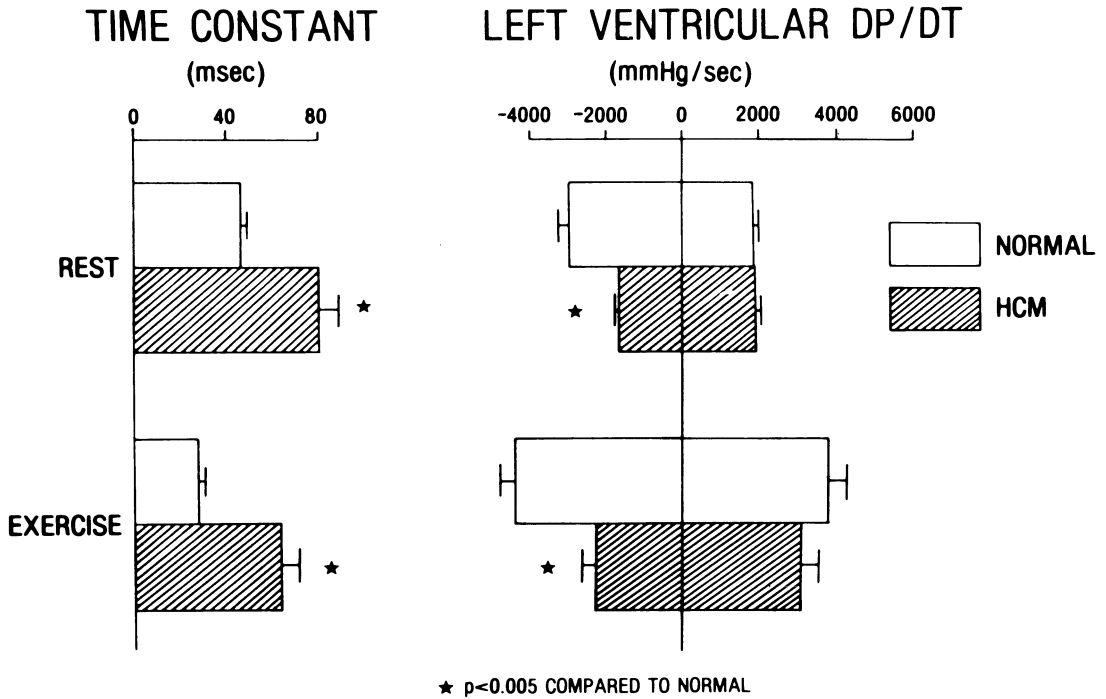
TABLE 13-1. Calculated Time Constants (TC) and Values<sup>a</sup> for the Nonzero Asymptote ( $P_B$ ) Obtained from Normal Subjects and from Patients with HCM\*

	TC (msec)	$P_B$ (mm Hg)
Normal rest	47 ± 2	-7.9 ± 0.8
HCM rest	81 ± 10 <sup>b</sup>	-28.1 ± 4.2 <sup>b</sup>
Normal exercise	28 ± 3	-5.9 ± 1.8
HCM exercise	54 ± 8 <sup>b</sup>	-24.4 ± 2.8 <sup>b</sup>

<sup>a</sup> ± standard error of the mean.

<sup>b</sup> p < 0.005, compared to normal subjects.

HCM = hypertrophic cardiomyopathy



for an entire cardiac cycle in both a normal subject and a patient with HCM. The nonlinear relationship during isovolumic relaxation clearly indicates the absence of monoexponential decay in the patient with HCM as opposed to the linear relationship shown in the normal subject.

*Discussion*

Generally, the monoexponential model that does not assume a zero asymptote more accurately describes the left ventricular pressure decline during isovolumic relaxation. As shown in Figure 13-7, the derived best-fit curves, both from the zero and the nonzero asymptote models, appear to fit the data relatively well. However, it is apparent from the residuals and standard deviation data shown in the bottom portion of that figure that the best fit is obtained with the equation that allows pressure to decay toward a *nonzero* baseline. As assessment of the residuals, representing the difference between actual data points and points on the derived curves, provides a direct and sensitive way to

FIGURE 13-8. Time constants and levels of peak positive and peak negative dp/dt obtained in normal subjects and patients with hypertrophic cardiomyopathy (HCM) studied at rest and during supine exercise. Brackets denote standard deviations.

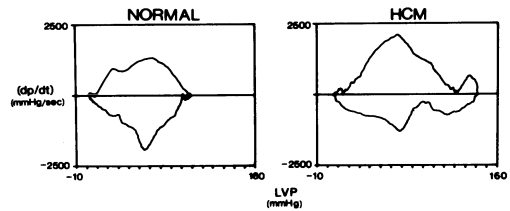


FIGURE 13-9. Phaseplane plots of left ventricular pressure (LVP) vs. its corresponding first derivative dp/dt shown from a normal subject and a patient with hypertrophic cardiomyopathy (HCM). Data from one cardiac cycle are shown for each plot.

determine the appropriateness of the monoexponential model to the data. Such residual plots complement statistical tests of goodness of fit that employ correlation coefficients and their level of significance. These correlation coefficients may be very near unity because of the limited data available, even when there are significant deviations of the actual pressure curve from a monoexponential decay. In the case of a truly monoexponential decay of left ventricular pressure during isovolumic relaxation, the residuals will show only random, minimum deviation attributable to experimental noise.

It is apparent from the data obtained in normal subjects that the time constants with the nonzero asymptote model are significantly higher than with the zero asymptote model. These higher time constants accrue from the negative values of  $P_B$ . A model that assumes a zero asymptote forces the derived curve to decline faster to achieve a zero asymptote, rather than decay at a slower rate to reach a negative nonzero asymptote.

The negative value for  $P_B$  obtained in normal ventricles is within the physiologic range expected to account for extramural forces on the heart. Because these forces are not routinely obtained during human cardiac catheterization, transmural pressure is not available for calculation of the time constant as it is in the open-chest animal model used by Weiss and coworkers to calculate the time constant of isovolumic relaxation. Thus, utilization of the nonzero asymptote model for calculation of the time constant is necessary when using clinical cardiac catheterization data, and results in a true characterization of isovolumic pressure decline when this decline is monoexponential. This nonzero asymptote model will not be affected by intrathoracic pressures that may shift the entire left ventricular pressure curve without actually altering the shape of the isovolumic pressure decline.

The application of the nonzero asymptote model to a select subset of patients with coronary artery disease [9, 14] illustrates that the model can be applied to disease states in which there is no evidence of gross asynchrony [11, 13] or abnormal myocardium. In these patients, the monoexponential model is suitable for the decay of left ventricular pressure during isovolumic relaxation and permits appropriate calculation of the time constant. The results show that during exercise the elevated LVEDP

in patients with coronary artery disease correlated with a time constant that was significantly elevated, compared to the findings for normal subjects exercised to the same workload, heart rate, and systolic blood pressure. In this setting, the time constant is a useful tool in identifying and quantitating an abnormality of isovolumic relaxation that correlates with conventional indices of abnormal diastolic performance. Attempts to apply the time constant of relaxation to the abnormal HCM diastolic function present in patients with HCM are not as successful [11–13].

Although the abnormal time constants calculated in HCM patients correlate with other manifestations of abnormal diastolic performance [15–18], such as peak negative  $dp/dt$  and LVEDP, the application of the monoexponential model to isovolumic pressure decline in these patients is often inappropriate. The phase-plane plots of left ventricular pressure vs. its first derivative indicate that there is no linear relationship between these two variables during isovolumic relaxation, as would have to apply if pressure decline during this interval were monoexponential. Attempts to determine the time constant in this case may reveal gross abnormalities during isovolumic relaxation, but have limited value in characterizing abnormal relaxation. In spite of relatively high correlation coefficients obtained from linear regression techniques, examination of the residuals, phase-plane plots, and values obtained for  $P_B$  will indicate that the monoexponential model is inappropriate. Unlike normal ventricles, the values for  $P_B$  obtained in these patients with HCM are often in an extremely unphysiologic range. These unphysiologic values are the mathematical result of forcing data that are not monoexponential in their decay to a monoexponential model.

In summary, it has been shown empirically that isovolumic pressure decline in normal ventricles is monoexponential. As a result of intrathoracic forces, and perhaps other uncharacterized factors, this monoexponential decline in pressure is best described by a model with a nonzero asymptote. Such a model accounts for shifts in the left ventricular pressure curve that do not alter the shape, i.e., the rate, of pressure decline in the left ventricle during isovolumic relaxation. This model may be appropriate for the calculation of the time constant of relaxation in certain subsets of patients with abnormal ventricular function, thereby serving as a useful

tool in determining the contribution of slow or incomplete relaxation to impaired diastolic performance. However, in other patients with abnormal ventricular function, such as those with HCM, application of the monoexponential model for calculation of the time constant is inappropriate. Suitability of the monoexponential model must be obtained from examination of phase-plane plots and the residuals around the best-fit curve.

### References

1. Weiss JL, Frederiksen JW, Weisfeldt ML (1976). Hemodynamic determinants of the time course of fall in canine left ventricular pressure. *J Clin Invest* 58:751-760.
2. Frederiksen JW, Weiss JL, Weisfeldt ML (1978). Time constant of isovolumic pressure fall: Determinants in the working left ventricle. *Am J Physiol* 235:H701-706.
3. Craig WE, Murgu JP (1980). Evaluation of isovolumic relaxation in normal man during rest, exercise, and isoproterenol infusion. *Circulation* 62(suppl II):II-92 (abstract).
4. Raff GL, Glantz SA (1981). Volume loading slows left ventricular isovolumic relaxation rate: Evidence of load dependent relaxation in the intact dog heart. *Circ Res* 48:813-824.
5. Thompson DS, Waldron CB, Coltart DJ, et al (1983). Estimation of time constant of left ventricular relaxation. *Br Heart J* 49:250-258.
6. Pasipoularides A, Palacios I, Frist W, et al (1985). Contribution of activation-inactivation dynamics to the impairment of relaxation in hypoxic cat papillary muscle. *Am J Physiol: Regulatory Integrative Comp Physiol* 248:R54-R62.
7. Pasipoularides A, Murgu JP, Miller JW, Craig WE. Nonobstructive left ventricular ejection pressure gradients in man. (Submitted for publication)
8. Sabbah HN, Stein PD (1986). Investigation of the theory and mechanism of the origin of the second heart sound. *Circ Res* 39:874-882.
9. Brown DL, Craig WE, Layton SA, et al (1981). Exercise induced abnormalities of left ventricular relaxation in coronary artery disease. *Circulation* 64(suppl IV):28 (abstract).
10. Murgu JP, Craig WE (1980). Relaxation abnormalities in hypertrophic cardiomyopathies. *Circulation* 62(suppl II):206 (abstract).
11. Craig WE, Pasipoularides A (1986). Ventricular diastolic dynamics: Effects of wall asynchrony on global relaxation indices. In *Proceedings of the 21st Annual Meeting of the Association for the Advancement of Medical Instrumentation*, Chicago, IL.
12. Murgu JP, Craig WE, Pasipoularides A (1982). The relationship between diastolic function and ejection in hypertrophic cardiomyopathy. In *Proceedings of Symposium on Diastolic Function of the Heart*, Hamburg, Germany.
13. Pagani M, Pizzinelli P, Gussoni M, et al (1983). Diastolic abnormalities of hypertrophic cardiomyopathy reproduced by asynchrony of the left ventricle in conscious dogs. *J Am Coll Cardiol* 1:641 (abstract).
14. Thompson DS, Waldron CB, Juul SM, et al (1982). Analysis of left ventricular pressure during isovolumic relaxation in coronary artery disease. *Circulation* 65:690-697.
15. Brutsaert DL, Housmans PR, Goethals MA (1980). Dual control of relaxation: Its role in the ventricular function in the mammalian heart. *Circ Res* 47:637-652.
16. Cohn PF, Liedtke AJ, Serur J, et al (1972). Maximal rate of pressure fall (peak negative dp/dt) during ventricular relaxation. *Cardiovasc Res* 6:263-267.
17. Karliner JS, Lewinter MM, Mahler F, et al (1977). Pharmacologic and hemodynamic influences on the rate of isovolumic left ventricular relaxation in the normal conscious dog. *J Clin Invest* 60:511-521.
18. Thompson DS, Wilmshurst P, Juul SM, et al (1983). Pressure-derived indices of left ventricular isovolumic relaxation in patients with hypertrophic cardiomyopathy. *Br Heart J* 49:259-267.

---

# 14. LOADING CONDITIONS AND LEFT VENTRICULAR RELAXATION

---

William H. Gaasch, Michael R. Zile, Alvin S. Blaustein, Oscar H.L. Bing

Relaxation refers to the process by which the myocardium returns to its initial or resting length and tension; in the intact heart the term refers to the process by which the left ventricle returns to its presystolic or end diastolic pressure and volume. Relaxation is controlled by a complex interaction between *deactivation* (the time-dependent decay of active-force-generation capacity) and *loading* conditions (forces affecting myocardial length and tension). These forces may be subdivided into loads that are applied early in the cardiac cycle (contraction loads) and those that are abruptly applied late in the cycle (relaxation loads) (Table 14-1). Our rationale for separating early and late loads rests in the experimental observation that the application of an early or contraction load results in a more prolonged relaxation, whereas the application of a late or relaxation load results in a premature and more rapid relaxation; this latter phenomenon has been called "load dependent relaxation" [1].

Attempts to evaluate relaxation in the intact left ventricle have evolved along two lines that use data from two periods of the cardiac cycle: the period between aortic valve closure and mitral valve opening (the isovolumic relaxation period); and the period immediately after mitral valve opening (the early diastolic filling period). The isovolumic and filling indices of relaxation include the isovolumic relaxation time, maximum negative  $dp/dt$ , relaxation time constant, peak filling rate, time to peak filling, wall thinning rate, and others [2]. It should be recognized, however, that all of these indices are influenced by complex interactions between deactivation and load, both of which are

modulated by neurohumoral, metabolic, and pharmacologic influences. Thus, these indices reflect the intensity of the "intrinsic" myocardial relaxing system only if the loading and other conditions are constant or at least considered in the analysis. Accordingly, the purpose of this chapter is to review the effects of acute changes in loading conditions on left ventricular relaxation. The effect of preload, systolic loads, and filling (lengthening) loads will be discussed following the general outline shown in Table 14-1.

## *Contraction Loads*

### PRELOAD

It has long been known that adjustments in left ventricular (LV) preload provide for variations in systolic performance according to the Frank-Starling mechanism; only recently, however, have the effects of preload on LV relaxation been defined [3]. The results from a variety of experimental models ranging from intact dogs to isolated cardiac muscles indicate that preload does not influence relaxation rate unless the intervention is also associated with a change in afterload.

*Intact Heart Studies.* By inserting a large-bore catheter into the LV apex of an anesthetized dog

TABLE 14-1. Loading conditions and Left Ventricular Relaxation

---

Contraction Loads
End diastole
Early systole
Relaxation Loads
Late ejection
Rapid filling period

---

Grossman, William, and Lorell, Beverly H. (eds.), *Diastolic Relaxation of the Heart*. Copyright © 1987. Martinus Nijhoff Publishing. All rights reserved.

and rapidly infusing blood into the LV during a single diastole, the effects of an abrupt increase in preload can be studied. Using a second catheter in the central aorta, LV systolic pressure can be held nearly constant by withdrawing aortic blood during systole. Thus, these single-beat, interventions allow an assessment of LV isovolumic relaxation rate during LV infusion only (both preload and afterload increase) or during an LV infusion with simultaneous withdrawal of aortic blood (preload increase with systolic unloading to provide an unchanged afterload) (Figure 14-1). Comparison of data from a control beat (immediately preceding the intervention beat) with data from a preloaded beat does not allow sufficient time for neurohumoral or reflex changes to influence the results.

LV pressure was measured in eight anesthetized dogs with a high fidelity micromanometer, and the isovolumic relaxation time constant ( $T$ ) was calculated according to the original method of Weiss and colleagues [4]; this method provides results that are similar to those obtained with other methods [5, 6]. Sixty-two paired beats (control vs. 8-12 ml volume infusion) were obtained. LV systolic pressure increased from  $112 \pm 2$  to  $128 \pm 3$  mm Hg ( $p < 0.05$ ), and there was a small, but significant increase in  $T$  from  $28.0 \pm 0.4$  to  $30.7 \pm 0.4$  msec ( $p < 0.05$ ). In an additional 23 paired beats (control vs. LV infusion plus aortic withdrawal), systolic pressure was held constant ( $109 \pm 2$  vs.  $107 \pm 2$ ,  $p = \text{NS}$ ), and there was no change in  $T$  ( $25.3 \pm 0.8$  vs.  $25.8 \pm 0.8$ ,  $p = \text{NS}$ ). Thus, an isolated increase in LV preload is not associated with a change in the relaxation time constant.

*Isolated Muscle Studies.* The independent effect of preload on relaxation can best be studied in physiologically sequenced isolated muscle preparations in which the loading sequence of the intact heart is simulated (i.e., isometric contraction is followed by shortening of the muscle and isometric relaxation precedes lengthening). In such studies, either the length or tension is controlled by means of an electronic servosystem and a digital computer; thus, total load (the sum of preload and afterload) can be held constant over a wide range of preload [7].

Isometric relaxation studies were performed in six rat LV papillary muscles and four right ventricular (RV) trabecular muscles from the

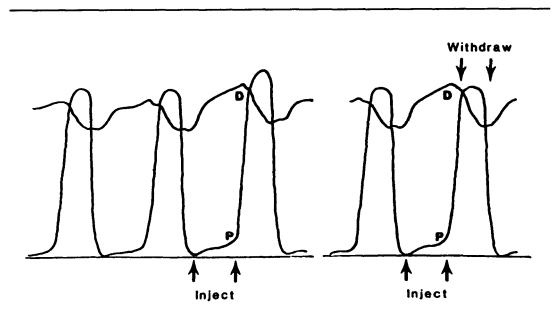


FIGURE 14-1. Example of the method used to define the effect of preload on the left ventricular isovolumic relaxation time constant. In the panel on the left volume is infused into the ventricle during a single diastole (inject); end-diastolic pressure (P) and dimension (D) increase, as does left ventricular systolic pressure. In the panel on the right a similar diastolic infusion is made, but in this case a rapid withdrawal of blood from the aortic cannula provides constant systolic pressure (despite the increment in preload). In protocol A, the time constant increased; in protocol B, there was no change in the time constant [3].

dog. In these experiments, preload was varied from 30% to 100% of resting tension at  $L_{\max}$ , and all comparisons were made at a constant total load. An example of a typical experiment is shown in Figure 14-2. In the panel on the left, lengthening occurs at a force equal to the preload; in the panel on the right, end-systolic length is maintained at minimal muscle length, and force is allowed to dissipate to a minimal value. In both types of experiments, the time course of isometric relaxation was clearly superimposable at the three different preloads. This was a consistent finding in all ten muscles [3]. Previous experiments likewise indicate that the maximum rate of isometric tension decline is independent of preload [8]. Thus, isometric relaxation (in the isolated muscle) and isovolumic relaxation (in the intact heart) are independent of preload.

The isolated muscle apparatus is also well suited to study the effects of preload on isotonic lengthening (lengthening at constant tension which is analogous to filling in the intact heart). An example of such an experiment is shown in the left panels of Figure 14-3. As was discussed above, these experiments are designed so that muscle lengthening occurs after isometric relaxation. The time course of isotonic leng-

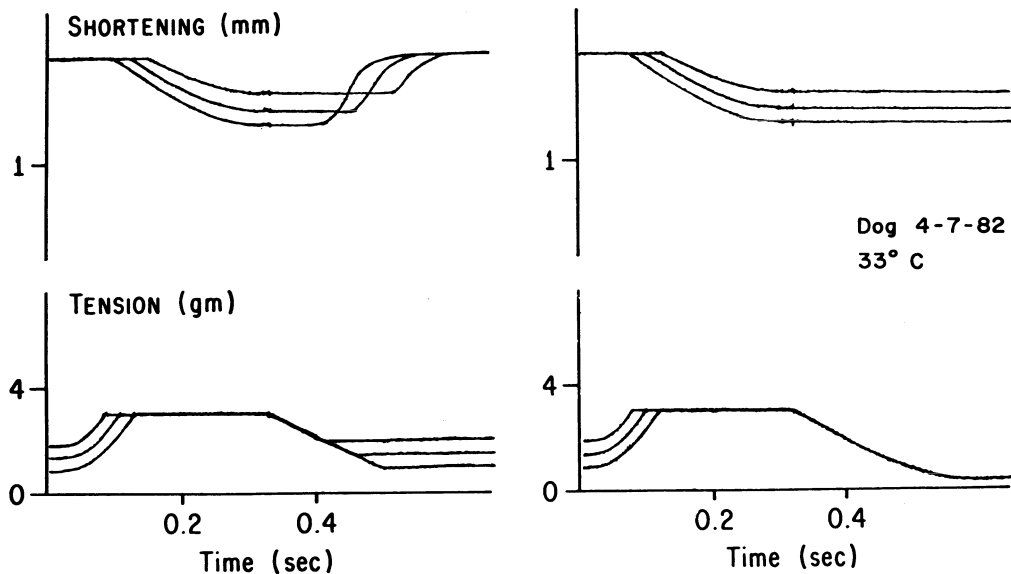


FIGURE 14-2. Isolated muscle studies with physiologically sequenced contractions in which the loading sequence seen in the intact heart is simulated. In the panel on the left, three superimposed contractions are displayed in which three values of preload are set before contraction. After stimulation, the computer-controlled system holds muscle length constant while force rises to a predetermined total load (isometric contraction period). After achieving total load, the system maintains force constant while shortening takes place (isotonic shortening). When minimum length is detected, constant length is maintained while force declines (isometric relaxation). Constant force is then maintained while lengthening takes place (isotonic relaxation). A similar contraction pattern is present in the panel on the right, except that minimum length is maintained until force dissipates to its lowest value. Despite variations in preload (at constant total load), isometric force decline records are superimposable. The studies were taken from right ventricular trabecular muscle in dogs; cross-sectional area =  $0.85 \text{ mm}^2$ ; stimulation rate =  $12/\text{min}$ ; temperature =  $33^\circ\text{C}$ . Shortening record was set to zero before each contraction.

thening (shown in the upper left panel of Figure 14-3) does not change with preload; this experiment indicates that neither isometric relaxation (lower panel) nor isotonic relaxation (upper panel) is influenced by preload. The maximum isotonic relaxation rate was studied in six rat papillary muscles and, as before, preload was varied while total load was held constant. As is shown in the right panel of Figure 14-3, the average values for maximum isotonic relaxation rate are independent of preload [9]. Note that the load on the muscle during isotonic relaxation (lengthening) is equal in all five experiments; if the lengthening load is not held constant, the lengthening rate may vary (see below).

#### SYSTOLIC LOAD

The effects of short-term alterations in LV systolic pressure on isovolumic relaxation rate have been studied in the intact dog heart by using steady state infusions of vasopressor agents or brief mechanical occlusions of the aorta (variably afterloaded and single isovolumic beats produced by cross-clamping the aorta). The pharmacologic studies are quite physiologic, but the results may be affected by baroreceptor or other reflex activity; in contrast, the aortic clamp experiments are less physiologic, but this method provides data that are not contaminated by neurohumoral or reflex mechanisms. In general, however, both types of experiments indicate that an increase in LV afterload results in an

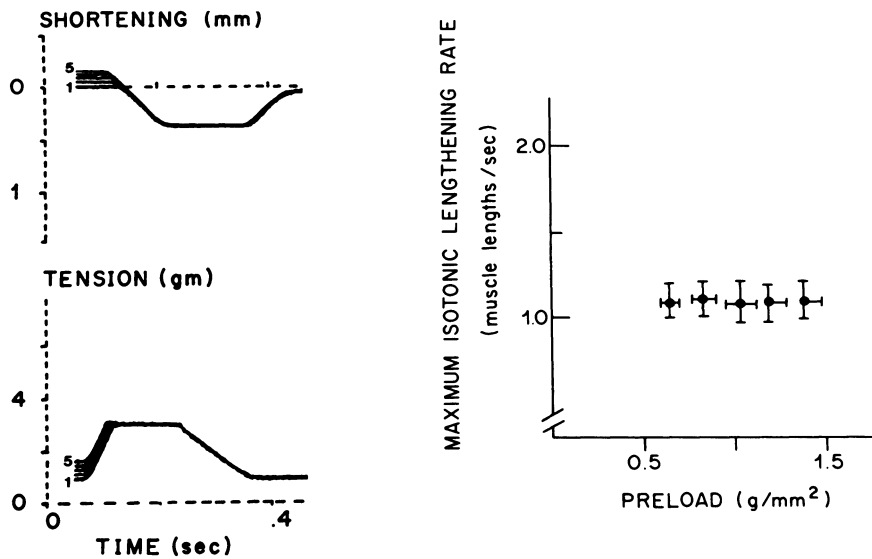


FIGURE 14-3. Effects of preload on isotonic relaxation. The example on the left demonstrates a progressive increase in preload and muscle length (both labeled 1 to 5); in this figure the shortening record was not set to zero before each contraction. Neither isometric or isotonic relaxation rates were affected by changes in preload, as shown by the superimposed force and length tracings. On the right, the average results from six papillary muscle experiments are shown. When preload was increased from 0.65 to 1.37  $\text{g}/\text{mm}^2$ , maximum isotonic relaxation rate was unchanged.

increase in the isovolumic relaxation time constant [10-15].

To determine the effects of an isolated increase in afterload, we placed a large vascular clamp around the descending aorta and produced variably afterloaded beats by clamping the descending aorta for three cardiac cycles. An example of a single experiment is shown in Figure 14-4. These experiments were performed in anesthetized open-chest dogs; LV pressure was measured with a high fidelity micromanometer and the relaxation time constant (T) was calculated according to the method of Weiss and coworkers [4]. The average results from a series ( $n = 6$  dogs) of aortic cross-clamp experiments are shown in Figure 14-5; these data reflect a direct relation between LV end-systolic pressure (the pressure at the onset of isovolumic relaxation) and the isovolumic relaxation time constant (T). Systolic pressure increased from  $124 \pm 6$  mm Hg in the control beat to  $176 \pm 11$  mm Hg in the third cross-clamp beat; T increased from  $20 \pm 2$  to  $30 \pm 4$  msec [12]. The results are qualitatively similar when peak systolic pressure is substituted for end-systolic pressure. It should be noted that the cross-clamp experiment does not cause a pure increase in afterload; end-diastolic pressure also shows a progressive rise after the first cross-clamp beat. However, since preload does not

affect the rate of isovolumic pressure decline, these results indicate a direct relation between systolic load and the relaxation time constant.

The effect of afterload on LV peak filling rate (auxotonic relaxation) was also studied in anesthetized dogs using the aortic cross-clamp technique. Segment length and minor axis dimension were measured with sonomicrometers, and the peak rate of increase of these parameters (during the rapid filling period) was taken as an index of LV peak filling rate. An example of a three-beat cross-clamp on LV pressure and segment length is shown in Figure 14-4; the inverse relation between peak pressure and rate of change of the minor axis dimension is shown in Figure 14-6. Both of these parameters (peak positive  $dL/dt$  and  $dD/dt$ ) were found to be inversely related to peak LV pressure

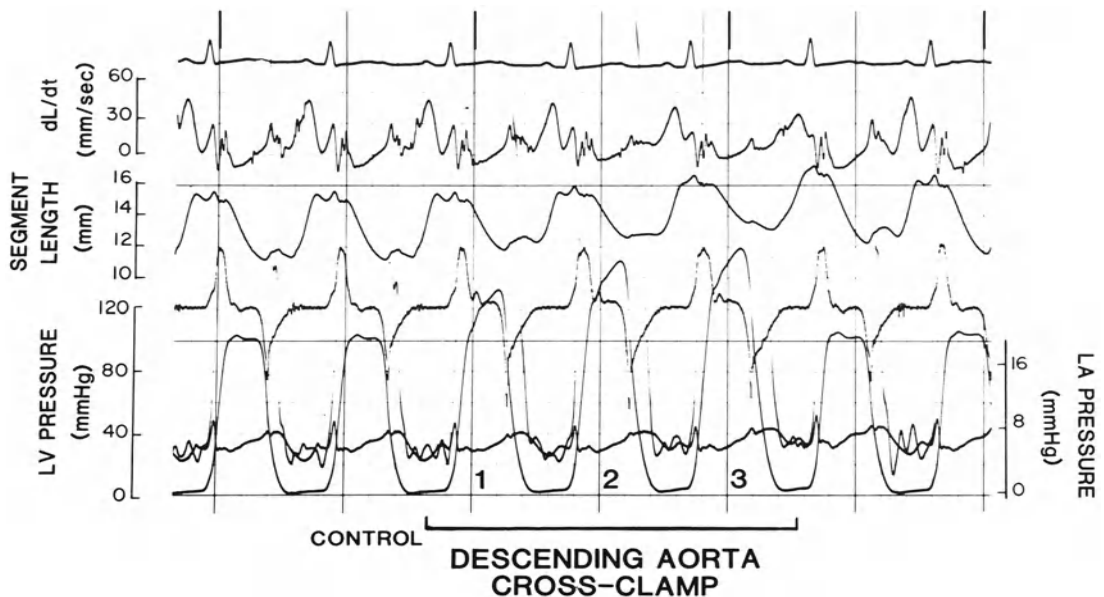


FIGURE 14-4. Example of the effects of a descending aortic cross-clamp. Left ventricular (LV) pressure (micromanometer), the first derivative of pressure ( $dp/dt$ ), LV midwall segment length (ultrasonic crystals) and the first derivative of length ( $dL/dt$ ) are shown; left atrial (LA) pressure and LV diastolic pressure are shown at high gain. With application of the descending aorta clamp, the LV systolic pressure and length progressively increase while fractional shortening and peak lengthening rate progressively decrease.

[16]. These data and those published by Bahler and Martin [13] indicate that during acute hemodynamic interventions, isovolumic relaxation rate and auxotonic relaxation rates are inversely related to LV systolic pressure.

The role of systolic pressure or afterload as a determinant of isovolumic relaxation was examined further by Hori and associates [14]. They produced variably afterloaded beats by clamping the ascending and descending aorta; the ascending aortic clamps manifest an earlier peaking pressure while the descending clamps produced a late peaking pressure (the peak systolic pressure was equal, but the time course of pressure differed in the two interventions). They then compared the relaxation rates in these

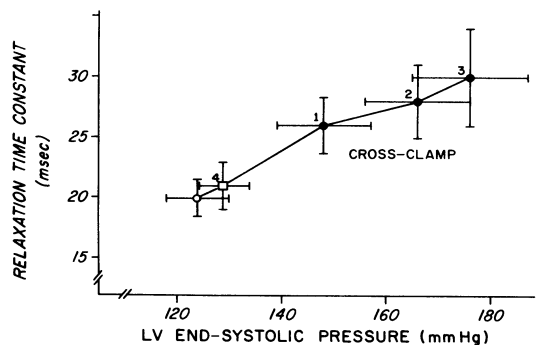


FIGURE 14-5. Relation between the relaxation time constant and left ventricular (LV) end-systolic pressure. After abrupt occlusion of descending thoracic aorta, both LV end-systolic pressure and relaxation time constant increase progressively (closed circles labeled 1, 2, and 3). Release of occlusion results in prompt return (open square, beat 4) toward control (open circle) value.

two interventions. These experiments in the anesthetized open-chest dog clearly demonstrate that a late peaking systolic pressure (descending aorta clamp) results in a substantial increase in T ( $74.5 \pm 2.5$  to  $121.8 \pm 10.2$  msec); however, an ascending aortic clamp with an early peak pressure (of the same magnitude) is associated with a relatively small increase in T ( $67.0 \pm 2.9$  to  $85.6 \pm 8.3$  msec). Based on these differences in relaxation between early and late peak pressure, Hori concluded that the "loading sequence is a major determinant of afterload-dependent relaxation in the intact canine heart."

It is important to recognize that Hori's ascending and descending clamp interventions are not the same as contraction and relaxation loads as defined by Brutsaert [1]. The loads applied by Hori were all applied early in the cardiac cycle (during contraction), and the time course of pressure varied depending on whether the clamp was applied to the ascending or descending aorta. In contrast, the manifestation of load-dependent relaxation as defined by Brutsaert requires the application of an abrupt load increment during the relaxation phase of the cardiac cycle.

### Relaxation Loads

#### LATE SYSTOLIC (LATE EJECTION) LOAD

The results of isolated muscle experiments performed by Brutsaert and associates, if extrapolated to the intact heart, indicate that the abrupt application of a lengthening force near the instant of aortic valve closure should precipitate premature and more rapid relaxation [1]; such an effect could be produced by reflected aortic pressure waves (near the end of ejection) or by a rapid engorgement of the coronary vasculature (just after aortic valve closure). Thus, the application of a late systolic load (at a time when myocardial force potential is low) produces a premature and rapid relaxation. This phenomenon, termed *load-dependent relaxation*, has not been extensively studied in the intact heart, but preliminary data indicate that the phenomenon can be demonstrated experimentally [17, 18].

Load-dependent relaxation was studied in the intact heart by using a computer-controlled servo-pump that was programmed to produce a rapid volume increment (quick stretch) at any time in the cardiac cycle. In five anesthetized dogs we attached the servo-pump to the LV apex

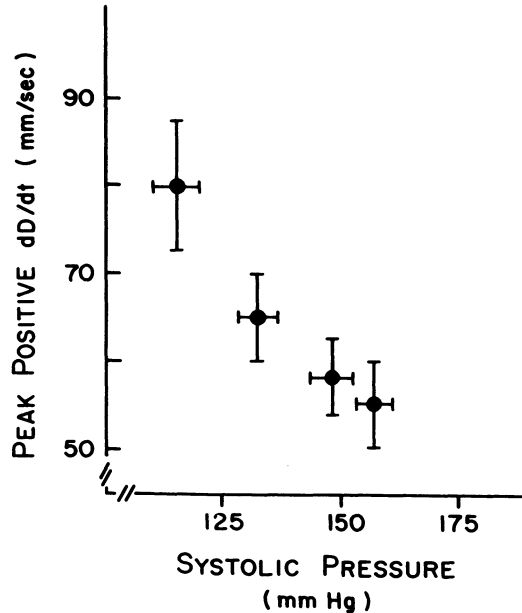


FIGURE 14-6. Relation between the peak rate of increase in minor axis dimension ( $dD/dt$ ) and left ventricular (LV) systolic pressure. After an abrupt occlusion of the descending thoracic aorta, LV systolic pressure increased, while peak positive  $dD/dt$  decreased. The upper left coordinate represents control.

and studied the effects of 6-ml increments in volume on LV relaxation; each volume increment or quick stretch was produced by infusing 6 ml into the LV within a 15-msec interval. Volume increments were given every 30 msec throughout systole so that the effects of an early (contraction) load could be contrasted with the effects of a late (relaxation) load. To prevent reflex or other feedback mechanisms from influencing our results, each quick stretch intervention was performed in a single beat, and the intervention beats were separated by 20 stabilization (control) beats. In both ejecting and isovolumic beats, a quick stretch after the first one-third of systole caused a premature onset of relaxation and a more rapid rate of pressure decline; duration of the relaxation phase was typically reduced by 10 to 15% [18]. An example of load-dependent relaxation in the intact heart is shown in Figure 14-7. These results confirm the presence of load-dependent relaxa-

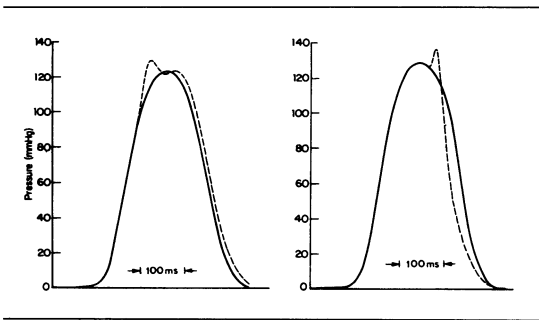


FIGURE 14-7. The effect of an abrupt volume increment on the time course of left ventricular pressure. The solid lines are control isovolumic beats, and the broken lines are intervention (quick-stretch) beats. In the panel on the left, the volume increment is given early in the contraction; in the panel on the right, the volume increment is given late in the contraction. In both experiments, 6 ml of warm blood were infused within 15 msec. The early volume infusion caused an abrupt increase in pressure, followed by a decline, and then a plateau before pressure began to fall toward the diastolic level. The onset of pressure decline was 12 msec later than control in the early intervention experiment. By comparison, the same volume increment given in late systole produced a quite different result. Here the pressure decline was earlier and much more rapid; peak negative  $dp/dt$  increased from 1742 mm Hg/second in the control beat to 3005 mm Hg/second in the intervention beat.

tion in the normal dog heart, but the significance of this phenomenon awaits further study.

#### RAPID FILLING (LENGTHENING) LOAD

Relaxation throughout the period of rapid ventricular filling (auxotonic relaxation) is especially difficult to assess because of the interdependencies of pressure and volume, neither of which is constant during this interval. Because the changes in ventricular volume greatly exceed the changes in pressure during this period, most attempts to characterize auxotonic relaxation utilize measurements of the rate of change of LV volume. As will be seen, factors independent of the relaxation process may influence filling. For example, left atrial pressure (or the transmitral pressure gradient) is known to influence transmitral flow and LV filling rate [15]; alterations in myocardial load or wall stress after the onset of filling may also act as a determinant of LV filling or myocardial lengthening rate [1]. In this section, we will review some of the

dynamics of rapid ventricular filling, and we will present data from isolated cardiac muscle experiments that indicate that myocardial lengthening rates are determined in part by the load on the muscle during lengthening. In contrast to preload, which may be considered an early or contraction load, the late (lengthening) loads are those that are present during the rapid filling period (during auxotonic relaxation).

*Intact Heart Studies.* Alterations in left atrial pressure, and the transmitral pressure gradient, are said to effect changes in LV filling rate without necessarily influencing the process of myocardial relaxation. Accordingly, Ishida and coworkers have made precise measurements of transmitral pressure and flow and isovolumic relaxation rate during acute alterations in LV preload and afterload; their studies shed considerable light on the determinants of peak filling rate [15].

An example of the effects of volume loading on LV filling dynamics in a conscious dog is shown in Figure 14-8. Transmitral flow was measured with an electromagnetic flowmeter while LV and left atrial pressures were measured with high fidelity micromanometers. This experiment clearly demonstrates that an increased left atrial pressure can result in an increased peak filling rate despite an increase in the time constant of isovolumic relaxation (indicating slower isovolumic relaxation). These investigators also studied the effects of a graded increase in afterload (angiotensin infusion) on filling and found that filling rate can be maintained in the presence of slowed isovolumic relaxation if the left atrial pressure is sufficiently high. Their observations provide a basis for the interpretation of altered filling rates in clinical and experimental studies of LV relaxation and filling. These studies do not, however, directly address the issue of myocardial loading conditions and the effect of load or wall stress on myocardial fiber lengthening during the diastolic filling period.

*Isolated Muscle Studies.* Isotonic relaxation (lengthening) in the isolated muscle preparation is analogous to auxotonic relaxation (filling) in the intact left ventricle; since the magnitude and timing of isolated muscle loads can be controlled precisely, the independent effect of load on isotonic relaxation can be assessed in a quantitative fashion. It should be recognized,

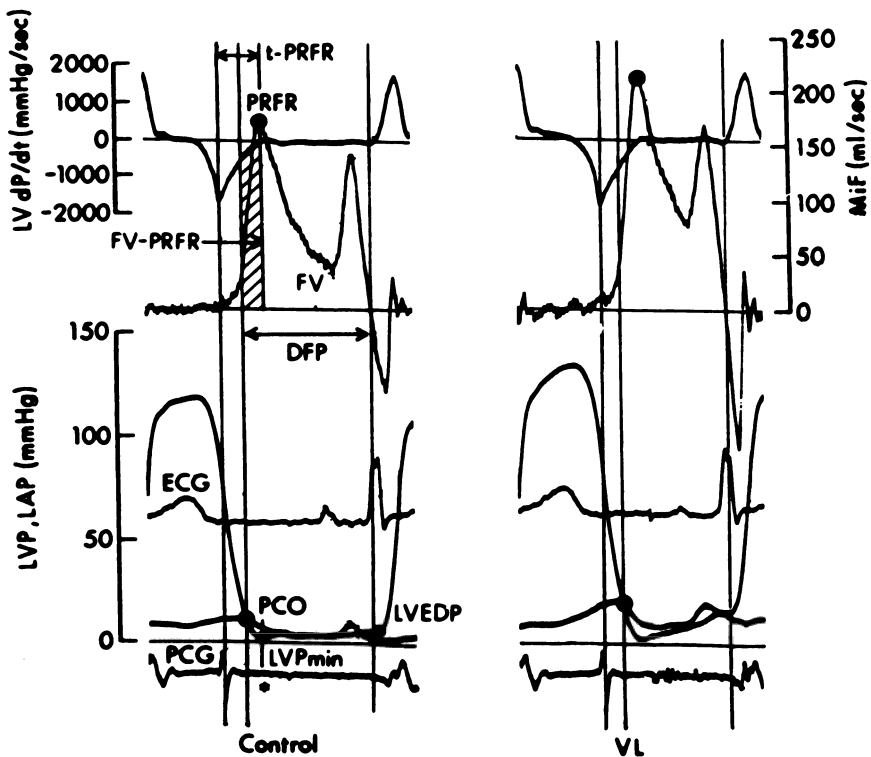


FIGURE 14-8. The effect of volume loading (VL) on left ventricular early filling dynamics in the conscious dog. Left ventricular pressure (LVP) and left atrial pressure (LAP) were measured with micromanometers and phasic transmitral flow (MiF) was measured with an electromagnetic flowmeter. After volume infusion, peak LVP increased from 121 to 135 mm Hg, and left ventricular end-diastolic pressure (LVEDP) increased from 6 to 16 mm Hg. Despite a decrease in isovolumic relaxation rate (the isovolumic relaxation-time constant increased from 28 to 32 msec), the peak rapid filling rate (PRFR) increased from 178 to 220 ml/second; this increase in filling rate occurred as a consequence of an increase in the transmitral pressure gradient from 6 to 8 mm Hg. (From Ishida et al. (15), with permission of the authors and the American Heart Association.)

however, that lengthening load in the isolated muscle is not strictly equivalent to left atrial pressure (in the presence of a small physiologic transmitral pressure gradient, the left atrial pressure exceeds the prevailing LV pressure during rapid filling). Thus, lengthening load experiments provide insight into the effects of variations in LV wall stress during rapid filling (the load that promotes fiber lengthening).

The effects of changes in lengthening load were studied in six physiologically sequenced rat papillary muscles. An example of a lengthening load experiment is shown in Figure 14-9. After isometric tension declined for a predetermined period of time, a series of force clamps (with

progressively larger load) was applied, thus raising the level of load borne by the muscle during isotonic lengthening. In this manner, the magnitude of the lengthening load could be changed while holding the time of application constant. Alternatively, the time of the load could be varied with a load of constant magnitude. As is shown in Figure 14-9, in the panels on the left, a progressive increase in lengthening load (from 1 to 4) resulted in a progressive increase in muscle lengthening rate [9]. The average data from all six muscles are shown in the right panel of Figure 14-9. This figure demonstrates the direct relation between lengthening load and lengthening rate. For a

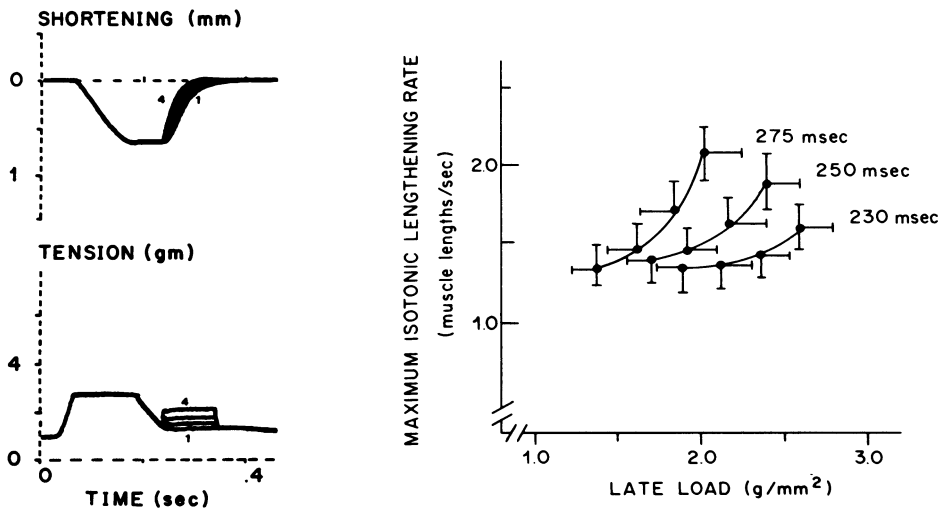


FIGURE 14-9. Effects of a change in the magnitude of lengthening load on isotonic lengthening rate. In the example on the left, isometric tension was allowed to fall for a predetermined period of time and a series of force clamps at progressively larger loads (labeled 1 to 4, with 4 being the highest) were applied, thus raising the level of load on the muscle during isotonic lengthening. On the right ( $n = 6$ ) are plotted the effects of load clamps applied at three points in time during isometric relaxation (230, 250, and 275 msec after muscle stimulation). At any given time, isotonic lengthening rate increased as the magnitude of load increased. The slope of the curvilinear relationship between isotonic lengthening rate and the magnitude of late load became steeper at later times during isometric relaxation. Thus, isotonic lengthening rate (at a common load) increased as the load was applied later in the course of tension decline.

given magnitude of late load, the rate of isotonic lengthening is greater as the load is applied later in the course of tension decline; this is presumably due to greater muscle deactivation near the end of isometric tension decline. These results, if extrapolated to the intact heart, indicate that loading the LV during the rapid filling period should enhance filling by promoting myocardial lengthening; in effect, filling promotes filling.

### Summary

In this chapter we emphasized the significant influence of loading conditions on LV relaxation. Changes in inotropic state, ischemia, hypertrophy, and a host of other factors also affect relaxation but were not discussed. Ventricular asynchrony is likewise beyond the scope of this chapter, but it should be recognized that complex loading interactions among fibers within the LV wall influence relaxation and filling in

ventricles that contract and relax nonsynchronously.

Intact heart and isolated muscle experiments indicate that changes in preload do not influence relaxation rates when systolic pressure or total load remains constant. It appears, therefore, that the relaxation changes that occur with volume loading are due to changes in systolic pressure or load. Indeed, an increase in systolic pressure may cause a substantial decrease in isovolumic relaxation rate—especially if there is a slow rise and a late peak in LV pressure. In contrast, an abrupt increase in late systolic load augments relaxation. Intact heart studies indicate that an abrupt load increment near the end of ejection results in premature and more rapid isovolumic relaxation, whereas an increase in left atrial pressure increases the filling rate; isolated muscle studies indicate that a load increment at the end of isometric relaxation causes an increase in isotonic relaxation periods. Thus, loading conditions during the periods of ejec-

tion, isovolumic relaxation, and filling can influence relaxation parameters in the normal heart and should be considered in clinical and experimental studies of LV relaxation.

### References

1. Brutsaert DL, Housmans PR, Goethals MA (1980). Dual control of relaxation: Its role in the ventricular function in the mammalian heart. *Circ Res* 47:637-652.
2. Brutsaert DL, Rademakers FE, Sys SU, et al (1985). Ventricular relaxation. In Levine HJ, Gaasch WH (eds): *The Ventricle*. Boston: Martinus Nijhoff, 1985.
3. Gaasch WH, Carroll JD, Blaustein AS, Bing OHL (1986). Myocardial relaxation: Effects of preload on the time course of isovolumetric relaxation. *Circulation* 73:1037-1041.
4. Weiss JL, Frederiksen JW, Weisfeldt ML (1970). Hemodynamic determinants of the time course of fall in canine left ventricular pressure. *J Clin Invest* 58:751-760.
5. Mirsky I (1984). Assessment of diastolic function: Suggested methods and future considerations. *Circulation* 69:836-841.
6. Yellin EL, Hori M, Chaim Y, et al (1986). Left ventricular relaxation in the filling and non-filling intact canine heart. *Am J Physiol* 250: H620-629.
7. Wiegner AW, Bing OHL (1982). Mechanics of myocardial relaxation: Application of a model to isometric and isotonic relaxation of rat myocardium. *J Biomech* 15:831-840.
8. Wiegner AW, Bing OHL (1978). Isometric relaxation of rat myocardium at end-systolic fiber length. *Circ Res* 43:865-869.
9. Zile MR, Gaasch WH, Wiegner AW, et al (1985). Mechanical determinants of the rate of isotonic lengthening in rat left ventricular myocardium. *Circulation* 72:III-184 (abstract).
10. Karliner JS, LeWinter MM, Mahler F, et al (1977). Pharmacologic and hemodynamic influences on the rate of isovolumic left ventricular relaxation in the normal conscious dog. *J Clin Invest* 60:511-521.
11. Gaasch WH, Blaustein AS, Andrias CW, et al (1980). Myocardial relaxation. II. Hemodynamic determinants of the rate of left ventricular isovolumic pressure decline. *Am J Physiol* 239:H1-6.
12. Blaustein AS, Gaasch WH (1983). Myocardial relaxation. VI. Effects of beta adrenergic tone and asynchrony on LV relaxation rate. *Am J Physiol* 244:H417-422.
13. Bahler RC, Martin P (1985). Effects of loading conditions and inotropic state on rapid filling phase of left ventricle. *Am J Physiol* 248:H523-533.
14. Hori M, Inoue M, Kitakaze M, et al (1985). Loading sequence is a major determinant of afterload-dependent relaxation in intact canine heart. *Am J Physiol* 249:H747-754.
15. Ishida Y, Meisner JS, Tsujioka K, et al (1986). Left ventricular filling dynamics: Influence of left ventricular relaxation and left atrial pressure. *Circulation* 74:187-196.
16. Zile MR, Blaustein AS, Gaasch WH (1985). In the normal left ventricle catecholamine induced changes in filling rate are mediated through changes in end systolic size. *Circulation* 72:III-88.
17. Goethals MA, Kersschot IE, Claes VA, et al (1980). Influence of abrupt pressure increments on left ventricular relaxation. *Am J Cardiol* 45:392, (abstract).
18. Gaasch WH, Ariel Y, McMahon TA (1986). Load-dependent relaxation in the intact left ventricle. *J Am Coll Cardiol* 7:243A, (abstract).

---

# 15. INFLUENCE OF PRESSURE AND VOLUME OVERLOAD ON DIASTOLIC COMPLIANCE

---

H.P. Krayenbuehl, O.M. Hess, M. Ritter, J. Schneider,  
E.S. Monrad, J. Grimm

Traditionally, the passive diastolic properties of the intact ventricle are assessed from the diastolic portion of the pressure-volume or pressure-length relationship. Compliance of the ventricular chamber refers to the ratio of change in volume ( $dV$ ) to a change in pressure ( $dP$ ). The reversed ratio represents chamber stiffness ( $dP/dV$ ). The relationship between P and V throughout diastole is curvilinear. It is popular to fit the P-V data to an exponential relation, although in many instances (and also in pressure and volume overload) the observed P-V coordinates may clearly deviate from a true exponential relationship. The slope of the pressure-volume relation is termed the constant of *chamber stiffness* and represents a nonnormalized quantity of diastolic stiffness.

Chamber stiffness is influenced by a variety of factors intrinsic or extrinsic to the ventricle [1, 2]. The basic determinant, however, is the ventricular myocardium whose structure may undergo important changes with the development of concentric and eccentric hypertrophy consequent to chronic pressure and volume overload. For the quantification of the true elastic properties of the myocardium, the pressure-volume data must be normalized for size, shape, and wall thickness. Thus, intrinsic *myocardial stiffness* is assessed from the diastolic stress-strain relationship, which is independent of chamber geometry.

The purpose of this chapter is to report on

determinations of left ventricular chamber and myocardial stiffness in patients with chronic left ventricular pressure and/or volume overload from aortic stenosis and/or aortic insufficiency. The diastolic functional data were compared with morphometric measurements from left ventricular endomyocardial biopsies carried out at catheterization [3, 4]. This comparison is of interest because in animal models when chronic pressure overload was experimentally induced an increase in myocardial stiffness has been shown to parallel an increase in myocardial connective tissue [5, 6].

## *Patients and Methods*

In a first study, 21 patients (mean age 47 years) with aortic valve disease underwent right and left heart catheterization as well as left ventricular endomyocardial biopsies before and 17.5 months (range 9 to 25) after successful aortic valve replacement [4]. There were ten patients with aortic stenosis (AS) six with aortic insufficiency (AI) and five with combined aortic valve lesion (AS + AI). Ten patients (mean age 36 years) with no or minimal heart disease served as control subjects. Informed consent was obtained from all patients.

The basic data for the assessment of left ventricular chamber and myocardial stiffness were derived from simultaneous left ventricular high-fidelity pressure and single-beam echocardiographic measurements. The pressure-echo tracings were digitized on a computer-assisted system. Left ventricular pressure, its first derivative ( $dP/dt$ ), left ventricular internal diameter, posterior wall thickness, midwall circumference

Supported by the Swiss National Science Foundation.  
Grossman, William, and Lorell, Beverly H. (eds.), *Diastolic Relaxation of the Heart*. Copyright © 1987. Martinus Nijhoff Publishing. All rights reserved.

(1), its first derivative ( $dl/dt$ ), and meridional wall stress were analyzed at a rate of 130 times per cardiac cycle.

Left ventricular chamber stiffness was evaluated from the diastolic (lowest left ventricular pressure to end-diastole) pressure-midwall circumference relationship, and myocardial stiffness was estimated from the meridional stress-strain relationship. Because deviations from an exponential curve can occur when filling and hence strain rates are enhanced [7], such as in AI [3] or in AS with increased left atrial driving pressure [8], a viscoelastic rather than a static elastic model with or without an asymptote was used to fit the pressure-circumference and the stress-strain data. Thus *diastolic chamber stiffness* was determined from the equation:

$$P = \alpha'(e^{\beta' l} - 1) + \eta'(dl/dt)$$

where  $P$  = left ventricular pressure (mm Hg);  $\alpha'$  = elastic constant (mm Hg);  $\beta'$  = constant of left ventricular chamber stiffness;  $l$  = left ventricular midwall circumference (cm);  $\eta'$  = constant of chamber viscosity (mm Hg·sec);  $dl/dt$  = lengthening rate of midwall circumference ( $\text{sec}^{-1}$ ). The three constants  $\alpha'$ ,  $\beta'$ , and  $\eta'$  were calculated by an iteration procedure using the nonlinear curve-fit program. For the assessment of *myocardial stiffness* calculation of stress and strain throughout the passive diastolic phase is required. Strain ( $\epsilon$ ) is determined either

according to the Lagrangian ( $\epsilon = \frac{l - l_0}{l_0}$ )

or the natural strain ( $\epsilon = \ln \frac{l}{l_0}$  definition), both of which include the estimation of a reference length at a transmural stress of zero. ( $l_0$ ). Because true  $l_0$  cannot be determined in humans at catheterization, we used as its index the midwall circumference at a wall stress of  $1 \text{ g/cm}^2$  ( $l_1$ ), which allows normalization of strain in ventricles of different sizes to a common preload. The reference midwall circumference,  $l_1$  was obtained by extrapolation of the viscoelastic stress-midwall circumference relationship according to the formula:

$$\sigma = \alpha^*(e^{\beta^* l} - 1) + \eta^* dl/dt$$

where  $\sigma$  = meridional wall stress ( $\text{g/cm}^2$ );  $\alpha^*$  = elastic constant ( $\text{g/cm}^2$ );  $\beta^*$  = slope of the

stress-circumference relationship;  $l$  = midwall circumference (cm);  $\eta^*$  = constant of viscosity ( $\text{g}\cdot\text{sec}/\text{cm}^2$ );  $dl/dt$  = lengthening rate of the midwall circumference ( $\text{sec}^{-1}$ ). The three constants  $\alpha^*$ ,  $\beta^*$ , and  $\eta^*$  were again determined by nonlinear regression analysis.

Once  $l_1$  was determined, the diastolic viscoelastic stress-strain relationship was calculated according to the formula

$$\sigma = \alpha(e^{\beta \epsilon} - 1) + \eta d\epsilon/dt$$

where  $\sigma$  = left ventricular meridional wall stress ( $\text{g/cm}^2$ );  $\alpha$  = elastic constant ( $\text{g/cm}^2$ );  $\beta$  = constant (and measure) of left ventricular myocardial stiffness;  $\epsilon$  = normalized strain (natural strain definition);  $\eta$  = constant of myocardial viscosity ( $\text{g}\cdot\text{sec}/\text{cm}^2$ );  $d\epsilon/dt$  = left ventricular strain rate ( $\text{sec}^{-1}$ ).  $\alpha$ ,  $\beta$ , and  $\eta$  were determined using the nonlinear regression analysis described above. We realize that others [2, 9, 10] did not use this classic way of determining the constant of myocardial stiffness via the estimation of the reference length of the unstressed muscle but assessed the stiffness constant of the muscle from the equation

$$E = \frac{d\sigma}{d\epsilon} = k_m \cdot \sigma + c$$

where  $E$  = modulus of myocardial elastic stiffness,  $\sigma$  = wall stress;  $\epsilon$  = strain;  $k_m$  = constant of myocardial stiffness; and  $c$  = intercept.

Because  $d\epsilon = dl/l$ , the estimation of the reference muscle length  $l_0$  is not required for the calculation of  $k_m$ . This certainly represents a methodological advantage. However, by the sole estimation of  $k_m$  with this technique, diastolic myocardial stiffness might be incompletely assessed. Both  $k_m$  and myocardial elastic stiffness values at similar levels of stress are necessary for full functional characterization of the diastolic muscle properties [11]. Unfortunately, in patients with chronic cardiac disease, observed diastolic stress values may not or only partially overlap with stress values of control subjects [10]; thus, evaluation of diastolic myocardial stiffness remains incomplete.

Left ventricular biplane cineangiography, to determine volume and estimate left ventricular muscle mass, as well as selective coronary arteriography, to exclude coronary artery disease, were carried out at the end of the catheterization [4]. Left ventricular endomyocardial biopsies

were obtained by the transeptal route. Quantitative evaluation was carried out by morphometry as described previously [3, 4]. In the ten control subjects no biopsies were performed. Normal values for morphometric data were obtained from autopsy specimens of subjects who had been healthy before they died in a traffic accident.

## Results

### HEMODYNAMICS

In all three types of aortic valve disease, systolic function was well preserved; the left ventricular angiographic ejection fraction was comparable with that of the control subjects both before and after aortic valve replacement. Left ventricular end-diastolic volume index (EDVI) was significantly increased to 173 ml/m<sup>2</sup> in AS + AI and to 217 ml/m<sup>2</sup> in AI and regressed ( $p < 0.05$ ) to 99 and 137 ml/m<sup>2</sup>, respectively. End-diastolic angiographic wall thickness (h) was significantly increased in AS (1.24 cm) and AS + AI (1.07 cm). After surgery, h decreased ( $p < 0.005$ ) to 1.0 cm in AS. This value was still slightly increased ( $p < 0.05$ ) as compared to control subjects (0.76 cm). In AS + AI (0.93 cm) and AI (0.79 cm), postoperative h did not differ from that of control subjects. In all three groups the angiographic muscle mass index that was increased preoperatively had decreased significantly following surgery, although it remained 36 to 46% above the value observed in control subjects. (81 g/m<sup>2</sup>). The ratio of left ventricular muscle mass to end-diastolic volume (LMM/EDV in g/ml) was increased ( $p < 0.01$ ) in AS (1.61) and slightly decreased in AI (0.75). In the three groups with aortic valve disease LMM/EDV after surgery (1.15, 1.10, and 0.86) was not significantly different from the ratio in the control subjects (0.98). Left ventricular peak systolic pressure (LVSP), which was increased in AS and AS + AI, decreased significantly after surgery. However, the postoperative LVSP in AS (150 mm Hg) was still higher ( $p < 0.05$ ) than that in control subjects (117 mm Hg).

### PASSIVE DIASTOLIC FUNCTION

The constant of left ventricular chamber stiffness,  $\beta'$ , did not differ significantly between the three groups with aortic valve disease and the control subjects. After surgery,  $\beta'$  decreased

only slightly in patients with AS or AI but significantly in those with AS + AI. In four of the ten patients with AS, preoperative  $\beta'$  was increased but after valve replacement (Figure 15-1) was decreased in three of them.

The constant of myocardial stiffness ( $\beta$ ) in patients with aortic valve disease was not significantly different from that in control subjects, (Figure 15-2). However, after surgery,  $\beta$  increased significantly in AS; the postoperative mean value was also significantly higher than that in control subjects. No significant changes of  $\beta$  were observed in AS + AI and in AI. Figure 15-3 shows the stress-strain relationship in a typical patient with AS. After valve replacement, the slope  $\beta$  of the stress-strain relationship increased, indicating an increase in myocardial stiffness. In the same patient, the constant of chamber stiffness decreased postoperatively.

### LEFT VENTRICULAR ENDOMYOCARDIAL BIOPSIES

Table 15-1 summarizes the morphometric findings. All three groups of those with aortic valve disease exhibited marked cellular hypertrophy, which decreased but did not normalize after surgery. Interstitial fibrosis (IF in %) was increased to a similar extent in the three groups with aortic valve disease. After surgery, IF increased significantly in AS; the two other groups showed only a trend for IF to increase. Left ventricular fibrous content (FC in g/m<sup>2</sup>) remained unchanged in all three groups (FC = IF · LMMI/100).

## Discussion

### PREOPERATIVE LEFT VENTRICULAR DIASTOLIC PROPERTIES

The present findings are in accordance with the observations of Peterson and coworkers [10] that non-normalized left ventricular chamber stiffness is increased in some but not all patients with chronic pressure overload from AS. In an earlier study, Grossman and colleagues [12] had described a consistent increase of the slope ( $\Delta P/\Delta D$ ) of the left ventricular pressure-diameter relation in late diastole in five patients with AS. The same authors also reported a moderate increase of  $\Delta P/\Delta D$  in aortic insufficiency [12], whereas in our patients with volume overload, chamber stiffness was normal or even slightly

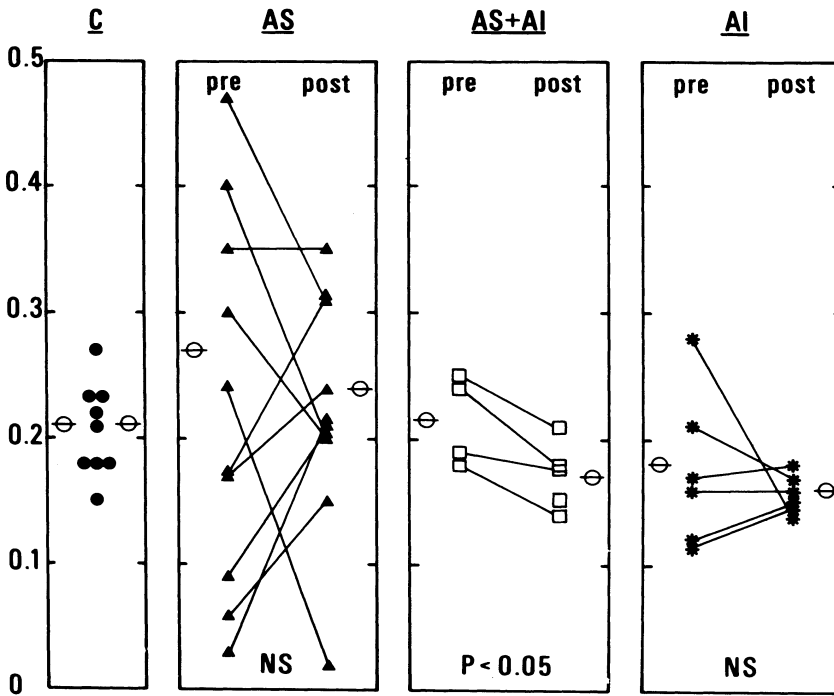


FIGURE 15-1. Left ventricular chamber stiffness constant  $\beta'$  in control subjects (C) and in patients with aortic valve disease before (pre) and after (post) aortic valve replacement. The mean values of  $\beta'$  in aortic stenosis (AS), combined aortic valve lesion (AS + AI) and aortic insufficiency (AI) were not different from those of control subjects before or after surgery. It should be noted that in three of four patients with AS and increased preoperative  $\beta'$ , this constant decreased substantially following valve replacement. In AS + AI,  $\beta'$  decreased significantly. In one patient with AS + AI,  $\beta'$  could not be determined preoperatively. NS = not significant.

TABLE 15-1. Left Ventricular Morphometric Findings in eight Controls Subjects, and in Patients with Aortic Stenosis (AS), Combined Aortic Valve Lesion (AS + AI), and Aortic Insufficiency (AI)

	MFD ( $\mu$ )	IF (%)	FC ( $g/m^2$ )
Controls (n = 8)	14	2	—
AS (n = 10) pre	31	15	28
AS post	26	26	31
AS + AI (n = 5) pre	31	15	25
AS + AI post	27	22	27
AI (n = 6) pre	31	19	30
AI post	27	24	29

\*  $p < 0.05$ .

\*\*  $p < 0.01$ .

MFD = muscle fiber diameter; If = interstitial fibrosis; FC = fibrous content.

smaller than in control subjects. The reason for an increased chamber stiffness in AS and a decreased chamber stiffness in AI must be sought primarily in the particular type of hypertrophy (i.e., concentric and eccentric) rather than in a fundamental difference of wall structure because preoperative IF and cell diameter did not differ. However, there was a marked difference in left ventricular geometry—mass/volume ratio and end-diastolic wall thickness were increased in AS.

Myocardial stiffness assessed from the slope

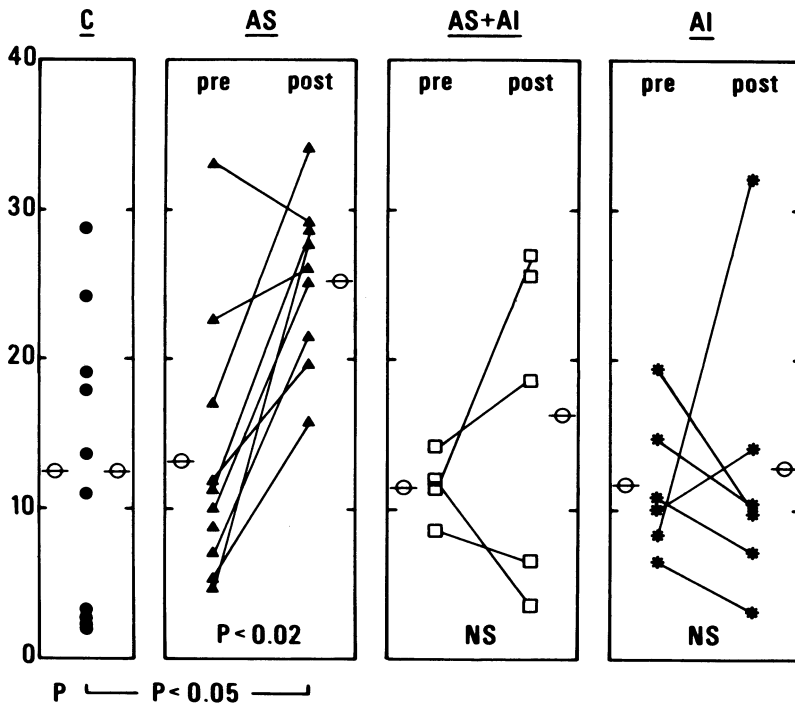


FIGURE 15-2. Left ventricular myocardial stiffness constant ( $\beta$ ) in control subjects, (C), and in patients with aortic valve disease before (pre) and after (post) aortic valve replacement. Prior to surgery  $\beta$  was no different in the three groups of aortic valve disease and in controls. After surgery,  $\beta$  increased significantly in aortic stenosis (AS), whereas in combined aortic valve lesion (AS + AI) and in aortic insufficiency (AI) the change of  $\beta$  was variable. In one patient with AS and in one patient with AS + AI,  $\beta$  could be determined only at the preoperative or the postoperative investigation, respectively. NS = not significant;  $\ominus$  = mean values.

( $\beta$ ) of the left ventricular stress-strain relationship showed quite a larger range in the control subjects. The preoperative values of  $\beta$  in the patients with aortic valve disease did not differ from those of controls. Previously, Peterson and associates [10] had reported an increased left ventricular myocardial stiffness in AS when left ventricular end-diastolic pressure was markedly increased, and Gaasch and coworkers [2] had found myocardial stiffness to be variable, i.e., normal or abnormal, in single patients with AS or AI.

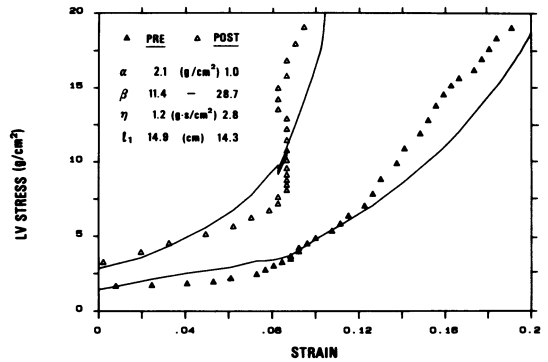


FIGURE 15-3. Preoperative and postoperative left ventricular (LV) stress-strain relationship in a patient with aortic stenosis. The slope  $\beta$  increased from 11.4 to 28.7 following aortic valve replacement indicating an increase in myocardial stiffness. In the same patient the slope of the pressure-midwall circumference relationship ( $\beta'$ ) had decreased from 0.47 to 0.31, indicating a postoperative decrease of chamber stiffness.

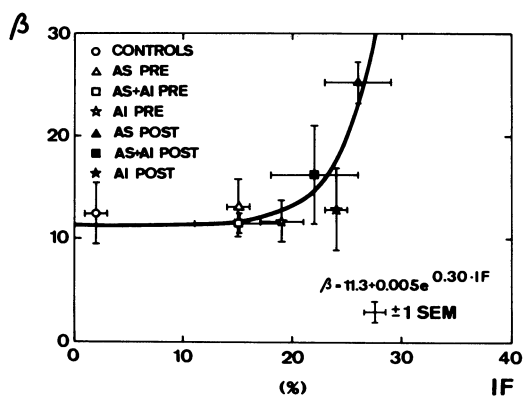


FIGURE 15-4. Myocardial stiffness constant ( $\beta$ ) versus interstitial fibrosis (IF in %) in control subjects and patients with aortic stenosis (AS), combined aortic valve lesion (AS + AI), and aortic insufficiency (AI) before (PRE) and after (POST) successful aortic valve replacement. Given are mean values  $\pm 1$  standard error of the mean (SEM). An exponential relationship exists between myocardial stiffness and IF whereby myocardial stiffness tends to increase once fibrosis exceeds 20%. In some patients (AI POST) myocardial stiffness remains normal although fibrosis increased to 24%. This suggests that in these patients with increased cavity size postoperatively, factors other than just IF might influence  $\beta$ .

Increased IF has been suspected to be at the origin of increased myocardial stiffness [2, 10]. Our morphometric findings at the preoperative investigation, however, document that IF in aortic valve disease may exceed that of control specimens from autopsies by a factor of almost up to ten without an alteration of myocardial stiffness.

#### POSTOPERATIVE LEFT VENTRICULAR DIASTOLIC PROPERTIES

Diastolic chamber stiffness reassessed within 25 months after aortic valve replacement decreased significantly in patients with combined aortic valve lesion and in three of four patients with AS in whom increased preoperative  $\beta'$  chamber stiffness became normal postoperatively. This decrease was associated with regression but not normalization of angiographic muscle mass and end-diastolic wall thickness, as well as with a trend of the mass/volume ratio to change toward the value in control subjects. The postoperative

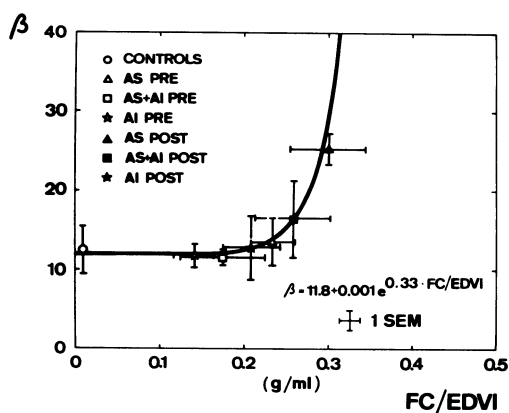


FIGURE 15-5. Myocardial stiffness constant ( $\beta$ ) vs. the ratio of fibrous content (FC in  $\text{g}/\text{m}^2$ ) and end-diastolic volume index (EDVI in  $\text{ml}/\text{m}^2$ ) in control subjects, patients with aortic stenosis (AS), combined aortic valve lesion (AS + AI), and aortic insufficiency (AI) before (PRE) and after (POST) successful aortic valve replacement. Given are mean values  $\pm 1$  standard error of the mean (SEM). An exponential relationship exists between myocardial stiffness and FC/EDVI, suggesting that myocardial stiffness is not only dependent on the amount of fibrous tissue but also on left ventricular geometry. This explains why myocardial stiffness is normal in patients with AI after surgery despite an interstitial fibrosis of 24% (see Figure 15-4); thus, a certain amount of fibrous tissue has a different influence on myocardial stiffness in a small and large ventricle.

change in chamber stiffness (see Figure 15-1) was opposite to that of myocardial stiffness, which increased in patients with aortic stenosis (see Figure 15-2). An explanation for this increase was provided by the postoperative morphometric measurements. In AS, IF increased after surgery, although left ventricular FC did not change. When all preoperative and postoperative data were combined a curvilinear relationship between  $\beta$  and IF (Figure 15-4) was observed [13]. As far as patients with pressure overload are concerned, the myocardial stiffness constant tended to increase once IF was larger than 20%. In AI, postoperative myocardial stiffness changed little although IF increased to 24%. This observation raised the possibility that the type of hypertrophy (concentric or eccentric) or distribution of a given amount of fibrous tissue around the left ventricular cavity

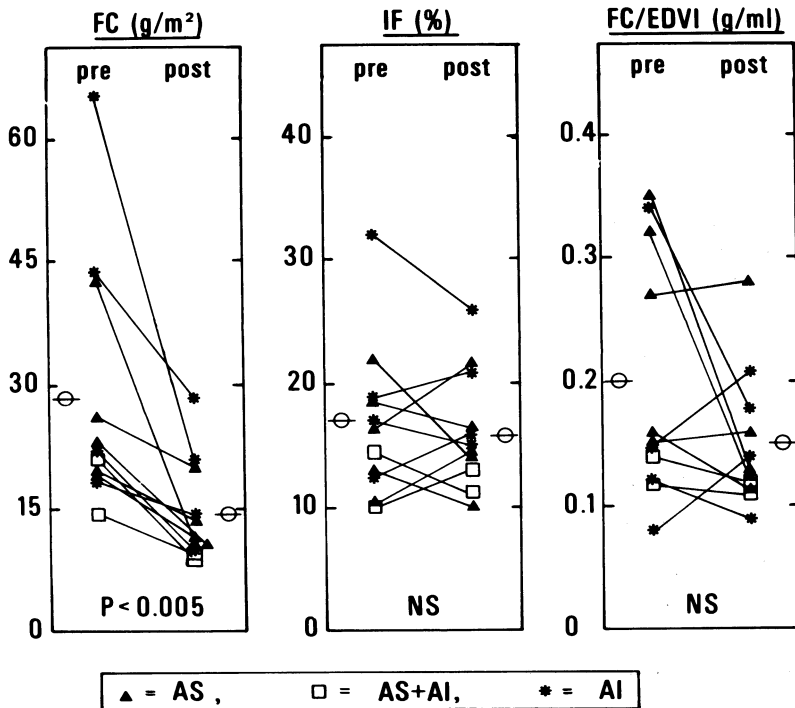


FIGURE 15-6. Left ventricular connective tissue in 11 patients with normal ejection fraction 70 months after aortic valve replacement. There is a significant decrease of fibrous content (FC), hence fibrosis is at least partially reversible late postoperatively. The relative interstitial fibrosis (IF) and the ratio FC/end-diastolic volume (EDVI) remained unchanged late after aortic valve replacement, suggesting that no major changes in the constant of myocardial stiffness ( $\beta$ ) occurred. However in three of four patients with a sizably increased preoperative FC/EDVI ratio, this ratio fell below 0.20 g/ml after surgery, and hence the preoperatively increased myocardial stiffness is presumed to have returned to an essentially normal value in these three instances. AS = aortic stenosis; AS + AI = combined aortic valve lesion; AI = aortic insufficiency; NS = not significant.

could also play a role as a determinant of myocardial stiffness. Indeed, when  $\beta$  was plotted versus the ratio FC/end-diastolic volume (EDVI) (in g/ml) a similar curvilinear relationship (Figure 15-5) was observed as for the relation between  $\beta$  and IF (see Figure 15-4). The break-off point where myocardial stiffness starts to rise is located at a FC/EDVI ratio of about 0.20 g/ml.

Whether an increased myocardial stiffness at an essentially normal chamber stiffness has a clinical significance is not clear. In any case, the increase of  $\beta$  in AS after surgery was associated with a decrease of resting left ventricular end-diastolic pressure from 19 to 15 mm Hg rather than an increase. However, one could imagine

that with increased left ventricular filling, filling pressure could rise abnormally when the muscle is stiffer than normal. In this respect, it is noteworthy that when patients with aortic valve replacement and normal resting ejection fraction were studied after undergoing bicycle exercise 14 months following surgery, 50% showed a pathologic increase of left ventricular end-diastolic pressure during stress [14].

The long-term outcome as to the level of left ventricular myocardial stiffness after correction of chronic pressure and volume overload is likely to be linked to whether FC persists or regresses as well as to the change of cavity size. Within the first 2 years after aortic valve replacement FC remained unchanged. In a recent study of 16

patients who had endomyocardial biopsies 70 months after aortic valve replacement, 11, whose postoperative left ventricular ejection fraction was well preserved (56–78%) (Figure 15–6), showed a decrease of FC from 28.7 to 14.4 g/m<sup>2</sup>. Thus, the possibility does exist that IF is, at least in part, reversible late after aortic valve replacement. The IF in % (16.9 and 16.2%) and the ratio FC/EDVI (0.20 and 0.15 g/ml, respectively) remained essentially unchanged, suggesting that the constant of myocardial stiffness ( $\beta$ ) did not change either. It should be noted, however, that in three of four patients with an increased preoperative FC/EDVI ratio, this ratio decreased below the critical value of 0.20 g/ml after surgery.

### Summary

The results of our studies can be summarized as follows:

Left ventricular chamber stiffness was increased in some but not all patients with chronic pressure overload from AS and tended to be decreased in chronic volume overload from AI.

Concentric hypertrophy with increased mass/volume ratio and end-diastolic wall thickness was the main determinant of increased chamber stiffness.

Left ventricular myocardial stiffness was within normal limits in both patients with AS and patients with AI.

Nine to 25 months following successful aortic valve replacement, myocardial stiffness increased in AS, but remained unchanged in AI.

The postoperative increase of myocardial stiffness was associated with a relative increase of IF, while left ventricular FC was unchanged. The magnitude of left ventricular FC relative to chamber size appeared to be the main determinant of myocardial stiffness.

In patients with normal ejection performance, left ventricular FC was partially reversible seventy of months following surgery; however, from the commensurate decrease of cavity size with the ratio FC/EDVI remaining unchanged, it is likely that there was little change of the myocardial stiffness constant ( $\beta$ ).

### Reference

1. Grossman W, McLaurin LP (1976). Diastolic properties of the left ventricle. *Ann Int Med* 84:316–326.
2. Gaasch WH, Bing OHL, Mirsky I (1982). Chamber compliance and myocardial stiffness in left ventricular hypertrophy. *Eur Heart J* 3(suppl A):139–145.
3. Hess OM, Schneider J, Koch R, et al (1981). Diastolic function and myocardial structure in patients with myocardial hypertrophy. *Circulation* 63: 360–371.
4. Hess OM, Ritter M, Schneider J, et al (1984). Diastolic stiffness and myocardial structure in aortic valve disease before and after valve replacement. *Circulation* 69:855–865.
5. Cooper G, Tomanek RJ, Ehrhardt JC, Marcus ML (1981). Chronic progressive pressure overload of the cat right ventricle. *Circ Res* 48:488–497.
6. Thiedemann KU, Holubarsch Ch, Medugorac I, Jacob R (1983). Connective tissue content and myocardial stiffness in pressure overload hypertrophy: A combined study of morphologic, morphometric, biochemical and mechanical parameters. *Basic Res Cardiol* 78:140–155.
7. Rankin JS, Arentzen CE, McHale PA et al (1977). Viscoelastic properties of the diastolic left ventricle in the conscious dog. *Circ Res* 41:37–45.
8. Murakami T, Hess OM, Gage JE, et al (1986). Diastolic filling dynamics in patients with aortic stenosis. *Circulation* 73:1162–1174.
9. Mirsky I (1976). Assessment of passive elastic stiffness of cardiac muscle: Mathematical concepts, physiologic and clinical considerations, directions of future research. *Progr Cardiovasc Dis* 18:277–308.
10. Peterson KL, Tsuji J, Johnson A, et al (1978). Diastolic left ventricular pressure-volume and stress-strain relations in patients with valvular aortic stenosis and left ventricular hypertrophy. *Circulation* 58:77–89.
11. Williams JF Jr, Potter RD (1981). Passive stiffness of pressure-induced hypertrophied cat myocardium. *Circ Res* 49:211–215.
12. Grossman W, McLaurin LP, Stefadouros MA (1974). Left ventricular stiffness associated with chronic pressure and volume overloads in man. *Circ Res* 35:793–800.
13. Hess OM, Ritter M, Schneider J, et al (1984). Diastolic function in aortic valve disease: Techniques of evaluation and pre-/postoperative changes. *Herz* 9:288–296.
14. Horstkotte D, Haerten K, Körfer R, et al (1983). Hemodynamic findings at rest and during exercise after implantation of different aortic valve prostheses. *Z Kardiol* 72:429–437.

---

## 16. INFLUENCE OF THE PERICARDIUM ON DIASTOLIC COMPLIANCE

---

Martin M. LeWinter

The influence of the pericardium on diastolic compliance is a function of the distensibility of the pericardium itself, the distensibility of the cardiac chambers, and the total volume contained within the cardiac chambers [1]. To illustrate the latter factor, it is reasonable to expect that at a given left ventricular volume, the influence of the pericardium on left ventricular compliance will be directly proportional to the volume contained within the other cardiac chambers, since it is the *total* cardiac volume that determines pericardial distention. An additional effect of the pericardium on diastolic compliance has to do with the fact that the intact pericardium has a substantial modulating influence on diastolic interaction between the ventricles, i.e., the amount of interaction is markedly reduced when the pericardium is removed [2, 3]. For some time, we have been particularly interested in examining both the distensibility of the pericardium and its influence on the diastolic pressure-volume relation of the cardiac chambers. We have not specifically studied diastolic ventricular interaction. However, our basic approach to assessing the influence of the pericardium on compliance is quite straightforward. We simply examine the intracavitary pressure-volume (or dimension) relation of a cardiac chamber before and after pericardiectomy. In this fashion, we determine the *net* effect of the pericardium on compliance; included in this net effect is the pericardial modulation of ventricular interac-

tion. This chapter will serve to review certain aspects of this work which have already been completed and, in addition, more recent work which is currently in progress.

### *Distensibility of the Pericardium*

We have examined this question in several ways. First, the material properties of specimens of both canine and human pericardium have been tested in vitro using a biaxial stretching device [4]. The key advantages of the biaxial technique, as opposed to prior studies using uniaxial loading, are that the tissue is subjected to more physiologic loading and the issue of anisotropy can be addressed directly. As shown in Figure 16-1, obtained from canine pericardium [4], the relation between tension and stretch ratio in both the X and Y directions is initially quite flat, but fairly abruptly makes a transition on a rather steep relationship. As also shown in this figure, there are differences between the tension-stretch relationship depending on the direction of loading, that is, the tissue is anisotropic. However, the amount of anisotropy is modest, averaging about a 20% difference between the two directions [4]. As shown in Figure 16-2, the canine pericardium displays substantial stress relaxation [4]. We do not detect any appreciable creep, however. More recently, we have performed similar tests on specimens of human pericardium obtained from patients undergoing coronary artery bypass surgery [5]. Qualitatively, the tension-stretch ratio relationships of human pericardium appear similar to those of the dog. The behavior of these specimens during creep and stress relaxation tests was also quite comparable to canine specimens. However, there *were* some differences

This research was sponsored by USPHS Grant No. 1R01 HL35309 (National Heart, Lung and Blood Institute) and by the Research Service of the Veterans Administration. Grossman, William, and Lorell, Beverly H. (eds.), *Diastolic Relaxation of the Heart*. Copyright © 1987. Martinus Nijhoff Publishing. All rights reserved.

between canine and human pericardium. First, human specimens are isotropic, as opposed to the mild anisotropy observed in canine pericardium. Second, human pericardium is about three times thicker than canine pericardium. Finally, when both canine and human data were fitted to an exponential of the form  $dT/da = \beta T$ , where  $T$  = tension,  $a$  = area of the specimen, and  $dT/da$  is equivalent to a tangent modulus of the tension-area relation, it was found that the tangent modulus was not significantly different between species. However, the constant  $\beta$  was slightly, but significantly, larger in the dog. The implication of the finding is that human pericardium is less extensible than canine at lower, but physiologic tensions (equivalent to a transpericardial pressure below about 12 mm Hg).

In a second approach to this question, we have examined directional lengthening of the in situ pericardium in open-chest dogs as a function of changes in the filling of the heart [6]. In this study, we implanted mutually orthogonal, pulsed-transit sonomicrometers on the surface of the pericardium to measure lengthening of short (approx. 1 cm) segments of the tissue. We also measured atrial pressures and the pericardial pressure, the latter with flat, air-filled balloons. As shown in Figure 16-3, the pericardium displays marked directional variability in lengthening. Specifically, as the heart size is varied by a combination of partial inferior vena caval occlusion and volume infusion, virtually all of the lengthening of the pericardium occurs along the circumferential axis of the heart, with essentially no change (in this case, actually a decrease) along the longitudinal axis. Results of another such experiment are shown graphically in Figure 16-4, in which pericardial pressure is plotted against pericardial strain in the circumferential and longitudinal directions; once again, all of the lengthening is in the circumferential direction.

These results are in marked contrast to the in vitro behavior of the canine pericardium described previously [4], in which only modest directional variability of lengthening was observed. This finding implies that in situ the pericardium is markedly influenced by factors other than its intrinsic material properties, most likely the shape change of the heart itself as its volume varies or the external attachments of the pericardium.

A more traditional way of examining peri-

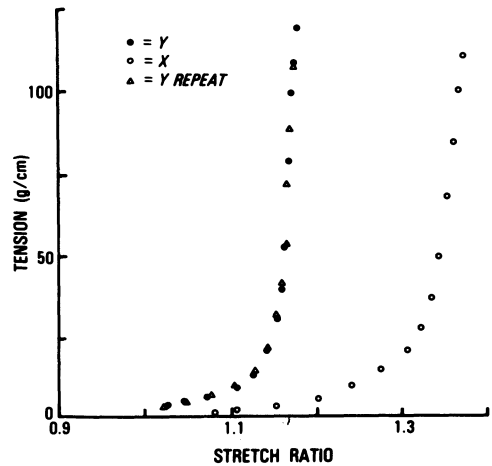


FIGURE 16-1. The relation between tension and stretch ratio (actual length  $\div$  unstressed length) in mutually orthogonal (X, Y) directions as the pericardium is subjected to biaxial loading. The procedure is to increase tension and length in one direction while keeping tension constant in the other direction, and then repeat the protocol for the other direction. (Reprinted from Lee et al. [4] by permission, American Journal of Physiology.)

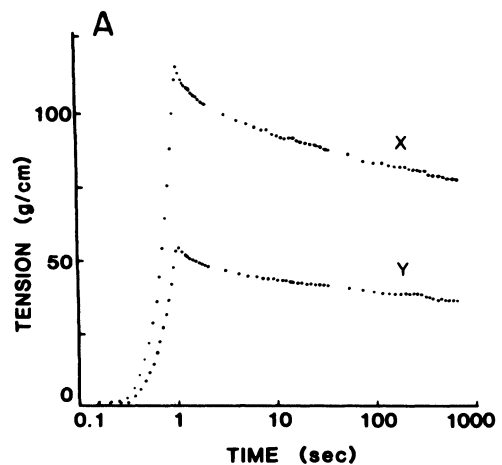


FIGURE 16-2. Stress relaxation testing of pericardium. The specimen is subjected to an abrupt increase in length and tension. Length is then held constant and tension allowed to vary with time. Note the progressive decrease in tension, indicative of stress relaxation. (Reprinted from Lee et al. [4] by permission, American Journal of Physiology.)

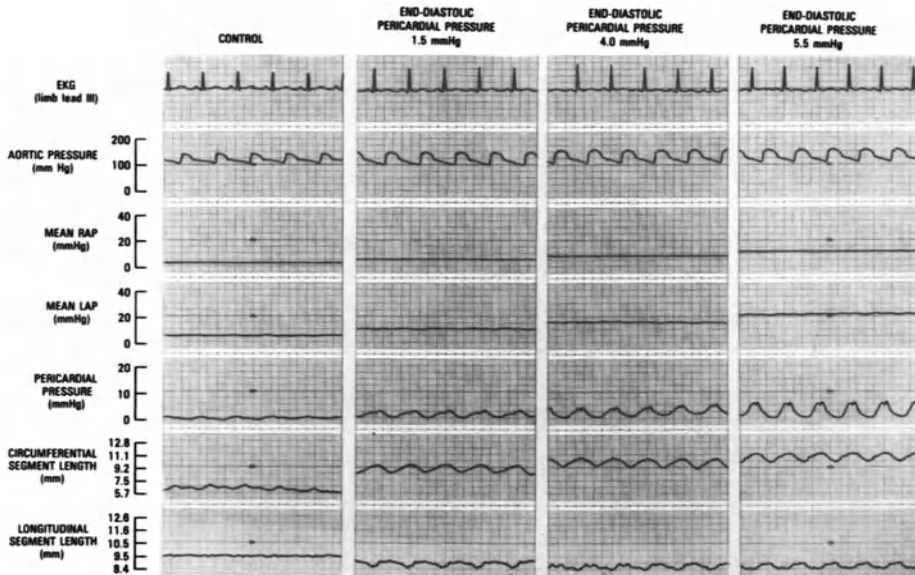


FIGURE 16-3. In vivo lengthening of canine pericardium. As heart size increases, the pericardium lengthens exclusively in the circumferential direction (see text). EKG = electrocardiogram; RAP = right atrial pressure; LAP = left atrial pressure. (Reprinted from Mann et al. [6] by permission, American Journal of Physiology.)

cardial distensibility is to examine its pressure-volume relation. The usual approach is to arrest the heart, empty it, and add known amounts of fluid to the pericardial sac while simultaneously measuring the pressure. The starting volume, which is the volume of the heart, is measured after completion of the experiment. An early example of such an experiment was published by Dr. Joseph Holt and coworkers [7], as shown in Figure 16-5. Here, the pericardial pressure-volume relation appears quite similar to the tension-stretch relation of the *in vitro* pericardium, that is, a very flat portion with an abrupt transition (or "knee") leading to a steep portion. However, note that the range of pericardial pressure measured was extremely large, reaching levels markedly above those present even with severe cardiac tamponade. More recently, we have reexamined this issue [8] and confined our measurements to smaller pressure ranges, as shown in Figure 16-6. When looked at in this

way, the transition to the steep portion of the pericardial pressure-volume relation in a normal dog, shown on the left, appears much more gradual. The pressure-volume relation on the right of Figure 16-6 was obtained in a dog with chronic cardiac dilation due to an intra-abdominal arteriovenous fistula. In this situation, the pericardial pressure-volume relation is markedly shifted to the right and less steep than normal. Thus, the pericardium accommodates a chronically enlarged heart by substantially increasing its volume and becoming more compliant. Further, in these same animals [8], the weight of the pericardium, normalized to body weight, is also increased, suggesting that these changes in the pressure-volume relation may be related, at least in part, to growth of the pericardial tissue.

### *Influence of the Pericardium on Cardiac Filling*

A number of investigators have studied the influence of the pericardium on diastolic compliance by determining the intracavitary pressure-volume relation of a cardiac chamber before and then after removing the pericardium [1, 9-11]. In most such studies, rather than

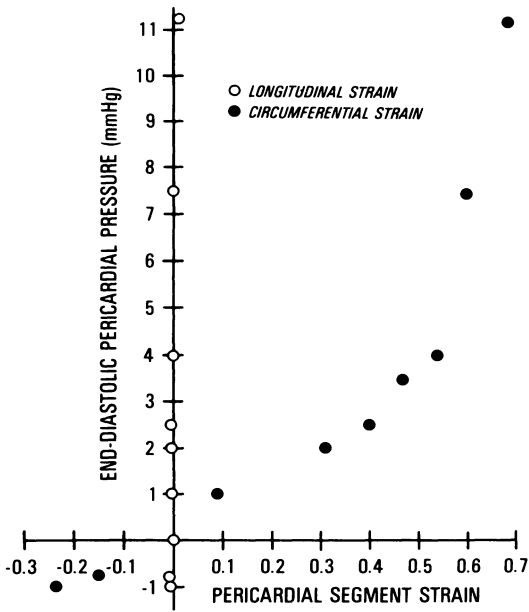


FIGURE 16-4. End-diastolic pericardial strain (actual length  $\div$  length at pericardial pressure of 0 mm Hg) is plotted against pericardial pressure (see text). (Reprinted from Mann et al. [6] by permission, American Journal of Physiology.)

measuring the absolute volume of the cardiac chamber, some surrogate for volume (usually a chamber dimension) is employed; in almost all instances, the chamber selected for study has been the left ventricle. A significant problem in certain of these studies is the fact that the pericardium has first been incised to allow for instrumentation of the heart and then resutured—a procedure which may result in an artifactual decrease in the compliance of the pericardium [11]. Nonetheless, as shown in Figure 16-7 [11], a downward or rightward shift of the diastolic pressure-dimension relation following pericardiectomy is what has been observed repeatedly for the left or right ventricle. Although its magnitude has varied, this shift can be used as a quantitative index of the effect of the pericardium on the compliance of the chamber in question.

Before reviewing some recent experiments we have performed to better understand the effect of the pericardium on cardiac filling, consider

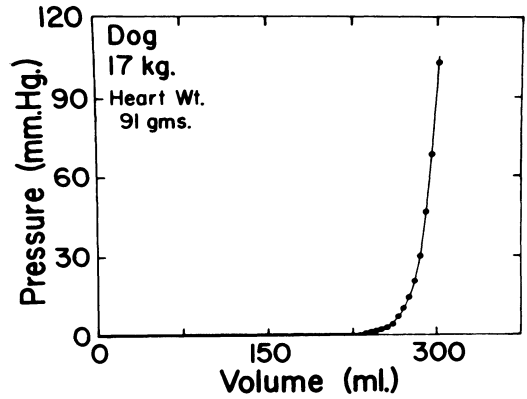


FIGURE 16-5. The pericardial pressure-volume relation (see text). (Reprinted from Holt et al. [7] by permission, American Heart Association.)

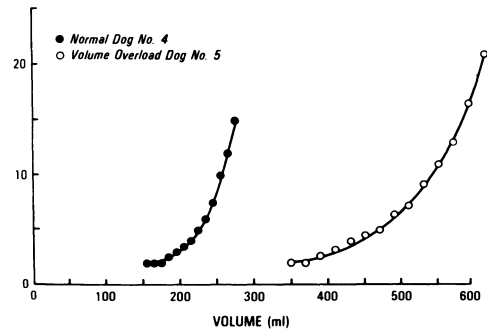


FIGURE 16-6. The pericardial pressure-volume relation in a normal dog (*left*) and a dog with chronic cardiac dilation (*right*). (Reprinted from Freeman and LeWinter [8] by permission, American Heart Association.)

first the following theoretical concepts. As shown in Figure 16-8 (top), the diastolic heart is envisioned as consisting of two balloons, an inner balloon representing the cardiac chambers(s) and an outer one representing the pericardium. The volume of the inner balloon can be varied directly, but that of the outer balloon varies passively in response to volume changes of the inner balloon. The goal is to predict the actual, or observed intracavitary

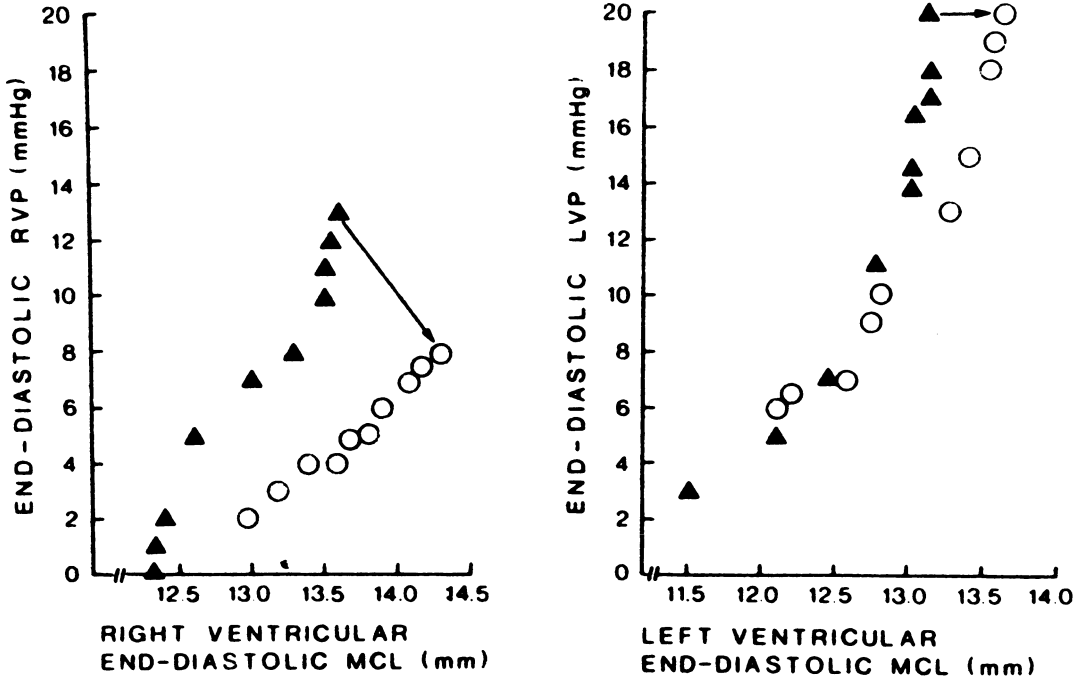


FIGURE 16-7. End-diastolic pressure-chord length (MCL) relations before (*closed triangles*) and after (*open circles*) pericardiectomy in the dog. (Reprinted from Stokland et al. [11] by permission, American Heart Association.)

pressure-volume relation of the inside balloon. Secondly, we would also like to predict what happens to the pressure-volume relation if the outer balloon is removed and what the contact, or normal surface pressure between the two balloons should be as the volume of the inner balloon is varied.

We propose that at any volume of the inside balloon, its intracavitary pressure is a function of the relative distensibility of both the inner and outer balloons. This is of course merely a re-statement of our introductory comments. Now consider two extreme cases (Figure 16-8, bottom). In the first case, the inner balloon, or cardiac chamber, is much less distensible than the outer balloon, or pericardium. In this case, the unconstrained cardiac chamber pressure-volume curve is represented by the upper solid line, and the pericardial pressure-volume curve by the lower solid line. More specifically, the

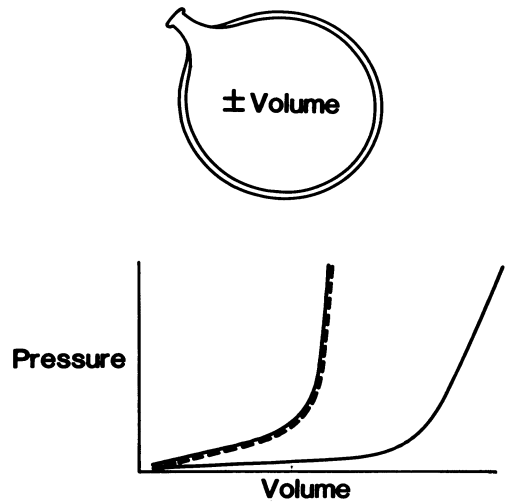


FIGURE 16-8. Schematic model of the diastolic heart (*top panel*) and pressure-volume curves of unconstrained cardiac chamber and pericardium (*solid lines*) and observed pressure-volume curve (*dashed line*).

pericardial pressure-volume relation is essentially flat, and the pressure is close to zero over the range of volumes of the inner balloon in which we are interested: a range of volumes that includes the steep portion of the inner balloon's pressure-volume relation. In this case, the outer balloon will have no influence on the pressure-volume relation of the inner balloon and the observed pressure-volume relation (shown in dashes) is identical to that of the unconstrained inner balloon. Obviously, removal of the outer balloon has no effect on the inner balloon's pressure-volume relation. Further, the contact pressure between the two balloons is zero over the range of volumes of interest. In the other extreme, the outer balloon is much less distensible than the inner balloon over the range of volumes of interest (which once again encompasses the steep portion of the less distensible balloon's pressure-volume relation) and the inner balloon's pressure-volume relation is flat with a pressure close to zero over this range of volume, i.e., the unconstrained chamber and pericardial pressure-volume curves in Figure 16-8 are now reversed (solid lines). In this case, the observed pressure-volume relation (dashed line) is determined completely by the outside balloon. Removal of the outside balloon results in a completely different observed pressure-volume relation (lower solid line), which again is flat with a pressure close to zero over the range of volumes of interest. Finally, in this case, the contact pressure between the two balloons is identical to the pressure in the inside balloon—as a quantitative manifestation of this, at any volume, the drop in pressure after pericardiectomy is equal to the intracavitary pressure present before pericardiectomy at that volume.

We know relatively little about the actual relationship between the pericardial pressure-volume relation and the pressure-volume relation of specific cardiac chambers. Further, as indicated previously, most such information has been obtained in the left ventricle and has been inferred from changes in its pressure-volume relation occurring after pericardiectomy. Nonetheless, we do know the following. The pericardium is less distensible than the left ventricle, at least at relatively high volumes, as shown by the sort of experimental results demonstrated in Figure 16-7. In this example from a study by Stokland and colleagues [11], a left ventricular end-diastolic pressure-segment length relation is plotted on the right side of the figure before

and after pericardiectomy. The relation shifts downward after pericardiectomy, but only at relatively high pressures. Interestingly, in this study a single example of a right ventricular end-diastolic pressure-segment length relation was presented, as shown on the left, and the downward shift after pericardiectomy seems to be larger in magnitude and to occur over a larger range of volumes (i.e., chord lengths) than that for the left ventricle. Insofar as the *lower end of the pressure-volume relation* is concerned, we know, based on the data shown previously (see Figure 16-5), that the pericardial pressure-volume relation, beginning at a volume equal to that of the empty heart, is very flat. We do not know, however, the *relative* distensibility of the pericardium and the cardiac chambers at the low end of their pressure-volume curves. If we assume that at low volumes the pericardium is much more distensible than the left ventricle and that the reverse is true at high volumes, there must be a transition zone over which the relation between left ventricular and pericardial distensibility reverses. If this is the case, for the left ventricle, we would predict the result shown by Stokland and associates [11]. On the other hand, if the right ventricle is substantially more compliant than the pericardium over a wide range of volumes extending to the low end of the curve, we would again predict the sort of result shown by Stokland and colleagues. Indeed, recent direct measurements of the pericardial pressure by Smiseth, Tyberg, and coworkers [12] suggest that for the right ventricle the extreme relationship shown earlier may apply: i.e., the right ventricle may be much more distensible than the pericardium at all volumes. These measurements indicate that the intracavitary pressure in the right side of the heart is identical to the pericardial pressure at all pressure levels, when the pericardial pressure is measured with flat balloons.

In examining the influence of the pericardium on cardiac filling, we have also recently been quite interested in the influence of the pericardium on the right ventricle and in attempting to systematically compare both ventricles. We have examined this question in two ways. First, in open-chest dogs [12] we implanted sonomicrometers to measure instantaneous lengths of approximately 1-cm segments of myocardium at three locations, the anterior left ventricular free wall and the right ventricular inflow and outflow tracts. Alternatively, we also measured

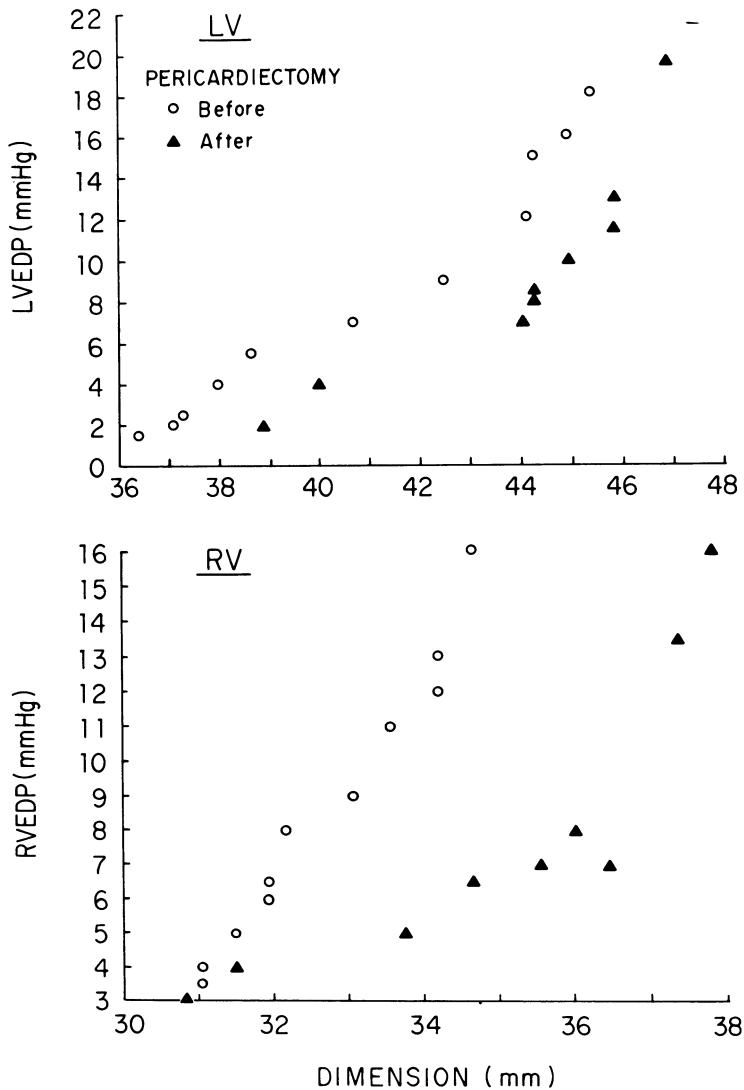


FIGURE 16-9. Right (RV) and left ventricular (LV) end-diastolic pressure-septal-lateral dimension relations before and after pericardiectomy. LVEDP = left ventricular end-diastolic pressure; RVEDP = right ventricular end-diastolic pressure.

right and left ventricular septal-lateral dimensions. We then generated end-diastolic pressure-length or dimension relations under steady-state conditions before and after pericardiectomy, using a combination of caval occlusion and rapid

infusion of dextran to vary cardiac filling. This technique has the advantage that the pericardium need only be minimally disrupted to implant the sonomicrometers. However, as with other studies of this type, we did not measure absolute right and left ventricular volumes. Our data indicate that the end-diastolic pressure-segment length (or dimension) relation differs between the right and left ventricles. As shown in Figure 16-9, after pericardiectomy the right

ventricular pressure-dimension relation shifted markedly downward, with a major change in its slope. In contrast, a downward shift of the left ventricular pressure-dimension relation also occurred, but it was proportionally smaller than that of the right ventricle and appeared to involve less of a slope change. Indeed, when we fitted these data to a simple linear model relating in end-diastolic pressure to dimension, we found that the right ventricular end-diastolic pressure-dimension relation demonstrated a substantial and significant reduction in slope after pericardiectomy; for the left ventricle, the change was statistically purely a parallel one, without a change in slope. Another way to look at these data is to compare the influence of the pericardium on the right and left ventricular end-diastolic pressures. Using data once again fitted to a linear relation between end-diastolic pressure and dimension, the proportion of end-diastolic pressure accounted for by the pericardium can be expressed as a function of the intracavitary end-diastolic pressure. Reflecting the different effect of pericardiectomy on the right and left ventricles, the proportion of left ventricular end-diastolic pressure accounted for by the pericardium remains fairly constant as end-diastolic pressure increases, whereas that for the right ventricle increases as end-diastolic pressure increases.

The second way in which we have examined the relative effect of the pericardium on right and left ventricular compliance employed a very different methodology. In brief, we used canine hearts freshly arrested with potassium chloride, isolated both the left and right sides of the heart by ligating all venous inflow and arterial outflow vessels, and inserted large-bore, multiple-side-hole catheters across the left and right atrioventricular valves via the superior vena cava and a left pulmonary vein. The only manipulation of the pericardium was an approximately 3-cm, loosely reapproximated incision, to allow ligation of the proximal pulmonary artery and aorta and in addition ligation of the proximal coronary arteries to prevent left-to-right shunting. After emptying both the left and right sides of the heart by suction, we filled both sides with warmed saline at equal rates sufficient to produce a left ventricular end-diastolic pressure of 25 mm Hg in about 1 minute.  $V_0$ , the volume at which the pressure was zero mm Hg, was carefully noted in both left and right sides of the heart. This procedure was then repeated

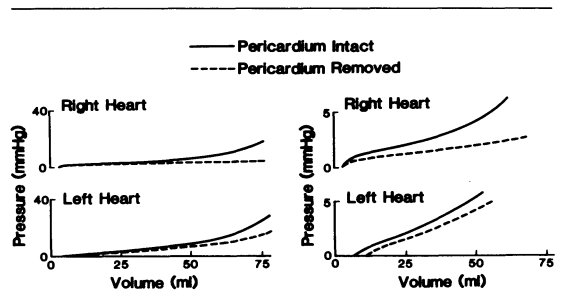


FIGURE 16-10. Right and left heart pressure-volume curves before and after pericardiectomy. On the left are shown low gain and on the right high gain pressure scales. Note the larger downward shift of the pressure-volume curve for the right heart and the modest rightward shift of  $V_0$  for the left heart.

after pericardiectomy. This technique has two major advantages. We can obtain precise and reproducible absolute right and left heart volumes and the pressure measurements, being static, are also quite precise. Typical results are shown in Figure 16-10, with the right heart pressure-volume relation before and after pericardiectomy shown on the top and the left heart on the bottom. For the left heart, we observed a moderately sized downward shift of the pressure-volume relation, which was evident even at low pressures. This shift consisted of both a decrease in slope and a rightward shift of the  $V_0$ , indicating a concomitant parallel shift. The downward shift of the right heart pressure-volume relation was uniformly extremely large and proportionally greater than that for the left ventricle and was also evident even at very low pressures. In this case, however, the downward shift consisted completely of a slope change, without a shift in  $V_0$ . Our goal here was to mimic the normal, physiologic, steady-state relationship between left and right heart volume, i.e., we assumed that these are normally equal over a wide range of volumes. Because this may not in fact be the case, we also performed this experiment using rates that gave right and left heart volumes differing by 10% in either direction—the results were no different. These results imply that the pericardium accounts for most of the right heart filling pressure, even within the physiologic range. However, without the pericardium, the right heart pressure-volume relation is not perfectly flat at low or physiologic pressures, a result which would be predicted by the direct

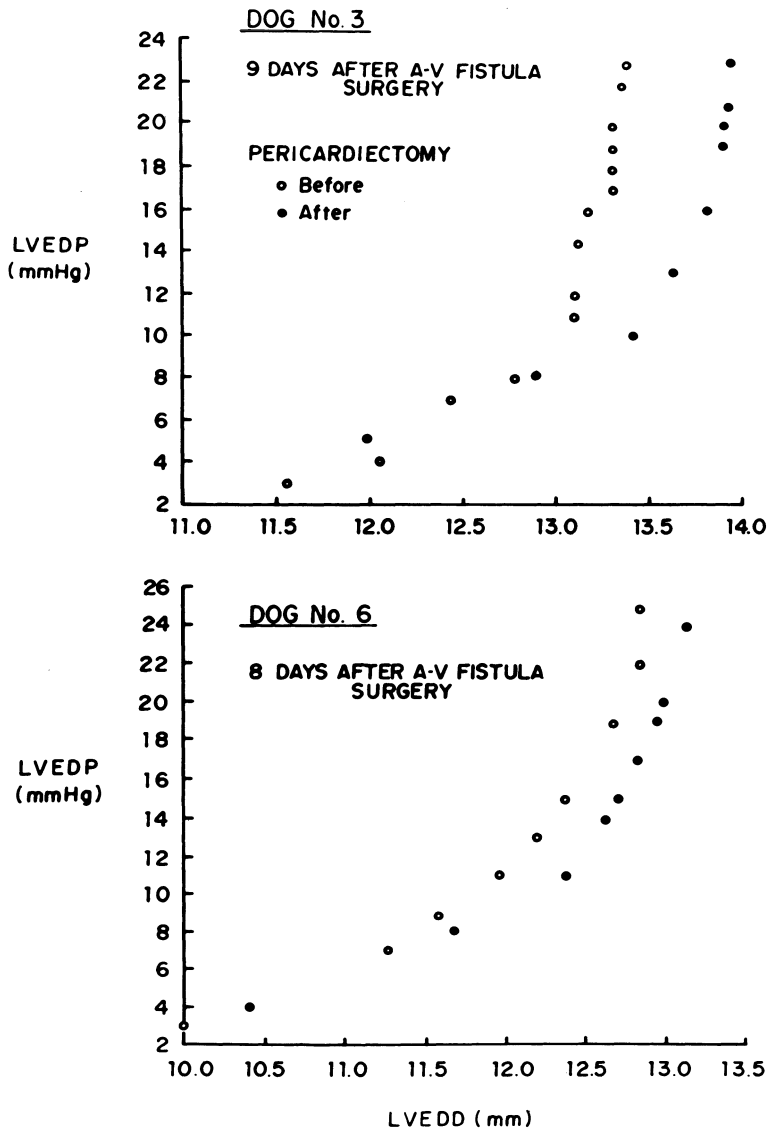


FIGURE 16-11. Left ventricular end-diastolic pressure-segment length relations before and after pericardiectomy at an early time after the production of chronic volume overload in dogs. (Reprinted from LeWinter and Pavelec [1] by permission, American Heart Association.) A-V = arteriovenous; LVEDP = left ventricular end-diastolic pressure; LVEDD = left ventricular end-diastolic dimension.

measurements of the pericardial pressure [12] cited previously. In other words, our results indicate that the right heart is not so distensible that the pericardium alone accounts for its diastolic pressure-volume relationship.

In summary, then, using two very different approaches to this problem, we found that the pericardium has significant effects on the filling of both sides of the heart and that these effects

differ both quantitatively and qualitatively. The pericardium influences the right heart much more than the left heart and indeed accounts for a very substantial proportion of the right heart diastolic pressure even at physiologic volumes. It does not appear to account for all of the right-heart diastolic pressure, however.

Finally, in relation to cardiac filling and the pericardium, we have also been interested in whether chronic cardiac dilation alters the relation between the pericardium and the cardiac chambers [1]. Previously (see Figure 16-6), we showed that the pericardium enlarges substantially and undergoes a change in its own compliance when the heart chronically dilates in dogs with systemic arteriovenous fistulas [8]. In these same animals, we have examined left ventricular end-diastolic pressure-segment length relations (again using sonomicrometry) before and after pericardiectomy at approximately 1 week and 6 weeks after production of the arteriovenous fistula [1]. At the early time, these animals had increased operating left ventricular end-diastolic pressures (usually 15-20 mm Hg) but no measurable hypertrophy, at least by heart weight/body weight ratio. At the later time, these animals continued to have high operating left ventricular end-diastolic pressures, but also had substantial hypertrophy and dilation with an average increase in heart weight body weight ratio of 40 to 50%. As shown in Figure 6-11, at the early time, pericardiectomy results in a downward shift of the end-diastolic pressure-segment length relation quite comparable to that shown earlier in normal dogs (see Figure 16-7). In contrast, at the later time, over the same range of end-diastolic pressure, there is no longer a detectable shift in the end-diastolic pressure-segment length relation after pericardiectomy. Thus, the alteration in the pressure-volume relation of the pericardium that is seen after chronic cardiac dilation is accompanied by a change in the influence of the pericardium on the filling of the left ventricle over a comparable range of end-diastolic pressure.

### Summary

To review our current understanding of the pericardium and its relation to cardiac filling, we believe the following points are accurate:

1. The *in situ* pericardium lengthens in a much

more complex fashion than would be predicted by its behavior *in vitro*.

2. The pericardial pressure-volume relation does not make as abrupt a transition from a relatively compliant to a noncompliant portion as has previously been thought. Further, when the heart dilates chronically, the pericardial pressure-volume relation changes substantially, perhaps in association with growth of the tissue in response to long-term stress.
3. The influence of the pericardium on filling is proportionally much more substantial on the right than the left side of the heart and indeed accounts for most, but not all, of the right-heart diastolic pressure at physiologic volumes.
4. With chronic cardiac dilation, the influence of the pericardium on diastolic compliance decreases over time when compared at similar diastolic pressures, at least insofar as the left side of the heart is concerned.

### References

1. LeWinter M, Pavelec R (1982). Influence of the pericardium on left ventricular end-diastolic pressure-segment length relations during early and later phases of experimental chronic volume overload in dogs. *Circ Res* 50:501-510.
2. Taylor RR, Covell JW, Sonnenblick EH, Ross J Jr (1967). Dependence of ventricular distensibility on filling of the opposite ventricle. *Am J Physiol* 213:711-718.
3. Janicki JS, Weber KT (1980). The pericardium and ventricular interaction, distensibility and function. *Am J Physiol* 238:H494-H503.
4. Lee MC, LeWinter MM, Freeman G, et al (1985). Biaxial mechanical properties of the pericardium in normal and volume overload dogs. *Am J Physiol* 249:H222-H230.
5. Lee MC, Fung YC, Shabetal R, LeWinter MM: (1986). Biaxial mechanical properties of the human pericardium and canine comparisons. *Am J Physiol* 253:H75-H82.
6. Mann DL, Lew W, Waldman L, et al (1986). *In vivo* mechanical behavior of canine pericardium. *Am J Physiol* 251:H349-H356.
7. Holt JP, Rhode EA, Kines H (1960). Pericardial and ventricular pressure. *Circ Res* 8:1171-1181.
8. Freeman G, LeWinter MM (1984). Pericardial adaptation during chronic cardiac dilation in dogs. *Circ Res* 54:294-300.
9. Hefner LL, Coghlan CH, Jones WB, Reeves TJ (1961). Distensibility of the dog left ventricle. *Am J Physiol* 201:97-101.

10. Glantz SA, Misbach GA, Moores WY, et al (1978). The pericardium substantially affects the left ventricular diastolic pressure-volume relationship in the dog. *Circ Res* (1978). 42:433-441.
11. Stokland O, Miller MM, Lekven J, Ilebakk A (1980). The significance of the intact pericardium for cardiac performance in the dog. *Circ Res* 47:27-32.
12. Smiseth OA, Frais MA, Kingma I, et al (1986). Assessment of pericardial constraint: The relation between right ventricular filling pressure and pericardial pressure measured after pericardiocentesis. *J Am Coll Cardiol* 7:307-314.
13. Assanelli D, Lew WYW, Shabetal R, LeWinter MM (1987). Influence of the pericardium on right and left ventricular filling in the dog. *Am J Physiol* (in press).

---

# 17. IMPLICATIONS OF PERICARDIAL PRESSURE FOR THE EVALUATION OF DIASTOLIC DYSFUNCTION

---

John V. Tyberg, Nairne W. Scott-Douglas, Iris Kingma,  
Mouhieddin Traboulsi, and Eldon R. Smith

An unappreciated change in pericardial pressure may alter the interpretation of measurements of left ventricular isovolumic relaxation and of the diastolic pressure-volume relationship both qualitatively and quantitatively. However, before these problems can be discussed it is necessary to define what is meant by pericardial pressure and to specify its magnitude.

### *The Concept of Pericardial Pressure*

As discussed in greater detail recently [1], some of the difficulty with the concept of pericardial pressure is semantic. That is, the important component of so-called pericardial constraint is not really "pressure" at all; it is vectorial and thus does not obey Pascal's law, which states that pressure applied to a fluid at any point is exerted equally in all directions. In the case of the interaction between the pericardium and the ventricle, the important component is a radial compressive contact stress. If this is true, it is easy to appreciate that (except when the pericardium contains an excess of fluid) pericardial constraint cannot be measured by a device that measures fluid pressure (e.g., liquid-filled catheter and conventional transducer or transducer-tipped catheter in a liquid-filled space). The compressive contact stress developed between

the heart and pericardium can only be measured by a transducer such as the balloon developed by Holt and his collaborators [2] (which is a transducer in the sense that an average stress exerted on the balloon is converted to pressure within the closed fluid-filled system) or an appropriate stress gauge, which can measure the small displacement of a minimally deformable material.

The foregoing interpretation is supported by a recent study from our laboratory [3], an investigation designed to compare the balloon and open catheter as alternative methods of measuring pericardial "pressure." The critical point in all our studies on pericardial pressure is the rationale that a static equilibrium of forces exists (momentarily) at the end of diastole when the ventricle is not moving. Since there is no motion, inertial and viscous contributions to pressure can be neglected and only the elastic component needs to be considered [4]. This equilibrium at the endocardium of the left ventricular free wall is illustrated in Figure 17-1. Intracavitary end-diastolic pressure exerts a given force on a unit area of endocardium. This force is exactly opposed by the sum of two forces applied to the same area: the force/area that the unsupported ventricle can sustain at this volume (i.e., the transmural pressure) plus the force due to the constraining action of the pericardium. The same concept is represented differently in Figure 17-2. This shows the diastolic portions of two pressure-diameter (volume) loops, the upper one recorded with an intact pericardium and the lower one (at the same end-diastolic diameter) after the pericardium has been opened and the lungs retracted. Because no

This study was supported by an Establishment Grant from the Alberta Heritage Foundation and an operating grant from the Alberta Heart and Stroke Foundation.

Grossman, William, and Lorell, Beverly H. (eds.), *Diastolic Relaxation of the Heart*. Copyright © 1987. Martinus Nijhoff Publishing. All rights reserved.

pressure or force is acting on the external surface of the heart in the latter condition, intracavitary pressure is equal to the transmural pressure under these circumstances. Then, if it can be assumed that the transmural pressure of the ventricle (i.e., ventricular distensibility) is not changed by removing the pericardium, the difference in pressure between the two curves is exactly equal to the pressure due to the effect of the pericardium ("pericardial pressure").

Using this rationale Smiseth and coworkers [3] showed that, whereas the balloon always recorded a pressure equal to this calculated value, the pressure measured via the open, liquid-filled catheter was very dependent on the amount of liquid in the pericardium. When the pericardium was empty, this pressure was approximately zero. As liquid was infused into the

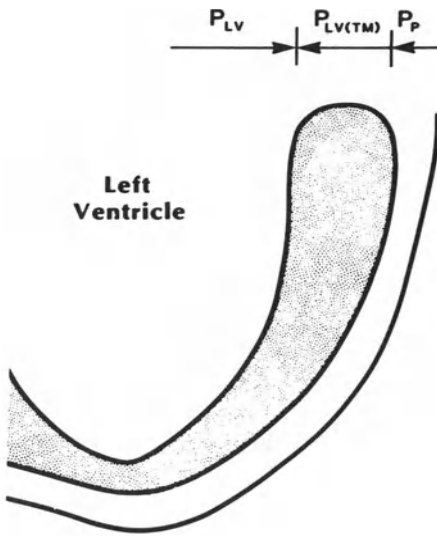


FIGURE 17-1. The static equilibrium of forces applied to a unit area of left ventricular free-wall endocardium at end-diastole. Intracavitary pressure ( $P_{LV}$ ) is exactly opposed by the transmural pressure ( $P_{LV(TM)}$ ) the ventricle can sustain at that volume plus the effective pressure ( $P_P$ ) of the pericardium (i.e., force per unit area). When the pericardium is opened widely and the lungs held back, intracavitary pressure is equal to transmural pressure because pericardial pressure is zero. (Compare Figure 17-2.) (Reproduced from Tyberg and Smith [1], with permission of the publisher.)

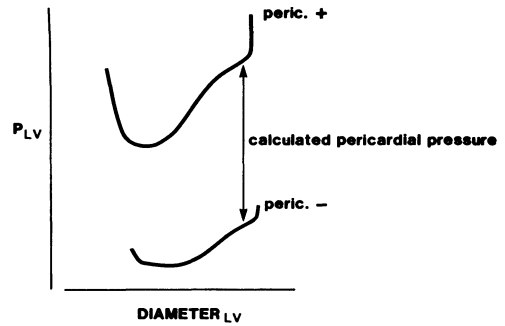


FIGURE 17-2. The diastolic portions of two left ventricular pressure-diameter loops recorded when the pericardium was intact (peric. +) and after the pericardium had been openly widely and the lungs retracted (peric. -). Because the lower loop measures transmural pressure directly (see text and Figure 17-1) and the upper loop reflects the sum of transmural pressure and the effect of the pericardium, the vertical distance between the two at end-diastole represents the effective, calculated pericardial "pressure." This value was used as the standard-of-reference against which balloon and catheter measurements of pericardial pressure were compared. Pressure measured via the balloon was equal to this standard-of-reference pressure regardless of the amount of liquid in the pericardium. (Reproduced from Smiseth *et al.* [3], with permission of the American Heart Association.)

pericardium (catheter) pressure rose rapidly but at least 30 ml was required before the difference between the pressure measured with the liquid-filled catheter and that measured by the balloon became statistically insignificant. The difference between the two methodological approaches to pericardial pressure was demonstrated most dramatically after the infusion was complete (Figure 17-3). Several small incisions were then quickly cut in the pericardium. Pressure recorded through the open catheter immediately fell toward zero even through the ventricle was still constrained by the pericardium (as indicated by the balloon measurement and the fact that the intracavitary pressure at this diameter was higher than it was after the pericardium had been opened widely).

Thus, the mechanical effect of the pericardium on diastolic filling (manifest by an increased intracavitary pressure at a given end-diastolic volume compared to the pressure at that volume when the pericardium is widely

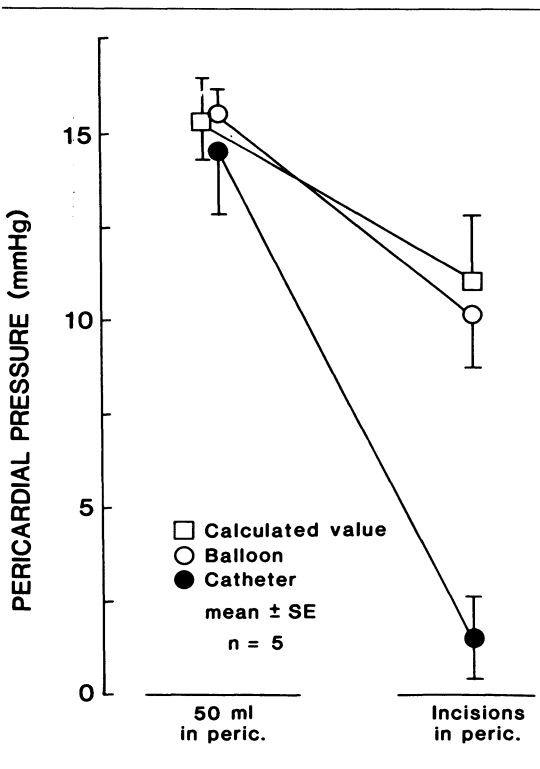


FIGURE 17-3. Experimental data showing that the pericardial balloon accurately measures the mechanical constraining effect of the pericardium even after several 1-cm incisions cut in the pericardium have allowed the liquid to escape. At the beginning of the experiment, 50 ml of saline was contained in the pericardial space. Pressures were measured with a flat liquid-containing Silastic rubber balloon and an open, multiple-side-hole catheter placed in the resealed pericardium. SE = standard error. (Reproduced from Smiseth et al. [3], with permission of the American Heart Association.)

open) can be measured accurately by a Holt-type balloon transducer. On the other hand, except when an excess volume of liquid is present, none of the conventional approaches that measure pressure in the pericardial liquid can measure the pericardial constraint accurately.

### *The Magnitude of Pericardial Pressure*

The magnitude of the pressure measured by the balloon transducer varies somewhat, depending on experimental conditions. In the balloon-catheter comparison [3], balloon pressure was 13

to 15 mm Hg at a left ventricular end diastolic pressure of 20 mm Hg, but in this study some augmentation of the pericardial effect was inevitable because the pericardium had to be sutured tightly and resealed. Similarly, although earlier studies clearly demonstrated the qualitative role of the pericardium on left ventricular diastolic filling, the magnitude of this effect was probably also somewhat overestimated because of the necessity to seal the pericardium [5] or because of the presence of significant instrumentation [6]. However, none of these concerns obtain with respect to the recently published determination of pericardial balloon pressure in patients [7]. In this study, immediately following sternotomy a small pericardial incision was made over the lateral border of the left ventricle. The balloon was placed between the ventricle and pericardium and its catheter secured with a single suture. Because the small pericardial incision was left gaping and since the volume of the balloon was relatively negligible, the possibility of an artificial constriction of the pericardium is not a concern. Thus, the finding that mean pericardial balloon pressure was approximately equal to mean right atrial pressure over a wide range (0 to 20 mm Hg) has considerable importance. First, left ventricular intracavitary end-diastolic pressure is not equal to transmural pressure. In fact, given the usual relationship between the diastolic pressure of the right and left ventricles, left ventricular transmural end-diastolic pressure (true preload) may be no more than half the magnitude of the intracavitary pressure. Second, there is no assurance that the change in transmural pressure can be predicted from the change in intracavitary pressure. Thus, left ventricular end-diastolic pressure and mean pulmonary-capillary wedge pressures may provide very poor estimates of the changes in left ventricular end-diastolic volume. Third, the good relationship between mean right atrial pressure and pericardial balloon pressure suggests that the Swan-Ganz triple-lumen catheter may be utilized in a modified way to estimate transmural pressure (i.e., mean pulmonary-capillary wedge pressure minus mean right atrial pressure). This approach has been promising in preliminary laboratory studies [8] and clinical studies are underway.

The approximately one-to-one relationship between right ventricular filling pressure and pericardial balloon pressure implies that right

ventricular transmural diastolic pressure is almost negligible or at least unmeasurable by this technique. Current laboratory studies suggest that, indeed, this is the case. When caval constriction and volume loading were used to vary right ventricular intracavitary end diastolic pressure from 2 to 20 mm Hg, transmural pressure only rose from 0 to 2.5 mm Hg, while right ventricular circumferential segment length increased 7%. Thus, the right ventricular transmural pressure-volume relationship apparently is very flat, and considerable changes in end-diastolic volume are apparently effected by difficult-to-measure changes in transmural pressure.

An important caveat must be stated here. All of the investigations discussed above have been of short duration. That is, one must not extrapolate from these studies to make inferences about chronic disease conditions. In particular, LeWinter and Pavalec [9] have demonstrated that removing the pericardium in dogs subjected to several weeks of shunt-induced volume overload affects the left ventricular pressure-volume relationship less than removal of the pericardium affects it in normal animals. Further clinical studies are required to define the importance of pericardial constraint in patients with chronic cardiac (chamber) dilatation.

### *The Relation of Pericardial Pressure to Indices of Left Ventricular Isovolumic Relaxation*

In the early studies of isovolumic relaxation Weiss and Weisfeldt clearly stated their assumption that pressure external to the ventricle was zero [10]. However, their simple semilogarithmic estimation of T (the time constant of isovolumic relaxation) has been employed under circumstances in which pericardial pressures was probably not negligible. In our laboratory, Frais and colleagues studied the effect of changing pericardial pressure in open-chest dogs with variable amounts of liquid in their pericardia [11]. The time constant of isovolumic relaxation was significantly and directly dependent on pericardial pressure as anticipated intuitively from the nature of the semilogarithmic relationship (addition of a constant pressure flattens the slope of the log pressure vs. time relationship which increases T). Other analytic approaches [12–14] proposed to circumvent the dependence on external pressure do provide

estimates of T that are less dependent on pericardial pressure. With respect to the latter methods, it is of interest that the parameters corresponding to the asymptotic value of pressure correlate significantly with pericardial pressure.

### *The Relation of Pericardial Pressure to Shifts in the Left Ventricular Diastolic Pressure-Volume Relationship*

Although Serizawa and coworkers [15] clearly demonstrated that the transient, pacing-induced decreases in the distensibility of ischemic myocardium may occur in the absence of the pericardium, the observations discussed above suggest that when there are acute changes in right ventricular filling pressure one might expect to see shifts in the left ventricular diastolic pressure-volume relationship of the same magnitude. Examples might include the effects of vasodilators such as sodium nitroprusside or nitroglycerin and interventions that raise arterial pressure such as angiotensin infusion or isometric hand grip exercise. Recently Kingma and associates in our laboratory examined the effect of nitroglycerin administration on patients in whom ventricular pressures were measured and left ventricular size was estimated using two-dimensional echocardiography [16]. Although most of these patients did not have markedly elevated left ventricular intracavitary pressures, nitroglycerin shifted the pressure-volume relationship significantly downward (Figure 17–4). Using right ventricular diastolic pressure as an estimate of pericardial pressure, transmural pressure was calculated at the beginning and the end of diastole. There was no evidence of a shift in the estimated transmural pressure-volume relationship, further suggesting that nitroglycerin does not change myocardial distensibility [17] and that the change in apparent diastolic compliance [18] can be accounted for, in large measure, by the concomitant change in pericardial pressure.

### *Summary*

We suggest that the pericardium is more important hemodynamically than previously appreciated because most earlier investigators failed to recognize that the mechanical effect of the pericardium normally cannot be assessed

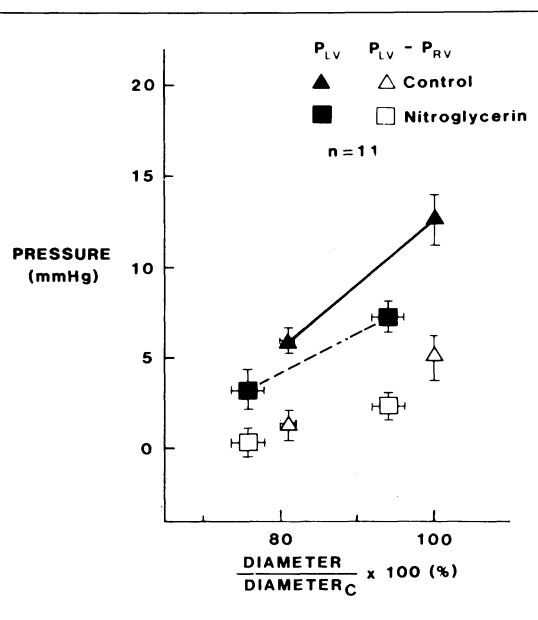


FIGURE 17-4. Left ventricular diastolic pressure-dimension data from patients given nitroglycerin. Pressures and diameters were measured at minimal diastolic pressure and at end-diastole. Left ventricular diameter was derived from a two-dimensional minor axis echocardiogram. Although nitroglycerin (triangles) shifted the intracavitary pressure dimension relationship significantly downward (closed symbols), no shift was observed when transmural pressure (open symbols) was calculated by using the instantaneous value of right ventricular pressure as an approximation of pericardial pressure.  $P_{LV}$  = intracavitary pressure;  $P_{LV} - P_{RV}$  = transmural pressure. (Reproduced from Kingma et al. [16], with permission of the publisher.)

by measuring the pressure of the liquid contained in the pericardial space. When the equivalent pressure (force/area) exerted by the pericardium is properly measured (as with a balloon), this pressure is found to be approximately equal to right atrial pressure in patients, as well as in experimental animals. This rather high value of pericardial pressure is important in the evaluation of diastolic dysfunction in at least two important ways. First, conventional (i.e., semilogarithmic) estimations of  $T$  are increased significantly when pericardial pressure is elevated. Second, some load-mediated changes in left ventricular diastolic compliance can be largely explained by changes in pericardial pressure.

## References

1. Tyberg JV, Smith ER (1987). On the interaction between the pericardium and the heart. In ter Keurs HEDJ, Tyberg JV: *Mechanics of the Circulation* Dordrecht/Boston-Lancaster: Martinus Nijhoff, 71-188.
2. Holt JP, Rhode EA, Kines H (1960). Pericardial and ventricular pressure. *Circ Res* 8: 1171-1181.
3. Smiseth OA, Fraiss MA, Kingma I, et al (1985). Assessment of pericardial constraint in dogs. *Circulation* 71:158-164.
4. Rankin JS, Arentzen CE, McHale PA, et al (1977). Viscoelastic properties of the diastolic left ventricle in the conscious dog. *Circ Res* 41:37-45.
5. Refsum H, Junemann M, Liopton MG, et al (1981). Ventricular diastolic pressure-volume relations and the pericardium: Effect of changes in blood volume and pericardial effusion in dogs. *Circulation* 64:997-1004.
6. Linderer T, Chatterjee K, Parmley WW, et al (1983). Influence of atrial systole on the Frank-Starling relation and the end-diastolic pressure-volume relation in the left ventricle. *Circulation* 67:1045-1053.
7. Tyberg JV, Tatchman GC, Smith ER, et al (1986). The relation between pericardial pressure and right atrial pressure: An intraoperative study. *Circulation* 73:428-432.
8. Douglas N, Kingma I, Smiseth O, et al (1984). Assessment of left ventricular preload during PEEP from pulmonary capillary wedge pressure and right atrial pressure in dogs. *Clin Invest Med* 7(suppl 3):41 (abstract).
9. LeWinter MM, Pavelec R: Influence of the pericardium on left ventricular end-diastolic pressure-segment relations during early and later stages of experimental chronic volume overload in dog. *Circ Res* 50:501-509.
10. Weiss JL, Frederiksen JW, Weisfeldt ML (1976). Hemodynamic determinants of the time-course of fall in canine left ventricular pressure. *J Clin Invest* 58:751-760.
11. Fraiss MA, Kingma I, Groves G et al (1983). The dependence of the time constant of left ventricular relaxation on pericardial pressure. *J Am Coll Cardiol* 1:627 (abstract).
12. Craig WE, Murgu JP (1980). Evaluation of isovolumic relaxation in normal man during rest, exercise and isoproterenol infusion. *Circulation* 62(suppl III):III-22 (abstract).
13. Thompson DS, Waldron CB, Juul SM, et al (1982). Analysis of left ventricular pressure during isovolumic relaxation in coronary artery disease. *Circulation* 65:690-697.
14. Thompson DS, Waldron CB, Coltart DJ, et al (1983). Estimation of time constant of left ventricular relaxation. *Br Heart J* 49:250-258.

15. Serizawa T, Carabello BA, Grossman W (1980). Effect of pacing-induced ischemia on left ventricular diastolic pressure-volume relations in dogs with coronary stenoses. *Circ Res* 46:430-439.
16. Kingma I, Smiseth OA, Belenkie I, et al (1986). A mechanism for the nitroglycerin-induced downward shift of the left ventricular diastolic pressure-diameter relationship of patients. *Am J Cardiol* 57:673-677.
17. Brodie BR, Chuck L, Klausner SC, et al (1976). Effects of sodium nitroprusside and nitroglycerin on tension prolongation of cat papillary muscle during recovery from hypoxia. *Circ Res* 39:596-601.
18. Braunwald E, Ross J Jr (1963). The ventricular end-diastolic pressure. *Am J Med* 34:147-150 (editorial).

---

## 18. COMPARATIVE EFFECTS OF ISCHEMIA AND HYPOXIA ON VENTRICULAR RELAXATION IN ISOLATED PERFUSED HEARTS

---

Carl S. Apstein, Laura F. Wexler, W. Mark Vogel, Ellen O. Weinberg,  
and Joanne S. Ingwall

Many experimental studies of left ventricular diastolic properties have utilized isolated perfused hearts subjected to either global ischemia or hypoxia. The isolated perfused heart model (see Figure 18-1) has several advantages. The pericardium is removed and the right ventricle is vented; thus, any pericardial or right ventricular interaction effect on left ventricular diastolic relaxation [1-4] is eliminated. Because the imposed ischemic or hypoxic condition is globally distributed throughout the myocardium, regional or segmental differences in contractility are eliminated, thus negating the effects on relaxation of "strong and weak segments in series" [6-7]. For these reasons, the isolated perfused heart model assesses the diastolic properties of the left ventricular chamber consisting of myocytes, connective tissue elements, interstitial fluid, and coronary vasculature.

This chapter will review the work from our laboratory that compares the effects of global ischemia and hypoxia on myocardial diastolic properties in isolated rat and rabbit hearts perfused with either Krebs buffer or whole blood [8-15]. Despite the common element of tissue hypoxia, our results show that ischemic and hypoxic perfusion conditions result in

opposite acute changes in left ventricular diastolic chamber compliance. We use the term *diastolic chamber compliance* to refer to left ventricular end-diastolic pressure relative to simultaneous diastolic volume, i.e., to the position of the diastolic pressure-volume curve. Thus, a change in diastolic chamber compliance could result from either a change in the slope of the pressure-volume curve or from a parallel shift in the position of the curve. Use of diastolic pressure at end-diastole yields an index of the extent of relaxation. The studies we review investigated the initial changes in ventricular diastolic chamber compliance with global hypoxia or ischemia, i.e., those changes that occurred within 5 minutes.

*Ischemia* means an abnormally low level of myocardial perfusion or coronary flow; arterial oxygen content is normal. Ischemia may be of the "demand" or "supply" variety. Demand ischemia occurs in the setting of a restricted coronary flow when an increase in myocardial oxygen demand occurs and exceeds the ability of the coronary circulation to provide adequate oxygenation. Supply ischemia occurs when there is a severe reduction in coronary flow, e.g., with a coronary occlusion or very severe stenosis, such that coronary flow is inadequate to support a resting level of myocardial work; in this setting, ischemia results from the reduction in oxygen supply without an increase in myocardial oxygen demand. These two types of ischemia have opposite acute effects on diastolic compliance. Supply ischemia results in an acute increase in

Supported by NIH grants HL31807, HL18318, HL26215 and AM01114.

Grossman, William, and Lorell, Beverly H. (eds.), *Diastolic Relaxation of the Heart*. Copyright © 1987. Martinus Nijhoff Publishing. All rights reserved.

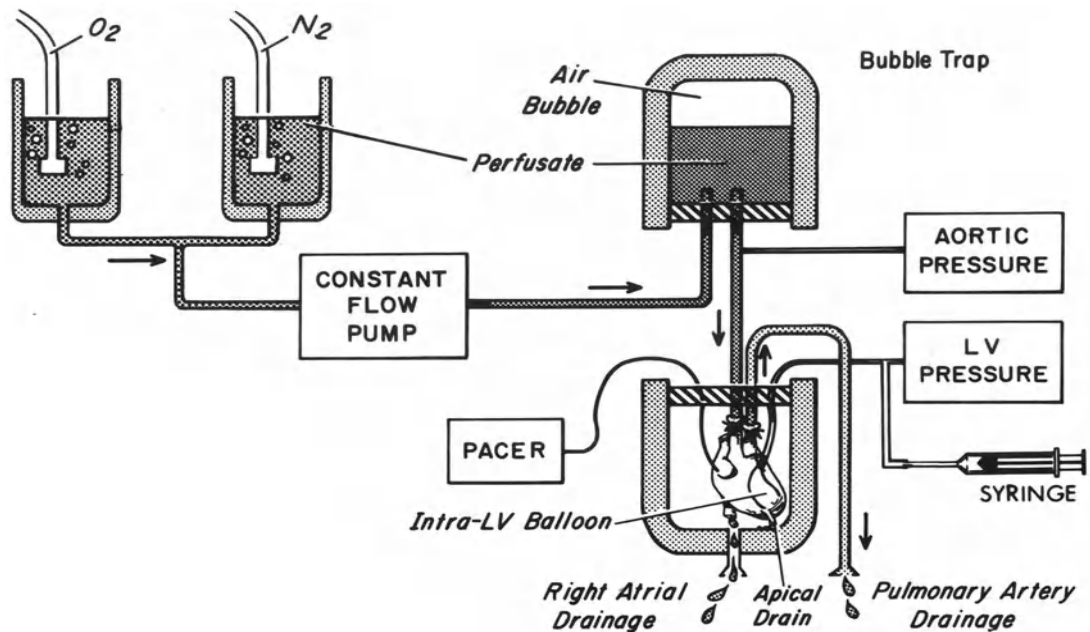


FIGURE 18-1. Isolated perfused heart preparation. The coronary arteries of the isolated heart are perfused retrograde via the aortic stump by a constant flow pump or at constant perfusion pressure. The left ventricle (LV) does isovolumic work against an intra-LV balloon tied at the mitral valve orifice. Two cannulas exit from the intra-LV balloon and lead to a pressure transducer and to a calibrated syringe by which known increments of volume can be added to the balloon as intra-LV pressure is recorded. A pacing catheter and temperature probe (not shown) enter the right ventricle via a right atrial incision. Coronary venous drainage is collected from a pulmonary artery catheter. An apical drain permits free drainage of thebesian venous effluent. The heart is perfused by Krebs-Henseleit buffer warmed to  $37^{\circ}\text{C}$  in water-jacketed reservoirs gassed with a mixture of 95%  $O_2$ , 5%  $CO_2$  or, for investigations of hypoxia, with 95%  $N_2$ , 5%  $CO_2$ . Air embolization is prevented by passing the perfusate through a bubble trap, and the heart is kept warm ( $36.0^{\circ} \pm 0.5^{\circ}\text{C}$ ) in a water-jacketed chamber. For perfusion with blood, the apparatus is modified such that the blood is recirculated and passes through a membrane oxygenator for appropriate gas equilibration.

ventricular diastolic chamber compliance, whereas demand ischemia causes an acute decrease in chamber compliance [14, 15]. This chapter will focus on the effects of supply ischemia.

In contrast to ischemia, *hypoxia* or hypoxemia indicates the presence of an abnormally low oxygen content. In this article we will use the term *hypoxia* to refer to myocardial hypoxia, resulting from hypoxic or hypoxemic perfusion, in contrast to ischemic perfusion. During hypoxia, myocardial perfusion (coronary flow) may be normal or increased depending on experimental conditions and the extent of coronary vasodilator reserve. Like demand ischemia,

hypoxia results in an acute decrease in diastolic chamber compliance [10-13].

The major differences between supply ischemia and hypoxia result from the differences in coronary flow between the two states, because tissue hypoxia is common to both perfusion conditions. During ischemia, coronary pressure and flow are reduced or absent and the coronary vasculature is collapsed. In contrast, during hypoxia the coronary circulation is normally pressurized, coronary flow may be increased, and the coronary vasculature is engorged due to coronary vasodilation. Because such coronary engorgement can influence diastolic ventricular

chamber stiffness and wall thickness, it has been called a coronary "erectile," "garden hose," or "turgor" effect [10–12, 16–20]. Thus, a major difference between the hypoxic and ischemic conditions is the reduction of coronary turgor during ischemia and a constant or increased coronary turgor during hypoxia. Our results show that differences in coronary turgor contribute to the differences between the effects of hypoxia and ischemia on chamber stiffness. The presence of myocardial perfusion during hypoxia also influences myocardial metabolism in ways that can affect myocardial relaxation.

### *Methodology*

#### ISOLATED HEART PREPARATION

The results reviewed in this article have been obtained with isolated rat or rabbit hearts perfused with Krebs-Henseleit buffer or blood [8–13]. The experimental preparation is shown in Figure 18–1. The coronary arteries were perfused retrograde via the cannulated aortic stump. The pericardium was removed and a cannula passed through the pulmonary artery into the right ventricle to drain that chamber and collect coronary venous effluent flow. Heart rate was held constant via a right ventricular pacing wire. Aortic pressure, which in this model is equivalent to coronary perfusion pressure, was measured via a transducer connected to a side arm of the aortic cannula. The left ventricle was decompressed by an apical drain which removes any thebesian venous drainage.

A highly compliant latex balloon was inserted into the left ventricle via the mitral orifice and tied in place at the atrioventricular groove. The balloon cannula was attached to a pressure transducer and also to a calibrated syringe, which was used to alter left ventricular volume to construct pressure-volume curves. In isovolumic experiments, balloon volume is held constant throughout the experiments such that changes in left ventricular end-diastolic pressure reflect changes in diastolic chamber compliance [8–12]. The perfusate was gassed with 95% O<sub>2</sub> 5% CO<sub>2</sub> for oxygenated experiments (pO<sub>2</sub> ≈ 500 mm Hg) and 95% N<sub>2</sub> 5% CO<sub>2</sub> (pO<sub>2</sub> ≈ 10–20 mm Hg) for hypoxia experiments. A coronary perfusion pressure of 80 to 100 mm Hg was used. Changes in end-diastolic wall thickness were assessed by means of a segment-length gauge sutured to the epicardium along the equator of the left ventricle. Since the left

ventricular balloon volume held the endocardial circumference constant, changes in the epicardial circumference reflected changes in wall thickness [11].

#### MEASUREMENT OF HIGH ENERGY PHOSPHATES AND INTRACELLULAR pH BY <sup>31</sup>P PHOSPHORUS NUCLEAR MAGNETIC RESONANCE (NMR)

To study the relationship between intracellular pH (pH<sub>i</sub>) and changes in chamber compliance, we utilized isolated rat hearts. The experimental preparation was similar to that described above, with the following modifications. The hearts were not paced. The preparation was suspended in a 20-mm (outer diameter) NMR tube and the venous effluent was allowed to bathe the heart. To ensure that all phosphorus NMR signals were of intracellular origin, the perfusate consisted of phosphate-free Krebs-Henseleit buffer. The aortic and left ventricular cannulas and a suction tube, which maintained a constant fluid level above the heart, were attached to long extension tubes inside a warmed water jacket. This "umbilical cord" was necessary to permit placement of the isolated heart inside the magnet. The methodology has been published in detail [13, 21].

<sup>31</sup>P NMR spectra were obtained during the last 1.9 minutes of each 2- 4-minute intervention. Myocardial adenosine triphosphate (ATP) and creatine phosphate (CP) content were calculated by integrating the resonance areas under the beta-ATP and CP peaks using the Nicolet integration program. ATP and CP were expressed as a percentage of the aerobic baseline ATP resonance area for each heart. Intracellular pH (pH<sub>i</sub>) was derived from the relationship between pH<sub>i</sub> and the position of the inorganic phosphate resonance peak [21–24].

### *Results*

#### CHANGES IN DIASTOLIC CHAMBER COMPLIANCE

Hypoxia and ischemia caused opposite initial changes in diastolic chamber compliance as illustrated in Figures 18–2 and 18–3. Figure 18–2 shows a left ventricular pressure tracing from an isolated isovolumic rabbit heart perfused at a constant coronary flow rate [10]. Prior to hypoxia, left ventricular end-diastolic pressure was 10 mm Hg. After 1 minute of hypoxic perfusion, diastolic chamber compliance de-

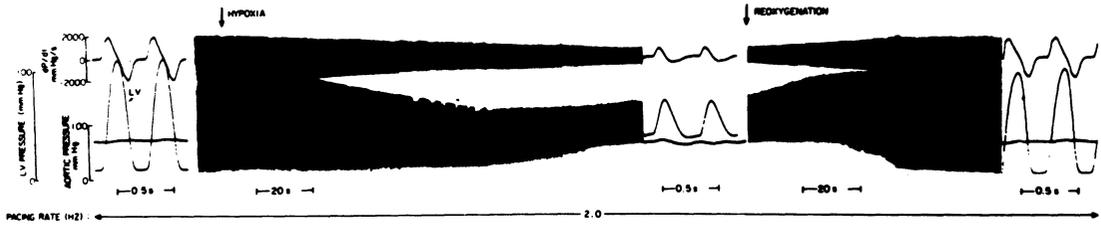


FIGURE 18-2. Effect of hypoxia at constant coronary flow on left ventricular diastolic chamber compliance. These pressure tracings were obtained from an isovolumic isolated rabbit heart perfused at a constant coronary flow of 30 ml/minute with Krebs buffer. The increase in left ventricular (LV) diastolic pressure during 2 min of hypoxia indicates a decrease in diastolic chamber compliance in this isovolumic preparation. Chamber compliance returned to the control level after reoxygenation. From Serizawa et al. [10], with permission.)

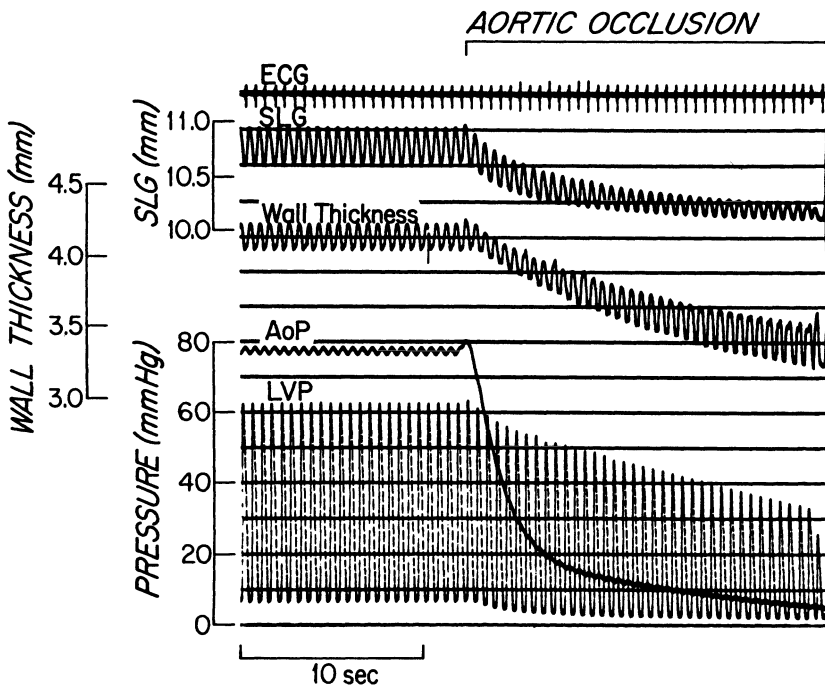


FIGURE 18-3. Effect of ischemia on left ventricular diastolic chamber compliance and diastolic wall thickness. From top to bottom, these tracings show a local electrocardiogram (ECG), epicardial segment length (SLG), left ventricular wall thickness (as measured with transmural ultrasonic crystals), coronary perfusion pressure (aortic pressure, AoP), and left ventricular pressure (LVP) at the onset of global ischemia (aortic occlusion). Segment length, wall thickness, and LV diastolic pressure all fell simultaneously with the decrease in perfusion pressure in this isovolumic buffer-perfused rabbit heart. Thus, in contrast to hypoxia (see Figure 18-2) ischemia caused an acute increase in diastolic chamber compliance. From Vogel et al. [11], with permission.)

creased as manifested by an increase in left ventricular end-diastolic pressure, which reached a value of 20 mm Hg after 2 minutes of hypoxia. This decrease in diastolic chamber compliance was completely reversed during reoxygenation. In contrast, Figure 18-3 demonstrates that acute ischemia abruptly increased diastolic chamber compliance [11]. With the onset of ischemia, there was a simultaneous decrease in left ventricular end-diastolic pressure, indicating an increase in diastolic chamber compliance in this isovolumic model.

In these ischemia experiments, "supply" ischemia was imposed; coronary perfusion was zero and heart rate was held constant. Thus, myocardial energy demand was not increased, but decreased due to the rapid decrease in contractility that occurred immediately after the onset of ischemia.

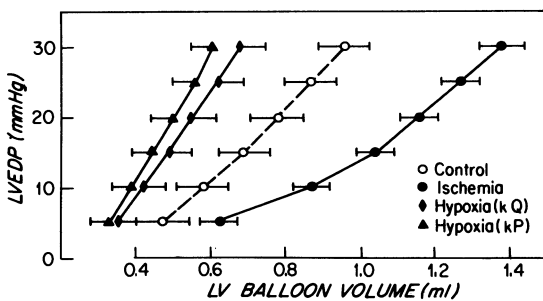


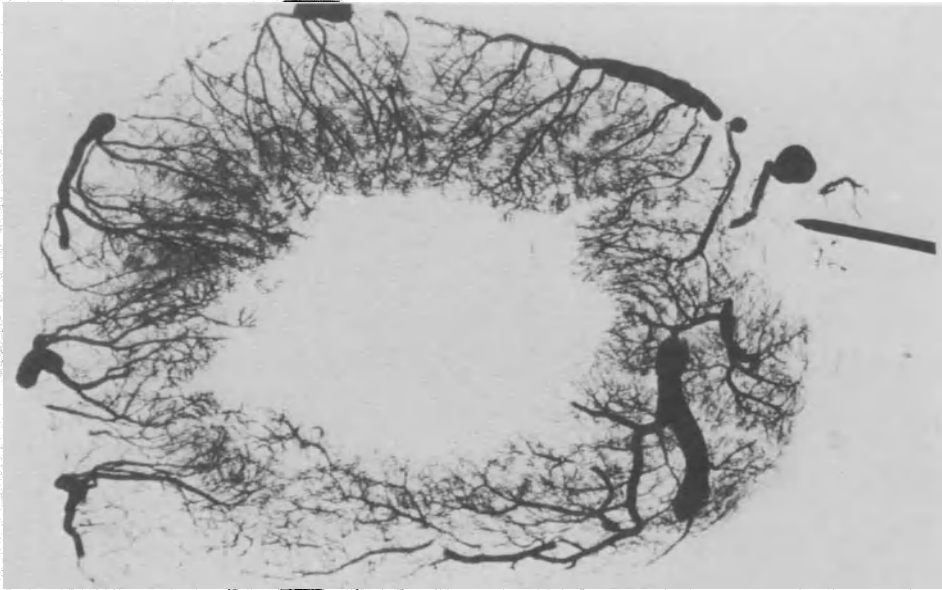
FIGURE 18-4. Effect of ischemia and hypoxia on the left ventricular (LV) diastolic pressure-volume relationship. Pressure-volume curves were generated in the same buffer-perfused rabbit hearts during an aerobic control period and after 2 minutes of global ischemia, hypoxia with constant coronary flow (kQ), and hypoxia with constant coronary perfusion pressure (kP). Left ventricular end-diastolic pressure (LVEDP) in mm Hg is plotted against left ventricular balloon volume in ml. The curve obtained during ischemia was shifted significantly to the right ( $p < 0.001$ ). During hypoxia at constant coronary flow the curve was shifted to the left ( $p < 0.001$ ). When flow was allowed to increase during hypoxia at constant perfusion pressure the curve was shifted further to the left compared to the curve obtained during hypoxia at constant coronary flow ( $p < 0.005$  kQ vs. kP at all points above LVEDP = 5 mm Hg). Points represent mean  $\pm$  standard error of the mean from 10 hearts (From Vogel et al. [11], with permission.)

Diastolic pressure-volume curves demonstrating the acute changes in chamber compliance with ischemia and hypoxia are shown in Figure 18-4. The diastolic pressure-volume curve generated after 2 minutes of global ischemia was shifted to the right relative to the control curve, and the slope was less steep, indicating an increase in left ventricular diastolic chamber compliance during acute total global ischemia. Two minutes of hypoxia under conditions of constant coronary flow caused a shift to the left and an increase in the slope of the diastolic pressure-volume curve, indicating a decrease in diastolic chamber compliance compared to the control state. Coronary resistance decreased during hypoxic perfusion. When coronary flow was allowed to increase during hypoxia, to maintain constant perfusion pressure, there was a significantly greater leftward shift in the position and slope of the diastolic pressure volume curve compared to hypoxia at constant coronary flow [11].

#### CHANGES IN DIASTOLIC WALL THICKNESS

Why should hypoxia and ischemia cause opposite initial changes in diastolic chamber compliance? We reasoned that the acute opposite changes in diastolic wall thickness and chamber compliance with ischemia and hypoxia could be caused by alterations of the coronary intravascular volume. The coronary vascular space occupies approximately 15% of the left ventricular wall [18]. The extensive nature of the coronary circulation is illustrated in Figure 18-5. Ischemia, by depressurizing the coronary vasculature, causes a collapse of the coronary vascular compartment. Conversely, hypoxia at a constant coronary perfusion pressure causes vasodilation, and coronary vascular engorgement [11].

An alteration in the size of the coronary vascular compartment is measured indirectly, by a change in diastolic wall thickness, as shown in Figure 18-3. In this typical ischemia experiment, diastolic wall thickness decreased simultaneously with the decrease in coronary perfusion pressure and increase in diastolic chamber compliance. The acute opposite changes in left ventricular diastolic chamber compliance with ischemia and hypoxia were accompanied by parallel changes in diastolic wall thickness as shown in Figure 18-6. At all intraventricular balloon volumes, diastolic thickness was decreased during global ischemia relative to control, but was increased relative to control during



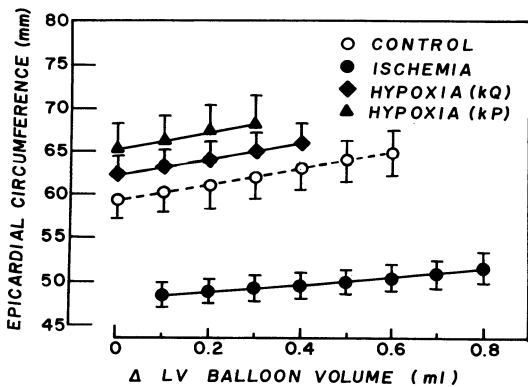
hypoxia at constant coronary flow. Wall thickness increased further when coronary flow was allowed to increase during hypoxia at constant perfusion pressure [11]. Thus, these changes in diastolic wall thickness were consistent with expected changes in the size of the coronary vascular compartment during ischemia and hypoxia.

**CHANGES IN CORONARY TURGOR**

To elucidate the influence of the coronary vasculature on chamber compliance, the coronary turgor and the myocardial fiber contribu-

FIGURE 18-5. The coronary vasculature. This photograph demonstrates the extensive nature of the coronary vasculature, which has been filled with contrast material in this left ventricular cross-section. The coronary vascular space accounts for 10 to 15% of myocardial wall volume [18], and provides the anatomical basis for the influence of coronary turgor on diastolic chamber compliance.

FIGURE 18-6. Effect of ischemia and hypoxia on left ventricular (LV) diastolic epicardial circumference. Diastolic epicardial circumference is plotted as a function of increasing LV balloon volume. Zero on the horizontal axis is that LV volume which produced a left ventricular end-diastolic pressure (LVEDP) of 5 mm Hg during the control period ( $0.58 \pm 0.07$  ml). Data were obtained during generation of the diastolic pressure volume curves shown in Figure 18-4. Diastolic epicardial circumference was decreased at all volumes during ischemia, suggesting a decrease in LV wall diastolic thickness. During hypoxia with constant coronary flow (kQ), diastolic epicardial circumference was increased at all volumes, suggesting increased diastolic wall thickness. When coronary flow was allowed to increase during constant perfusion pressure hypoxia (kP), diastolic epicardial circumference was shifted to higher values at each volume. The same LV balloon volume range was not employed during all interventions because balloon volume was not increased beyond the value which produced an LVEDP of 35 mm Hg. (From Vogel et al. [11], with permission.)



tions to diastolic compliance were assessed in a series of experiments under oxygenated conditions where coronary dynamics were varied in the absence of hypoxia [11]. We used adenosine to produce coronary vasodilation, measured the effect on diastolic wall thickness and diastolic chamber compliance under oxygenated conditions, and compared the results to those which occurred during hypoxia. The effects of adenosine on diastolic chamber compliance and diastolic wall thickness under oxygenated conditions are shown in Figure 18-7. Adenosine infusion at a constant perfusion pressure of 80 mm Hg increased coronary flow by 50%, from 31 to 47 ml/minute. The diastolic pressure-volume compliance curve measured during adenosine infusion was significantly shifted to the left, relative to control, without a change in slope. Diastolic wall thickness increased by approximately 4% during the adenosine infusion. These results show that when coronary dilation occurs at a constant coronary perfusion pressure, coronary flow increases, vascular engorgement occurs, wall thickness increases, and diastolic chamber compliance decreases independently from any hypoxic effect [11].

We have recently obtained similar results in an isolated blood-perfused rabbit heart preparation, which was subjected to an experimental hypertensive crisis. When the coronary perfusion pressure was raised from the control value of 70 mm Hg to hypertensive levels (130 mm Hg), there was an immediate increase in coronary flow, and diastolic wall thickness and a decrease in diastolic chamber compliance, thus demonstrating the acute effects of arterial hypertension on diastolic myocardial properties via a mechanism of increased coronary turgor [25].

To determine whether the changes in coronary turgor could account entirely for the ventricular compliance changes observed during ischemia and hypoxia, we performed a series of experiments in which adenosine infusion or hypoxia was imposed while coronary flow was held constant to minimize any coronary turgor effect (Figure 18-8). Coronary perfusion pressure during control aerobic perfusion was 84 mm Hg. Hypoxia and adenosine infusion each caused a comparable degree of vasodilation and a 30% decrease in coronary perfusion pressure. However, hypoxia caused a significant shift of the diastolic pressure-volume curve to the left, but adenosine infusion, despite an equal degree of coronary vasodilation, had no effect on the diastolic pressure-volume relation-

ship. Figure 14-8B shows that diastolic wall thickness was increased at all balloon volumes during hypoxia, but was unchanged during adenosine infusion when coronary flow was held constant. These results indicate that the increase in diastolic chamber stiffness with hypoxia at constant coronary flow cannot be explained by increased coronary turgor due to coronary vasodilation, because an equal degree of vasodilation with adenosine altered neither wall thickness nor chamber stiffness when coronary flow was held constant. We therefore concluded that a hypoxia-induced metabolic alteration was responsible for the decrease in diastolic chamber compliance during hypoxic perfusion [11].

#### HYPOXIA WITH SUPERIMPOSED ISCHEMIA

The conclusion that hypoxic perfusion caused a metabolically based decrease in chamber compliance, independent of coronary turgor, must be reconciled with our observation that ischemia, which also caused tissue hypoxia, resulted in an acute increase in diastolic chamber compliance (see Figures 18-3, 18-4). In an attempt to clarify the mechanisms responsible for the opposite compliance changes with hypoxia and ischemia, we performed an experiment in which the ischemic and hypoxic conditions were superimposed in the same heart. In these experiments, after an initial 2-minute ischemia and 10-minute recovery period, a hypoxic decrease in diastolic compliance was induced with 2 minutes of hypoxic perfusion; then, during the phase of decreased hypoxic compliance, the ischemic condition was superimposed by halting all coronary flow. Simultaneous<sup>21</sup>P NMR spectroscopy defined the concomitant intracellular pH and high energy phosphate changes that occurred [13].

The effects on diastolic compliance of global ischemia or hypoxia alone, and of global ischemia superimposed on hypoxia, are shown in Figure 18-9. After the control diastolic pressure-volume relationship was defined, the hearts were first made transiently globally ischemic to define the magnitude of the coronary turgor effect. The pressure-volume curve shifted markedly to the right within 5 seconds of the onset of ischemia, which was consistent with a decrease in coronary turgor. A small additional rightward shift occurred between 5 seconds and 2 minutes of ischemia. The rightward shift of the pressure-volume curve indicated a substantial increase in diastolic chamber compliance with 2 minutes of ischemia. The

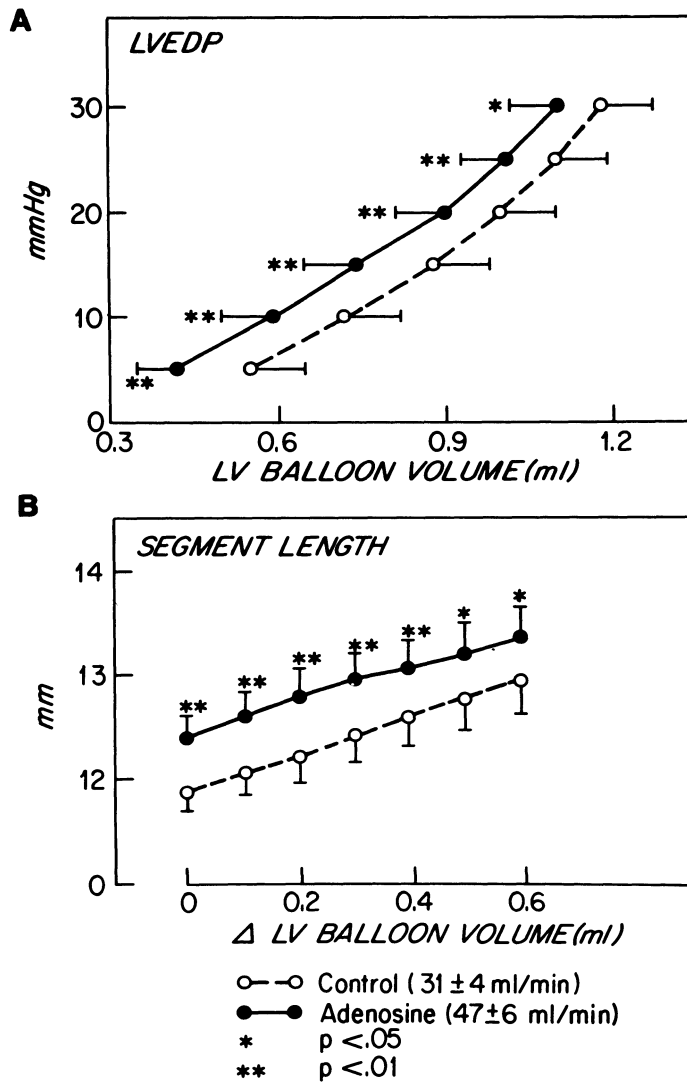


FIGURE 18-7. Effects of adenosine infusion (at constant perfusion pressure) on the left ventricular (LV) diastolic pressure-volume relationship and on diastolic epicardial segment length in buffer-perfused rabbit hearts. Panel A shows the plot of left ventricular end-diastolic pressure LVEDP vs. LV balloon volume. Points were obtained from six hearts during control conditions and during infusion of  $10^{-4}$  M adenosine. Aortic perfusion pressure was constant at 80 mm Hg; numbers in parentheses indicate coronary flow in the two conditions. During adenosine infusion, the curve shifted to the left, indicating a decrease in diastolic chamber compliance. Panel B shows diastolic epicardial segment length as a function of increasing LV balloon volume. Points were obtained during generation of the pressure-volume curves shown in panel A. Zero volume is that which produced LVEDP = 5 mm Hg during the control period. During adenosine infusion, epicardial segment length was increased at all LV balloon volumes, suggesting that wall thickness had increased. Values given in both panels are means  $\pm$  standard error of the mean. (From Vogel et al. [11], with permission.)

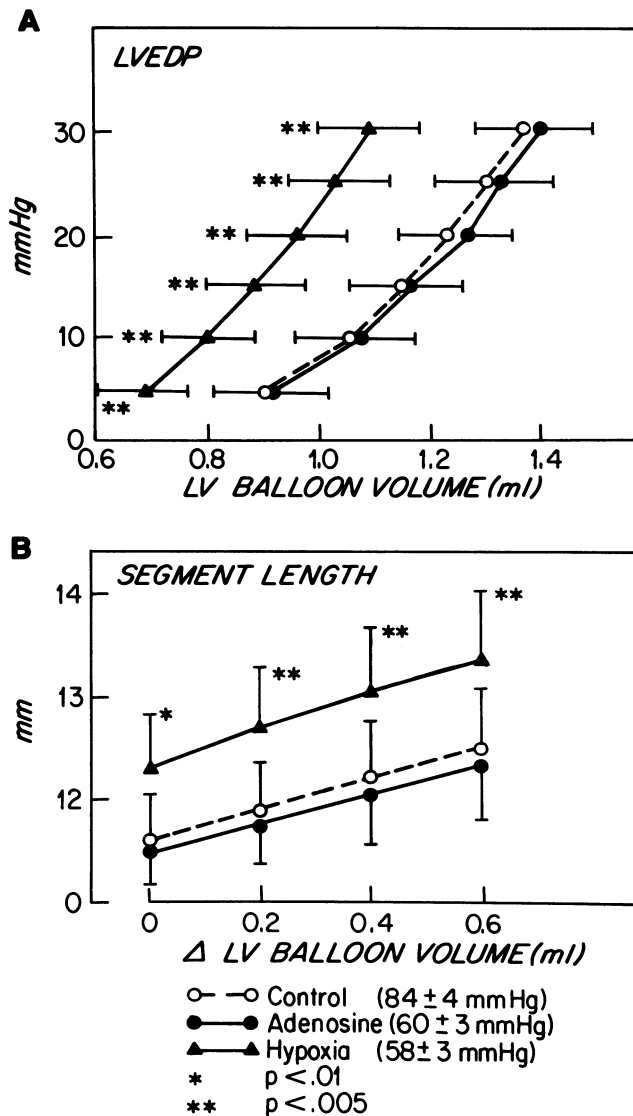


FIGURE 18-8. Effects of adenosine and hypoxia (at constant coronary flow) on the left ventricular (LV) diastolic pressure-volume relationship and on epicardial segment length in buffer-perfused rabbit hearts. Panel A shows the plot of left ventricular end-diastolic pressure (LVEDP) vs. LV balloon volume. Points were obtained from six hearts during control conditions, during hypoxia, or during  $10^{-4}$  M adenosine infusion. Coronary flow was constant at 30 ml/minute during all conditions; numbers in parentheses indicate coronary perfusion pressure in the various conditions. During hypoxia the diastolic pressure-volume curve was shifted to the left, but the adenosine infusion had no significant effect on the diastolic pressure-volume curve despite an equal degree of vasodilation. Panel B shows epicardial diastolic segment length as a function of increasing left ventricular balloon volume. Points were obtained during generation of the diastolic pressure-volume curves shown in panel A. During hypoxia, diastolic segment length was increased at each ventricular balloon volume, but adenosine had no significant effect. Symbols designate the same conditions in both panels. (From Vogel et al. [11], with permission.)

hearts were then reperfused at the control flow rate for 10 minutes and the diastolic pressure volume curve returned to its original position, verifying recovery to baseline diastolic chamber compliance. The hearts were then made hypoxic for 2 minutes at constant coronary flow; this resulted in a marked decrease in diastolic chamber compliance as indicated by a leftward shift of the pressure-volume curve.

While in this state of decreased compliance secondary to hypoxia, the hearts were made globally ischemic, i.e., coronary flow was turned off, to superimpose ischemia on the hypoxia-induced decreased compliance condition. After 5 seconds of ischemia, the pressure-volume curve had shifted to the right, indicating an increase in compliance, consistent with a decrease in coronary turgor as result of coronary flow cessation. However, after a total of 2 minutes of global ischemia superimposed on the "stiff" hypoxic ventricle, the diastolic pressure-volume curve shifted much further to the right to a position similar to that observed after 2 minutes of ischemia alone. Thus, acute ischemia completely reversed the decrease in chamber compliance caused by hypoxia. Although the rightward shift of the diastolic pressure-volume curve after 5 seconds of ischemia was consistent with a coronary turgor effect, the subsequent further rightward shift during 2 minutes of ischemia was too large to be explained by a decrease in coronary turgor and suggested an additional ischemic metabolic factor.

To define metabolic processes that could contribute to the differences in compliance during ischemia and hypoxia, we performed a series of experiments utilizing  $^{31}\text{P}$  NMR spectroscopy. Table 18-1 reports hemodynamic and metabolic data from a series of rat heart perfusion experiments similar to the rabbit heart experiments reported in Figure 18-9. Isolated buffer-perfused rat hearts were exposed to acute (2 to 4-min.) periods of ischemia or hypoxia. In these experiments, the intraventricular balloon-volume was adjusted to produce an initial left ventricular end-diastolic pressure (LVEDP) of  $20 \pm 1$  mm Hg under control, oxygenated conditions. After acute ischemia, LVEDP decreased to  $11 \pm 2$  mm Hg, indicating an acute increase in diastolic chamber compliance. In contrast, after acute hypoxia, LVEDP increased to  $48 \pm 3$  mm Hg, indicating an acute decrease in diastolic chamber compliance. These differences in diastolic chamber compliance cannot be explained by differences in the con-

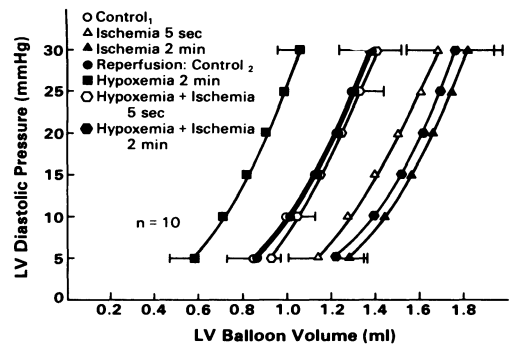


FIGURE 18-9. Changes in diastolic chamber compliance (DCC) with global ischemia superimposed on hypoxia. Diastolic pressure-volume (P-V) curves obtained during seven sequential interventions in each of seven hearts. After 5 seconds of global ischemia, the left ventricular (LV) diastolic P-V curve shifted to the right ( $\Delta$ ) indicating the increase in DCC attributable to loss of the "erectile effect." After a total of 2 minutes of global ischemia, there was an additional shift of the P-V curve to the right ( $\blacktriangle$ ). Reperfusion for 10 minutes returned the P-V curve to its original control position ( $\bullet$ ). After 2 minutes of hypoxia, the P-V curve shifted to the left ( $\blacksquare$ ) indicating a decrease in DCC. Global ischemia was then superimposed on hypoxia by turning off coronary flow. After 5 seconds, the P-V curve shifted to the right ( $\square$ ) indicating an increase in DCC. This shift was similar to that seen after 5 seconds of ischemia in the nonhypoxic heart and is consistent with an acute decrease in coronary turgor. After a total of 2 minutes of ischemia superimposed on hypoxia, there was a marked additional shift of the P-V curve to the right ( $\bullet$ ) such that DCC after 2 minutes of ischemia super-imposed on hypoxia was almost the same as DCC after 2 minutes of ischemia alone ( $\blacktriangle$ ), i.e., the decrease in DCC resulting from hypoxia was completely reversed by 2 minutes of global ischemia. (From Wexler et al. [13], with permission.)

centrations of the high energy phosphate compounds. As the data in Table 18-1 indicate, there were no significant differences between the ischemic or hypoxic states with respect to myocardial levels of ATP, CP, or inorganic phosphate.

Two major differences between the ischemia and hypoxia periods, which may be related to the differences in diastolic chamber compliance, were the degree of intracellular acidosis and the amount of contractile work, or energy demand, that persisted during ischemia and hypoxia.

TABLE 18-1. Comparison of Acute Ischemia and Hypoxia

	Control	Ischemia	Hypoxia	<i>p</i> *
LV developed pressure (mm Hg)	160 ± 8	6 ± 1	58 ± 3	< .001
LVEDP (mm Hg)	20 ± 1	11 ± 2	48 ± 3	< .001
Heart rate	245 ± 10	184 ± 25	112 ± 14	< .025
HR × LV Dev P (× 10 <sup>-3</sup> )	39.3 ± 3.0	1.16 ± 0.03	6.44 ± 0.91	< .005
pHi	7.03 ± 0.02	6.87 ± 0.03	6.99 ± 0.01	< .01
ATP	100%	91 ± 6%	94 ± 9%	NS
CP	138 ± 7%	45 ± 10%	66 ± 5%	NS
P <sub>i</sub>	45 ± 7%	145 ± 14%	136 ± 12%	NS

\* *p* values compare ischemia vs. hypoxia by Student's unpaired *t* test. LV = left ventricle; EDP = end-diastolic pressure; HR = heart rate; Dev P = developed pressure; pHi = intracellular pH; ATP = adenosine triphosphate; CP = creatine phosphate; P<sub>i</sub> = inorganic phosphate. ATP, CP, and P<sub>i</sub> values are expressed relative to the 100% control ATP content.

During acute ischemia intracellular pH decreased from the control value of 7.03 to 6.87, (*p* < 0.01); that is, the proton concentration increased by approximately 32%. In contrast, during acute hypoxia, there was no significant change in intracellular pH relative to the control condition.

These differences in intracellular pH most likely contribute to the observed differences in contractile function and myocardial oxygen demand during ischemia and hypoxia. During 2 minutes of ischemia, the product of heart rate times left ventricular developed pressure (an index of myocardial energy demand) decreased to 3% of control, but during acute hypoxia this index of energy demand persisted at 17% of the control level. Thus, during acute hypoxia approximately six times the rate of energy utilization was present relative to the acute ischemia condition. Despite this higher rate of energy utilization during hypoxia, tissue high-energy phosphate levels were comparable during acute ischemia and hypoxia; this observation suggests that rates of high energy phosphate synthesis must be greater during hypoxia than ischemia and is consistent with an inhibition of glycolysis during ischemia secondary to tissue acidosis and lactate accumulation [26, 27].

### Discussion

The results just reviewed show that acute global supply ischemia and hypoxia cause opposite early changes in diastolic chamber compliance: ischemia increases compliance and hypoxia decreases it. Furthermore, the superimposition of the ischemic condition completely reversed the compliance decrease, which had occurred in

hearts that were made hypoxic. Thus the factors that increase diastolic compliance with ischemia appear to outweigh those favoring a decrease in compliance during hypoxia.

The factors that best explain the differences in diastolic chamber compliance observed during these two types of acute tissue hypoxia include: (1) the presence of a pressurized coronary vascular tree during hypoxia in contrast to coronary vascular collapse during global supply ischemia; (2) the development of intracellular acidosis and its effect on Ca<sup>2+</sup>-activated tension during ischemia but not during hypoxia; and (3) decreased Ca<sup>2+</sup> resequestration by the sarcoplasmic reticulum during tissue hypoxia induced by either ischemia or hypoxia.

### ROLE OF CORONARY VASCULAR COLLAPSE ON DIASTOLIC CHAMBER COMPLIANCE

During global supply ischemia, coronary flow ceases, wall thickness diminishes, and the left ventricle becomes more compliant. In contrast, during hypoxia, coronary flow continues, coronary vascular collapse does not occur, and the coronary turgor effect to maintain diastolic left ventricular wall stiffness is maintained [11, 12]. This coronary turgor factor may be largely responsible for the opposite initial changes in diastolic chamber compliance after 2 minutes of ischemia compared with 2 minutes of hypoxia. Coronary vascular collapse may also contribute to the observed reversal by superimposed ischemia of the hypoxic-induced decrease in diastolic chamber compliance.

However, changes in coronary turgor cannot entirely explain the changes in diastolic compliance that we observed when ischemia was superimposed on hypoxia (see Figure 18.9). In a

constant coronary flow preparation, early hypoxia was associated with a decrease in coronary perfusion pressure (indicating a fall in coronary resistance, compatible with hypoxia-induced vasodilation), but with an increase in wall thickness. The increase in wall thickness and associated decrease in chamber compliance could not be attributed to coronary vasodilation because administration of adenosine, which induced a degree of vasodilation equal to that observed during hypoxia, caused no change in chamber compliance or wall thickness when coronary flow was held constant (see Figure 18-8) [11]. These observations suggested that another factor such as persistent actin-myosin cross-bridge cycling, i.e., incomplete relaxation, may contribute to the decrease in diastolic chamber compliance during hypoxia.

Since the decrease in chamber compliance during early hypoxia cannot be attributed solely to a coronary vascular turgor effect, collapse of the coronary vasculature with the onset of ischemia superimposed on the hypoxic heart, would be expected to result in only a partial reversal of the early hypoxic compliance decrease, as we observed after 5 seconds of superimposed ischemia in the hypoxic heart (see Figure 18-9). However, the further rightward shift of the diastolic pressure-volume curve, completely reversing the hypoxic compliance decrease after 2 minutes of superimposed ischemia (see Figure 18-9), requires additional explanation.

#### ROLE OF INTRACELLULAR ACIDOSIS

Differences in the degree of intracellular acidosis may be another factor affecting the early opposite changes in diastolic chamber compliance in response to hypoxia and ischemia and may also play a role in the reversal of the hypoxic compliance decrease by ischemia. We observed that after 2 minutes of ischemia,  $\text{pH}_i$  decreased by 0.16 pH units. In contrast, after 4 minutes of hypoxia,  $\text{pH}_i$  was not significantly different from control (see Table 18-1), presumably because continuous coronary flow maintained washout of the excess  $\text{H}^+$  generated during anaerobic metabolism. Our results are comparable to those obtained in other recent NMR studies. The value for control  $\text{pH}_i$  measured by NMR in other studies of isolated perfused rabbit and rat hearts has been reported to be between 7.07 and 7.18 [23, 24, 28, 29]. Garlick and coworkers [23] reported a decrease in  $\text{pH}_i$  of approximately 0.2 pH units after 2

minutes of ischemia, which is similar to our results. Mathews and associates [28] reported only a small drop in  $\text{pH}_i$  after 4 minutes of hypoxia (approximately 0.05 pH units), and a recent report by Allen and colleagues [30], shows little change in  $\text{pH}_i$  after 4 minutes of exposure to cyanide. Thus, it appears that  $\text{pH}_i$  falls significantly after 2 minutes of global ischemia, but little, if at all, after 4 minutes of hypoxia.

The effect of acidosis on myocardial contractility and on intracellular  $\text{Ca}^{2+}$  has been studied extensively [31-38]. Changes in intracellular pH have been shown to alter the sensitivity of the contractile proteins to  $\text{Ca}^{2+}$ , i.e., a decrease in pH shifts the  $\text{pCa}$ -force relationship such that tension development at any given  $\text{Ca}^{2+}$  level is markedly decreased [33-37]. Using the aequorin technique, Allen and coworkers [38] have shown that when isolated papillary muscles are made acidotic by perfusion with high  $\text{pCO}_2$  buffer, intracellular calcium increases at the same time active tension is decreasing. This suggests that the inhibitory effect of  $\text{H}^+$  on myofibrillar  $\text{Ca}^{2+}$  sensitivity is sufficiently potent to offset the potentially positive inotropic effect of an increase in cytosolic  $\text{Ca}^{2+}$ .

These observations of the effect of pH on  $\text{Ca}^{2+}$ -activated tension development may also be relevant to diastolic function in view of recent evidence that cytosolic  $\text{Ca}^{2+}$  persists throughout diastole at levels sufficient to account for some resting myofilament activation [39-41]. Thus, the acidosis that occurs after 2 minutes of ischemia may contribute to the observed increase in diastolic chamber compliance, i.e., there may be some decrease in residual diastolic "tone" during ischemia because of a pH-mediated decrease in myofilament sensitivity to  $\text{Ca}^{2+}$ .

#### ROLE OF SARCOPLASMIC RETICULAR $\text{Ca}^{2+}$ RESEQUSTRATION

The decrease in diastolic chamber compliance during hypoxia may be related to an increase in diastolic  $\text{Ca}^{2+}$  availability resulting from impaired  $\text{Ca}^{2+}$  resequstration by the sarcoplasmic reticulum [42-47]. Thus, the effect of intracellular acidosis to decrease  $\text{Ca}^{2+}$  activated tension may contribute to the reversal of the hypoxic compliance decrease by superimposed ischemia. Further support for this hypothesis comes from studies of isolated papillary muscle preparations in which pretreatment with acidotic buffer was shown to prevent or delay the

development of hypoxic contracture [48–50]. Bing and colleagues [49] suggested that the mechanism was related to the decrease in contractile function that occurred when the muscles were bathed with acidotic buffer, the slower rate of ATP depletion leading to a slower rate of contracture development. In addition, Greene and Weisfeldt [48] demonstrated a protective effect of acidosis against hypoxic contracture in the absence of contractile activity, supporting the concept of a direct effect of  $H^+$  on  $Ca^{2+}$ -activated resting or diastolic tension during hypoxia.

Thus, the opposite acute changes in diastolic chamber compliance with acute hypoxia and global supply ischemia can be explained by considering which of the following elements are present: (a) *a pressurized coronary vasculature*, which decreases diastolic chamber compliance by the “coronary turgor” effect; (b) *tissue hypoxia*, which may result in an increase in cytosolic calcium level due to impairment of sarcoplasmic reticular resequestration of  $Ca^{2+}$ ; and (c) *tissue acidosis*, which decreases  $Ca^{2+}$ -activated tension development. With hypoxia, a pressurized coronary vasculature and tissue hypoxia are present, and acidosis is absent or minimal; the net effect is a rapid decrease in diastolic chamber compliance. With global supply ischemia, the coronary vasculature is acutely decompressed, resulting in an immediate increase in diastolic chamber compliance due to the loss of the “coronary erectile” or “turgor” effect. In addition, rapid development of acidosis may decrease any resting diastolic  $Ca^{2+}$ -activated tone, outweighing the effects of any increase in cytosolic calcium availability. The complete reversal of the hypoxic compliance decrease by superimposed ischemia can reasonably be attributed to the same two factors: coronary vascular collapse with loss of the turgor effect and intracellular acidosis which, by decreasing the sensitivity of the myofilament to  $Ca^{2+}$ , reversed the effects of increased diastolic cytosolic  $Ca^{2+}$  levels associated with tissue hypoxia.

#### ROLE OF PERSISTENT MYOCARDIAL ENERGY DEMAND

Another difference between the acute ischemic and hypoxic states is the level of myocardial contractile function and energy demand, which was six times greater during hypoxia than during ischemia (see Table 18–1). An association between increased myocardial energy de-

mand and decreased compliance has been noted in previous studies which compared “demand” and “supply” ischemia. Demand ischemia, induced by pacing tachycardia in the setting of a restricted coronary flow, resulted in a higher level of myocardial energy demand than did supply ischemia (coronary occlusion); demand ischemia was associated with an acute decrease in diastolic compliance, whereas supply ischemia caused an acute increase in compliance [14, 15, 46, 51–57, 69]. The data in Table 18–1 do not suggest a mechanism by which increased energy demand might contribute to the acute compliance difference between ischemia and hypoxia; high energy phosphate levels were equally affected in both states. One might speculate that the higher level of contractile work during hypoxia relative to ischemia decreased a critical cytosolic ATP pool to a greater extent during hypoxia than during ischemia. If this is the case, the decrease in this cytosolic ATP pool was undetected by our measurement of total cellular ATP. Because of compartmentalization and possible impairment of ATP transport from mitochondria to the cytosol during hypoxia and ischemia, the measured decrease in total cellular ATP may underestimate the decrease in ATP available to the sarcolemmal and sarcoplasmic reticular calcium pumps [70–73]. Thus, the lack of a difference in total ATP levels during hypoxia and ischemia (see Table 18–1) does not definitively exclude a greater depletion of a critical cytosolic ATP pool as a result of the greater level of contractile function during hypoxia relative to ischemia. In addition, it is possible that turnover rates of ATP or CP, rather than their steady state contents, may differ in hypoxia and ischemia.

It is also possible that the higher level of contractile function during hypoxia relative to ischemia is simply secondary to the greater intracellular acidosis associated with ischemia. In this case, the difference in contractile function between hypoxia and ischemia may simply reflect the difference in cell pH and not contribute per se to the observed difference in diastolic chamber compliance.

*Clinical Correlations.* The changes in diastolic chamber compliance that we have observed with acute global hypoxia and ischemia in the isolated perfused heart are probably related to alterations in diastolic myocardial properties observed in patients with ischemic heart disease.

The decrease in diastolic compliance, which

occurred after 2 minutes of hypoxia in the isolated heart, is strikingly similar to the time course and magnitude of the shift in the diastolic pressure-volume curve seen after pacing-induced angina in patients with coronary artery disease or pacing-induced ischemia in dogs with coronary arterial stenoses [51–57]. In both cases there is persistent coronary flow to the hypoxic region so that coronary “turgor” is maintained and tissue acidosis is minimized. The mechanism for decreased compliance in models of pacing-induced ischemia may be the same as that causing the early hypoxic compliance decrease, i.e., an increase in intracellular calcium availability secondary to impaired resequestration of  $\text{Ca}^{2+}$  by the sarcoplasmic reticulum resulting in incomplete relaxation [15].

In contrast to global hypoxia and the pacing-induced “demand” ischemia model, the acute increase in diastolic chamber compliance observed after acute global supply ischemia in the isolated heart is comparable to the increase in diastolic chamber compliance or diastolic segment length relative to diastolic ventricular pressure observed after an acute coronary ligation in intact animals [58–66]. Global supply ischemia in the isolated heart and a complete coronary occlusion share the common features of an immediate collapse of the coronary vasculature in the ischemic region (loss of coronary turgor) and an acute marked tissue acidosis [24, 67–69], both of which would be expected to initially increase diastolic chamber compliance as has been observed.

In summary, global hypoxia and ischemia have been shown to have opposite initial effects on diastolic chamber compliance, despite the presence of tissue hypoxia during both conditions. The different acute compliance changes with ischemia and hypoxia appear to be related to differences in coronary turgor, intracellular pH, and myocardial energy demand.

### References

1. Glantz SA, Misbach GA, Moores WY, et al (1978). The pericardium substantially affects the left ventricular diastolic pressure-volume relationship in the dog. *Circ Res* 42:433–441.
2. Ross J Jr (1979). Acute displacement of the diastolic pressure-volume curve of the left ventricle: Role of the pericardium and the right ventricle. *Circulation* 59:32–27.
3. Lorell BH, Palacios I, Daggett WM, et al (1981). Right ventricular distension and left ventricular compliance. *Am J Physiol* 240: H87–H98.
4. Maruyama Y, Ashikawa K, Isoyama S, et al (1983). Mechanical interactions between four heart chambers with and without the pericardium in canine hearts. *Circ Res* 50:86–100.
5. Waters DD, Da Luz P, Wyatt HL, et al (1977). Early changes in regional and global left ventricular function induced by graded reductions in regional coronary perfusion. *Am J Cardiol* 39:537–543.
6. Wiegner AW, Allen GJ, Bing OHL (1978). Weak and strong myocardium in series: Implications for segmental dysfunction. *Am J Physiol* 235:H776–H783.
7. Brutsaert DL, Rademakers FE, Sys SV (1984). Triple control of relaxation: Implications in cardiac disease. *Circulation* 69:190–196.
8. Apstein CS, Deckelbaum L, Mueller M, et al (1977). Graded global ischemia and reperfusion: Cardiac function and lactate metabolism. *Circulation* 55:864–872.
9. Apstein CS, Mueller M, Hood WB Jr (1977). Ventricular contracture and compliance changes with global ischemia and reperfusion and their effect on coronary resistance in the rat. *Circ Res* 41:206–217.
10. Serizawa T, Vogel WM, Apstein CS, Grossman W (1981). Comparison of acute alterations in left ventricular relaxation and diastolic chamber stiffness induced by hypoxia and ischemia. *J Clin Invest* 68:91–102.
11. Vogel WM, Apstein CS, Briggs LL, et al (1982). Acute alterations in left ventricular diastolic chamber stiffness: Role of the “erectile” effect of coronary arterial pressure and flow in normal and damaged hearts. *Circ Res* 51:465–478.
12. Vogel WM, Briggs LL, Apstein CS (1985). Separation of inherent diastolic myocardial fiber tension and coronary vascular “erectile” contribution to wall stiffness of rabbit hearts damaged by ischemia, hypoxia, calcium paradox and reperfusion. *J Mol Cell Cardiol* 17:57–70.
13. Wexler LF, Weinberg EO, Ingwall JS, Apstein CS (1986). Acute alterations in diastolic left ventricular chamber distensibility: Mechanistic differences between hypoxemia and ischemia in isolated perfused rabbit and rat hearts. *Circ. Res.* 59:515–528.
14. Isoyama S, Lorell BH, Grice WN, et al (1985). Increased diastolic chamber stiffness during simulated angina in isolated hearts. *Circulation* 72(suppl III):III–72.
15. Apstein CS, Grossman W (1987). Opposite initial effects of supply and demand ischemia on left ventricular diastolic compliance: The ischemia-diastolic paradox. *J Mol Cell Cardiol* 19:119–128.

16. Salisbury PF, Cross CE, Rieben PA (1960). Influence of coronary artery pressure upon myocardial elasticity. *Circ Res* 8:794-800.
17. Bourdillon PD, Poole-Wilson PA (1982). The effects of verapamil, quiescence and cardioplegia on calcium exchange and mechanical function in ischemic rabbit myocardium. *Circ Res* 50:360-368.
18. Morgenstern C, Holjes U, Arnold G, Lochner W (1973). The influence of coronary pressure and coronary flow on intracoronary blood volume and geometry of the left ventricle. *Pfluegers Arch* 340:101-111.
19. Olson CO, Attarian EE, Jones RN, et al (1981). The coronary pressure-flow determinants of left ventricular compliance in dogs. *Circ Res* 49:856-865.
20. Shine KI, Douglas AM, Ricchiuti N (1976). Ischemia in Isolated ventricular septae: Mechanical events. *Am J Physiol* 231:1225-1232.
21. Ingwall JS (1982). Phosphorus nuclear magnetic resonance spectroscopy of cardiac and skeletal muscle. *Am J Physiol* 242:H729-H744.
22. Moon RB, Richards H (1973). Determination of intracellular pH as observed by  $^{31}\text{P}$  magnetic resonance. *J Biol Chem* 248:7276-7278.
23. Garlick PB, Ratta GK, Seely PJ (1979). Studies of acidosis in the ischemic heart by phosphorus nuclear magnetic resonance. *Biochem J* 184:547-554.
24. Jacobus WE, Pores IH, Lucas SK, et al (1982). Intracellular acidosis and contractility in the normal and ischemic heart as examined by  $^{31}\text{P}$  NMR. *J Mol Cell Cardiol* 14(suppl 3):13-20.
25. Wexler LW, Grice WN, Huntington M, et al (1986). Effect of hypertensive coronary perfusion pressure on left ventricular diastolic chamber stiffness. *Circulation* 74(suppl II):II-288 (abstract).
26. Neely JR, Feuvray D (1982). Metabolic products and myocardial ischemia. *Am J Pathol* 102:282-291.
27. Rovetto JM, Lamberton WF, Neely JR (1975). Mechanisms of glycolytic inhibition in ischemic rat hearts. *Circ Res* 37:742-751.
28. Mathews PM, Radda GK, Taylor DJ (1981). A  $^{31}\text{P}$  NMR study of metabolism in the hypoxic perfused rat heart. *Trans Biochem Soc* 9:236-237.
29. Flaherty JT, Weisfeldt ML, Bulkley BH, et al (1982). Mechanisms of ischemic myocardial cell damage assessed by phosphorus  $^{31}\text{P}$  nuclear magnetic resonance. *Circulation* 65:561-571.
30. Allen DG, Morris PG, Orchard CH (1983). A transient alkalosis precedes acidosis during hypoxia in ferret heart. *J Physiol* 34:58-59P.
31. Tsien RW (1976). Possible effects of hydrogen ions in ischemic myocardium. *Circulation* 53 (suppl 1):14-16.
32. Poole-Wilson PA (1978). Measurement of myocardial intracellular pH in pathological states. *J Mol Cell Cardiol* 10:511-526.
33. Mandel F, Kranias RG, DeGende AG, et al (1982). The effect of pH on the transient state kinetics of  $\text{Ca}^{2+}$ - $\text{Mg}^{2+}$ -ATPase of cardiac sarcoplasmic reticulum. *Circ Res* 50:310-317.
34. Donaldson SKB, Hermansen L (1978). Differential, direct effects of  $\text{H}^{+}$  on  $\text{Ca}^{2+}$ -activated force of skinned fibers from the soleus, cardiac and adductor magnus muscles of rabbits. *Pfluegers Arch* 376:55-56.
35. Fabiato A, Fabiato F (1978). Effects of pH on the myofilaments and the sarcoplasmic reticulum of skinned cells from cardiac and skeletal muscle. *J Physiol* 276:233-255.
36. Donaldson SKB, Bond E, Seeger L, et al (1981). Intracellular pH vs  $\text{Mg ATP}^{2-}$  concentration: Relative importance as determinants of  $\text{Ca}^{2+}$ -activated force generation of disrupted rabbit cardiac cells. *Cardiovasc Res* 15:268-275.
37. Allen DG, Orchard CH (1983). The effects of changes of pH on intracellular calcium transients in mammalian cardiac muscle. *J Physiol* 335:555-567.
38. Allen DG, Eisner DA, Orchard CH (1984). Factors influencing free intracellular calcium concentration in quiescent ferret ventricular muscle. *J Physiol* 350:615-630.
39. Lakatta EG, Lappe DL (1981). Diastolic scattered light fluctuation, resting force and twitch force in mammalian cardiac muscle. *J Physiol* 35:369-394.
40. Matsubara I, Yagi N, Endoh M (1982). The state of cardiac contractile proteins during the diastolic phase. *Jpn Circulation J* 46:44-48.
41. Stern MD, Kort AA, Bhatnagar GM, Lakatta EG (1983). Scattered-light intensity fluctuations in diastolic rat cardiac muscle caused by spontaneous  $\text{Ca}^{2+}$ -dependent cellular mechanical oscillations. *J Gen Physiol* 82:119-153.
42. First WH, Palacios I, Powell WH Jr (1978). Effect of hypoxia on myocardial relaxation in isometric cat papillary muscle. *J Clin Invest* 61:1218-1224.
43. Nayler WG, Yopez CE, Poole-Wilson PA (1978). The effect of  $\beta$ -adrenoreceptor and calcium $^{2+}$  antagonist drugs on the hypoxia-induced increase in resting tension. *Cardiovasc Res* 12:666-674.
44. Nayler WG, Poole-Wilson PA, Williams A (1979). Hypoxia and calcium. *J Mol Cell Cardiol* 11:683-706.
45. Nayler WG, Williams A (1978). Relaxation in heart muscle: Some morphologic and biochemical considerations. *Eur J Cardiol* 7(suppl):35-50.
46. Grossman W, Barry WH (1980). Diastolic pressure-volume relations in the diseased heart. *Fed Proc* 39:148-155.

47. Harding DP, Poole-Wilson PA (1980). Calcium exchange in rabbit myocardium during and after hypoxia: Effect of temperature and substrate. *Cardiovasc Res* 14:435-445.
48. Greene HL, Weisfeldt ML (1977). Determinants of hypoxic and post-hypoxic myocardial contracture. *Am J Physiol* 232:526-533.
49. Bing OHL, Brooks WW, Messer JV (1973). Heart muscle viability following hypoxia: Protective effect of acidosis. *Science* 180:1297-1298.
50. Poole-Wilson PA, Lakatta EG, Nayler WG (1977). The effects of acidosis on myocardial function and the uptake of calcium during and after hypoxia. *Clin Sci Molec Med* 52:2-3P.
51. Dwyer EM (1970). Left ventricular pressure-volume alterations and regional disorders of contraction during myocardial ischemia induced by atrial pacing. *Circulation* 42:1111-1122.
52. McLaurin LP, Rolett SL, Grossman W (1973). Impaired left ventricular relaxation during pacing induced ischemia. *Am J Cardiol* 32:751-757.
53. Barry WH, Brooker JZ, Alderman EL, Harrison DC (1974). Changes in diastolic stiffness and tone of the left ventricle during angina pectoris. *Circulation* 49:255-263.
54. Mann T, Brodie BR, Grossman W, McLaurin LP (1977). Effects of angina on the left ventricular diastolic pressure volume relationship. *Circulation* 55:761-766.
55. Mann T, Goldberg S, Mudge GH Jr, Grossman W (1979). Factors contributing to altered left ventricular diastolic properties during angina pectoris. *Circulation* 52:14-20.
56. Serizawa T, Carabello BA, Grossman W (1980). Effect of pacing induced ischemia on left ventricular diastolic pressure-volume relations in dogs with coronary stenoses. *Circ Res* 46:430-439.
57. Bourdillon PD, Lorell BH, Mirsky I, et al (1983). Increased regional myocardial stiffness of the left ventricle during pacing-induced angina in man. *Circulation* 67:316-323.
58. Tennant R, Wiggers CJ (1985). Effect of coronary occlusion on myocardial contraction. *Am J Physiol* 112:351-361.
59. Forrester JS, Diamond G, Parmley WE, Swan HJC (1972). Early increase in left ventricular compliance after infarction. *J Clin Invest* 51:598-603.
60. Theroux P, Franklin D, Ross J Jr, Kemper WS (1974). Regional myocardial function during acute coronary artery occlusion and its modification by pharmacologic agents in the dog. *Circ Res* 35:825-908.
61. Theroux P, Ross J Jr, Franklin D, et al (1977). Regional myocardial function and dimensions early and late after myocardial infarction in the unanaesthetized dog. *Circ Res* 40:158-165.
62. Tyberg JV, Forrester JS, Wyatt HL, et al (1974). An analysis of segmental ischemic dysfunction utilizing the pressure length loop. *Circulation* 49:748-754.
63. Pirzada FA, Ekong EA, Vokonas PS, et al (1976). Experimental myocardial infarction. XIII. Sequential changes in left ventricular pressure-length relationship in the acute phase. *Circulation* 53:970-974.
64. Vokonas PS, Pirzada FA, Hood WB Jr (1976). Experimental myocardial infarction. XII. Dynamic changes in sequential mechanical behavior of infarcted and non-infarcted myocardium. *Am J Cardiol* 37:853-859.
65. Weiner JM, Apstein CS, Arthur JH, et al (1976). Persistence of myocardial injury following brief periods of coronary occlusion. *Cardiovasc Res* 10:678-686.
66. Hess OM, Osakada G, Lavelle JF, et al (1983). Diastolic myocardial wall stiffness and ventricular relaxation during partial and complete coronary occlusions in the conscious dog. *Circ Res* 52:387-400.
67. Reagan TJ, Effros RM, Haider B, et al (1976). Myocardial ischemia and cell acidosis: Modification by alkali and the effects on ventricular function and cation composition. *Am J Cardiol* 37:501-507.
68. Cobbe SM, Poole-Wilson PA (1980). The time of onset and severity of acidosis in myocardial ischemia. *J Mol Cell Cardiol* 12:745-760.
69. Momomura S, Ingwall JS, Parker JA, et al (1985). The relationships of high energy phosphates, tissue pH, and regional blood flow to diastolic distensibility in the ischemic dog myocardium. *Circ. Res.* 57:822-835.
70. Apstein CS, Deckelbaum L, Hagopian L, Hood WB Jr (1978). Acute cardiac ischemia and reperfusion. Contractility, relaxation and glycolysis. *Am J Physiol* 235:H637-H648.
71. Bricknell OL, Daries PS, Opie LH (1981). A relationship between adenosine triphosphate, glycolysis and ischemic contracture in the isolated rat heart. *J Mol Cell Cardiol* 13:941-945.
72. Gudbjarnson S, Mathes P, Raven KG (1970). Functional compartmentation of ATP and creatine phosphate in heart muscle. *J Mol Cell Cardiol* 1:325-339.
73. Shrago E, Shug AL, Sul H, et al (1976). Control of energy production in myocardial ischemia. *Circ Res* 38(Suppl 1):175-79.

---

# 19. EFFECTS OF HYPOXIA ON RELAXATION OF THE HYPERTROPHIED VENTRICLE

---

Beverly H. Lorell, Laura F. Wexler, Shin-ichi Momomura, Ellen Weinberg,  
Joanne Ingwall, and Carl S. Apstein

Cardiac hypertrophy is a compensatory response to chronic pressure-overload of the heart. However, studies in both animal models and in patients provide evidence that adaptive pressure-overload cardiac hypertrophy may be associated with an increased susceptibility to the development of diastolic dysfunction during ischemia or hypoxia. In this regard, Bache and coworkers have shown that left ventricular end-diastolic pressure rises in response to ischemia induced by pacing tachycardia in dogs with chronic left ventricular hypertrophy [1]. Similarly, Fifer and coworkers have recently shown that patients with normal coronary arteries and pressure-overload hypertrophy due to aortic stenosis demonstrate a striking rise in left ventricular diastolic pressure and an impairment of left ventricular relaxation during transient angina induced by pacing tachycardia [2]. It is likely that these transient changes in diastolic function in hearts with pressure-overload hypertrophy are related in part to the development of global left ventricular subendocardial ischemia. Coronary vascular reserve appears to be impaired in dogs with chronic aortic stenosis and in patients with pressure-overload hypertrophy [3–5]. Furthermore, relative hypoperfusion of the subendocardium has been shown in dogs with aortic stenosis in whom metabolic evidence of ischemia was induced by pacing tachycardia [1].

The rise in left ventricular diastolic pressure

during ischemia in the presence of cardiac hypertrophy is very similar to that observed during demand ischemia in patients with coronary stenoses [6] and in animal models with regional coronary stenoses [7] or with global low-flow ischemia with superimposed tachycardia [8].

Thus, the rise in left ventricular diastolic pressure seen in response to ischemia in the presence of cardiac hypertrophy may simply reflect the effects of ischemia per se, due to impaired coronary reserve. However, it is not known whether hypertrophied myocardium is more susceptible to developing diastolic dysfunction in response to any degree of ischemic or hypoxic stress, compared with nonhypertrophied myocardium. Previous studies suggest that hypertrophied cardiac muscle is characterized by an intrinsic prolongation of the duration of the intracellular calcium transient [9]. Thus, it is possible that hypertrophied cardiac muscle is predisposed to develop a more profound impairment of diastolic relaxation in response to any level of ischemic or hypoxic stress.

Consequently, this chapter will describe studies that were carried out to test the hypothesis that hearts with chronic pressure-overload left ventricular hypertrophy (LVH) demonstrate a more severe impairment of left ventricular relaxation in response to transient hypoxia in comparison with controls.

## *Methods*

We compared hearts from hypertensive uninephrectomized Wistar-Kyoto rats treated with

deoxycorticosterone and increased salt intake (DOC-salt rats) with hearts from aged-matched normotensive control rats treated with uninephrectomy alone [10]. Thirteen control rats and 12 hypertensive rats (LVH group) were studied. At age 15 weeks, the *in vivo* tail-cuff pressure in the LVH group was significantly higher than in the control group ( $201 \pm 24$  vs.  $129 \pm 14$  mm Hg,  $p < 0.05$ ). The LV/body weight ratio was greater in the LVH group compared with the controls ( $3.19 \pm 0.36$  vs.  $1.89 \pm 0.19$ ,  $p < 0.05$ ).

The effects of brief hypoxia (3 minutes) were studied in an isolated Krebs buffer-perfused rat heart preparation [11]. Buffer was delivered by a constant flow pump to the coronary arteries through a cannula in the aortic stump. Because the rate of coronary flow was constant, mean coronary perfusion pressure was proportional to the coronary vascular resistance. A thin-walled latex balloon was inserted into the left ventricular cavity and attached to a micromanometer catheter. In this preparation, left ventricular balloon volume was held constant. Thus, changes in left ventricular diastolic pressure reflect changes in left ventricular diastolic distensibility. Left ventricular thebesian drainage was vented by an apical drain. Coronary venous efflux was collected via a drain in the pulmonary artery. Heart rate was held constant at 4 Hz by a right ventricular pacemaker, and temperature was held constant at 37°C and monitored with an intraventricular temperature probe.

Coronary flow was divided by left ventricular wet weight and expressed as ml/minute per gram. Left ventricular relaxation rate was estimated by calculation of the time constant (T) using the derivative method of Raff and Glantz [12]. In this model, the extrapolated baseline pressure ( $P_B$ ) reflects the asymptote to which pressure would fall if decay continued indefinitely and is an estimate of the extent of relaxation. The fit of data points to this model was excellent with a correlation coefficient 0.99 or greater. Arterial and venous perfusion samples were analyzed for lactate concentration by the specific enzymatic method of Apstein and coworkers [13].

Before each experiment, the heart was perfused by oxygenated buffer for 30 minutes. Left ventricular balloon volume was adjusted at baseline so that left ventricular end-diastolic pressure was 10 mm Hg under aerobic conditions in both the LVH and control groups. This

balloon volume was maintained unchanged throughout the subsequent experiment. At baseline, coronary flow in the control group was adjusted to achieve a mean coronary perfusion pressure of 100 mm Hg, and flow was fixed at that level throughout the experiment. In the chronic hypertensive LVH group, coronary flow was adjusted to achieve a mean coronary perfusion pressure of 150 mm Hg under baseline conditions and was fixed at that level of flow throughout the experiment. These differing levels of coronary flow and baseline perfusion pressures were selected to approximate the *in vivo* mean coronary perfusion pressures to which the groups were chronically exposed, and because pilot studies indicated that this approach would achieve comparable coronary flow per gram left ventricular weight in both groups.

At the end of the 30-minute stabilization period, measurements of left ventricular pressure, coronary perfusion pressure, coronary flow, and arterial and coronary venous lactate content were made. After baseline measurements, the coronary perfusate was switched to buffer equilibrated with a 5% CO<sub>2</sub>-95% nitrogen gas mixture. Hemodynamic recordings were made continuously during 3 minutes of hypoxia, and arterial and coronary venous lactate samples were obtained during the final 15 seconds of the 3-minute period of hypoxia. Heart weight was measured after recovery under aerobic conditions for 15 minutes. The wet weight: dry weight ratio was also determined.

### Results

Under baseline conditions, left ventricular systolic pressure was significantly higher in the LVH group ( $171 \pm 18$  vs.  $103 \pm 13$  mm Hg,  $p < .05$  than in the controls), and left ventricular developed pressure per unit of left ventricular mass was also higher in the LVH group than in the control group ( $134 \pm 23$  vs.  $109 \pm 22$  mm Hg/g,  $p < 0.05$ ). By experimental design, left ventricular end-diastolic pressure was identical in the LVH and control groups at baseline ( $11.0 \pm 1.5$  vs.  $10.1 \pm 1.0$  mm Hg,  $p = \text{NS}$ ). At baseline, coronary flow rate was  $20 \pm 5.0$  (ml/min) per gram in the control group and  $17.6 \pm 3.6$  (ml/min) per gram in the LVH group,  $p = \text{NS}$ . Neither group had metabolic evidence of myocardial lactate production at baseline.

At baseline, there were no differences be-

tween the LVH group and the control group in any indices of either the rate or extent of left ventricular relaxation during aerobic conditions.

Figure 19-1 shows the response to brief hypoxia of a typical experimental heart from the control group and from the LVH group. In both groups, hypoxia resulted in an expected fall in left ventricular systolic pressure, but left ventricular systolic pressure was significantly higher (75%) in the LVH group compared with the control group. Left ventricular contractility as assessed by LV positive  $dP/dt/P$  was depressed to a similar extent. Left ventricular developed pressure per unit of left ventricular mass during hypoxia was also similar ( $24 \pm 7$  vs.  $19 \pm 5$  mm Hg/g,  $p = \text{NS}$ ). In addition, the extent of coronary vasodilation induced by hypoxia as assessed by the change in coronary vascular resistance was identical in both groups.

However, as illustrated in Figure 19-2, in response to brief hypoxia, left ventricular end-diastolic pressure rose to a significantly higher level in the LVH group than in the control group ( $37.0 \pm 5.3$  vs.  $22.0 \pm 5.0$  mm Hg,  $p < 0.001$ ). The increase in left ventricular end-diastolic pressure during hypoxia, normalized per unit of left ventricular mass, was also greater in the LVH group than in the control group ( $22 \pm 5$  vs.  $14 \pm 6$  mm Hg/g,  $p < 0.005$ ). Indices of the rate of left ventricular relaxation, including negative  $dP/dt/P$ , and T were depressed during hypoxia but did not differ between the LVH and control groups. However, the extent of left ventricular relaxation during hypoxia as assessed by the asymptote  $P_B$  to which left ventricular pressure declined was significantly more impaired in the LVH group than in the control group ( $33.0 \pm 6.7$  vs.  $22.2 \pm 4.7$  mm Hg,  $p < 0.001$ ).

Both the LVH and the control groups showed evidence of anaerobic metabolism during hypoxia, but the extent of myocardial lactate production was comparable in both groups. Similarly, there were no differences in the left ventricular wet weight: dry weight ratio between the LVH and control group, suggesting that there was no difference in the extent of the edema induced by hypoxia.

These experiments showed that brief hypoxia results in a much greater rise in left ventricular diastolic pressure and impairment of the extent of left ventricular relaxation in hypertrophied rat hearts than in nonhypertrophied controls. These differences in diastolic function during

hypoxia did not appear to be related to differences in myocardial perfusion per unit of left ventricular weight or to the degree of glycolytic flux. To determine why hypoxia causes a greater impairment of left ventricular relaxation in hypertrophied hearts, a series of preliminary experiments has been done to assess high-energy-phosphate metabolism using  $^{31}\text{P}$  nuclear magnetic resonance (NMR) spectroscopy. We hypothesized that the greater impairment of diastolic function in response to hypoxia in hypertrophied hearts could be related to a more rapid depletion of high energy phosphates in hypertrophied hearts in comparison with controls or to differences in the degree of intracellular acidosis induced by hypoxia.

To test these hypotheses, we studied isovolumic buffer-perfused hypertrophied and control rat hearts prepared in the manner described above [14]. Measurements of mechanical function and high-energy-phosphate levels were correlated during 12 minutes of hypoxic buffer perfusion. Hemodynamic measurements and  $^{31}\text{P}$  NMR spectra were obtained at baseline and every 2 minutes during the 12 minutes of hypoxia. Adenosine triphosphate (ATP) and creatine phosphate levels were derived from the integrated areas of the beta-phosphate resonance peak of ATP and from the creatine phosphate resonance peak. Intracellular pH was derived from the position of the inorganic phosphate peak. During 12 minutes of hypoxia, there was a significant and comparable fall in left ventricular systolic pressure in the LVH and control groups. As seen in the rat heart experiments described above, there was a significantly greater rise in left ventricular diastolic pressure at constant volume in the group with LVH in comparison with the control group. However, the rate and extent of decline of ATP were similar in the LVH and control groups in response to 12 minutes of hypoxia. The rate of decline of creatine phosphate was also similar in both groups. In response to 12 minutes of hypoxia, there was a very small but comparable fall in intracellular pH of less than 0.1 pH unit in both groups [14].

### *Discussion*

These experiments suggest that a greater impairment of the extent of diastolic relaxation occurs in hypertrophied hearts in comparison with nonhypertrophied control hearts in re-

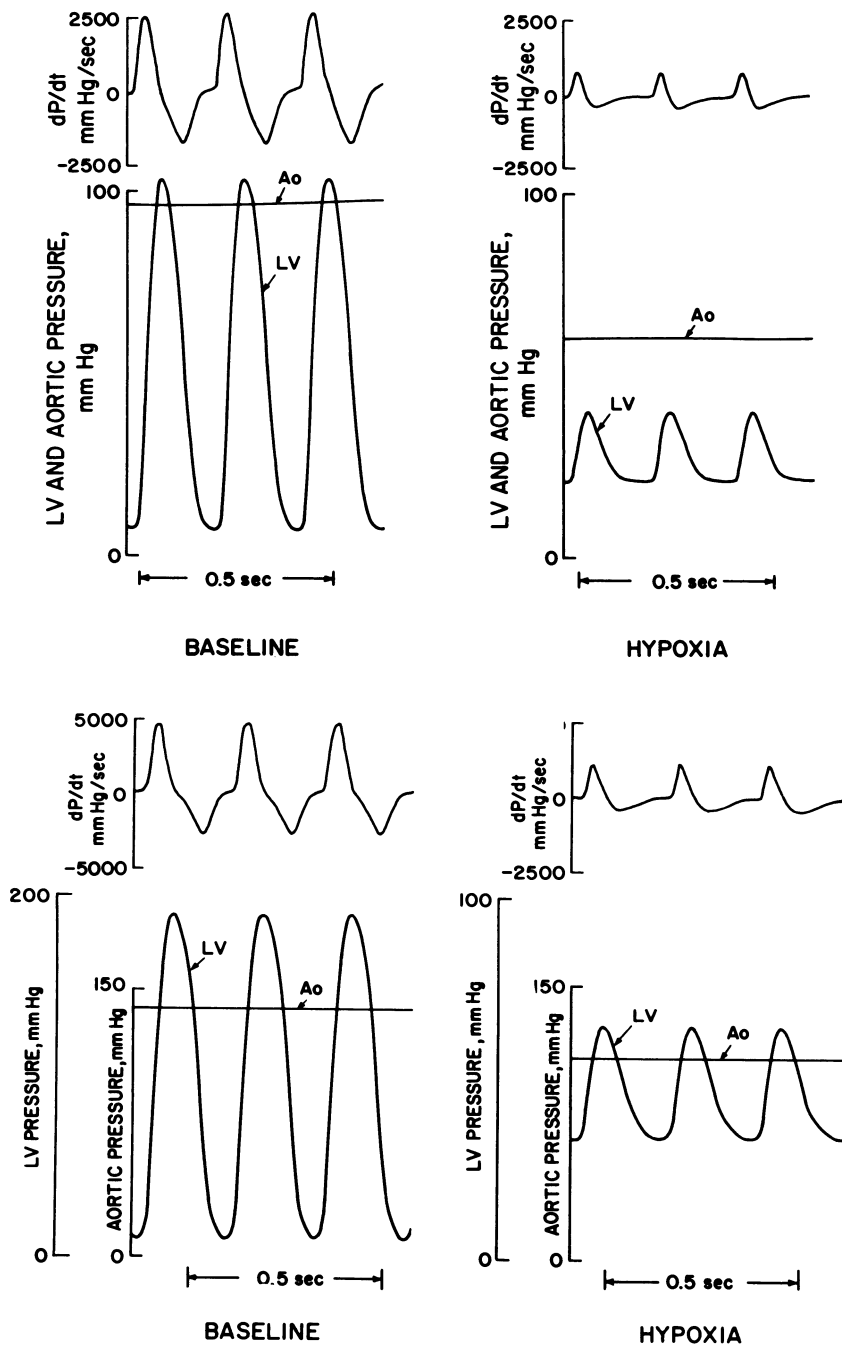


FIGURE 19-1. Left ventricular (LV) and aortic (A.) (coronary perfusion) pressure at baseline and in response to 3 minutes of hypoxia. Experiments from the control group (*upper panel*) and LVH group (*lower panel*) are shown. Brief hypoxia was associated with a fall in LV systolic pressure and LV dp/dt, and coronary vasodilation evident as a fall in coronary perfusion pressure in both groups. Coronary flow rate per gram was identical in both groups. Left ventricular end-diastolic pressure was identical at baseline, but there was a much greater rise in LV end-diastolic pressure in response to hypoxia in the LVH group than in the control group. (From Lorell et al. [10], with permission.)

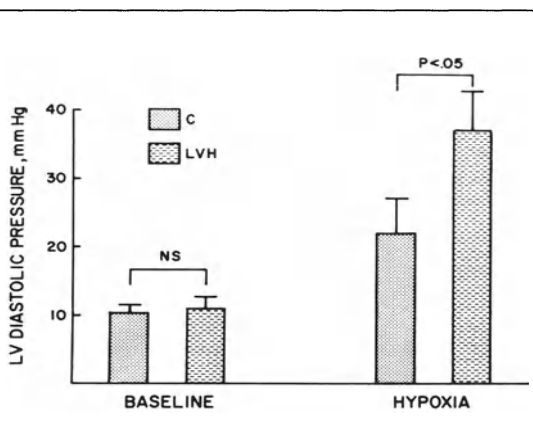


FIGURE 19-2. Left ventricular (LV) end-diastolic pressure at baseline and in response to 3 minutes of hypoxia. During aerobic baseline conditions, LV diastolic pressure was comparable in the control and LVH groups, and this level of diastolic pressure was achieved at comparable left ventricular balloon volumes. However, the rise in LV diastolic pressure in response to hypoxia was significantly greater in the LVH group than in the controls. This suggests that hearts with cardiac hypertrophy show a greater impairment of diastolic distensibility, compared with control hearts, in response to an identical brief hypoxic stress. NS = not significant.

response to an identical brief hypoxic stress. Furthermore, our preliminary data using  $^{31}\text{P}$  NMR spectroscopy suggest that differences in high-energy-phosphate depletion and intracellular acidosis do not account for the greater impairment of diastolic function which occurs in hypertrophied hearts in response to brief hypoxia.

#### POSSIBLE MECHANISMS

Several mechanisms might account for differences in the diastolic response to hypoxia seen in hypertrophied and control hearts in our study. Vogel and coworkers [15] have previously shown a powerful erectile hydraulic effect of the coronary vasculature on diastolic function in both buffer and blood-perfused isovolumic hearts. Although great efforts were taken in this experiment to achieve comparable coronary flow per gram of left ventricular weight in both groups during aerobic and hypoxic conditions, it is not possible to exclude a greater contribution of coronary turgor to the hypoxia-induced decrease in diastolic distensibility in the hypertrophied hearts. Furthermore, although the flow

per gram of left ventricular weight was comparable in both groups, we cannot exclude the possibility that there were differences in subendocardial flow and for that matter, in subendocardial high-energy-phosphate levels, between these groups.

Secondly, the influence of loading conditions on the rate and extent of relaxation in the hypertrophied and control hearts should be considered. Under well-oxygenated conditions, diastolic relaxation is profoundly influenced by the magnitude and temporal dispersion of systolic load on cardiac muscle [16-18]. Although left ventricular systolic pressure clearly differed in the control and LVH groups in our experiments, the observation that both the rate and extent of relaxation were identical in these groups during the well-oxygenated baseline state strongly suggests that "afterload mismatch" with excessively high systolic wall stress was not operative in the left ventricular hypertrophy group. Furthermore, in these isovolumic hearts with vented right ventricles, the influence of pericardial and right ventricular constraint on diastolic function and relaxation was not operative.

#### CHANGES IN FORCE INACTIVATION

Studies of isolated heart muscle indicate that myocardial relaxation during hypoxia is load-independent and is primarily regulated by the processes that influence the dissipation of cross-bridge attachment [19]. These biochemical processes that influence the rate and extent of force inactivation are as yet incompletely understood but appear to depend in part on the ATP-dependent rate and capacity of calcium sequestration by the sarcoplasmic reticulum and, to a lesser extent, by processes that influence calcium flux across the sarcolemma [20].

In our experiments, differences in myocardial calcium availability for diastolic cross-bridge interaction could account for the greater impairment of left ventricular diastolic distensibility and extent of relaxation that was observed in hypertrophied hearts relative to controls during hypoxia. There is evidence that pressure-overloaded hypertrophied cardiac muscle may be characterized by intrinsic changes in the duration of the active state and intracellular calcium regulation. Studies of isolated sarcoplasmic reticulum from hearts with advanced cardiac hypertrophy have shown a decrease in both the rate and total binding activity of calcium by the

sarcoplasmic reticulum [21]. Furthermore, studies of intracellular calcium transients using the aequorin injection technique have strongly suggested that chronic pressure overload hypertrophy in both human and animal models is associated with a significant prolongation of the time course of the intracellular calcium transient in association with prolongation of the time course of both tension development and relaxation [9, 22]. Such changes in intracellular calcium regulation may represent a salutary adaptation of hypertrophied muscle under aerobic conditions, which permits the sustained development of high systolic pressure and facilitates the development of increased work by the hypertrophied heart.

However, our current working hypothesis is that such adaptations of intracellular calcium regulation may make hypertrophied myocardium more sensitive to the development of cytosolic calcium overload, resulting in an impaired extent of diastolic cross-bridge inactivation during interventions such as hypoxia, which impair the energy-dependent regulation of cytosolic calcium.

If cardiac hypertrophy is characterized by an intrinsic prolongation of the calcium transient, any depression of sarcoplasmic reticulum calcium sequestration or sarcolemmal pump function by hypoxia may promote profound diastolic calcium overload and severe depression of the extent of relaxation. Thus, the hypertrophied myocardium may be susceptible to an adverse interplay between intrinsic changes in cytosolic calcium regulation and the imposition of any ischemic or hypoxic stress.

To address this hypothesis directly, it will be necessary to have the ability to directly measure rapid changes in cytosolic calcium in nonhypertrophied and hypertrophied heart muscle under aerobic and hypoxic conditions. Because other interventions such as temperature and heart rate can profoundly influence high-energy-phosphate availability and calcium regulation, it will be particularly important to assess changes in cytosolic calcium under physiologic conditions in normothermic, working, and beating hearts. This requirement is important because studies of isolated cardiac muscle using the aequorin technique have shown that the presence of hypothermia and a slow rate of depolarization appear to protect against any early change in either diastolic muscle tension or change in the calcium transient during hypoxia [23].

In summary, brief hypoxia is associated with a more profound impairment of the extent of left ventricular relaxation in hypertrophied rat hearts than in nonhypertrophied controls. The rise in left ventricular diastolic pressure observed with pressure-overload hypertrophy appears to be related to a greater impairment of diastolic force inactivation for any degree of glycolytic flux or high-energy-phosphate depletion than is seen in the absence of hypertrophy.

## References

1. Bache RJ, Arentzen CE, Simon AB, Vrobel TR (1984). Abnormalities in myocardial perfusion during tachycardia in dogs with left ventricular hypertrophy: Metabolic evidence for myocardial ischemia. *Circulation* 69:409.
2. Fifer MA, Bourdillon PD, Lorell BH (1986). Altered left ventricular diastolic properties during pacing-induced angina in patients with aortic stenosis. *Circulation* 74:675.
3. Marcus ML, Doty DB, Hiratzka LF, et al (1982). Decreased coronary reserve: A mechanism for angina pectoris in patients with aortic stenosis and normal coronary arteries. *N Engl J Med* 307:1362.
4. Pichard AD, Gorlin R, Smith H, et al (1981). Coronary flow studies in patients with left ventricular hypertrophy of the hypertensive type. *Am J Cardiol* 47:547.
5. Bache RJ, Arentzen CE, Simon AB, Vrobel TR (1984). Abnormalities in myocardial perfusion in dogs with left ventricular hypertrophy: Metabolic evidence for myocardial ischemia. *Circulation* 69:409.
6. Bourdillon PD, Lorell BH, Mirsky I, et al (1983). Increased regional myocardial stiffness of the left ventricle during pacing-induced angina in man. *Circulation* 67:316.
7. Serizawa T, Carabello BA, Grossman W (1980). Effect of pacing-induced ischemia on left ventricular diastolic pressure-volume relations in dogs with coronary stenoses. *Circ Res* 46:430.
8. Ioyama S, Lorell BH, Grice WN, et al (1985). Increased diastolic chamber stiffness during simulated angina in isolated hearts. *Circulation* 72:III-72 (abstract).
9. Gwathmey JK, Morgan JP (1985). Altered calcium handling in experimental pressure-overload hypertrophy in the ferret. *Circ Res* 57:836.
10. Lorell BH, Wexler LF, Momomura S, et al (1986). The influence of pressure overload left ventricular hypertrophy on diastolic properties during hypoxia in isovolumically contracting rat hearts. *Circ Res* 58:653.
11. Apstein CS, Mueller M, Hood WB Jr (1977). Ventricular contracture and compliance changes

- with global ischemia and reperfusion, and their effect on coronary resistance in the rat. *Circ Res* 41:206.
12. Raff GL, Glantz SA (1981). Volume loading slows left ventricular isovolumic relaxation rate. *Circ Res* 48:813.
  13. Apstein CS, Puchner E, Brachfeld N (1970). Improved automated lactate method. *Anal Biochem* 38:20.
  14. Wexler LF, Lorell BH, Momomura S, et al (1985). Cardiac hypertrophy: Hemodynamic and metabolic  $^{31}\text{P}$ -NMR response to hypoxia. *Circulation* 72:III-337 (abstract).
  15. Vogel WM, Apstein CS, Briggs LL, et al (1982). Acute alterations in left ventricular diastolic chamber stiffness. *Circ Res* 51:465.
  16. LeCarpentier YC, Chuck LHS, Housmans PR, et al (1979). Nature of load dependence of relaxation in cardiac muscle. *Am J Physiol* 237: H455.
  17. LeCarpentier Y, Martin JL, Gastineau, P, Hatt PY (1982). Load dependence of mammalian heart relaxation during cardiac hypertrophy and heart failure. *Am J Physiol* 242:H855.
  18. Brutsaert DL, Rademakers FE, Sys SU (1984). Triple control of relaxation: Implications in cardiac disease. *Circulation* 69:521.
  19. Chuck LH, Goethals MA, Parmley WW, Brutsaert DL (1981). Load insensitive relaxation caused by hypoxia in mammalian cardiac muscle. *Circ Res* 48:797.
  20. Nayler WG, Poole-Wilson PA, Williams A (1979). Hypoxia and calcium. *J Mol Cell Cardiol* 11:683.
  21. Sordahl LA, McCollum WB, Wood WG, Schwartz A (1973). Mitochondria and sarcoplasmic reticulum function in cardiac hypertrophy and failure. *Am J Physiol* 224:497.
  22. Allen DG, Orchard CH (1983). Intracellular calcium concentration during hypoxia and metabolic inhibition in mammalian ventricular muscle. *J Physiol* 339:107.

---

## 20. RELAXATION AND DIASTOLIC DISTENSIBILITY OF THE REGIONALLY ISCHEMIC LEFT VENTRICLE

---

William Grossman

### *Diastolic Function During Angina Pectoris*

Normal left ventricular contraction and relaxation are dependent upon an appropriate balance between myocardial oxygen supply and demand. In the clinical setting, myocardial ischemia is commonly associated with left ventricular dysfunction. It has been observed by many investigators that a transient, reversible rise in left ventricular diastolic pressure commonly accompanies angina pectoris [1–4]. This increase in diastolic pressure could be due simply to an increase in diastolic volume, resulting from contractile failure of ischemic myocardium and an increased residual volume. Alternatively, the increased diastolic pressure might reflect decreased diastolic distensibility of the left ventricular chamber, with a higher diastolic pressure being needed to achieve the same degree of end-diastolic sarcomere stretch. These potential mechanisms for the increased diastolic pressure that characterizes angina pectoris are illustrated in Figure 20–1. The rise in diastolic pressure seen in patients with angina pectoris has been studied extensively by clinical investigators [5–14], and there is now widespread agreement that the phenomenon results from *both* decreased left ventricular diastolic distensibility and impaired contractile function. As shown by Sasayama and coworkers [9], the left ventricular diastolic pressure-volume relationship curve shifts upward and slightly to the right during angina pectoris. This shift apparently represents

a direct upward shift of the pressure-segment length relationship for ischemic myocardium and a rightward or Frank-Starling shift for the remaining nonischemic myocardium (Figure 20–2).

Studies of left ventricular pressure-volume relations during pacing-induced angina pectoris have shown that the normal heart responds to pacing tachycardia with an increase in inotropic state as well as a downward shift in the diastolic pressure-volume relationship [15], as seen in Figure 20–3A. However, in the presence of coronary stenoses, pacing tachycardia is associated with a progressive decrease in the myocardial oxygen supply-demand ratio (demand ischemia), and this is manifested by impaired contractile function as well as an upward shift in the left ventricular diastolic pressure-volume relationship (Figure 20–3B).

Clinical studies of *regional* myocardial function have been carried out using echocardiographic techniques. In one study, Bourdillon and coworkers [11] examined the relationship between left ventricular diastolic pressure and posterior wall thickness in patients with coronary artery disease and impairment of the coronary circulation supplying the inferior and posterior left ventricular myocardium. Angina pectoris was induced by pacing tachycardia and resulted in a transient elevation in left ventricular end-diastolic pressure, which gradually returned to the control value over a period of 1 to 3 minutes following termination of the tachycardia. When left ventricular diastolic pressure was plotted throughout diastole against simultaneous wall thickness, it was noted that diastolic pressure was higher during angina for any

Grossman, William, and Lorell, Beverly H. (eds.), *Diastolic Relaxation of the Heart*. Copyright © 1987. Martinus Nijhoff Publishing. All rights reserved.

value of posterior wall thickness. This was interpreted as signifying a reduction in regional distensibility of the ischemic myocardium, because a passive rise in left ventricular diastolic pressure should have resulted in greater diastolic stretching and therefore a *thinner* wall at the higher diastolic pressure. In association with this upward shift in the relationship between left ventricular diastolic pressure and instantaneous wall thickness, Bourdillon and co-workers [11] found that the peak rate of posterior wall thinning actually fell. Because other investigators have shown that a higher left ventricular diastolic pressure induced by volume loading leads to a higher left ventricular diastolic filling rate and a greater peak rate of posterior wall thinning, the actual *fall* in peak rate of posterior wall thinning in association with angina pectoris (despite a higher diastolic pressure) strongly supported the concept that myocardial relaxation was impaired. In this study, Dr Israel Mirsky contributed an analysis of radial stress-strain relations for the ischemic myocardium. His analysis indicated that there was an increased residual stiffness in the ischemic region during angina pectoris, as compared to the control state [11].

Others have examined the left ventricular diastolic pressure-volume relation during demand ischemia induced by bicycle exercise. Carroll and coworkers [12-13] have shown that a similar upward and rightward shift of the left ventricular diastolic pressure-volume relation is obtained during angina pectoris induced by exercise, whereas patients with coronary occlusion and completed myocardial infarction (left ventricular scar) do not show any change in diastolic distensibility during exercise. (Dr. Carroll's findings are presented in detail in Chapter 22.) Because exercise is associated with catecholamine release, which should theoretically improve myocardial relaxation, the worsening of relaxation and impairment of diastolic distensibility seen in these patients during exercise strongly suggests that myocardial ischemia has a primary role in controlling diastolic relaxation and distensibility.

### Distensibility vs. Diastolic Compliance

The term *distensibility* has been preferred by our group over the term *diastolic compliance*. Compliance and its opposite, stiffness, are terms with rigorous definitions in physical science.

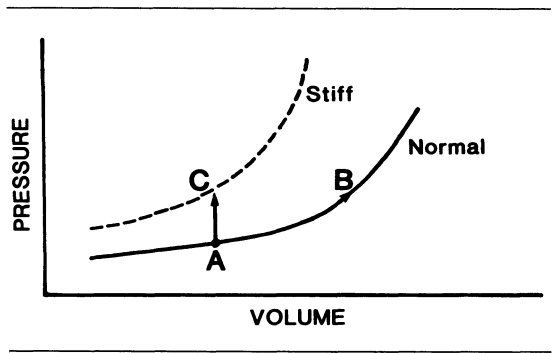


FIGURE 20-1. Left ventricular diastolic pressure-volume relations for a normal heart (lower solid curve) and for a heart with a stiff left ventricle (upper dashed curve). An increase in left ventricular diastolic pressure is seen during angina pectoris. This could potentially be explained by either an increase in diastolic chamber volume (A → B) without alteration in diastolic stiffness or an increase in diastolic stiffness (A → C) without change in diastolic chamber volume.

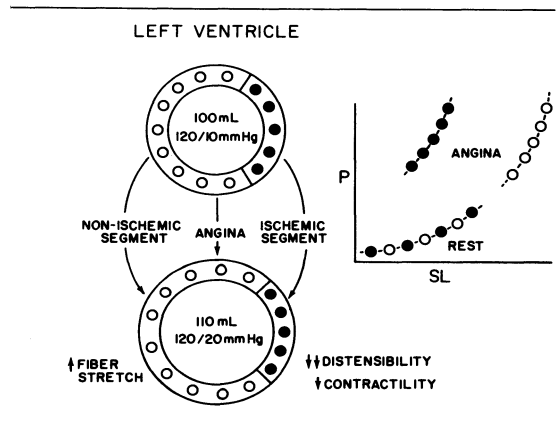


FIGURE 20-2. Physiologic changes in the left ventricular myocardium during angina pectoris. Left: the myocardial segment distal to an obstructed coronary artery (*closed circles*) becomes ischemic during angina and exhibits decreased diastolic distensibility. Left ventricular diastolic pressure increases, stretching the non-ischemic segment (*open circles*). Right: plots of left ventricular diastolic pressure (P) against segment length (SL) show equivalent diastolic properties for both the normal and potentially ischemic myocardium at rest. However, only the ischemic segment shows reduced distensibility during angina, while the nonischemic segment moves to a higher and steeper portion of a single pressure-segment length relation. (From Grossman [1], with permission.)

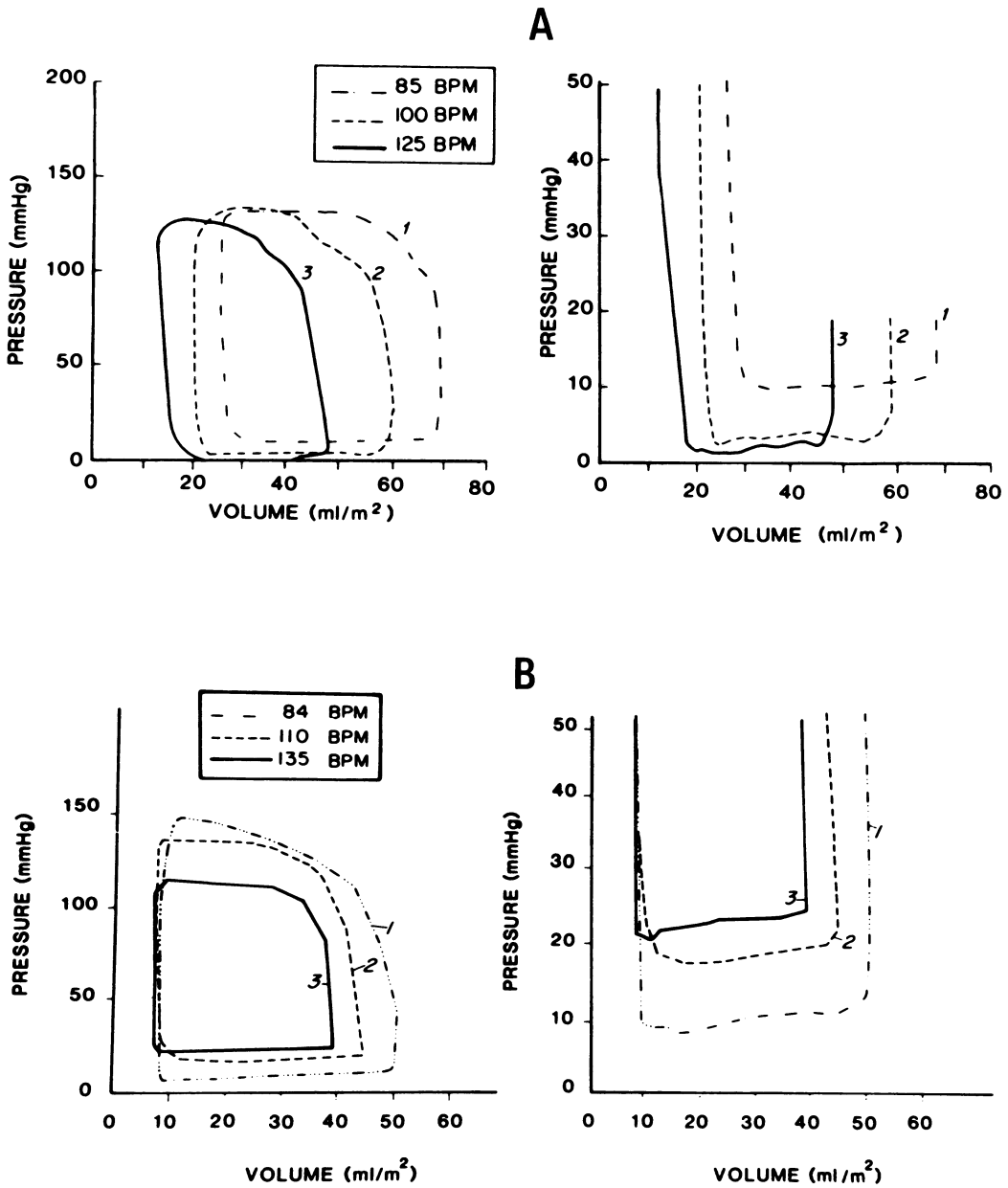


FIGURE 20-3. Left ventricular pressure-volume relations during pacing tachycardia in a patient with normal coronary arteries (A) and a patient with coronary artery disease (B). As can be seen, in the normal heart, pacing tachycardia causes a leftward shift of the end-systolic pressure-volume point (increased inotropy) as well as a downward and leftward shift of the diastolic pressure-volume relation. In the patient with coronary artery disease, pacing tachycardia induced angina pectoris and both a decrease in inotropy (reduction in left ventricular end-systolic pressure at nearly constant end-systolic volume) as well as an upward shift in the diastolic pressure-volume relation. (From Aroesty, et al. [15], with permission.)

Compliance refers to the *slope* of the pressure-volume or stress-strain relationship, and a left ventricular chamber may be considered to have reduced compliance when the increment in diastolic volume associated with a unit rise in diastolic pressure is reduced, compared to a baseline value. Although the terms *compliance* and *stiffness* are useful and are widely used in the discussion of left ventricular diastolic properties, strict adherence to their physical definitions creates potential problems in interpretation of experimental data. For example, in Figure 20-1, the upper curve (labeled "stiff") shows upward displacement *and* increased slope compared to the lower curve. For reasons just discussed, this higher curve represents a decrease in diastolic compliance (increased stiffness). We use the term *distensibility* to indicate a change in diastolic properties of the left ventricular chamber such that a higher diastolic pressure is needed to fill the ventricle to the same volume. Accordingly, the upper curve in Figure 20-1 also shows decreased diastolic distensibility. However, let us suppose that the upper curve in Figure 20-1 was produced simply by an upward displacement of the diastolic pressure-volume relation depicted in the lower ("normal") curve, as shown in Figure 20-4. Such a *parallel shift* would not represent a change in diastolic compliance defined strictly as a change in the slope of the pressure-volume relationship. However, a parallel shift would meet our definition of altered distensibility, because a higher dia-

stolic pressure was needed to achieve the same diastolic volume. In general, parallel shifts in the diastolic pressure-volume relation reflect changes in extrinsic constraints to ventricular filling (Table 20-1). Complex dynamic changes in relaxation rate and other factors reflecting energy-requiring processes may also produce shifts of the dynamic diastolic pressure-volume relation that are apparently parallel in nature. For instance, slowing of left ventricular relaxation may result in a relative elevation in left ventricular diastolic pressure early in diastole, compared to the pressure late in diastole. This could alter the early diastolic pressure-volume relation relative to the late diastolic pressure-volume relation, giving an upward displacement of the entire diastolic pressure-volume relation with either no change in slope, or even a *decrease* in slope of the entire relationship due to the early diastolic pressure-volume relation being shifted higher than the late diastolic pressure-volume relation, as seen in Figure 20-4.

### *Determinants of Ventricular Diastolic Distensibility*

Left ventricular diastolic distensibility is influenced by a multiplicity of factors. These may be considered as factors extrinsic to the ventricular chamber or factors intrinsic to the ventricular myocardium (see Table 20-1). A summary of

TABLE 20-1. Factors that Influence Ventricular Diastolic Distensibility

- 
- |     |  |
|-----|--|
| I.  | Factors Extrinsic to the Ventricular Chamber   |
| A.  | Pericardial properties   |
| B.  | Loading of the contralateral ventricle   |
| C.  | Coronary vascular turgor (erectile effect)   |
| D.  | Extrinsic compression by tumor, pleural pressures, etc.  |
| II. | Factors Intrinsic to the Ventricular Chamber   |
| A.  | Passive elasticity of the ventricular wall (stiffness or compliance when myocytes are completely relaxed)  |
| 1.  | Thickness of ventricular wall, and composition of ventricular wall (muscle, fibrosis, amyloid, hemosiderin), including both endocardium and myocardium |
| 2.  | Temperature, osmolality  |
| B.  | Active elasticity of ventricular wall due to residual cross-bridge activation (cycling and/or latch state) through part or all of diastole:            |
| 1.  | Slow relaxation affecting early diastole only  |
| 2.  | Incomplete relaxation affecting early, mid- and end-diastolic distensibility   |
| 3.  | Diastolic tone, contracture, or rigor  |
| C.  | Elastic recoil (diastolic suction)   |
| D.  | Viscoelasticity (stress relaxation, creep)   |
-

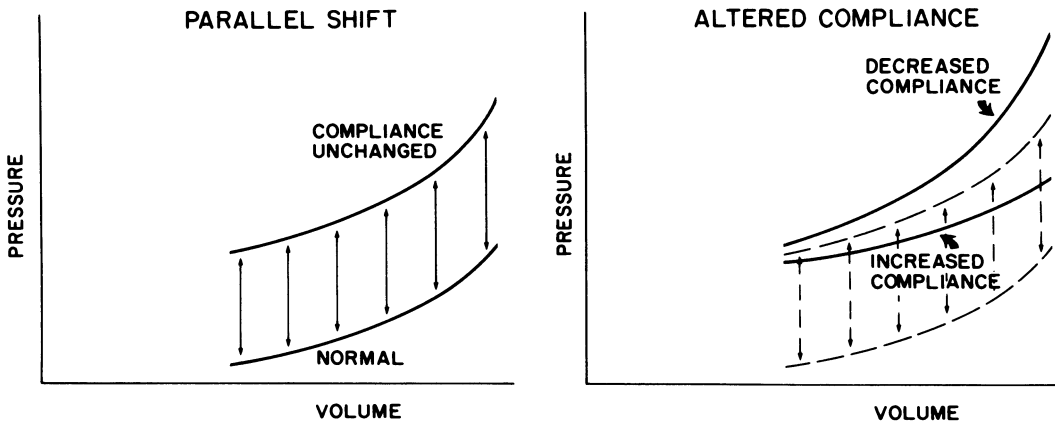


FIGURE 20-4. Schematic illustration of the difference between diastolic distensibility and altered compliance. On the left, the left ventricular diastolic pressure-volume relation has undergone a parallel upward shift. Distensibility is decreased (higher diastolic pressure required to fill the ventricle to the same chamber volume) although compliance (the slope of the pressure-volume relation) is unchanged. On the right, superimposed on the parallel upward shift are curves whose slopes are steeper (decreased compliance) or less steep (increased compliance) than either of the two parallel pressure-volume curves. This illustrates the importance of distinguishing distensibility from compliance, because the curve labeled "increased compliance" nevertheless exhibits decreased distensibility compared to the normal pressure-volume relation.

factors *intrinsic* to the ventricular myocardium that are important as determinants of the left ventricular diastolic pressure-volume relation are presented in Table 20-1. As can be seen, passive elasticity of the ventricular wall is influenced by the thickness of the ventricular wall as well as its composition (muscle, fibrosis, amyloid, hemosiderin). Thus, infiltration with fibrous tissue or amyloid decreases the passive elasticity of the ventricular wall and leads to an increase in diastolic chamber stiffness when myocytes are completely relaxed. An important consideration in the analysis of ventricular diastolic chamber distensibility relates to the contribution of *active elasticity* of the ventricular wall. Active elasticity may be considered the result of residual cross-bridge activation (cycling and/or latch state) through part or all of diastole. Active elasticity may be due to slow relaxation (affecting early diastole only) or incomplete relaxation, affecting early, mid-, and end-diastole. The mechanisms for these changes in "active" diastolic elasticity are the subject of much recent investigation, and most of the chapters in this book touch on one or more of the potential mechanisms involved.

### *Experimental Model of Angina Physiology*

To determine the mechanisms responsible for decreased distensibility of the ischemic myocardium in patients with angina pectoris, we undertook to develop an experimental model that simulated the physiology of angina pectoris [16-21]. In the dog, sudden coronary occlusion produces primary ischemia of myocardial tissue, and results in a rapid and complete loss of contractility for the ischemic segment. This is quite different from the situation seen during demand ischemia in patients with angina pectoris. Cineangiographic and echocardiographic studies during angina pectoris induced by pacing tachycardia [5, 8, 9, 11] show depression of contractile force, but rarely show akinesia or dyskinesia of myocardium that had previously contracted normally. Coronary stenoses placed proximally on the left anterior descending and circumflex coronary arteries can be made quite severe without interfering with resting myocardial function. Indeed, a 90% constriction (diameter) of both the proximal left anterior descending and circumflex coronary arteries in

the dog was not associated with depression of resting contractile function [16–19]. In our experimental model of angina physiology, proximal stenoses are placed on the left anterior descending and circumflex coronary arteries to reduce antegrade flow (measured by electromagnetic flowmeter) to approximately 50% of the resting value. Microsphere studies [20] show that such stenoses do not reduce resting myocardial perfusion in the affected areas, presumably due to collateral supply. Contractile function is normal in these segments, but tachycardia (1.7–2.0 times resting heart rate) for 2 to 3 minutes induces transient “demand ischemia,” which is physiologically similar to the ischemia seen during angina-of-effort in patients with coronary artery disease. Following discontinuation of pacing and the return of the heart rate to the control level, left ventricular diastolic pressure remains elevated, and the diastolic pressure-volume relation curve is shifted up-

ward. As seen in Figure 20–5, there is no change in right ventricular diastolic pressure in this experimental model (open pericardium, open-chest anesthetized dogs). The left ventricular diastolic pressure-volume relation is shifted upward (Figure 20–6), with left ventricular diastolic pressure higher for any given volume. Examination of these pressure-volume curves emphasizes the advantage of the term *distensibility* as defined above, as opposed to terminology related to chamber compliance. As can be seen, it would be difficult to assess the slopes of the diastolic pressure-volume relations as exemplified for the individual beats displayed. Also displayed in Figure 20–6 are left ventricular diastolic pressure-volume curves (dashed lines) at rest and following pulmonary artery constriction. It is apparent that in this open-pericardium model there is little evidence for ventricular diastolic interaction. Substantial overload of the right ventricle is produced by constriction of the

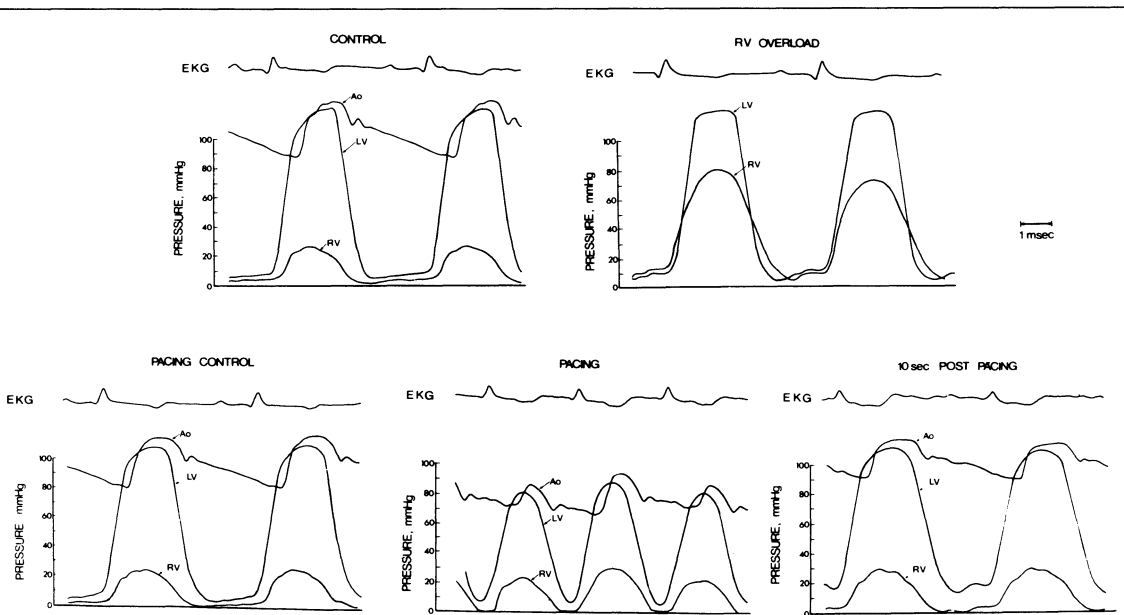


FIGURE 20–5. Left (LV) and right (RV) ventricular pressures during control (*upper left*), pulmonary artery constriction (*upper right*), control with 90% stenoses on left anterior descending and circumflex coronary arteries (*lower left*), pacing tachycardia (*lower middle*), and postpacing (*lower right*) in the presence of coronary stenoses. Left ventricular diastolic pressure is increased following pacing tachycardia in the presence of coronary stenoses. (From Serizawa, et al. [16], with permission.)

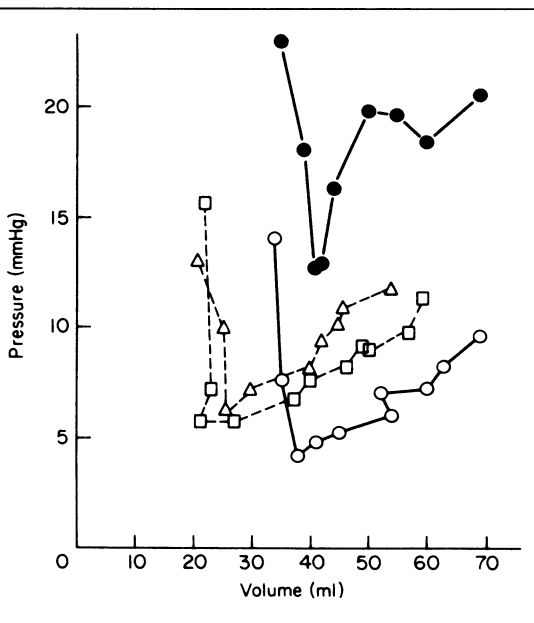


FIGURE 20-6. Left ventricular diastolic pressure-volume relations from the experiment shown in Figure 20-5. The diastolic pressure-volume relation in the presence of coronary stenoses (*open circles*) is shifted upward (*closed circles*) following pacing tachycardia. In the absence of coronary stenoses (*open squares*), the relation is affected minimally following pulmonary artery constriction sufficient to produce a marked rise in right ventricular systolic pressure (*open triangles*) in this open-chest, open-pericardium model. Dashed lines = diastolic pressure-volume curves at rest and following pulmonary artery constriction.

pulmonary artery, shown by the pressure tracings in Figure 20-5; however, in the absence of the pericardium this does not have a substantial effect on the diastolic pressure-volume relation for the left ventricle. This contrasts to the substantial elevation of left ventricular diastolic pressure relative to volume seen during demand ischemia in the same dogs.

When ultrasonic crystals are used to measure myocardial segment lengths in the affected regions, the diastolic pressure-segment length relationship can be assessed. As shown in Figure 20-7, during pacing tachycardia in dogs with coronary stenoses, the diastolic pressure-segment length relationship shifts upward and to the left (curve 2). After 3 minutes of demand

ischemia, termination of pacing is followed by a series of curves (curves 3-6), which show an upward and rightward shift indicative of decreased distensibility as well as some ventricular dilatation.

### *End-Diastolic Distensibility*

Using this experimental model, inferior vena cava occlusion can be employed as a technique to obtain multiple end-diastolic pressure-segment length points, thus allowing inscription of the end-diastolic pressure-segment length relation. This technique has been used by Rankin and co-workers at Duke and is discussed fully in Chapter 12. As Figure 20-8 illustrates, following 2 to 3 minutes of pacing tachycardia to induce demand ischemia, there is alteration in regional myocardial function such that the end-diastolic pressure-segment length relationship is shifted upward, while the end-systolic pressure-segment length relationship is shifted downward. This set of findings documents both decreased distensibility and decreased contractility of the affected myocardial tissue during demand ischemia. These alterations in function are transient, and completely normal function is restored within 1 to 2 minutes following termination of the tachycardia stress.

The intravenous administration of caffeine during pacing tachycardia markedly potentiates the upward shift in left ventricular diastolic pressure-segment length relations that follows termination of the tachycardia [17]. However, administration of an equal intravenous dose of caffeine during pacing tachycardia in dogs *without coronary stenoses* has no effect on the diastolic pressure-segment length relationship. The potentiation of diminished myocardial distensibility by caffeine is consistent with caffeine's known properties of decreasing diastolic calcium uptake by sarcoplasmic reticulum and increasing calcium sensitivity of the myofilaments (as discussed in Chapter 4). Thus, caffeine may exacerbate a diastolic calcium overload state induced by demand ischemia. Caffeine increases myocardial contractility, and it is conceivable that the increased contractility exacerbated the intensity of the demand ischemia. However, caffeine was equally effective in potentiating decreased diastolic distensibility when administered immediately prior to termination of the pacing tachycardia and did not

need to be present during the period of tachycardia stress.

### *Primary Ischemia vs. Demand Ischemia*

It is interesting that in several studies, primary myocardial ischemia produced by coronary occlusion either had no effect or produced an increase in diastolic myocardial distensibility of the affected region [22–24]. In studies comparing demand ischemia and primary ischemia [19, 20], it was found that while demand ischemia usually produced an upward shift in the diastolic pressure-segment length relation, brief primary ischemia, induced by coronary occlusion, produced no change or a slight downward and rightward shift in the diastolic pressure-segment length relation. Rankin and coworkers (Chapter 12) have observed similar changes with primary ischemia, although they have shown that when stress-strain analysis is applied, myocardial stiffness appears to have increased. The explanation for this substantial difference in diastolic behavior is uncertain, but available data provide some clues. As has been pointed out by other investigators, there are many important points of difference between primary ischemia (abrupt reduction in coronary blood flow) and demand ischemia (increased myocardial oxygen requirement in the setting of restricted coronary inflow). First, primary ischemia is associated with a rapid reduction in contractile activity, and severe primary ischemia, which occurs following coronary occlusion, results in cessation of contractile activity for the affected myocardium. It is known that this rapid cessation of myocardial contractile activity is not simply due to a reduction in high energy phosphate production within the affected myocardium. Instead, other factors (e.g., accumulation of inorganic phosphate, hydrogen ion, and a decrease in erectile forces that provide diastolic loading for the sarcomeres) are presumably of major importance in this cessation of contractile activity. In contrast, demand ischemia is associated with continued excitation-contraction coupling and continued development of systolic contractile force, albeit at a reduced level. The cessation of contractile activity with severe primary ischemia means that there is no cross-bridge cycling in systole and therefore no substrate for "impaired relaxation." In addition, rapid accumulation of hydrogen ion in the myo-

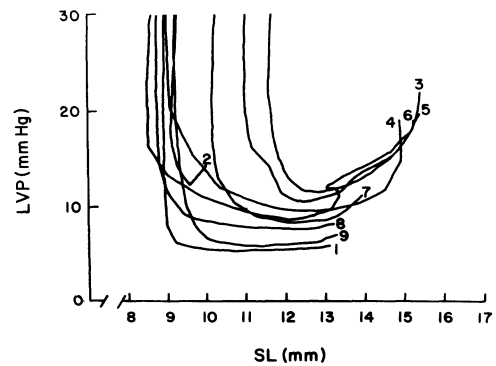


FIGURE 20-7. Diastolic left ventricular pressure (LVP)-segment length (SL) relations in the distribution of the left anterior descending artery in a dog with a 90% proximal stenosis on the left anterior descending artery and circumflex coronary arteries. Curve 1 = pre-pacing; curve 2 = during pacing; curve 3 = first postpacing beat; curve 4 = second postpacing beat; curve 5 = third postpacing beat; curve 6 = fifth postpacing beat; curve 7 = tenth postpacing beat; curve 8 = 30 seconds postpacing; curve; curve 9 = 1 minute postpacing. (From Momomura, et al. [18], with permission.)

cardium distal to a coronary occlusion results in a substantial fall in myocardial pH, and this decline in myocardial pH is 236% greater than the decline in pH seen with demand ischemia of the same duration [20]. As discussed earlier in this book (Chapters 3 and 4), acidosis shifts the force-calcium curve for the myofilaments such that a lower force is produced for any given calcium concentration. Thus, acidosis has a relaxing effect on the myofilaments, which would tend to counteract any decreased distensibility that might otherwise be associated with primary ischemia. An additional factor that characterizes primary ischemia and that may in part account for the absence of altered diastolic distensibility with this type of ischemia concerns the erectile or turgor contribution of coronary blood flow (see Table 20-1). Coronary blood flow and coronary perfusion pressure add an erectile component to myocardial and ventricular stiffness. This turgor component is presumably preserved in demand ischemia, but is strikingly diminished in primary ischemia [25]. It is also possible that differences in high energy phosphate levels within the myocardium in primary vs. demand ischemia could account for

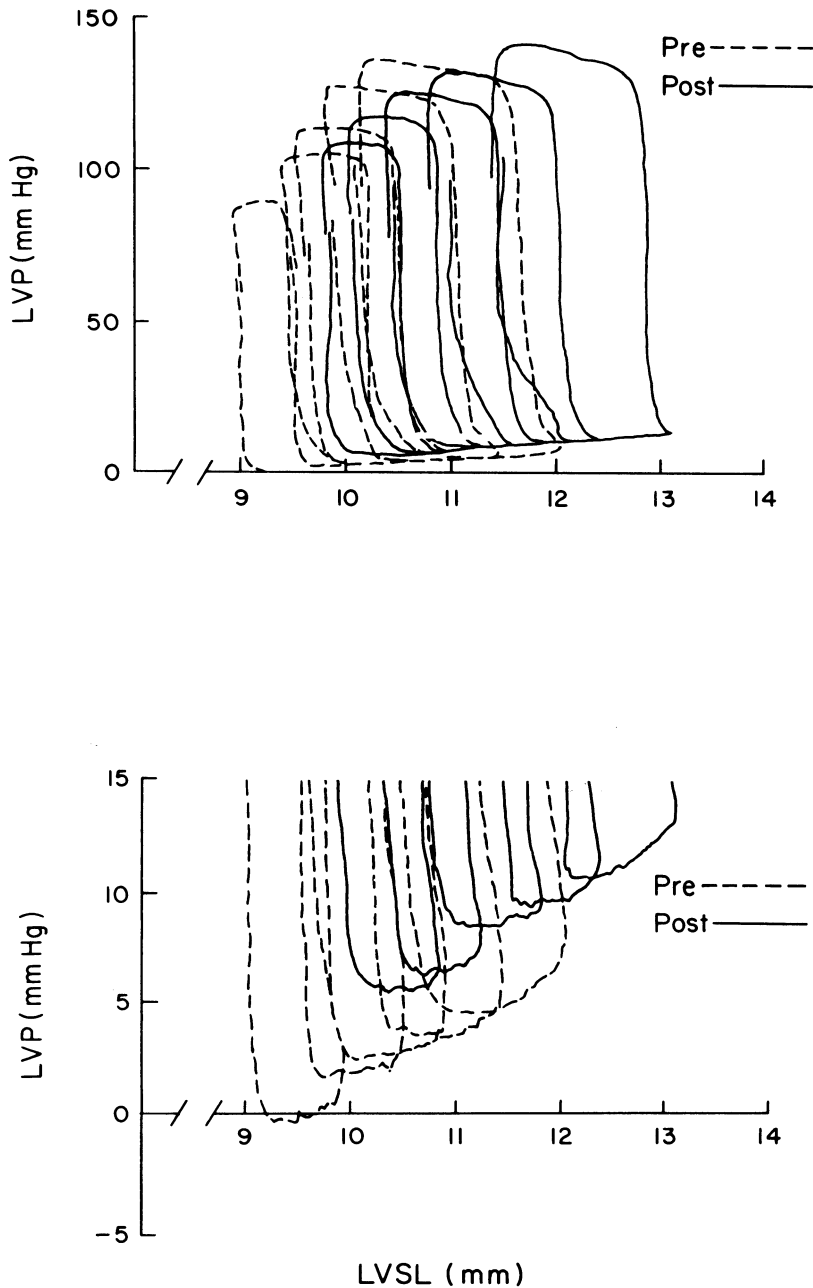


FIGURE 20-8. Left ventricular pressure (LVP)–segment length (LVSL) relations before (pre) and immediately following (post) pacing tachycardia in dogs with coronary stenoses. Multiple diastolic pressure–segment length plots were obtained in each state by using vena cava occlusion to produce a prompt decline in left ventricular preload, as well as unloading of the right ventricle. The end-diastolic pressure–volume relation is clearly shifted upward in the overlap portion of the curves. (From Momomura, et al. [18], with permission.)

the observed differences in diastolic distensibility. However, a careful examination of this from our laboratory [20] found that myocardial adenosine triphosphate (ATP) levels show little decline with 3 minutes of either primary or demand ischemia in the intact dog heart. It is still possible that compartmentalization of ATP differs in these two forms of ischemia, and it is noteworthy that creatine phosphate was much lower in myocardial samples from hearts affected by primary ischemia than those with demand ischemia. This suggested that ATP levels in hearts subjected to primary ischemia might have been relatively well preserved due to glycolytic synthesis of ATP, as opposed to mitochondrial production of ATP in hearts subjected to demand ischemia. Glycolytic ATP may be more effective than aerobically produced ATP in protecting against abnormalities of diastolic relaxation [26, 27].

It must be pointed out that these findings were obtained in experimental animals without prior chronic exposure to coronary stenosis and myocardial ischemia. In humans with long-standing coronary stenosis, sudden complete coronary occlusion by balloon infection during PTCA may be associated with an *upward* shift in the LV diastolic P-V relation, as discussed by Dr. Serrays in Chapter 25. This difference from the response to acute coronary occlusion in the unprepared heart may reflect the presence of well developed collateral flow as well as chronic changes in myocardial metabolism in myocardium subjected to repeated ischemia, as discussed by Drs. Ponleur and Rousseau in Chapter 24. Further studies will be needed to clarify the mechanisms responsible for these apparent differences.

### References

- Grossman W (1985). Why is the left ventricular diastolic pressure increased during angina pectoris? *J Am Coll Cardiol* 5:607-608.
- Muller O, Rorvik K (1958). Hemodynamic consequences of coronary heart disease with observations during anginal pain and on the effect of nitroglycerin. *Br Heart J* 20:302-310.
- Parker JD, DiGiogi S, West RO (1966). A hemodynamic study of acute coronary insufficiency precipitated by exercise: With observations on the effect of nitroglycerin. *Am J Cardiol* 17:470-483.
- O'Brien KP, Higgs LM, Glancy DL, Epstein SE (1969). Hemodynamic accompaniments of angina: A comparison during angina induced by exercise and by atrial pacing. *Circulation* 39:735-743.
- Dwyer EM Jr (1970). Left ventricular pressure-volume alterations and regional disorders of contraction during myocardial ischemia induced by atrial pacing. *Circulation* 42:1111-1122.
- McLaurin LP, Rolett EL, Grossman W (1973). Impaired left ventricular relaxation during pacing induced ischemia. *Am J Cardiol* 32:752-757.
- Barry WH, Brooker JZ, Alderman EL, Harrison DC (1974). Changes in diastolic stiffness and tone of the left ventricle during angina pectoris. *Circulation* 49:255-263.
- Mann T, Brodie BR, Grossman W, McLaurin LP (1977). Effect of angina on the left ventricular diastolic pressure-volume relationship. *Circulation* 55:761-766.
- Sasayama S, Nonogi H, Miyazaki S, et al (1985). Changes of diastolic properties of the regional myocardium during pacing-induced ischemia in human subjects. *J Am Coll Cardiol* 5:599-606.
- Lorell BH, Turi Z, Grossman W (1981). Modification of left ventricular response to pacing tachycardia by nifedipine in patients with coronary artery disease. *Am J Med* 71:667-675.
- Bourdillon PD, Lorell BH, Mirsky I, et al (1983). Increased regional myocardial stiffness of the left ventricle during pacing-induced angina in man. *Circulation* 67:316-323.
- Carroll JD, Hess OM, Hirzel HO, Krayenbuehl HP (1983). Exercise-induced ischemia: The influence of altered relaxation on early diastolic pressures. *Circulation* 67:521-527.
- Carroll JD, Hess OM, Hirzel HO, et al (1985). Left ventricular systolic and diastolic function in coronary artery disease: effects of revascularization on exercise-induced ischemia. *Circulation* 72:119-129.
- McCans JL, Parker JO (1973). Left ventricular pressure-volume relationships during myocardial ischemia in man. *Circulation* 48:775-785.
- Aroesty JM, McKay RG, Heller GV, et al (1985). Simultaneous assessment of left ventricular systolic and diastolic dysfunction during pacing-induced ischemia. *Circulation* 71:889-900.
- Serizawa T, Carabello BA, Grossman W (1980). Effect of pacing-induced ischemia on left ventricular diastolic pressure-volume relations in dogs with coronary stenoses. *Circ Res* 46:430-439.
- Paulus WJ, Serizawa T, Grossman W (1982). Altered left ventricular diastolic properties during pacing-induced ischemia in dogs with coronary stenosis: Potentiation by caffeine. *Circ*

- Res 50:218–227.
18. Momomura SI, Bradley AB, Grossman W (1984). Left ventricular diastolic pressure-segment length relations and end-diastolic distensibility in dogs with coronary stenoses: An angina physiology model. *Circ Res* 55:203–214.
  19. Paulus WJ, Grossman W, Serizawa T, et al (1985). Different effects of two types of ischemia on regional left ventricular systolic and diastolic function. *Am J Physiol* 248:H719–H728.
  20. Momomura SI, Ingwall J, Parker JA, et al (1985). The relationships of high energy phosphates, tissue pH and regional blood flow to diastolic distensibility in the ischemic dog myocardium. *Circ Res* 57:822–835.
  21. Bourdillon PD, Paulus WJ, Seizawa T, Grossman W (1986). Effects of verapamil on regional myocardial diastolic function in pacing-induced ischemia in dogs. *Am J Physiol* 251:H834–H840.
  22. Forrester JS, Diamond G, Parmley WW, Swan HJC (1972). Early increase in left ventricular compliance after myocardial infarction. *J Clin Invest* 51:598–603.
  23. Tyberg JV, Forrester JS, Wyatt HL, et al (1974). An analysis of segmental ischemic dysfunction utilizing the pressure-length loop. *Circulation* 49:748–754.
  24. Palacios I, Johnson RA, Newell JB, Powell WJ Jr (1976). Left ventricular end-diastolic pressure-volume relation with experimental acute global ischemia. *Circulation* 53:428–436.
  25. Vogel WM, Apstein CS, Briggs LL, et al (1982). Acute alterations in left ventricular diastolic chamber stiffness. Role of the “erectile” effect of coronary arterial pressure and flow in normal and damaged hearts. *Circ Res* 51:465–478.
  26. Bricknell OL, Daries PS, Opie LH (1981). A relationship between adenosine triphosphate, glycolysis and ischemic contracture in isolated rat heart. *J Mol Cell Cardiol* 13:941–945.
  27. Apstein CS, Deckelbaum L, Hagopian L, Hood WB (1978). Acute cardiac ischemia and reperfusion: Contractility, relaxation and glycolysis. *Am J Physiol* 235:H637–648.

---

PART IV. CLINICAL  
DISORDERS OF  
DIASTOLIC RELAXATION  
AND COMPLIANCE

---

---

## 21. ALTERED DIASTOLIC DISTENSIBILITY DURING ANGINA PECTORIS

---

Shigetake Sasayama

Numerous studies have been done in both clinical and experimental settings to describe the acute hemodynamic and left ventricular volume changes during ischemia. Although it has been well accepted that an increase in left ventricular filling pressure relative to volume is the characteristic feature of the pacing-induced [1–4] or exercise-induced [5–7] ischemia in the ventricle with limited coronary reserve, controversy has continued on the underlying mechanisms of these changes. Some investigators accounted for an increased left ventricular end-diastolic pressure by an increase in diastolic volume with depressed myocardial contractility, whereby the ventricle moves up toward a higher and steeper portion of the pressure-volume curve [8, 9], while others have emphasized the altered diastolic distensibility of the left ventricular chamber, with the distortion of the entire pressure-volume relation resulting in higher pressures at any given volume [1, 10, 11]. Mann and coworkers [2] studied diastolic left ventricular pressure-volume curves before and immediately following rapid atrial pacing in patients with significant coronary artery stenoses and demonstrated that both impaired left ventricular systolic performance and altered left ventricular diastolic properties play a role in producing elevated left ventricular diastolic pressure during ischemia. The relative contributions of these two mechanisms were assessed by Aroesty and colleagues [12] using radio-nuclide angiography. Using serial pressure-volume analysis in conjunction with pressure

recordings, they demonstrated that the ischemic response to pacing tachycardia involves both systolic and diastolic dysfunction but that diastolic impairment precedes systolic depression. From the latter finding, these investigators suggested that impaired diastolic performance is the first manifestation of ischemia.

Proposed mechanisms for the upward shift of the pressure-volume relation include impaired left ventricular relaxation, altered elastic and viscous properties, and changes in properties extrinsic to the left ventricle [11, 13]. In studying the diastolic properties of the diseased human left ventricle, Ross [14] emphasized consideration of the interaction of the left ventricle with the right ventricle as well as with the pericardium. The pericardium has been thought to affect the pressure-volume relation by coupling left and right ventricular pressure [14–17]. However, studies that reproduced the upward shift of the left ventricular pressure-volume relation in dogs with coronary stenosis in the absence of the pericardium [3] militate against its role in this phenomenon.

On the other hand, even without a distinct role for the pericardium, right ventricular filling can have an effect on elevating left ventricular end-diastolic pressure due to factors such as septal displacement, increased septal stiffness, or stretching of common fibers. Hess and coworkers [18] offered further evidence for this connection, showing that the upward shift of the diastolic pressure-volume curve during complete coronary occlusion in the conscious dog was prevented by reduction in right ventricular pressure and volume with obstruction of the inferior vena cava. In the more recent study of Momomura and associates [19], vena caval

*Grossman, William, and Lorell, Beverly H. (eds.), Diastolic Relaxation of the Heart. Copyright © 1987. Martinus Nijhoff Publishing. All rights reserved.*

occlusion failed to abolish the upward shift of pressure-length relations following pacing tachycardia in open-chest dogs with high grade stenoses, even when right ventricular pressure was reduced to zero. These findings led the authors to conclude that extrinsic compression of the left ventricle by the right ventricle is unlikely to be responsible for the upward shift. Although many issues have been raised as described above, much more information is needed before we can define with certainty the mechanisms underlying alternations in the shape and position of left ventricular diastolic pressure-volume curves during angina.

Cardiac ischemia is essentially regional in nature, and its analysis should be directed to the regional as well as the global function of the ventricle for a comprehensive understanding of the mechanics of myocardial ischemia. In animal experiments, varieties of methods provide sufficiently accurate measures of differing dimensions of regional performance [20, 21]. However, the methodologies are substantially limited for quantitative evaluation of such regional function in humans. For this purpose, we developed a computer-assisted image processing system that allowed us to relate the shift in the left ventricular pressure-volume relation to a regional change in distensibility during pacing-induced angina in patients with coronary artery disease [4, 22-24].

### *Cineangiographic Techniques and Analysis of Ventricular Mechanics*

Patients with coronary artery disease and effort angina were studied [23]. At the time of diagnostic cardiac catheterization, left ventricular cineangiography was performed in the 30-degree right anterior oblique projection at a filming rate of 60 frames per second using a high-fidelity micromanometer-tipped catheter, which allowed the simultaneous measurement of left ventricular pressure during ventriculography. Heart rate was increased incrementally with cardiac pacing by 30 beats/minute every 2 minutes until angina pectoris developed or a ventricular rate of 150 beats/minute was achieved. Pacing was then stopped and a second angiogram was obtained on cessation of pacing in the same manner as in the control state.

The left ventricular images on cine film were transferred to a computer through a flying-spot

scanner. The ventricular boundary was delineated using the image-processing system we developed [4]. The ventricular silhouette area of the digitized image was calculated from the amount of pixels surrounded by the ventricular boundary. Left ventricular volumes were calculated by the area-length method. The calculated volume of each frame was synchronized to corresponding pressure throughout the cardiac cycle and the pressure-volume loop was obtained. Sequential ventricular silhouettes were superimposed on the end-diastolic frame throughout the cardiac cycle by using external reference markers. We chose the geometric center of gravity of the cavity as the fixed reference point to which the inward movement of the ventricular wall can be related. In each superimposed ventricular image, radial grids were drawn from the center of gravity of the end-diastolic silhouette to the endocardial margin. Measurement of the length of each grid line throughout

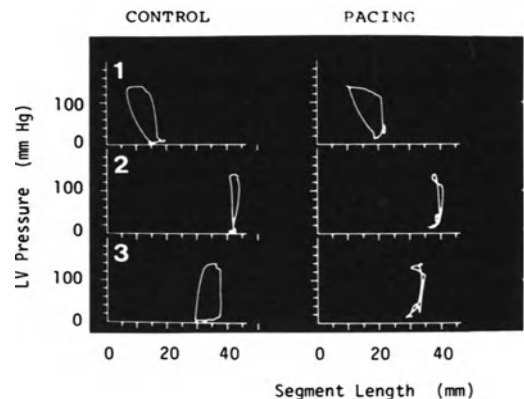


FIGURE 21-1. To analyze regional wall motion of the left ventricle, radial grids are drawn from the geometric center of gravity of the end-diastolic silhouette to the endocardial margin. Each of the 128 radial grid lines represents the segmental systolic centripetal motion of a given point of the ventricular circumference. Three segments representing normal (1), central ischemic (2), and potentially ischemic areas (3) were selected. The pressure-length loops were constructed from the simultaneous pressure-length data for each segment. The left panel shows the resting state, the right panel shows the condition after rapid cardiac pacing. LV = left ventricular. (From Sasayama, et al. [22], with permission).

the cardiac cycle allowed for analysis of contraction and relaxation of specific segments of the left ventricular myocardium.

We analyzed the effect of pacing stress on the segmental contraction of normal sections perfused with patent coronary arteries and of potentially ischemic regions corresponding to known coronary lesions. In the latter, active shortening was preserved at rest, but acute reversible abnormalities in segment shortening were provoked when oxygen requirements exceeded a fairly constant level.

The lengths of the given radial grid of the normal and the ischemic regions of each frame were also related to the corresponding pressure to obtain pressure-length loops simultaneously in two different portions of the left ventricular wall (Figure 21-1).

### *Effect of Ischemia on Global and Regional Function of the Left Ventricle*

All patients showed significant coronary artery stenosis or obstruction and developed typical anginal pain during pacing tachycardia. In the postpacing beats, the heart rate did not change significantly. Left ventricular peak systolic pressure remained unchanged, while end-diastolic

pressure increased from  $10 \pm 3$  mm Hg to  $23 \pm 9$  mm Hg ( $p < 0.005$ ). Although there were no consistent changes in left ventricular end-diastolic volume, end-systolic volume uniformly increased. Stroke volume was unaltered, but the ejection fraction was reduced significantly (Table 21-1). Rapid cardiac pacing elicited short-term reversible abnormalities in segmental function in the postpacing ventriculogram. Active contraction was maintained at rest in the ischemic segment, although the coronary reserve was critically limited. End-diastolic length remained unchanged in the postpacing beat, and stroke excursion was decreased by 62% ( $p < 0.01$ ). In the normally perfused segment, end-diastolic length was augmented by 14% from the control value ( $p < 0.005$ ) and was associated with a 23% increase ( $p < 0.05$ ) in stroke excursion (see Table 21-1) [23, 24].

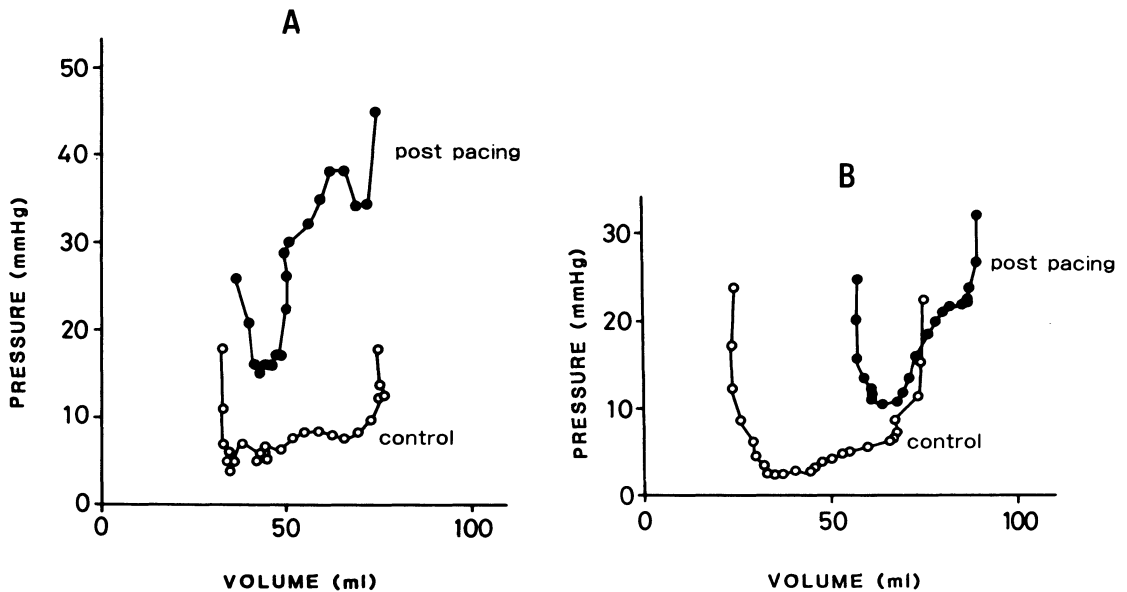
### *Left Ventricular Chamber Stiffness and Distensibility of the Regional Myocardium*

When global left ventricular compliance was analyzed by the diastolic pressure-volume relation, there were two different responses. In four of the seven patients, the pressure-volume

TABLE 21-1. Hemodynamic Data Before and After Pacing

	Control	Postpacing before N	Postpacing after N	(C-P)	Significance (p) (C-N)	(P-N)
Normal segment length						
End-diastolic	26.1 ± 5.2	29.7 ± 6.1	27.4 ± 4.6	< 0.01	NS	< 0.05
End-systolic	16.2 ± 5.9	17.3 ± 5.9	14.3 ± 3.3	< 0.05	NS	< 0.05
Extent of shortening	9.9 ± 2.0	12.2 ± 3.4	13.1 ± 3.3	< 0.05	< 0.05	< 0.05
Ischemic segment length						
End-diastolic	29.3 ± 7.2	29.4 ± 6.0	29.3 ± 5.2	NS	NS	NS
End-systolic	18.0 ± 9.6	25.2 ± 6.8	20.7 ± 3.2	< 0.01	NS	< 0.05
Extent of shortening	11.4 ± 5.2	4.3 ± 1.8	8.7 ± 3.1	< 0.01	NS	< 0.05
Heart rate	74 ± 12	74 ± 15	90 ± 19	NS	< 0.05	< 0.05
Left ventricular pressure						
Peak	148 ± 29	162 ± 27	134 ± 20	< 0.01	NS	< 0.05
End-diastolic	10 ± 5	23 ± 9	13 ± 7	< 0.01	NS	< 0.05
Left ventricular volume						
End-diastolic	99 ± 29	113 ± 27	97 ± 22	< 0.05	NS	< 0.01
End-systolic	35 ± 21	52 ± 20	35 ± 14	< 0.05	NS	< 0.01
Stroke volume	64 ± 14	61 ± 19	62 ± 16	NS	NS	NS
Ejection fraction	66 ± 10	54 ± 13	64 ± 12	< 0.05	NS	< 0.01

N = nifedipine; NS = not significant; C-P = comparison between control and post-pacing; C-N = comparison between control and post-pacing with nifedipine; P-N = comparison between postpacing before and after pretreatment with nifedipine. (From Nonogi et al. [24], with permission.)



curves shifted upward in the postpacing beat (Figure 21-2A), while in the remaining three patients the curve shifted more to the right (Figure 21-2B).

Despite these variabilities in ischemic responses of the left ventricular chamber, the displacement of the regional diastolic pressure-length relation of normal and ischemic segments during pacing induced ischemia was entirely uniform. Figure 21-3 illustrates representative plots of left ventricular pressure against normal and ischemic segment lengths throughout passive ventricular filling for the same patients shown in Figure 21-2. The increase in left ventricular diastolic pressure was accompanied by comparable increases in end-diastolic length in normal segments. Thus, the normal segment appeared to be operating at the higher portion of a single pressure-length curve. In ischemic segments, pressure was higher for any given segment length in the postpacing beat, and the pressure-length curves shifted upward, indicating regional alteration in diastolic properties of the ischemic myocardium.

In the ischemic myocardium, the sarcomere may be overstretched with disengagement and rupture of the actin filaments [25], resulting in the greater limitation of the preload reserve.

FIGURE 21-2. Left ventricular diastolic pressure-volume relations before (*open circles*) and after (*closed circles*) rapid cardiac pacing in two representative patients with coronary artery disease who developed angina during cardiac pacing. The entire curve shifted directly upward in some patients (A), and the curve shifted upward and more to the right in others (B). (From Sasayama, et al. [23], with permission).

Thus, an additional ischemic insult with pacing stress in patients with preexisting coronary artery disease, will result in a less marked change in diastolic length in the ischemic region than in the normal region.

Bourdillon and coworkers [26] derived a radial stiffness modulus from the simultaneous thickness and pressure data using a new approach to the assessment of regional myocardial stiffness. This method permitted the assessment of the material properties of a single ischemic region of the left ventricular myocardium in the clinical setting. The stiffness modulus thus obtained was shown to increase during pacing induced angina. These authors concluded that this regional increase in myocardial stiffness contributed to the upward shift in pressure-wall thickness and pressure-volume relationships during ischemia, together with a decreased rate of wall thinning and slow active-pressure decay.

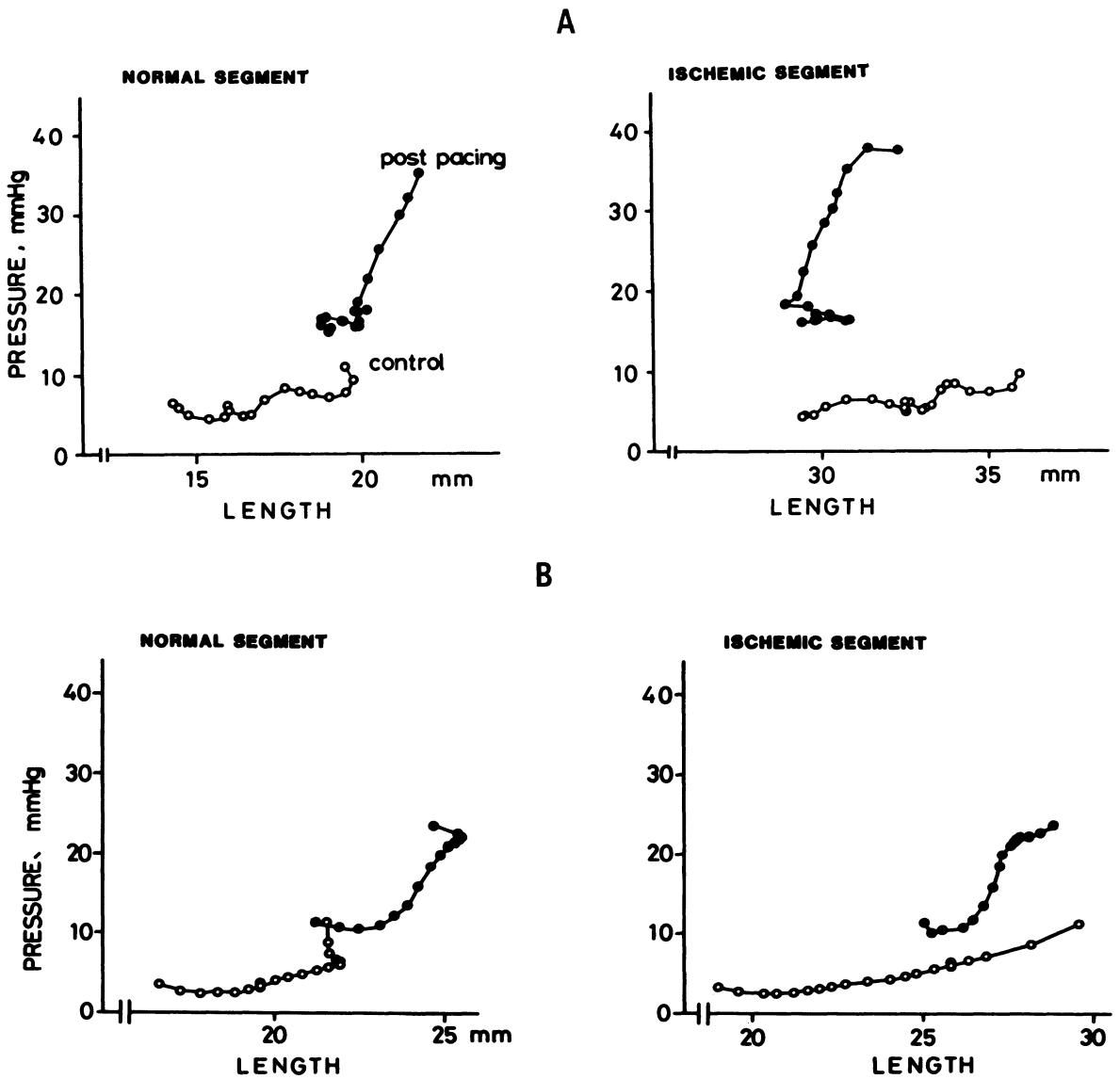


FIGURE 21-3. Plots of left ventricular pressure against normal and ischemic segment lengths before (*open circles*) and after (*closed circles*) rapid cardiac pacing. Despite different responses in the pressure-volume loops, changes in the pressure-length relation are uniform in both cases A and B: the normal segment moves up to the higher portion of the single pressure-length relation, and the ischemic segment shifts upward directly so that pressure is higher at any given length. (From Sasayama, et al. [23], with permission.)

More recently, similar changes in the regional constant of elastic stiffness were documented in response to transient abrupt coronary occlusion in humans during angioplasty of the stenosis in a single, proximal, left anterior, descending coronary artery [27]. These abnormalities in diastolic function were shown to persist after the procedure when normal blood flow and systolic function had been completely restored.

### *Mechanism of an Increase in Diastolic Stiffness*

The precise mechanism for an increase in myocardial stiffness with ischemia remains speculative at present. Hess and colleagues [18] studied the sequential effects of both partial and complete coronary occlusions on diastolic properties of the left ventricle in a conscious dog and demonstrated that myocardial wall stiffness was not changed during coronary occlusion when systolic wall thickening was reduced but maintained, whereas it increased significantly during complete occlusion when there was systolic wall thinning. Accordingly, they concluded that the changes in myocardial stiffness were dependent on systolic overstretch of the ischemic region. Subsequent experiments of Paulus and co-workers [28] showed that the radial stiffness was less during coronary occlusion than after pacing tachycardia in the presence of a coronary stenosis. Thus, repeated systolic stretch of the segment subserved by an occluded coronary artery was assumed to prevent an increase in diastolic stiffness by either breaking or preventing the formation of rigor bonds within the ischemic cells.

It has been shown that relaxation in heart is a complex phenomenon. The transition from the active to the resting state requires a reduction in the cytosolic concentration of  $\text{Ca}^{2+}$ , achieved by a rapid sequestration into the sarcoplasmic reticulum and the return of some  $\text{Ca}^{2+}$  to the extracellular phase. The energy required for this process is derived from the hydrolysis of adenosine triphosphate (ATP) via a calcium-activated ATPase in the limiting membranes of the sarcoplasmic reticulum.

A failure of muscle to relax in hypoxic state may involve a rise in cytosolic  $\text{Ca}^{2+}$  to such a level that the rapid  $\text{Ca}^{2+}$  accumulating activity of the sarcoplasmic reticulum is inadequate, in association with a rapid decline in the tissue

stores of ATP and creatine phosphate and in the respiratory activity of their mitochondria.

It is generally agreed that the decline in high energy phosphate reserves of heart muscle could lead to a slowed rate of calcium accumulation from the cytosol [29]. A raised cytosolic calcium level surrounding the contractile proteins and the decreased availability of ATP for actin-myosin cross-bridge dissociation may be responsible for increased stiffness of the ischemic myocardium [29].

### *Effect of a Calcium Antagonist on Diastolic Properties of the Ischemic Myocardium*

As discussed previously, the increased cytosolic  $\text{Ca}^{2+}$  concentration depletes the hypoxic muscle of its energy stores and limits the availability of ATP for cross-bridge relaxation. The residual cross-bridges within the contractile units remaining throughout diastole could cause diastolic interaction of the contractile elements and a reversible form of contracture. In the isolated rabbit heart such myocardial contracture and accumulation of calcium were prevented by the calcium antagonist nifedipine [30].

We also studied the effects of nifedipine on regional systolic and diastolic dysfunction during pacing-induced ischemia in patients with coronary artery disease [24, 31]. The left ventriculograms were obtained in the control and postpacing periods both before and after treatment with nifedipine. All patients developed typical angina during pacing tachycardia before administration of nifedipine but not after taking the drug.

With nifedipine, a postpacing increase in end-diastolic pressure was markedly attenuated, with a reduction in left ventricular systolic pressure. The responses of the regional myocardium to the same pacing stress were markedly reduced (Figure 21-4). The upward shift of the diastolic pressure-length relation of the regional ischemic segment and movement of the control segment toward a higher portion of the single relation were remarkably attenuated or abolished in the postpacing beats after the administration of nifedipine (Figure 21-5), (see Table 21-1).

These data suggest that prevention of myocardial cell calcium overload by nifedipine appears to be a major mechanism for an im-

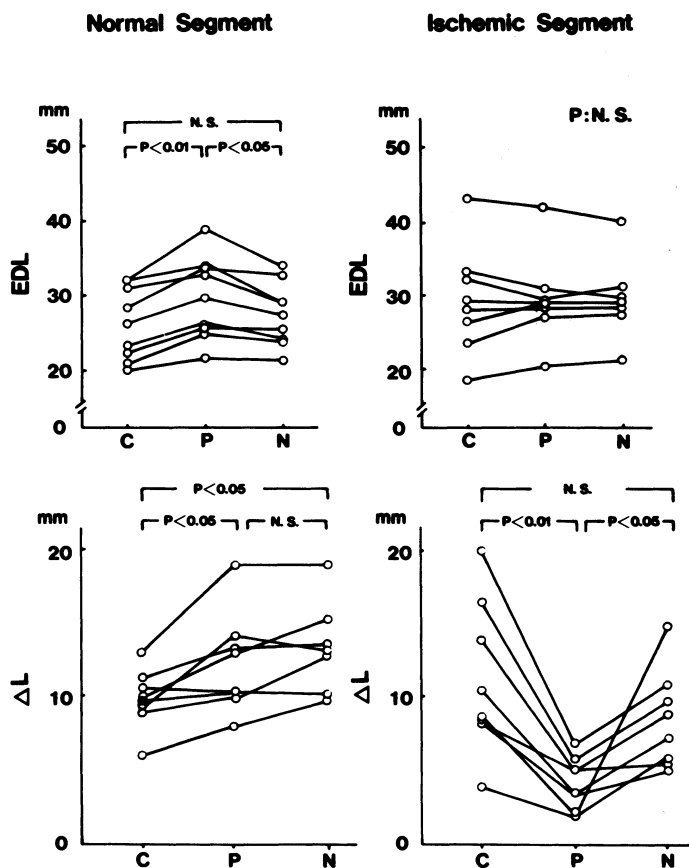


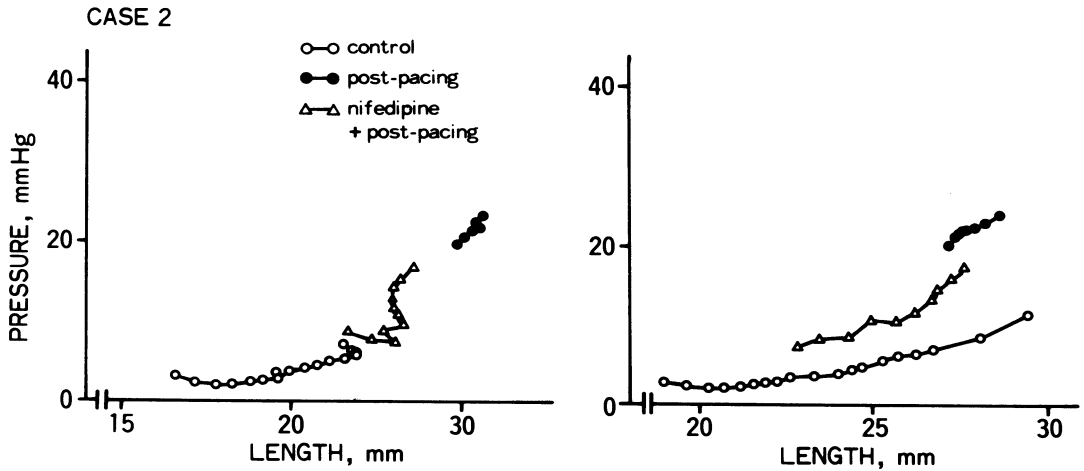
FIGURE 21-4. Regional myocardial responses to pacing stress before and after treatment with nifedipine. Individual changes in end-diastolic length (EDL) and extent of segment shortening ( $\Delta L$ ) of normal and ischemic regional myocardial segments in response to pacing stress before and after treatment with nifedipine, C = control; P = post pacing; N = nifedipine + post pacing N.S. = not significant. (From Sasayama, et al. [31] with permission.)

provement in the ischemic changes in diastolic properties of the left ventricle. Conversely, caffeine, which prolongs intracellular calcium availability through both impaired calcium sequestration by the sarcoplasmic reticulum and increased calcium influx through the sarcolemma, has been shown to markedly potentiate the pacing-induced upward shift of the pressure-volume relationship in the canine ventricle with coronary stenosis [32].

#### *Interaction of Ischemic and Nonischemic Myocardium*

Animal experiments have shown that ischemia due to coronary stenosis has substantially different effects on regional wall motion and sequential diastolic mechanics than does ischemia due to coronary occlusion [18, 19]. These studies emphasized the creep phenomenon associated with repeated systolic stretching by adjacent nonischemic myocardium or quantitative interaction of systolic performance during ischemia as factors determining diastolic properties of the ischemic myocardium.

On the other hand, when global left ventricular ischemia was induced by constriction of left main coronary artery in the conscious dog, left ventricular chamber compliance was de-



creased as evidenced by a leftward shift of the diastolic pressure-volume strain relationship without systolic bulging or dyssynchronous systolic shortening. These results were thought to suggest that the mechanical changes during diastole induced by global left ventricular ischemia (creep and increased myocardial stiffness) were identical to those that occur during regional ischemia and that the regional abnormalities were also the direct result of ischemia rather than the result of mechanical interactions between ischemic and nonischemic regions of the ventricle [33]. Segmental function analysis of the left ventriculograms in the clinical setting, revealed the direct upward shift in the diastolic pressure-length plots of the ischemic segment, which implies an altered distensibility in the regional ischemic myocardium. This in turn contributed to an augmented preload of the normally perfused regions of the same ventricle which moved toward a higher portion of the single diastolic pressure-length curve [23] (see Figure 21-3, 21-5).

In summary, our study of the mechanisms involved in the altered diastolic distensibility during angina pectoris in patients with coronary artery disease led to the following observations. During attacks of pacing-induced angina, left ventricular end-diastolic pressure increased characteristically. Increases in filling pressure were associated with two types of shift in the left ventricular diastolic pressure-volume curve, either directly upward or upward and more to

the right. The segmental diastolic pressure-length relationship of the ischemic region consistently shifted upwards, while that of the normal segment moved to a higher portion of a single curve. These observations suggest that a complex interaction between changes in the mechanical properties of the regional myocardium might be responsible for the net global changes in ventricular chamber compliance. Increased diastolic stiffness of the ischemic myocardium most likely results from incomplete relaxation and increased cytosolic  $Ca^{2+}$  concentrations due to low availability of the ATP, necessary for actin-myosin cross-bridge dissociation and calcium sequestration. This concept was supported by the observation that the calcium antagonist nifedipine substantially attenuated the upward shift of the diastolic pressure-length relationship of the regional ischemic segment. (From Sasayama, et al. [31], with permission.)

the right. The segmental diastolic pressure-length relationship of the ischemic region consistently shifted upwards, while that of the normal segment moved to a higher portion of a single curve. These observations suggest that a complex interaction between changes in the mechanical properties of the regional myocardium might be responsible for the net global changes in ventricular chamber compliance. Increased diastolic stiffness of the ischemic myocardium most likely results from incomplete relaxation and increased cytosolic  $Ca^{2+}$  concentrations due to low availability of the ATP, necessary for actin-myosin cross-bridge dissociation and calcium sequestration. This concept was supported by the observation that the calcium antagonist nifedipine substantially attenuated the upward shift of the diastolic pressure-length relationship of the regional ischemic segment.

## References

1. Dwyer EM Jr (1970). Left ventricular pressure-volume alterations and regional disorders of contraction during myocardial ischemia induced by atrial pacing. *Circulation* 42:1111-1122.
2. Mann T, Brodie BR, Grossman W, McLaurin LP (1977). Effect of angina on the left ventricular diastolic pressure-volume relationship. *Circulation* 55:761-766.
3. Serizawa T, Carabello BA, Grossman W (1980). Effect of pacing-induced ischemia on left ventricular diastolic pressure-volume relations in dogs with coronary stenoses. *Circ Res* 46:430-439.
4. Fujita M, Sasayama S, Kawai C, et al (1981). Automatic processing of cineventriculograms for analysis of regional myocardial function. *Circulation* 63:1065-1074.
5. Carroll JD, Hess OM, Hirzel HO, Krayenbuehl HP (1983). Exercise-induced ischemia: The influence of altered relaxation on early diastolic pressures. *Circulation* 67:521-528.
6. Tomoike H, Franklin D, McKown D, et al (1978). Regional myocardial dysfunction and hemodynamic abnormalities during strenuous exercise in dogs with limited coronary flow. *Circ Res* 42:487-496.
7. Sharma B, Goodwin JF, Raphael MK, et al (1976). Left ventricular angiography on exercise: A new method of assessing left ventricular function in ischemic heart disease. *Br Heart J* 38:59-70.
8. Parker JO, Ledwich JR, West RO, Case RB (1969). Reversible cardiac failure during angina pectoris: Hemodynamic effects of atrial pacing in coronary artery disease. *Circulation* 39:745-757.
9. McCans JL, Parker JO (1973). Left ventricular pressure-volume relationships during myocardial ischemia in man. *Circulation* 48:775-785.
10. McLaurin LP, Rolett EL, Grossman W (1973). Impaired left ventricular relaxation during pacing-induced ischemia. *Am J Cardiol* 32:751-757.
11. Grossman W, Mann JT (1978). Evidence for impaired left ventricular relaxation during acute ischemia in man. *Eur J Cardiol* 7(suppl):239-249.
12. Aroesty JM, McKay RG, Heller GV, et al (1985). Simultaneous assessment of left ventricular systolic and diastolic dysfunction during pacing-induced ischemia. *Circulation* 71:889-900.
13. Grossman W, McLaurin LP (1976). Diastolic properties of the left ventricle. *Ann Intern Med* 84:316-326. 1976.
14. Ross J Jr (1979). Acute displacement of the diastolic pressure-volume curve of the left ventricle: Role of the pericardium and the right ventricle. *Circulation* 59:32-37.
15. Glantz SA, Misbach GA, Moores WY, et al (1978). The pericardium substantially affects the left ventricular diastolic pressure-volume relationship in the dog. *Circ Res* 42:433-441.
16. Janicki JS, Weber KT (1980). Factors influencing diastolic pressure-volume relation of the cardiac ventricles. *Fed Proc* 39:133-140.
17. Refsum B, Junemann M, Lipton MJ, et al (1981). Ventricular diastolic pressure-volume relations and the pericardium: Effects of changes in blood volume and pericardial effusion in dogs. *Circulation* 64:997-1004. 1981.
18. Hess OM, Osakada G, Lavelle JF, et al (1983). Diastolic myocardial wall stiffness and ventricular relaxation during partial and complete coronary occlusions in the conscious dog. *Circ Res* 52:387-400.
19. Momomura S, Bradley AB, Grossman W (1984). Left ventricular diastolic pressure-segment length relations and end-diastolic distensibility in dogs with coronary stenoses: An angina physiology model. *Circ Res* 55:203-214.
20. Theroux P, Franklin D, Ross J Jr, Kemper WS (1974). Regional myocardial function during acute coronary artery occlusion and its modification by pharmacologic agents in the dog. *Circ Res* 35:896-908.
21. Sasayama S, Franklin D, Ross J Jr, et al (1976). Dynamic changes in left ventricular wall thickness and their use in analyzing cardiac function in the conscious dog: A study based on a modified ultrasonic technique. *Am J Cardiol* 38:870-879. 1976
22. Sasayama S, Nonogi H, Fujita M, et al (1984). Analysis of asynchronous wall motion by regional pressure-length loops in patients with coronary artery disease. *J Am Coll Cardiol* 4:259-267.
23. Sasayama S, Nonogi H, Miyazaki S, et al (1985). Changes in diastolic properties of the regional myocardium during pacing-induced ischemia in human subjects. *J Am Coll Cardiol* 5:599-606.
24. Nonogi H, Sasayama S, Miyazaki S, et al (1985). Modification of pacing-induced alterations in diastolic properties of the regional myocardium by nifedipine in patients with coronary artery disease. *Heart Vessels* 1: 232-238.
25. Crozatier B, Ashraf M, Franklin D, Ross J Jr (1977). Sarcomere length in experimental myocardial infarction: evidence for sarcomere overstretch in dyskinetic ventricular regions. *J Mol Cell Cardiol* 9:785-797.
26. Bourdillon PD, Lorell BH, Mirsky I, et al (1983). Increased regional myocardial stiffness

- of the left ventricle during pacing-induced angina in man. *Circulation* 67:316–323.
27. Wijns W, Serruys PW, Slager CJ, et al (1986). Effect of coronary occlusion during percutaneous transluminal angioplasty in humans on left ventricular chamber stiffness and regional diastolic pressure-radius relations. *J Am Coll Cardiol* 7:455–463.
  28. Paulus WJ, Grossman W, Serizawa T, et al (1985). Different effects of two types of ischemia on myocardial systolic and diastolic function. *Am J Physiol* 248:H719–H728.
  29. Nayler WG, Williams A (1978). Relaxation in heart muscle: Some morphological and biochemical considerations. *Eur J Cardiol* 7(suppl): 35–50.
  30. Henry PD, Schuchlieb R, Davis J, et al (1977). Myocardial contracture and accumulation of mitochondrial calcium in ischemic rabbit heart. *Am J Physiol* 233: H677–H684.
  31. Sasayama S, Nonogi H, Asanoi H, et al (1986). Effects of nifedipine on pacing-induced ischemia: Modification of regional myocardial function and coronary hemodynamics. In Lichtlen PR (ed): *New Therapy of Ischemic Heart Disease and Hypertension*. Amsterdam: Excerpta Medica, pp 137–146.
  32. Paulus WJ, Serizawa T, Grossman W (1982). Altered left ventricular diastolic properties during pacing-induced ischemia in dogs with coronary stenoses: Potentiation by caffeine. *Circ Res* 50:218–227.
  33. Visner MS, Arentzen CE, Parrish DG, et al (1985). Effects of global ischemia on the diastolic properties of the left ventricle in the conscious dog. *Circulation* 71:610–619.

---

## 22. DIASTOLIC FUNCTION DURING EXERCISE-INDUCED ISCHEMIA IN MAN

---

John D. Carroll, Otto M. Hess, Hans Peter Krayenbuehl

Diastolic pressures frequently increase dramatically during ischemia. The mechanism for the pressure increase has been the subject of many clinical and experimental studies [1–5]. Impaired relaxation has been shown in humans during pacing-induced ischemia [2]. The alterations in left ventricular pressure decay may be important in elevating diastolic pressures, producing the upward shift in the diastolic pressure-volume relation, and impairing the time course and extent of left ventricular filling.

Many episodes of ischemia, with or without angina, occur during exercise, particularly in the patient with stable, chronic coronary artery disease. Therefore, dynamic exercise was used in our studies to induce ischemia [6–11]. The use of micromanometer pressures and biplane cineangiographic volumes allowed us to acquire high-quality data for subsequent analysis.

Studies were undertaken both to quantify the abnormalities in left ventricular function during exercise and to understand the mechanisms important in producing these functional abnormalities. Certain patient groups were of particular interest and useful in achieving these goals. The first were patients who were found to have no significant cardiovascular abnormalities. They represent our control group and are believed to show normal or near normal left ventricular function during exercise. The second group were patients with severe coronary artery disease with inducible ischemia. Their exercise hemodynamics allow a characterization of ische-

mia to be contrasted with control subjects. The third group were patients who had had successful bypass surgery. They provided an opportunity to assess the efficacy of surgery in reversing diastolic and relaxation abnormalities. Furthermore, with the aid of intraoperative biopsies, the role of chronic structural changes and abnormalities in passive muscle compliance can be assessed. Finally, a fourth group were patients with past myocardial infarction, but without inducible ischemia. During exercise, this group, like the ischemia group, had an inhomogenous contraction pattern that may, by itself, affect left ventricular pressure decay and other diastolic properties.

### *Methods*

#### PATIENT POPULATION

The characteristics of the patients studied have been reported previously in detail [6–11]. The *control group* consisted of five patients who had no or minimal cardiovascular disease. All were undergoing catheterization because of atypical chest pain.

The *ischemia group*, consisting of 23 patients, had significant coronary artery disease (greater than 50% diameter narrowing of at least one coronary artery). Fifteen had three-vessel disease, five had two-vessel disease, and three had single-vessel narrowings. All had exercise-induced regional-wall motion abnormalities with a fall in ejection fraction. Fourteen had accompanying angina.

The *bypass group*, consisting of 24 patients, had stable angina refractory to medical therapy before surgery. Six had two-vessel disease and the remainder had three-vessel disease. All had

exercise-induced ischemia at the time of preoperative catheterization. All patients subsequently underwent bypass surgery with a total of 83 distal anastomoses placed. After an average of 7.7 months following surgery, cardiac catheterization was completed with a repeat exercise study. These patients were selected on the basis of improved symptoms after surgery (only five had any angina) and having 81/83 patent grafts.

The *scar group*, consisting of five patients, had a prior infarction with a large akinetic/dyskinetic area with reduced left ventricular ejection fraction on a resting angiogram. None showed a new wall-motion abnormality with exercise. None had angina, two had normal coronary arteries, and three had one-vessel disease of the coronary artery appropriate to the site of prior infarction.

#### CARDIAC CATHETERIZATION

Informed consent was obtained from all patients. Premedication consisted of 10 mg of chlordiazepoxide. Cardiovascular medications were withheld for 12 to 24 hours before catheterization.

Patients were evaluated by catheterization of the right and left sides of the heart and biplane cineangiography at rest and during supine bicycle exercise. Left ventricular pressure was measured with a Millar pigtail angiographic catheter introduced from the femoral artery. Pressures were recorded at a paper speed of 250 mm/second (Figure 22-1). Mean right atrial pressure was recorded in some patients with a fluid-filled catheter.

Biplane left ventricular cineangiograms were obtained at a filming rate of 50 frames/second. Volumes were calculated by the area-length method. Each angiographic frame had a digital time corresponding to time marks on the pressure recordings.

#### EXERCISE PROTOCOL

All patients underwent bicycle exercise testing before catheterization to determine achieved workload and exercise limitations. At catheterization, pressures were recorded before and after each patient's feet were strapped to the bicycle device. After the resting angiogram and a subsequent 12- to 15-minute pause, patients began to exercise at a low level. Workloads were increased progressively until either angina or other limiting symptoms occurred or until a predicted submaximal heart rate was achieved.

Scar group and control group patients generally achieved the target heart rate. Bypass group patients followed the same exercise protocol they had followed before surgery to match external workloads. Exercise duration and maximal workload were, therefore, identical for both studies. At the point of peak exercise, pressures were again recorded and simultaneous cineangiography was completed. Coronary arteriograms were obtained by the Judkins technique after exercise.

#### DATA ANALYSIS

Methods of analysis have been described previously in detail [6-11]. In summary, resting and exercise data were derived from well-opacified beats that were not immediately postextrasystolic. Pressure tracings were digitized. The characteristics of isovolumic pressure decay were derived from the linear regression of pressure and  $dP/dt$  coordinates (Figure 22-2). Thus two variables,  $T$ , representing the negative reciprocal of the slope, and  $P_B$ , representing the pressure-axis intercept, were derived for each patient at rest and during exercise.

Ventricular volumes were calculated from frame-by-frame analysis of biplane angiograms. Three-point smoothing of volume calculations was performed, and the peak rate of filling was identified. End-diastolic, end-systolic volumes, and ejection fraction were calculated.

The left ventricular pressure at the time unopacified blood first entered the ventricle was measured and denoted mitral valve opening pressure. This was used as an index of the left atrial pressure, which plays a key role in determining filling rates.

Diastolic pressure-volume relations for rest and exercise data were constructed for each patient. To permit comparisons, we derived mean diastolic pressure-volume relations for each group at rest and during exercise. Three diastolic pressure-volume coordinates were used, including the early diastolic pressure nadir, end-diastole, and the time half way through the filling period (Figure 22-3).

Rest and exercise data within groups and between preoperative and postoperative studies were tested for significant differences by use of the paired  $t$  test. Differences between groups were tested with an unpaired  $t$  test. Data on figures are mean  $\pm$  standard error of the mean (SEM), while those in the text are mean  $\pm$  standard deviation (SD).

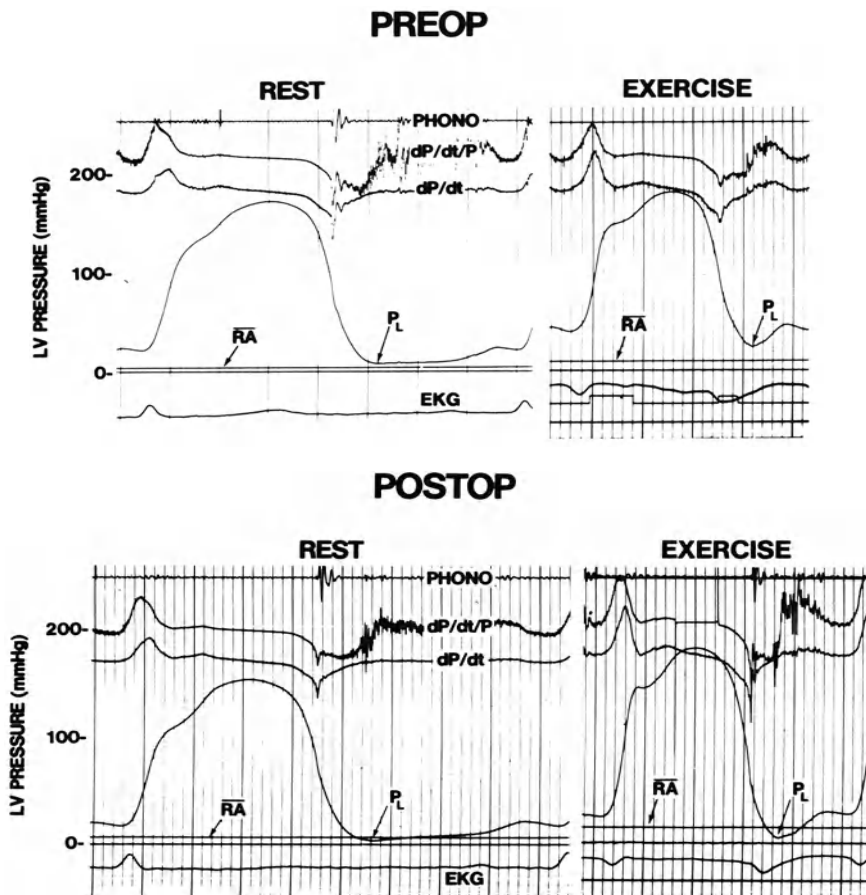


FIGURE 22-1. Left ventricular (LV) pressure tracings at rest and during exercise-induced ischemia from one patient with severe triple-vessel disease. Before surgery, there was a dramatic rise in diastolic pressures. During postoperative exercise, the early diastolic pressure nadir,  $P_L$ , did not increase, yet end-diastolic pressure did. Cineangiography revealed severe anterior hypokinesis during preoperative exercise, but no new asynergy during postoperative exercise. Pressure-volume relations were constructed (see Figure 22-7)  $\overline{RA}$  = right atrial pressure; EKG = electrocardiogram (From Carroll et al [10], with permission.)

## Results

### CONTROL GROUP

During exercise, the control group had no significant change in end-diastolic volume ( $96$

$\pm 6$  to  $102 \pm 11$  ml/m<sup>2</sup>), whereas the end-systolic volume decreased from  $35 \pm 5$  to  $28 \pm 6$  ml/m<sup>2</sup> ( $p < 0.05$ ) and ejection fraction increased from  $64 \pm 3$  to  $73 \pm 4\%$  ( $p < 0.01$ ). Heart rate increased from  $70 \pm 18$  to  $120 \pm 21$  beats per minute ( $p < 0.01$ ).

Left ventricular pressure decay was accelerated, with  $T$  decreasing from  $48 \pm 14$  to  $26 \pm 6$  ms ( $p < 0.05$ ) and no change in  $P_B$  ( $0 \pm 1$  to  $3 \pm 11$  mm Hg) (see Figure 22-2). The early diastolic pressure nadir decreased insignificantly during exercise ( $11 \pm 6$  to  $4 \pm 5$  mm Hg). No change in left ventricular end-diastolic pressure (LVEDP) occurred ( $18 \pm 8$  to  $20 \pm 9$  mm Hg). The increased LVEDP at rest and during exercise was due to leg elevation.

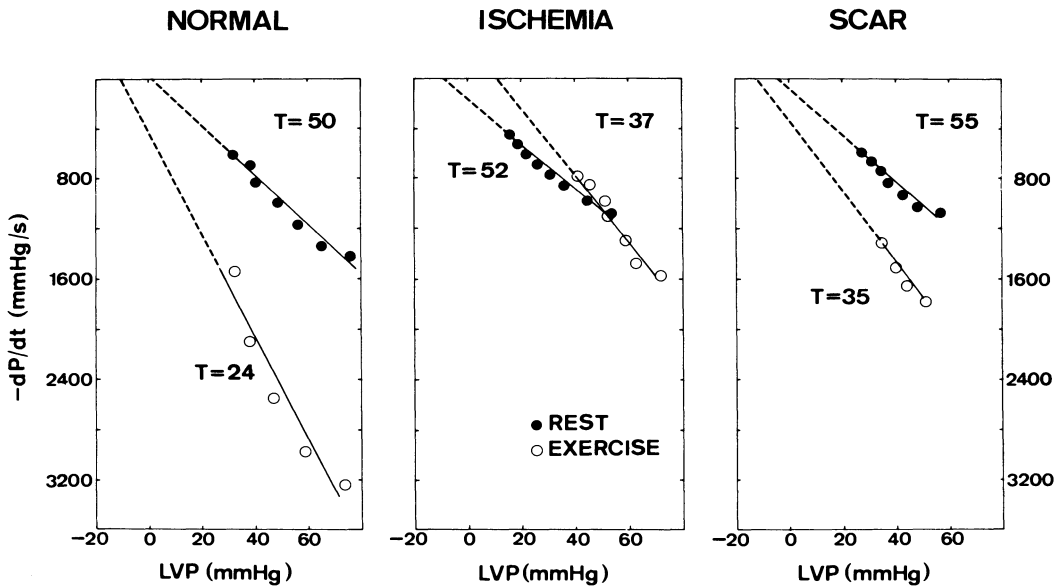


FIGURE 22-2. Left ventricular pressure (LVP) and negative dP/dt coordinates from the isovolumic relaxation period in representative patients in three of the groups. The negative reciprocal of the slope, T, decreased during exercise in all three patients, but much more in the control patient. The pressure-axis intercept,  $P_B$ , significantly increased during exercise with the patient developing ischemia. The scar group patient had pressure decay characteristics during exercise that were not normal, but clearly different from the patient with ischemia. (From Carroll et al. [6], with permission.)

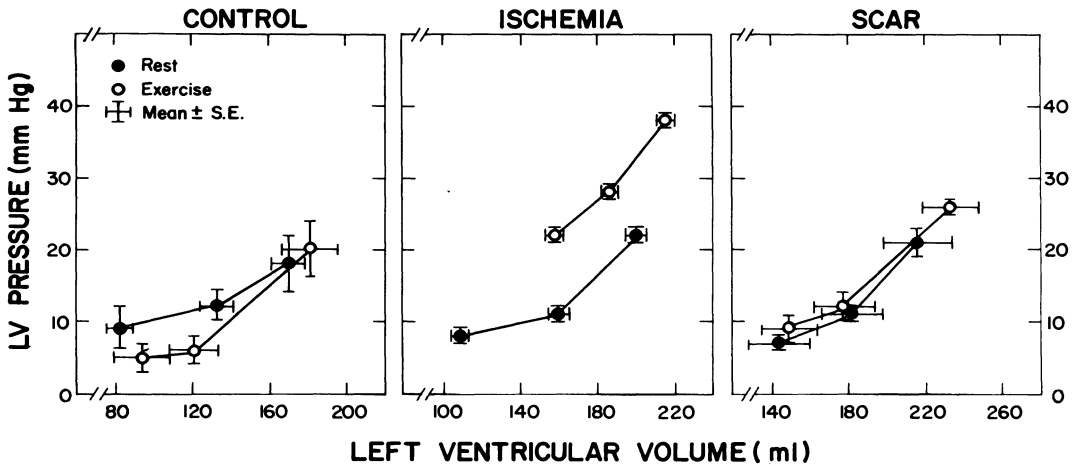


FIGURE 22-3. Diastolic pressure-volume relations from three groups are shown for both the resting state and during exercise. Coordinates of pressure and volume are averages at three diastolic points. The control group had a tendency for a downward shift in the early diastolic coordinate. The ischemia group had a clear upward shift during exercise. There was no shift for the scar group, yet end-diastolic pressure increased. (From Carroll et al [7], with permission.)

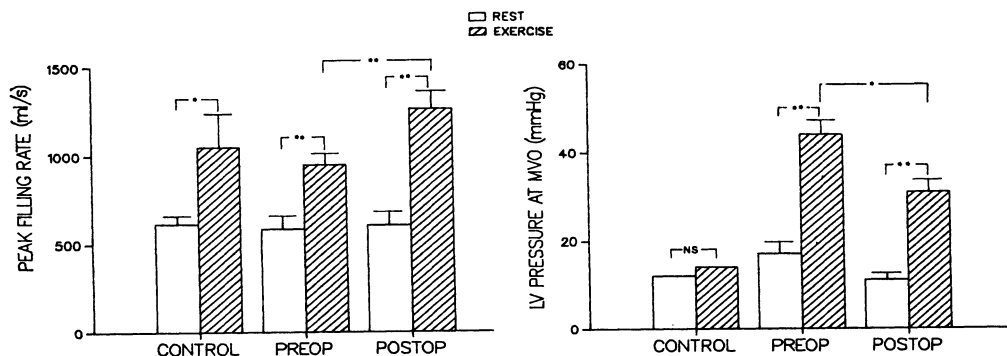


FIGURE 22-4. Left ventricular filling dynamics in three groups of patients. During exercise, the control group had an increase in peak filling rate (*left panel*) without a change in the index of left atrial pressure, the pressure at which mitral valve opening (MVO) occurred (*right panel*). The preoperative patients with exercise-induced ischemia, also had an increase in peak filling rate, yet the pressure at mitral valve opening was grossly elevated. Postoperatively, peak filling rate increased during exercise to a level greater than that during preoperative exercise. Yet, MVO pressure still increased although less than it increased preoperatively. \* =  $p < 0.05$ ; \*\* $p < 0.001$ ; NS = not significant (From Carroll et al [7], with permission.)

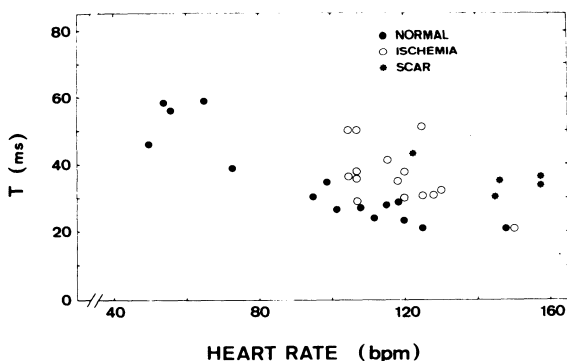


FIGURE 22-5. In the control group (*solid circles*), the negative reciprocal of the slope, T, and heart rate are strongly correlated at rest and during graded exercise. Exercise coordinates from the ischemia group (*open circle*) and scar group (*asterisks*) had a prolonged T, relative to heart rate. (From Carroll et al [6], with permission.)

The diastolic pressure-volume relationship showed a slight downward shift in early diastole during exercise in the control groups (see Figure 22-3). Peak filling rate increased from  $615 \pm 163 \pm 318$  ml/sec ( $p < 0.05$ ) (Figure 22-4). Mitral valve opening pressure was unchanged ( $12 \pm 7$  to  $14 \pm 10$  mm Hg). The filling period decreased from  $430 \pm 150$  to  $200 \pm 69$  ms ( $p < 0.05$ ) during exercise. The filling volume increased from  $104 \pm 11$  to  $126 \pm 20$  ml ( $p < 0.05$ ).

#### ISCHEMIA GROUP

In contrast to the control group, there was an increase in end-diastolic volume ( $105 \pm 11$  to  $116 \pm 11$  ml/m<sup>2</sup>,  $p < 0.001$ ) and in end-systolic volume from  $40 \pm 8$  to  $57 \pm 11$  ( $p < 0.001$ ). The ejection fraction fell from  $62 \pm 6$  to  $51 \pm 8\%$  ( $p < 0.001$ ). Heart rate increased from  $67 \pm 13$  to  $119 \pm 14$  ( $p < 0.001$ ).

Left ventricular pressure decay was accelerated with T decreasing from  $55 \pm 9$  to  $37 \pm 8$  ms ( $p < 0.001$ ), yet the exercise value was significantly elevated compared to the control group value ( $p < 0.05$ ) (Figures 22-2, 22-5). In addition,  $P_B$  rose from  $-10 \pm 7$  to  $+11 \pm 8$  mm Hg ( $p < 0.001$ ). The early diastolic pressure nadir increased significantly during exercise from  $9 \pm 3$  to  $21 \pm 5$  mm Hg ( $p < 0.001$ ). LVEDP rose from  $22 \pm 6$  to  $38 \pm 7$  mm Hg ( $p < 0.001$ ). The diastolic pressure-volume relationship showed a large upward shift throughout diastole (see Figure 22-3).

Right atrial pressure rose from  $5 \pm 2$  to  $13 \pm 5$  mm Hg ( $p < 0.001$ ) during exercise in the 11 patients for whom data existed. Pressure-

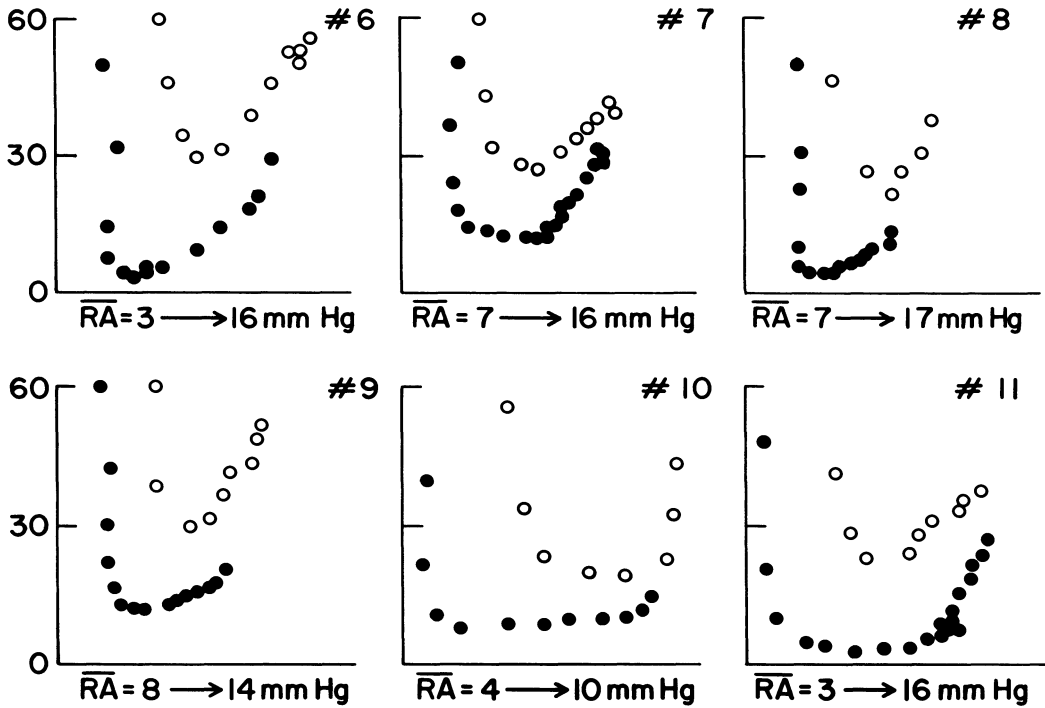


FIGURE 22-6. Left ventricular diastolic pressure-volume relations are shown at rest (*solid circles*) and during exercise (*open circles*) in six patients with exercise-induced ischemia. All had an upward shift with ischemia. The right atrial pressure rose significantly in these patients, raising the possibility of pericardial restraint and/or ventricular interaction being one mechanism involved in the alteration in left ventricular chamber compliance. Yet, in other patients there were inconsistent changes in right atrial pressure that did not correlate with changes in left-sided pressure-volume relations.

volume relations in several of these patients are shown in Figure 22-6.

Peak filling rate increased from  $697 \pm 219$  to  $1035 \pm 309$  ml/second ( $p < 0.001$ ) (see Figure 22-4). Mitral valve opening pressure was markedly elevated during exercise ( $14 \pm 6$  to  $35 \pm 9$  mm Hg). The filling period decreased from  $470 \pm 150$  to  $190 \pm 40$  ms ( $p < 0.001$ ). Yet, unlike the control group, filling volume fell from  $118 \pm 25$  to  $101 \pm 35$  ml ( $p < 0.001$ ).

#### BYPASS GROUP

During preoperative exercise the findings for the bypass group were similar to those of the ischemia group. During postoperative exercise there was still an increase in end-diastolic volume ( $108 \pm 25$  to  $115 \pm 27$  ml/m<sup>2</sup> ( $p < 0.01$ ), although less, in absolute terms, than preoperatively. End-systolic volume, on the other hand, did not change during postoperative exercise ( $44 \pm 18$  to  $46 \pm 21$ ) and ejection fraction rose slightly from  $59 \pm 11$  to  $61 \pm 11\%$  ( $p < 0.05$ ). Heart rate was greater during

postoperative exercise ( $129 \pm 19$  vs.  $115 \pm 11$ ,  $p < 0.001$ ).

Left ventricular pressure decay was accelerated, with T decreasing from  $52 \pm 11$  to  $30 \pm 9$  ms ( $p < 0.001$ ). The exercise value postoperatively was less than it was preoperatively ( $30 \pm 9$  vs.  $37 \pm 9$  ms,  $p < 0.01$ ). In addition,  $P_B$ , which rose preoperatively during exercise, did not rise during postoperative exercise ( $-10 \pm 10$  to  $-7 \pm 12$  mm Hg). The early diastolic pressure nadir increased significantly during preoperative exercise from  $9 \pm 4$  to  $21 \pm 8$  mm Hg ( $p < 0.001$ ), but during post-

operative exercise it was stable ( $5 \pm 3$  to  $6 \pm 3$  mm, mm Hg). LVEDP still rose from  $17 \pm 4$  to  $25 \pm 10$  mm Hg ( $p < 0.001$ ) during postoperative exercise, although the increase was less compared to preoperative exercise (see Figure 22-1).

The left ventricular diastolic pressure-volume relation showed no shifts during postoperative exercise. Yet, the bypass group patients did have an increased end-diastolic pressure, which appeared appropriate for the increase in end-diastolic volume (Figure 22-7).

In nine patients, right atrial pressure increased during postoperative exercise from  $4 \pm 2$  to  $10 \pm 4$  mm Hg ( $p < 0.001$ ), which was unchanged from preoperative exercise.

Peak filling rate increased from  $604 \pm 235$  to  $1260 \pm 319$  ml/second ( $p < 0.001$ ) and was greater during postoperative exercise than preoperative exercise (1260 vs. 950 ml/second,  $p < 0.01$ ). Mitral valve opening pressure was markedly elevated during exercise preoperatively ( $17 \pm 6$  to  $44 \pm 10$  mm Hg,  $p <$

$0.001$ ), but less so during postoperative exercise ( $11 \pm 4$  to  $31 \pm 9$ ,  $p < 0.001$ ).

#### SCAR GROUP

There was no change in end-diastolic volume ( $111 \pm 16$  to  $116 \pm 15$  ml/m<sup>3</sup>) and in end-systolic volume ( $57 \pm 10$  to  $55 \pm 12$  ml/m<sup>2</sup>) during exercise, and ejection fraction also did not change ( $49 \pm 3$  to  $52 \pm 7\%$ ). Heart rate increased from  $74 \pm 16$  to  $138 \pm 20$  ( $p < 0.01$ ).

Left ventricular pressure decay was accelerated during exercise with T decreasing from  $66 \pm 10$  to  $37 \pm 3$  ms ( $p < 0.05$ ); however, the exercise value was significantly elevated compared to the control group value ( $p < 0.05$ ) (Figures 22-2, 22-5). In contrast,  $P_B$  was stable. The early diastolic pressure nadir was also unchanged during exercise ( $11 \pm 3$  to  $8 \pm 3$  mm Hg). LVEDP rose insignificantly during exercise, from  $21 \pm 5$  to  $26 \pm 3$  mm Hg.

The left ventricular diastolic pressure-volume relation showed no shifts during exercise in the

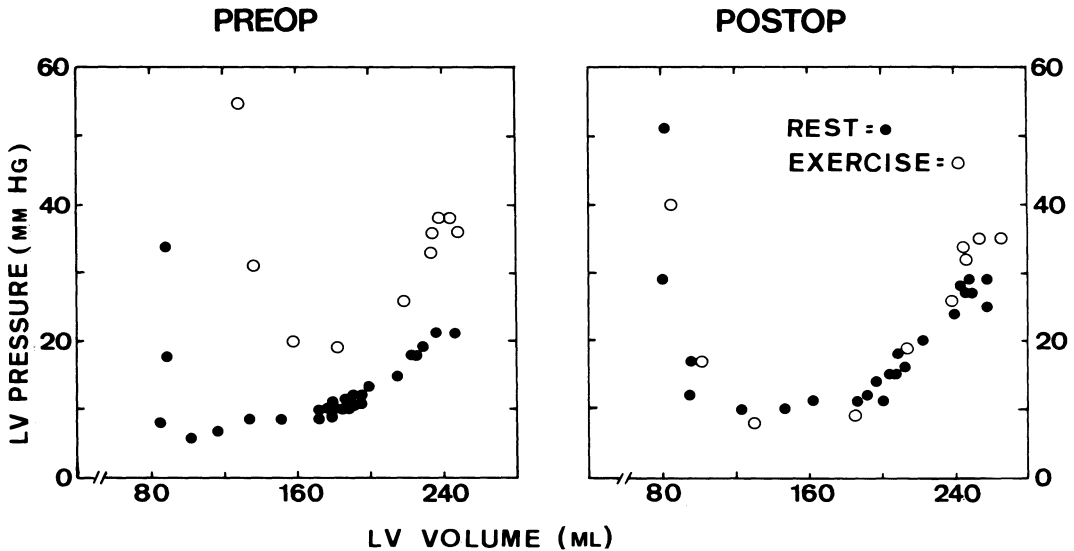


FIGURE 22-7. The left ventricular diastolic pressure-volume relation before bypass surgery demonstrated an upward shift during exercise-induced ischemia. Postoperatively, there was no shift and end-diastolic pressure increased with a slight increase in end-diastolic volume.

scar group. However, the scar group patients did have the slight increase in end-diastolic pressure that appeared appropriate for the increase in end-diastolic volume (see Figure 22-3).

Right atrial pressure was  $4 \pm 3$  at rest and  $4 \pm 4$  mm Hg during exercise. Peak filling rate increased from  $590 \pm 209$  to  $1185 \pm 161$  ml/second ( $p < 0.01$ ). Mitral valve opening pressure did not increase significantly during exercise ( $13 \pm 5$  to  $21 \pm 13$  mm Hg). The filling period decreased from  $440 \pm 180$  ms at rest to  $160 \pm 30$  ms with exercise ( $p \pm 0.05$ ). The filling volume increased from  $97 \pm 15$  to  $117 \pm 18$  ml ( $p < 0.05$ ).

## Discussion

### NORMAL ADJUSTMENTS IN DIASTOLIC FUNCTION DURING EXERCISE

Augmented pump function is required during exercise to produce the increase in cardiac output to match the increased metabolic needs. In diastole, adjustments in pressure decay and filling dynamics occur which shorten the isovolumic relaxation period, increase total transmitral flow in an abbreviated filling period, and maintain low diastolic pressures. Alterations in autonomic tone undoubtedly play a vital role in these adjustments in diastolic function. It is well-established that myocardial relaxation is directly accelerated by beta-adrenergic receptor activation [12-15]. Alterations in heart rate and loading conditions may also facilitate adjustments in diastolic, as well as systolic function, during exercise [12, 16, 17].

### DIASTOLIC PRESSURE DURING ISCHEMIA

Patients in the ischemia group had increases in pressure throughout diastole. In early diastole, the nadir was elevated far beyond the limit of a normal pressure at end-diastole. This was unique in the ischemia group; patients in the scar and bypass groups often increased end-diastolic pressure, but never minimum diastolic pressure during exercise. The resultant effects on left atrial and pulmonary venous pressure would clearly be of the magnitude to produce pulmonary edema, if sustained with prolonged ischemia. By study design, patients with significant mitral regurgitation during exercise were excluded. Therefore, the acute increase in diastolic pressure was primarily related to altera-

tions in left ventricular chamber compliance. Several mechanisms for this acute rise in pressure will be discussed.

### EFFECT OF ISCHEMIA ON RELAXATION

The alterations in left ventricular relaxation during exercise-induced ischemia are probably related to changes in the multiple determinants of relaxation [12, 18]. The abnormal systolic dynamics of ischemia, including asynchrony and increased end-systolic volume, are factors that combine with direct disruption of muscle relaxation to produce the reduced rate, and perhaps extent, of pressure decay. The myocardium may never completely relax between systoles, especially since diastole is so brief during exercise. In addition, with the high incidence of triple-vessel disease in this study, it is reasonable to suggest that global ischemia occurred in many subjects.

Delayed and incomplete relaxation translates, at the ventricular or chamber level, into slow pressure decay that fails to achieve a pressure level expected for a totally relaxed chamber [6]. During exercise, the effects of ischemia are superimposed on the hemodynamics of exercise with changes in heart rate, contractile state, and loading conditions [16, 17]. Pressure decay was actually accelerated in many patients with exercise-induced ischemia. Yet, when compared to a control group, the true extent of abnormal pressure decay during exercise-induced ischemia was apparent. A problem does arise when comparing only the ischemia group to the control group. Those with exercise-induced ischemia may also have chronic abnormalities of both passive and active chamber compliance. Therefore, two groups with coronary artery disease, but no ischemia during exercise, were also studied.

### EFFECT OF AN AKINETIC SCAR ON RELAXATION

The presence of a large akinetic area or ischemic region may impair the rate of pressure decay simply because of the inhomogenous contraction/relaxation pattern. A temporal disruption in the contraction/relaxation pattern is associated with a prolongation of pressure decay [12]. In this study the scar group demonstrated a different form of regional abnormality, which was associated with a prolonged resting T. During exercise the ejection fraction did not increase, and the large end-systolic chamber size

did not decrease. Pressure decay acceleration occurred, as shown by a decrease in  $T$  and no change in  $P_B$ . Yet, the reduction in  $T$  was not to normal levels expected for the fast heart rate (see Figure 22-5). Nevertheless, the adjustment in pressure decay was adequate, in the scar group, to maintain low early diastolic pressures. Therefore, ischemia has unique effects on pressure decay that cannot simply be explained by the abnormal pattern of regional contraction/relaxation. The acutely ischemic myocardium itself appears to be a key determinant in the rise of left ventricular diastolic pressure during exercise.

The monoexponential model of pressure decay used in this study fits pressure and  $dP/dt$  coordinates from the isovolumic period. The  $T$  value from this method is not directly comparable to the tau value derived from relating the natural logarithm of pressure to time [19]. It is not clear if there is one best method for describing pressure decay. In some patients with congestive cardiomyopathy there is a poor linear fit of  $dP/dt$  and  $P$  coordinates [13]. No significant deviations from linearity were seen using the  $P$  vs.  $dP/dt$  method in these patients with coronary artery disease and large regional-wall motion abnormalities. The average correlation coefficient during exercise-induced ischemia remained 0.99 [6].

#### EFFECT OF REVASCULARIZATION ON RELAXATION

Abnormal pressure decay in the left ventricle, along with other hemodynamic abnormalities, can be greatly improved by revascularization. As demonstrated in Figure 22-1, the change can be easily seen in the left ventricular pressure contour. During postoperative exercise both  $T$  and  $P_B$  were improved, yet were often not identical to normal values. Persistent abnormalities in pressure decay may be related to the persistent inability to decrease end-systolic volume during exercise, residual inhomogeneities of contraction and relaxation, myocardial hypertrophy and interstitial fibrosis, and subclinical ischemia.

#### DIASTOLIC PRESSURE-VOLUME RELATION

The rise in diastolic pressures during ischemia is not simply due to an increase in end-diastolic volume, i.e., it is not merely a preload-dependent change in left ventricular chamber stiffness [20-23]. Chamber dilatation did occur in many of our subjects during exercise-induced

ischemia, yet the diastolic pressure-volume relations curve showed an upward shift, indicating an acute shift in chamber stiffness. This has been reported previously in pacing-induced angina [1, 4, 24]. Although abnormal pressure decay has been demonstrated in both pacing- and exercise-induced ischemia, other factors could contribute to this acute alteration in chamber stiffness.

Viscous factors are important to consider, especially in exercise-induced ischemia where filling rates are increased and diastole is quite brief. In addition, viscous effects are also proportional to intrinsic myocardial stiffness [25]. Many of the patients in our study had intraoperative biopsies that revealed increased interstitial fibrosis, which could elevate muscle stiffness [11].

#### THE PERICARDIUM AND VENTRICULAR INTERACTION

The normal pericardium resists stretch if there is a significant and acute increase in total intrapericardial volume [26]. The atria and right ventricle may dilate acutely from the elevation of left ventricular filling pressures during ischemia. If total intrapericardial volume increases so that intrapericardial pressure rises above its normal low values, an acute pericardial effect on left ventricular chamber properties may become manifest [27-32]. A parallel upward shift in the diastolic pressure-volume relation, as seen in Figure 22-8, would be produced. Tyberg and coworkers have pointed out the close correlation of right atrial and pericardial pressures in a group of patients after thoracotomy [32].

During exercise-induced ischemia, unlike pacing-induced ischemia, there is a marked rise in right atrial pressures. During exercise, the patients were supine, with legs slightly elevated, which increased right- as well as left-sided pressures and, presumably, total intrapericardial volume. As seen in Figure 20-6, there are examples of large increases in right atrial pressure in patients with massive upward shifts in the left ventricular diastolic pressure-volume relation. Yet, we have also noted a lack of consistency in the presence of elevated right atrial pressures during exercise-induced ischemia, a lack of correlation between the degree of increase in right atrial pressure and pressure-volume shift, and a clear inconsistency in patients studied postoperatively. Then, right atrial pressure still increased in most patients,

yet there were no or minimal upward shifts in the left ventricle's diastolic pressure-volume relation. Other factors may elevate right atrial pressure, e.g., right ventricular ischemia, tricuspid regurgitation, and postoperative changes in the external constraints of the left ventricle. Thus, while it is probably true that some patients have a "pericardial effect" during ischemia, the frequency, consistency, and relative contribution to the rise in diastolic pressures remain in question.

#### CHRONIC CHANGES IN PASSIVE CHAMBER COMPLIANCE IN CORONARY ARTERY DISEASE

Patients in the bypass and scar groups did not have a shift in the diastolic pressure-volume relation during exercise. The rest and exercise data are basically on the same relation, indicating stable chamber properties. End-diastolic pressure increased in many of these patients, which, according to the pressure-volume relation, appeared to be caused by a simple increase in end-diastolic chamber size, i.e., a preload-dependent change in chamber stiffness. The absolute increase in end-diastolic pressure was often great with a small increase in volume, indicating the steepness of the pressure-volume relation [22]. Fibrosis, either localized as a postinfarction scar, or patchy in areas served by severely diseased vessels, is a common feature of these two groups. Intraoperative biopsies, as Hess reported [11], also show myocardial hypertrophy, even in the absence of systemic hypertension.

Chronic changes in chamber compliance need to be considered in interpreting exercise hemodynamics. The acute changes in chamber compliance, produced by ischemia, are superimposed on any chronic changes. The resultant elevation of diastolic pressures was predicted to be dramatic, and often was. Sasayama and co-workers have shown that the ischemic region of the left ventricle has an upward shift in its pressure-segment length relation; the nonischemic region had no shift, but simply moved to a higher pressure on the same pressure-segment length relation [33]. Thus, within the same ventricle, acute and chronic changes in compliance may be observed.

#### FILLING DYNAMICS

If the left ventricle becomes stiffer acutely during ischemia, filling should be altered [34, 35]. In addition, exercise will alter filling,

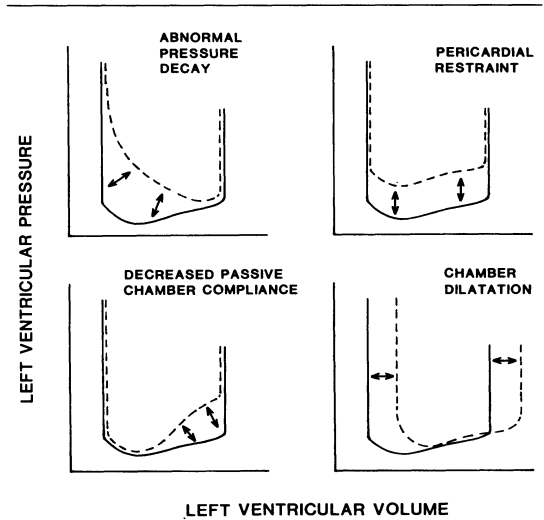


FIGURE 22-8. Schematic representation of left ventricular diastolic pressure-volume relations showing the types of changes involved in patients with coronary artery disease. Abnormal pressure decay from disrupted myocardial relaxation appears to be the central process in exercise-induced ischemia. Chronic changes in chamber compliance are relevant in many patients with coronary artery disease. Pericardial restraint may be operative during ischemia, yet the data are indirect and, at this time, not specific. (From Carroll et al [13], with permission.)

potentially causing an active suction of blood into the left ventricle in early diastole [36, 37]. Alterations do occur during exercise-induced ischemia, but in a complex way that is not reflected in peak filling rates, interpreted in isolation of other factors. Given that the atrial-ventricular pressure gradient is a major factor in the determination of filling, the role of left atrial pressure, the driving pressure for filling, must be addressed [38, 39]. In the ischemia group, the pressure responsible for mitral valve opening increased substantially during exercise. This did not occur in the scar group and control group and was lower in the bypass group. Thus, the atrial driving pressure for early filling may offset abnormalities of relaxation, which, when unopposed, would tend to slow early filling. Experimental data supporting this reasoning come from the elegant studies of Yellin and others [38, 40].

Left ventricular filling dynamics are markedly

altered after revascularization. The bypass group had increased peak filling rates during post-operative exercise, concomitant with improved pressure decay. Yet, the persistent increase in the pressure at mitral valve opening suggests that filling dynamics remain abnormal. In addition, the pattern of filling remains abnormal, with reduced rates in the second half of diastole [7]. This may reflect the chronic structural alterations that determine passive chamber stiffness. Revascularization would not be expected to reverse the increased amount of interstitial fibrosis that is seen in many patients.

#### TYPE OF ISCHEMIA

Exercise-induced ischemia has unique features, as discussed above and further studied in animal models [16, 17]. The resultant left ventricular dysfunction is often profound. The imbalance in myocardial oxygen supply and demand primarily involves an increase in the determinants of myocardial oxygen consumption. Yet a reduction in coronary flow may also accompany exercise, as demonstrated by the study of Gage [41]. These considerations of the way ischemia is produced are important. As demonstrated by Paulus and coworkers [42], the regional dysfunction, both systolic and diastolic, is different for coronary occlusion vs. pacing-induced ischemia with a coronary stenosis. Ischemia in humans is further modified by the anatomic and physiologic diversity of coronary artery disease.

#### *Summary and Conclusions*

During exercise the duration of diastole is brief, frequently less than 200 msec. In the normal left ventricle, an acceleration of pressure decay maintains low diastolic pressures, augments filling rates, and, therefore, is important in increasing stroke volume during exercise.

During exercise in a patient with coronary artery disease, ischemia may occur and exercise hemodynamics are disrupted. Using micromanometer-measured left ventricular pressure, and ventricular volumes, calculated from biplane cineangiograms, left ventricular function at rest and during exercise was studied in 57 patients. Exercise-induced ischemia produced dramatic increases in diastolic pressures and an upward shift in the diastolic pressure-volume relation. Central to these changes was abnormal myocardial relaxation with impaired left ventricular pressure decay. However, the isovolu-

mic relaxation period was not prolonged, and the filling period was not abbreviated, during exercise-induced ischemia because of the early opening of the mitral valve when intraventricular pressure was still over 30 mm Hg. Rapid filling proceeded when pressure decay was incomplete from the previous systole. Exercise studies in patients after bypass surgery and in patients with scars from distant myocardial infarction were useful in clarifying confounding factors. For example, asynchrony of contraction and relaxation, ventricular interaction, pericardial restraint, and chronic changes in passive chamber compliance may also further compromise diastolic function during exercise. In patients with coronary artery disease without ischemia during exercise, LVEDP, but not early diastolic pressures, rose during exercise. The increase in pressure was appropriate for a slight increase in end-diastolic volume in a ventricle with a steep pressure-volume relation.

Thus, the acute abnormalities of diastolic relaxation in exercise-induced ischemia are intertwined with the hemodynamics of exercise and superimposed on the chronic passive chamber abnormalities frequently seen in coronary artery disease.

#### *References*

1. Barry WH, Brooker JZ, Alderman EL, et al (1974). Changes in diastolic stiffness and tone of the left ventricle during angina pectoris. *Circulation* 49:255-263.
2. Mann T, Goldberg S, Mudge GH, Grossman W (1979). Factors contributing to altered left ventricular diastolic properties during angina pectoris. *Circulation* 59:14-18.
3. Paulus WJ, Serizawa T, Grossman W (1982). Altered left ventricular diastolic properties during pacing-induced ischemia in dogs with coronary stenoses. *Circ Res* 50:218-227.
4. Dwyer EM (1970). Left ventricular pressure-volume alterations and regional disorders of contraction during myocardial ischemia induced by atrial pacing. *Circulation* 42:1111-1122.
5. Grossman W, Serizawa T, Carabello BA (1980). Studies of the mechanisms of altered left ventricular diastolic pressure-volume relationship. *Eur Heart J* 1(suppl A):141-147.
6. Carroll JD, Hess OM, Hirzel HO, et al (1983). Exercise-induced ischemia: The influence of altered relaxation on early diastolic pressures. *Circulation* 67:521-528.
7. Carroll JD, Hess OM, Hirzel HO, et al (1983). Dynamics of left ventricular filling at rest and

- during exercise. *Circulation* 68:59-67.
8. Carroll JD, Hess OM, Studer NP, et al (1983). Systolic function during exercise in patients with coronary artery disease. *J Am Coll Cardiol* 2:206-216.
  9. Carroll JD, Hess OM, Hirzel HO, et al (1983). Inconsistency of changes in right atrial pressure during exercise-induced left ventricular ischemia. *Circulation* 68(suppl 3):102 (abstract).
  10. Carroll J, Hess OM, Hirzel HO, et al (1985). Left ventricular systolic and diastolic function in patients with coronary artery disease: Effects of revascularization on exercise-induced ischemia. *Circulation* 72:119-129.
  11. Hess OM, Schneider J, Carroll JD, et al (1983). Myocardial structure of ventricular segments with and without exercise-induced wall motion abnormalities in patients with coronary artery disease. *J Am Coll Cardiol* 1:734 (abstract).
  12. Brutsaert DL, Rademakers FE, Sys SU (1984). Triple control of relaxation: Implications in cardiac disease. *Circulation* 69:190-196.
  13. Carroll JD, Lang RM, Neumann AL, et al (1986). The differential effects of positive inotropic and vasodilator therapy on diastolic properties in congestive cardiomyopathy. *Circulation* 74:815-825.
  14. Parmley WW, Sonnenblick EH (1968). Relation between mechanics of contraction and relaxation in mammalian cardiac muscle. *Am J Physiol* 216:1084-1091.
  15. Blaustein AS, Gaasch WH, Carroll JD, et al (1981). Systolic load dependency of left ventricular relaxation is influenced by beta adrenergic tone and abnormal synchrony. *Am J Cardiol* 47:410.
  16. Tomoike H, Franklin D, McKown D, et al (1978). Regional myocardial dysfunction and hemodynamic abnormalities with strenuous exercise in dogs with limited coronary flow. *Circ Res* 42:487-496.
  17. Horowitz LD, Peterson DF, Bishop VS (1978). Effect of regional myocardial ischemia on cardiac pump performance during exercise. *Am J Physiol* 234:H157-H162.
  18. Hess OM, Osakada G, Lavelle JF, et al (1983). Diastolic myocardial wall stiffness and ventricular relaxation during partial and complete coronary occlusions in the conscious dog. *Circ Res* 52:387-400.
  19. Mirsky I (1984). Assessment of diastolic function: Suggested methods and future considerations. *Circulation* 69:836-841.
  20. Grossman W, *Mcaurin* LP (1976). Diastolic properties of the left ventricle. *Ann Intern Med* 84:316-326.
  21. Grossman W (1985). Why is left ventricular diastolic pressure increased during angina pectoris. *J Am Coll Cardiol*:607-608.
  22. Gaasch WH, Levine HJ, Quinones MA, et al (1976). Left ventricular compliance: Mechanisms and clinical implications. *Am J Cardiol* 38:645-653.
  23. Glantz SA, Parmley WW (1978). Factors which affect the diastolic pressure-volume curve. *Circ Res* 42:171-180.
  24. Mann T, Brodie BR, Grossman W, et al (1977). Effect of angina on the left ventricular diastolic pressure-volume relationship. *Circulation* 55:761-766.
  25. Pouleur H, Karliner JS, LeWinter MM, Covell JW (1979). Diastolic viscous properties of the intact canine left ventricle. *Circ Res* 45:410.
  26. Shabetai R (1981). *The Pericardium*. New York: Grune and Stratton.
  27. Mirsky I, Rankin JS (1979). The effects of geometry, elasticity, and external pressure on the diastolic pressure-volume and stiffness-stress relations. How important is the pericardium? *Circ Res* 44:601-611.
  28. Janicki JS, Weber KT (1980). The pericardium and ventricular interaction, distensibility, and function. *Am J Physiol* 238:H494-H503.
  29. Grossman W, Barry WH (1980). Diastolic pressure-volume relations in the diseased heart. *Fed Proc* 39:148-155.
  30. Shirato K, Shabetai R, Bargava V, et al (1978). Alterations of left ventricular diastolic pressure-segment length relation produced by the pericardium: Effects of cardiac distension and afterload reduction in conscious dogs. *Circulation* 57:1191-1198.
  31. Spadaro J, Bing OHL, Gaasch WH, et al (1981). Pericardial modulation of right and left ventricular diastolic interaction. *Circ Res* 48:233-238.
  32. Tyberg JV, Taichman GC, Smith ER, et al (1986). The relationship between pericardial pressure and right atrial pressure: an intraoperative study. *Circulation* 73:428-432.
  33. Sasayama S, Nonogi H, Miyazaki S, et al (1985). Changes in diastolic properties of the regional myocardium during pacing-induced ischemia in human subjects. *J Am Coll Cardiol* 5:599-606.
  34. Reduto LA, Wickemeyer WJ, Young B, et al (1981). Left ventricular diastolic performance at rest and during exercise in patients with coronary artery disease. *Circulation* 63:1228-1237.
  35. Bonow RD, Bacharach SL, Green MV, et al (1981). Impaired left ventricular diastolic filling in patients with coronary artery disease: Assessment with radionuclide angiography. *Circulation* 64:315-323.
  36. Sonnenblick EH (1980). The structural basis and importance of restoring forces and elastic recoil for the filling of the heart. *Eur Heart J* 1(suppl A):107.

37. Sabbah HN, Stein PD (1981). Pressure-diameter relations during early diastole in dogs: Incompatibility with the concept of passive left ventricular filling. *Circ Res* 48:357-365.
38. Yellin EL, Sonnenblick EH, Frater RWM (1980). Dynamic determinants of left ventricular filling An overview. In Baan J, Arntzenius AC, Yellin EL (eds): *Cardiac Dynamics*. The Hague: Martinus Nijhoff, pp 145-158.
39. Noble MIN, Nilne EN, Goerke R, et al (1969). Left ventricular filling and diastolic pressure-volume relations in the conscious dog. *Circ Res* 24:269-283.
40. Ishida Y, Meisner JS, Tsujioka K, et al (1984). Peak rapid filling rate may not reflect left ventricular relaxation properties when left atrial pressure compensates for changes in loading conditions. *Circulation* 70(suppl II):349 (abstract).
41. Gage J, Hess OM, Murakami T, Krayenbuehl HP (1986). Vasoconstriction of stenotic coronary arteries during dynamic exercise in patients with classic angina pectoris: Reversibility by nitroglycerin. *Circulation* 1986:73:865.
42. Paulus WJ, Grossman W, Serizawa T, et al (1985). Different effects of two types of ischemia on myocardial systolic and diastolic function. *Am J Physiol* 248:H719-H728.

---

## 23. LEFT VENTRICULAR FILLING IN ISCHEMIC AND HYPERTROPHIC HEART DISEASE

---

Robert O. Bonow

Impairment of left ventricular diastolic function develops commonly in patients with coronary artery disease or hypertrophic cardiomyopathy, stemming from disorders of ventricular relaxation, filling, and distensibility. These factors may contribute substantially to the clinical manifestations of these disease processes. Hence, numerous hemodynamic, angiographic, and non-invasive techniques have been applied to the study of left ventricular diastolic properties. Much attention has been focused recently on the filling phase of diastole, because left ventricular filling lends itself to analysis by noninvasive techniques. The applications and limitations of such analysis are examined in this chapter.

### *Determinants of Left Ventricular Filling*

Rapid diastolic filling of the left ventricle represents the complex interaction of the passive elastic properties determining left ventricular distensibility, such as fibrosis and hypertrophy, and the dynamics of left ventricular relaxation, encompassing both inactivation-dependent and load-dependent effects [1–4]; these include myocardial ischemia [5–10], sympathetic tone [11–14], extent of systolic fiber shortening [1, 2] afterload [1, 2], regional inhomogeneity or asynchrony [10, 15–22], and the rate and extent of coronary blood flow [1, 4]. During the onset of the rapid filling period, left ventricular pressure continues to subside despite the abrupt increase in volume, indicating that active left ventricular relaxation continues beyond the isovolumic phase and well into the diastolic

filling period, and that alterations in the rate and extent of left ventricular relaxation may have a significant impact on the subsequent filling phase [23–26]. The interdependence between relaxation and rapid filling is further shown by the load-dependent effects of the rapid filling phase itself. Thus, relaxation is influenced importantly by the dynamics of the filling process, including the driving pressure between the left atrium and the left ventricle [27] and factors determining myocardial wall tension after mitral valve opening [1], such as ventricular volume and wall thickness. Moreover, prolonged or incomplete relaxation produces persistent interaction of contractile units, resulting in increased myocardial tone during the filling phase, thereby altering left ventricular diastolic pressure-volume relations [9, 24, 28, 29]. Thus, left ventricular distensibility is determined not only by fixed, passive properties of the ventricular myocardium but also by potentially reversible alterations in left ventricular filling dynamics resulting from impaired relaxation [23, 24].

### *Measurement of Left Ventricular Filling*

We have used radionuclide angiographic methods both in the noninvasive laboratory and in the catheterization laboratory to evaluate left ventricular filling properties. Left ventricular filling is assessed from high-temporal-resolution time-activity curves representing relative left ventricular volume changes throughout the average cardiac cycle (Figure 23–1). Indices describing the rapid-filling period include the peak rate of filling, the time interval from end-systole to the occurrence of peak filling rate, and, in patients with a discernible diastasis

*Grossman, William, and Lorell, Beverly H. (eds.), Diastolic Relaxation of the Heart. Copyright © 1987. Martinus Nijhoff Publishing. All rights reserved.*

interval, the relative contributions of rapid filling and atrial systole to total left ventricular stroke volume [30–33]. Because peak filling rate is computed in left ventricular counts per second, this variable is usually normalized for the number of counts at end-diastole and expressed as end-diastolic counts per second (EDV/sec) [31].

There are potential pitfalls in the use of radionuclide angiographic methods to evaluate left ventricular filling, and prerequisite technical considerations must be borne in mind, including acquisition methods, framing rates, temporal smoothing effects, normalization parameters, and the influence of heart rate and systolic performance on the resulting data [34, 35]. For example, expressing peak filling rate in terms of EDV/sec creates a “diastolic” index that is influenced markedly by the ejection fraction. Such effects must be considered when comparing patient groups or assessing effects of interventions.

In addition, it is often difficult in clinical studies to ascertain the individual mechanism or mechanisms responsible for disturbed left ventricular filling, even when sophisticated studies are performed in the setting of the cardiac catheterization laboratory, because of the many factors contributing to the complex interrelation of left ventricular passive elastic properties, inactivation, and loading. Hence, the evaluation of left ventricular diastolic function using noninvasive techniques is inherently more difficult, because of the inability to obtain instantaneous pressure-volume and pressure-time coordinates. It is important to note that the radionuclide angiographic volume curve can also be obtained in the catheterization laboratory during simultaneous pressure recordings [26, 36–40], which allows the construction of multiple high-temporal-resolution pressure-volume loops (Figure 23–2). This combination of invasive and noninvasive methodologies not only permits correlation of the noninvasive indices of left ventricular filling with the more accepted hemodynamic indices, but also provides greater versatility in the study of ventricular diastolic function, because a large number of interventions may be investigated after a single radioisotope dose, without the limitations of multiple angiographic contrast injections.

Although it is not possible to obtain definitive data noninvasively, regarding mechanisms for impaired left ventricular filling in patients

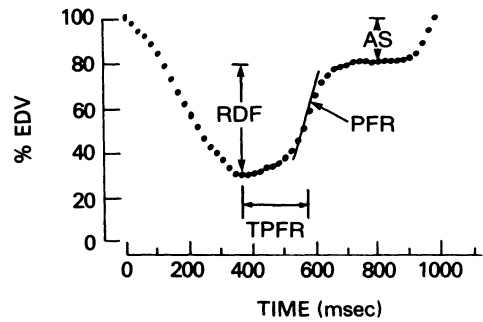


FIGURE 23–1. High-temporal-resolution time-activity curve obtained from radionuclide angiography. Each point represents 20 msec. Variables used to assess left ventricular rapid diastolic filling include peak filling rate (PFR), measured as the peak slope of a third-order polynomial fit to the rapid filling phase; time-to-peak-filling rate (TPFR) measured from end-systole; and the contribution of rapid diastolic filling (RDF) and atrial systole (AS) expressed as a percent of stroke volume. EDV = end-diastolic volume.

with ischemic or hypertrophic heart disease, it is possible to study the prevalence of diastolic filling disorders at rest compared to a normal control population and to determine the potential for reversal of these abnormalities after appropriate interventions. Assuming no change in heart rate or left ventricular systolic function, an improvement in left ventricular filling after an intervention to reduce ischemia or improve coronary flow would suggest that reduced diastolic filling under basal conditions was related to potentially reversible alterations in one or more determinants of left ventricular relaxation.

### *Left Ventricular Filling in Ischemic Heart Disease*

When radionuclide angiographic methods are applied to a series of patients with coronary artery disease, the majority have evidence of impaired left ventricular filling under basal conditions [31, 41–46] manifested by reduced peak filling rate, prolonged time-to-peak-filling rate, or both (Figure 23–3). Over a wide spectrum of ventricular function, there is a direct correlation between peak filling rate and left ventricular ejection fraction (Figure 23–4). This relation would be expected on a physiologic basis. In patients with coronary artery

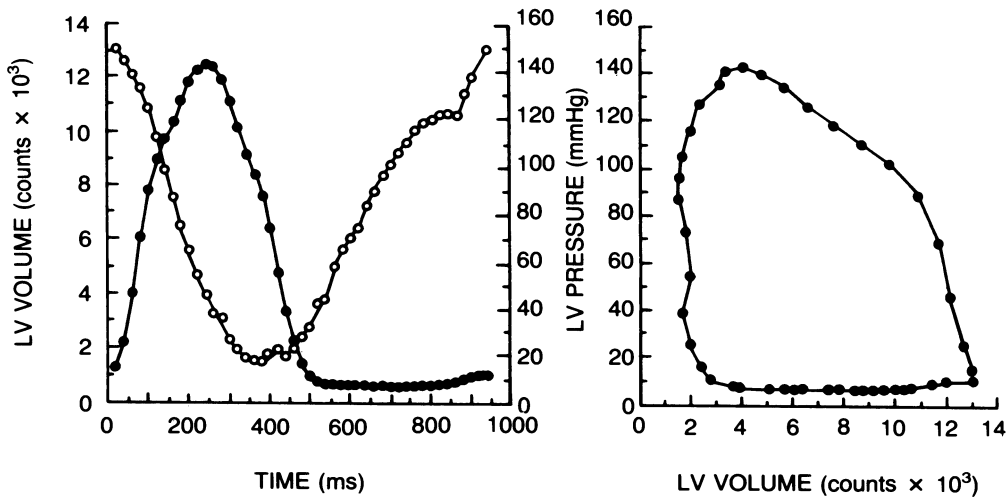


FIGURE 23-2. Simultaneous electrocardiogram-gated left ventricular (LV) volume and pressure curves and the resultant pressure-volume loop obtained in a patient with hypertrophic cardiomyopathy using a portable gamma camera and a micromanometer-tipped catheter.

disease and depressed left ventricular systolic function, regional fibrosis or ischemia would both decrease distensibility and impair ventricular relaxation on the basis of load-dependent mechanisms such as reduced systolic shortening [1, 2] and increased regional nonuniformity [10, 20–22]; myocardial ischemia, if present, would also reduce myocardial inactivation [5–10]. In this setting, progressive reduction in systolic performance would be associated with progressive deterioration in diastolic performance. In addition, peak filling rate measured by this method is usually normalized by end-diastolic volume (as in Figure 23-4), producing a filling variable that is ejection-fraction-dependent [35]. Alternative normalization schemes might be less dependent on the extent of systolic shortening. From these physiologic and methodologic considerations, it is evident that most patients with coronary artery disease and left ventricular systolic dysfunction will be likely to manifest impaired left ventricular filling. However, even among patients with normal ejection fractions at rest, peak filling rate is reduced compared to normal subjects matched for heart rate and ejection fraction (see

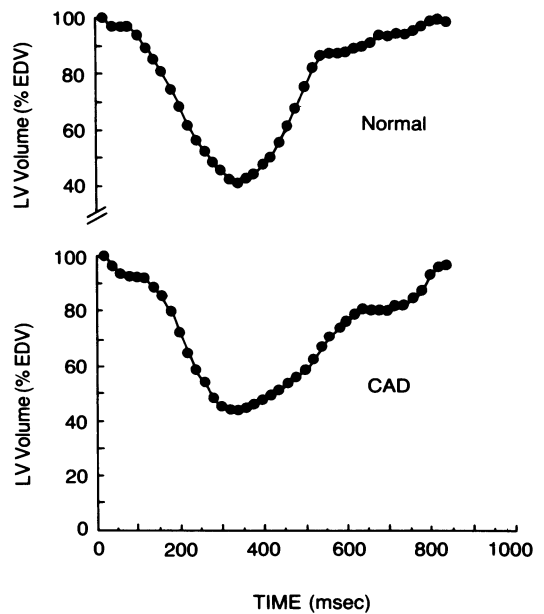
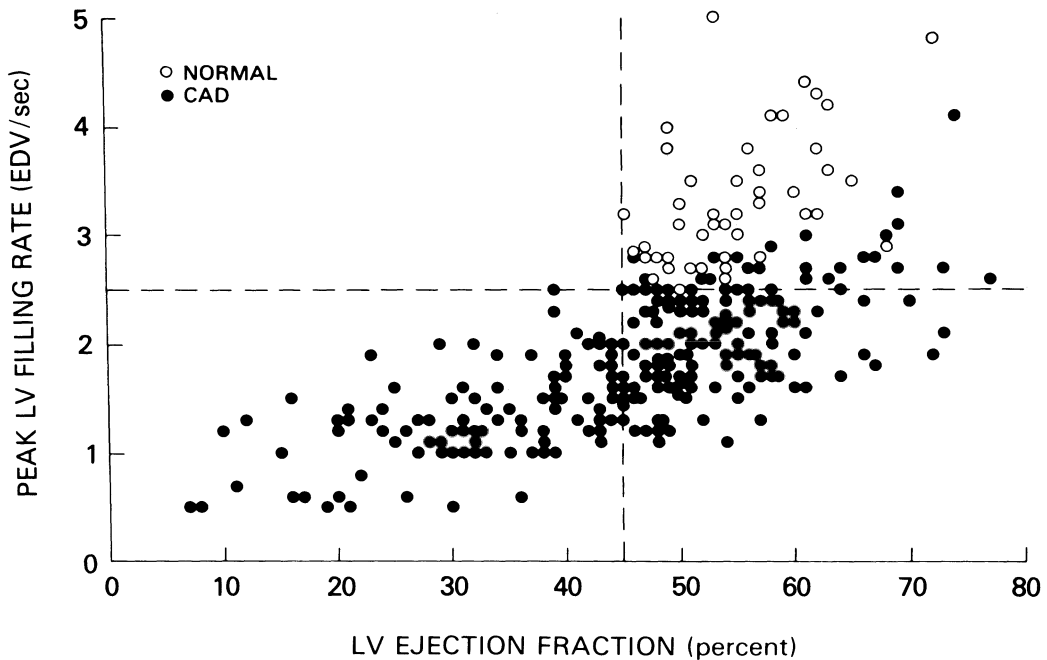


FIGURE 23-3. Left ventricular time-activity curves at rest in a patient with isolated stenosis of the right coronary artery (CAD) and a normal subject matched for age, heart rate, and ejection fraction. Rapid filling is impaired in the patient with CAD despite the findings of normal global and regional systolic function, normal resting electrocardiogram, no history of myocardial infarction, and no angina pectoris at the time of study. EDV = end-diastolic volume.



Figures 23-3, 23-4). Because the rate and extent of rapid diastolic filling decline significantly as a function of age in normal subjects [47, 48], correction for age is also necessary. Recent data indicate that even after accounting for age effects, patients with coronary disease have a reduced rate of rapid filling and a prolonged time-to-peak-filling rate compared to normal volunteers [49] and that these abnormalities under resting conditions persist even when those patients with previous myocardial infarction, abnormal resting electrocardiograms (ECG), and regional wall motion abnormalities are excluded from analysis [31, 49]. Although the prevalence of impaired diastolic filling at rest in such patients has differed among various studies [31, 41-46] (presumably reflecting differences in techniques and in patient selection), most investigators concur that left ventricular filling is impaired under resting conditions, in the absence of overt evidence of myocardial ischemia, in many patients with coronary artery disease and normal left ventricular systolic function [31, 41-45].

To investigate whether such disorders of rapid diastolic filling might be reversible, we

FIGURE 23-4. Peak left ventricular (LV) filling rate plotted as a function of LV ejection fraction for 231 consecutive patients with coronary artery disease (CAD) and 45 normal volunteers. All patients studied were free from cardiac medications EDV = end-diastolic volume. (Reproduced from Bonow et al. [31], with permission of the American Heart Association.)

studied a consecutive series of patients with single-vessel coronary artery disease before and after percutaneous transluminal coronary angioplasty (PTCA) [50]. Selection criteria included a normal resting ECG (absence of Q waves), normal global and regional left ventricular systolic function, and no history of myocardial infarction, to exclude patients with evidence of clinically overt myocardial fibrosis; absence of rest angina; and normal left ventricular internal cavity dimensions and wall thickness by echocardiography. All patients underwent radionuclide angiography free from cardiac medications both before and after PTCA; in the majority of patients, these studies were performed 1 day before and repeated 2 days after PTCA. Despite the selection of patients with normal regional and global systolic function at rest, left ven-

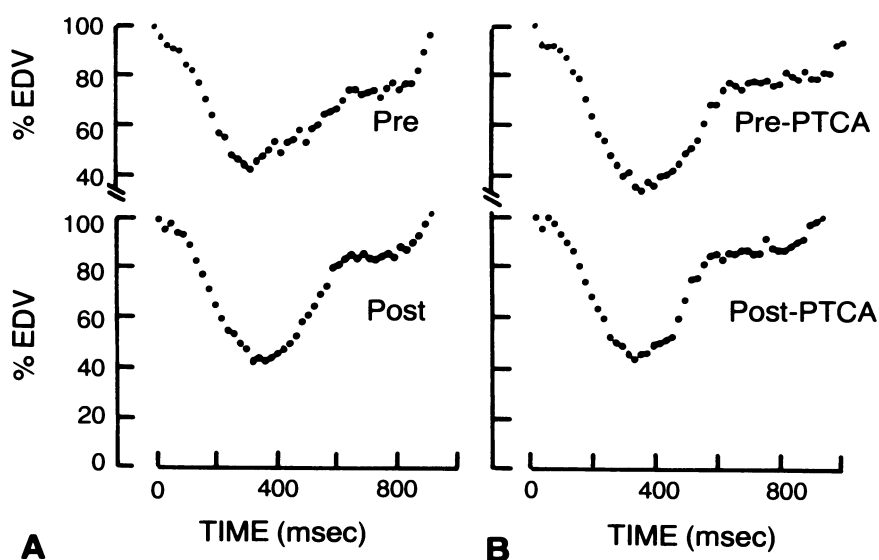


FIGURE 23-5. Left ventricular time-activity curves obtained at rest before (Pre) and after (Post) successful percutaneous transluminal coronary angioplasty (PTCA) in two patients (A and B) with single-vessel coronary artery disease. Ejection fraction and heart rate were not altered by PTCA, but the rate and timing of diastolic filling improved after PTCA. EDV = end-diastolic volume. (Reproduced from Bonow et al. [80], with permission of the American Heart Association.)

tricular filling was impaired in 68% of patients. After PTCA, heart rate and indices of systolic function (such as ejection fraction and peak ejection rate) were unchanged at rest, but rapid diastolic filling improved; peak filling rate increased and time to peak filling rate decreased (Figure 23-5). A possible mechanism of this effect on left ventricular filling is enhanced left ventricular relaxation stemming from reversal of subclinical myocardial ischemia or from the mechanical, load-dependent effect of an increased rate of early diastolic coronary blood flow [1]. These findings indicate that in many patients with coronary artery disease and normal global and regional systolic function, impaired rapid filling at rest does not represent a fixed abnormality but may be a reversible manifestation of myocardial ischemia or reduced coronary flow.

Impaired left ventricular filling in coronary

artery disease may also be modified by pharmacologic interventions. Peak filling rate increases and prolonged time to peak filling rate decreases after short-term oral verapamil therapy, both at rest and during maximum exercise [51]. In contrast, left ventricular filling properties at rest and exercise are not altered significantly by propranolol [51]. Verapamil-induced improvement in indices of rapid diastolic filling is observed despite significant reduction in ejection fraction at rest and in heart rate both at rest and with exercise, both of which would be expected to aggravate, rather than enhance, these indices. These observations are comparable to the combined hemodynamic and contrast angiographic findings of Lorell and coworkers [52], who demonstrated improved left ventricular relaxation and diastolic pressure-volume relations during pacing-induced ischemia in patients with coronary artery disease after the acute administration of sublingual nifedipine. Similarly, intravenous diltiazem depressed myocardial contractility but improved left ventricular relaxation and early diastolic filling in patients with coronary artery disease in the study of Murakami and colleagues [53].

The calcium channel blocking agents may enhance left ventricular filling by reducing myocardial ischemia and/or increasing myocardial blood flow directly—mechanisms identical

to those postulated for improved rapid filling after PTCA. However, the precise mechanism of action of these drugs is exceedingly difficult to determine because they also affect several additional load-dependent factors, including reduction in afterload, depression of left ventricular contractile performance, changes in heart rate, and possible alterations in left atrial pressure. The calcium channel blocking drugs may also have direct effects on reducing intracellular  $\text{Ca}^{2+}$  availability, thereby decreasing the severity of intracellular  $\text{Ca}^{2+}$  overload and facilitating the inactivation process. Such possible direct effects cannot be dissociated in clinical studies from the complex interaction of these agents on ischemia, coronary flow, and loading conditions. However, under some experimental conditions, impaired myocardial relaxation during hypoxia appears to be reversible and may be modified by intracellular  $\text{Ca}^{2+}$  availability [6, 54]. In addition, impaired myocyte relaxation resulting from exposure to a high concentration of  $\text{Ca}^{2+}$  can be either reversed by verapamil or prevented by pretreatment with verapamil [55]. Whether reduced myocardial inactivation during acute ischemia may be improved directly by agents that inhibit  $\text{Ca}^{2+}$  flux across the myocardial cell membrane remains to be determined.

### Left Ventricular Filling in Hypertrophic Heart Disease

Left ventricular diastolic function is altered in disease states characterized by left ventricular hypertrophy, and impaired rapid filling has been demonstrated by radionuclide angiography in over 70% of patients with hypertrophic cardiomyopathy, despite the common observation of normal or supranormal indices of systolic function [32, 56]. As in ischemic heart disease, rapid filling in hypertrophic cardiomyopathy is influenced both by the passive elastic properties of the left ventricle [24, 28, 57–59] and by the dynamics of left ventricular relaxation [60–65]. The morphologic disorders in this disease contribute to increased left ventricular chamber stiffness and decreased distensibility; these include increased myocardial mass, foci of myocardial fibrosis, and possibly myocardial cellular disorganization (Figure 23–6). In addition, several potential factors could influence left ventricular relaxation adversely (see Figure 23–6). Experimental studies indicate that sarcoplasmic reticulum uptake of  $\text{Ca}^{2+}$  may be

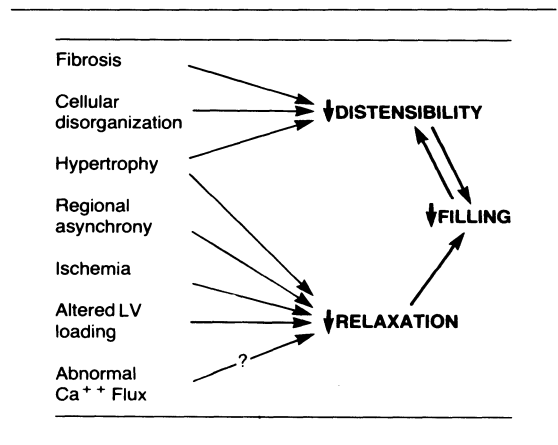


FIGURE 23–6. Determinants of impaired left ventricular (LV) filling in hypertrophic cardiomyopathy.

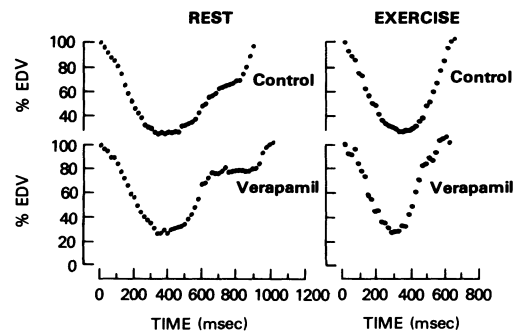


FIGURE 23–7. Left ventricular time-activity curves at rest and during exercise in a patient with hypertrophic cardiomyopathy before (control) and after oral verapamil therapy. At rest, verapamil results in shortening of the isovolumic relaxation period, increased rate and extent of rapid diastolic filling, reduced time to peak filling rate, and reduced contribution of atrial systole. Peak filling rate and time-to-peak-filling rate are also improved during exercise. Each point represents 20 msec. (Reproduced from Bonow [74], with permission of the American Journal of Cardiology.)

reduced in the setting of myocardial hypertrophy [66–68], and there is also increasing evidence that myocardial ischemia occurs commonly in hypertrophic cardiomyopathy in the absence of associated coronary artery disease [69, 70]. In addition to these two possible inactiva-

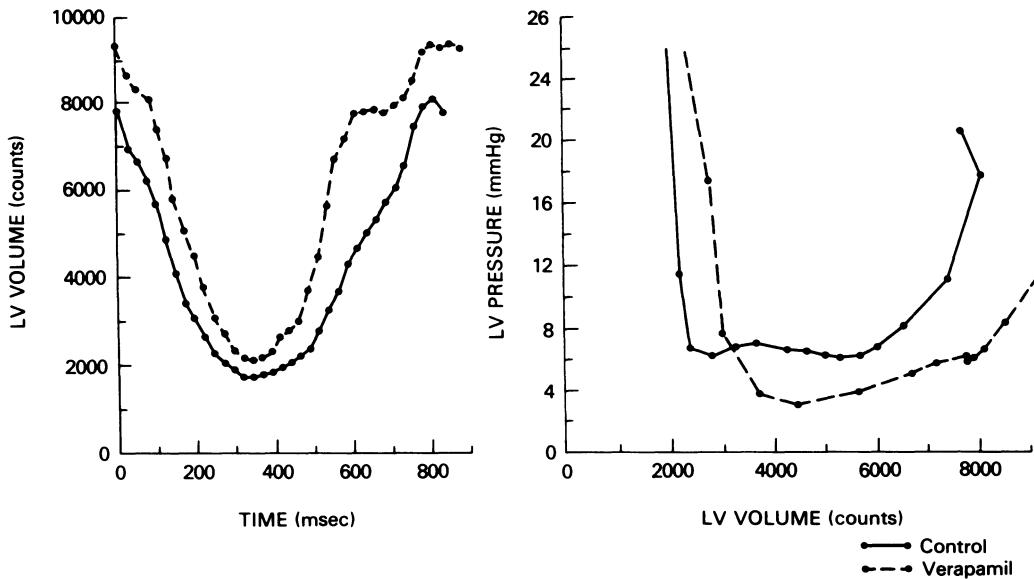


FIGURE 23-8. Left ventricular (LV) volume curves (*left panel*) and pressure-volume relations (*right panel*) obtained using a nonimaging scintillation probe and a micromanometer-tipped catheter in a patient with hypertrophic cardiomyopathy. Intravenous verapamil results in increased rate and extent of rapid filling, reduced contribution of atrial systole, and an increase in both end-diastolic volume and stroke volume. These changes are associated with a downward and rightward shift in the pressure-volume relation. Each point represents 25 msec. (Reproduced from Bonow, et al. [37], with permission of the American Heart Association.)

tion-dependent mechanisms, left ventricular relaxation may be disturbed in hypertrophic cardiomyopathy on the basis of load-dependent effects, including the rate and extent of coronary blood flow [69, 70] regional left ventricular nonuniformity [4, 71], decreased myocardial wall tension at the time of mitral valve opening [1, 4], altered afterload [1, 2], and altered contractile state [72]. Any or all of these potential mechanism may be operative in hypertrophic cardiomyopathy. Impaired relaxation and filling of the hypertrophied left ventricle result in elevated end-diastolic pressure despite normal or reduced end-diastolic volume and contribute importantly to the spectrum of symptoms experienced by patients with this disease.

The rate and extent of rapid filling is reduced in hypertrophic cardiomyopathy, time-to-peak-filling rate is prolonged, and the contribution of atrial systole to left ventricular stroke volume is increased [32, 56]. The isovolumic relaxation period, which is increased significantly in patients with hypertrophic cardiomyopathy compared to normal subjects [60-65], is the principal determinant of prolonged time-to-peak-filling rate [65], providing additional evidence that impaired left ventricular relaxation contributes importantly to the disturbances in rate, extent, and timing of rapid diastolic filling.

Verapamil, which is effective in relieving symptoms in patients with hypertrophic cardiomyopathy [73], improves these indices of left ventricular relaxation and filling (Figure 23-7), during both short-term and long-term therapy [32, 56, 71, 74, 75]. Combined hemodynamic and radionuclide angiographic studies indicate that enhanced left ventricular filling during verapamil administration is usually associated with improved indices of left ventricular relaxation (reduced time constant of relaxation) and diastolic-pressure volume relations (Figure 23-8) [37], despite significant negative inotropic effects. Similar improvement in left ventricular relaxation, filling, and pressure-volume rela-

tions have been observed during acute administration of nifedipine [76–78]. Enhanced left ventricular relaxation and filling by calcium channel blocking agents may be mediated by amelioration of intracellular calcium overload (either directly or indirectly via reduction in ischemia), increased coronary blood flow, reduction in left ventricular asynchrony, or other beneficial effects on left ventricular loading conditions. Enhanced left ventricular filling after verapamil administration correlates with objective symptomatic improvement [75], suggesting that improved left ventricular relaxation and filling are important mechanisms by which many patients experience symptomatic improvement during treatment with verapamil. In contrast, beta blockers do not appear to affect left ventricular diastolic performance to an important extent in hypertrophic cardiomyopathy [56, 77, 79].

### *Regional Asynchrony and Left Ventricular Filling*

Numerous studies have related impaired left ventricular relaxation and filling to nonuniform regional function in ischemic heart disease [10, 15–22, 42, 44, 80, 81]. Using radionuclide angiographic methods, abnormal left ventricular filling to has been found to be related significantly to regional asynchrony.

In the absence of apparent regional wall-motion disturbances at rest, regional systolic events are synchronous, but diastolic filling is asynchronous [42, 44, 80], and the magnitude of regional diastolic asynchrony correlates with severity of depression in global peak filling rate [44, 80]. The improvement in global left ventricular filling after successful PTCA in patients with single-vessel disease and normal systolic function is associated with a significant reduction in the degree of asynchronous diastolic function (Figure 23–9) [80]. Thus, diastolic asynchrony may be reversible and related to regional myocardial ischemia or regional reduction in coronary flow.

In patients with overt regional wall-motion abnormalities, the magnitude of systolic asynchrony has an additional impact on global left ventricular filling; the severity of systolic asynchrony correlates significantly in such patients with the prolongation in global time to peak filling rate [81]. These findings indicate that

regional asynchrony, representing a potential load-dependent effect on left ventricular relaxation [4], contributes to impaired global left ventricular filling in patients with ischemic heart disease. In patients with apparently normal global and regional systolic function, regional diastolic asynchrony is evident and, in many patients, may be reversed by interventions such as PTCA. When fibrosis or ischemia result in overt regional wall-motion disturbances, global left ventricular relaxation and filling are further delayed by the compounding effect of superimposed regional systolic asynchrony.

These concepts appear to pertain to hypertrophic cardiomyopathy as well; impaired left ventricular filling is related to substantial systolic and diastolic asynchrony, and the severity of diastolic asynchrony correlates with the depression in global peak filling rate [71]. Improvement in left ventricular filling parameters during verapamil therapy is associated with more uniform regional function [71], suggesting that verapamil's beneficial effects in hypertrophic cardiomyopathy may be mediated in part by reduction in asynchrony.

In view of the significant decline in rapid diastolic filling that occurs as a function of the normal aging process, we have recently assessed the effect of aging on left ventricular diastolic asynchrony in normal subjects ranging in age from 18 to 77 [48]. With advancing age, the magnitude of left ventricular diastolic asynchrony significantly increased, and the degree of asynchrony correlated with the age-related depression in both rate and extent of rapid filling [83]. These findings suggest that, as in coronary artery disease and hypertrophic cardiomyopathy, severity of diastolic asynchrony may contribute importantly to impaired global left ventricular filling in normal aging subjects.

### *Summary*

Evaluation of rapid diastolic filling in patient populations with coronary artery disease and hypertrophic cardiomyopathy indicates that disorders of left ventricular filling are prevalent even under resting conditions and are related to the degree of underlying regional systolic and diastolic asynchrony. The observation that impaired rapid filling in many such patients is not fixed, but may be reversible after appropriate therapeutic interventions, is evidence that left ventricular filling is influenced markedly by in-

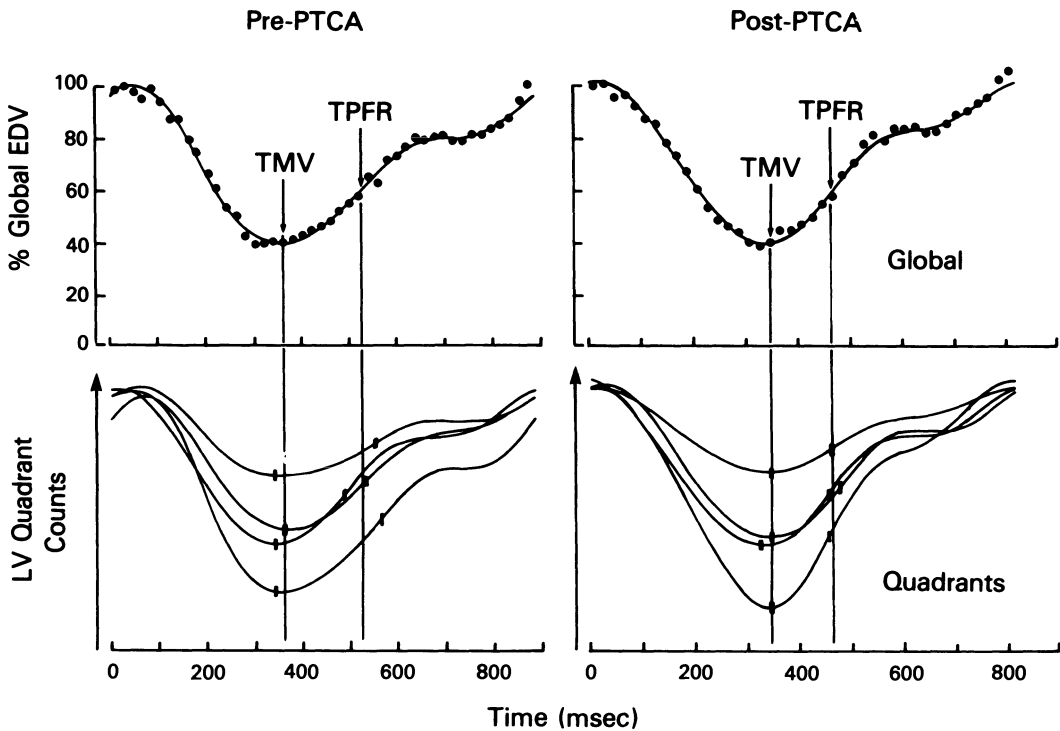


FIGURE 23-9. Regional variation in time to minimum volume (TMV) and time to peak filling rate (TPFR) in a patient before and after percutaneous transluminal coronary angioplasty (PTCA). Global time-activity curves are presented in the top panels and four quadrant curves (after three-harmonic filtering) in the bottom panels. Vertical lines indicate global TMV and TPFR, and heavy vertical bars indicate individual quadrant TMV and TPFR. Homogeneous values of TMV indicate relative regional systolic synchrony. However, variation among quadrants in TPFR before PTCA indicates considerable diastolic asynchrony, which was reduced after PTCA. This was associated with a decrease in global time to peak filling rate after PTCA and an increase in global peak filling rate. (Reproduced from Bonow, et al. [80], with permission of the American Heart Association.)

activation-dependent or load-dependent determinants of ventricular relaxation. Although abnormal rapid diastolic filling generally reflects altered ventricular relaxation, it must be emphasized that such disorders do not specifically indicate impaired inactivation, as filling dynamics are influenced by numerous loading factors as well as by the passive elastic properties of the left ventricle. It follows that definitive statements regarding the mechanisms responsible for impaired left ventricular diastolic function in these disease states, or for changes in diastolic function after interventions, cannot be determined by analysis of ventricular filling indices alone, especially if this assessment is made using noninvasive methods. Nonetheless,

in the proper setting, the evaluation of left ventricular filling may provide important insights into disease processes characterized by myocardial ischemia or hypertrophy.

### References

1. Brutsaert DL, Housmans PR, Goethals MA (1980). Dual control of relaxation: Its role in the ventricular function in the mammalian heart. *Circ Res* 47:637-652.
2. Gaasch WH, Blaustein AS, Andrias CW, et al (1980). Myocardial relaxation. II. Hemodynamic determinants of the left ventricular isovolumic pressure decline. *Am J Physiol* 239: H1-H6.
3. Raff GL, Glantz SA (1981). Volume loading

- slows left ventricular isovolumic relaxation rate: Evidence of load-dependent relaxation in the intact dog heart. *Circ Res* 48:813-824.
4. Brutsaert DL, Rademakers FE, Sys SU (1984). Triple control of relaxation: Implications in cardiac disease. *Circulation* 69:190-196.
  5. McLaurin LP, Rolett EL, Grossman W (1973). Impaired left ventricular relaxation during pacing induced ischemia. *Am J Cardiol* 32:751-757.
  6. Henry PD, Shuchleib R, Davis J, et al (1977). Myocardial contracture and accumulation of mitochondrial calcium in ischemic rabbit heart. *Am J Physiol* 233:H677-H684.
  7. Nayler WC, Williams A (1978). Relaxation in heart muscle: some morphological and biochemical considerations. *Eur J Cardiol* 7 (suppl):35-50.
  8. Frist WH, Palacios I, Powell WJ Jr (1978). Effect of hypoxia on myocardial relaxation in isometric cat papillary muscle. *J Clin Invest* 61:1218-1224.
  9. Mann T, Goldberg S, Mudge GH, et al (1979). Factors contributing to the altered left ventricular diastolic properties during angina pectoris. *Circulation* 59:14-20.
  10. Kumada T, Karliner JS, Pouleur H, et al (1979). Effects of coronary occlusion on early ventricular diastolic events in conscious dogs. *Am J Physiol* 237:H542-H549.
  11. Parmley WW, Sonnenblick EH (1969). Relation between mechanics of contraction and relaxation in mammalian cardiac muscle. *Am J Physiol* 216:1084-1091.
  12. Morad M, Rolett EL (1972). Relaxing effect of catecholamines on mammalian heart. *J Physiol (Lond)* 244:537-558.
  13. Karliner JS, LeWinter MM, Mahler F, et al (1977). Pharmacologic and hemodynamic influences on the rate of isovolumic left ventricular relaxation in the normal conscious dog. *J Clin Invest* 60:511-521.
  14. Morad M, Weiss J, Cleeman L (1978). The inotropic action of adrenaline on cardiac muscle: Does it relax or potentiate tension? *Eur J Cardiol* 7(suppl):53-62.
  15. Gibson DG, Prewitt TA, Brown DJ (1976). Analysis of left ventricular wall movement during isovolumic relaxation and its relation to coronary artery disease. *Br Heart J* 38:1010-1019.
  16. Ludbrook PA, Byrne JD, Tiefenbrunn AJ (1981). Association of asynchronous protodiastolic segmental wall motion with impaired left ventricular relaxation. *Circulation* 64:1201-1211.
  17. Pouleur H, Rousseau MF, van Eyll C, et al (1984). Assessment of regional left ventricular relaxation in patients with coronary artery disease: Importance of geometric factors and changes in wall thickness. *Circulation* 69:696-702.
  18. Green MV, Jones-Collins BA, Bacharach SL, et al (1984). Scintigraphic quantitation of asynchronous myocardial motion during the left ventricular isovolumic relaxation period: A study in the dog during acute ischemia. *J Am Coll Cardiol* 4:72-79.
  19. Gaasch WH, Blaustein AS, Bing OHL (1985). Asynchronous (early segmental) relaxation of the left ventricle. *J Am Coll Cardiol* 5:891-897.
  20. Sasayama S, Nonogi H, Miyazaki S, et al (1985). Changes in diastolic properties of the regional myocardium during pacing-induced ischemia in human subjects. *J Am Coll Cardiol* 5:599-606.
  21. Grossman W (1985). Why is left ventricular diastolic pressure increased during angina pectoris? *J Am Coll Cardiol* 5:607-608.
  22. Takeuchi M, Fujitani K, Kurogane K, et al (1985). Effects of left ventricular asynchrony on time constant and extrapolated pressure of left ventricular pressure decay in coronary artery disease. *J Am Coll Cardiol* 6:597-602.
  23. Gaasch WH, Cole JS, Quinones MA, et al (1975). Dynamic determinants of left ventricular diastolic pressure-volume relations in man. *Circulation* 51:317-323.
  24. Grossman W, Barry WH (1980). Diastolic pressure-volume relations in the diseased heart. *Fed Proc* 39:148-155.
  25. Gewirtz H, Ohley W, Walsh J, et al (1983). Ischemia-induced impairment of left ventricular relaxation: Relation to reduced diastolic filling rates of the left ventricle. *Am Heart J* 105:72-80.
  26. Magorien DJ, Shaffer P, Bush C, et al (1984). Hemodynamic correlates of timing intervals, ejection rate and filling rate derived from the radionuclide angiographic volume curve. *Am J Cardiol* 53:567-571.
  27. Ishida Y, Meisner JS, Tsujioka K, et al (1986). Left ventricular filling dynamics: Influence of left ventricular relaxation and left atrial pressure. *Circulation* 74:187-196.
  28. Grossman W, McLaurin LP 1976. Diastolic properties of the left ventricle. *Ann Int Med* 84:316-326.
  29. Glantz SA, Parmley WW 1978. Factors which affect the diastolic pressure-volume curve. *Circ Res* 42:171-180.
  30. Bacharach SL, Green MV, Borer JS, et al (1980). Left ventricular peak ejection rate, peak filling rate, and ejection fraction: Frame rate requirements at rest and during exercise. *J Nucl Med* 20:189-193.
  31. Bonow RO, Bacharach SL, Green MV, et al (1981). Impaired left ventricular diastolic filling

- in patients with coronary artery disease: Assessment with radionuclide angiography. *Circulation* 64:315-323.
32. Bonow RO, Frederick TM, Bacharach SL, et al (1983). Atrial systole and left ventricular filling in patients with hypertrophic cardiomyopathy: Effect of verapamil. *Am J Cardiol* 51:1386-1391.
  33. Green MV, Findley SF, Bonow RO, et al (1984). The amount of early left ventricular filling in resting normal subjects and patients with coronary artery disease and normal systolic function. In *Computers in Cardiology*. Long Beach, CA: IEEE Computer Society, pp 215-217.
  34. Bacharach SL, Green MV, Borer JS (1979). Instrumentation and data processing in cardiovascular nuclear medicine: Evaluation of ventricular function. *Semin Nucl Med* 9:257-274.
  35. Bonow RO, Bacharach SL. Left ventricular diastolic function: evaluation by radionuclide ventriculography. In Pohost GM (ed): *New Concepts in Cardiac Imaging 1987*. Chicago: Year Book, pp 107-137.
  36. Magorien DJ, Shaffer P, Bush CA, et al (1983). Assessment of left ventricular pressure-volume relations using gated radionuclide angiography, echocardiography, and micromanometer pressure recordings. *Circulation* 67:844-853.
  37. Bonow RO, Ostrow HG, Rosing DR, et al (1983). Verapamil effects on left ventricular systolic and diastolic function in patients with hypertrophic cardiomyopathy: Pressure-volume analysis with a nonimaging scintillation probe. *Circulation* 68:1062-1073.
  38. McKay RG, Aroesty JM, Heller GV, et al (1984). Left ventricular pressure-volume diagrams and end-systolic pressure-volume relations in human beings. *J Am Coll Cardiol* 3:301-312.
  39. Bonow RO, Ostrow HG, Rosing DR, et al (1984). Dynamic pressure-volume alterations during left ventricular ejection in hypertrophic cardiomyopathy: Evidence for true obstruction to left ventricular outflow. *Circulation* 70(suppl II):11-17 (abstract).
  40. Aroesty JM, McKay RG, Heller GV, et al (1985). Simultaneous assessment of left ventricular systolic and diastolic dysfunction during pacing-induced angina. *Circulation* 71:899-900.
  41. Polak JF, Kemper AJ, Bianco JA, et al (1982). Resting early peak diastolic filling rate: A sensitive index of myocardial dysfunction in patients with coronary artery disease. *J Nucl Med* 23:471-478.
  42. Miller TR, Goldman KJ, Sampathkumaran KS, et al (1983). Analysis of cardiac diastolic function: Application to coronary artery disease. *J Nucl Med* 24:2-7.
  43. Mancini GBJ, Slutsky RA, Norris SL, et al (1983). Radionuclide analysis of peak filling rate, filling fraction, and time to peak filling rate: Response to supine bicycle exercise in normal subjects and patients with coronary artery disease. *Am J Cardiol* 51:43-51.
  44. Yamagishi T, Ozaki M, Kumada T, et al (1984). Asynchronous left ventricular diastolic filling in patients with isolated disease of the left anterior descending coronary artery: Assessment with radionuclide ventriculography. *Circulation* 69:933-942.
  45. Bryhn M (1984). Abnormal left ventricular filling in patients with sustained myocardial relaxation: Assessment of diastolic parameters using radionuclide angiography and echocardiography. *Clin Cardiol* 7:639-646.
  46. Poliner LR, Farber SH, Glaeser DH, et al (1984). Alteration of diastolic filling rate during exercise radionuclide angiography: A highly sensitive technique for detection of coronary artery disease. *Circulation* 70:942-950.
  47. Miyatake K, Okamoto M, Kinoshita N, et al (1984). Augmentation of atrial contribution to left ventricular inflow with aging as assessed by intracardiac Doppler flowmetry. *Am J Cardiol* 53:586-589.
  48. Bonow RO, Vitale DF, Bacharach SL, et al (1987). Effects of aging on left ventricular regional function and global ventricular filling in normal human subjects. *J Am Coll Cardiol* (in press).
  49. Borow RO, Pace L, Bacharach SL, et al (1987). Impaired left ventricular filling in patients with coronary artery disease: Correction for age effect. *J Am Coll Cardiol* 9: UA (abstr).
  50. Bonow RO, Kent KM, Rosing DR, et al (1982). Improved left ventricular diastolic filling in patients with coronary artery disease after percutaneous transluminal coronary angioplasty. *Circulation* 66:1159-1167.
  51. Bonow RO, Leon MB, Rosing DR, et al (1982). Effects of verapamil and propranolol in left ventricular systolic function and diastolic filling in patients with coronary artery disease: Radionuclide angiographic studies at rest and during exercise. *Circulation* 65:1337-1350.
  52. Lorell BH, Turi Z, Grossman W (1981). Modification of left ventricular response to pacing tachycardia by nifedipine in patients with coronary artery disease. *Am J Med* 71: 667-675.
  53. Murakami T, Hess OM, Krayenbuehl HP (1985). Left ventricular function before and after diltiazem in patients with coronary artery disease. *J Am Coll Cardiol* 5:723-730.
  54. Greene HL, Weisfeldt ML (1977). Determinants of hypoxic and posthypoxic myocardial

- contracture. *Am J Physiol* 232:H526–H533.
55. Lorell BH, Barry WH (1984). Effects of verapamil on contraction and relaxation of cultured chick embryo ventricular cells during calcium overload. *J Am Coll Cardiol* 3:341–348.
  56. Bonow RO, Rosing DR, Bacharach SL, et al (1981). Effects of verapamil on left ventricular systolic function and diastolic filling in patients with hypertrophic cardiomyopathy. *Circulation* 64:787–796.
  57. Gaasch WH, Battle WE, Oboler AA, et al (1972). Left ventricular stress and compliance in man: With special reference to normalized ventricular function curves. *Circulation* 45:746–762.
  58. Mirsky I, Cohn PF, Levine JA, et al (1974). Assessment of left ventricular stiffness in primary myocardial disease and coronary artery disease. *Circulation* 50:128–136.
  59. Gaasch WH, Levine HJ, Quinones MA, et al (1976). Left ventricular compliance: Mechanisms and clinical implications. *Am J Cardiol* 38:645–653.
  60. Sanderson JE, Gibson DG, Brown DJ, et al (1977). Left ventricular filling in hypertrophic cardiomyopathy: An angiographic study. *Br Heart J* 39:661–670.
  61. Sanderson JE, Traill TA, St. John Sutton MG, et al (1978). Left ventricular relaxation and filling in hypertrophic cardiomyopathy: an echocardiographic study. *Br Heart J* 40:596–601.
  62. St. John Sutton MG, Tajik AJ, Gibson DG, et al (1978). Echocardiographic assessment of left ventricular filling and septal and posterior wall dynamics in idiopathic hypertrophic subaortic stenosis. *Circulation* 57:512–520.
  63. Hanrath P, Mathey DG, Siegert R, et al (1980). Left ventricular relaxation and filling in different forms of left ventricular hypertrophy: an echocardiographic study. *Am J Cardiol* 45:15–23.
  64. Alvares RF, Shaver JA, Gamble WH, et al (1984). Isovolumic relaxation period in hypertrophic cardiomyopathy. *J Am Coll Cardiol* 3:71–81.
  65. Betocchi S, Bonow RO, Bacharach SL, et al (1986). Isovolumic relaxation period in hypertrophic cardiomyopathy: assessment by radionuclide angiography. *J Am Coll Cardiol* 7:74–81.
  66. Sordahl LA, McCollum WB, Wood WG, et al (1973). Mitochondria and sarcoplasmic reticulum function in cardiac hypertrophy and failure. *Am J Physiol* 224:497–502.
  67. Ito Y, Suko J, Chidsey CA (1974). Intracellular calcium and myocardial contractility. V. Calcium uptake of sarcoplasmic reticulum fractions in hypertrophied and failing rabbit hearts. *J Mol Cell Cardiol* 6:237–247.
  68. Lecarpenter Y, Martin JL, Gastineau P, et al (1982). Load dependence of mammalian heart relaxation during cardiac hypertrophy and heart failure. *Am J Physiol* 242:H855–H861.
  69. Pasternac A, Noble J, Streulens Y, et al (1982). Pathophysiology of chest pain in patients with cardiomyopathies and normal coronary arteries. *Circulation* 65:778–689.
  70. Cannon RO, Rosing DR, Maron BJ, et al (1985). Myocardial ischemia in patients with hypertrophic cardiomyopathy: Contribution of inadequate vasodilator reserve and elevated left ventricular filling pressures. *Circulation* 71:234–243.
  71. Bonow RO, Vitale DF, Bacharach SL, et al (1987). Left ventricular regional left asynchrony and impaired global ventricular filling in hypertrophic cardiomyopathy: Effect of verapamil. *J Am Coll Cardiol* 9:1108–1116.
  72. Pouleur H, Rousseau MF, van Eyll C, et al (1983). Force-velocity-length relations in hypertrophic cardiomyopathy: Evidence for normal or depressed myocardial contractility. *Am J Cardiol* 52:813–817.
  73. Rosing DR, Condit JR, Maron BJ, et al (1981). Verapamil therapy: A new approach to the pharmacologic treatment of hypertrophic cardiomyopathy. III. Effects of long-term administration. *Am J Cardiol* 48:545–553.
  74. Bonow RO (1985). Effect of calcium channel blocking agents on left ventricular diastolic function in hypertrophic cardiomyopathy and in coronary artery disease. *Am J Cardiol* 55:172B–178B.
  75. Bonow RO, Dilsizian V, Rosing DR, et al (1985). Verapamil-induced improvement in left ventricular diastolic filling and increased exercise tolerance in patients with hypertrophic cardiomyopathy: Short- and long-term effects. *Circulation* 72:853–864.
  76. Lorell BH, Paulus WJ, Grossman W, et al (1982). Modification of abnormal left ventricular diastolic properties by nifedipine in patients with hypertrophic cardiomyopathy. *Circulation* 65:499–507.
  77. Senn M, Hess OM, Krayenbuehl HP (1982). Nifedipin in der Behandlung der hypertrophen, nicht-obstruktiven Kardiomyopathie. *Schweiz Med Wochenschr* 112:1312–1317.
  78. Paulus WJ, Lorell BH, Craig WE, et al (1983). Comparison of the effects of nitroprusside and nifedipine on diastolic properties in patients with hypertrophic cardiomyopathy: Altered left ventricular loading or impaired muscle inactivation? *J Am Coll Cardiol* 2:879–886.
  79. Hess OM, Grimm J, Krayenbuehl HP (1983). Diastolic function in hypertrophic cardiomyopathy: Effects of propranolol and verapamil on diastolic stiffness. *Eur Heart J* 4(suppl F):47–56.
  80. Bonow RO, Vitale DF, Bacharach SL, et al

- (1985). Asynchronous left ventricular regional function and impaired global diastolic filling in coronary artery disease: Reversal after coronary angioplasty. *Circulation* 71:297-307.
81. Bonow RO, Vitale DF, Bacharach SL, et al (1985). Effect of regional systolic and diastolic asynchrony on global left ventricular filling in coronary artery disease. *Circulation* 72(suppl III):III-481 (abstract).

---

## 24. REGIONAL DIASTOLIC DYSFUNCTION IN CORONARY ARTERY DISEASE: CLINICAL AND THERAPEUTIC IMPLICATIONS

---

Hubert Pouleur, Michel F. Rousseau

Alterations in left ventricular diastolic function, such as reduction in the rate of pressure-decrease during isovolumic relaxation, impaired rate of rapid filling, or upward shift of the diastolic pressure-volume relation, are found in most patients with coronary artery disease [1–9]. These abnormalities are particularly severe during angina [2, 8], but they are also frequently evident in the absence of clinical signs of ischemia [3–6, 9, 10]. It has also been shown that these altered diastolic properties may be improved by several therapeutic interventions [6, 9–11].

Controversy still exists, however, regarding the pathophysiologic mechanisms underlying these abnormalities, as well as regarding their clinical relevance. It has, indeed, been suggested that the slowing in the rate of isovolumic pressure fall or the shift of the diastolic pressure-volume relation, rather than reflecting true impairment in myocardial relaxation, might merely represent mechanical artifacts caused by asynchronous wall motion, reduced coronary perfusion pressure or interaction between the cardiac chambers and the pericardium [12–14]. Nevertheless, during the last few years, studies combining simultaneous measurements of the

regional and global diastolic function have been performed in animal models of high-demand ischemia [15, 16] and in patients with ischemic heart disease [9, 10, 17, 18]. Their results support the hypothesis that, in angina pectoris, regional myocardial stiffness is increased and relaxation is impaired in response to pacing-induced ischemia. These studies have also provided evidence that in the presence of a sufficient mass of acutely or chronically ischemic myocardium, the dynamic compliance of the left ventricular chamber itself is reduced.

This chapter will review some of these studies and will then focus specifically on the possible relationship between coronary artery disease, impaired regional diastolic function, and the functional status of the patient. To assess the clinical relevance of the information derived from these previous studies, it is necessary to correlate objective assessments of diastolic function with clinical parameters such as functional capacity, incidence of congestive heart failure, prognosis, and mortality. So far, none or very little of this work has been done. Some of our preliminary data may therefore provide an *avant-goût* of what might be found in larger controlled studies.

This work was supported, in part, by a grant SPPS 83/88-51 from the Belgian Government. The technical help of Mr Jean Etienne, Christian van Eyll and Henri Van Mechelen and the careful secretarial assistance of Mrs Véronique Heirman are also gratefully acknowledged. Grossman, William, and Lorell, Beverly H. (eds.), *Diastolic Relaxation of the Heart*. Copyright © 1987. Martinus Nijhoff Publishing. All rights reserved.

### *Relation Between Regional Myocardial Stiffness, Regional Relaxation, and Coronary Perfusion*

Complete coronary occlusion usually results only in transient alteration of the left ventricular

isovolumic relaxation rate [13]. In this setting, the ischemic area creeps and may function during diastole in the steep part of its passive stress-strain relation [14], but there is no evidence that its distensibility is reduced by an active mechanism.

In contrast, when ischemia is produced in open-chest dogs by increasing myocardial energy demand in the presence of coronary stenoses, there is an increase in muscle stiffness, that can be potentiated by caffeine [15, 16]. Thus, the change in physical property of the myocardium induced by high-demand ischemia appears directly related to an impairment of the active relaxation process or, in other words, to an incomplete inactivation of the myocardial cell. High-demand myocardial ischemia may impair intracellular metabolism in such a way that the rate of calcium sequestration by the sarcoplasmic reticulum or calcium efflux across the sarcolemma is reduced, resulting in a persistent interaction of contractile proteins throughout diastole and in an increased "active" diastolic stiffness [16].

Several clinical studies have confirmed that these mechanisms are also operative in patients with angina pectoris. Bourdillon and coworkers [17], using simultaneous high-fidelity left ventricular pressure recording and M-mode echocardiography, reported that during pacing-induced angina a decreased rate of posterior wall thinning and a displacement of the diastolic pressure/wall thickness relation develop, identical to that observed in dogs. Sasayama and colleagues [18], using angiographic techniques, also showed a reduction in myocardial distensibility in ischemic regions.

In our laboratory, we examined patients with angina to determine if the same phenomenon of delayed or incomplete inactivation might also be present, although with a reduced severity, between anginal episodes. For that purpose, we computed regional left ventricular wall stress during isovolumic relaxation in patients with coronary artery disease [10], by simultaneously measuring high-fidelity left ventricular pressure, angiographic ventricular dimensions, and wall thickness. We observed that in noninfarcted areas perfused by stenosed arteries ("Ischemic" Area, Figure 24-1), the rate of decrease in wall stress was significantly slower than the rate of decrease in pressure. Moreover, the residual regional wall stress at the time of mitral valve opening was increased in areas perfused by stenosed arteries ( $30 \pm 19$  standard deviation

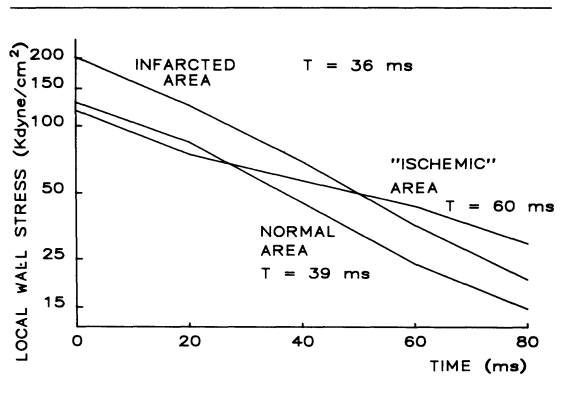


FIGURE 24-1. Time-course of regional wall stress fall during isovolumic relaxation in three different areas of a left ventricle. The rate of stress fall is reduced in the area perfused by a stenosed coronary artery ("Ischemic" Area).  $T$  = the time constant of the monoexponential relation fitted into the data points.

[SD]  $\text{kdyne/cm}^2$  vs.  $9 \pm 5 \text{ kdyne/cm}^2$  in normal areas;  $p < 0.001$ ). These data, therefore, indicate that the rate of myocardial relaxation remained abnormal between anginal episodes in the territory perfused by diseased vessels. This suggests that the abnormalities in diastolic function observed in the basal state and in response to high-demand ischemia probably share a common origin: impaired inactivation caused by abnormalities in intracellular metabolism.

In this perspective, the impaired diastolic properties in ischemic heart disease would not be an "all or none" phenomenon, triggered only by high-demand ischemia, but rather a continuous process of varying intensity. It has been shown, using radiolabeled metabolites, that anerobic metabolism is sometimes present in the basal state in patients with coronary artery disease [19-21]. Other abnormalities that can be detected at rest in these patients include the myocardial release of glutamine and alanine and an increased uptake of glutamic acid [21-22]. Thus, regional myocardial metabolism appears chronically disturbed in patients with angina pectoris either because of chronic underperfusion of viable areas or because of incomplete recovery of the underperfused areas between anginal episodes. It can be suspected, therefore, that such alterations in intracellular metabolism may be directly responsible for the incom-

plete inactivation of the cells, particularly if the energy-yielding pathways used for relaxation are disturbed. Repeated or prolonged ischemic episodes followed by reperfusion result in a persistent depression of the systolic function or "stunning" of the myocardium [23]; the presently available data suggest that the most sensitive marker of the "stunned myocardium" might well be an impairment in regional diastolic relaxation and distensibility.

### *Relation Between Impaired Regional Relaxation and Global Ventricular Dynamic Compliance*

To assess the influence of the active relaxation process on myocardial stiffness, it has been proposed that the rate of tension fall from the time-constant of isovolumic pressure fall be evaluated and then the values of residual wall stress be computed during diastole, which, in this method, is also alleged to decay exponentially. This procedure may be a good approximation in normal ventricles but will lead to large errors in ischemic heart disease for three reasons.

First, the time-course of the decrease in isovolumic pressure underestimates the severity of local impairment in relaxation rate and will therefore also underestimate the values of residual wall stress [10]. This can lead to errors of 100% (as in Figure 24-1) or more. Second, there may be a dissociation between the *rate* and *extent* of myocardial relaxation [16], so that after some time the tension no longer decays exponentially but remains constant. Experimentally, this situation has been observed after caffeine administration [16]. A similar phenomenon, related to a reduction in the maximum binding capacity of the sarcoplasmic reticulum, might also occur during ischemia. Third, the values of regional residual wall stress obviously depend not only on their rate of decay but also on their absolute value at the start of the decay. This intuitive point has been totally neglected in most analyses, and this again may lead to large errors, particularly when hypokinetic or akinetic areas are present in which the radius of curvature remains large and in which the wall remains thin at the end of ejection. For example in Figure 24-1, the residual wall stress in the infarcted area is greater than normal, although its rate of decay is actually faster. The time-constant of isovolumic pressure fall should, therefore, not be used to predict the dynamic

left ventricular compliance, because it imperfectly reflects the numerous factors, some active, some passive, that contribute to maintain high levels of regional wall forces until diastolic filling begins. These forces impede the filling of the cavity either actively, by creating a kind of "mini-systole" and by generating external work [24] or passively, because wall distensibility is reduced by the increased resting tension. At identical values of venous return, the presence of these impeding forces will increase left atrial pressure and shift the left ventricular diastolic pressure-volume relation upward [8, 9, 18]. The fact that these shifts have been noted in animals with the chest and the pericardium opened [15, 16] confirms that the changes observed in patients can be explained primarily by the impaired regional relaxation rather than by a pericardial effect. Nevertheless, it can also be predicted intuitively that a certain amount of myocardium must be underperfused before modifications of the global diastolic function can be detected. Recent work has been able to demonstrate, in patients, these relations between the amount of myocardium "at risk" and the global left ventricular diastolic function [27].

In 20 patients with angina pectoris, but without prior myocardial infarction, we examined the relations between the number of ventricular segments with an impaired diastolic distensibility and the dynamic chamber compliance [9]. Because regional wall stress is tedious to evaluate, we computed a simpler index of regional distensibility, the regional peak filling rate. For that purpose, the angiographic data were digitized manually, frame by frame, as described previously [25]. Regional wall motion was assessed in eight ventricular segments (four anterior and four inferior), and the rate of change in a segmental area was computed after data smoothing. A depressed regional peak filling rate in at least one ventricular segment was detected in 75% of the patients with angina studied in the basal state. It must be remembered, however, that regional and global peak filling rates are dependent not only on the physical properties of the myocardium but also on the pressure gradient between the atrium and the ventricle [26]. Consequently, an increased preload can preserve normal values of regional peak filling rate in spite of a significant impairment in regional relaxation. This reduces the sensitivity of this index but its specificity to detect impaired regional diastolic function re-

mains excellent. Indeed, in all patients in whom depression in regional peak filling rate was detected, the left ventricular filling pressure was normal or increased, making false-positive results unlikely. The interesting observation of this study is that a relation between the extent of the alterations in regional peak filling rate and the dynamic left ventricular compliance was evident. Despite comparable end-diastolic volume, the patients with angina pectoris whose ventricles had at least three segments with a reduced peak filling rate, had, indeed, significant increases in mean left ventricular filling pressure ( $14 \pm 4$  vs.  $8 \pm 3$  in normal subjects;  $p < 0.01$ ) and upward shifts of their left ventricular diastolic pressure-volume relation during rapid filling when compared with normal subjects or with patients with less severe alterations in regional distensibility (Figure 24-2).

Another proof of the direct relation between the amount of underperfused myocardium and the severity of the impairments in diastolic function was provided by the work of McKay and coworkers [27]. In their study, the total thallium score during exercise was used as an index of the mass of ischemic myocardium. They found an excellent rank correlation ( $r = 0.90$ ) between total thallium score and the post-pacing increase in left ventricular end-diastolic pressure. Recently, we have also reported a similar relation between the total thallium score measured during exercise and the left ventricular end-diastolic pressure measured in the basal state [28]. Patients with the highest thallium score during exercise also had, in the basal state, the slowest rate of isovolumic pressure fall, the smallest lactate extraction fraction, and the largest myocardial release of alanine and glutamine [28]. These data support the hypothesis that regional abnormalities in diastolic function directly reflect the presence of viable but underperfused areas.

In summary, all data available so far are compatible with the hypothesis that myocardial metabolism is impaired in myocardial areas perfused by stenosed coronary vessels, not only during acute ischemic episodes but also in the basal state between ischemic episodes. These metabolic abnormalities are the most likely cause of the incomplete inactivation of the myocardium in these areas. As expected, some correlation exists between the size of the underperfused area, the increase in left ventricular

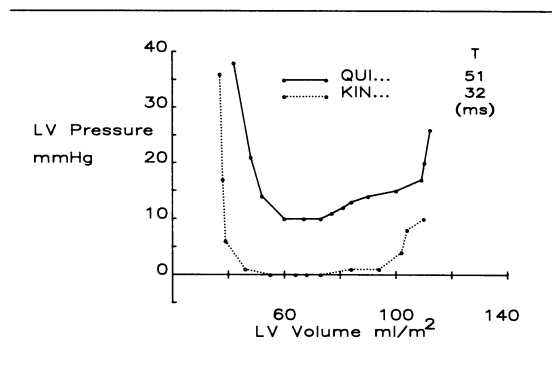


FIGURE 24-2. Diastolic left ventricular (LV) pressure-volume relation in two patients with angina pectoris and comparable systolic function. Neither patient had a prior myocardial infarct, but regional peak filling rate was reduced in three ventricular segments in the patient QUI..., whereas patient KIN... had an entirely normal regional function during diastolic filling. T = time constant of isovolumic pressure fall.

filling pressure, and the reduction in left ventricular compliance. The clinical implications of these alterations in left ventricular regional relaxation will now be examined.

### *Clinical and Therapeutic Implications*

The persistence of a significant amount of active myocardial tension during diastole may have clinically relevant consequences by different mechanisms [29]. By impeding coronary perfusion, impaired myocardial relaxation may create a vicious circle, worsening regional ischemia and further increasing the diastolic tone. Thus, impaired relaxation might theoretically trigger a progressive deterioration of the myocardial performance, at first limited to diastole but eventually extending to systolic performance. Another consequence of the reduced diastolic distensibility is the increase in cardiac filling pressure and the pulmonary vascular congestion. Some clinical manifestations of heart failure may therefore be more directly related to the diastolic dysfunction than to the systolic dysfunction.

From this perspective, one aspect that we feel is particularly worth investigating is the adaptive changes in ventricular volume and pressure during exercise. An adequate relaxation is, indeed, of paramount importance to ensure optimal ventricular filling during tachycardia

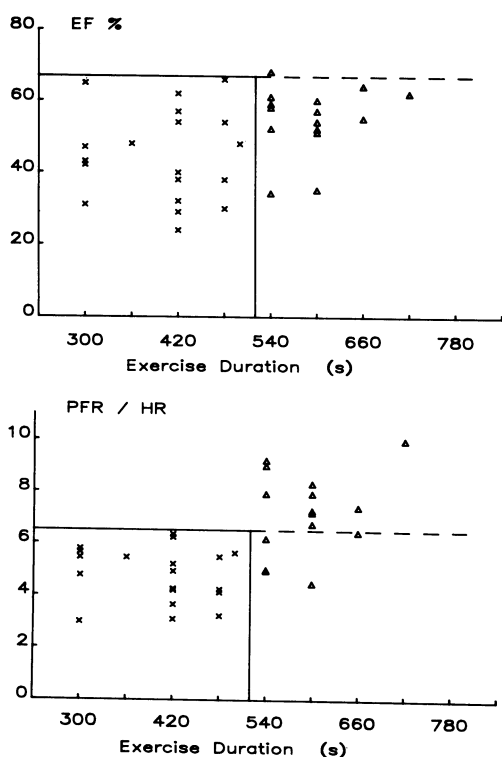


FIGURE 24-3. Relationship between maximal exercise duration and resting ejection fraction (EF) or resting peak filling rate normalized for resting heart rate (PFR/HR). All 34 patients had a previous anterior myocardial infarction. The correlation between EF and exercise duration was weak ( $r = 0.37$ ), and the separation of the patients with good exercise tolerance (triangles: group B) from those with reduced exercise capacity (crosses: group A) was also poor with this index of systolic function. The correlation of exercise duration with the index of diastolic function was slightly better ( $r = 0.59$ ), and 83% of the patients could be correctly classified by this index.

and abbreviation of the length of diastole. An impaired relaxation should, therefore, limit the preload reserve that can be used in upright exercise [30], requiring the cardiac output to be increased by an excessive tachycardia and necessarily limiting the maximal load achieved. Accordingly, the fact that the maximal oxygen uptake during exercise correlates poorly with the indices of systolic function such as the ejection fraction might be partially related to the difference in diastolic performance between

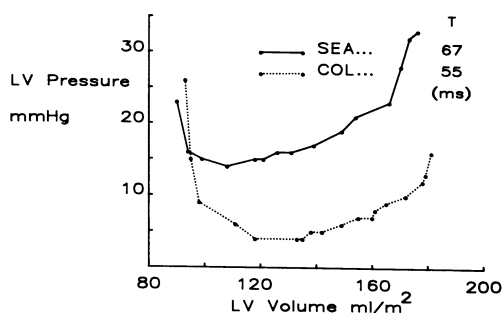


FIGURE 24-4. Typical left ventricular (LV) diastolic pressure-volume relation at rest in a patient from group A (SEA... , continuous line) and in a patient from group B (COL... , dotted line). Systolic function was similar in both patients, but dynamic diastolic compliance and exercise duration (420 vs. 540 seconds) were reduced in patient SEA.

patients.

To verify this hypothesis, we analyzed the exercise test data of 34 patients with left ventricular dysfunction caused by a prior anterior myocardial infarction. The exercise tests had been performed on a bicycle ergometer with a 20-watt increase in load every minute [31]. The day following the test, a left ventriculogram with simultaneous recording of high-fidelity left ventricular pressure was performed. Angiographic data were processed as already described. As shown by Figure 24-3, the resting ejection fraction was of little value in predicting exercise duration in these patients. In contrast, an index of diastolic distensibility, such as the peak rapid filling rate normalized for the resting heart rate (Figure 24-3) or for the left ventricular end-diastolic pressure, allowed a good separation of the patients able to exercise more than 9 minutes (group B) from those with a reduced exercise tolerance (group A) (Figure 24-3). The number of ventricular segments with a reduced regional peak filling rate was greater in group A patients than in group B patients (average 4.2 vs. 2.6 segments/patient in group B;  $p < 0.01$ ) and the mean left ventricular filling pressure was also elevated at rest ( $19.2 \pm 7.4$  vs.  $14.0 \pm 3.7$  mm Hg;  $p < 0.02$ ) in group A patients. Moreover, when patients with similar left ventricular volumes were compared, an impairment in diastolic compliance was obvious in the patients in group A (see Figure 24-4).

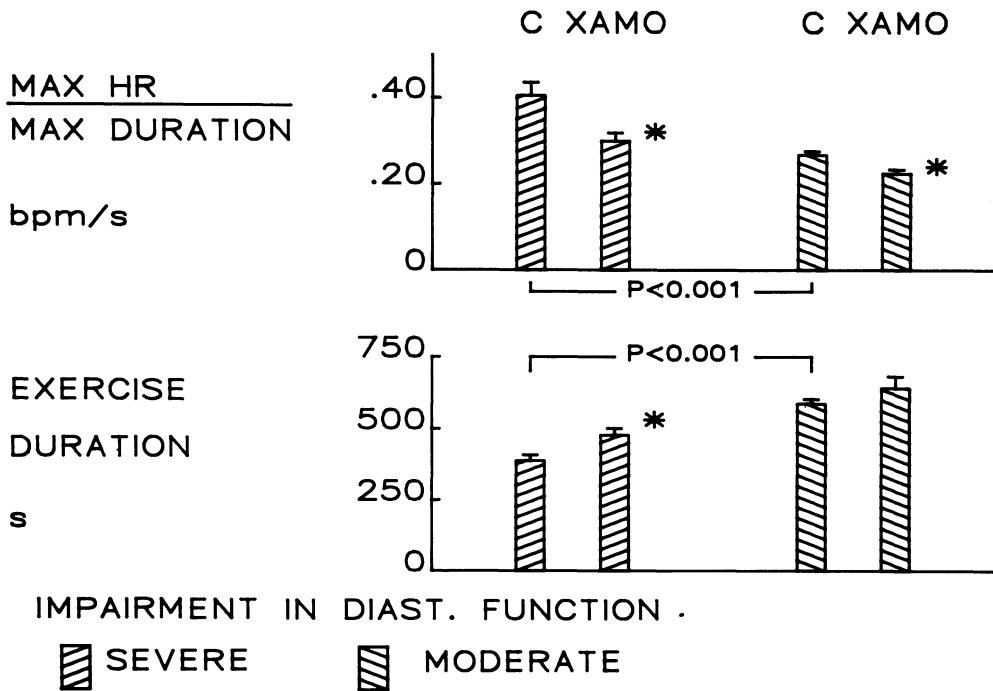


FIGURE 24-5. Maximal heart rate at peak exercise normalized for exercise duration in patients with severe (group A) or moderate (group B) diastolic dysfunction, before (C) or during long-term xamoterol (XAMO) therapy. There was an inappropriate tachycardia and a reduced exercise duration in group A, both of which were improved by xamoterol therapy.

Another difference between groups, which might have an important physiologic significance, was noted when examining the heart rate changes during exercise: to achieve the same load, the heart rate was higher in group A than in group B. Accordingly, the maximal heart rate normalized for the maximal load was inappropriately high in patients with severe diastolic dysfunction ( $0.41 \pm 0.10$  bpm/second of exercise in group A vs.  $0.27 \pm 0.028$  bpm/second of exercise in group B [ $p < 0.001$ ]). Such data suggest that, in ischemic heart disease, alterations in dynamic regional distensibility affect the cardiac response during exercise and may play a functional role, independently of the systolic function.

Consequently, one might wonder if therapeutic interventions aimed at improving myocardial relaxation could have some future promise. The intravenous administration of xamoterol [32], a new  $\beta_1$ -adrenoceptor partial agonist, acutely improves myocardial relaxation and reduces diastolic wall stress while producing only modest changes in the ejection fraction or in end-systolic volume [33]. Twenty-three of the 34

patients illustrated in Figure 24-3 received xamoterol orally for 3 months (200 mg b.i.d.). Exercise tests and ventriculography were then repeated under therapy. As can be seen in Figures 24-5 and 24-6, xamoterol therapy improved exercise duration and reduced exercise tachycardia in these patients. Figure 24-6 indicates that global systolic pump function was little affected at rest by this therapy, as shown by the lack of change in ejection fraction. Diastolic function on the other hand, consistently improved. The typical changes in diastolic pressure-volume relation during xamoterol treatment are illustrated in Figure 24-7. Xamoterol therapy significantly reduced the filling pressures (average reduction in left ventricular end-diastolic pressure for the whole group: from  $24 \pm 7$  to

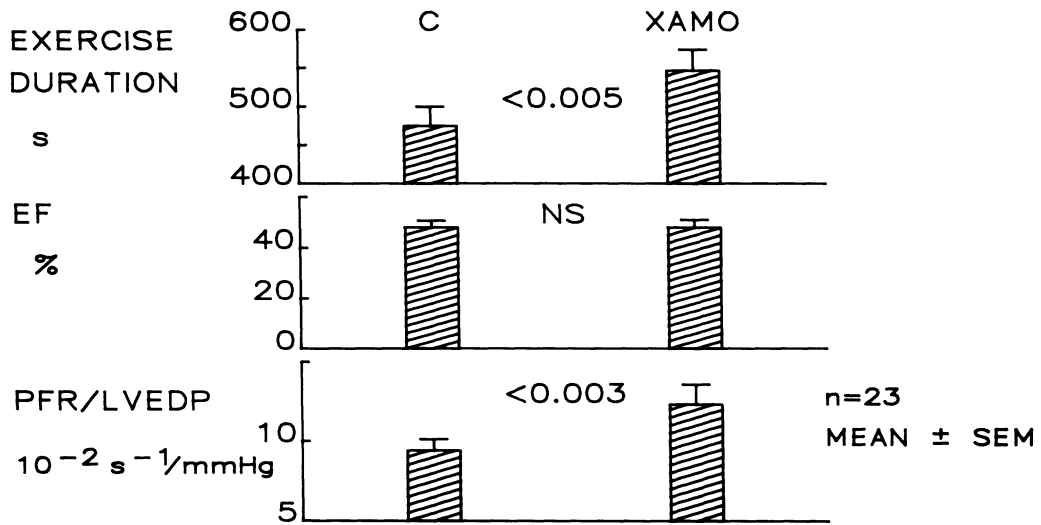


FIGURE 24-6. Exercise duration, resting ejection fraction (EF) and resting peak filling rate normalized for preload (PFR/LVEDP) before (C) and during long-term xamoterol (XAMO) treatment. NS = not significant.

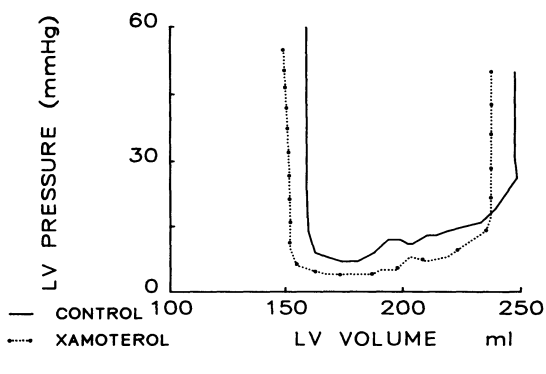
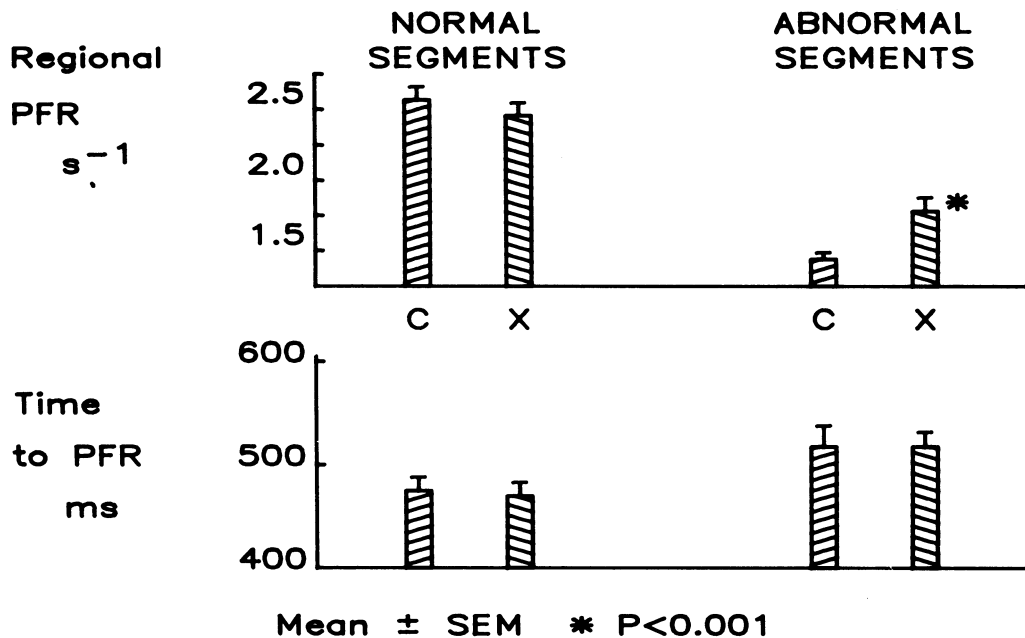


FIGURE 24-7. Typical changes in diastolic pressure-volume loop induced in one patient from group A by long-term xamoterol therapy.

$17 \pm 7$  mm Hg;  $p < 0.001$ ) and improved the dynamic ventricular compliance during rapid filling. It is also noteworthy that despite the preload reduction, regional peak filling rates improved significantly in areas with a reduced distensibility (Figure 24-8). Since a preload

reduction normally reduces the filling rate [26], this observation suggests that xamoterol therapy had significantly improved myocardial distensibility in these areas. Further, when preload changes were taken into account, the global peak filling rate appeared improved during treatment (see Figure 24-6). Again, the parallel improvement in exercise tolerance and in diastolic function during xamoterol therapy adds another argument in favor of the functional importance of these alterations of diastolic function. Finally, it is interesting to note that myocardial lactate extraction fraction increased during treatment with xamoterol, from  $20 \pm 17$  to  $30 \pm 15\%$  ( $p < 0.01$ ), whereas lactate extraction tended to be reduced in a similar group of placebo-treated patients ( $22 \pm 6$  to  $6 \pm 20\%$ ). Thus, the improvement in diastolic function was accompanied by an indirect evidence that underperfused areas may also have improved their aerobic metabolism.

Other therapeutic interventions have been shown to improve myocardial diastolic function acutely in patients with ischemic heart disease, either in basal state or after angina. They include administration of calcium-antagonists such as nifedipine, verapamil, or nicardipine [9, 10, 11, 34] or the infusion of other inotropes such as milrinone [35]. The mechanisms by which these agents can improve diastolic distensibility are beyond the scope of this review.



Xamoterol and milrinone could improve the calcium reuptake of the sarcoplasmic reticulum through cyclic adenosine monophosphate mediated mechanisms. Calcium antagonists may reduce myocardial ischemia and myoplasmic calcium-overload, responsible for the increased diastolic tone. Intravenous administration of nicardipine performed in separate groups of patients with angina pectoris improved myocardial metabolism acutely, reducing regional lactate production evaluated by the infusion of radiolabeled lactate, and reducing amino-acid release. It is tempting to consider that such an improvement in aerobic metabolism was responsible for the selective improvement in regional relaxation observed after nicardipine infusion in other studies [9, 10]. Whatever mechanisms are involved, these promising results show that it is possible to improve diastolic function in patients with ischemic heart disease, and that this may have useful clinical consequences.

### Conclusions

Regional diastolic dysfunction in coronary artery disease appears to be caused by an incomplete inactivation of the myocardium in under-

FIGURE 24-8. Effects of xamoterol (X) on regional peak filling (PFR) rate and on time to peak filling rate. Despite the significant preload reduction during treatment, peak filling rate was unchanged in normal segments and improved in areas with impaired distensibility. C = before xamoterol therapy.

perfused areas. The alterations in diastolic behavior of the left ventricle, such as asynchronous diastolic wall motion, prolongation of isovolumic relaxation, reduced peak filling rate, and shifts of the pressure-volume relation, are likely to be the direct consequences of impairment in regional myocardial relaxation. In addition, the alterations in dynamic ventricular compliance that are evident during severe ischemia and even in the basal state when large myocardial areas are underperfused chronically, appear able to limit the functional capacity of these patients.

### References

1. Papapietro SE, Coghlan HC, Zissermann D, et al (1979). Impaired maximal rate of left ventricular relaxation in patients with coronary artery disease and left ventricular dysfunction. *Circulation* 59:984-991.
2. McLaurin LP, Rolett EL, Grossman W (1973).

- Impaired left ventricular relaxation during pacing-induced ischemia. *Am J Cardiol* 32:751-757.
3. Rousseau MF, Veriter C, Detry JMR, et al (1980). Impaired early left ventricular relaxation in coronary artery disease. Effects of intracoronary nifedipine. *Circulation* 62:764-772.
  4. Rousseau MF, Pouleur H, Detry JMR, Brasseur LA (1981). Relationship between changes in left ventricular inotropic state and relaxation in normal subjects and in patients with coronary artery disease. *Circulation* 64:736-743.
  5. Bonow RO, Bacharach SL, Green MV, et al (1981). Impaired left ventricular diastolic filling in patients with coronary artery disease: Assessment with radionuclide cineangiography. *Circulation* 64:315-323.
  6. Bonow RO, Vitale DF, Bacharach SL, et al (1985). Asynchronous left ventricular regional function and impaired global diastolic filling in patients with coronary artery disease: Reversal after coronary angioplasty. *Circulation* 71:297-307.
  7. Reduto LA, Wickmeyer WJ, Young JB, et al (1981). Left ventricular diastolic performance at rest and during exercise in patients with coronary artery disease: Assessment with first-pass radionuclide angiography. *Circulation* 63:1228-1237.
  8. Mann T, Goldberg S, Mudge GH, Grossman W (1979). Factors contributing to altered left ventricular diastolic properties during angina pectoris. *Circulation* 59:14-20.
  9. Pouleur H, Rousseau MF, van Eyll C, et al (1986). Impaired regional diastolic distensibility in coronary artery disease: Relations with dynamic left ventricular compliance. *Am Heart J* 112:721-728.
  10. Pouleur H, Rousseau MF, van Eyll C, Charlier AA (1984). Assessment of regional left ventricular relaxation in patients with coronary artery disease: Importance of geometric factors and changes in wall thickness. *Circulation* 69:696-702.
  11. Lorell BH, Turi Z, Grossman W (1981). Modification of left ventricular response to pacing tachycardia by nifedipine in patients with coronary artery disease. *Am J Med* 71:667-675.
  12. Ludbrook PA, Byrne JD, Tiefenbrunn AJ (1981). Association of asynchronous protodiastolic segmental wall motion with impaired left ventricular relaxation. *Circulation* 64:1201-1211.
  13. Kumada T, Karliner J, Pouleur H, et al (1979). Effects of acute coronary occlusion on early ventricular diastolic events in conscious dogs. *Am J Physiol* 237:H542-H549.
  14. Ross J Jr (1979). Acute displacement of the diastolic pressure-volume curve of the left ventricle: Role of the pericardium and the right ventricle. *Circulation* 59:32-37.
  15. Serizawa T, Carabello BA, Grossman W (1980). Effect of pacing-induced ischemia on left ventricular diastolic pressure-volume relations in dogs with coronary stenoses. *Circ Res* 46:430-439.
  16. Paulus WJ, Serizawa T, Grossman W (1982). Altered left ventricular diastolic properties during pacing-induced ischemia in dogs with coronary stenoses: Potentiation by caffeine. *Circ Res* 50:218-227.
  17. Bourdillon PD, Lorell BH, Mirsky I, et al (1983). Increased regional myocardial stiffness of the left ventricle during pacing-induced angina in man. *Circulation* 67:316-323.
  18. Sasayama S, Nonogi H, Miyazaki S, et al (1985). Changes in diastolic properties of the regional myocardium during pacing-induced ischemia in human subjects. *J Am Coll Cardiol* 5:599-606.
  19. Gertz EW, Wisneski JA, Neese R, et al (1981). Myocardial lactate metabolism: evidence of lactate release during net chemical extraction in man. *Circulation* 63:1273-1279.
  20. Wisneski JA, Gertz EW, Neese RA, et al (1985). Dual carbon-labeled isotope experiments using D-(6-<sup>14</sup>C)glucose and L-(1, 2, 3-<sup>13</sup>C<sub>3</sub>) lactate: A new approach for investigating human myocardial metabolism during ischemia. *J Am Coll Cardiol* 5:1138-1146.
  21. Rousseau MF, Vincent MF, Van Hoof F, et al (1984). Effects of nicardipine and nisoldipine on myocardial metabolism, coronary blood flow and oxygen supply in angina pectoris. *Am J Cardiol* 54:1189-1194.
  22. Mudge GH Jr, Mills RM, Taegtmeier H, et al (1976). Alterations of myocardial amino-acid metabolism in chronic ischemic heart disease. *J Clin Invest* 58:1185-1192.
  23. Braunwald E, Kloner RA (1982). The stunned myocardium: Prolonged, postischemic ventricular dysfunction. *Circulation* 66:1146-1149.
  24. Suga H (1979). External mechanical work from relaxing ventricle. *Am J Physiol* 236:H494-H497.
  25. van Eyll C, Pouleur H, Charlier AA, et al (1984). Interest of quantitative diastolic regional wall motion analysis in ischemic heart disease. In *Computers in Cardiology*. Salt Lake City: IEEE Computer Society, pp 219-222.
  26. Ishida Y, Meisner JS, Tsujioka K, et al (1986). Left ventricular filling dynamics: Influence of left ventricular relaxation and left atrial pressure. *Circulation* 74:187-196.
  27. McKay RG, Aroesty JM, Heller GV, et al (1984). The pacing stress test reexamined: Correlation of pacing-induced hemodynamic changes with the amount of myocardium at risk. *J Am Coll Cardiol* 3:1469-1481.

28. De Kock M, Melin JA, Pouleur H, Rousseau MF (1986). Alterations in myocardial metabolism and function at rest in stable angina pectoris: Relations with the amount of exercise-induced thallium-201 perfusion defect. *Catheterization and Cardiovascular Diagnosis* 12: 391–398.
29. Grossman W, Barry WH (1980). Diastolic pressure-volume relations in the diseased heart. *Fed Proc* 39:148–155.
30. Rodeheffer RJ, Gerstenblith G, Becker LC, et al (1984). Exercise cardiac output is maintained with advancing age in healthy human subjects: Cardiac dilatation and increased stroke volume compensate for a diminished heart rate. *Circulation* 69:203–213.
31. Melin JA, Piret LJ, Vanbutsele RJM, et al (1981). Diagnostic value of exercise electrocardiography and thallium myocardial scintigraphy in patients without previous myocardial infarction: a Bayesian approach. *Circulation* 63:1019–1024.
32. Nuttall A, Snow HM (1982). The cardiovascular effects of ICI 118, 587: A  $\beta_1$ -adrenoceptor partial agonist. *Br J Pharmacol* 77:381–388.
33. Rousseau MF, Pouleur H, Vincent MF (1983). Effects of a cardioselective  $\beta_1$  partial agonist (Corwin) on left ventricular function and myocardial metabolism in patients with previous myocardial infarction. *Am J Cardiol* 51:1267–1274.
34. Bonow RO, Leon MB, Rosing DR, et al (1981). Effects of verapamil and propranolol on left ventricular systolic function and diastolic filling in patients with artery disease. Radionuclide angiographic studies at rest and during exercise. *Circulation* 65:1337–1350.
35. Monrad ES, McKay RG, Baim DS, et al (1984). Improvement in indexes of diastolic performance in patients with congestive heart failure treated with milrinone. *Circulation* 70(6): 1030–1037.

---

# 25. EJECTION, FILLING AND DIASTASIS DURING TRANSLUMINAL OCCLUSION IN MAN: CONSIDERATION ON GLOBAL AND REGIONAL LEFT VENTRICULAR FUNCTION

---

Patrick W. Serruys, William Wijns, Federico Piscione, Pim de Feyter,  
and Paul G. Hugenholtz

An extensive literature exists that describes the acute changes in hemodynamics and left ventricular function following coronary occlusion in animals [1–4]. Much less, however, is known in humans. Extrapolating results from animals to humans is potentially difficult, because in humans preexisting atherosclerotic coronary disease and a unique distribution of collateral circulation [5–7] may influence the findings. Until recently, measurement of left ventricular geometry and hemodynamics early after an abrupt occlusion of a major coronary artery has not been feasible in humans. Percutaneous transluminal coronary angioplasty (PTCA), however, now provides a unique opportunity to study the time course of these variables during the transient interruption of coronary flow in the balloon occlusion sequence in patients with single-vessel disease and without angiographically demonstrable collateral circulation [8–10].

## *Study Population and Protocol*

### STUDY POPULATION

After a preliminary study to confirm the absence of effects of nonionic contrast media (metriza-

*Grossman, William, and Lorell, Beverly H. (eds.), Diastolic Relaxation of the Heart. Copyright © 1987. Martinus Nijhoff Publishing. All rights reserved.*

mid [Amipaque]) on left ventricular function, permission was obtained from the Thoraxcenter Ethics Committee to perform left ventricular angiography during balloon inflation at PTCA. All patients involved in the study gave informed consent, and no complications related to the research procedure occurred. Fourteen patients with coronary artery disease undergoing PTCA, with the following selection criteria, were studied:

1. Isolated, obstructive lesion of one coronary artery (10, left anterior descending; 3, right coronary; 1, left circumflex), without angiographically demonstrable collateral circulation.
2. Normal left ventricular wall motion at rest, as determined at prior diagnostic catheterization.
3. No intraventricular conduction abnormalities on the resting electrocardiogram (ECG),

Four patients had mild essential hypertension and an elevated left ventricular end-diastolic pressure (LVEDP  $\geq 25$  mm Hg). Standard antianginal therapy was allowed until the day of the study.

During the PTCA procedure, the number of transluminal occlusions performed per patient was  $4.9 \pm 2.2$  (mean  $\pm$  [SD]). The average

duration of each occlusion was  $51 \pm 12$  second and the total occlusion time during the whole procedure was  $252 \pm 140$  seconds.

#### STUDY PROTOCOL

Left ventricular pressure was recorded during ventriculography (30-degree right anterior oblique view at 50 frames/second) carried out before balloon dilatation, at a mean occlusion time of 20 seconds during the second dilatation, at a mean occlusion time of 48 seconds during the fourth dilatation, and at a mean of 12 minutes after the last dilatation. Angiography during the fourth dilatation was performed in only 10 patients. A total of three to ten occlusions were performed, and the duration of balloon inflation ranged from 15 to 75 seconds. Each consecutive balloon inflation was made only when end-diastolic pressure and left ventricular pressure-derived isovolumic parameters of contractility and relaxation, which were available on-line during the procedure [11, 12], had returned to basal values. Care was taken to maintain uniform patient position relative to x-ray equipment during sequential angiograms, which were performed with the breath held in shallow inspiration.

### Methods

#### ANALYSIS OF PRESSURE-DERIVED INDICES DURING SYSTOLE AND DIASTOLE

Left ventricular pressure was measured with a Millar micromanometer catheter and digitized at 250 samples/second. Combined analog and digital filtering resulted in an effective time constant of less than 10 msec. This employed an updated version of the beat-to-beat program described previously [11, 12].

Peak left ventricular pressure, LVEDP, peak negative  $dP/dt$ , peak positive  $dP/dt$ , and the relation between  $dP/dt/P$  and  $P$  linearly extrapolated to  $P = 0$  ( $V_{max}$ ) were computed on line after a data acquisition of 20 seconds.

A new technique has been implemented for the off-line beat-to-beat calculation of the relaxation parameters [13], using a semilogarithmic model:

$$P(t) = P_0 e^{-t/T}$$

The  $P_0$  and  $T$  parameters are estimated from a

linear least-squares fit of  $\ln P = -t/T + \ln P_0$ , starting from the time of peak  $-dP/dt$ :

- a. fit of first 40 msec ( $n = 8$ ),  $\tau_1$ , biexponential [13].
- b. fit after the first 40 msec ( $n = 8$ ),  $\tau_2$ , biexponential [13].
- c. fit of all points ( $n = 8$ ),  $T$ , monoexponential.

Isovolumic relaxation period was defined as the time interval between the aortic valve closure and the mitral valve opening. This latter was defined during left ventriculography, as occurring in the last frame preceding the entry of nonopacified blood into the left ventricle from the left atrium. The left ventricular pressure corresponding to this frame was considered to reflect left atrial pressure [14].

#### ANALYSIS OF REGIONAL AND GLOBAL LEFT VENTRICULAR FUNCTION

*Ejecting Dynamics.* A complete cardiac cycle was analyzed frame by frame from each angiogram. The ventricular contours were automatically detected by an analysis system [15] and the instantaneous volume calculated according to Simpson's rule. End-diastolic and end-systolic volumes, cardiac index, stroke index and ejection fraction, and the derivative of volume relative to time ( $dV/dt$ ) were derived. End-diastolic pressure was defined as that point on the pressure trace at which the derivative of the pressure first exceeded 200 mm Hg/second [11] and in all cases coincided with the maximal measured left ventricular volume.

End-systole was defined, with reference to the pressure tracing, at the occurrence of the dicrotic notch of the central aortic pressure. To analyze the regional left ventricular function, the computer generated a system of coordinates along which the left ventricular wall displacement is determined frame by frame in 20 segments (Figure 25-1). The definition of the 20 segmental coordinates was derived from the mean trajectories of endocardial sites in 23 normal individuals [16] and generalized as a mathematical expression amenable to automatic data processing [17, 18].

Segmental volume was computed from the local radius ( $R$ ) and the height of each segment ( $1/10$  of left ventricular long axis length [ $L$ ]) according the formula:  $\frac{1}{20} \pi R^2 L$ . When

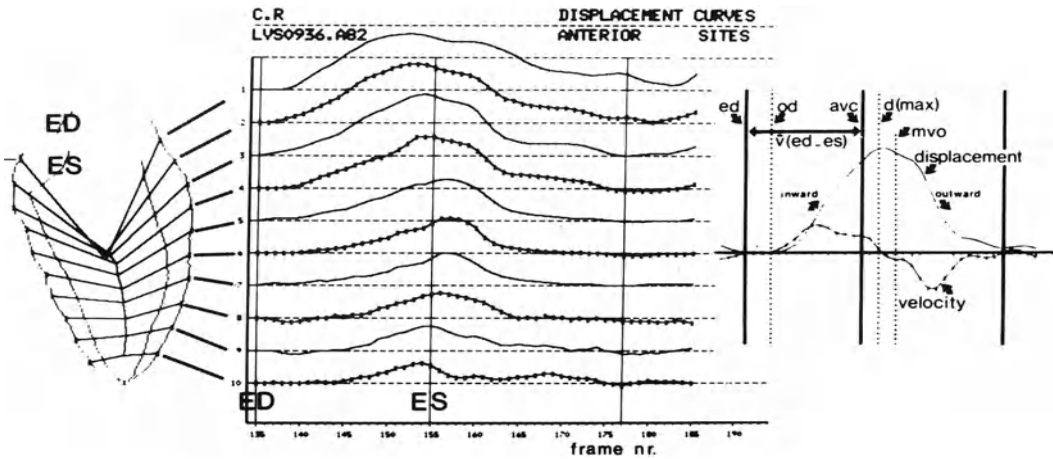


FIGURE 25-1. End-diastolic and end-systolic left ventricular contours, as detected by the automated analysis system. On these silhouettes is superimposed a system of coordinates along which segmental left ventricular wall displacement is detected. Left ventricular wall velocity (first derivative of wall displacement) is derived from these data. ed-end-diastole; es-end-systole; od-onset of displacement;  $\bar{v}(ed-es)$ -mean ejection-phase wall velocity;  $d(max)$ -maximal inward wall displacement; mvo-mitral valve opening.

normalized for end-diastolic volume, the systolic segmental volume change can be considered as a parameter of regional pump function (Figure 25-2). During systole this parameter expresses quantitatively the contribution of a particular segment to global ejection fraction, termed *regional contribution to global ejection fraction* or CREF [17]. The sum of the values for all 20 segments equals the global ejection fraction.

Segmental wall velocity was computed as the first derivative of the instantaneous displacement function. Mean ejection phase wall velocity ( $V$ ) for each segment was calculated from end-diastole to end-systole ( $V_{ed-es}$ ) (Figure 25-1).

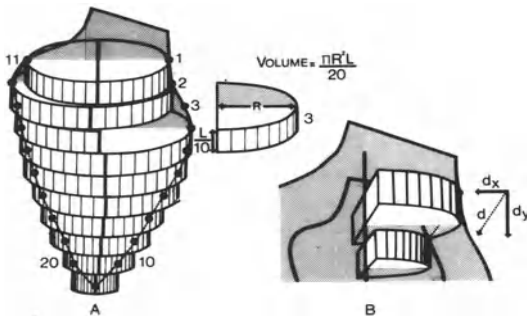


FIGURE 25-2. Method for computing regional contribution to ejection fraction (CREF): volume of each segment (slice volume) is computed according to the formula shown in the figure. The systolic volume change is derived from the regional displacement and is mainly a consequence of the decrease of radius ( $R$ ) of a half slice, which is expressed by the  $x$ -component ( $d_x$ ) of the displacement vector ( $d$ ). L-left ventricular, long-axis length, extending from base to apex.

*Filling Dynamics.* Peak segmental inward and outward velocity was calculated as the first derivative relative to time of the segmental wall displacement after a three point smoothing function had been applied to the data (see Figure 25-1). Peak ejection rate was taken as the lowest  $dV/dt$  after end-diastole; peak global filling rate as the peak  $dV/dt$  after mitral valve opening and the time to peak filling rate was the time interval between the aortic valve closure and the peak  $dV/dt$ . The time interval was measured between the occurrence of the global peak filling rate and the peak velocity of segmental outward displacement (Figure 25-3). We defined  $\Sigma \Delta t_1$  as the sum of the absolute

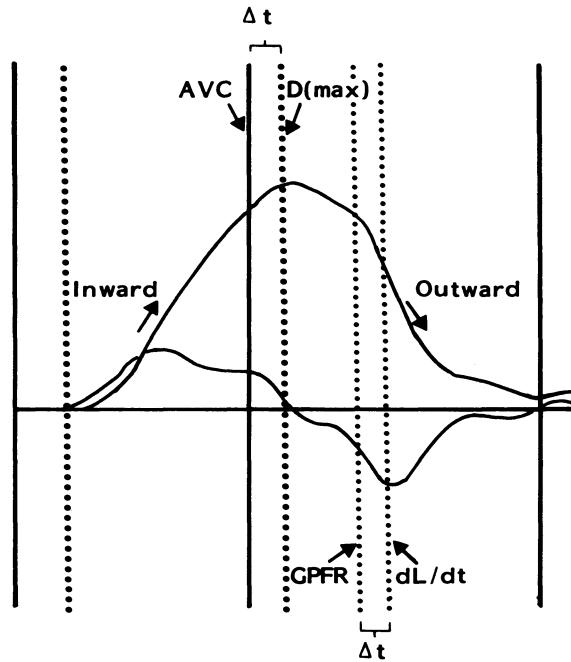


FIGURE 25-3. Segmental wall displacement and its first derivative are superimposed to show the temporal relationship between inward and outward phases with the aortic valve closure (AVC). The time intervals ( $\Delta t$ ) between AVC and the maximal inward wall displacement,  $D(\max)$ , and between the occurrence of global peak filling rate (GPFR) and the peak velocity of outward displacement ( $dL/dt$ ) were measured in every segment.

values of the time differences between global peak filling rate and peak velocity of segmental outward displacement;  $\Sigma\Delta t_1/Dt$  was  $\Sigma\Delta t_1$ , normalized for diastolic time. We defined  $\Sigma\Delta t_2$  as the sum of the absolute values of the time differences between aortic valve closure and peak segmental inward displacement (see Figure 25-3) and  $\Sigma\Delta t_2/ET$  was  $\Sigma\Delta t_2$ , normalized for ejection time. The terms  $\Sigma\Delta t_1$ ,  $\Sigma\Delta t_1/Dt$ ;  $\Sigma\Delta t_2$ ,  $\Sigma\Delta t_2/ET$  are thus indexes reflecting variations in the synchrony of ventricular filling and contraction, respectively.

**Diastasis.** This part of the study includes the 10 patients (1 female and 9 males) who underwent a PTCA of a left anterior descending coronary artery stenosis. One of the 10 patients was excluded because the small number of available data points due to a higher heart rate precluded analysis of the diastolic function. Thus simultaneous left ventricular pressure and volume were obtained after a median occlusion of 20 seconds (range 15–27) during the second dilatation in nine patients and after a median occlusion of 48 seconds (range 46–59) during the fourth dilatation in five patients.

In this subset of patients, the length of the 20 segmental radii defined by the model was measured frame by frame and among them, we selected for analysis six radii located either in the core of the ischemic segment (anterior, anterolateral, and apical radius), or in the non-ischemic segment (anterobasal and posterobasal radius), as well as the inferior radius immediately adjacent to the ischemic segment (Figure 25-4). The linear correlation coefficients between repeated measurements of radius length in 20 patients ranged from 0.96 to 0.99 (SEE = 0.4 to 1.4%) for the same operator and from 0.91 to 0.99 (SEE = 0.4 to 2.3%) for two different operators.

For the evaluation of the global chamber stiffness, the left ventricular pressure (P) and

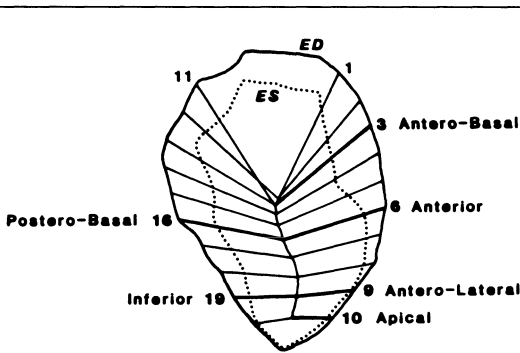


FIGURE 25-4. The end-diastolic (ED) and end-systolic (ES) contours of a left ventriculogram during transluminal occlusion are displayed with the system of the 20 radii along which regional wall displacement was determined. For the analysis of regional diastolic function, we selected radii 6, 9, and 10 within the ischemic zone, radii 3 and 16 within the nonischemic zone, and radius 19 in the adjacent inferior zone.

volume ( $V$ ) data obtained every 20 msec starting at the lowest diastolic pressure and ending at the end-diastolic pressure were fitted by a simple elastic model:  $P = \alpha \ell^{\beta V} + C$ , where  $\alpha$  = intercept (mm Hg),  $\beta$  = constant of elastic chamber stiffness, and  $C$  = baseline pressure (mm Hg). The three constants of this equation ( $\alpha$ ,  $\beta$ ,  $C$ ) were determined using an iteration procedure until the beat nonlinear curve fit was obtained [19].

For the evaluation of the regional chamber stiffness, the left ventricular pressure and the segment radius length ( $L$ ) data were fitted in a similar way for each of the six (1, 2, . . . n) analyzed segmental radii:

$$P = \alpha_n e^{\beta_n L} + C_n,$$

where  $\beta_n$  represents the regional elastic stiffness constant for a given radius. The same approach was applied previously by others to pressure-length relations obtained either by ultrasonic subendocardial crystals [20] or by contrast ventriculography [21, 22].

**Statistical Analysis.** Results are given for all patients and the subgroup analyzed after 50 seconds of occlusion as either mean  $\pm$  SD or as median values using analysis of variance for

repeated measurements. Comparisons between preangioplasty, postangioplasty, and 20-second occlusion conditions were performed in 10 patients. The data obtained before angioplasty, after 50-second occlusion, and after angioplasty were compared in the appropriate subgroup of five patients. In both cases, when overall significance was found, multiple comparisons were used to delineate which paired comparisons were significantly different at the 0.05 level. The relationship between peak filling rate and the regional indexes reflecting asynchrony of contraction and filling were analyzed by regression analysis.

## Results

### GLOBAL LEFT VENTRICULAR FUNCTION DURING SYSTOLE AND DIASTOLE

Volumes, pressures, and derived parameters measured before, during, and after transluminal occlusion are listed in Table 25-1. There was no important change in heart rate during the PTCA procedure. The pattern of change in peak left ventricular pressure, LVEDP, peak positive  $dP/dt$ , and  $V_{max}$ , however, suggests a progressive depression in myocardial mechanics without any indication of an early peak.

In contrast, within four of five beats after occlusion, a deformation appeared in the ascending limb of the negative  $dP/dt$  curve (Figure 25-5), and in the next 10 seconds this deformation in the negative  $dP/dt$  curve gradually increased so that the irregularity in the negative  $dP/dt$  curve reached the same height as peak negative  $dP/dt$  which had progressively decreased to its nadir. In the next 20 to 50 seconds, peak negative  $dP/dt$  began to return towards control levels with a resolution of the irregularity in the ascending limb of negative  $dP/dt$ . As 50 seconds, peak negative  $dP/dt$  recovered to 77% of the preocclusion value, and the deformity was no longer present.

This deformation of the negative  $dP/dt$  signal at the early phase of the occlusion means that the time course of left ventricular pressure decay deviates substantially from the monoexponential model usually proposed and it means also that asynchronous contraction or relaxation may be involved at the very beginning of the transluminal occlusion. Therefore biexponential fitting of the pressure curve was computed during the isovolumic relaxation, primarily on the basis

TABLE 25-1. Global Systolic Function Before PTCA, 20 and 50 Seconds After the Onset of Occlusion, and After PTCA

Variables	Before PTCA		20-Second Occlusion (total group; n = 14)	50-Second Occlusion (subgroup; n = 9)	After PTCA	
	Total Group (n = 14)	Subgroup (n = 9)			Subgroup (n = 9)	Total Group (n = 14)
Heart rate (bpm)	62 ± 16	59 ± 18	61 ± 13	62 ± 14	63 ± 11	64 ± 11
End-diastolic volume (ml/m <sup>2</sup> )	81 ± 15	79 ± 14	81 ± 15	81 ± 16	78 ± 11	77 ± 11
End-systolic volume (ml/m <sup>2</sup> )	31 ± 9	29 ± 7	37 ± 9 <sup>b</sup>	41 ± 9 <sup>b</sup>	26 ± 15	27 ± 7 <sup>a</sup>
Stroke volume (ml/m <sup>2</sup> )	50 ± 11	49 ± 11	44 ± 12 <sup>a</sup>	39 ± 14 <sup>a</sup>	52 ± 10	50 ± 9
Ejection fraction (%)	61 ± 8	62 ± 6	54 ± 8 <sup>b</sup>	48 ± 12 <sup>b</sup>	66 ± 6	64 ± 7
Mean systolic ejection rate (ml/sec)	129 ± 24	127 ± 24	125 ± 32	116 ± 67	165 ± 48	147 ± 27
Peak ejection rate (ml/sec)	251 ± 97	255 ± 106	222 ± 69	185 ± 61 <sup>a</sup>	248 ± 77	240 ± 68
Time to peak ejection rate (msec)	172 ± 44	175 ± 50	172 ± 56	153 ± 34	170 ± 88	166 ± 76
Peak ejection rate (SV/sec)	5 ± 1	5.4 ± 1	5 ± 0.7	5 ± 0.9	5 ± 0.6	4.7 ± 0.6
Peak ejection rate (EDV/sec)	3 ± 0.8	3.3 ± 0.9	2.7 ± 0.5	2.3 ± 0.5 <sup>b</sup>	3.2 ± 0.5	3 ± 0.5
End systolic pressure (mm Hg)	95 ± 18	92 ± 22	90 ± 19	98 ± 24	91 ± 15	90 ± 14
Peak LVP (mm Hg)	154 ± 30	151 ± 35	142 ± 29	145 ± 37	148 ± 24	147 ± 21
Peak Positive dP/dt (mm Hg <sup>-1</sup> )	1403 ± 304	1356 ± 257	1312 ± 320	1278 ± 317	1442 ± 384	1412 ± 333
V <sub>max</sub> (s <sup>-1</sup> )	39 ± 9	40 ± 8	39 ± 9	34 ± 10 <sup>a</sup>	43 ± 12	42 ± 11
Tau <sub>1</sub> (msec)	55 ± 8	55 ± 6	79 ± 17 <sup>b</sup>	68 ± 16 <sup>b</sup>	56 ± 7	54 ± 7
Tau <sub>2</sub> (msec)	44 ± 7	43 ± 7	51 ± 8 <sup>a</sup>	59 ± 8 <sup>b</sup>	45 ± 8	45 ± 9
IRP msec	71 ± 18	77 ± 18	85 ± 16 <sup>a</sup>	80 ± 17	77 ± 16	71 ± 15
MVO pressure (mm Hg)	19 ± 5	18 ± 3	23 ± 8	25 ± 6 <sup>a</sup>	19 ± 5	21 ± 6
MVO volume (ml/m <sup>2</sup> )	37 ± 9	35 ± 7	41 ± 9 <sup>a</sup>	45 ± 10 <sup>b</sup>	30 ± 6	31 ± 8
Peak filling rate (ml/sec)	311 ± 83	296 ± 84	234 ± 82 <sup>a</sup>	225 ± 93 <sup>a</sup>	297 ± 117	277 ± 109
Time to peak filling rate (msec)	128 ± 20	133 ± 22	145 ± 38	151 ± 26	130 ± 18	126 ± 23
Peak filling rate (SV/sec)	6.5 ± 1	6 ± 0.9	5.9 ± 1	6 ± 2	5.8 ± 0.8	5.7 ± 1
Peak filling rate (EDV/sec)	4 ± 1	3.7 ± 0.8	3 ± 8 <sup>a</sup>	2.8 ± 0.7 <sup>b</sup>	3.8 ± 0.9	3.6 ± 1
P <sub>min</sub> (mm Hg)	10 ± 5	8 ± 3	11 ± 4	16 ± 6 <sup>b</sup>	8 ± 5	8 ± 4
Volume at P <sub>min</sub> (ml/m <sup>2</sup> )	51 ± 13	48 ± 11	53 ± 10	55 ± 10	45 ± 11	45 ± 9
MRVI (ml/sec)	179 ± 82	198 ± 78	98 ± 78 <sup>b</sup>	104 ± 69 <sup>b</sup>	161 ± 131	138 ± 113
EDP (mm Hg)	22 ± 8	18 ± 6	22 ± 7	29 ± 5 <sup>b</sup>	21 ± 5	20 ± 6
EDV (ml/m <sup>2</sup> )	81 ± 15	79 ± 14	81 ± 15	81 ± 16	78 ± 11	77 ± 11

<sup>a</sup>  $p < 0.05$ , compared with before PTCA, paired Student's  $t$  test.

<sup>b</sup>  $p < 0.005$ , compared with before PTCA, paired Student's  $t$  test.

PTCA = percutaneous transluminal coronary angioplasty; SV = stroke volume; EDV = end-diastolic volume; LVP = left ventricular pressure; dP/dt = rate of change of pressure; V<sub>max</sub> = maximal velocity of the contractile element (dP/dt/P linearly extrapolated to P = 0); Tau<sub>1</sub> and tau<sub>2</sub> = time constant of relaxation (biexponential fitting) Tau<sub>1</sub>, fit of the first 40 msec; Tau<sub>2</sub> fit after 40 msec; IRP = isovolumic relaxation period; MVO = mitral valve opening; P<sub>min</sub> = minimal left ventricular diastolic pressure; MRVI = mean rate of volume inflow during the time interval between MVO and P<sub>min</sub>; EDP = end-diastolic pressure.

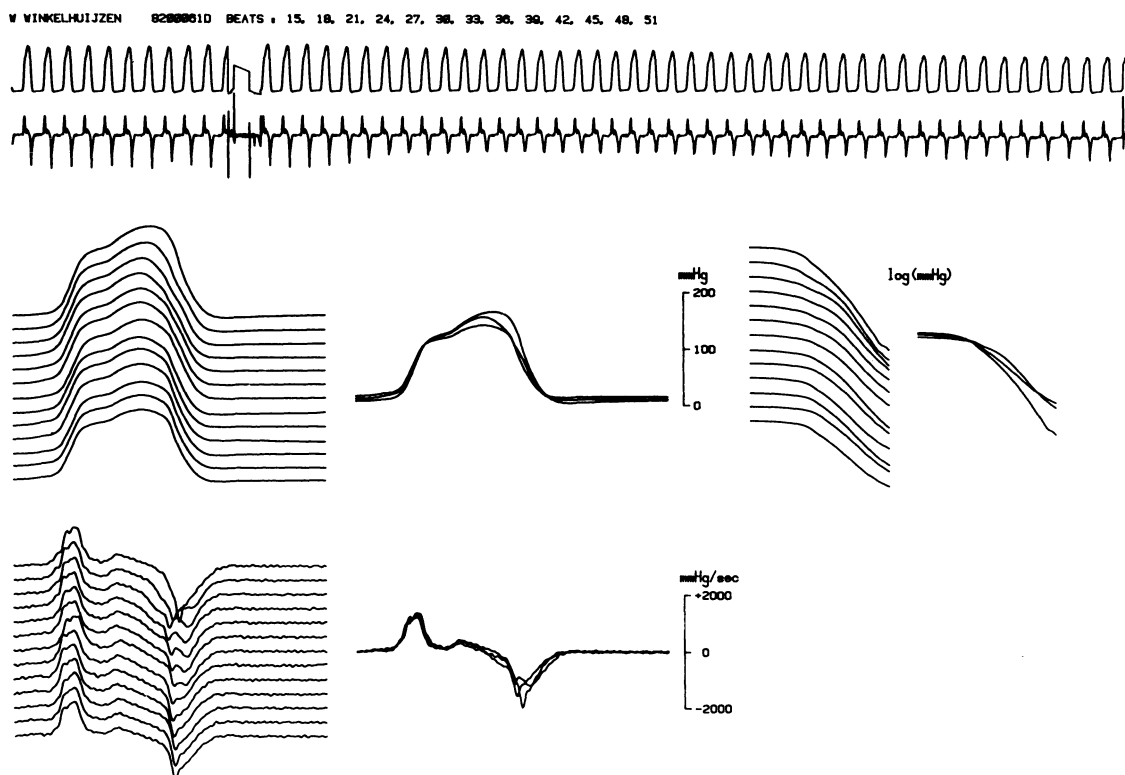


FIGURE 25-5. Effects of coronary artery occlusion on left ventricular pressure (mm Hg) and positive and negative  $dP/dt$  (mm Hg/sec). The break in the recording at beat 15 corresponds to inflation of the balloon. On the left side are displayed the left ventricular pressure and positive and negative  $dP/dt$  of individual beats [15, 18, 21, and so forth], while the natural logarithm of the pressure is shown on the right side. Notice the decrease in negative  $dP/dt$  associated with an irregularity in the upstroke of the negative  $dP/dt$  curve. After 30 seconds (beat 42), peak negative  $dP/dt$  starts to return toward a more normal shape of the signal.

that the pressure curve when plotted on semi-logarithmic paper was noted to follow two straight lines rather than the one predicted by the monoexponential mode.

The first half of Table 25-1 summarizes the results of the relaxation parameters. An example of the frame-to-frame analysis of left ventricular volume before and during ischemia induced by balloon inflation is shown in Figure 25-6 with its derivative ( $dV/dt$ ). The global indexes of the

ejection phase decreased during the two periods of coronary occlusion; the ejection fraction fell from 61% to 54% over 20 seconds ( $p < 0.005$ ) and from 62% to 48% ( $p < 0.005$ ) over 50 seconds, this reduction being mainly due to the increase in end-systolic volume over 20 seconds (from  $31 \pm 9$  ml/m<sup>2</sup> to  $37 \pm 9$ ;  $p < 0.005$ ) and 50 seconds (from  $29 \pm 7$  ml/m<sup>2</sup> to  $41 \pm 9$ ;  $p < 0.005$ ). Consequently, the stroke volume was significantly decreased from  $50 \pm 11$  ml/m<sup>2</sup> to  $44 \pm 12$  ( $p < 0.05$ ) during the first period of occlusion and from  $49 \pm 11$  ml/m<sup>2</sup> to  $39 \pm 14$  ( $p < 0.05$ ) during the second. A slight but not significant reduction in peak ejection rate was observed over 20 seconds, but after 50 seconds it was decreased from  $255 \pm 106$  ml/m<sup>2</sup> to  $185 \pm 61$  ( $p < 0.05$ ) (Figure 25-7). Normalization for end-diastolic volume and stroke volume did not render the change in peak ejection rate at 20 seconds significant. In parallel to the prolongation of  $\tau_1$  and  $\tau_2$ , the isovolumic relaxation period increased from  $71 \pm 18$  msec to  $85 \pm$

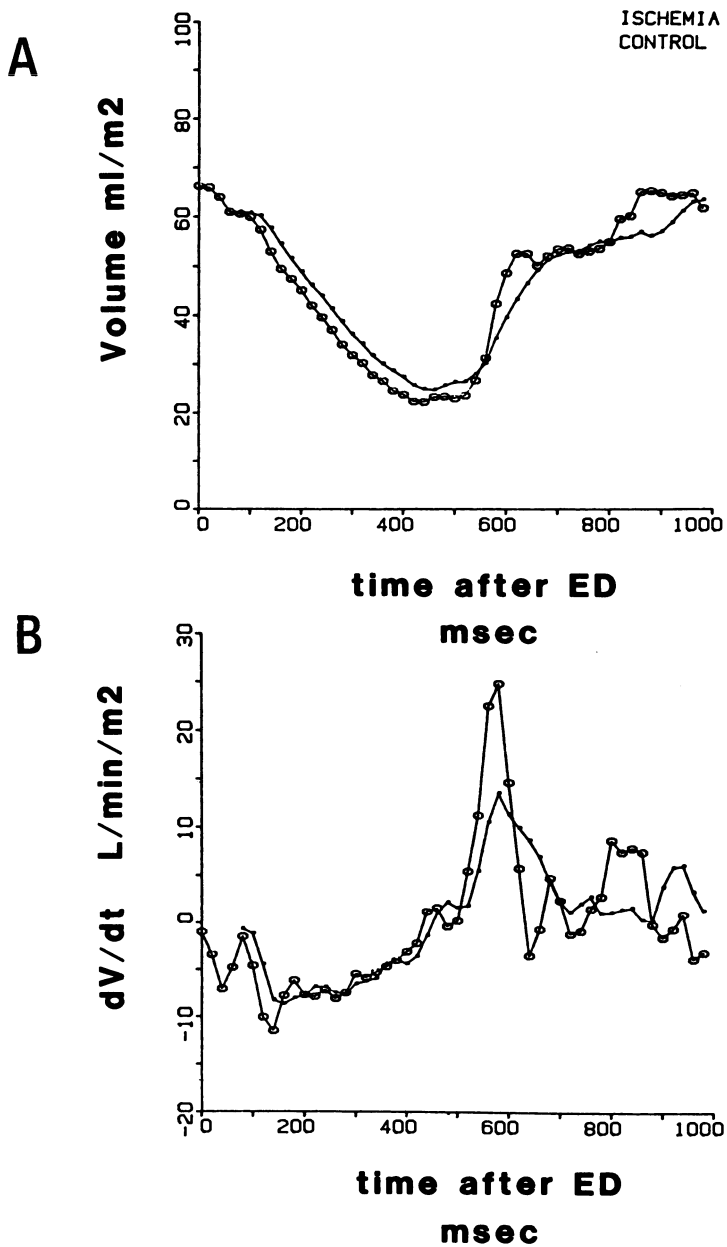


FIGURE 25-6. A. Left ventricular volume curves for the same patient, derived from angiographic volumes every 20 msec throughout a complete cardiac cycle, before and during transluminal occlusion. B. Instantaneous left ventricular volume derivative ( $dV/dt$ ) curves for the same patient, measured every 20 msec throughout a complete cardiac cycle, before and during transluminal occlusion. During ischemia a decrease in peak  $dV/dt$  was observed. ED = end-diastole, (● = ischemia; ○ = control).

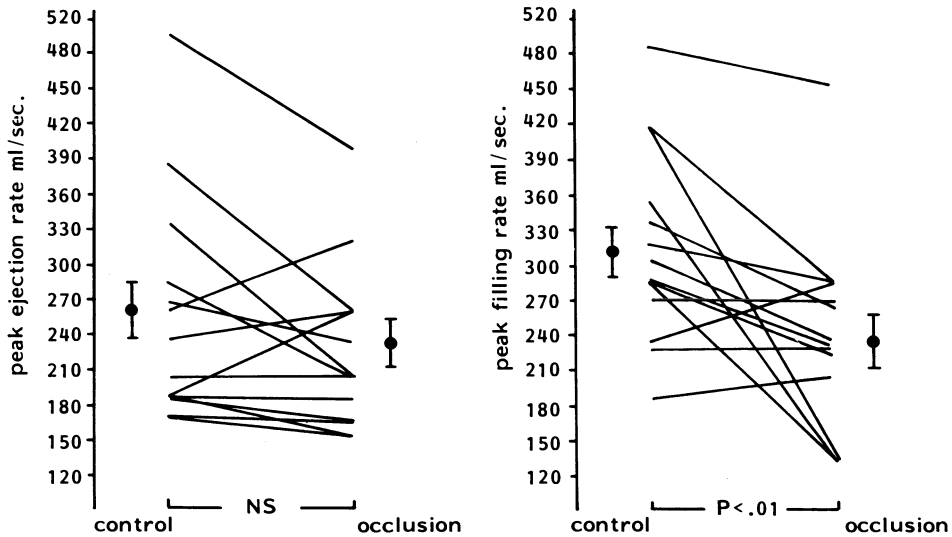


FIGURE 25-7. Individual and mean changes ( $\pm$ SEM) in peak ejection rate and peak filling rate during transluminal occlusion (20 msec). Only the peak filling rate showed a significant decrease during the early phase of coronary occlusion. NS = not significant.

16 ( $p < 0.05$ ) over 20 seconds and from  $77 \pm 18$  msec to  $80 \pm 17$  ( $p = \text{NS}$ ) over 50 seconds. The left ventricular pressure at the time of mitral valve opening increased from  $19 \pm 5$  mm Hg to  $23 \pm 8$  ( $p = \text{NS}$ ) over 20 seconds and from  $18 \pm 3$  mm Hg to  $25 \pm 6$  ( $p < 0.05$ ) over 50 seconds. Peak filling rate was reduced from  $311 \pm 85$  ml-sec to  $234 \pm 82$  ( $p < 0.05$ ) after 20 seconds of ischemia and from  $296 \pm 84$  ml/second to  $225 \pm 93$  ( $p < 0.05$ ) after 50 seconds. When normalized for stroke volume, peak filling rate was unchanged after 20 and 50 seconds of occlusion, whereas after normalization for end-diastolic volume (EDV) it was significantly decreased after 20 (from  $4 \pm 1$  EDV/second to  $3 \pm 0.8$ ;  $p < 0.05$ ) and 50 seconds (from  $3.7 \pm 0.8$  EDV/second to  $2.8 \pm 0.7$ ;  $p < 0.005$ ). The mean rate of volume inflow, measured during the early filling period between the mitral valve opening, and the occurrence of minimal diastolic pressure, declined significantly both at 20 (from  $179 \pm 82$  ml/second to  $98 \pm 78$ ;  $p < 0.005$ ) and 50 seconds (from  $198 \pm 94$  ml/second to  $104 \pm 69$ ;  $p < 0.005$ ) from the onset of occlusion.

The left ventricular volume at the lowest diastolic pressure as well as at end-diastole did not change significantly during and after angioplasty while the lowest diastolic ( $p < 0.05$ ) and the end-diastolic ( $p < 0.01$ ) pressures were increased in the subgroup of patients studied after 50 seconds of anterior descending coronary artery occlusion. The increase in pressure relative to volume during transluminal occlusion resulted in an upward shift of the entire pressure-volume relation, as shown for two representative patients (patients 2 and 7) in Figure 25-8A and 25-8B. In only two instances (patients 6 and 9), did we observe a shift downward and to the right of the pressure-volume relation.

The calculated parameters of global chamber stiffness showed a similarly increased constant of elastic stiffness ( $\beta$ ) after 20 seconds as well as after 50 seconds of occlusion (Table 25-2). The baseline pressure (C) increased significantly ( $p < 0.01$ ) only after 50 seconds of coronary occlusion. No change in the intercept ( $\alpha$ ) was observed (see Table 25-2). All patients but one showed an increase in chamber stiffness during coronary occlusion which, after the procedure, returned to values not significantly different from the preangioplasty value. However, the postangioplasty elastic constant remained higher than the control value in five instances. This is

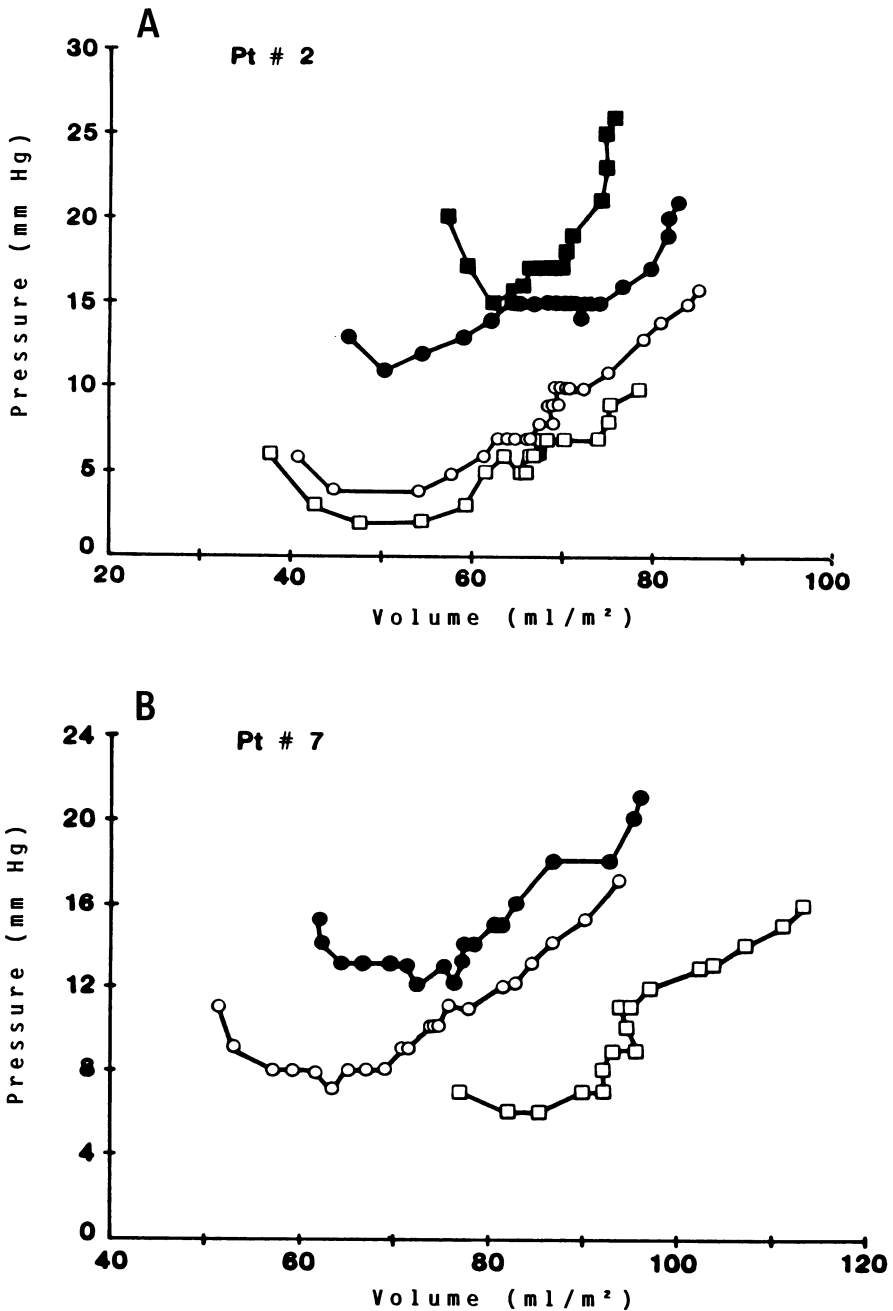


FIGURE 25-8. Diastolic pressure-volume relation in two representative patients. Note the upward shift of the relation during coronary occlusion. In patient 2(A), the postangioplasty relation returned towards control, whereas it remains shifted upwards in patient 7 (B). open squares = preangioplasty; closed circles = 20-second occlusion; closed squares = 50-second occlusion; open circles = postangioplasty.

TABLE 25-2. Global Left Ventricular Chamber Stiffness (Simple Elastic Model)<sup>a</sup>

	Intercept ( $\alpha$ ) (mm Hg)	Constant of Elastic Stiffness ( $\beta$ )	Baseline pressure (C) (mm Hg)
ALL patients (n = 9)	NS	<sup>b</sup>	NS
Pre-PTCA	4.6 ± 4.9	0.0273 ± 0.017	-1.4 ± 9.5
20-second occlusion	1.2 ± 3.3	0.0621 ± 0.026 <sup>b</sup>	5.2 ± 8.3
Post-PTCA	1.2 ± 1.5	0.0529 ± 0.037	2.8 ± 4.7
Subgroup (n = 5)	NS	<sup>c</sup>	<sup>c</sup>
Pre-PTCA	5.3 ± 5.9	0.0214 ± 0.007	-5.8 ± 7.4
50-second occlusion	0.2 ± 0.3	0.0605 ± 0.015 <sup>b</sup>	9.4 ± 2.7 <sup>c</sup>
Post-PTCA	1.9 ± 1.8	0.0396 ± 0.027	0.8 ± 5.6

<sup>a</sup> Values given are mean ± 1 standard deviation; overall and paired (vs. pre-PTCA).

<sup>b</sup>  $p < 0.05$ .

<sup>c</sup>  $p < 0.01$ .

PTCA = percutaneous transluminal coronary angioplasty; NS = not significant.

further illustrated in Figure 25-8 as the pressure-volume relation obtained after the procedure is nearly superimposed on the control curve in patient 2 (Figure 25-8A) whereas the post-angioplasty curve remains shifted upwards in patient 7 (Figure 25-8B).

#### REGIONAL INDEXES OF LEFT VENTRICULAR EJECTION AND FILLING AND REGIONAL PRESSURE-RADIUS LENGTH RELATIONS

The profound effect of a 20-second occlusion of the left anterior descending artery (LAD) on left ventricular wall motion and its time sequence is shown in Figure 25-9. The delay in onset of displacement with respect to end-diastole as well as the timing relationship between the aortic valve closure and the occurrence of the maximal wall displacement is illustrated in Figure 25-9. The onset of displacement of the anterior and inferior wall was not significantly affected after 20 seconds of LAD occlusion. On the contrary, the moment of maximal wall displacement for the anterior wall shifted from end-systole to early diastole. The anterolateral segment (nos. 6 and 7) and the apical segment (nos. 9 and 10) of the anterior wall, as well as the apical segment (nos. 20 and 19) of the inferior wall appeared to be most affected. Parallel to this shift in peak inward wall displacement, a delay was observed in the occurrence of peak velocity of outward displacement ( $dL/dt$ ) with respect to aortic valve closure, particularly in the apical region (segments 10 and 20 in Figure 20-10). The absolute value of the  $dL/dt$  was reduced in the ischemic segments (Figure 25-10). In the non-

ischemic segments, a compensatory increase in  $dL/dt$  was observed.

To test whether this decrease in the absolute value of  $dL/dt$  was in fact intrinsically related to a reduction in the amplitude of the peak outward displacement, we normalized segmental  $dL/dt$  for the corresponding value of maximal outward displacement. After normalization we observed an increase in the ischemic segments, whereas no major changes were apparent in the nonischemic segments (see Figure 25-10). Therefore, a relationship between the asynchrony of segmental  $dL/dt$  and the reduction of global peak filling rate was sought by measuring the sum of the absolute values of the time differences from global peak filling rate to the occurrence of peak  $dL/dt$  in each of the 20 segments ( $\Sigma\Delta t_1$ ). This sum increased significantly during both the first (from  $572 \pm 194$  msec to  $940 \pm 264$ ;  $p < 0.005$ ) and the second occlusion (from  $546 \pm 198$  msec to  $842 \pm 224$ ;  $p < 0.005$ , as well as  $\Sigma\Delta t_1/Dt$ , thus indicating an asynchrony in filling (Table 25-3). To elucidate whether the decrease in global peak filling rate was related to the asynchrony in regional peak filling rate rather than to other causes, we correlated global peak filling rate with  $\Sigma\Delta t_1$  and found a significant negative correlation ( $r = -0.68$ ;  $p < 0.001$ ), demonstrating that a greater degree of asynchrony was associated with a reduction in peak filling rate (Figure 25-11). To determine whether the asynchrony in regional filling was an isolated phenomenon or the effect of a temporal nonuniformity in inward wall displacement, we quantified this systolic nonuniformity by mea-

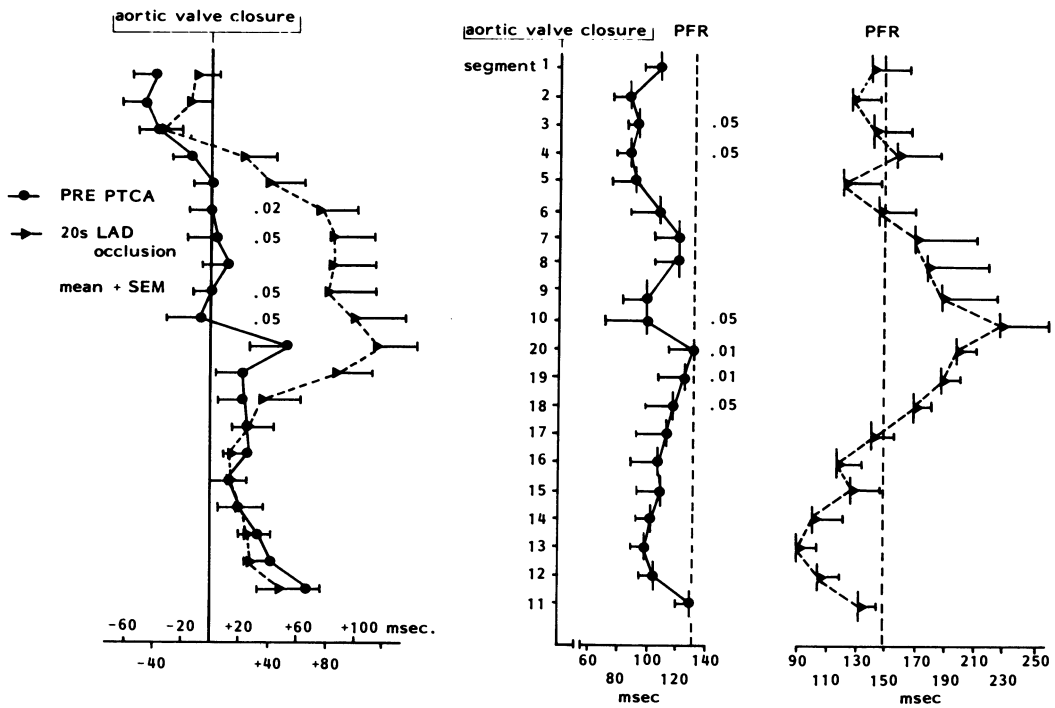


FIGURE 25-9. Left panel: Time relationship between aortic valve closure and the occurrence of maximal inward wall displacement before and after 20 msec of occlusion of the left anterior descending artery (LAD). Middle panel: Time relationship between aortic valve closure and the occurrence of peak velocity of segmental outward displacement before and after 20 seconds of occlusion of the left anterior descending artery. Right panel: Global peak filling rate (PFR).

TABLE 25-3. Measurement of Regional Asynchrony in Inward and Outward Wall Displacement Before PTCA, 20 and 50 Seconds After the Onset of Occlusion, and After PTCA

Variables	Before PTCA		20-Second Occlusion (total group; n = 14)	50-Second Occlusion (subgroup; n = 9)	After PTCA	
	Total Group (n = 14)	Subgroup (n = 9)			Subgroup (n = 9)	Total Group (n = 14)
$\Sigma \Delta t_1$ (msec)	572 ± 194	546 ± 198	940 ± 264 <sup>b</sup>	842 ± 224 <sup>b</sup>	495 ± 179	645 ± 355
$\Sigma \Delta t_2$ (msec)	965 ± 348	948 ± 415	1442 ± 314 <sup>b</sup>	1472 ± 370 <sup>a</sup>	985 ± 171	978 ± 281
$\Sigma \Delta t_1$ /diastolic time	1.1 ± 0.7	1.3 ± 0.8	1.8 ± 0.8 <sup>b</sup>	1.9 ± 1 <sup>b</sup>	1.3 ± 0.7	1.2 ± 0.6
$\Sigma \Delta t_2$ /ejection time	2.6 ± 0.9	2.8 ± 0.7	4.2 ± 0.9 <sup>b</sup>	4.5 ± 0.9 <sup>a</sup>	3 ± 0.9	2.8 ± 0.8

<sup>a</sup>  $p < 0.05$ , compared with before PTCA, paired student's  $t$  test.

<sup>b</sup>  $p < 0.005$ , compared with before PTCA, paired Student's  $t$  test.

$\Sigma \Delta t_1$  = sum of the time intervals between global peak filling rate and peak velocity of segmental outward displacement (dL/dt);  $\Sigma \Delta t_2$  = sum of the time intervals between aortic valve closure and segmental peak inward displacement.

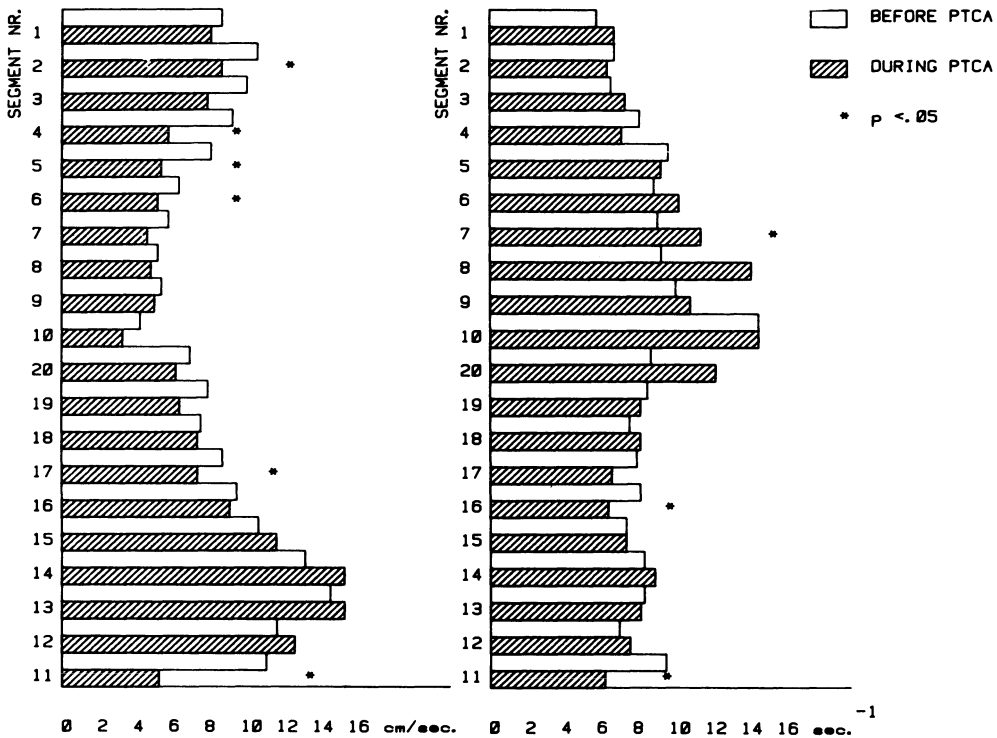


FIGURE 25-10. Left panel: Mean changes in peak velocity of segmental outward displacement ( $dL/dt$ ) in 10 anterior and 10 posterior segments before and during occlusion of the left anterior descending artery. Right panel: Mean changes in the ratio  $dL/dt$ /maximal outward displacement in 10 anterior and 10 posterior segments before and during occlusion of the left anterior descending artery.

During the time relationship between end-systole and the occurrence of the segmental peak inward displacement. The sum of the absolute time differences between aortic valve closure and the peak regional inward wall displacement ( $\Sigma\Delta t_2$ ) was used as an index of systolic asynchrony, and during coronary occlusion both  $\Sigma\Delta t_2$  and  $\Sigma\Delta t_2/ET$  increased in the same fashion as  $\Sigma\Delta t_1$  and  $\Sigma\Delta t_1/Dt$  (see Table 25-3). In addition, we found a significant correlation ( $r = 0.66$ ;  $p < 0.001$ ) between  $\Sigma\Delta t_2$  and  $\Sigma\Delta t_1$  (Figure 25-12), suggesting an interdependence between the asynchrony of contraction and the abnormalities of filling dynamics. Further supportive evidence for the interrelationship between contraction

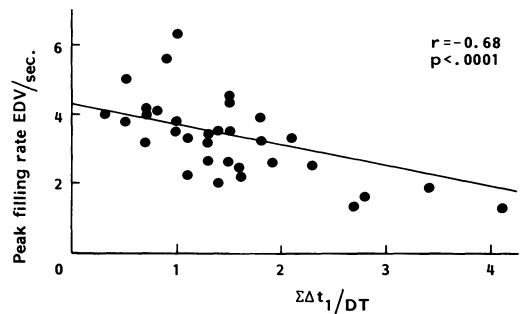


FIGURE 25-11. The negative correlation between the global normalized peak filling rate and the  $\Sigma\Delta t_1$ /diastolic time (DT) as an index of segmental asynchrony in filling, in patients with left anterior descending artery disease. EDV = end-diastolic volume.

and filling was given by the significant negative correlation between the global peak filling rate and  $\Sigma\Delta t_2$  ( $r = -0.73$ ;  $p < 0.001$ ) (Figure 25-13).

Thus the greater the asynchrony in the pattern of contraction, the greater the decrease in peak filling rate. All these data indicate that the asynchrony in the occurrence of the regional filling, with subsequent decreases in peak filling rate, reflects nonuniformity of left ventricular contraction and occurs within 20 seconds of the onset of ischemia. To further elucidate the dynamic interplay between asynchrony in contraction and abnormalities in the early diastolic phase, we correlated  $\Sigma\Delta t_2$  with parameters of the relaxation phase and these latter parameters with the peak filling rate. A significant correlation was observed between  $\Sigma\Delta t_2$  and  $\tau_1$  ( $r = 0.75$ ,  $p < 0.0001$ ) and between  $\tau_1$  and the duration of isovolumic relaxation period ( $r = 0.58$ ;  $p < 0.0001$ ). On the other hand, no correlation or only weak correlations were observed between parameters of the relaxation phase and peak filling rate (Table 25-4).

*Regional Pressure-Radius Length Relation.*

There was no significant difference during the procedure in the length at end-diastole of the various segmental radii. Plots of the left ventricular pressure against a representative radius within the ischemic segment (radius 6, 9, or 10) are shown in Figure 25-14. During occlusion, the slope of the pressure-radius length relation increased; this was often accompanied by an upward shift. The postangioplasty curves either showed a return towards the control relation or remained parallel to the curves during occlusion. The latter was mainly observed in patients 4, 6, 7, and 9, all of whom had persistent global increased chamber stiffness after the procedure, as mentioned earlier.

TABLE 25-4. Correlation Between Parameters of Left Ventricular Relaxation and Filling

Comparison	Correlation Coefficient	p value
Tau <sub>1</sub> -PFR	-0.33	0.06
Tau <sub>2</sub> -PFR	-0.152	0.37
IRP-PFR	-0.53	0.009
MVO*-PFR	-0.23	0.2

\* = pressure.  
 PFR = peak filling rate; IRP = isovolumic relaxation period;  
 MVO = mitral valve opening.

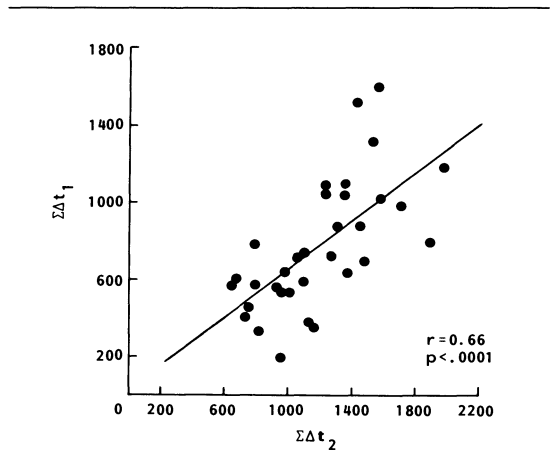


FIGURE 25-12. The correlation between the  $\Sigma\Delta t_1$  index of segmental asynchrony in filling and the  $\Sigma\Delta t_2$  index of segmental asynchrony in contraction. This correlation suggests an interdependence between the asynchrony of contraction and abnormal diastolic filling properties.

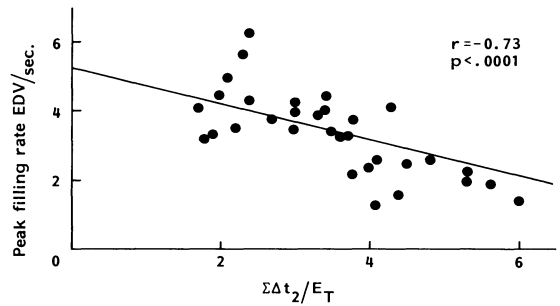


FIGURE 25-13. The negative correlation between the global normalized peak filling rate and the  $\Sigma\Delta t_2$ /ejection time ( $E_T$ ) as an index of segmental asynchrony in contraction, in patients with left anterior descending artery disease. EDV = end-diastolic volume.

These relations were fitted with the same elastic model used for calculation of the global chamber stiffness. The changes in the constant of regional chamber stiffness ( $\beta_n$ ) showed a marked and persistent increased stiffness in the ischemic segment as well as in the adjacent inferior segment (radius 19). The regional stiffness in the nonischemic segments was not significantly affected by the coronary occlusions

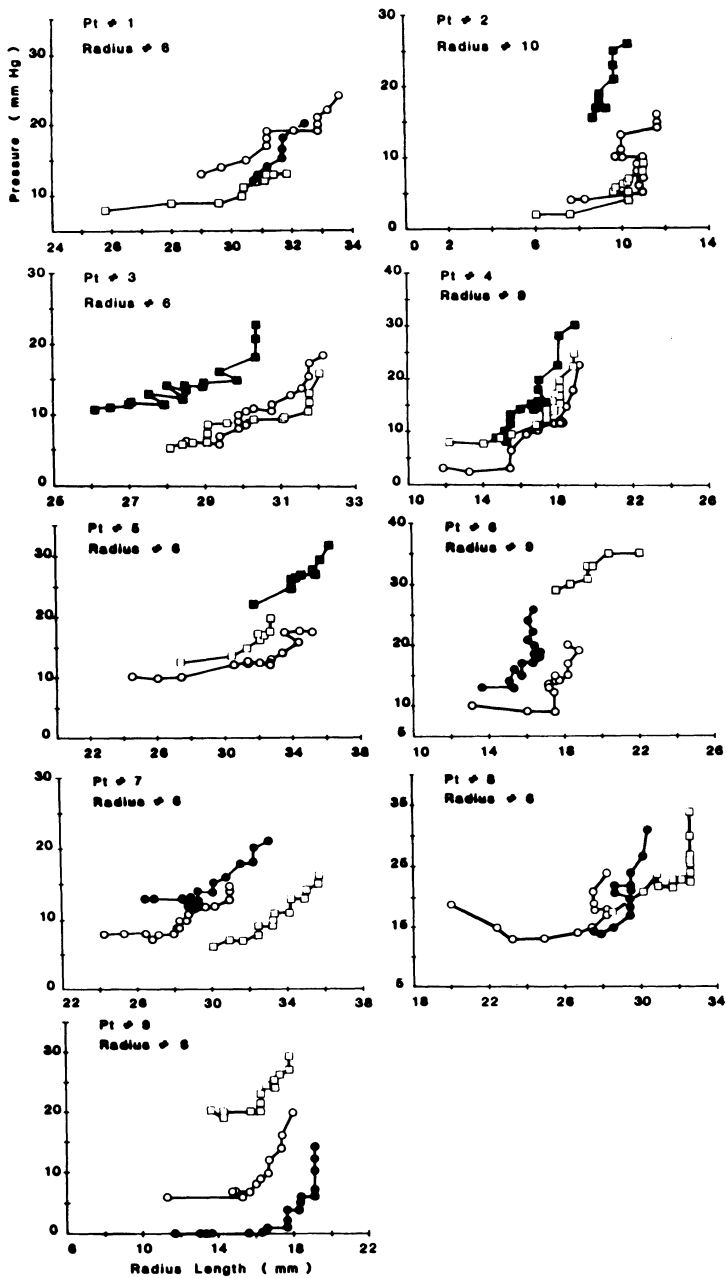


FIGURE 25-14. Plots of left ventricular pressure against the radius length in the ischemic zone. During occlusion, the slope of this relation increased as compared to preangioplasty. The postangioplasty curves showed either a return towards the control relation or remained parallel to the curves observed during occlusion (patients 4, 6, 7, 9). (Symbols are the same as in the Figure 25-8.)

(Table 25-5). There were also no significant changes in the nonlinear elastic constant ( $\beta_n$ ). Similar shifts in the baseline pressure (C) as for the global diastolic function were observed since the same left ventricular pressure data were used for both calculations of global and regional chamber stiffness.

### Discussion

#### MYOCARDIAL ISCHEMIA, TRANSIENT ASYNERGY, AND ALTERED RELAXATION

The earliest (1-15 seconds after occlusion) and most sensitive hemodynamic indicator of regional perfusion deficit proved to be an impairment in early relaxation, with an extreme prolongation of  $\tau_1$ , the time constant of the early relaxation phase. If the premise of the two time constant models previously described [13] is correct, then the early change in  $\tau_1$  with constant  $\tau_2$  represents an exacerbation in the asynchrony of relaxation.

This is illustrated by the change in negative  $dP/dt$  and wall displacement induced by a 20-second coronary occlusion (Figure 25-15). Within four or five beats after occlusion, a distinct deformation appears in the ascending limb of the negative  $dP/dt$  curve and in the next 10 seconds this deformation reaches the same height as peak  $-dP/dt$ , which in the meantime has progressively decreased to its nadir. Accompanying this change in negative  $dP/dt$ , the ischemic segments exhibit a biphasic inward-outward wall displacement that occurs after valve closure and peak negative  $dP/dt$ . During the remainder of relaxation and rapid filling, the ischemic segments display a second wave of inward wall displacement. The beginning of this second wave of inward wall displacement in early diastole corresponds closely in time to the irregularity in  $dP/dt$ . In the same way, the peak inward displacement of the control segment is consistently observed near the notching in the  $dP/dt$ . Shortly after this point, the pressure ceases to have a relaxation time constant  $\tau_1$  and abruptly switches to  $\tau_2$ . On the other hand, after 50 seconds of occlusion the majority of the ischemic segments were akinetic, exhibiting an increased regional stiffness, whereas  $\tau_1$ , the time constant of the early relaxation phase tended to return toward less abnormal values. At 50 seconds, the deformity in negative  $dP/dt$  was no longer present.

#### MODELS OF ASYNERGY AND IMPAIRED RELAXATION

The connection between transient asynergy, myocardial ischemia, and alteration in the time course of relaxation was pointed out as early as 1969 by Tyberg and coworkers [23], who designed an experimental model consisting of two papillary muscles in series. They demonstrated that when one muscle of the pair was hypoxic, but still contracting, it was disturbing the time course of the total tension fall generated by the two muscles, much more than when one of the muscles in series was not contracting at all and infinitely stiff [23]. More recent studies in conscious animals after experimental coronary occlusion have indicated that ventricular dyssynchrony due to late systolic contraction and relaxation in different regions can produce marked effects on the linearity and maximal rate of pressure fall in the left ventricle [21, 23-25]. The time course and magnitude of changes in global parameters of left ventricular function following coronary occlusion in our patients are similar to those previously reported in conscious animals after experimental coronary occlusion [1, 2, 25]. Progressive and gradual decreases in parameters of systolic function accompanied very early changes in the rate of left ventricular pressure decay. The biexponential approximation of the isovolumic pressure fall is consistent with an asynchrony of regional myocardial contraction or relaxation [13]. Changes in parameters of isovolumic pressure fall were most pronounced during the first half of occlusion and slightly less at the end of occlusion. In our study, one of the earliest changes in epicardial wall motion was a decrease in the extent of shortening while velocity of early shortening was maintained. These results are similar to the earliest changes of motion of left ventricular mid-wall ultrasonic crystals during ischemia in conscious dogs as reported by Pagani and colleagues [1].

Our angiographic observations suggest that a similar phenomenon occurs in the intact human heart during acute ischemia. At 20 seconds, there was late systolic outward displacement of the ischemic and active inward displacement of the nonischemic segments. Conversely, the early diastolic inward displacement of the ischemic segments must correspond to an accelerated outward displacement of the normal segment. Ultimately, the ischemic zone after 20 seconds of ischemia appears to act as an additional elas-

TABLE 25-5. Regional Left Ventricular Chamber Stiffness ( $\beta_n$ )

Zone/Radius	Nonischemic Anterobasal/3	Anterior/6	Ischemic anterolateral/9	Apical 10	Adjacent Inferior/19	Nonischemic posterobasal/16
All patients (n = 9)	NS	NS	<sup>a</sup>	NS	NS	NS
Pre-PTCA	1.59	3.92	3.11	2.93	2.76	4.03
20-second occlusion	3.03	4.03	5.63	4.97	6.59	5.01
Post-PTCA	2.73	2.59	6.45 <sup>a</sup>	7.16	5.98	3.64
Subgroup (n = 5)	NS	NS	<sup>b</sup>	<sup>b</sup>	<sup>b</sup>	NS
Pre-PTCA	1.59	3.45	2.81	1.09	1.52	2.59
50-second occlusion	4.13	4.81	5.39	6.16	7.56 <sup>a</sup>	5.54
Post-PTCA	1.98	3.71	5.59	7.16	6.93	4.35

<sup>a</sup>  $p < 0.05$ .<sup>b</sup>  $p < 0.01$ .

+ = the statistical significance was borderline at the 0.05 level.

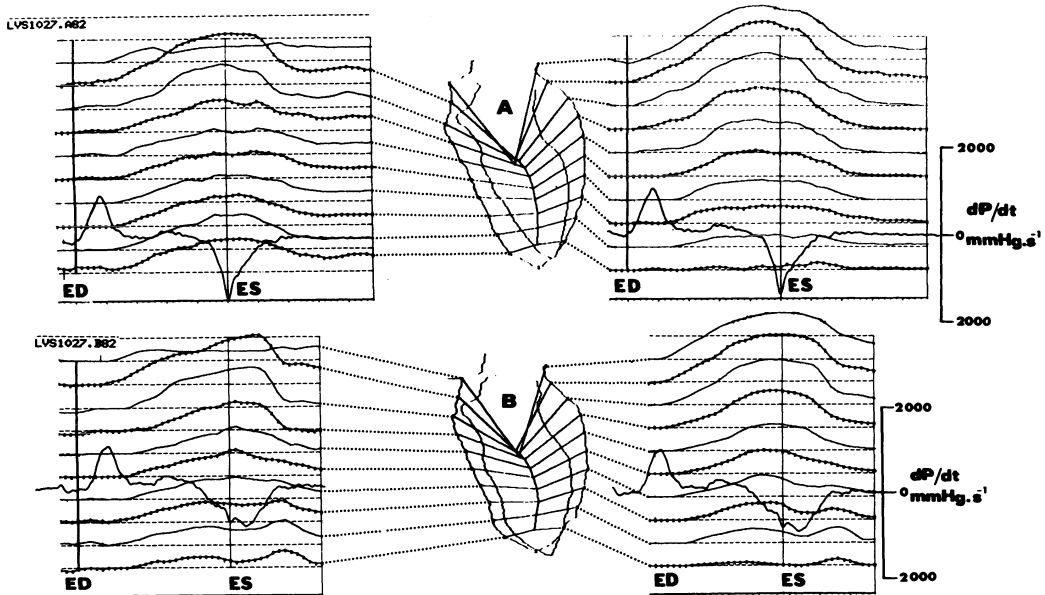
 $\beta_n$  = constant of regional elastic stiffness—median values are given, overall and paired (vs. pre = PTCA); PTCA = percutaneous transluminal coronary angioplasty; NS = not significant.

FIGURE 25-15. Left ventricular wall displacement studied in 20 separate segments, ten in the anterior (*right*) and ten in the inferoposterior wall (*left*). A typical example of the relation between segmental wall displacement and  $dP/dt$  curve is observed before PTCA (A) and after 20 seconds (B) of left anterior descending artery occlusion: after 20 seconds of occlusion, the notch in the  $dP/dt$  curve corresponds to a second wave of inward wall displacement in the anteroapical and inferoapical segments. ED = end-diastole; ES = end-systole.

tic element, in series with the actively contracting and relaxing nonischemic segment. This mechanism is consistent with the model of left ventricular pressure relaxation recently proposed by our group [13], which assumes that the observed time constant  $\tau_1$  results from the combined action of that fraction of the myocardium in the process of relaxing and the re-

maining fraction in which relaxation has not yet been initiated. After 40 seconds of ischemia, despite paradoxical lengthening (epicardial wall motion) throughout systole, early diastolic shortening was still observed consistent with a markedly diminished yet persistent tension becoming manifest only after a decline in the load imposed upon the region by the remainder of the effectively contracting ventricle.

#### UNCOORDINATED SEGMENTAL CONTRACTION AS A CAUSE OF IMPAIRED FILLING DYNAMICS

Variability in the temporal sequence of regional left ventricular contraction in normal subjects has been previously observed and attributed to variations in the sequence of electrical activation or to other factors playing an important role in determining ventricular geometry such as ventricular volume and fiber orientation [26, 27]. In patients with coronary artery disease, the completion of ejection was found to be delayed, whereas the onset of ejection was not, and the severity of coronary artery disease was positively correlated with the persistence of these contraction abnormalities into early diastolic [28]. During spontaneous angina, a significant prolongation of left ventricular ejection time with an accompanying shortening of diastole has also been observed [29]. All these observations dictate that studies of relaxation and filling in early diastole should be correlated with the pattern of contraction

*Determinants of Filling Dynamics.* It has been suggested that the peak filling rate is dependent on the rate of left ventricular relaxation and on the left atrial pressure [30]. Under normal conditions, the relaxing left ventricle produces a rapid change in the atrioventricular pressure gradient, which is the driving force for inflow [31]. Thus a prolonged relaxation phase, as observed during acute ischemia, causes a delay in the development of the atrioventricular pressure gradient, and, consequently, a greater left atrial pressure is required to open the mitral valve. In fact we observed a consistent delay in the relaxation rate occurring 20 seconds after the onset of ischemia and concomitantly both the isovolumic relaxation period and the left atrial pressure required for mitral valve opening increased. The significant relationship existing between  $\Sigma\Delta t_2$  and  $\tau_1$  and between this latter parameter and the duration of the isovolumic

relaxation period suggests that, during acute ischemia, the atrioventricular dynamic interplay occurring during the early diastole is affected by the asynchronous left ventricular contraction. Yellin and coworkers [30] demonstrated in the dog that under conditions of similar left atrial pressure at valve opening, the prolongation of the time constant of relaxation decreases the rate and amplitude of filling, whereas under conditions of similar left ventricular pressure during relaxation, an increase of left atrial pressure increases the amplitude of early filling. Thus the lack of correlation between peak filling rate and any single parameter of the relaxation phase, such as time constants of relaxation, isovolumic relaxation period, or mitral valve opening pressure, was expected because these latter parameters, during acute ischemia, are changing in opposite direction.

A decrease in peak filling rate has been extensively reported in patients with coronary artery disease with or without previous myocardial infarction. Until recently no data were available in the literature regarding the relationship between global and regional left ventricular filling. Yamagishi and associates [32] investigated this relationship using radionuclide angiography in normal subjects and in patients with left anterior descending coronary artery disease without previous myocardial infarction and found differences in peak filling rate differentiating normal subjects from those with coronary artery disease. To explain this difference, they analyzed regional filling dynamics and identified asynchrony in regional filling as a major determinant of the decrease in peak filling rate. The sum of the absolute time differences between the global and regional peak filling rates was inversely correlated to the global peak filling rate and proposed as an index of asynchrony in diastolic filling. More recently Bonow and colleagues [33] studied with radionuclide angiography the relationship between regional left ventricular diastolic asynchrony and global diastolic filling, before and after PTCA in patients with single-vessel coronary artery disease. Before PTCA, impaired global diastolic filling was found and was related to regional variations in the timing of left ventricular relaxation and filling determined by variations in phase among sectors and by regional quadrant analysis. In addition, they demonstrated a negative correlation between the magnitude of global peak filling rate and the extent of regional

asynchrony. Reevaluation 1 day to 1 month after PTCA showed an improvement of the above mentioned changes in diastolic global and regional function.

*Role of Asynchronous Contraction.* In the present study, we demonstrated that ischemia occurring early during coronary occlusion severely alters filling dynamics and that the major determinant of this change is asynchrony in regional filling. This diastolic asynchrony was secondary to a nonuniformity of inward wall displacement, but the crucial question remains whether this diastolic asynchrony was a direct, intrinsic manifestation of altered relaxation properties of the myocardium (inactivation) or a consequence of dysfunction of the contractile properties of the myocardium (activation) [34, 35].

#### EFFECT OF CORONARY OCCLUSION ON LEFT VENTRICULAR CHAMBER STIFFNESS AND REGIONAL DIASTOLIC PRESSURE-RADIUS RELATIONS

The third major finding of the present study was that ischemia induced by complete occlusion of the left anterior descending coronary artery increased the regional chamber stiffness of the ischemic anterior wall, even during an occlusion as short as 20 seconds. Parallel to this increase in regional stiffness, the global stiffness of the left ventricle increased significantly. In experimental studies [36–38], an increase in global chamber stiffness was only seen when the area rendered ischemic was large, such as during acute occlusion of the left anterior descending coronary artery.

The baseline pressure (constant C) increased slightly from  $-1.4$  to  $5.2$  mm Hg after 20 seconds and from  $-5.8$  to  $9.4$  mm Hg after 50 seconds of acute coronary occlusion (see Table 25–2). This increase in baseline pressure reflects the upward shift of the diastolic pressure-volume relation during coronary occlusion, which was thus  $6.6$  mm Hg after 20 seconds and  $15.2$  mm Hg after 50 seconds.

Twelve minutes after the end of the procedure, including repeated (three to ten) and brief (15–75 seconds) occlusions, the parameters of global and regional systolic function had returned to baseline, as shown from the indices of isovolumic contraction, relaxation, and segmental wall motion. In contrast, the parameters of

regional diastolic function were still abnormal (see Table 25–5), whereas the constant of global chamber stiffness and the baseline pressure remained slightly elevated. This suggests the postischemic diastolic abnormalities persist even when complete recovery of systolic function and relaxation has already occurred.

*Significance of the Upward Shift in Pressure-Volume and Pressure-Radius Relations.* The significance of the upward shift in the pressure-volume and/or pressure-radius length relations is still the subject of controversy. In the various previous studies [21, 22, 36–41], this shift was attributed to any or a combination of the following factors: changes in intrinsic diastolic myocardial stiffness, delayed left ventricular relaxation, loss of elastic recoil due to ventricular asynergy, changes in right ventricular-pericardial constraints, and coronary perfusion. A limitation of the present study is that we cannot address directly these specific issues. For instance, fitting of the pressure-volume relation by a simple elastic model, as we did, does not allow one to infer that the intrinsic diastolic properties of the myocardium were affected by acute coronary occlusion because this would require analysis of left ventricular stress and strain [42]. Regional wall thickness measurements are needed, which cannot be obtained accurately at 20-msec intervals from the left ventricular angiocardiograms. Also, the strain data should be normalized for a reference unloaded muscle length, i.e., at a transmural pressure of 0 mm Hg, and this cannot be obtained easily during cardiac catheterization in man.

As far as extrinsic factors are concerned, we feel that the coronary perfusion, or the so-called “erectile effect,” is not likely to account for the increased stiffness of the ischemic segment. During coronary occlusion of the left anterior descending artery, inflation of the dilatation balloon results on average in a 44% decrease in regional blood flow [43], thereby reducing the myocardial wall blood volume. Likewise, the postangioplasty measurements were obtained at a time where any increased myocardial turgor due to reactive hyperemia had dissipated [43]. Interestingly, the increase in regional stiffness observed in the adjacent inferior segment could be related to an increased turgor as the collateral flow to that area might increase during left anterior descending occlusion [44].

*Comparison with Animal Models of Acute Low-Flow Ischemia.* Coronary angioplasty mimics the experimental coronary occlusion in the animal laboratory and induces transient acute low-flow ischemia. In this animal model, Hess and coworkers [22] showed that "myocardial wall stiffness is increased during complete coronary occlusion when there is systolic thinning of the ischemic wall." In these conscious chronically instrumented dogs, the ischemic alteration in the intrinsic diastolic properties of the muscle resulted in an upward shift of the pressure-volume curve. They observed an average 27% increase in diastolic wall stiffness, which compares well with the 35% increase in global chamber stiffness after 50 seconds of anterior descending coronary artery occlusion in the present data. It may be emphasized that in the animal study, the upward shift of the pressure-volume curve was prevented by inferior vena caval obstruction. This emphasizes the modulating role of the right ventricular loading conditions and the ventricular interaction, which can offset the increase in pressure.

Thus, the observed changes in global and regional diastolic chamber stiffness are in accordance with previous experimental work [20, 22, 37], demonstrating an increase in the myocardial stiffness during coronary occlusion.

*Mechanism of Increased Myocardial Stiffness.* The mechanism by which ischemia increases the myocardial stiffness remains speculative and may depend on the pathophysiology [36] and the duration [45] of a given ischemic condition. In the acute coronary occlusion model [22, 37], systolic overstretch of the akinetic muscle fibers by adjacent nonischemic myocardium was thought to be responsible for the diastolic thinning of the ischemic wall and the increase in resting muscle length. This "creep" effect causes the ischemic myocardium to operate at a higher point on the pressure-sarcomere length relation and thus at an increased stiffness level. Although we observed no significant changes in end-diastolic volume throughout the procedure, it cannot be excluded that creep may have occurred. Echocardiographic evidence of wall thinning during angioplasty and during attacks of variant angina supports this hypothesis [8, 46]. The other major mechanism refers to the concept of residual diastolic actin-myosin-interaction [47]. An increase in cytosolic  $Ca^{2+}$  and a decrease in adenosine triphosphate available for cross-bridge dissociation could result in the

presence of an abnormal myocardial "tone." This mechanism is unlikely after prolonged occlusion because the ischemic segment becomes akinetic or dyskinetic and systolic cross-bridge formation is probably minimal or absent. However, after 20 seconds of occlusion, we observed asynchrony and late shortening of the ischemic wall [43, 45], which were shown to affect the stiffness of rat heart trabeculae [48]. Also, the persistent abnormalities in diastolic function seen after the procedure could be related to an abnormal myocardial tone despite normalization of the rate of relaxation. As recently emphasized [21, 36], such failure of complete myofilament inactivation implies a reduced extent of relaxation, which is not necessarily synonymous with a reduced rate of relaxation, as measured from the time constant of isovolumic left ventricular pressure decay.

Finally, it should be realized that the increase in the calculated stiffness constant could also be related to an increased resistance to early filling. It was shown recently in humans that early diastolic filling can be kept normal during ischemia despite delayed relaxation and loss of elastic recoil (increase in end-systolic volume) by increasing the left atrial driving pressure [49]. Under these conditions, the diastolic properties of the myocardium would be better characterized by a viscoelastic model rather than by a simple elastic stress-strain relation [50, 51].

We used a simple elastic model because the present angiocardiographic data did not allow proper quantitation of the strain rates, which are essential for determining diastolic viscous effects. Therefore, our calculated stiffness constant includes both elastic and viscous forces. Interestingly, we found similar increases in the constant of elastic chamber stiffness after 20 and 50 seconds of occlusion, whereas left ventricular asynchrony and late shortening of the ischemic wall were observed only at 20 seconds. This increased chamber stiffness observed only at 20 seconds may only be apparent and related more to an increase in viscous resistance to early filling, although asynchrony and late shortening have been shown to affect the stiffness of rat heart [51].

CONCLUSION: PTCA AS AN ISCHEMIC MODEL?

*Early Wall Motion During Acute Ischemia: How to Interpret?* Recently we evaluated the

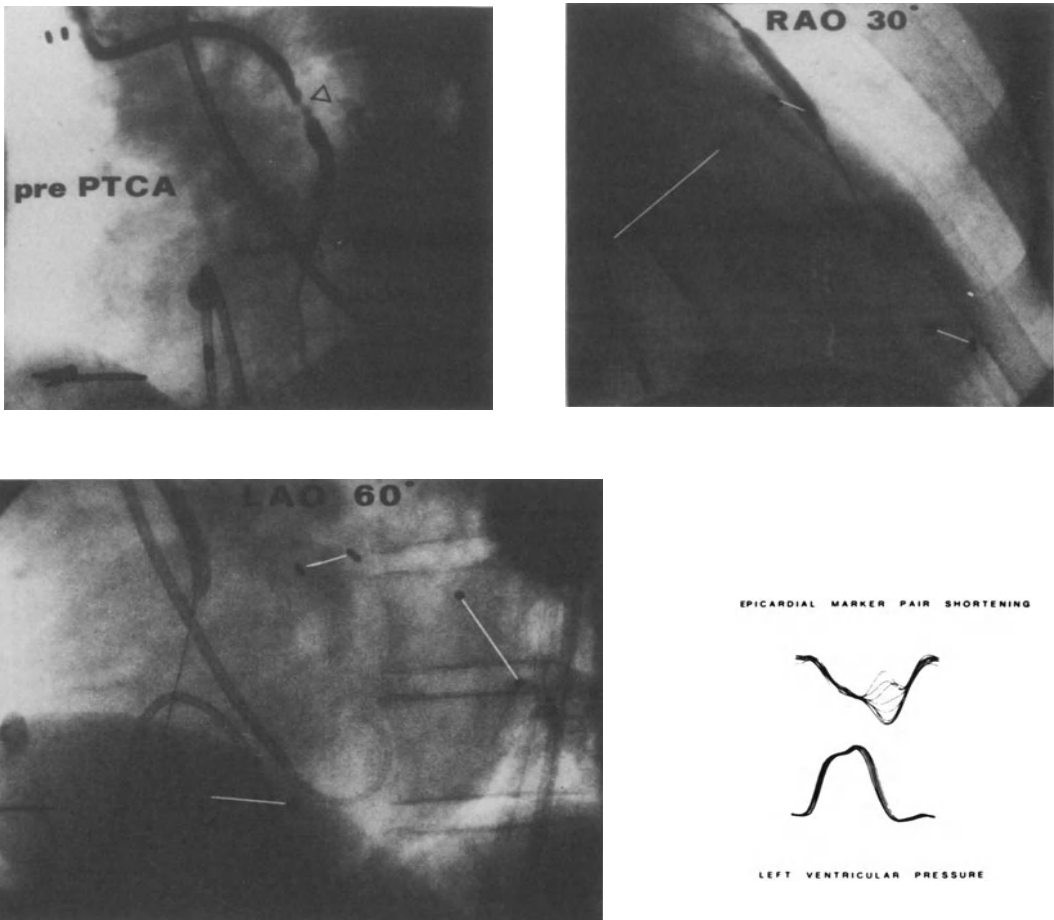


FIGURE 25-16. Angiogram of left anterior descending bypass graft stenosis and markers before PTCA (A). Panels B and C show the inflated angioplasty catheter in place in RAO 30° and LAO 60°, respectively. Panel D shows changes in epicardial marker pair shortening in the region of the bypass graft and left ventricular pressure during graft occlusion. The W phenomenon is evident.

beat-to-beat myocardial shortening changes accompanying acute coronary occlusion in one patient, who was undergoing PTCA of a coronary artery bypass graft and in whom pairs of epicardial wall markers had been placed at the time of his original cardiac surgery [45]. Their motion reflecting epicardial transverse shortening was characterized, in ischemic myocardium, by the early appearance of a late systolic

lengthening, followed by an early diastolic shortening (Figure 25-16). We referred to this biphasic motion as the "W" phenomenon due to its morphologic characteristics, transient duration, and frequency of appearance in studies of endocardial wall-thickness motion during regional ischemia. This polyphasic wall-motion pattern appears to be similar to that described by Wiegner and coworkers [48], who studied the interaction of normal and hypoxic myocardial muscles in series. They identified a biphasic pattern of motion of the hypoxic muscle analogous to that observed in the ischemic region of the intact left ventricle (Figure 25-17). The early lengthening phase of the hypoxic muscle was attributed to a prema-

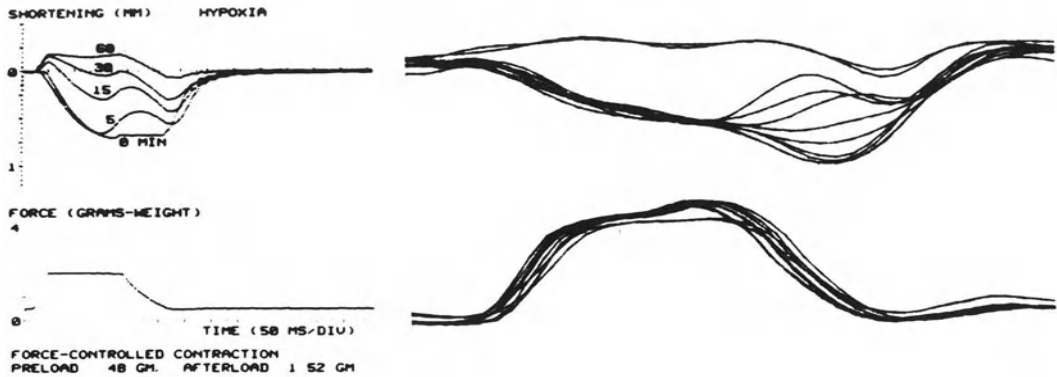


FIGURE 25-17. Biphasic pattern of motion of isolated hypoxic muscle studied under the condition of normal and hypoxic muscle in series (Modified from Weigner et al [48], with permission.)

ture onset of force decline, and the second late shortening phase was ascribed to either a persisting contractile force of the muscle or a manifestation of stored force from elastic recoil of previously stretched passive muscle elements. Furthermore, they indicated the possible negative role of late shortening on filling dynamics. Similar types of wall motion abnormalities have been described in animals [1, 2, 4, 52] and during chronic ischemia in humans [53, 54]. In our angiographic study, the frame-by-frame analysis of the anterior wall displacement during brief occlusion of left anterior descending artery also showed a variety of biphasic wall motion patterns. After 17 seconds of occlusion, some of the segments adjacent to the ischemic area exhibited the W phenomenon, whereas the segment located in the core of the ischemic area exhibited a late inward-wall displacement in early diastole. This phenomenon was mirrored by an accelerated outward displacement of the normal segment. Ultimately, the interaction between ischemic and nonischemic segments results in segmental asynchrony in the occurrence of peak velocity of outward displacement. Because this parameter reflects the segmental peak filling rate, an asynchrony in segmental outward displacement corresponds to the asynchrony in the filling phase with consequent changes in the global peak filling rate.

In summary, our study demonstrates that short periods of ischemia, induced by balloon inflation, cause an early disruption of the normal sequence of inward-outward segmental displacement in the ischemic segments. This phenomenon is characterized by an early lengthening

occurring during late systole with late shortening occurring during early diastole. These data in part confirm an "asynchronous contraction" occurring during brief periods of ischemia [55] and, in particular, demonstrate, the close relationship existing between uncoordinated contraction and the impairment of filling dynamics.

*Are there Clinical Implications for the PTCA Procedure?* We can conclude that repeated complete coronary occlusions of the left anterior descending coronary artery in conscious humans are associated with profound alterations in diastolic chamber stiffness, which persist well after restoration in myocardial blood flow and a normal systolic function. Further work is needed to document the time course of the recovery to a normal regional diastolic function and to address the responsible derangement of sub-cellular metabolism because the mechanisms of the observed abnormalities are not yet fully understood.

From the clinical point of view, many factors have contributed to increase the extent and severity of iatrogenic ischemia during angioplasty: longer balloon inflation time, dilatation of multiple lesions during a single setting and inclusion of patients with unstable angina or impaired left ventricular function. This has prompted studies attempting to modify ische-

mic changes induced by balloon inflation by means of various intervention [9, 56, 57].

Along with our previous studies [43, 45], the present data suggest that the analysis of diastolic function may prove to be a sensitive tool in assessing the possibly deleterious effects of repeated coronary occlusions during angioplasty and could be a useful end point in evaluating the efficacy of "cardioprotective" intervention.

## References

- Pagani M, Vatner S, Brig H, Braunwald E (1978). Initial myocardial adjustments to brief periods of ischemia and reperfusion in the conscious dog. *Circ Res* 43:83-91.
- Kumada T, Karliner JS, Pouleur H, et al (1979). Effects of coronary occlusion on early ventricular diastolic events in conscious dogs. *Am J Physiol* 237:H542-H549.
- Gaasch WH, Bernard SA (1977). The effects of acute changes in coronary blood flow on left ventricular end-diastolic wall thickness: An echocardiographic study. *Circulation* 56:593-597.
- Forrester JS, Wyatt HL, de Luz PL, et al (1976). Functional significance of regional ischemic contraction abnormalities. *Circulation*; 54:64-70.
- Rentrop KP, Cohen M, Blanke H, Phillips RA (1985). Changes in collateral filling immediately after controlled coronary artery occlusion by an angioplasty balloon in human subjects. *J Am Coll Cardiol* 5:587-592.
- Probst P, Zangl W, Pachinger O (1985). Relation of coronary arterial occlusion pressure during percutaneous transluminal coronary angioplasty to presence of collaterals. *Am J Cardiol* 55:1264-1269.
- Meier B, Luethy P (1984). Coronary wedge pressure as predictor of recruitable collateral arteries. *Circulation* 70(suppl II):266.
- Das SK, Serruys PW, vd Brand M, et al (1983). Acute echocardiographic changes during percutaneous coronary angioplasty and their relationship to coronary blood flow. *J Cardiovasc Ultrasonogr* 2:269-271.
- Serruys PW, vd Brand M, Brower RW, Hugenholtz PG (1983). Regional cardioplegia and cardioprotection during transluminal angioplasty, which role for nifedipine? *Eur Heart J* 4:115-21.
- Sigwart U, Grbic M, Payot M, et al (1985). Ischemic events during coronary artery balloon obstruction. In Rutishauser W, Roskamm H (eds): *Silent Myocardial Ischemia*. Roskamm; Berlin: Springer Verlag, pp 29-36.
- Meester GT, Bernard N, Zeelenberg C, et al (1975). A computer system for real time analysis of cardiac catheterization data. *Cathet Cardiovasc Diagn* 1:112-23.
- Meester CT, Zeelenberg C, Bernard N, Gorter S (1974). Beat to beat analysis of cardiac catheterization data. In *Computers in Cardiology*. Los Angeles: IEEE Computer Society, pp 63-65.
- Brower RW, Meij S, Serruys PW (1983). A model of asynchronous left ventricular relaxation predicting the bi-exponential pressure decay. *Cardiovasc Res* 17:482-488.
- Fioretti P, Brower RW, Meester GT, Serruys PW (1980). Interaction of left ventricular relaxation and filling during early diastole in human subjects. *Am J Cardiol* 46:197-203.
- Slager CJ, Reiber JHC, Schuurbiens JCH, Meester GT (1978). Contouromat—A hard-wired left ventricular angio processing system: Design and application. *Comp Biomed Res* 11:431-502.
- Slager CJ, Hooghoudt TEH, Reiber JCH, et al (1980). Left ventricular contour segmentation from anatomical landmark trajectories and its application to wall motion analysis. In *Computers in Cardiology*. Los Angeles: IEEE Computer Society, pp 347-350.
- Hooghoudt TEH, Slager CJ, Reiber JHC, et al (1980). "Regional contribution to global ejection fraction" used to assess the applicability of a new wall motion model to the detection of regional wall motion in patients with asynergy. In *Computers in Cardiology*. Los Angeles: IEEE Computer Society, pp 253-256.
- Slager CJ, Hooghoudt TEH, Serruys PW, et al (1982). Automated quantification of left ventricular angiograms. In Short MD, et al (eds): *Physical techniques in Cardiological Imaging*. Bristol, Eng. A Hilger Ltd, pp 163-172.
- Hess OM, Grimm J, Krayenbuehl HP (1979). Diastolic simple elastic and viscoelastic properties of the left ventricle in man. *Circulation* 59:1178-1187.
- Theroux P, Franklin D, Ross J Jr, Kemper WS (1974). Regional myocardial function during acute coronary artery occlusion and its modification by pharmacologic agents in the dog. *Circ Res* 35:896-908.
- Sasayama S, Nonogi H, Migazaki S, et al (1985). Changes in diastolic properties of the regional myocardium during pacing-induced ischemia in human subjects. *J Am Coll Cardiol* 5:599-606.
- Hess OM, Koch R, Bamert C, Krayenbuehl HP (1980). Regional wall stiffness during acute myocardial ischemia in the canine left ventricle. *Eur Heart J* 1:435-443.
- Tyberg JV, Parmley MW, Sonnenblick EH (1969). In vitro studies of myocardial asynchrony and regional hypoxia. *Circulation* 25: 569-579.

24. Theroux P, Ross J Jr, Franklin D, et al (1977). Regional myocardial infarction in the unanesthetized dog. *Circ Res* 40:158-165.
25. Theroux P, Ross J Jr, Franklin D, et al (1976). Regional myocardial function in the conscious dog during acute coronary occlusion and responses to morphine, propranolol, nitroglycerine and lidocaine. *Circulation* 53:302-314.
26. Clayton PD, Bulawa WF, Klausner SC, et al (1979). The characteristic sequence for the onset of contraction in the normal human left ventricle. *Circulation* 59:671-679.
27. Klausner SC, Blair TJ, Bulawa WF, et al (1982). Quantitative analysis of segmental wall motion throughout systole and diastole in the normal human left ventricle. *Circulation* 65:580-590.
28. Holman LB, Wynne J, Idoine J, Neill J (1980). Disruption in the temporal sequence of regional ventricular contraction. I. Characteristics and incidence in coronary artery disease. *Circulation* 61:1075-1083.
29. Ferro G, Piscione F, Carella G, et al (1984). Systolic and diastolic time intervals during spontaneous angina. *Clin Cardiol* 7:588-592.
30. Yellin EL, Yoran C, Sonnenblick EH, Frater RWM (1980). The relation between left ventricular relaxation and early diastolic filling in the intact dog heart. *Eur Heart J* 1(suppl B):179-180.
31. Yellin EL, Peskin C, Yoran C, et al (1981). Mechanism of mitral valve motion during diastole. *Am J Physiol* 214:H389-H400.
32. Yamagishi T, Ozaki M, Kumada T, et al (1984). Asynchronous left ventricular diastolic filling in patients with isolated disease of the left anterior descending coronary artery: assessment with radionuclide ventriculography. *Circulation* 69:933-942.
33. Bonow RO, Vitale DF, Bacharach SL, et al (1985). Asynchronous left ventricular regional function and impaired global diastolic filling in patients with coronary artery disease: reversal after coronary angioplasty. *Circulation* 71:297-307.
34. Brutsaert DL, Housemans PR, Goethals MA (1980). Dual control of relaxation: Its role in the ventricular function in the mammalian heart. *Circ Res* 47:637-652.
35. Brutsaert DL, Rademakers FE, Sys SV (1984). Triple control of relaxation: Implications in cardiac diseases. *Circulation* 69:190-196.
36. Paulus WJ, Grossman W, Serizawa T, et al (1985). Different effects of two types of ischemia on myocardial systolic and diastolic functions. *Am J Physiol* 1985; 248:H719-H728.
37. Hess OM, Osakada G, Lavelle JF, et al (1983). Diastolic myocardial wall stiffness and ventricular relaxation during partial and complete coronary occlusion in the conscious dog. *Circ Res* 52:387-400.
38. Grossman W, Serizawa T, Carabello BA (1980). Studies on the mechanism of altered left ventricular diastolic pressure-volume relations during ischemia. *Eur Heart J* 1(suppl):141-147.
39. Bourdillon PD, Lorell BH, Mirsky I, et al (1983). Increased regional myocardial stiffness of the left ventricle during pacing-induced angina in man. *Circulation* 67:316-323.
40. Shirato K, Shabetai R, Bhargava V, et al (1978). Alteration of the left ventricular diastolic pressure segment length relation produced by the pericardium: Effects of cardiac distension and afterload reduction in conscious dogs. *Circulation* 57:1191-1198.
41. Serizawa T, Carabello BA, Grossman W (1980). Effect of pacing-induced ischemia on left ventricular diastolic pressure-volume relations in dogs with coronary stenoses. *Circ Res* 46:430-439.
42. Glantz SA, Parmley WW (1978). Factors which affect the diastolic pressure-volume curve. *Circ Res* 42:171-180.
43. Serruys PW, van den Brand M, Mey S, et al (1984). Left ventricular performance, regional blood flow, wall motion and lactate metabolism during transluminal angioplasty. *Circulation* 70:25-36.
44. Wahr DW, Ports TA, Botvinick EH, et al (1985). The effects of coronary angioplasty and reperfusion on distribution of myocardial flow. *Circulation* 72:334-343.
45. Jaski BE, Serruys PW (1985). Epicardial wall motion and left ventricular function during coronary graft angioplasty in humans. *J Am Coll Cardiol* 6:695-700.
46. Distante A, Rovai D, Picano E, et al (1984). Transient changes in left ventricular mechanics during attacks of Prinzmetal's angina. *Am Heart J* 107:465-472.
47. Nayler WG, Williams A (1978). Relaxation in heart muscle: Some morphological and biochemical considerations. *Eur J Cardiol* 7(suppl):35-50.
48. Wiegner AW, Allen GJ, Bing OHL (1978). Weak and strong myocardium in series: Implications for segmental dysfunction. *Am J Physiol* 235:H776-H783.
49. Carroll JD, Hess OM, Hirzel HO, Krayenbuehl HP (1983). Dynamics of left ventricular filling at rest and during exercise. *Circulation* 68:59-67.
50. Rankin JS, Arentzen CE, McHale PA, et al (1977). Viscoelastic properties of the diastolic left ventricle in the conscious dog. *Circ Res* 41:37-45.

51. Pouleur H, Karliner JS, Le Winter MM, Covell JW (1979). Diastolic viscous properties of the intact canine left ventricle. *Circ Res* 45:410–419.
52. Heijndrickx GR, Millard RW, McRitchie RJ, et al (1975). Regional myocardial function and electrophysiological alterations after brief coronary artery occlusion in conscious dogs. *J Clin Invest* 56:978–985.
53. Gibson DJ, Prewitt TA, Brown DT (1976). Analysis of left ventricular wall movement during isovolumic relaxation and its relation to coronary artery disease. *Br Heart J* 38:1010–1019.
54. Sasayama S, Nonogi H, Fujita M, et al (1984). Analysis of asynchronous wall motion by regional pressure length loops in patients with coronary artery disease. *J Am Coll Cardiol* 1984; 4:256–267.
55. Gaasch WH, Blaustein AS, Bing OHL (1985). Asynchronous (segmental early) relaxation of the left ventricle. *J Am Coll Cardiol* 5:891–897.
56. Doorey AJ, Mehmel HC, Schwartz FX, Kübler W (1985). Amelioration by nitroglycerin of left ventricular ischemia induced by percutaneous transluminal coronary angioplasty: Assessment by hemodynamic variables and left ventriculography. *J Am Coll Cardiol* 6:267–274.
57. McDonald FM, Fuchs M, Kreuzer J, et al (1985). Hemodynamic and antiarrhythmic protective effects of intracoronary perfusion during percutaneous transluminal coronary angioplasty. *Eur Heart J* 6:284–293.

---

# 26. DIASTOLIC VENTRICULAR FUNCTION IN PRIMARY AND SECONDARY HYPERTROPHY: THE INFLUENCE OF VERAPAMIL

---

W.H. Bleifeld

Left ventricular diastolic function is of clinical importance [1], because disturbed relaxation results in impaired left ventricular filling and an increase of left ventricular filling pressure with breathlessness during exercise or at rest. Although hypertrophy in highly trained athletes does not appear to be accompanied by abnormalities of systolic or diastolic function as evaluated from the end-diastolic pulmonary artery pressure [2], patients with left ventricular hypertrophy due to pressure overload or primary myocardial disease usually manifest increased filling pressure and, depending on the degree of their disease, may exhibit clinical signs of left heart failure.

Calcium channel blocking agents have been shown not only to relax vascular smooth muscle [2a], but also to improve the relaxation of the myocardial muscle [3] and are now widely used in the treatment of hypertrophic cardiomyopathy [4, 5]. In the following study, we examined diastolic function in different forms of left ventricular hypertrophy as well as the acute and chronic effects of verapamil on left ventricular relaxation, hemodynamics and exercise capacity in patients with hypertrophic cardiomyopathy.

### *Patient Population*

For the evaluation of diastolic function in left

ventricular hypertrophy, 76 patients were divided into three groups: Group I was recruited from 28 healthy subjects (15 males, 13 females), and served as the control population. Group II consisted of 24 patients (9 males, 15 females) with hypertrophic obstructive cardiomyopathy (HOOCM). At the time of investigation, no drug therapy was given and 22 were in sinus rhythm. In Group III, 24 patients with chronic pressure overload (CPO) were studied. Six patients had valvular aortic stenosis, while in the remaining 18 patients, left ventricular hypertrophy (septal and posterior wall thickness by echocardiography > 21 mm) was the result of arterial hypertension [6].

In a second study, the effect of 0.15 mg/kg intravenous verapamil was assessed in 11 patients (5 males, 6 females) with hypertrophic cardiomyopathy (HCM), diagnosed by echocardiographic, hemodynamic, and angiographic criteria, before and 7 minutes after injection of the drug. Coronary artery disease was excluded. Six patients had outflow obstruction at rest or after provocation (HOOCM), while five persons had no left ventricular outflow tract gradient (HNOOCM). In addition, 14 patients with left ventricular hypertrophy as a result of arterial hypertension were tested [7].

Finally, the effect of long-term oral therapy with verapamil (40 mg three times daily increasing to 120 mg four times daily for 7 weeks) was examined in 18 patients with HCM (12 HOOCM; 6 HNOOCM). One patient was in atrial fibrillation. Three patients had mitral insufficiency [8].

*Grossman, William, and Lorell, Beverly H. (eds.), Diastolic Relaxation of the Heart. Copyright © 1987. Martinus Nijhoff Publishing. All rights reserved.*

### Methods

For the measurement of instantaneous left ventricular pressures, an 8F-tip manometer was inserted into the left ventricle, and pressure was recorded simultaneously with the echocardiogram.

M-mode echocardiograms of the left ventricle were recorded with a paper speed of 50 mm/second analyzed by use of an x-y-reader and a computer [9]. In the noninvasive studies aortic valve closure was taken from the first component of the second heart sound ( $A_2$ ) in the phonocardiogram. The percent of diameter change (FS) was calculated from the end-diastolic (DD) and the end-systolic (DS) diameters according to the following formula:

$$\frac{DD - DS}{DD} \times 100 = \text{FS}(\%)$$

In addition, septal and posterior wall thickness at the time of end-diastole and the velocity of circumferential shortening ( $V_{CFmax}$ ) were calculated. End-diastolic left ventricular dimension (DD) was measured at the peak of the R-wave and end-diastolic dimension at the time point of aortic valve closure. From the difference between the time of end-systolic diameter (t-DS) and the time of mitral valve opening (t-MO) the interval (t-DS) - (t-MO) was calculated. The change in regional dimension during isovolumic relaxation ( $D_{IVR}$ ) was measured as the difference between the left ventricular dimension at the time point of aortic valve closure ( $A_2$ ) and that at mitral valve opening. The dimensional increase during left ventricular filling ( $D_{LVF}$ ) was measured as the dimensional increase from the time point of mitral valve opening to the peak of the following R-wave. The peak rate of diastolic posterior wall thinning in mm/second was calculated as  $dpW \text{ min}/dt$ . Cardiac output and pulmonary artery pressures were measured with a Swan-Ganz thermodilution catheter advanced to the pulmonary artery. Cardiac output was measured in triplicate by thermodilution. Pulmonary artery pressure measurements were based on the analysis of five consecutive cycles. Arterial blood pressure was taken from cuff manometer. Exercise was performed on a braked bicycle ergometer with the patient supine. Maximal work rate in the individual patient was calculated by summing the work rate in kmp/min (W) of each exercise step achieved.

Diastole was divided into the following parts:

1. Isovolumic relaxation (IVR), from closure of the aortic valve ( $AOC/A_2$ ) to opening of the mitral valve.
2. The rapid filling phase (RFP), from opening of the mitral valve to the end of the rapid early diastolic diameter increase, defined as the time when the peak rate of dimension had increased to 50% of the maximum. Thus, a calculation of the duration of RFP (t-RF) and the diameter change during RFP ( $D_{RF}$ ) was possible.

### Results

#### DIASTOLIC FUNCTION IN DIFFERENT FORMS OF HYPERTROPHY

Left ventricular diameter-time curves in control subjects and patients with pressure-overload are shown in Figure 26-1A. It is obvious that the IVR time is prolonged in HOCM. There is a very early diameter increase at the expense of that during RFP. The duration of the RFP was decreased, but not significantly prolonged in patients with HCM. Almost identical changes were observed in patients with CPO compared to control subjects (Figure 26-1B).

The mean values for all groups are demonstrated in Figure 26-2, which shows that the duration of isovolumic relaxation was significantly increased in both HOCM and CPO. During the RFP, (Figure 26-3A), the duration and diameter change were significantly reduced compared to normals. No alterations were observed during the slow filling phase and atrial contraction (Figure 26-3B).

#### ACUTE EFFECT OF VERAPAMIL ON DIASTOLIC FUNCTION

To test the hypothesis that verapamil has favorable effects on diastolic function of the left ventricle, the effect of intravenous verapamil on global and regional left ventricular relaxation and filling was examined in 11 patients with HCM and in 14 patients with left ventricular hypertrophy due to arterial hypertension (CPO) by the use of echocardiography and phonocardiography. While parameters of systolic function such as heart rate, blood pressure, end-systolic dimension, and fractional shortening were not altered in patients with HCM after 0.15 mg/kg of intravenous verapamil, IVR and the change

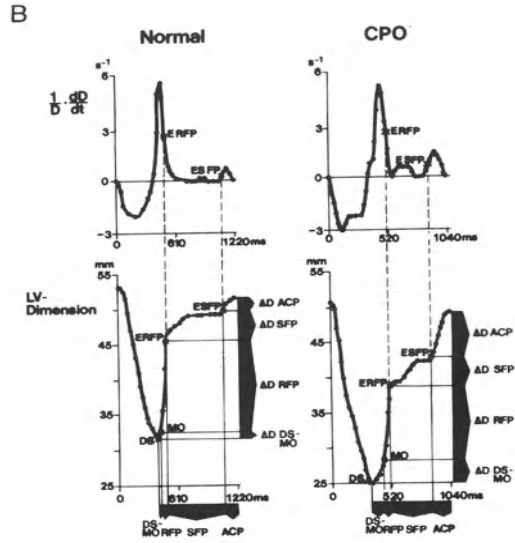
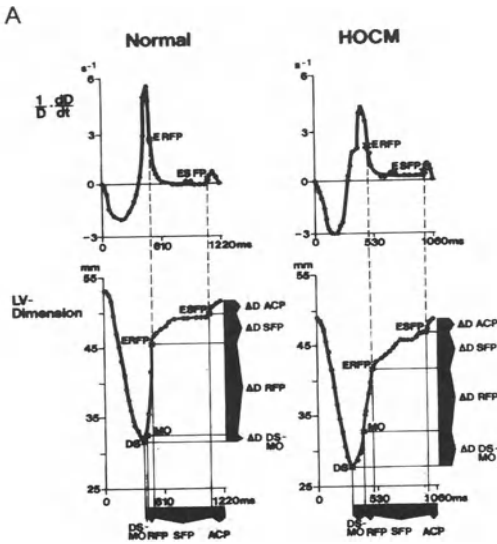
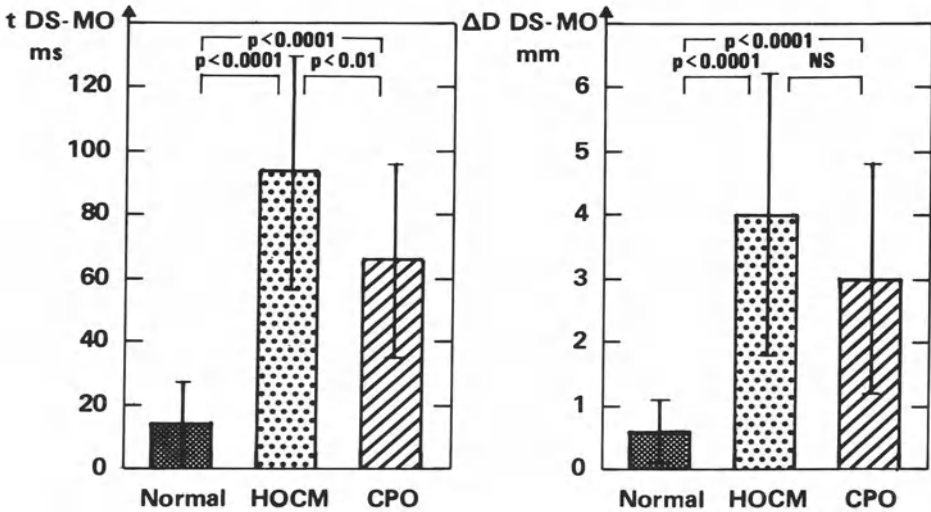


FIGURE 26-1. Left ventricular (LV) diameter-time curves for normal subjects, a patient with hypertrophic obstructive cardiomyopathy (HOCM) (A), and a patient with chronic pressure overload (CPO) (B). ERFP = early rapid filling phase; ESFP = L<sub>1</sub> ΔD ACP = L<sub>2</sub>; ΔD SEP = L<sub>3</sub>; ΔD DSMO = L<sub>4</sub>. L<sub>1</sub> end diastolic filling period; L<sub>2</sub> diameter change during atrial contraction; L<sub>3</sub> diameter change during slow filling phase; L<sub>4</sub> diameter change from end-systolic diameter to mitral opening.

FIGURE 26-2. Duration of isovolumic relaxation for all groups. HOCM = hypertrophic obstructive cardiomyopathy; CPO = chronic pressure overload; tDS-MO = L<sub>1</sub>; ΔD DS-MO = L<sub>2</sub>; NS = not significant. L<sub>1</sub> time from end systolic diameter to mitral opening; L<sub>2</sub> diameter change from end systolic to mitral opening.



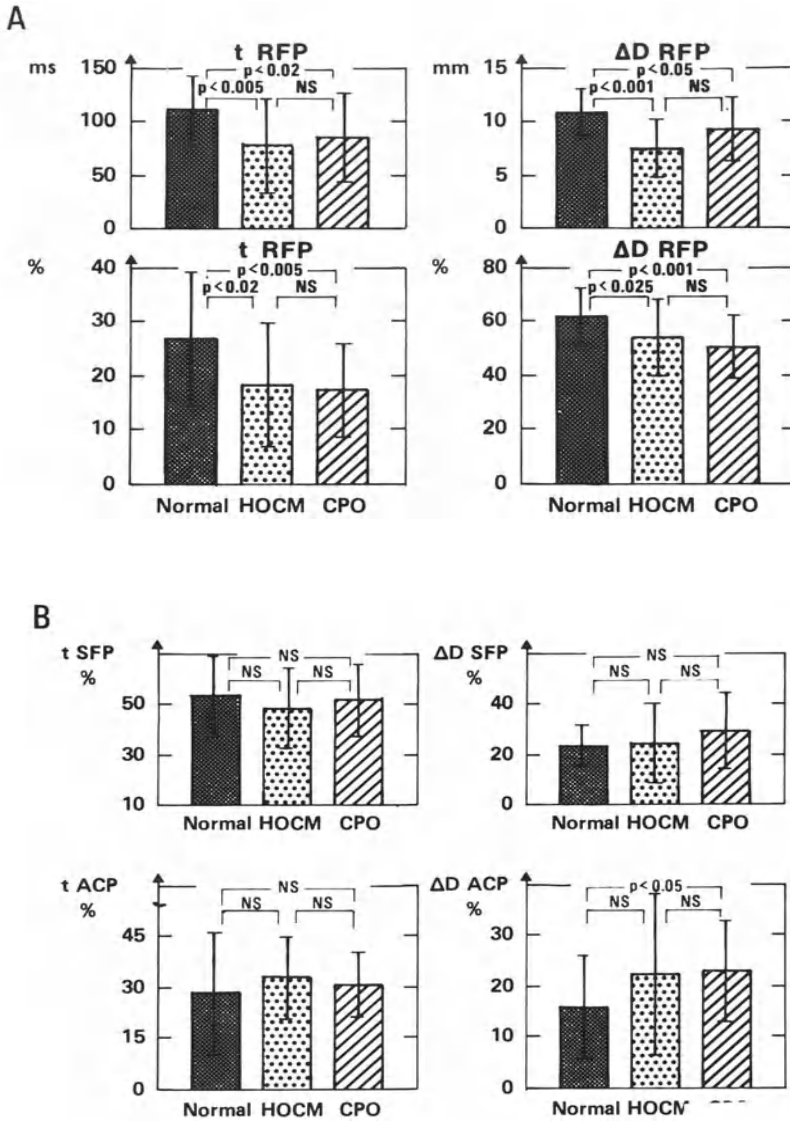


FIGURE 26-3. Data on the rapid (A) and slow (B) filling phase for all groups. HOcm = chronic obstructive hypertrophic cardiomyopathy CPO = chronic pressure overload; t RFP = L<sub>1</sub>; ΔD RFP = L<sub>2</sub>; t SFP = L<sub>3</sub>; ΔD SFP = L<sub>4</sub>; t ACP = L<sub>5</sub>; ΔD ACP = L<sub>6</sub>; NS = not significant. L<sub>1</sub> time of rapid filling period; L<sub>2</sub> diameter change during rapid filling period; L<sub>3</sub> time of slow filling period; L<sub>4</sub> diameter change during slow filling period; L<sub>5</sub> time of atrial contraction; L<sub>6</sub> diameter change during atrial contraction.

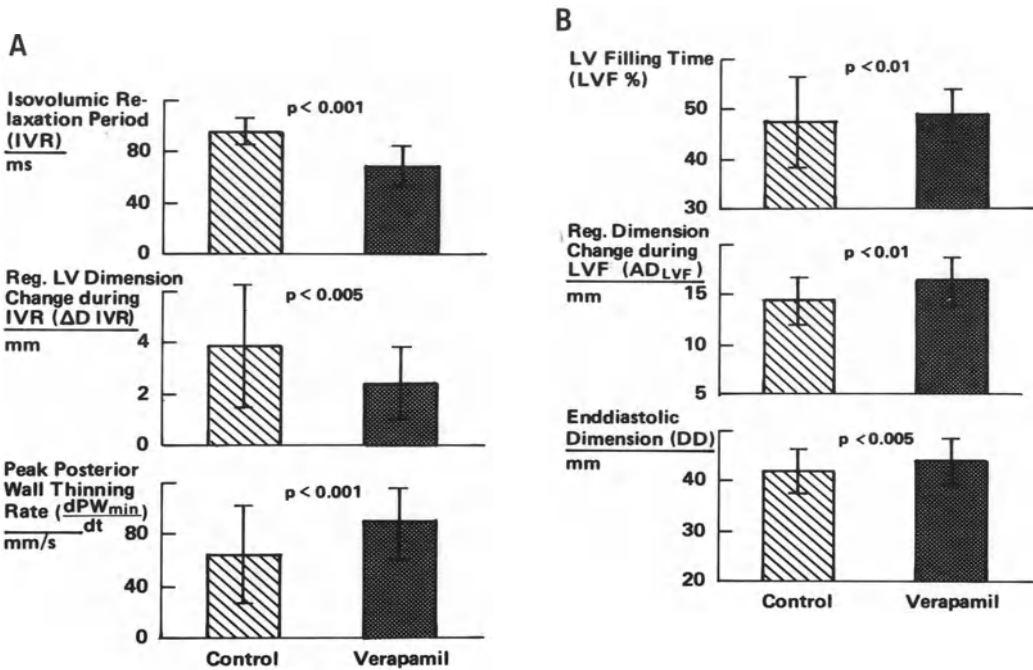


FIGURE 26-4. Influence of verapamil on isovolumic relaxation period (IVR), change in regional (reg.) left ventricular (LV) dimension, and peak posterior wall-thinning rate (A); as well as on other LV filling parameters (B).

in dimension during IVR were decreased significantly and the posterior wall thinning rate was increased (Figure 26-4A). Total left ventricular filling time, regional and global dimension increased slightly, but significantly during left ventricular filling (Figure 26-4B). Similar changes were observed in patients with CPO (Figure 26-5A, B).

#### EFFECTS OF CHRONIC VERAPAMIL ADMINISTRATION

The results of the acute administration of verapamil formed the basis for a further study evaluating the effect of chronic high-dose verapamil administration on left ventricular performance at rest and during exercise in 18 patients with hypertrophic cardiomyopathy (see Patient Population). The mean resting intraventricular gradient was  $53 \pm 21$  mm Hg and after provocation  $95 \pm 49$  mm Hg. Before the study, medication was stopped for at least 3 days. After baseline measurements, verapamil 40 mg three

times daily was initiated and increased to a maximum of 120 mg six times daily. Repeat hemodynamic investigation was performed at an average treatment duration of 7 weeks and was done 2 hours after the morning dose. The results are shown in Figures 26-6 and 26-7. Heart rate decreased significantly during rest and maximum exercise in comparison with baseline, as was observed for mean arterial pressure and systemic vascular resistance during exercise. Stroke volume index increased at rest and during maximum exercise. As a consequence of the improvement of diastolic filling, pulmonary artery end-diastolic pressure was lower in comparison with baseline (24 vs. 32 mm Hg) (see Figure 26-7), and pulmonary vascular resistance was also lower at maximum exercise. The maximum work rate was improved by about 25% from an average of 626 to 779W.

#### Discussion

The study of patients with different forms of left ventricular hypertrophy has shown that primary (HCM) and secondary hypertrophy (CPO) are

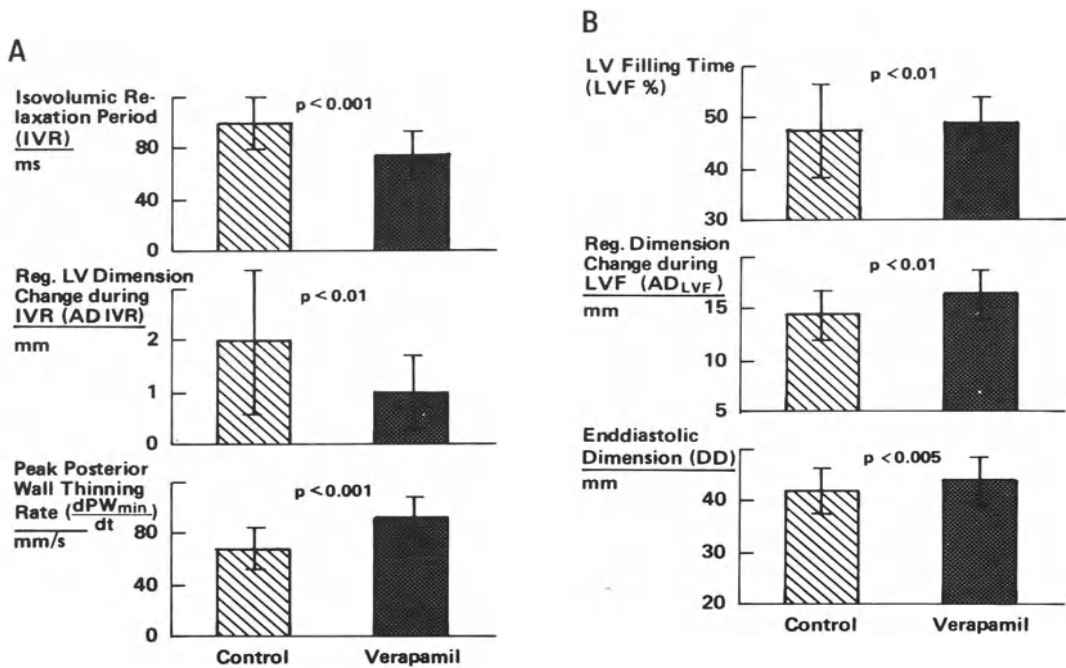


FIGURE 26-5. Effect of verapamil on global (A) and regional (B) left ventricular filling in arterial hypertension. Abbreviations as in Figure 26-4.

both accompanied by impairment of left ventricular diastolic function [6] in terms of a prolongation of left ventricular relaxation time. This is accompanied by an abnormal increase of regional diameter during relaxation compared to healthy patients. Thus, abnormal relaxation is nonspecific for HCM, but appears to be due to a pathologic hypertrophic process in the myocardium independent of its cause.

Previous studies from our own laboratory [2], evaluating the exercise hemodynamics of highly trained athletes, showed no abnormal increase of pulmonary end-diastolic pressure as a marker of impaired left ventricular diastolic function.

In the study of acute effects of verapamil on prolonged IVR in patients with HCM and CPO [7], significant shortening of IVR and an increased rate of left ventricular filling were observed and were associated with a smaller increase in regional ventricular dimension during IVR compared to the measurement before verapamil. These changes are an expression of the improvement in global and regional left ventricular relaxation. None of the extramyocardial determinants of relaxation, such as heart rate, systolic pressure, systolic volume, and left

atrial pressure [1, 10-14] were altered following the administration of verapamil either in HCM or in CPO. Thus, the beneficial effects of verapamil on diastolic function are not related to the specific anatomic features of HOCM and HCM.

Experimental studies suggest that impaired relaxation of the heart muscle may be caused by a depletion of high-energy phosphate reserves in the heart muscle due to hypoxia- or ischemia [3, 15]. In fact, thallium scintigrams of patients with hypertrophic cardiomyopathy in our own laboratory exhibited reversible defects [16].

The findings of an increase in regional left ventricular diameter change during IVR in left ventricular hypertrophy compared to normal is in accordance with the angiographic findings of Sanderson and coworkers [10], who observed an early geometric alteration of the base of the left ventricle during relaxation, suggesting regional dyssynchrony of contraction and relaxation in HCM. The suggestion that a pathologic type of hypertrophy, independent of its cause, is ac-

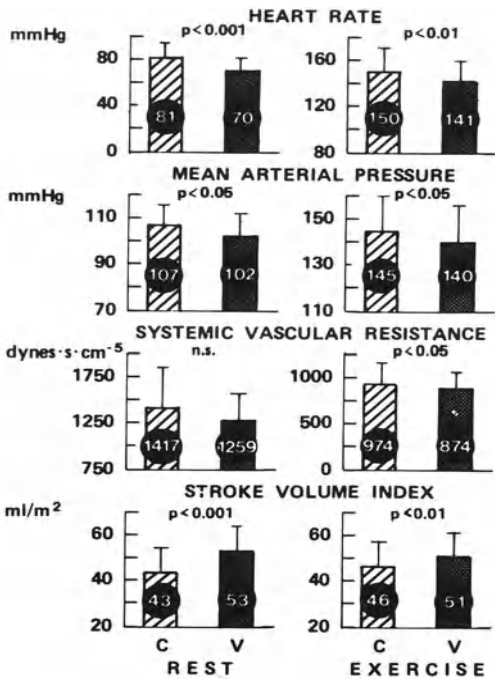


FIGURE 26-6. Hemodynamic parameters at rest and at peak exercise before and after long-term (7 weeks) verapamil (V) therapy. C = control subjects; n.s. = not significant.

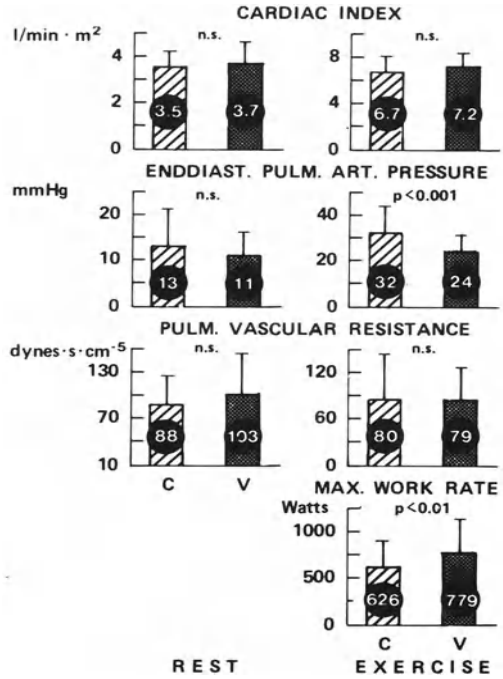


FIGURE 26-7. Hemodynamic parameters at rest and at peak exercise before and after long-term (7 weeks) verapamil (V) therapy. C = control subjects; n.s. = not significant.

accompanied by an impairment of IVR, and diastolic filling is also underlined by the results of Spirito and associates [17]. They found a progressive increase in the time from minimum left ventricular dimension to mitral valve opening from mild to severe left ventricular hypertrophy compared to normal subjects. Panidis and colleagues [18] added an interesting observation regarding three patients with apical HCM, in whom they showed abnormalities of peak filling rate and disturbed systolic function in terms of a decrease of left ventricular ejection fraction during exercise in this variant of HCM.

Long-term therapy (7 weeks) with oral verapamil in HCM patients [8] showed a beneficial effect on left ventricular hemodynamics at rest and during exercise. Whereas left ventricular systolic performance in terms of stroke volume index improved at rest and at maximal exercise, pulmonary artery end-diastolic pressure de-

creased during maximal exercise by 33% compared with baseline. The improvement in systolic function is certainly, in part, a consequence of the vasodilating action of verapamil, as pointed out by other investigators [19, 20]. Similar observations as in our study have been obtained by Chatterjee and coworkers [21] and Bonow and associates [22]. Exercise performance was increased significantly, probably due to a fall in pulmonary pressures during exercise, which may have resulted in an amelioration of dyspnea.

The effects of verapamil in terms of improvement of left ventricular relaxation are suggested by a shortened IVR, an increased rate of left ventricular filling, and the increased velocity of left ventricular wall thinning. The significant reduction of heart rate during exercise may have contributed to the relief of subendocardial ischemia. Favorable effects of high-dose, long-

term verapamil therapy in HCM on left ventricular hemodynamics and exercise capacity have also been reported by Spicer and coworkers [23]. In 32 patients with HCM treated for an average of  $13 \pm 6$  months, a significant decrease in the septal/left ventricular posterior wall-thickness ratio and a significant shortening of IVR were noted. These alterations were accompanied by marked symptomatic improvement in terms of relief of dyspnea and angina as well as dizziness, whereas syncope was not affected.

As a consequence of these favorable experiences with the short- and long-term administration of verapamil, this calcium channel blocker is now used widely for the therapy of HCM. Controversial results with another calcium channel blocker, nifedipine, have been reported. Although Lorell and associates [24] observed in an echocardiographic study an improvement of diastolic function in terms of a downward shift of the left ventricular diastolic pressure-volume curve in the presence of unaltered left ventricular systolic and diastolic dimensions after the administration of nifedipine, Betocchi and colleagues [25] could not demonstrate any beneficial effect on left ventricular outflow tract obstruction and diastolic function. They observed, in contrast, in patients with normal pulmonary arterial wedge pressures and/or significant left ventricular outflow tract gradients a deterioration following nifedipine. Cserhalmi and coworkers [26], however, found a significant reduction in the A/H-ratio in the apexcardiogram and symptomatic improvement following nifedipine and propranolol. Kurnik and associates [27] found no influence of nifedipine on myocardial stiffness and elastic stiffness in a micromanometric pressure and ventriculographic study 30 minutes after administration of nifedipine. They proposed, however, that in those patients with signs of ischemia, nifedipine may improve left ventricular diastolic filling.

Thus, it may be reasonable to suggest that, depending on the intrinsic properties of the particular calcium channel blocking drug on the myocardium and on the peripheral circulation, differences may exist between the individual compounds of this category. Recently, Suwa and coworkers [28] found with diltiazem that IVR and the time to peak velocity of circumferential fiber shortening during diastole decreased significantly in patients with HCM, and the peak velocity of fiber shortening was enhanced, whereas the beta-blocker propranolol

had no effect in the same patient population. Therefore, further studies will need to elucidate the particular properties of the different calcium channel blocking drugs on systolic and diastolic function in cardiac hypertrophy.

*Summary:* To test the hypothesis that impairment of diastolic function is not a pathognomonic feature of HCM, but also present in pathologic, secondary cardiomyopathy, 76 patients were studied by use of echocardiography and phonocardiography, and a semiautomatic analysis of the diametertime course. Because calcium channel blockers like verapamil result in a relaxation of smooth muscle and myocardial muscle, the acute effect of 0.15 mg/kg intravenous verapamil was examined in 11 patients with HCM diagnosed by echocardiographic, hemodynamic, and angiographic criteria. Finally, the effect of chronic verapamil therapy (40 mg three times daily increasing up to 120 mg four times daily) on left ventricular hemodynamics at rest during exercise, and on exercise capacity was examined in 18 patients with HCM.

IVR was increased significantly in both HOCM and CPO compared to normal subjects and was accompanied by an abnormal increase in left ventricular diameter during relaxation. During the absolute and relative rapid filling phase, the left ventricular diameter increase was reduced compared to the control population. Thus, impaired diastolic function in terms of prolonged isovolumic relaxation seems to be a uniform feature of pathologic left ventricular hypertrophy, independent of its cause.

Prolonged left ventricular IVR was shortened significantly following the intravenous administration of verapamil. This was accompanied by a smaller increase in regional left ventricular dimension during left ventricular relaxation, while the peak rate of posterior wall thinning, as well as the change in left ventricular dimension during the left ventricular filling period and the duration of the relative filling period increased significantly. Left ventricular hemodynamics at rest and during exercise after 7 weeks of oral verapamil therapy showed a 33% decrease of pulmonary artery end-diastolic pressure during maximal exercise (mean 32 mm Hg to 24 mm Hg  $p < 0.001$ ), accompanied by an increase in the stroke volume index. Exercise capacity also improved significantly.

From these studies, it is concluded that verapamil, the prototype calcium channel blocking

drug, is an effective therapeutic agent for patients with primary and secondary left ventricular hypertrophy. Its effects include enhanced diastolic function, improved systolic function with reduction of the left ventricular outflow tract obstruction, and increase in exercise capacity with reduction of symptoms. Because controversial results have been reported about the effect of nifedipine on diastolic function, left ventricular hemodynamics, and clinical symptoms, further studies are needed to elucidate the particular properties of different calcium channel blockers in left ventricular hypertrophy.

### References

1. Grossman W, McLaurin LP (1976). Diastolic properties of the left ventricle. *Ann Intern Med* 84:316–326.
2. Markworth P, Bleifeld W (1982). Regulation des Herzminutenvolumens ausdauertrainierter Spitzensportler. *Z Kardiol. Suppl* 178 (abstr).
- 2a. Fleckenstein A, Nakayama K, Fleckenstein-Grün G, Byon YK (1975) Interactions of vasoactive ions and drugs with Ca-dependent excitation-contraction coupling of vascular smooth muscle. In Carafoli et al (eds): *Calcium Transport in Contraction and Secretion*. Amsterdam: North-Holland, p 555.
3. Nayler WG, Williams A (1978). Relaxation in heart muscle: Some morphological and biochemical considerations. *Eur J Cardiol (suppl)* 7:35–50.
4. Kaltenbach M, Hopf R, Keller M (1976). Calciumantagonistische Therapie bei hypertroph-obstruktiver Kardiomyopathie. *Dtsch Med Wochenschr* 101:1284–1287.
5. Kuhn H, Thelen U, Leuner C, et al (1980). Long-term treatment of hypertrophic non-obstructive cardiomyopathy (HNCM) with verapamil. *Z Kardiol* 69:669–675.
6. Hanrath P, Mathey DG, Siegert R, Bleifeld W (1980). Left ventricular relaxation and filling pattern in different forms of left ventricular hypertrophy: An echocardiographic study. *Am J Cardiol* 45:15–23.
7. Hanrath P, Mathey DG, Kremer P, et al (1980). Effect of verapamil on left ventricular isovolumic relaxation time and regional left ventricular filling in hypertrophic cardiomyopathy. *Am J Cardiol* 45:1258.
8. Hanrath P, Schlüter M, Sonntag F, et al (1983). Influence of verapamil therapy on left ventricular performance at rest and during exercise in hypertrophic cardiomyopathy. *Am J Cardiol* 52:544.
9. Krebs W, Hanrath P, Bleifeld W, Effert S (1977). Rechnergestützte Auswertung von M-Mode-Echokardiogrammen. *Herz-Kreislauf* 9: 519–525.
10. Sanderson JE, Gibson DG, Brown DJ, Goodwin JF (1977). Left ventricular filling in hypertrophic cardiomyopathy: An angiographic study. *Br Heart J* 39:661–670.
11. Cohn PF, Liedtke AJ, Serur J, et al (1972). Maximal rate of pressure fall (peak negative dP/dt) during ventricular relaxation. *Cardiovasc Res* 6:263–267.
12. Weisfeldt ML, Scully HE, Frederiksen J, et al (1974). Hemodynamic determinants of maximum negative dP/dt and periods of diastole. *Am J Physiol* 227:613–621.
13. Benchimol A, Ellis JG (1967). A study of the period of isovolumic relaxation in normal subjects and in patients with heart disease. *Am J Cardiol* 19:196–206.
14. Papapietro HC, Coughlan D, Zissermann RO, et al (1979). Impaired maximal rate of left ventricular relaxation in patients with coronary artery disease and left ventricular dysfunction. *Circulation* 59:984–90.
15. Mathey D, Bleifeld W, Franken G (1974). Left ventricular relaxation and diastolic stiffness in experimental myocardial infarction. *Cardiovasc Res* 8:583–692.
16. Hanrath P, Mathey D, Montz R, et al (1981). Myocardial thallium-201 imaging in hypertrophic obstructive cardiomyopathy. *Eur Heart J* 2:177–185.
17. Spirito P, Maron BJ, Chiarella F, et al (1985). Diastolic abnormalities in patients with hypertrophic cardiomyopathy: relation to magnitude of left ventricular hypertrophy. *Circulation* 72:310.
18. Panidis IP, Nestico P, Hakki AH, et al (1986). Systolic and diastolic left ventricular performance at rest and during exercise in apical hypertrophic cardiomyopathy. *Am J Cardiol* 57:356.
19. Singh BN, Roche AHG (1977). Effects of intravenous verapamil on hemodynamics in patients with heart disease. *Am Heart J* 94: 593–599.
20. Ferlinz J, Easthope JL, Aronow WS (1979). Effects of verapamil on myocardial performance in coronary disease. *Circulation* 59:313–319.
21. Chatterjee K, Raff G, Anderson D, Parmley WW (1982). Hypertrophic cardiomyopathy—therapy with slow channel inhibiting agents. *Prog Cardiovasc Dis* 25:193–210.
22. Bonow RO, Dilsizian V, Rosing DR, et al (1985). Verapamil-induced improvement in left ventricular diastolic filling and increased exercise tolerance in patients with hypertrophic cardiomyopathy: Short- and long-term effects.

- Circulation 72:853.
23. Spicer RL, Rocchini AP, Crowley DC, Rosenthal A (1984). Chronic verapamil therapy in pediatric and young adult patients with hypertrophic cardiomyopathy. *Am J Cardiol* 53:1614.
  24. Lorell BH, Paulus WJ, Grossman W, et al (1982). Modification of abnormal left ventricular diastolic properties by nifedipine in patients with hypertrophic cardiomyopathy. *Circulation* 65:499.
  25. Betocchi S, Bonow RO, Bacharach SL, et al (1982). Isovolumic relaxation period in hypertrophic cardiomyopathy: assessment by radionuclide angiography. *J Am Coll Cardiol* 7:74.
  26. Cserhalmi L, Assmann I, Glavanov M, et al (1984). Langzeittherapie der hypertrophischen obstruktiven und nichtobstruktiven Kardiomyopathie mit nifedipin im Vergleich zu Propranolol. (Long-term therapy of hypertrophic obstructive and non-obstructive cardiomyopathy with nifedipine in comparison to propranolol). *Z Gesamte Inn Med* 39:330.
  27. Kurnik PB, Courtois MR, Ludbrook PA (1986). Effect of nifedipine on intrinsic myocardial stiffness in man. *Circulation* 74:126.
  28. Suwa M, Hirota Y, Kawamura K (1984). Improvement in left ventricular diastolic function during intravenous and oral diltiazem therapy in patients with hypertrophic cardiomyopathy: An echocardiographic study. *Am J Cardiol* 54:1047.

---

# 27. FAILURE OF INACTIVATION OF HYPERTROPHIED MYOCARDIUM: A CAUSE OF IMPAIRED LEFT VENTRICULAR FILLING IN HYPERTROPHIC CARDIOMYOPATHY AND AORTIC STENOSIS

---

Walter J. Paulus, Stanislas U. Sys, Paul Nellens, Guy R. Heyndrickx,  
and Eric Andries

Impaired left ventricular filling has been observed in hypertrophic cardiomyopathy [1–5] and in pressure overload hypertrophy [1, 4, 6–12]. This impairment of left ventricular filling has been related to slow left ventricular pressure decay [13, 14], which prolongs isovolumic relaxation and impedes left ventricular inflow [15, 16]. A slow left ventricular pressure decay, persisting into the left ventricular filling phase can be explained by a failure of myocardial inactivation [17, 18], which causes incomplete myoplasmic calcium reuptake and favors persistent diastolic cross-bridge interaction and contractile tension generation. A failure of myocardial inactivation of the hypertrophied left ventricle could be induced by a shift of certain critical proteins involved in excitation-contraction coupling towards isomeric forms with slower enzyme kinetics and an altered calcium sensitivity [19, 20].

Calcium channel blocking agents improve left ventricular isovolumic pressure decay and filling dynamics in hypertrophic cardiomyopathy [5, 13, 17], possibly by correcting a myocardial calcium-overload state [21–23], which could result from an imbalance between myo-

plasmic calcium influx and deficient myoplasmic calcium reuptake. To further evaluate a failure of myocardial inactivation as a cause of impaired relaxation and filling of the hypertrophied left ventricle, we investigated the influence of post-extrasystolic potentiation on left ventricular relaxation in aortic stenosis and hypertrophic cardiomyopathy. A premature contraction increases calcium influx, which augments calcium availability at the contractile sites and causes postextrasystolic potentiation [24]. The effect of postextrasystolic potentiation on left ventricular relaxation appears to be the sum of opposing influences; namely, increased intracellular calcium, which delays left ventricular relaxation, and smaller end-systolic dimensions and load, which enhance left ventricular relaxation. In the intact dog heart, these opposing influences counterbalance, resulting in no overall effect of postextrasystolic potentiation on left ventricular relaxation [25]. In humans, the results are conflicting: in coronary artery disease patients, isovolumic and early diastolic left ventricular pressure decay were significantly slower after postextrasystolic potentiation [26], whereas in noncoronary artery disease patients there was no relation between postextrasystolic potentiation of contractility and postextrasystolic isovolumic pressure decline [27]. In our studies, postextrasystolic potentiation affected

left ventricular isovolumic pressure decay, left ventricular diastolic pressure waveforms, and left ventricular filling dynamics differently in patients with pressure-overload hypertrophy or hypertrophic cardiomyopathy in comparison with normal control subjects.

*Isovolumic Left Ventricular Pressure Decay and Diastolic Left Ventricular Pressure-Wave Forms in Hypertrophic Cardiomyopathy and Pressure-Overload Hypertrophy*

Left ventricular isovolumic relaxation and filling dynamics of hypertrophic cardiomyopathy and pressure-overload hypertrophy have been analyzed by curve fits to isovolumic left ventricular pressure data points to derive a time constant of pressure decay [13, 14, 28, 29], by sequential analysis of diastolic left ventricular cavity volumes using contrast or radionuclide left ventricular angiograms [2, 5, 12], by calculation of left ventricular internal dimension lengthening or posterior wall-thinning rates from left ventricular echocardiograms [3, 4, 6–11] and by measurement of early diastolic peak flow velocity and deceleration from Doppler mitral flow velocity recordings [30, 31].

A single time constant derived from a monoexponential curve fit was originally used as an afterload independent index of isovolumic left ventricular pressure decay in anesthetized dogs [32]. Subsequently, however, the time constant of isovolumic left ventricular pressure decay was found to be dependent on left ventricular afterload in a similar experimental preparation [33, 34]. Moreover, several mathematical pit-falls and conceptual problems arose when calculating a time constant of isovolumic left ventricular pressure decay, especially in hypertrophic cardiomyopathy and in aortic stenosis [14, 29, 35]. These problems included:

1. Deviations from an exponential decay of the isovolumic left ventricular relaxation pressure in hypertrophic cardiomyopathy and aortic stenosis. When a variable (e.g., left ventricular pressure) decays exponentially, its first derivative (e.g.,  $dp/dt$ ) must follow a course that is also exponential but of opposite convexity. In many patients with hypertrophic cardiomyopathy (Figure 27–1) or aortic stenosis (Figure

27–2), the upper portion of isovolumic left ventricular pressure decay does not follow an exponential course because the corresponding portion of the negative  $dp/dt$  signal is linear or has a convexity equal to the left ventricular pressure decay. Similar findings have been reported during coronary occlusion and after intracoronary isoproterenol infusion [36, 37]. To overcome the problem of deviations from a monoexponential decay and to improve on the curve fit's correlation coefficient, a biexponential curve fit with an inflection point at 40 msec was proposed [38], the concept of a nonzero asymptote of the exponential decay was introduced [39], or more elaborate fitting procedures such as polynomial methods were used [17].

2. The lack of an exact marker on the left ventricular pressure signal of the starting point of the isovolumic relaxation period. Digitization of isovolumic left ventricular pressure data points usually starts at peak negative  $dp/dt$ , which is assumed to correspond to the onset of the isovolumic relaxation period. In many cases of aortic stenosis and hypertrophic cardiomyopathy, peak negative  $dp/dt$  does not appear as a sharp inflection but rather as a series of transients with a peak value sometimes occurring at the beginning and sometimes at the end of the series.

3. Variable endpoints to the curve fits used to calculate the time constant of isovolumic left ventricular pressure decay. Time constants of isovolumic left ventricular pressure decay have been calculated using as endpoint either a left ventricular pressure which equaled left ventricular end-diastolic pressure plus 10 mm Hg, or a left ventricular pressure which equaled the v wave of a pulmonary capillary wedge or left atrial pressure tracing. Shifting the end point of the curve fit, however, greatly alters the value of the time constant of isovolumic left ventricular pressure decay [40]. These findings are relevant to hypertrophic cardiomyopathy and aortic stenosis, in which left ventricular end-diastolic pressure is high because of reduced left ventricular compliance and in which accompanying mitral regurgitation could shorten the isovolumic relaxation period.

In our studies (Tables 27–1, 27–2), left ventricular pressure was digitized from a point corresponding to the last peak of the negative

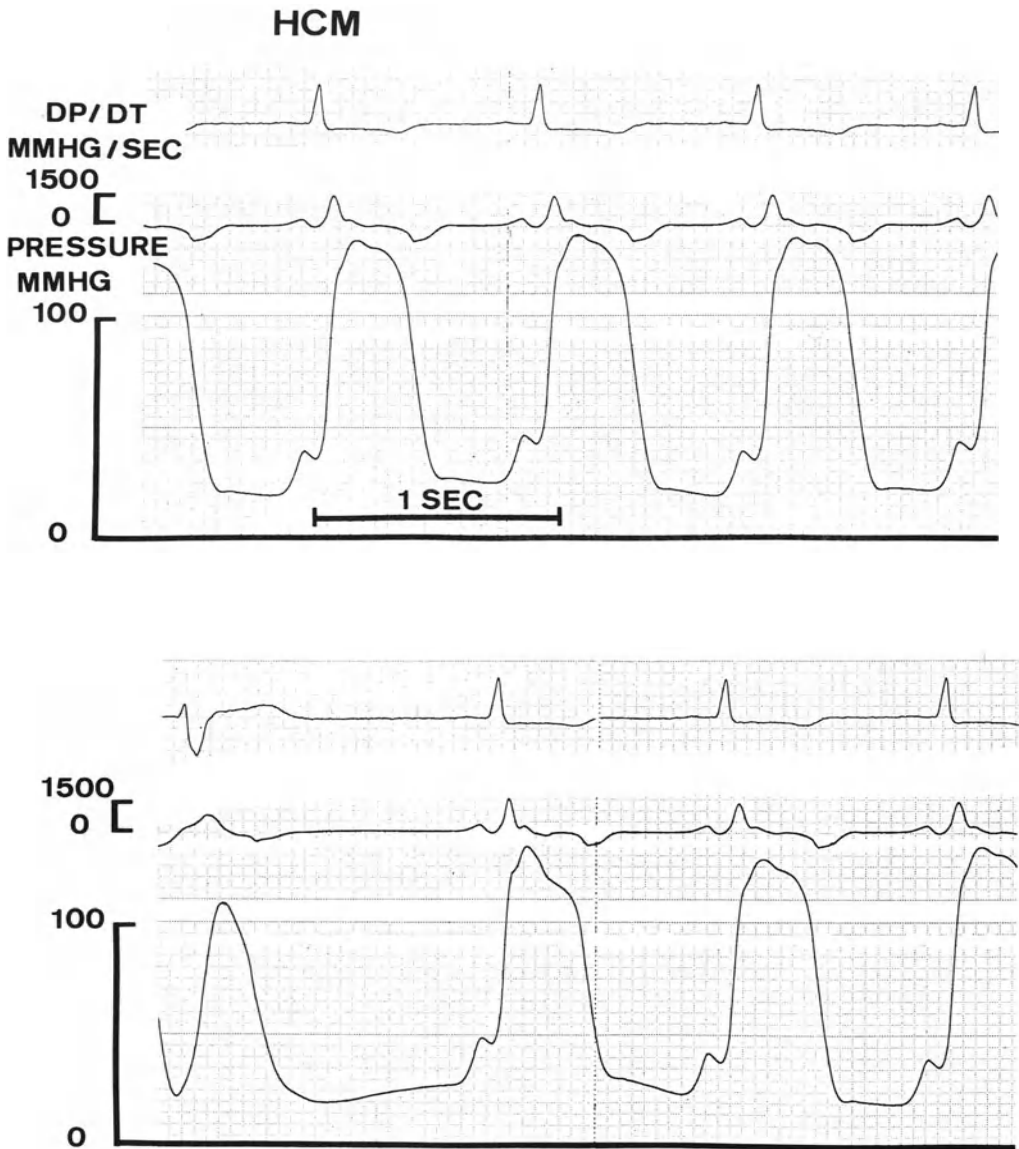


FIGURE 27-1. Electrocardiogram, left ventricular micromanometer-tip-catheter pressure tracing and its first derivative (dp/dt) recorded in a patient with a nonobstructive form of hypertrophic cardiomyopathy (HCM) during normal sinus rhythm (*upper panel*) and after a premature ventricular beat (*lower panel*). During normal sinus rhythm and especially after the potentiated beat (*second beat of the lower panel*), the diastolic pressure has an abnormal waveform with persistent decay throughout early and mid-diastole and a minimum diastolic pressure, which occurs just before the onset of the following "a" wave. After the potentiated beat, the diastolic pressure waveform becomes more abnormal with an earlier transition from fast to slow left ventricular pressure decay. During regular sinus rhythm, the terminal portion of the negative dp/dt signal has a downward convexity implying nonexponential decay of the corresponding portion of the left ventricular pressure signal.

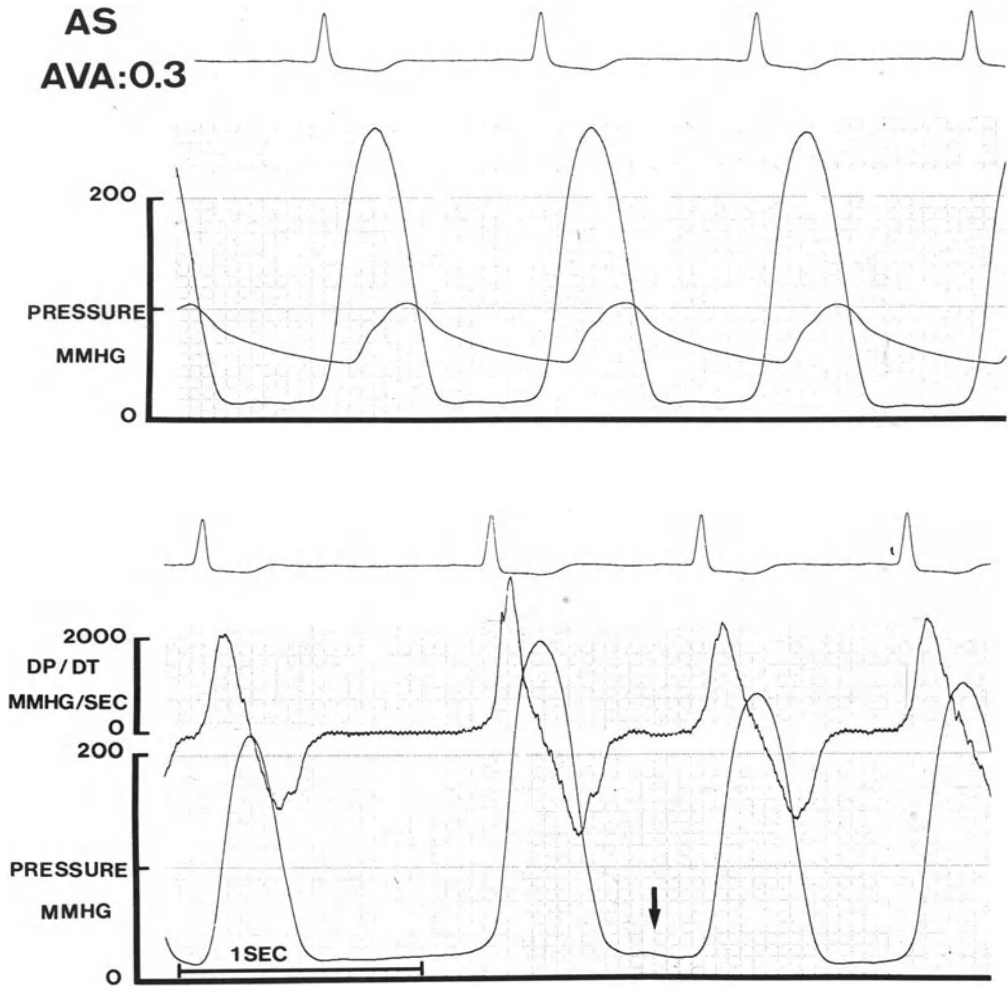


FIGURE 27-2. Electrocardiogram, systemic arterial pressure (*upper panel*), left ventricular micromanometer-tip-catheter pressure and its first derivative ( $dp/dt$ ) (*lower panel*) recorded in a patient with critical aortic stenosis (AS) (AVA = Aortic valve area =  $0.3 \text{ cm}^2$ ) during regular sinus rhythm (*upper panel*) and after a premature ventricular beat (*lower panel*). The terminal portion of the negative  $dp/dt$  signal rises linearly implying non-exponential decay of the corresponding portion of the left ventricular pressure signal. Peak negative  $dp/dt$  does not appear as a single sharp inflection but rather as a series of transients. The time constant analysis was started not at the lowest value of the negative  $dp/dt$  signal but after the series of transients. After postextrasystolic potentiation, the diastolic pressure waveform shifts to an abnormal morphology without a fast-filling wave but with persistent slow pressure decay into late diastole (*arrow*).

$dp/dt$  signal to a left ventricular pressure value which equaled left ventricular end-diastolic pressure. A biexponential curve fit was used with an inflection point, which could be moved in the interval ranging from 30 to 50 msec past

the starting point of the analysis. The inflection point was moved to optimize the correlation coefficient of both segments of the biexponential curve fit. Such a partitioning of the curve fit into two segments allows separation of an upper part

TABLE 27-1. Comparison of Hemodynamic Indices of Left Ventricular Relaxation in Controls, Hypertrophic Cardiomyopathy, and Pressure-Overload Hypertrophy Induced by Aortic Stenosis<sup>a</sup>

	Control	HCM (n = 12)	AS (n = 12)
T1 (msec) (38)	46.0 ± 1.3 (n = 8)	55.2 ± 8.1 <sup>b</sup>	53.1 ± 5.6 <sup>b</sup>
T2 (msec) (38)	40.1 ± 3.0 (n = 8)	51.6 ± 7.0 <sup>b</sup>	45.8 ± 3.9 <sup>b</sup>
ϕ (degrees)	71.4 ± 6.4 (n = 11)	40.9 ± 7.2 <sup>b</sup>	38.9 ± 5.0 <sup>b</sup>

<sup>a</sup> Values given are mean ± standard error of the mean.

<sup>b</sup> *p* < 0.01 vs. control.

HCM = hypertrophic cardiomyopathy; AS = aortic stenosis; T1 = time constant of left ventricular pressure decay from peak negative dp/dt to 40 msec after peak negative dp/dt; T2 = time constant of left ventricular pressure decay from 40 msec after peak negative dp/dt to a pressure on the downslope equal to left ventricular end-diastolic pressure; ϕ = phase of the first Fourier harmonic of the left ventricular diastolic pressure wave.

TABLE 27-2. Influence of Postextrasystolic Potentiation on Hemodynamic and Doppler-Echocardiographic Left Ventricular Relaxation Indices<sup>a</sup>

	HCM (NSR)	HCM (PESP)	AS (NSR)	AS (PESP)
T1 (n = 12) (msec)	55.2 ± 8.1	53.7 ± 6.8	53.1 ± 5.6	70.4 ± 5.4 <sup>c</sup>
T2 (n = 12) (msec)	51.6 ± 7.0	54.8 ± 7.1	45.8 ± 3.9	57.9 ± 3.3 <sup>c</sup>
ϕ (n = 12) (degrees)	40.9 ± 7.2	21.1 ± 6.5 <sup>b</sup>	38.9 ± 5.0	23.1 ± 4.5 <sup>c</sup>
	HCM and AS (NSR)		HCM and AS (PESP)	
PFVE (n = 11) (m/sec)	0.63 ± 0.20		0.54 ± 0.06 <sup>b</sup>	
DEF (n = 11) (m/sec <sup>2</sup> )	5.5 ± 0.6		3.7 ± 0.7 <sup>b</sup>	

HCM = hypertrophic cardiomyopathy; AS = aortic stenosis; T1, T2, and ϕ = time constants of upper (T1) and lower (T2) parts of the left ventricular pressure decay, phase (ϕ) of the first Fourier harmonic of the left ventricular diastolic pressure wave; PFVE = peak flow velocity in early diastolic; DEF = Deceleration of early diastolic flow.

<sup>a</sup> Values given are mean ± SEM.

<sup>b</sup> *p* < 0.05 vs. NSR.

<sup>c</sup> *p* < 0.01 vs. NSR.

of left ventricular pressure decay, which tends to deviate from an exponential course in hypertrophic cardiomyopathy and aortic stenosis, from a lower part, which follows an exponential decline. Left ventricular pressure decay was digitized and analyzed up to a left ventricular pressure that equaled left ventricular end diastolic pressure. By choosing this end point, the analysis of time constants of left ventricular pressure decay is in continuity with the Fourier transform, which was applied to the diastolic left ventricular pressure data points. This end point is easily definable but fails to separate isovolumic left ventricular pressure data points from pressure data points recorded during left ventricular inflow. This distinction, however, lacks physiologic significance at the myocardial level. Myocardial relaxation does not proceed isometrically during the isovolumic relaxation period because of left ventricular shape changes [41], which alter myocardial wall tension and

because of the recoil of series elastic elements [42] such as intercalated discs (43) or connective tissue. In our studies the time constants (T1 and T2) of both segments of a biexponential curve fit to left ventricular pressure decay were significantly larger in patients with hypertrophic cardiomyopathy and aortic stenosis compared to control subjects (see Table 27-1). An optimal correlation coefficient (*r* > 0.99) was always achieved for T2. The correlation coefficient of T1 was lower in hypertrophic cardiomyopathy (*r* > 0.97) and in aortic stenosis (*r* > 0.98) because of deviations from an exponential course of the upper part of left ventricular pressure decay.

Diastolic left ventricular pressure waveforms have received less attention and have not been assessed quantitatively despite previous reports of an abnormal pattern of diastolic left ventricular pressure wave form in some patients with hypertrophic cardiomyopathy [13, 14, 17].

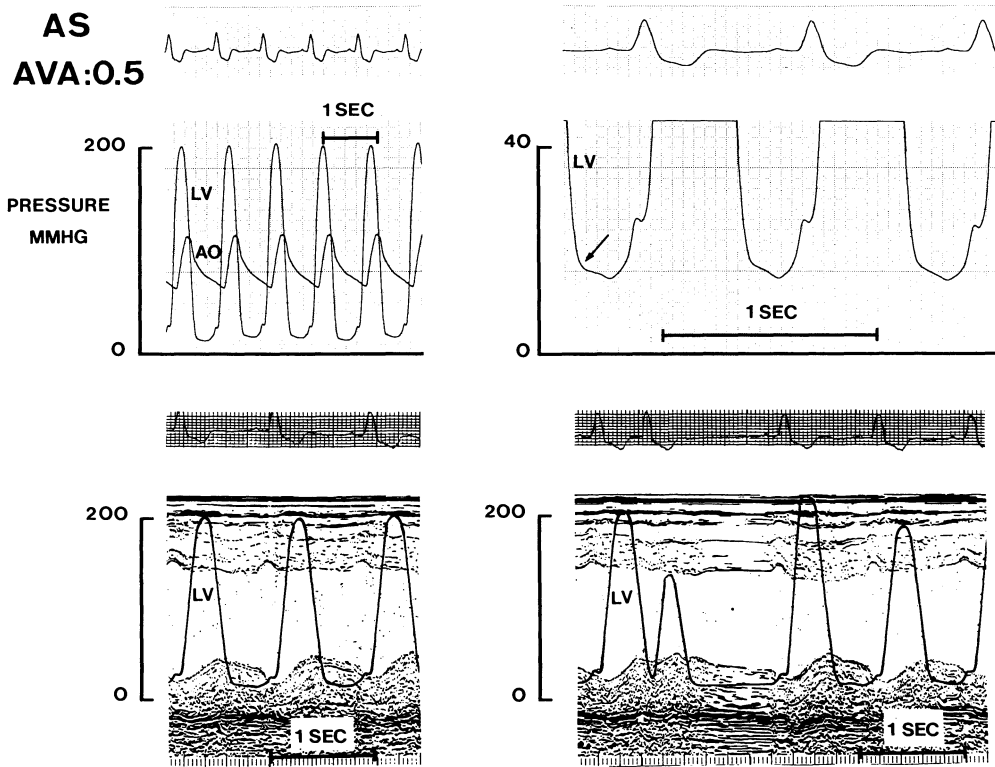


FIGURE 27-3. Left ventricular (LV) micromanometer-tip-catheter pressure and M-mode echocardiograms recorded in a patient with critical aortic stenosis (AS) (AVA = aortic valve area =  $0.5 \text{ cm}^2$ ). The upper left panel shows electrocardiogram, systemic arterial (AO) and LV micromanometer-tip pressures during regular sinus rhythm. The upper right panel shows a large-scale, fast-paper-speed recording of the diastolic LV pressure waves, which show a persistent decay into late diastole and a point of minimum diastolic LV pressure just prior to the "a" wave of the following beat. The small arrow marks the transition on the LV pressure tracing from fast to slow pressure decay. This transition is consistent with incomplete myocardial relaxation, possibly related to altered calcium sensitivity of proteins involved in myocardial calcium reuptake. The lower left panel shows LV pressure and M-mode echocardiogram during regular sinus rhythm. During the abnormal early and mid-diastolic LV pressure decay there is no septal wall thinning and little posterior wall thinning. The larger part of lengthening of left ventricular internal dimension is caused by the atrial contraction. The lower right panel shows a premature beat and the first and second postextrasystolic beat. During the diastole which immediately follows the premature beat, the diastolic LV pressure wave returns to a normal configuration and early diastolic septal and posterior wall thinning reappears. After the first potentiated beat, the diastolic wave returns to an abnormal waveform with a persistent decay into late diastole and a small mid-diastolic LV pressure rise superimposed on it. The latter occurs in the absence of any posterior wall thinning, and is suggestive of a diastolic aftercontraction, which has been observed in experimental pressure-overload hypertrophy of the ferret [19].

This pressure wave persistently declined into mid-diastole without a fast early-diastolic filling phase (see Figure 27-1). Such a slow decay of left ventricular pressure persisting into mid-diastole supports the concept of left ventricu-

lar inflow obstruction in hypertrophic cardiomyopathy [15] and explains the decreased peak left ventricular filling rate and the prolonged time to peak left ventricular filling [1-5]. It remained unclear whether such persistent early

diastolic left ventricular pressure decay was specific to hypertrophic cardiomyopathy as a cause of impaired left ventricular filling. We recently observed similar abnormal early diastolic pressure waveforms in patients with pressure-overload hypertrophy caused by aortic stenosis (Figure 27-3). This slow early diastolic pressure decline explains the previously reported reduction of peak left ventricular filling rate and prolongation of time to peak left ventricular filling, which were observed in pressure-overload hypertrophy caused by aortic stenosis [1, 12].

The diastolic pressure waveform was quantitatively assessed by Fourier transform of the diastolic pressure signal in a series of normal control subjects and in patients with aortic stenosis and hypertrophic cardiomyopathy. Diastolic left ventricular pressure was digitized from the end point of the time constant analysis (a pressure on the descending limb of the left ventricular pressure wave equal to left ventricular end-diastolic pressure) to left ventricular end-diastolic pressure. The digitized diastolic left ventricular pressure data points were subsequently processed by Fourier transform. These boundaries of the diastolic pressure wave provided an equal starting point and end point for the Fourier transform. This turned the diastolic pressure wave into a continuous variable and avoided discontinuities, which would have induced a loss of resolution of the Fourier transform. The phase of the first Fourier harmonic was an adequate discriminant between diastolic left ventricular pressure waves recorded in normal control subjects and in patients with hypertrophic cardiomyopathy or pressure-overload hypertrophy caused by aortic stenosis. The slower the early diastolic left ventricular pressure decay, the lower the value of the phase of the first Fourier harmonic. Patients with hypertrophic cardiomyopathy or aortic stenosis had a significantly lower phase value than normal control subjects (see Table 27-1). However, patients with the lowest phase values did not have the longest time constants and the phase of the first Fourier harmonic was not significantly correlated with the time constants of left ventricular pressure decay. It therefore appears that the rate of left ventricular relaxation and the completeness of left ventricular relaxation are not necessarily equally disturbed in hypertrophic cardiomyopathy and aortic stenosis.

A similar dissociation between rate and

extent of left ventricular relaxation has been observed in pacing-induced ischemia in dogs with coronary stenoses after caffeine administration [44]. Caffeine administration during pacing ischemia failed to further prolong the time constant of isovolumic left ventricular pressure decay, but caused marked upward shifting of the diastolic left ventricular pressure-volume relation suggestive of persistent diastolic cross-bridge interaction caused by incomplete muscle inactivation [45]. Such a dissociation between rate and extent of left ventricular relaxation could be explained by different effects of ischemia and of hypertrophy on enzyme kinetics or on calcium sensitivity of certain critical proteins involved in excitation-contraction coupling [20]. When diastolic left ventricular pressure decay persists into mid-diastole (see Figures 27-1, 27-3), an inflection point appears on the downslope of the left ventricular pressure recording, which separates an upper segment of fast left ventricular pressure decay from a lower segment of slow left ventricular pressure decay (see arrow in upper right panel of Figure 27-3). On simultaneous micromanometer recordings of left ventricular pressure and Doppler flow recordings across the mitral valve, the inflection point (see thin arrow in the last beat of Figure 27-4) appears to be unrelated to left ventricular inflow, which starts earlier, and is therefore unrelated to altered viscoelastic properties [46, 47] caused by left ventricular expansion. The inflection point more likely marks the transition from slow to incomplete left ventricular relaxation. The former may be explained by slower enzyme kinetics, the latter by altered calcium sensitivity of certain proteins involved in excitation-contraction coupling.

### *Postextrasystolic Potentiation Reveals Failure of Myocardial Inactivation in Hypertrophic Cardiomyopathy and Pressure Overload Hypertrophy*

To evaluate a failure of myocardial inactivation as a cause of impaired relaxation and filling of the hypertrophied left ventricle, we investigated the influence of postextrasystolic potentiation on left ventricular relaxation in hypertrophic cardiomyopathy and pressure-overload hypertrophy. A premature cardiac contraction augments myo-

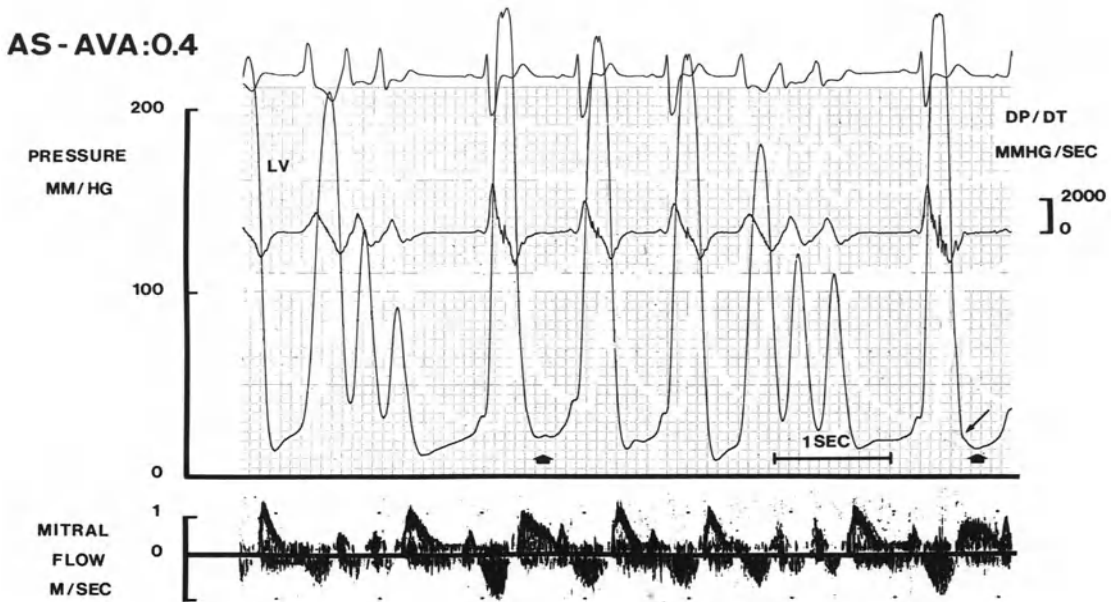


FIGURE 27-4. Left ventricular micromanometer-tip-catheter pressure, dp/dt and Doppler echocardiographic mitral-valve flow velocity recorded in a patient with severe aortic stenosis (AS) (AVA = aortic valve area =  $0.4 \text{ cm}^2$ ). The tracings are recorded during two runs of three premature beats, which are separated by three regular sinus rhythm beats. During the diastoles, which follow the first postextrasystolic beat (*thick arrows*), there is abnormal LV pressure decay in early diastole, reduced peak early diastolic mitral flow velocity, and reduced deceleration of early diastolic flow. The abnormal early diastolic LV pressure decay, observed after the first postextrasystolic beat, impedes early diastolic LV inflow. The thin arrow on the last beat marks the transition from fast to slow pressure decay. This transition is unrelated to mitral inflow, which starts earlier but is probably related to biphasic myocardial tension decay.

cardiac calcium influx. This increases activator calcium for the following beat and results in potentiation of contractile performance [24]. The higher myoplasmic calcium content of the potentiated beat challenges the calcium reuptake capacity of the myocardial inactivating system and, in the presence of an inactivation dependent relaxation pattern, this could result in a slow and eventually an incomplete myocardial relaxation. In the intact heart, the effect of postextrasystolic potentiation on left ventricular relaxation is the sum of opposing influences; namely, enhanced inotropic state and altered preload or afterload. In anesthetized dogs, there is no overall effect of postextrasystolic potentiation on left ventricular relaxation [25]. In patients with coronary artery disease postextrasystolic potentiation slows isovolumic and early

diastolic left ventricular pressure decay [26], whereas in patients without coronary artery disease there is no relation between postextrasystolic potentiation of contractility and postextrasystolic isovolumic pressure decline [27].

In our studies, postextrasystolic potentiation prolonged the time constants  $T_1$  and  $T_2$  in aortic stenosis but not in hypertrophic cardiomyopathy (see Table 27-2). This difference could be accounted for by:

1. Differences in left ventricular afterload: In patients with aortic stenosis, left ventricular afterload consists mainly of the resistance of the stenotic aortic valve. In patients with hypertrophic cardiomyopathy, left ventricular afterload consists of the arterial impedance in nonobstructive forms of hypertrophic cardio-

myopathy and a late systolic loading increment caused by outflow tract obstruction superimposed on the arterial impedance in patients with an obstructive form of hypertrophic cardiomyopathy. When the left ventricle faces a mainly resistive load of a stenotic aortic valve, peak myocardial tension occurs earlier in systole at the time of peak ejection velocity [48]. In the absence of end-systolic loading increments, there is no end-systolic imbalance between myocardial load and myocardial tension generation and therefore a favorable situation exists in aortic stenosis for an inactivation-dependent pattern of left ventricular relaxation. Postextrasystolic potentiation does not alter the resistive load of the stenotic aortic valve. After postextrasystolic potentiation, left ventricular relaxation therefore continues to proceed in accordance to myocardial inactivation, which is slower because of the reuptake of a larger amount of myoplasmic calcium after postextrasystolic potentiation. Wave reflections [49], the arterial capacitance [50], and eventually outflow tract obstruction [51] cause end-systolic loading increments in hypertrophic cardiomyopathy, which promote a load-dependent relaxation pattern of the left ventricle. Postextrasystolic potentiation further augments this end-systolic loading increment by a more forceful distention of the large arteries, which increases the capacitive component of the arterial load, by altering wave reflections and by increasing outflow tract obstruction. This compensates for slower myocardial inactivation so that the time constants of left ventricular relaxation remain unaltered after postextrasystolic potentiation.

2. The extent of left ventricular hypertrophy: in aortic stenosis the left ventricle is uniformly hypertrophied, whereas in hypertrophic cardiomyopathy, left ventricular hypertrophy is variable ranging from limited involvement of the basal septum to concentric involvement of the left ventricle [52, 53]. In hypertrophic cardiomyopathy, the normal myocardium can partially correct for the abnormal relaxation mechanics of the hypertrophied portions and offset changes of a global left ventricular relaxation index like a time constant of pressure decay.

After postextrasystolic potentiation, the phase of the first Fourier harmonic was significantly increased in patients with aortic stenosis and hypertrophic cardiomyopathy but remained

unaltered in normal control subjects. Small increments of the phase of the first Fourier harmonic corresponded to slowing of the early diastolic left ventricular pressure decay and blunting of the fast-filling phase (see Figure 27-4). Large increments implied a shift of the diastolic pressure wave to a waveform with persistent diastolic left ventricular pressure decay, an absent fast-filling phase and a minimum diastolic pressure, which occurred just before the onset of the subsequent wave (see Figure 27-1, 27-2). That such incomplete left ventricular relaxation can be induced by postextrasystolic potentiation is explained by a transient failure of myocardial inactivation. This may be caused by the increased myoplasmic calcium content after postextrasystolic potentiation and by alterations of certain critical proteins involved in excitation-contraction coupling that developed during the hypertrophy process. The excessive systolic load of aortic stenosis causes reduced sarcomere shortening, which accelerated the declining phase of the calcium transient by increasing the affinity of troponin-C for calcium [54]. Such a change of the calcium transient could be a signal for induction of isoform shifts of certain proteins involved in the myocardial activation-inactivation process.

When larger increments of the phase of the first Fourier harmonic were observed after postextrasystolic potentiation, the potentiated beat was often followed by a transient episode of *pulsus alternans* [55] (see Figure 27-2). This episode of *pulsus alternans* can be explained by deficient myoplasmic calcium reuptake in the diastole that followed the potentiated beat. This reduces the amount of activator calcium for the second postextrasystolic beat which therefore becomes the weaker beat of the *pulsus alternans* series. Systolic performance of the second postextrasystolic beat was inferior to systolic performance during regular sinus rhythm. This implies that incomplete left ventricular relaxation after postextrasystolic potentiation is not only related to the increased amount of activator calcium after postextrasystolic potentiation but also to a transient depression of the calcium reuptake mechanism itself. A transient resetting of the calcium sensitivity of the sarcoplasmic reticular calcium pump could explain these findings [56, 57].

The abnormal diastolic left ventricular pressure waveform after postextrasystolic potentiation raises concern about catheter entrapment,

especially at the small end-systolic left ventricular volumes which are observed during postextrasystolic potentiation. The following findings however argue against catheter entrapment:

1. On left ventricular cavity echocardiograms recorded simultaneously with the tip-micromanometer left ventricular pressure signal, end-systolic cavity dimensions of the premature ventricular beat and of the potentiated beat were equal (see Figure 27-3). Despite equal end-systolic dimensions, abnormal diastolic left ventricular pressure waveforms were observed only after the potentiated beat, and not in the diastole that immediately followed the premature ventricular contraction. This finding argues against left ventricular catheter entrapment caused by small end-systolic left ventricular dimensions as the cause of the abnormal left ventricular pressure waveform after postextrasystolic potentiation.

2. Mitral-valve Doppler flow measurements recorded together with the tip-micromanometer left ventricular pressure signals showed after postextrasystolic potentiation a reduction and slowing of the early left ventricular filling phase (see Table 27-2). This coincided with the slow early diastolic left ventricular pressure decay (see Figure 27-4). These simultaneous mitral-valve Doppler flow recordings confirm the functional importance of the abnormal diastolic left ventricular pressure waveform in terms of left ventricular inflow obstruction.

3. Similar diastolic pressure waveforms have been recorded on simultaneous pulmonary capillary wedge tracings.

Apart from catheter entrapment, respiratory variations could influence the diastolic left ventricular pressure signals. To quantify the influence of respiratory variations, the digitized data points of the diastoles recorded during 5 minutes of continuous sinus rhythm and quiet respiration were averaged. For each patient the average diastole recorded during regular sinus rhythm was subsequently compared to the digitized data points of diastoles recorded after postextrasystolic potentiation, using statistical rank testing. The influence of respiratory variation on the diastolic pressure waveform was significantly smaller than the alteration in diastolic pressure waveform that occurred after postextrasystolic potentiation.

### *Aortic Stenosis: A Model of Inactivation-Dependent Relaxation*

Myocardial relaxation is determined by a dual control mechanism, cardiac muscle loading and cardiac muscle inactivation [58]. This hypothesis of a dual control of myocardial relaxation provides a conceptual framework but does not address the relative importance of each mechanism as a cause of disturbed left ventricular relaxation observed in certain pathologic conditions, such as hypertrophic cardiomyopathy and pressure-overload hypertrophy. Table 27-3 summarizes the influence of altered left ventricular loading and of altered myocardial activation on left ventricular pressure decay and filling for the normal left ventricle and for the hypertrophied left ventricle of hypertrophic cardiomyopathy and of pressure-overload hypertrophy induced by aortic stenosis.

Reducing left ventricular afterload (see Table 27-3) reduces the time constant of left ventricular pressure decay of the normal left ventricle [33, 34] and of the left ventricle in hypertrophic cardiomyopathy [17]. In aortic stenosis, an infusion of nitroprusside sufficient to cause a 30 mm Hg reduction of peak left ventricular pressure did not alter the time constant of isovolumic left ventricular pressure decay [59]. Load-dependent left ventricular pressure decay therefore appears to be present in the normal left ventricle and in hypertrophic cardiomyopathy but absent in pressure-overload hypertrophy caused by aortic stenosis. The stenotic aortic valve imposes a predominantly resistive load on the hypertrophied left ventricle and disconnects it from end-systolic loading increments caused by arterial capacitance or wave reflections. This pattern of left ventricular loading favors an inactivation-dependent course of left ventricular pressure decay in aortic stenosis.

Reduction of left ventricular afterload improves left ventricular filling in the normal left ventricle and in hypertrophic cardiomyopathy [17] but not in aortic stenosis [59]. This improvement of left ventricular filling in the normal left ventricle and in hypertrophic cardiomyopathy is explained by the smaller end-systolic volume, which augments internal restoring forces or elastic recoil of the left ventricular wall [58, 60-62]. The presence of elastic recoil of the left ventricular wall is consistent with a load-dependent relaxation pattern, which makes myocardial lengthening

TABLE 27-3. Influence of load and activation on left ventricular (LV) pressure decay and filling in hypertrophic cardiomyopathy (HCM) and Aortic Stenosis (AS)

	NML	HCM	AS
Reducing LV afterload	T ↓	T ↓	T ↔
	PFR ↑	PFR ↑	PFR ↔
Calcium channel blocker	T ↓	T ↓	
	PFR ↑	PFR ↑ ↑	
After PESP	T ↔	T ↔	T ↑
	PFR ↔	PFR ↓	PFR ↓

(Table 27-2)

T = time constant; PFR = peak filling rate; NML = normal left ventricle; PESP = postextrasystolic potentiation.

sensitive to the small loading changes induced by internal restoring forces. The unaltered left ventricular filling in aortic stenosis, despite smaller end-systolic dimensions during nitroprusside infusion, implies that elastic recoil of the hypertrophied left ventricular wall does not contribute to left ventricular filling. Outward wall motion during filling of the hypertrophied left ventricle in aortic stenosis is therefore only determined by left ventricular inflow, which is a function of the instantaneous pressure difference between the left atrium and the left ventricle [12, 63]. Slow inactivation-dependent left ventricular pressure decay of the hypertrophied left ventricle in aortic stenosis reduces the pressure gradient for inflow across the mitral valve in early diastole and causes sluggish outward motion of the left ventricular wall.

The influence of myocardial activation on left ventricular relaxation was investigated by the administration of calcium channel blocking agents and by the analysis of left ventricular relaxation after postextrasystolic potentiation (see Table 27-3). The administration of verapamil leaves relaxation and lengthening mechanics of cat papillary muscles unaltered [58], consistent with a load-dependent relaxation pattern. In anesthetized dogs, verapamil causes only small reductions of the time constant of left ventricular relaxation [64]. These changes have been ascribed, however, to improved myocardial inactivation and not to altered left ventricular loading. In hypertrophic cardiomyopathy a comparative analysis of nifedipine and nitroprusside on isovolumic left ventricular relaxation revealed equal reductions of the time constant of left ventricular pressure decay [17], which implies that nifedipine exerts its bene-

ficial action on left ventricular isovolumic relaxation through peripheral vasodilatation. In the same study the beneficial effect of nifedipine on left ventricular filling significantly exceeded the effect of nitroprusside despite equal reductions in end-systolic dimensions [17]. This finding is consistent with the appearance of an inactivation-dependent relaxation pattern during the left ventricular filling phase. Therefore in hypertrophic cardiomyopathy both load-dependent and inactivation-dependent features are present with a load-dependent pattern of isovolumic relaxation and an inactivation-dependent pattern of the left ventricular filling phase.

The analysis of left ventricular relaxation after postextrasystolic potentiation provides further evidence about the influence of myocardial activation on subsequent relaxation. In the normal left ventricle, the time constant of the left ventricular pressure decay and left ventricular filling rate remain unaltered after postextrasystolic potentiation, consistent with a load-dependent pattern of left ventricular relaxation [25]. In hypertrophic cardiomyopathy, postextrasystolic potentiation did not affect the time constant of isovolumic relaxation but slowed early diastolic left ventricular pressure decay. These findings are in line with the effects of calcium channel blocking drugs in hypertrophic cardiomyopathy; namely, a load-dependent pattern during isovolumic relaxation and a predominant influence of myocardial inactivation during early diastolic filling. In aortic stenosis, postextrasystolic potentiation prolongs the time constant of left ventricular pressure decay and reduces early diastolic left ventricular inflow and filling. These effects are consistent with an inactivation-dependent pattern of both isovolu-

mic relaxation and early diastolic filling and are explained by an imbalance between the increased amount of activator calcium, which enters the myoplasm during postextrasystolic potentiation and the depressed inactivation of hypertrophied myocardium.

In conclusion, the impairment of left ventricular filling in hypertrophic cardiomyopathy and in pressure-overload hypertrophy of aortic stenosis has been related to slow left ventricular pressure decay. This slow left ventricular pressure decay, which prolongs isovolumic relaxation and impedes left ventricular inflow, is probably caused by persistent diastolic cross-bridge interaction related to a failure of inactivation of hypertrophied myocardium. This failure of myocardial inactivation is deduced from:

1. The absence of load-dependent relaxation of the hypertrophied left ventricle in aortic stenosis [59].

2. The beneficial effect of calcium channel blocking drugs on left ventricular filling in hypertrophic cardiomyopathy [17].

3. The worsening of left ventricular filling after postextrasystolic potentiation in hypertrophic cardiomyopathy and in aortic stenosis (see Table 27-2).

Such a failure of myocardial inactivation, which gradually developed during the hypertrophy processes, could be explained by alterations of enzyme kinetics or of calcium sensitivity of certain critical proteins involved in excitation-contraction-relaxation coupling.

## References

1. Stewart S, Mason DT, Braunwald E (1968). Impaired rate of left ventricular filling in idiopathic hypertrophic subaortic stenosis and valvular aortic stenosis. *Circulation* 37:8-14.
2. Sanderson JE, Gibson DG, Brown DJ, Goodwin JF (1977). Left ventricular filling in hypertrophic cardiomyopathy: An angiographic study. *Br Heart J* 39:661-670.
3. St John Sutton MG, Tajik AM, Gibson DG, et al (1978). Echocardiographic assessment of left ventricular filling and septal and posterior wall dynamics in idiopathic hypertrophic subaortic stenosis. *Circulation* 57:512-520.
4. Hanrath P, Mathey DG, Siegert R, Bleifeld W (1980). Left ventricular relaxation and filling pattern in different forms of left ventricular hypertrophy: An echocardiographic study. *Am J Cardiol* 45:15-23.
5. Bonow RO, Dilsizian V, Rosing DR, et al (1985). Verapamil-induced improvement in left ventricular diastolic filling and increased exercise tolerance in patients with hypertrophic cardiomyopathy: Short- and long-term effects. *Circulation* 72:853-864.
6. Gibson DG, Traill TA, Hall RJC, Brown DJ (1979). Echocardiographic features of secondary left ventricular hypertrophy. *Br Heart J* 41:54-59.
7. Friedman MJ, Sahn DJ, Burriss HA, et al (1979). Computerized echocardiographic analysis to detect abnormal systolic and diastolic left ventricular function in children with aortic stenosis. *Am J Cardiol* 44:478-486.
8. Fifer MA, Borow KM, Colan SD, Lorell BH (1985). Early diastolic left ventricular function in children and adults with aortic stenosis. 5:1147-1154.
9. Fouad FM, Tarazi RC, Gallagher JH, et al (1980). Abnormal left ventricular relaxation in hypertensive patients. *Clin. Sci.* 59:411S-414S.
10. Inouye I, Massie B, Loge D, et al (1984). Abnormal left ventricular filling: An early finding in mild to moderate systemic hypertension. *Am J Cardiol* 53:120-126.
11. Smith VE, Schulman P, Karimeddini MK, et al (1985). Rapid ventricular filling in left ventricular hypertrophy: II, Pathologic hypertrophy. *J Am Coll Cardiol* 5:869-874.
12. Murakami T, Hess OM, Gage JE, et al (1986). Diastolic filling dynamics in patients with aortic stenosis. *Circulation* 6:1162-1174.
13. Lorell BH, Paulus WJ, Grossman W, et al (1982). Modification of abnormal left ventricular diastolic properties by nifedipine in patients with hypertrophic cardiomyopathy. *Circulation* 65:499-507.
14. Murgu JP, Craig WE (1980). Relaxation abnormalities in hypertrophic cardiomyopathy. *Circulation* 62(suppl III):316 (abstract).
15. Goodwin JF (1980). Hypertrophic cardiomyopathy: A disease in search of its own identity. *Am J Cardiol* 45:177-180.
16. Betocchi S, Bonow RO, Bacharach SL, et al (1986). Isovolumic relaxation period in hypertrophic cardiomyopathy: assessment by radio-nuclide angiography. *J Am Coll Cardiol* 7:74-81, 1986.
17. Paulus WJ, Lorell BH, Craig WE, et al (1983). Comparison of the effects of nitroprusside and nifedipine on diastolic properties in patients with hypertrophic cardiomyopathy: Altered left ventricular loading or improved muscle inactivation? *J Am Coll Cardiol* 2:879-886.

18. Paulus WJ, Nellens P, Heyndrickx GR, Andries E (1986). Effects of long-term treatment with amiodarone on exercise hemodynamics and left ventricular relaxation in patients with hypertrophic cardiomyopathy. *Circulation* 74:544-554.
19. Gwathmey JK, Morgan JP (1985). Altered calcium handling in experimental pressure overload hypertrophy in the ferret. *Circ Res* 57:836-843.
20. Entman ML, Van Winkle WB, McMillin-Wood JB (1985). The biochemistry of excitation-contraction coupling: Implications with regard to pump failure. In Levine HJ, Gaasch WH (eds): *The Ventricle: Basic and Clinical Aspects*. Boston: Martinus Nijhoff, pp 63-77.
21. Lossnitzer K, Janke J, Hein B, et al (1975). Disturbed myocardial calcium metabolism: a possible pathogenetic factor in the hereditary cardiomyopathy of the Syrian hamster. In Fleckenstein A, Rona G (eds): *Recent Advances in Studies on Cardiac Structure and Function*. Baltimore: University Park Press, pp 207-217.
22. Lorell BH, Barry WH (1984). Effects of verapamil on contraction and relaxation of cultured chick embryo ventricular cells during calcium overload *J Am Coll Cardiol* 3:341-348.
23. Rouleau JL, Chuck LHS, Hollosi G, et al (1982). Verapamil preserves myocardial contractility in the hereditary cardiomyopathy of the Syrian hamster. *Circ Res* 50:405-412.
24. Johnson EA (1979). Force-interval relationship of cardiac muscle. In Berne RM, Sperlakis N, Geiger SR (eds): *Handbook of Physiology II. The Cardiovascular System*. Bethesda, MD: American Physiological Society, 475-496.
25. Blaustein AS, Gaasch WH, Adam D, Levine HJ (1981). Myocardial relaxation. V. Postextrasystolic contraction-relaxation in the intact dog heart. *Circulation* 64:345-351.
26. Carroll JD, Widmer R, Hess OM, et al (1983). Left ventricular isovolumic pressure decay and diastolic mechanics after postextrasystolic potentiation and during exercise. *Am J Cardiol* 51:583-590.
27. Nakamura Y, Konishi T, Nonogi H, et al (1986). Myocardial relaxation in atrial fibrillation *J Am Coll Cardiol* 7:68-73.
28. Eichhorn P, Grimm J, Koch R, et al (1982). Left ventricular relaxation in patients with left ventricular hypertrophy secondary to aortic valve disease. *Circulation* 65:1395-1404.
29. Hess O, Job JG, Kraft A, Krayenbuehl HP (1984). Is left ventricular relaxation delayed in patients with aortic stenosis? *Circulation* 70 (suppl II):303 (abstract)
30. Takenaka K, Dabestani A, Gardin JM, et al (1986). Left ventricular filling in hypertrophic cardiomyopathy: A pulsed doppler echocardiographic study. *J Am Coll Cardiol* 7:1263-1271.
31. Spirito P, Maron BJ, Bonow RO (1986). Non-invasive assessment of left ventricular diastolic function: Comparative analysis of doppler echocardiographic and radionuclide angiographic techniques. *J Am Coll Cardiol* 7:518-526.
32. Weiss JL, Frederiksen JW, Weisfeldt ML (1976). Hemodynamic determinants of the time course of fall in canine left ventricular pressure. *J Clin Invest* 58:751-760.
33. Gaasch WH, Blaustein AS, Andrias CW, et al (1980). Myocardial relaxation. II. Hemodynamic determinants of the rate of left ventricular isovolumic pressure decline. *Am J Physiol* 239:H1-H6.
34. Raff GL, Glantz SA (1981). Volume loading slows left ventricular isovolumic relaxation rate: Evidence of load-dependent relaxation in the intact dog heart. *Circ Res* 48:813-824.
35. Mirsky I (1984). Assessment of diastolic function: suggested methods and future considerations. *Circulation* 69:836-841.
36. Serizawa, T (1978). An experimental study of left ventricular isovolumetric relaxation period: On the fitting of left ventricular pressure fall to exponential function: *Tokyo J Med Sci* 85: 295-308.
37. Pagani M, Pizzinelli P, Gussomi M, et al (1983). Diastolic abnormalities of hypertrophic cardiomyopathy reproduced by asynchrony of the left ventricle in conscious dogs *J Am Coll Cardiol* (abstract).
38. Rousseau MF, Veriter C, Detry JR, et al (1980). Impaired early left ventricular relaxation in coronary artery disease: effects of intracoronary nifedipine. *Circulation* 62:764-772.
39. Craig WE, Murgo JB (1980). Evaluation of isovolumic relaxation in normal man during rest, exercise and isoproterenol infusion. *Circulation* 62(suppl III):192 (abstract).
40. Martin G, Gimeno JV, Cosin J, Guillem MI (1984). Time constant of isovolumic pressure fall: New numerical approaches and significance *Am J Physiol* 247:H283-H294.
41. Gibson DG, Doran JH, Traill TA, and Brown DJ (1978). Regional abnormalities of left ventricular wall movement during isovolumic relaxation in patients with ischemic heart disease. *Eur J Cardiol* 7(suppl):251-264.
42. Parmley WW, Sonnenblick EH (1967). Series elasticity of heart muscle: Its relation to contractile element velocity and proposed muscle models. *Circ Res* 20:112-123.
43. Winegrad S, Weisberg A, MacClellan G (1980). Are restoring forces important to relaxation? *Eur Heart J* 1(suppl A):59-65.
44. Paulus WJ, Serizawa T, Grossman W (1982). Altered left ventricular diastolic properties during pacing-induced ischemia in dogs with

- coronary stenoses: Potentiation by caffeine. *Circ Res* 50:218–227.
45. Grossman W, Barry WH (1980). Diastolic pressure-volume relations in the diseased heart. *Fed Proc* 39:18–25.
  46. Pouleur H, Karliner JS, LeWinter MM, Covell JW (1979). Diastolic viscous properties of the intact canine left ventricle. *Circ Res* 45:410–419.
  47. Hess OM, Schneider J, Koch R, et al (1981). Diastolic function and myocardial structure in patients with myocardial hypertrophy. *Circulation* 63:360–371.
  48. Paulus WJ, Claes VA, Brutsaert DL (1976). Physiological loading of isolated mammalian cardiac muscle. *Circ Res* 39:42–53.
  49. O'Rourke MF (1982). *Arterial Function in Health and Disease* Edinburgh: Churchill Livingstone.
  50. Paulus WJ, Claes VA, Brutsaert DL (1980). End-systolic pressure-volume relation estimated from physiologically loaded cat papillary muscle contractions. *Circ Res* 47:20–26.
  51. Wiggle ED, Sasson Z, Henderson MA, et al (1985). Hypertrophic cardiomyopathy: The importance of the site and the extent of hypertrophy. A review. *Prog Cardiovasc Dis* 28: 1–83.
  52. Maron BJ, Gottdiener JS, Epstein SE (1981). Patterns and significance of distribution of left ventricular hypertrophy in hypertrophic cardiomyopathy. *Am J Cardiol* 48:418–428.
  53. Shapiro LM, MacKenna WJ (1983). Distribution of left ventricular hypertrophy in hypertrophic cardiomyopathy: A two-dimensional echocardiographic study. *J Am Coll Cardiol* 2:437–444.
  54. Housmans PR, Lee NKM, Blinks JR (1983). Active shortening retards the decline of the intracellular calcium transient in mammalian heart muscle. *Science* 221:159–161.
  55. Hess OM, Surber EP, Ritter M, Krayenbuehl HP (1984). Pulsus alternans: Its influence on systolic and diastolic function in aortic valve disease. *J Am Coll Cardiol* 4:1–47.
  56. Fabiato A (1983). Calcium-induced release of calcium from the cardiac sarcoplasmic reticulum. *Am J Physiol* 245:C1–C14.
  57. Levitsky DO, Benevolensky DS (1986). Effects of changing  $Ca^{2+}$  to  $H^{+}$  ratio on  $Ca^{2+}$  uptake by sarcoplasmic reticulum. *Am J Physiol* 250: H360–H365.
  58. Brutsaert DL, Housmans PR, Goethals MA (1980). Dual control of relaxation: its role in the ventricular function in the mammalian heart. *Circ Res* 47:637–652.
  59. Diver DJ, Royal HD, Aroesty JM, et al (1985). Load independence of abnormal diastolic function in patients with aortic stenosis. *J Am Coll Cardiol* (in press).
  60. Brecher GA (1958). Critical review of recent work on ventricular diastolic suction. *Circ Res* 6:554–566.
  61. Sabbah HN, Stein PD (1981). Pressure-diameter relations during early diastole in dogs: incompatibility with the concept of passive left ventricular filling. *Circ Res* 48:357–364.
  62. Bahler RC, Martin P (1985). Effects of loading conditions and inotropic state on rapid filling phase of left ventricle. *Am J Physiol* 248:H523–H533.
  63. Ishida Y, Meisner JS, Tsujioka K, et al (1986). Left ventricular filling dynamics: influence of left ventricular relaxation and left atrial pressure. *Circulation* 74:187–196.
  64. Carroll JD, Blaustein AS, Donaldson JT, et al (1981). Verapamil uncouples contraction-relaxation in the canine left ventricle. *Circulation* 64 (suppl IV):211 (abstract).

---

# INDEX

---

- Acidosis**  
diastolic chamber compliance and, 180  
ischemic/hypoxic contracture and, 75  
reperfusion/reoxygenation contracture and, 77
- Actin**  
calcium sensitivity in contractile system and, 31  
coronary vascular collapse and diastolic chamber compliance and, 180
- Actomyosin cross-bridge cycle, and economy of concentration and relaxation, 44–45**
- Adenosine, in diastolic chamber compliance studies, 175**
- Adenosine diphosphate (ADP), and calcium pump of sarcoplasmic reticulum (SR), 11**
- Adenosine triphosphatase (ATPase) calcium pump of sarcoplasmic reticulum (SR) and, 11, 12, 98**  
ischemic/hypoxic contracture and, 74  
isomyosin composition and, 42  
regional myocardial heterogeneity and isometric relaxation and, 39  
reperfusion/reoxygenation contracture and, 79  
thyroid state in cardiac hypertrophy and calcium and, 102–103
- Adenosine triphosphate (ATP) brief periods of ischemia and, 80**  
2,3-butanedione monoxime (BDM) in hypoxia and, 69–70  
calcium-force relation in contraction and, 30–31  
calcium regulation of contraction and, 18  
cellular mechanisms of relaxation and, 3, 5, 6, 8  
calcium role in relaxation and deficit in, 14  
hypoxia and hypertrophied left ventricular levels of, 187, 189  
hypoxia and myocardial levels of, 67, 178  
ischemic contracture and calcium level and, 33, 34, 35, 36, 37  
ischemic/hypoxic contracture and acidosis and, 75  
myocardial energy demands during hypoxia and ischemia and, 181  
primary ischemia vs. demand ischemia and, 202  
relaxation and, 212  
thyroid state in cardiac hypertrophy and calcium and, 102
- Afterload, left ventricular filling dynamics and, 231**  
isovolumic relaxation and, 137–138
- Amrinone, and light and tension responses in cat papillary muscle, 19, 22**
- Angina pectoris diastolic distensibility during, 207–215**  
diastolic function during, 193–194, 245  
distensibility vs. diastolic compliance in, 194–196  
experimental model of, 197–199  
ventricular diastolic distensibility determinants in, 196–197
- Angioplasty, *see* Percutaneous transluminal coronary angioplasty (PTCA)**
- Angiotensin, and rapid load studies, 139**
- Aortic insufficiency (AI) diastolic compliance in, 143**  
hemodynamics of, 145  
load dependence of relaxation and, 93  
postoperative left ventricular diastolic properties in, 148–150  
preoperative left ventricular diastolic properties in, 145–148
- Aortic stenosis diastolic compliance in, 143**  
hemodynamics of, 145
- Aortic valve replacement, and diastolic properties, 14448–150**
- ARL-115, and force decline during relaxation, 90**
- Beta-agonists, and light and tension responses in cat papillary muscle, 19**
- 2,3-butanedione monoxime (BDM) adenosine triphosphate (ATP) concentration and creatine phosphate (CP) levels and, 69–70**  
contracture development and, 67  
extracellular calcium level and ryanodine and, 69  
reoxygenation after hypoxia and, 70–71  
reoxygenation-induced gain in calcium and, 69
- Bypass surgery, and diastolic function during exercise-induced ischemia, 217–218, 222–223**
- Caffeine intracellular calcium action and, 20, 98**  
cellular mechanisms of relaxation and, 5–6, 8  
end-diastolic distensibility and, 199  
ischemic/hypoxic contracture and, 74–75  
light and tension responses in cat papillary muscle with, 22
- Calcium adrenergic stimulation of, 29**  
aequorin measurement of intracellular, 18–19, 21  
arrhythmias and contractile activity with, 60–62  
ATPase reaction and, 11, 12  
2,3-butanedione monoxime (BDM) in hypoxia and, 69–70  
cardiac hypertrophy and intracellular, 97–106  
cellular mechanisms of relaxation

- and, 3, 5–8  
 cholinergic stimulation of, 29–30  
 contractile system and  
 variable sensitivity to,  
 27–32  
 cyclic adenosine monophosphate  
 (cAMP) and sensitivity to,  
 28–29  
 excitation-contraction coupling  
 phases and, 17  
 fluorescent probe measurement  
 of, 4 hypoxia and  
 hypertrophied left  
 ventricular levels of,  
 189–190  
 hypoxia and reoxygenation and,  
 23–24  
 ischemic contracture and level of,  
 33–37, 178  
 ischemic/hypoxic contracture  
 and, 73–74, 77  
 left ventricular filling and, 236  
 load dependence of  
 relaxation and, 87–91  
 model for contraction regulation  
 with, 17–18  
 release from sarcoplasmic  
 reticulum (SR) of, 12  
 relaxation abnormalities and  
 fluxes in, 12–14, 212  
 reperfusion/reoxygenation  
 contracture and, 77–78, 79  
 resting sarcomere length and  
 calcium-force relations with,  
 31–32  
 sarcoplasmic reticulum (SR) and  
 diastolic release of, 49–62  
 sarcoplasmic reticulum (SR) and  
 uptake of, 3, 8, 11–12  
 scattered light intensity  
 fluctuations (SLIF)  
 measurement of, 50, 55, 56,  
 59  
 smooth muscle tonic tension  
 development and, 24–25  
 sodium exchange with, *see*  
 Sodium-calcium exchange  
 spontaneous oscillations in  
 intracellular (CaOs), 50–55  
 troponin and sensitivity to, 27–  
 28
- Calcium antagonist  
 coronary artery disease and,  
 251–252  
 diastolic properties of ischemic  
 myocardium and, 212–213
- Calcium channel-blocking agents  
 hypertrophic conditions and,  
 281, 291  
 left ventricular filling and,  
 235–236, 238  
 light and tension responses in cat  
 papillary muscle with, 22
- Calcium, spontaneous oscillations in  
 intracellular (CaOs), 50
- arrhythmias and, 60–62  
 characteristics of, in single  
 cardiac cells, 50–52  
 diastolic tonus and, 52–55  
 systolic function interference  
 from, 55–60
- cAMP, *see* Cyclic adenosine  
 monophosphate (cAMP)
- Chamber stiffness  
 determination of, 144  
 influences in, 143  
 regional myocardial distensibility  
 and, 209–212  
 relaxation and, 169
- Contractile proteins (CP)  
 force, decline during relaxation  
 and, 90  
 load dependence of relaxation  
 and, 87
- Contraction  
 actomyosin cross-bridge cycle  
 and, 44–45  
 adenosine triphosphate (ATP)  
 concentration and calcium-  
 force relation in, 30–31  
 adrenergic stimulation of calcium  
 and, 29  
 cholinergic stimulation of  
 calcium and, 29–30  
 cyclic adenosine monophosphate  
 (cAMP) and calcium  
 sensitivity in, 28–29  
 economy of relaxation and,  
 41–42, 43  
 ischemic, and calcium level,  
 33–37  
 loading conditions and, 133–138  
 measures of, in relaxation studies,  
 4 percutaneous transluminal  
 coronary angioplasty (PTCA)  
 and, 272–273  
 phases of, 17  
 regional myocardial heterogeneity  
 and, 39–47  
 reperfusion/reoxygenation, 77–79  
 resting sarcomere length and  
 calcium-force relations in,  
 31–32  
 sarcoplasmic reticular control of,  
 11–14  
 thermal measurements and  
 interpretation in, 40–41  
 variable calcium sensitivity and,  
 27–32
- Contraction load, 85–87
- Coronary artery disease  
 calcium channel blockers in, 291  
 compliance changes in, 226  
 left ventricular filling in, 235,  
 272  
 myocardial stiffness, relaxation,  
 and coronary perfusion in,  
 245–247  
 relaxation impairment and global  
 ventricular compliance in,  
 247–248
- Creatine phosphate (CP)  
 2,3-butanedione monoxime  
 (BDM) in hypoxia and,  
 69–70  
 diastolic chamber compliance  
 and, 181  
 hypoxia and hypertrophied left  
 ventricular levels of, 187  
 hypoxia and myocardial levels of,  
 67, 178  
 relaxation and, 212
- Creep phenomenon, 118, 213, 274
- Cyanide, and calcium levels in  
 ischemic contracture, 34, 35
- Cyclic adenosine monophosphate  
 (cAMP)  
 calcium regulation of contraction  
 and, 18  
 calcium sensitivity in contractile  
 system and, 28–29  
 coronary artery disease treatment  
 and, 253  
 ischemic/hypoxic contracture  
 and, 74  
 light and tension responses in cat  
 papillary muscle with, 19
- Cyclic guanosine monophosphate  
 (cGMP), and calcium  
 sensitivity in contractile  
 system, 29, 30
- Deactivation, in relaxation, 133
- Demand ischemia, 169–170,  
 200–202
- 2-deoxyglucose (2DG), and calcium  
 levels in ischemic contracture,  
 34, 35
- Diastole  
 angina pectoris and, 193–194,  
 245  
 chronic volume overload and,  
 119–123  
 coronary artery disease and  
 compliance changes in, 226  
 coronary artery disease and  
 regional dysfunction in,  
 245–253  
 coronary vascular collapse and  
 chamber compliance in,  
 179–180  
 distensibility vs. compliance with  
 angina pectoris in, 194–196  
 exercise-induced ischemia and,  
 217–227  
 factors for data acquisition on,  
 111–112  
 intrathoracic pressure or force  
 external to heart in,  
 112–113  
 ischemia and hypoxia and  
 chamber compliance in,  
 171–173  
 ischemia and hypoxia and wall

- thickness in, 173–174  
 ischemia and stiffness in, 79–81  
 ischemia with superimposed  
 ischemia and, 175–179  
 ischemic and nonischemic  
 myocardium interaction in,  
 213–215  
 ischemic-induced creep in, 118,  
 213 measurement of  
 properties of, 111–116  
 myocardial ischemia and,  
 116–119  
 normalization of force and  
 dimension data in, 114–116  
 percutaneous transluminal  
 coronary angioplasty  
 (PTCA) and, 256, 259–265  
 pericardial influence on  
 compliance in, 151–160  
 pericardial pressure for evaluation  
 of, 163–167  
 pressure and volume data over full  
 physiologic range in, 113  
 pressure and volume overload and  
 compliance in, 143–150  
 sarcoplasmic reticulum (SR) and  
 calcium release in, 49–62  
 spontaneous oscillations in  
 intracellular calcium (CaOs)  
 and tonus of, 52–55  
 unified approach to ventricular  
 function quantification in,  
 116  
 verapamil and, 281–289  
**Diastolic chamber stiffness**  
 coronary artery disease and,  
 247–248  
 distensibility vs., 194–196  
 percutaneous transluminal  
 coronary angioplasty  
 (PTCA) and, 258–259, 268  
 relaxation and, 169  
**Dibutyryl cAMP**, in light and  
 tension responses in cat  
 papillary muscle, 19  
**Digitalis**, in light and tension  
 responses in cat papillary  
 muscle, 19  
**Diltiazem**, and reperfusion/  
 reoxygenation contracture, 77  
**Distensibility**  
 angina and, 207–215  
 cinangiographic techniques in  
 analysis of, 208–209  
 determinants of ventricular,  
 196–197, 207  
 diastolic compliance vs., 194–  
 196  
 end-diastolic, 199–200  
 experimental model of angina  
 physiology with, 198  
 left ventricular chamber stiffness  
 and regional myocardial,  
 209–212  
 pericardial, 151–153
- Excitation**, phases of, 17
- FCCP**, and calcium and tension  
 mechanism, 24  
**Frank-Starling mechanism**, and left  
 ventricular preload, 133
- Glycosides**, in cellular mechanisms  
 of relaxation, 6–8  
**Guanosine triphosphate (GTP)**, and  
 calcium sensitivity in  
 contractile system, 30
- Hydrogen ion**  
 diastolic chamber compliance  
 and, 181  
 intracellular calcium action and,  
 22  
 ischemia with coronary artery  
 occlusion and, 80  
 reperfusion/reoxygenation  
 contracture and, 78  
**Hypertrophy**, cardiac  
 human heart muscle models in,  
 104–106  
 hypoxia and relaxation in,  
 185–190  
 intracellular calcium handling  
 and, 97–106  
 left ventricular filling in,  
 236–238, 291–302  
 left ventricular isovolumic  
 relaxation and, 128–130,  
 131  
 nifedipine and, 288  
 pressure-overload right ventricle  
 model in, 97–101  
 thyroid state and, 101–104  
 verapamil and, 281, 282,  
 285–288  
**Hypoxia**  
 adenosine triphosphate (ATP)  
 concentration and creatine  
 phosphate (CP) levels in,  
 69–70  
 2,3-butanedione monoxime  
 (BDM) in reoxygenation  
 recovery after, 70–71  
 calcium and mechanism of,  
 23–24  
 contracture in, 73–77  
 diastolic chamber compliance in,  
 171–173  
 diastolic wall thickness in,  
 173–174  
 hypertrophied ventricular  
 relaxation and, 185–190  
 myocardial effects of, 67,  
 181–182  
 relaxation and, 67–72, 169–182  
 superimposed ischemia with,  
 175–179
- supply ischemia differentiated  
 from, 170–171
- Ischemia**  
 adenosine triphosphate (ATP)  
 levels in, 202  
 calcium antagonist and  
 myocardial properties in,  
 212–213  
 calcium level and contracture in,  
 33–37  
 contracture in, 73–77  
 demand ischemia, 169–170  
 diastolic chamber compliance in,  
 171–173  
 diastolic mechanics in, 116–119,  
 217–227  
 diastolic stiffness and, 79–81  
 diastolic wall thickness in,  
 173–174  
 exercise-induced, and diastolic  
 function, 217–227  
 hypoxia with superimposed,  
 175–179  
 left ventricular diastolic pressure  
 and, 185, 209  
 left ventricular filling in,  
 232–236  
 myocardial energy demands with,  
 181–182  
 primary vs. demand, 200–202  
 supply ischemia, 169–170  
 ventricular relaxation and,  
 169–182  
**Ischemic/hypoxic contracture**,  
 73–77  
 acidosis and, 75  
 caffeine and, 74–75  
 calcium and, 73–74, 77  
 definition of, 73  
 rigor and, 75–77  
**Ischemia-induced diastolic creep**,  
 118, 213  
**Isobutylmethylxanthine**, and light  
 and tension responses in cat  
 papillary muscle, 19  
**Isoproterenol**  
 diastolic sarcoplasmic reticulum  
 calcium and, 58, 59  
 force decline during relaxation  
 and, 90  
 intracellular calcium action and,  
 20, 98  
 light and tension responses in cat  
 papillary muscle with, 19
- Lanthanum**, and ischemic/hypoxic  
 contracture, 74  
**Left ventricle**  
 aortic valve disease  
 hemodynamics and, 145  
 aortic valve replacement and, 150  
 coronary artery disease and

- diastolic dysfunction in, 245
- diastolic distensibility and, 202
- diastolic function during angina pectoris and, 193–194
- diastolic mechanics of volume overload in, 121–123
- exercise-induced ischemia and diastolic function in, 219, 221, 222–223, 226
- hypoxia and relaxation in hypertrophy of, 185–190
- ischemia and diastolic pressure in, 185, 209
- isovolumic relaxation of, 125–132
- loading conditions and relaxation of, 133–142
- myocardial stiffness assessment and, 143–144
- percutaneous transluminal coronary angioplasty (PTCA) effects on, 255–277
- pericardial influences on diastolic compliance in, 157–158
- pericardial pressure measures and, 165, 166
- preload conditions in, 133–135
- rapid filling load and, 139
- systolic load studies of, 135–138
- vena caval occlusion studies of normal function in, 123
- Left ventricular filling**
  - coronary artery disease and, 248–249
  - determinants of, 231
  - hypertrophic heart disease and, 236–238, 291–302
  - ischemic heart disease and, 232–236
  - measurement of, 231–232
  - percutaneous transluminal coronary angioplasty (PTCA) and, 257–258, 265–270, 272–273
  - regional asynchrony and, 238
- Lidoflazine, and reperfusion/reoxygenation contracture, 77**
- Load dependence of relaxation, 83–95, 133, 138–141**
  - afterload twitches in, 83–84
  - contraction load vs., 85–87
  - intact ventricle and, 91–95
  - in isolated cardiac muscle, 83–87
  - late systolic load in, 138–139
  - load-clamped twitches in, 84–85
  - mechanisms of, 87–91
  - mitral (MI) and aortic valvular insufficiency (AI) and, 93–95
  - rapid filling load in, 139–141
- Magnesium**
  - calcium levels in ischemic contracture and, 36
  - reperfusion/reoxygenation contracture and, 77
- Manganese, and reperfusion/reoxygenation contracture, 78**
- Milrinone**
  - coronary artery disease and, 251, 252
  - light and tension responses in cat papillary muscle with, 19
- Mitral insufficiency (MI), and load dependence of relaxation, 93–95**
- Myocardial stiffness**
  - aortic valve disease and, 145
  - calculation of, 144
  - coronary artery disease and, 245–247
  - definition of, 143
  - percutaneous transluminal coronary angioplasty (PTCA) and, 273–275
  - postoperative left ventricular diastolic properties in, 149–150
  - preoperative left ventricular diastolic properties in, 146–147
  - primary ischemia and, 200
- Myocardium**
  - cellular mechanisms of relaxation and, 3, 6
  - diastolic function during angina pectoris and, 193–194
  - hypoxia and effects on, 67
- Myosin**
  - calcium sensitivity in contractile system and, 28, 31
  - coronary vascular collapse and diastolic chamber compliance and, 180
  - economy of contraction and relaxation and, 42
  - force decline during relaxation and, 89–91
  - regional myocardial heterogeneity and isometric relaxation and, 39, 40, 45–46
  - thyroid state in cardiac hypertrophy and calcium and, 103
- Nicardipine, and coronary artery disease, 251, 252**
- Nifedipine**
  - coronary artery disease and, 251
  - diastolic properties of ischemic myocardium and, 212–213
  - hypertrophic conditions with, 288
  - left ventricular filling and, 235, 238
- Ouabain**
  - diastolic sarcoplasmic reticulum calcium and, 58
- reperfusion/reoxygenation contracture and, 78**
- Papaverine, and light and tension responses in cat papillary muscle, 19**
- Percutaneous transluminal coronary angioplasty (PTCA)**
  - asynchronous contraction in, 273
  - clinical implications for, 276–277
  - coronary occlusion models of impaired relaxation in, 270–272
  - ejecting dynamics during, 256–257
  - filling dynamics with, 257–258
  - global chamber stiffness in, 258–259
  - left ventricular chamber stiffness and, 273–274
  - left ventricular filling on, 234–235, 236, 238
  - regional pressure-radius length relations in, 265–270
  - relaxation parameters in, 261–253
  - uncoordinated segmental contraction in, 272–273
  - wall motion during acute ischemia on, 274–277
- Pericardial pressure**
  - concept of, 163–165
  - diastolic dysfunction evaluation with, 163–167
  - magnitude of, 165–166
  - measurement of contact stress in, 163–165
- Pericardium**
  - cardiac filling and, 153–160
  - chronic cardiac dilatation and, 160
  - diastolic compliance and, 151–160
  - distensibility of, 151–153, 207
  - exercise-induced ischemia and diastolic function and, 225–226
  - right ventricular compliance and, 156–158
- pH**
  - hypoxia and hypertrophied left ventricular, 187
  - hypoxia and reoxygenation and, 23
  - ischemic/hypoxic contracture and, 73–74, 179
  - phosphorus nuclear magnetic resonance (NMR) measurement of, 171
- Phenylephrine, and intracellular calcium action, 22**
- Phosphates**
  - hypoxia and reoxygenation and, 23

- ischemia with coronary artery occlusion and, 80
  - Phosphodiesterase, in ischemic/hypoxic contracture, 74
  - Potassium
    - diastolic sarcoplasmic reticulum calcium and, 59
    - hypoxia and myocardial levels of, 67
    - reperfusion/reoxygenation contracture and, 78
  - Preload, left ventricular (LV)
    - intact heart studies of, 133–134
    - isolated muscle studies of, 134–135
  - Pressure overload
    - intracellular calcium and, 97–101
    - verapamil and, 281, 282
  - Propranolol, and ischemic/hypoxic contracture, 74
  - PTCA, *see* Percutaneous transluminal coronary angioplasty (PTCA)
  
  - Rapid filling load
    - intact heart studies of, 139
    - isolated muscle studies of, 139–141
  - Relaxation
    - actomyosin cross-bridge cycle and, 44–45
    - akinetin scar and, 224–225
    - calcium fluxes and abnormalities in, 12–14, 212
    - cellular mechanisms of, 3–8
    - coronary artery disease and, 245–247, 248–249
    - economy of contraction and, 41–42
    - exercise-induced ischemia and diastolic function and, 224
    - force decline during, 89–91
    - hypoxia and, 67–72, 169–182
    - ischemia and, 169–182
    - late systolic load and, 138–139
    - left ventricular filling and, 231
    - left ventricular isovolumic, 125–132
    - lengthening of muscle during, 87
    - loading conditions and left ventricular, 133–142
    - load dependence of, 83–95
    - measures of, 4
    - model for calcium regulation of, 17–18
    - percutaneous transluminal coronary angioplasty (PTCA) and, 261–263, 270–272
    - pericardial pressure in left ventricular isovolumic, 166
    - phases of, 5, 6
    - rapid filling load and, 139–141
    - regional myocardial heterogeneity and, 39–47
    - reperfusion/reoxygenation contracture and delay in, 78
    - revascularization and, 225
    - sarcoplasmic reticular control of, 11–14, 87
    - systolic pressure or afterload and, 137–138
    - velocity measurements and interpretation in, 83
    - verapamil and, 287–288
  - Reperfusion/reoxygenation contracture, 77–79
  - Right ventricle
    - economy of contraction and relaxation and, 42
    - diastolic distensibility and, 202
    - exercise-induced ischemia and diastolic function in, 221–222, 223, 224, 225–226
    - intracellular calcium and pressure overload in, 97–101
    - isometric relaxation studies of, 134
    - pericardial influences on diastolic compliance in, 156–158
    - pericardial pressure magnitude and, 165–166
  - Ryanodine
    - cellular mechanisms of relaxation and, 6
    - intracellular calcium action and, 20, 98
  - Sarcolemma
    - cellular mechanisms of relaxation and, 3, 5
    - excitation-contraction coupling phases and, 17
    - hypoxia and reoxygenation and, 23
  - Sarcomere
    - calcium sensitivity in contraction and length of, 31–32
    - ischemia and myocardial distensibility and, 210
  - Sarcoplasmic reticulum (SR)
    - adenosinetriphosphatase (ATPase) and, 98
    - calcium release from, 12
    - calcium uptake and, 3, 8, 11–12
    - cellular mechanisms of relaxation and, 3, 8
    - control of contraction and relaxation and, 11–14, 27
    - coronary artery disease treatment and, 253
    - diastolic chamber compliance and, 180–181, 182
    - diastolic release of calcium in myocardium and, 49–62
    - excitation-contraction coupling phases and, 17
    - hypoxia and hypertrophied left ventricular levels of calcium in, 189–190
  - hypoxia and reoxygenation and, 23
  - ischemia with coronary artery occlusion and, 80
  - ischemic/hypoxic contracture and, 74, 75
  - left ventricular filling and calcium and, 236
  - load dependence of relaxation and, 87
  - myocardial energy demands during hypoxia and ischemia and, 181
  - scattered light intensity fluctuations (SLIF)
    - measurement of calcium in, 50, 55, 56, 59
  - spontaneous oscillations in intracellular calcium (CaOs) in, 50–60
  - thyroid state in cardiac hypertrophy and calcium and, 102, 103
- Scar group after prior infarction, and diastolic function during exercise-induced ischemia, 218, 223–224
- Smooth muscle tonic tension
  - development, and calcium, 24–25
- Sodium
  - cellular mechanisms of relaxation and, 5–6, 8
  - excitation-contraction coupling phases and, 17
  - hypoxia and myocardial levels of, 67
- Sodium-calcium exchange
  - calcium levels in ischemic contraction and, 36
  - diastolic sarcoplasmic reticulum calcium and, 58
- Sulmazole, and intracellular calcium action, 22
- Supply ischemia, 169–170
- Systole
  - left ventricular (LV) load during, 135–138
  - percutaneous transluminal coronary angioplasty (PTCA) and, 256, 259–265
- 
- Theophylline, and light and tension responses in cat papillary muscle, 19, 22
- Thyroid hormone, and calcium in cardiac hypertrophy, 101–104
- TNI, and calcium sensitivity in contractile system, 29, 30, 31
- Transluminal angioplasty, *see* Percutaneous transluminal coronary angioplasty (PTCA)
- Troponin

- adenosine triphosphate (ATP)-
  - concentration and calcium-force relation and, 31
  - calcium and relaxation and, 17, 18, 20, 22, 100
  - calcium sensitivity in contractile system and, 27–28, 31
  - excitation-contraction coupling phases and, 17
  - force decline during relaxation and, 89
  - thyroid state in cardiac hypertrophy and calcium and, 103
- UDCG-115, and force decline during relaxation, 90
- Vanadate, and light and tension responses in cat papillary muscle, 19
- Vasopressor agents, and left ventricular systolic load, 135–138
- Vena caval occlusion
  - pericardial size studies with, 152
  - ventricular volume studies with, 113, 123
- Verapamil
  - chronic administration of, 285
  - coronary artery disease and, 251
  - diastolic ventricular function and, 281–289
  - hypertrophic conditions and, 282, 285–288
  - ischemic/hypoxic contracture and, 74
  - left ventricular filling and, 235, 236, 237
  - left ventricular relaxation and, 287–288
  - reperfusion/reoxygenation contracture and, 77
- Volume overload
  - diastolic compliance and pressure and, 143–150
  - diastolic mechanics of, 116, 119–123
- Xamoterol, in coronary artery disease, 250–251, 252